TIGRANYAN
Robert Edmondovich

Issues of electromagnetobiology

MOSCOW
FIZMATLIT ®

TABLE OF CONTENTS

I. Theory and experiment

II. Technical support for experiments on bioeffects of microwave

Preface

Monograph by R. E. Tigranyan “Issues of electromagnetobiology”
is devoted to the study of the mechanisms of biological action of electromagnetic radiation in the decimeter microwave range. The author of the monograph analyzes theoretical and experimental material,
describing the mechanical-acoustic effects of pulsed EMR in model and biological objects. Based on the theory of thermoelastic
excitation of microwave acoustic oscillations by pulsed EMR and the formation of capillary waves, the author of the monograph proposed an original hypothesis about the occurrence of phase synchronism in biological periodic structures, leading to multiple local accumulation of energy in these structures. Such local accumulation of energy can lead to disruption of the integrity of cellular

structures, which is revealed by the analysis of electron microscopic
photographs of biological objects that were exposed to EMR.

In the 60s of the twentieth century, a number of scientists suggested that the sensory auditory effects of pulsed microwave EMR
can be determined by the mechanism of thermoelastic vibrations of head tissue. To identify the mechanisms of auditory sensations
in humans, associated with the absorption of energy from microwave EMR pulses,
by the formation of thermal impulses in the tissues of the head, the generation of resonant mechanical vibrations and their further conduction through the bone-tissue pathway into the cochlea of the hearing organ, R. E. Tigranyan developed
electronic models of hearing objects observed in natural experiments
effects. The author showed that individual acts of interaction of electromagnetic radiation with a biological object can be combined
into a single system, similar to radio systems, and present it in the form of a communication channel for transmitting and receiving information.
This approach, taking into account the characteristics of a biological object, allowed
calculate equivalent system parameters that model the main sensory auditory effects of pulsed EMR.

The monograph consists of two parts, each of which contains several chapters. Part I - “Theory and Experiment” - contains
information from the radio engineering course necessary to understand the processes of conversion of microwave energy when it is absorbed by biological
structures (chapter 1). The second chapter is devoted to the results of studies of excited mechanical vibrations in model liquids
and biological objects. Chapter 3 presents material on the occurrence of phase matching and the excitation of capillary waves

on periodic biological structures as the basis of the mechanism
biological action of microwave. Chapter 4 contains experimental
data on the study of auditory microwave effects in natural experiments and on
electronic models. The second part - “Technical support for experiments on
microwave bioeffects” - contains
information and practical diagrams developed by the author
microwave generators with broadband modulation, various types of irradiators,
a new direction has been developed for the creation of miniature irradiators and
microwave generators on a semiconductor base. Considered
methods of life support, retrieval of useful information and determination
specific absorbed power synchronously with irradiation. First chapter
is devoted to the consideration of long lines as the basis for the formation
irradiators of various types. The second chapter discusses various
types of waves and waveguides, resonators that implement them and allow
make the optimal design for a particular experiment. Chapter 3 is devoted to
the selection of parameters and design of modulated
Microwave generators with wide variability. Chapters 4–6 are devoted to the
creation of hardware systems for research
in laboratory conditions. Chapter 7 provides standards for permissible
emissions and frequency standards.

The book is written in simple and understandable language and contains extensive illustrative material. Based on the relevance of the topic and the novelty of the factual material, the monograph can be recommended
for publication as a teaching aid for students
Universities with a specialty in “Biophysics”. Author of the monograph, Tigranyan Robert Edmondovich, Doctor of Physical and Mathematical Sciences, for scientific contribution to the field of biophysics of microwave EMR in 1994 was
elected full member of the Association of European Scientists
electromagnetobiology.

Responsible Editor -
Laureate of the USSR State Prize,
Chief Researcher
Institute of Cell Biophysics RAS,
Doctor of Biological Sciences, Professor
Chemeris Nikolai Konstantinovich.

Preface by the author

This book “Issues of electromagnetobiology” is mainly
contains materials from scientific research and design developments of the
author, carried out by him in the period 1970–1990. At the institute
biological physics of the USSR Academy of Sciences in Pushchino and published
in monographs and preprints published in very small editions, inaccessible to the
general reader. It is this circumstance, as well as
the almost complete absence today of generalizing works in the field
studies of the mechanisms of biological action of microwave decimeter range
prompted the author to write this book, despite
prescription

The book is preceded by a concise volume of information from the classic
course "Fundamentals of Radio Engineering" to demonstrate the possibility
representation of the impact of the microwave electromagnetic field on biological
structures in the form of a communication channel for transmitting information and,
as a consequence, the search and description of equivalent parameters of
biological systems when considering the mechanisms of biological action
Microwave fields. It is the attraction of analogies between microwave devices
and biological periodic structures made it possible to assume the possibility of
phase synchronism occurring when mechanical vibrations are excited in these
structures, and then to confirm using electron microscopy the presence of
bunches of mechanical energy on a biological periodic structure due to

phasing of capillary waves. This provides an explanation for the “resonance”
effects observed by many authors, when the difference
between the size of the object and the wavelength of mechanical vibrations
reaches several orders of magnitude. Complete absence of industrial hardware
systems for biophysical research for 40-50 years
ago, and now, in many ways, it hampers the development of biophysical research
with microwave radiation. Faced in due time
with this problem, the author of the book considered it his duty to introduce in a
separate section material devoted to issues of development and creation
modulated microwave generators based on laboratory measuring instruments
generators of domestic and foreign production and medical devices for microwave
therapy, as well as systems for retrieving information and life support for objects.
Methods and methods are described
calculation and design in research laboratories
guiding structures, many of which can be considered
as irradiators for biophysical experiments.

The book also includes the results of the author's research on the effect of ultra-weak doses of external vibrations and excited capillary waves by microwave pulses on similar periodic structures, which have not been published anywhere before.

The book is intended for biologist students, graduate students and teachers, as well as specialists in non-biological specialties who are starting to study modern problems of electromagnetobiology. The author thanks all the employees of the IBP Microwave Irradiation Service

USSR Academy of Sciences for participation in the work.

Doctor of Physical and Mathematical Sciences,
full member of the Association of European
Scientists in Electromagnetic Biology

TIGRANYAN Robert Edmondovich

Part I

THEORY AND EXPERIMENT

Chapter 1

SIGNALS AND INFORMATION IN BIOLOGICAL STRUCTURES

Introduction

The evolution of all forms of living matter on Earth from the moment of its origin proceeded against the background of the action of natural electromagnetic radiation (EMR). Like any environmental component, the electromagnetic field (EMF) of natural origin participated in the formation of living matter.

Over the past hundred years, artificial sources of electromagnetic radiation have been created, the power levels of which are many orders of magnitude higher. exceed the natural “electromagnetic background” of the environment person.

The equilibrium in interaction that has developed in the process of evolution natural EMF and biological elements is thus the norm, violations of which can lead to negative biological element consequences.

Currently, microwave electronics are firmly took its place in the national economy and in everyday life.

Entire branches have emerged in industry using the energy of ultra-high frequency electromagnetic oscillations. This is, first of all turn, various technological processes using the property substances actively absorb the energy of high-frequency electromagnetic vibrations. These include methods for obtaining high temperatures under sterile conditions, methods for increasing grades food products, drying, sterilization, etc. It is this property of various objects, including biological ones, that actively absorb the energy of electromagnetic fields (EMF) microwaves attract the close attention of researchers in various specialties, and, first of all, biologists. Since the creation of various artificial sources of microwave EMF, the question has arisen about their biological significance, degree of impact on biological objects, firstly queue per person. At the same time, questions arose regarding developing measures to protect against the effects of this physical factor on human body.

Until relatively recently, almost all work in the field of research into the biological effects of microwave EMFs was carried out in continuous radiation mode. This situation was due to on the one hand, the use of microwave oscillation energy in industrial

laziness and medicine as an influencing physical factor in
heating of the deep layers of an object. On the other side,
lack of sufficiently powerful microwave generators suitable for use in experiments and
operating in pulsed mode,
did not allow extensive research in this direction.

As a result of the rapid development of electronics and the emerging need to solve new problems, especially of an applied nature,
Currently, the dominant position is occupied by pulsed
microwave installations and systems. The operation of these installations has put
Researchers face new challenges, in particular, determining threshold power values that are safe for humans, which in turn
turn entailed the need to study the action of pulsed
Microwave EMF on biological objects at all levels of the organization.
This circumstance was also caused by the fact that when irradiated with
pulsed microwave EMFs, effects that were previously unknown began to be noted.
when exposed to continuous radiation [1, 2].

There is a need to study the effect of pulsed and intermittent EMFs of high and ultra-high frequencies (HF and microwave) on a biological object.
Firstly, almost all modern microwave devices and systems
operate in pulse mode, or in a mode characterized by instantaneous step changes in radiated power.
Such devices and systems include radar
stations, radio relay lines, television transmitters, systems
navigation, etc. Secondly, any instantaneous change in value
any parameter of an actively operating external factor, such as
as a rule, causes a more pronounced response from the perceiving system. Moreover, a substance acting as an acceptor often does not respond to the absolute value of some

parameter of the current external factor, but to change (or
rate of change) of this value, that is, the pulsed radiation mode turns out to be a more pronounced impact factor than
continuous or quasi-continuous. And in this sense it seems
tempting and very promising consideration of pulsed microwave
radiation and its absorption by biological systems as a channel
communications for the transmission of information, sufficiently and fully considered in radio engineering.

Radio engineering is a vast field of science and technology, which provides a person with ample opportunities for transmitting information over long distances using electromagnetic waves. In a general sense, in the broad sense of the word information -

is a collection of information about the world around a person, about the
person. Much of this information is transmitted using
radio equipment.

However, radio engineering as a science could only be born with the discovery electromagnetic field, which is a set of interconnected, time-varying fields - electric and magnetic

thread. The basic theory of this field was developed and published in 1873 by the English scientist D.C. Maxwell. Experimentally electromagnetic waves were first obtained by the German physicist G. Hertz, who published his results in 1880. The listed works formed the basis for the creation of radio engineering means of information transmission using electromagnetic waves.

Broadcasting messages is just one of the several branches of radio engineering and has a special name - radio communication

Despite the various areas of application, the use of electromagnetic waves as a means of transmitting information over a distance is based on general principles. When studying the basics of radio engineering From the very beginning, it is important to gain a general understanding of these principles and the radio engineering processes underlying them. Special Attention must be paid to the following:

1) *In what form must the information be provided in order to could it be transmitted using electromagnetic waves?*

2) *What is the essence of the main radio engineering processes during transmission of information using electromagnetic waves?*

3) *What technical means must be used to ensure the transmission of information using electromagnetic waves?*

In scattered articles, attempts were made to theoretically examine the observed effects, in some cases the observed effects were considered as a response of biological structures when irradiation with non-thermal doses of microwave EMF, and the irradiation itself with this began to be called informational. The author of this book did an attempt to consider these issues by searching for analogies between some technical microwave systems and biological objects, having similar architectonics and, therefore, allowing to a certain extent, transfer of ideas about the resonant formation of ongoing processes in technical non-resonant structures to their biological analogues.

Consideration of some biological structures as equivalent analogues of radio engineering devices made it possible to describe many effects observed in psychophysical experiments are categories and concepts of the theory of quadripoles and on this basis give an explanation of the auditory effects of microwave frequencies. Moreover, this approach allowed us to subsequently abandon experiments on humans and switch to physical models.

Considering microwave EMF as a source of information, and a biological object as a receiver of information, we will define the basic concepts, transmission methods, characteristics and structure of the communication channel to transfer information to a biological object when it is irradiated EMF Microwave.

1.1. Information and message. Source and recipient of information

Initially, the term *information* covered the totality of information transmitted between people orally, written or in some other way; Usually this was information about some events, phenomena or objects. Then the content of the term was expanded; Now information is any information that is

the object of the following operations: transfer, distribution, transformation, storage or direct use. Exchange of such
information is carried out not only between people, but also between
by man and machine, between various technical devices, in the animal and plant world.

The form of presenting information is called a message. For example, information can be transmitted via letter or telegram; the message in this case is text - a sequence of letters, numbers and other characters.

When sending a message, you can always specify *the sender of the message* and *the recipient* to whom it is addressed.

When irradiating biological objects with microwave EMF by the sender
message (source) we will consider the microwave EMF source, including a microwave generator, transmission line and irradiator, and the recipient -
biological object.

1.2. Electromagnetic waves

To transfer information from a source to a recipient, it is necessary to transmit messages containing this information. Messages on
distance can be transmitted using any material
carrier or physical process occurring over time.

In radio engineering, the material carrier is electromagnetic waves. We present here only some information about these waves,
which are most important for obtaining an overview
about the essence and possibilities of transmitting information using electronic magnetic waves.

Consider a conductor of finite length through which a constant current passes. In the space surrounding the conductor, there will be
there is a static magnetic field. If the current is slowly reduced to zero, then at each fixed point in space about
conductor magnetic field strength will also slowly
decrease to zero. In this case, they say that the energy contained in the field
will be returned to the power source. A similar picture is observed
and in the case when the current and its direction periodically change
with a small frequency: the field periodically appears and disappears when

the current increases, and the energy of the magnetic field also increases, with a decrease current, the field energy returns to the source.

However, with increasing frequency of changes in magnitude and direction The current picture described changes significantly. Discussed above the process of periodic movement of energy from a source to the field surrounding the conductor and back occurs only in a limited region of space immediately adjacent to the conductor. Part of the energy is radiated in all directions from the conductor in the form *electromagnetic waves.*

An important parameter of an electromagnetic wave propagating at speed c is *the wavelength.* If the frequency of the periodic changes in current in the conductor f, then the period of this change is T = 1/f. The length of the direct path traversed by an electromagnetic wave emitted by a conductor in time T is called the wavelength and is denoted symbol ÿ, i.e.

$$ÿ = c/f. \quad (I.1)$$

For example, in a vacuum , the speed of propagation of an electromagnetic wave is c0 = 3 108 m/s; if the frequency of the current in the conductor f = 3 103 Hz , then in accordance with (I.1), the wavelength emitted by it is ÿ = 105 m.

At the frequency of the current “feeding” the conductor f = 3 109 Hz = 3 GHz we will have ÿ = 10 cm.

If we denote the geometric length of the conductor by the symbol l , then a significant part of the energy of the current source will be radiated into the surrounding space only if l/ÿ ÿ 1. Therefore, when At low frequencies, enormous lengths of conductors would be required to ensure effective radiation. That is why in radio engineering Electromagnetic oscillations with fairly short will lengths are used as message carriers. Such waves turned out to be possible to radiate effectively using special conductor systems of acceptable sizes. Systems of conductors that are created specifically for emitting electromagnetic waves are called

transmitting antennas.

The frequency range of currents feeding transmitting antennas currently used in radio engineering extends from 104 to 1012 Hz; these frequencies are called *high* or *radio frequencies;* Electromagnetic waves with such frequencies are called *radio waves.* Radio waves with different frequencies travel differently in near-Earth and outer space. The frequency of radio waves used as a message carrier significantly affects also on the principles of designing the necessary radio engineering devices. Therefore, taking into account the characteristics of propagation, generation and radio frequency radiation is usually divided into ranges, the names of which are given in the table. Division of radio waves into ranges in radio communications is established by the International Radio Communications Regulations (Table 1.1).

Table 1.1

Radio frequency and radio wave bands

Radio frequency range	Borders the range	radio wave range	Borders the range
1st (Extremely Low ELF) 3–30 Hz 2nd (Ultra		1st (Decamegameter) 2nd	100–10 mm
Low ELF) 3rd (Infra Low ELF)	30–300 Hz	(Megameter) 3rd	10–1 mm
0.3–3 kHz 4th (Very Low VLF) 3–30 kHz		(Hectokilometer) 1000–100 km	
		4th (Miriameter) 5th	100–10 km
5th (Low LF) 30–300 kHz 6th (Mid MF) 0.3–2		(Kilometer) 6th	10–1 km
MHz 7th (High HF) 3–30 MHz 8th (Very High		(Hectometer) 7th	1–0.1 km
VHF) 30–300 MHz 9th (Ultra-High UHF) 0.3–3		(Decameter) 8th (Meter)	100–10 m
GHz 10th (Ultra-High Microwave) 11th (Ultra-High		9th (Decimeter) 10th	10–1 m
EHF) 30–300 GHz		(Centimeter) 11th	1–0.1 m
	3–300 GHz	(Millimeter)	10–1 cm
			10–1 mm
12th (Hyper-high HHF)	300–3000 GHz	12th (Decimmillimeter) 1–0.1 mm	

It should be noted that modern radio engineering is characterized by tendency to switch to shorter waves, i.e. to higher radio frequencies, which is explained by the following: 1) with increasing frequency the geometric dimensions of the antennas are reduced, and also ensures emission of radio waves in the desired direction, which is of great practical importance (it is possible to increase the distance over which information is transmitted with the same power of the oscillation source); 2) the level of extraneous electromagnetic radiation turns out to be lower, caused by lightning discharges, discharges in power lines, broken contacts in current collectors of electric trains, etc.; such third-party emissions, called interference, cause distortions in transmitted messages; 3) if not taken special measures, the implementation of which requires additional technical means, then radio waves cannot be used to simultaneously transmit several different messages to different recipients with the same frequency, since the message intended for one recipient will be a third party (interference) for another; That's why each “message source-receiver” pair must be allocated its own operating frequency, and with the growth of such pairs, the number of simultaneously used operating frequencies increases; 4) some messages are possible transmit with good quality only when used enough high operating frequencies, first of all, this applies, for example, to television images, for transmission of which to the present Nowadays, the meter and decimeter radio wave ranges are used.

Note also that shorter wavelength ranges occupy wider frequency range. So, the width of the kilometer range waves 3 105–3 104 = 27 104 Hz ; and the width of the range of shorter centimeter waves 3 1010–3 109 = 27 109 Hz .

1.3. Information transmission system

So, we will assume that the electromagnetic wave is emitted at the point in space where the source of the message is located. If this wave When distributed, it reaches the point where the recipient of the message is located, then it can be used as a message carrier. However, for this it is necessary to ensure that certain conditions are met. Let us briefly describe each of them.

Generation of high-frequency oscillations. An electromagnetic wave is formed due to radiation from the antenna when feeding it with high frequency current. Therefore, the first condition is providing the possibility of using electromagnetic waves as message carriers, there is a need to generate (create) such oscillations of electric current using technical devices; These devices are called high-frequency oscillation generators. As a rule, harmonic is used oscillation, which is the following function of time:

$$i(t) = Im \sin(2\ddot{y}ft + \ddot{y}), \quad (I.2)$$

where Im is *the amplitude;* f —frequency; ÿ is *the initial phase* of oscillation, describing in this case the change in time of the value of the electric current i(t).

In what follows, instead of f, we will also use the notation *angular frequency* ÿ = 2ÿf; Im, f and ÿ are the parameters of the harmonic fluctuations. The parameter T = 1/f is called *the period.*

A harmonic oscillation, the frequency of which belongs to any radio frequency range (see Table 1.1), is called *a radio frequency oscillation.* Development of radio frequency generation devices vibration is an important task for radio engineering.

Modulation of high frequency oscillations. The second condition that ensures the possibility of using electromagnetic wave as a message carrier, is as follows: it is necessary to introduce

transmitted message. This process is usually called *modulation* radio frequency vibration; it must also be carried out using a device called *a modulator.* Harmonic frequency oscillations subject to modulation for the purpose of transmitting information, called *the carrier frequency.*

Thus, modulation is a change in values over time any parameters of the carrier vibration - amplitude, frequency or phases.

RECEPTION OF RADIO WAVES The third condition that ensures the possibility of transmitting information using electromagnetic waves is as follows: at the point in space where the recipient is located information, it is necessary to convert a propagating electromagnetic wave into oscillations of electric current or voltage.

This conversion is usually carried out *by the receiving antenna;* we can say that the receiving antenna carries out an inverse transformation: the propagating electromagnetic wave induces an EMF in it, ideally representing an oscillation whose shape exactly matches the shape of the modulated radio signal supplied to the transmitting antenna.

Detection. To receive a transmitted message from received modulated radio signal, you must first isolate the modulating signal. To do this, the received radio signal is subjected to a transformation inverse to the transformation carrier oscillation during modulation. This transformation is called *detection* or *demodulation,* and the device performing it is *a detector* or *demodulator.* The implementation of this transformation is the fourth condition that ensures the possibility transmitting information using electromagnetic waves. Ideally In this case, at the output of the detector it is possible to obtain a modulating control signal u(t), which can be converted into a received signal message. The received message is presented to the recipient.

Modulation of high-frequency radiation and subsequent demodulation (detection) in an information receiver (radio receiver) agreed upon in advance, i.e. it is known in advance with what device inside the radio receiver and how detection occurs useful signal and in what form the selected signal appears. When applied to biological structures, it is impossible to demand the introduction of modulation *a priori,* if only because the structure is not known, which will play the role of a demodulator. But in any case, when When irradiated, a biological object will heat up due to the absorption of microwave EMF energy. But this is also information! Obviously, that until all the subtleties of the mechanisms of biological the effects of microwave EMF with various modulation methods will not structures of a biological object that can play a role have been identified demodulator (even in a formalized form), until then it will be impossible to talk about the information impact of microwave EMF on biological structures. Thus, it is first necessary to become familiar with the characteristics of the signals themselves that occur when the impact of microwave EMF on biological structures, with their spectra, energy, and then, based on information about the characteristics of the biological objects, about the processes that arise and occur in them, when absorbing microwave EMF energy, make a “stitching” of all necessary interaction parameters.

A set of radio engineering devices that carry out these processes, i.e. the transfer of information from the source of information to the recipient, is called *the information transmission system* (Fig. 1.01). Here It is useful to emphasize that the carrier oscillator, modulator and the transmitting antenna are the main elements *of the transmitter,* and the receiving antenna, amplifier and detector are *the receiver. Line*

Rice. 1.01. Block diagram of the information transmission system

transmission is the medium in which electromagnetic waves propagate from the transmitter to the receiver. Such a system can ensure the transfer of information over significant distances between
source and recipient.

Comparing the presented information transmission system with the traditional method of irradiating biological objects with microwave EMF,
one can be convinced of their complete analogy. However, the question arises - what structure in a biological object, as in a receiver of information,
plays the role of a detector. The answer is that there is no such structure as such.
It was shown in [3] that when bimolecular phospholipid membranes with alamethicin are irradiated with a microwave field at a frequency of 0.9 GHz
a reversible decrease in conductivity is observed (up to one order of magnitude
and more) membranes. The authors note the thermal nature of the effect, and a decrease in the conductivity of the system is equivalent to heating the channels
at 12 ўC. An increase in the temperature of the object when the field is turned on (or, which is the same, under the action of single pulses) and then a drop in temperature upon switching off form a thermal pulse. Comparison
in the time of the graph of changes in conductivity given by the authors
membranes with the beginning and end of the generation of microwave oscillations, i.e. with the formation of a microwave pulse, shows that the process of forming a thermal pulse can be considered as a formalized
detection function - membrane conductivity change curve
is essentially the envelope of the microwave pulse (Fig. 1.02).

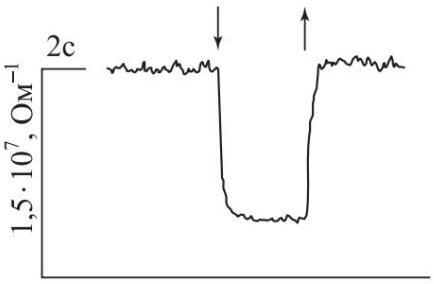

Rice. 1.02. Changes in the conductivity of phospholipid membranes modified with alamethicine when irradiated with an HF EMF pulse of power 8 W in 1 M KCl solution. The arrows indicate the moments turning on (ÿ) and turning off (ÿ) the field

The same effect was obtained when irradiating samples in a strip line in the carrier frequency range 0.2–0.82 GHz with various modifiers [91].

1.4. Signals and information. Signal characteristics

Basic definitions. All signals, with the exception of random ones, *are regular.* They are expressed in a certain way function of time. The image is like this functions (time diagram) gives a visual representation of *the signal shape. Random (irregular) signals* cannot be represented by a predetermined time function, since they change randomly over time.

Regular signals are divided into *periodic* and *non-periodic.* The first ones are repeated at regular intervals, called period T, and if the repetition is interrupted at some part of the observation time, then the signal is classified as non-periodic. It is characteristic that periodic oscillations carry information only in one period.

The analysis of periodic signals and radio circuits is carried out not only by a time method, but also by a spectral method, which is based on the decomposition of signals into a trigonometric Fourier series.

The purpose of time analysis is to determine the change in signal shape by *the response* (reaction) of the circuit to *the influence exerted on it.* The spectral method allows you to identify changes in the signal by transforming the spectrum by a given circuit. Both methods give the same result, But it is advisable to use temporary for a complex signal spectrum, and spectral for a simple one.

The concept of spectra of periodic signals. Let us turn to the voltage of a periodic signal of arbitrary shape. Instant its value u is equal to the sum of an infinitely large number of harmonic components:

constant component U0 equal to the average signal value for a period;

instantaneous value of the sinusoidal voltage of the first harmonic u1, whose frequency ÿ1 is equal to the signal repetition frequency ÿ, amplitude U1m and initial phase ÿ1;

instantaneous value of sinusoidal voltage u2 of the second gar- monics with frequency ÿ2 = 2ÿ, amplitude U2m and initial phase ÿ2;

instantaneous value of the sinusoidal voltage of the third harmonic u3 with frequency ÿ3 = 3ÿ, amplitude U3m and initial phase ÿ3,
.. ., i.e.

u = U0 + u1 + u2 + u3 + ... = U0 + U1m sin(ÿ1t + ÿ1) +
+ U2m sin(ÿ2t) + ÿ2) + U3m sin(ÿ3t + ÿ3) + ...

Using the sign of the sum of n terms $\sum_{n=1}^{\ddot{y}}$ where n is any integer number from 1 to ÿ, we get an abbreviated representation of the series:

$$u = U0 + \sum_{n=1}^{\ddot{y}} Unm \sin(n\ddot{y}t + \ddot{y}n). \qquad (I.3)$$

To illustrate this dependence in Fig. 1.03, *and* it is shown that if at any moment t we add three sinusoidal voltages u1, u2, u3, respectively having periods T1, T2 = T1/2,
T3 = T1/3, amplitudes U1m, U2m, U3m and initial phases ÿn = ÿt1, 2ÿt2, 3ÿt3, then you get a non-sinusoidal voltage u with the same period T, like the first harmonic (T = T1).

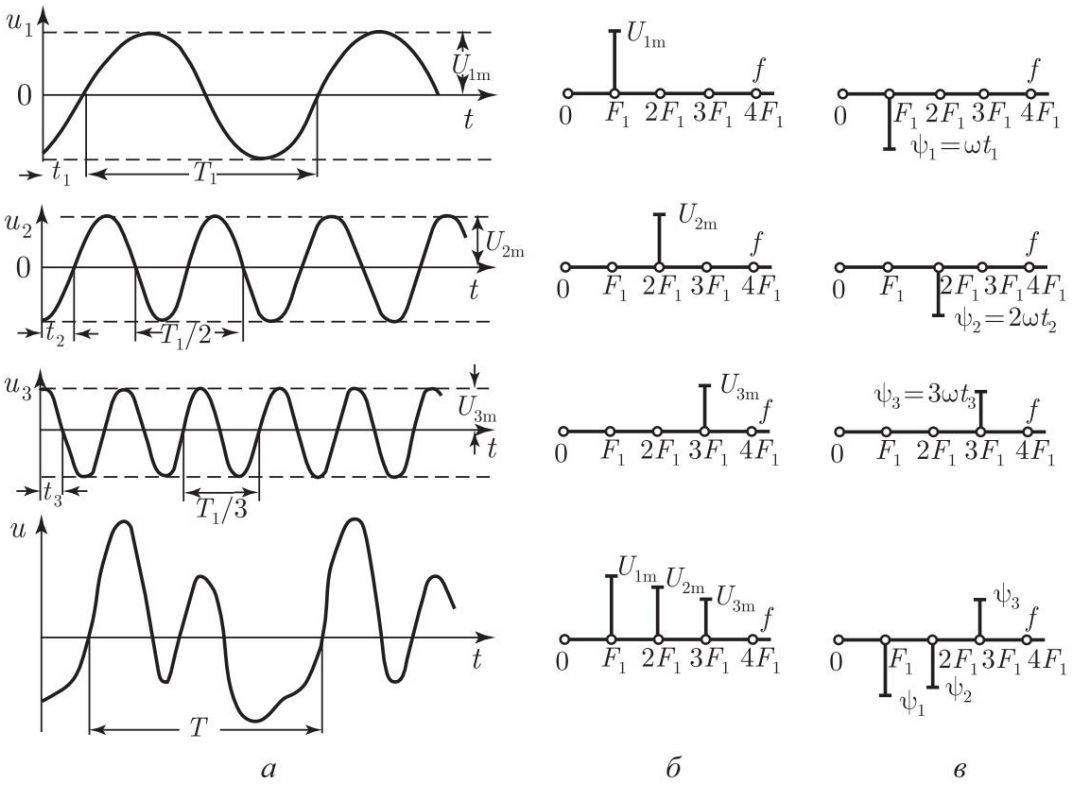

Rice. 1.03. Timing diagrams (a), amplitude-frequency spectrum *(b)* and phase-frequency spectrum *(c)* of a periodic non-sinusoidal signal

All harmonic components together form *a spectrum signal,* depicted by two diagrams, one of which is

is called *the amplitude-frequency spectrum,* and the other is called *the phase-frequency spectrum.* In these diagrams, the x-axis forms a frequency scale f = nf1, and segments whose length are plotted on the ordinate axis is proportional to the amplitude Unm (for the amplitude-frequency spectrum, rice. 1.03, b) or the initial phase ÿn (for the phase-frequency spectrum, rice. 1.03, c) the corresponding nth harmonic.

It is possible to exclude the initial phases of harmonics from the Fourier series if use transform

$$U_{nm}\sin(n\ddot{y}t + \ddot{y}n) = U_{nm}\sin n\ddot{y}t\cos\ddot{y}n + U_{nm}\cos n\ddot{y}t\sin\ddot{y}n =$$

$$= U_{nm}\sin n\ddot{y}t + U_{nm}\cos n\ddot{y}t,$$

where $U_{nm} = U_{nm}\cos\ddot{y}n$ ÿ $U_{nm} = U_{nm}\sin\ddot{y}n$ - constant values, expressing, respectively, the voltage amplitudes of the nth harmonic for sine and cosine components.

Now the Fourier series (I.3) takes the form

$$u = U0 + \sum_{n=1}^{\ddot{y}} IN_{nm}\sin n\ddot{y}t + \ddot{y}\sum_{n=1} IN_{nm}\cos n\ddot{y}t. \qquad (I.4)$$

This notation is especially convenient in the case of a signal with a so-called even or odd time function. *Called* even a function that has the same values f(t) for numerically equal and opposite sign values of the argument t, i.e. f(t) = f(ÿt). These properties are possessed by the cosine (cos ÿt) and any signal u, symmetrical about the ordinate axis 0u [see. rice. 1.04, a, where cos ÿ1 = cos(ÿÿ1) and u(t1) = u(ÿt1)]. Properties of *an odd* function has a sine (sin ÿt) and every signal u symmetric with respect to origin of coordinates 0 (Fig. 1.4, b). What is characteristic of an odd function is that that it has numerically equal and opposite sign values for numerically equal and opposite sign arguments [in Fig. 1.04, *b* sin(ÿ2) = ÿ sin(ÿÿ2) and u(t2) = ÿu(ÿt2)].

All this leads to the conclusion that *the spectral function of the "even" the signal contains only constant and cosine components,* *and* the *"odd" signal has only sine components; If* *If the signal is expressed by an arbitrary function of time, then in it There are both series of components: both sine and cosine.*

It is characteristic that *the spectrum of periodic signals is not continuous,* and *lined,* i.e. *between adjacent lines of the spectrum there are "gaps" as wide as the signal repetition rate* F = 1/T.

In studies of the effects of microwave EMF on biological structures, three main irradiation modes have emerged:

1) mode of continuous generation (CG) of microwave oscillations;
2) amplitude-modulated (AM) microwave EMF;
3) pulse-modulated (IM) EMF SWM.

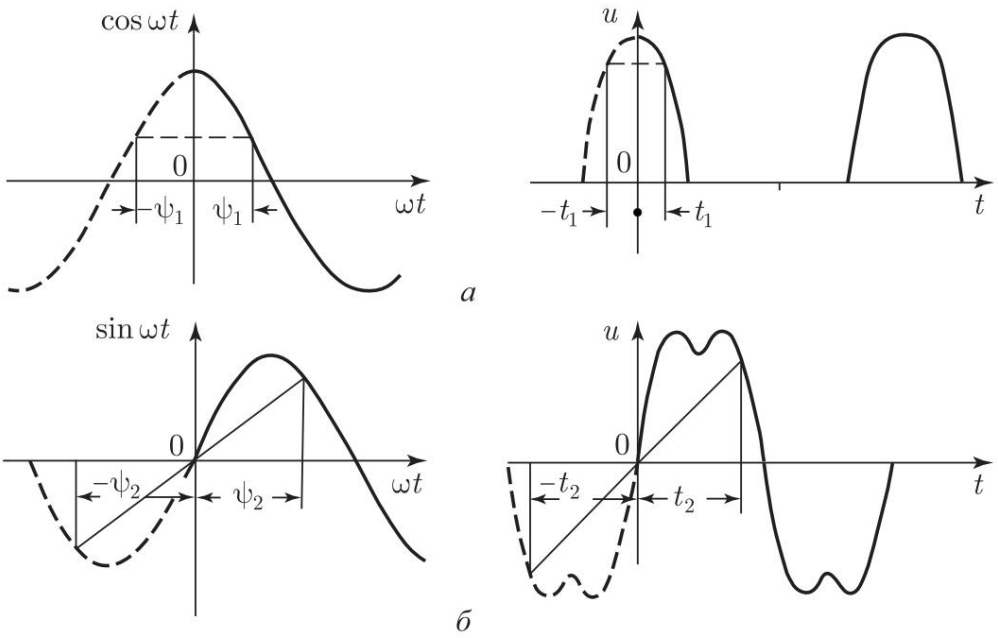

Rice. 1.04. Even *(a)* and odd (b) functions

The energy regime of NG is represented by one spectral component (Fig. 1.03, b), and nothing except the release of heat occurs when EMF energy is absorbed by a microwave biological object.

1.5. Amplitude modulated (AM) analysis signal

Let us assume that the control signal changes according to a harmonic law, and the radio signal is modulated in amplitude by this control signal, i.e., *the increase in the amplitude of the radio signal occurs in proportion to the increase in the control signal.* Let's consider the time (Fig. 1.05, a) and spectral (Fig. 1.05, b) voltage diagrams of the control signal uÿ and radio signal u. Until time t = t0, the

control voltage remains constant (uy = U0), therefore the radio signal voltage retains a sinusoidal shape at the carrier frequency ÿ0 = 2ÿf0, amplitude U0m and initial phase, which is assumed to be zero 1):

$$u = U0m \sin ÿ0t.$$

This corresponds on the amplitude-frequency spectrum of the control signal to the vertical segment U0 located opposite the frequency ÿ = 0, and on the spectrum of the radio signal to the vertical segment U0m located opposite the frequency scale point ÿ = ÿ0.

1) In the future, to simplify the recording, the initial phases of the initial oscillations are often taken equal to zero.

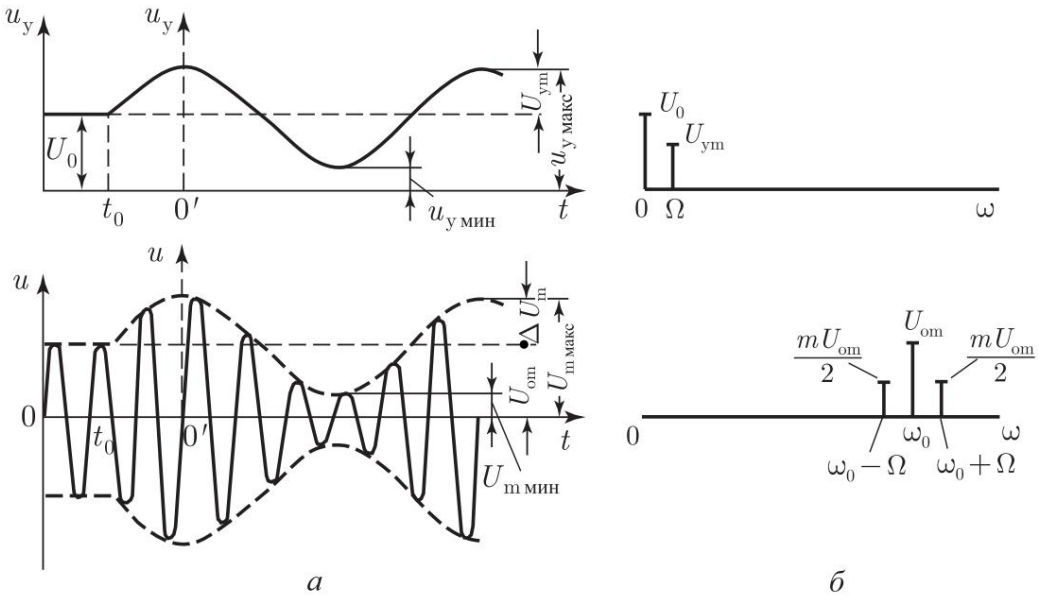

Rice. 1.05. Temporaŕya) and spectral *(b)* diagrams of the manager (and radio signals with AM sinusoidal voltage

The control voltage, starting from t = t0, changes according to a sinusoidal law. To identify the temporal and spectral functions of signals during modulation, we move the start of the time count to point 0 (Fig. 1.05, a), where the control voltage uÿ is maximum

(uÿ = Uÿ max). Then the voltage uÿ is the sum of the original U0 and the co-sinusoidal uym cosÿt, i.e. equation for the instantaneous value
control voltage will be

$$uÿ = U0 + Uÿm \cos ÿt,$$

where Uym is the amplitude of change in the control signal;
ÿ = 2ÿF is the frequency of the control signal.

At time t = 0 we get cosÿt = 1 and uy = U0 + Uym = uy max.

Undistorted amplitude modulation means that between
direct proportionality is observed between the amplitude of the radio signal voltage Um *and the control voltage uÿ .* That's why

$$Um = U0m + ÿUm \cos ÿt,$$

where ÿUm is the maximum increment in the amplitude of the radio signal relative to the initial value U0m.

Multiplying Um by sin ÿ0t, we obtain the instantaneous voltage value
radio signal:

$$u = Um \sin ÿ0t = (U0m + ÿUm \cos ÿt) \sin ÿ0t. \qquad (I.5)$$

On the timing diagrams (Fig. 1.05, a) the modulation is depicted as follows:
starting from moment 0 to the DC voltage U0 of the control
signal uÿ, a cosine voltage with amplitude is added
Uym and frequency ÿ, and in the radio signal oscillations of the carrier frequency ÿ0

continue as before, but their amplitude changes relative to
U0m by the value ÿUm cosÿt. These changes in amplitude, corresponding to *the envelope of the radio signal,* are depicted by dash-dotted lines. It should be remembered that the envelope of a radio signal is an imaginary curve that outlines the boundaries of changes in amplitude, and not
the vibrations themselves.

Meaning addiction

$$\sin ÿ0t \cos ÿt = \sin(ÿ0 + ÿ)t + \sin(ÿ0 - ÿ)t,$$

equation (I.5) is reduced to the form

$$u = U0m \sin ÿ0t + ÿUm \sin ÿ0t \cos ÿt = U0m \sin ÿ0t + \frac{ÿUm}{2} \sin(ÿ0 + ÿ)t + \frac{ÿUm}{2} \sin(ÿ0 - ÿ)t. \quad (I.6)$$

The depth of amplitude modulation is judged by *the modulation coefficient*

$$m = \frac{ÿUm}{U0m}$$

which shows what fraction of the carrier voltage amplitude
frequency U0m is the increment in the amplitude of the modulated voltage ÿUm.

When there is no modulation, then ÿUm = 0 and $m = \frac{ÿUm}{U0m} = 0$. When equal
ÿUm = U0m coefficient m = = 1, and the amplitude of the radio signal
varies from minimum $U_{m\,min} = U0m - ÿUm = 0$ to maximum
$U_{m\,max} = U0m + ÿUm = 2U0m$. If the modulation coefficient m > 1,
then ÿUm > U0m and distortion occurs, called *overmodulation.*

By introducing the value ÿUm = mU0m into expression (I.6) , we obtain

$$u = U0m \sin ÿ0t + \frac{mU0m}{2} \sin(ÿ0 + ÿ)t + \frac{mU0m}{2} \sin(ÿ0 - ÿ)t. \quad (I.7)$$

From equation (I.7) it follows that if sinusoidal oscillations
carrier frequency ÿ0 amplitude modulated by harmonic
control signal with frequency ÿ, then the result is non-sinusoidal oscillations, which consist of three sinusoidal ones:
oscillations of the carrier frequency ÿ0 with amplitude U0m, oscillations of the upper
lateral frequency ÿ0 + ÿ with amplitude $\frac{mU0m}{2}$ and oscillations of the lower
side frequency ÿ0 - ÿ with amplitude $\frac{mU0m}{2}$. As we see, it cannot be
said that amplitude-modulated oscillations are obtained by adding a high (carrier) to the oscillations

frequency ÿ0 of oscillations of low frequency ÿ. Actually in AM
vibration does not have a low frequency component, it contains all components
high-frequency (in this case these are frequencies ÿ0, ÿ0 + ÿ, ÿ0 - ÿ).
At the same time, it is confirmed that the periodic non-sinusoidal

a signal, such as an AM radio signal, consists of a series of sinusoidal oscillations.

In the spectrum of the control signal, modulation is expressed by a vertical segment of height Uym at frequency ÿ, and on the spectral diagram of the radio signal - by two vertical segments of height mU0m/2
each at frequencies ÿ0 ÿ ÿ and ÿ0 + ÿ. Name "side frequencies"
explained by the fact that the spectral lines of these frequencies are located
on both sides of the carrier frequency.

In Fig. Figure 1.06 shows time and spectral voltage diagrams of the carrier frequency uÿ, upper side frequency uÿ b, lower
side frequency unb and the resulting radio signal u, equal to the sum of the instantaneous voltage values un, uv b and unb .

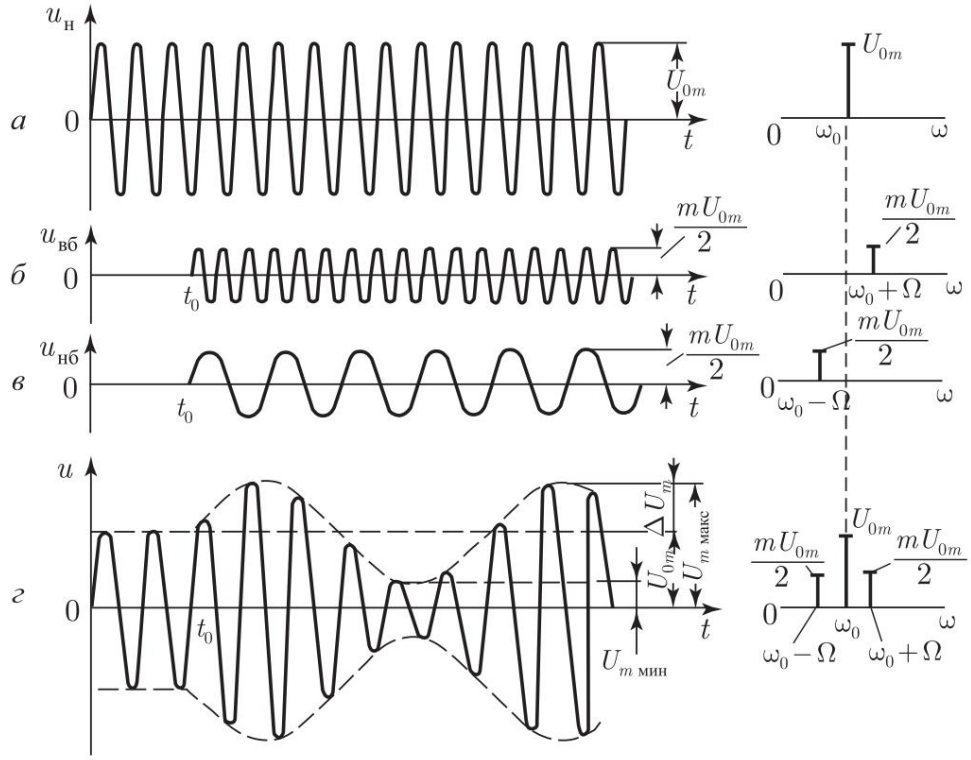

Rice. 1.06. Time and spectral diagrams of voltages of the carrier frequency (a), upper *(b)* and lower *(c)* side frequencies and the resulting
radio signal *(g)*

Before the control signal changes (t<t0), the modulation coefficient m and the amplitudes of the side frequencies mU0m/2 are equal to zero, i.e. no
oscillations of side frequencies, and the resulting voltage is a purely sinusoidal voltage of the carrier frequency (u = uÿ). When modulation occurs (m > 0), sinusoidal voltages arise

side frequencies with constant amplitudes mU0m/2, but since the side frequencies are different and not equal to the carrier, the phase shift between
the voltage components un, uub and unb are continuously changing.
The amplitude of the resulting radio signal changes accordingly.

When all three voltages are in phase, they are completely added and the amplitude of the radio signal is maximum:

$$U0m + \frac{mU0m}{2\,2} + \frac{mU0m}{} = U0m + mU0m = U0m + \ddot{y}Um = Um \quad \text{max.}$$

After half the modulation period, both side-frequency voltages will already be in antiphase with the carrier frequency voltage, and therefore the amplitude of the radio signal will be minimal:

$$U0m \ddot{y} \quad \frac{mU0m}{2\,2} + \frac{mU0m}{} = U0m \ddot{y} mU0m = U0m \ddot{y} \ddot{y}Um = Um \text{ min.}$$

Consequently, *the change in the amplitude of the radio signal occurs as a result of the fact that sinusoidal oscillations of side frequencies are added to the sinusoidal oscillations of the carrier frequency.*

Real control signals uÿ are more complex than purely harmonic ones: their spectrum contains frequencies from minimum ÿmin to maximum ÿmax (Fig. 1.07, a). If there were only two frequencies in this spectrum, say ÿ1 and ÿ2, then due to the first oscillations of the carrier frequency ÿ0 one pair of side frequencies ÿ0 + ÿ1 and ÿ0 ÿ ÿ1 would be added, and due to the second is another pair ÿ0 + ÿ2 and ÿ0 ÿ ÿ2. Similarly, in the general case (Fig. 1.07, b) for each harmonic component of the control signal there is one pair of side frequencies in the radio signal and therefore the spectrum of the radio signal, in addition to the carrier frequency ÿ0, contains a band lower side frequencies (from ÿ0 ÿ ÿmin to ÿ0 ÿ ÿmax) and a band of upper side frequencies (from ÿ0 + ÿmin to ÿ0 + ÿmax). Modulation factor m for each pair of side frequencies ÿ0 ± ÿ is directly proportional amplitude of that component of the control signal spectrum that corresponds to a given frequency ÿ, and since m 1, then the height spectral line of any side frequency radio signal mU0m/2 is not may be more than half the height of the carrier spectral line frequency U0m.

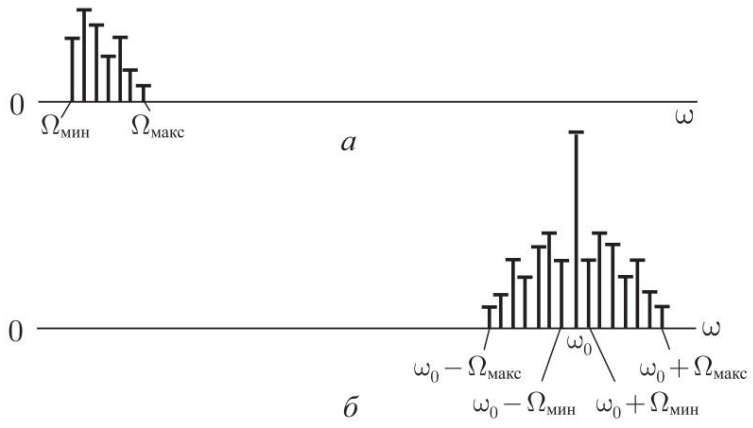

Rice. 1.07. Spectral diagrams of the control signal *(a)* and the corresponding AM radio signal *(b)*

The width of the radio signal spectrum ÿÿsp is of great practical importance. If we subtract from the maximum frequency of this spectrum ÿ0 + ÿmax its minimum frequency ÿ0 ÿ ÿmax, then we make sure that with amplitude modulation, the width of the radio signal spectrum is doubled greater than the maximum frequency of the control signal spectrum:

$$ÿÿsp = (ÿ0 + ÿmax) ÿ (ÿ0 ÿ ÿmax) = 2ÿmax. \quad (I.8)$$

1.6. Pulse Modulation (IM)

It is widely used in microwave transmitting devices.
pulse modulation (PM), when the envelope of the modulated oscillation has the form of rectangular pulses (Fig. 1.08, a). Main
the parameters of oscillations during MI are the amplitude of the AI pulses, their duration ÿI, repetition period TI or repetition frequency
FI = 1/TI. The rectangular shape of the modulating pulses provides maximum energy of the IM signal at a given amplitude, which
is very important, since in real conditions the amplitude values
voltage or current are limited by the electrical or thermal strength of the devices and the properties of their cathodes.

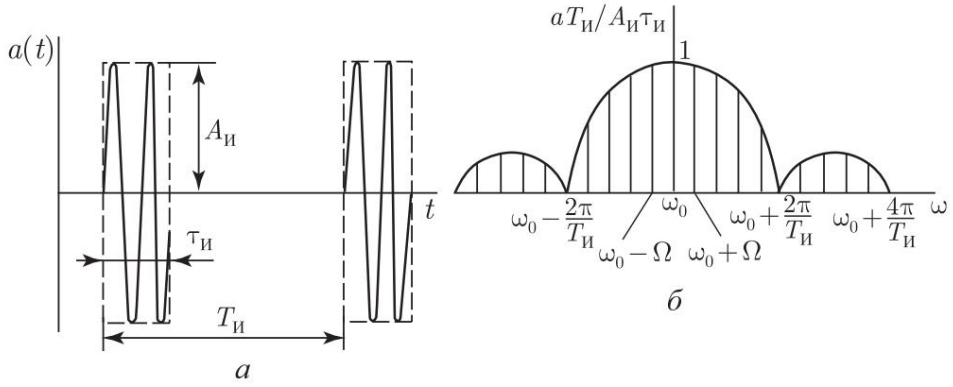

Rice. 1.08. Pulse-modulated signal *(a)* and its spectrum *(b)*

The spectrum of a pulse-modulated oscillation consists of a carrier and two side stripes:

$$a(t) = Aÿ \frac{ÿÿ}{YOU} \sin ÿ0t + \frac{1}{Pi} \sum_{n=1}^{ÿ} \frac{\sin(nÿt/2)}{n} \sin(ÿ0 + nÿ)t + \frac{1}{Pi} \sum_{n=1}^{ÿ} \frac{\sin(nÿt/2)}{n} \sin(ÿ0 ÿ nÿ)t , \quad (I.9)$$

where ÿ = 2ÿFÿ.

The width of the spectrum of the radio signal, as with any type of AM, turns out to be twice the width of the spectrum of the modulating signal. Usually in the absence of any special requirements for the signal, it is considered that

that the channel bandwidth required to pass a sequence of rectangular radio pulses can be determined
How

$$2\ddot{y}f = 2/\ddot{y}\ddot{y}, \quad (I.10)$$

i.e., in the spectrum all components of the order of magnitude are neglected
n > 2ÿ/ÿÿÿ = SI, where SI = TI/ÿÿ - duty cycle.

Important energy characteristics of a transmitter operating in pulse mode are pulse, peak and average
power.

Transmitter impulse power is the power developed
transmitter during the pulse

$$PI = \frac{1}{\ddot{y}\ddot{y}} \int_0^{\ddot{y}\ddot{y}} p(t)\, dt,$$

where p(t) is the power for one period of high-frequency oscillations.

With a rectangular pulse shape p(t) during the pulse time there is no changes, and the pulse power coincides with the peak Pÿ, i.e., with the power developed by the transmitter during one RF period corresponding to the maximum amplitude of the modulating envelope 1).
Since you can directly measure both peak and pulse
power is difficult, the concept of average has become widespread
power

$$Psv = PI/SI. \quad (I.11)$$

The average power of a transmitter operating in pulse mode determines the thermal conditions of both the transmitter itself and the individual
its elements.

Typically, IM is carried out in one or more power circuits
microwave generator using special pulsed power supply devices - and pulsed modulators.

Since in any MI circuit there are parasitic reactances and in them
Energy is inevitably stored; it is impossible to ensure an ideal rectangular shape of modulating voltage pulses. Real impulses are characterized by finite durations of the forward

front ÿf and decay ÿc of the pulse, as well as a certain unevenness of the flat top ÿu (Fig. 1.09). Usually under duration
the leading edge of the modulating pulse ÿf is understood as the time for
which voltage increases from 0.05 to 0.95 UI, and over the duration
ÿÿ is the time during which the voltage drops to 0.05 UI. Duration
pulse ÿI is determined at the level of 0.05 UI.

Requirements for the shape of modulating pulses depend on the type
microwave generator used, on the duration of installation processes

1) Due to the imperfectly rectangular shape of real radio pulses, usually PI < Pp.

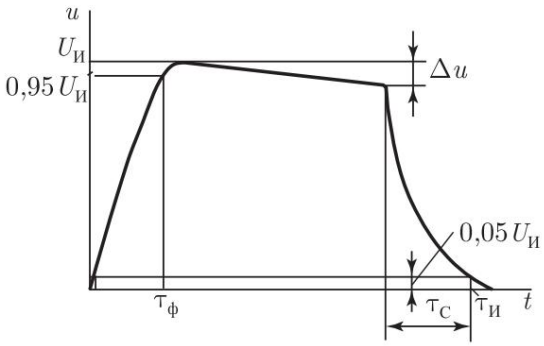

Rice. 1.09. Real shape of the modulating pulse

new high frequencies in it -

oscillations and their breakdown. Duration of the leading edge ÿf should not be less than the time tust for establishing microwave oscillations. Experiments show that

tust (100 ÷ 150)Tvch, (I.12)

where Twh = 1/f; f is the frequency of microwave oscillations [78].

Modulating parameters impulse is usually determined relations

ÿÿ = (0.1 ÷ 0.2)ÿÿ, ÿc = (0.2 ÷ 0.3)ÿÿ. (I.13)

Thus, taking into account tst, the real shape of the microwave radio pulse schematically it will look like:

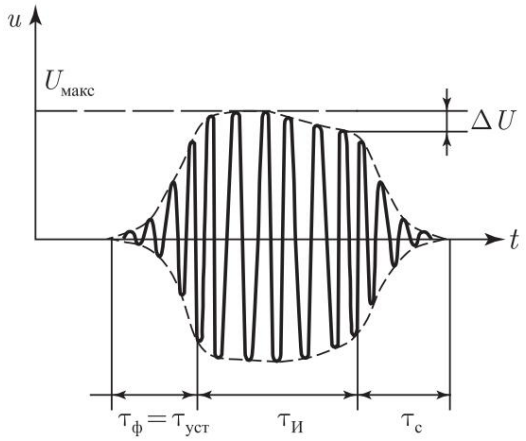

Rice. 1.10. Schematic representation of the actual shape of a microwave radio pulse

Chapter 2

EXCITED MECHANICAL OSCILLATIONS IN BIOLOGICAL STRUCTURES

Introduction

Currently, researchers are of great interest
so-called non-thermal effects of the electromagnetic field (EMF)
ultrahigh frequency (microwave) [4–8], which occur when exposed to
on biological objects with low-energy doses insufficient for
any significant thermal heating. These effects may
be local and (or) short-term in nature [8].

Until relatively recently, almost all work in the field of research into the biological effects of microwave EMFs was carried out
in continuous irradiation mode. Naturally, over the course of decades, a very definite attitude has developed towards this physical factor as a heat producer. Effects Caused
by the action of continuous microwave radiation, were identified as thermal, or nonspecific, and the primary mechanism was
the action of the heat released when absorbing the falling
to a microwave energy facility. From this point of view, at one time there were Permissible radiation exposure standards were developed, and the concept of “thermal” and “non-thermal” doses was introduced. Subsequent rapid development of electronics led to the emergence of powerful pulsed devices and microwave systems. At the same time, effects began to be noted that were previously unknown when exposed to continuous radiation, despite the significantly lower level of average value of microwave emitted power. Exploitation
these installations posed new challenges for researchers to
determining threshold power values that are safe for humans.

To date, extensive material has accumulated in the field
research on the bioeffects of pulsed microwave EMFs. The levels of specific power used vary from 10ÿ6 to 106 W/cm2, biological objects are studied at all levels of organization. And so
no less, despite the ever-increasing scientific
research flow of information, mechanism of biological action
pulsed microwave EMF needs clarification. Moreover, due to the diversity of objects and the even greater diversity of irradiation conditions,
The effects observed by various researchers are often diametrically opposed and difficult to reproduce.

An analysis of literary data in recent years shows that to date there has been a tendency to move away from old ideas about the nature of the observed effects.

Suggestions have been made about the existence of subtle mechanisms for converting energy absorbed by a biological object pulsed EMF microwave and the presence of a transfer connection between the external EMF and the observed effect. And it's not just about about the influence of strong pulsed EMFs, but also very weak ones, providing an internal field in the object only slightly exceeding thermal noise [9].

As a rule, the implementation of the effects observed when exposed to on a biological object with pulsed microwave EMF, using continuous irradiation with a power flux density (PPD) equal to the average value of this parameter during pulsed irradiation is not succeeds. In many experiments, frequency and spatial dependences of effects are observed [10, 11].

One of the interesting effects of pulsed microwave EMF is the phenomenon of radio sound - human perception of the envelope of a pulse-modulated microwave field. Lin [12] proposed thermoelastic theory to explain this effect. According to Lin, mechanical vibrations human heads, caused by thermal expansion due to the absorbed pulse power of microwave EMF, due to the presence of bone conduction, ultimately act on the hearing aid, causing sensation of sound. Having calculated the resonant frequency and pressure of sound vibrations, Lin came to the conclusion that the magnitude of this pressure is sufficient to form an auditory image.

The fact that low heating of tissues (less than 0.1ÿC) during the action weak non-thermal doses, microwave EMF can generate significant physiological changes that cannot be explained by an increase in temperature, Adie also points out. In his work [13] Adey suggests the existence of reinforcing mechanisms, ensuring the transfer of effects on living cells.

From the point of view of searching for mechanisms of biological action of pulsed EMF microwaves, the phenomenon of radio sound is a large interest. The fact that there are zero beats between the acoustic signal and harmonics of the pulse repetition frequency of microwave EMF [14, 15] also allows us to put forward as a possible mechanism of action excitation of mechanical vibrations in the tissues of the skull and consider the phenomenon of radio sound as a particular manifestation of a general property, inherent in all biological objects, and in the light of this assumption, consider experimental data that cannot be explained neither by thermal theory nor by the hypotheses considered in literature. Similar manifestations of pulsed microwave EMF can be would be called anomalies, and by the term "anomaly" we will understand not only the result of a specific impulse action Microwave EMF. If we do not observe effects interpreted

as thermal, this does not mean that heat production does not have
places. The question is different - what part of the absorbed electromagnetic energy and in what transformation leads to the emergence of effects interpreted as non-thermal? Taking as a working hypothesis
excitation of mechanical vibrations, it was natural to turn
to the analysis of works devoted to the direct effects of ultrasonic non-thermal doses on biological objects, and the selection of results,
obtained on similar objects under the influence of ultrasonic
vibrations and when irradiated with pulsed microwave EMFs. Thus,
By the term “anomaly” we mean effects that have an analogue
when the same object is exposed to ultrasonic (sound) vibrations.
Note that this definition is not entirely accurate. Below
it will be shown that for a certain ratio between the power
in the microwave EMF pulse and pulse repetition rate manifestation
the thermal effect can be compensated by the expected action of mechanical vibrations.

Analysis of literature data allows us to come to the conclusion that
the observed specific effects have much in common with the results of work on the effects of ultrasound on biological objects.
And what, from the point of view of thermal theory, is an anomaly at
when an object is exposed to pulsed microwave EMF, when the same object is exposed to ultrasonics, it is a pattern, at least
at least for the objects discussed in this book. Thus, for further consideration of the issue, it is necessary to accept that
part of the electromagnetic energy absorbed by a biological object and converted into heat is transformed into the energy of mechanical vibrations. Let us also assume that the temperature change curve
the object must have a sharply nonlinear character during its action
microwave EMF pulse, that is, a thermal pulse must be formed in the object. It can be assumed that this property should be
common to all biological objects capable of one way or another
absorb high frequency electromagnetic energy. It is interesting to compare the hypothesis put forward with the mechanism of propagation of a thermal pulse in solids, which manifests itself in the presence of
heater or heat converter and heat receiver.
One of the ways to create a thermal pulse is to use the power of a pulsed microwave source by absorbing it
in a thin metal film deposited on one surface of a dielectric crystal. In this case, the integral thermal impulse,
arriving at the receiver corresponds to the input power at low
crystal sizes. This indicates that the transport mechanism
energy is indeed thermal [16]. The use of microwave power pulses as a heat source is indicated
also in [17]. It is noted here that agreement for different
studied substances between the velocities corresponding to the observed times of arrival of thermal pulses and the predicted

phonon energy propagation speeds clearly shows that
using the speed of propagation of acoustic energy when
description of undissipated thermal energy in dielectric crystals is completely justified. This statement plays a big role
role in the proposed mechanism, given that a large number of biological objects have an ordered structure, that is
the front of the thermal impulse in such objects can be negligible
small

Possibility of exciting mechanical vibrations in some
individual objects is shown in [18, 19, 20, 21]. Thus, we see the presence of a fairly large number of theses and provisions that served as starting points for the formation
hypotheses about the presence of intense mechanical vibrations excited in organic and inorganic compounds when exposed to
microwave EMF pulses.

Consideration of qualitatively adequate observed effects when
the action on a biological object of microwave EMF pulses and ultrasound will make it possible to identify the physical quantities acting on the object under study, the numerical values of which will allow
to assessing the contribution of mechanical vibrations excited by pulses Microwave EMF, in the formation of specific effects. Thus,
a hypothesis is put forward about the mechanical nature of the specific action of pulsed microwave EMFs, while, however, the effect of heat as
an independent influencing factor causing certain shifts in the functioning of the object is not excluded. It is only assumed that the mechanical

fluctuations can play a leading role.

2.1. Examples of anomalous biological effects pulsed EMF microwave

Using literature data, we will show that the kinetics of the studied parameters of some biological objects under thermal
action and when exposed to pulses of microwave EMF are mutually inverse. In this case, we will limit ourselves to considering the action of pulsed EMFs Microwaves that do not cause any noticeable total heating
object, and we will try to identify, in the light of the proposed hypothesis, the mechanism of the biological action of these fields. In [22] it is shown that
that when a frog tibial nerve preparation is irradiated with microwave EMF pulses synchronously with the latent period, they decrease
speed of excitation wave propagation and potential amplitude
actions (AP). In this case, results were obtained that contradict
on the one hand, ideas about the amount of absorbed power,
on the other hand, data on quantitative and qualitative changes,

observed in a similar object under thermal influence [23]
and exposure to continuous microwave EMF [24].

According to [23], when a frog nerve preparation is heated from 0°C to +20°C, the speed of propagation of the excitation wave increases and the dependence of this parameter on temperature is approximately linear. The same picture occurs for the amplitude
PD (Fig. 2.01, 2.02). Here it is necessary to point out what is happening seasonal dependence of the values of measured parameters. In work [24] shows the effect of continuous microwave EMF radiation on speed propagation of the excitation wave and amplitude of the AP of the nerve preparation frogs. With an average power flux density (APFD) equal to
11 mW/cm2, increase in the speed of propagation of the excitation wave was +16% in 30 minutes, the heating of the drug by the 30th minute was 2ÿC. According to B.N. Veprintsev, when such preparations are heated to 2°C the increase in the speed of propagation of the excitation wave is within +6 ÷ 19%. Comparison of results in this case
speaks of the thermal effect of microwave EMF. In work [22] at frequency field pulse repetition rate equal to 20 Hz, and PPMav = 100 mW/cm2 within 60 minutes, the heating of the nerve was 1ÿC, the propagation speed excitation waves decreased by 35 ÷ 46%, AP amplitude decreased by 93 ÷ 95% (Fig. 2.03, 2.04).

It should be noted that these data were obtained by irradiation object during the latent period during the entire irradiation time (phased exposure, Fig. 2.05, a).

When the drug is irradiated with microwave EMF pulses with the same parameters in the post-latent period (Fig. 2.05, b), the observed effects disappear. This result cannot be explained in any way from the point of view thermal theory, since in both cases the amount of absorbed
the object of energy was one and the same. For slight heating
a frog nerve preparation under experimental conditions close to those described is also indicated in [25]. From this we can assume
that part of the absorbed energy of microwave EMF pulses triggers an unknown mechanism of inhibition of the propagation of the excitation wave, leading to an anomalous effect. Noteworthy is the
the fact that the development of recorded changes in the observed parameters is preceded by a certain period of time, during which the values
these parameters are close to normal. This means that such a mechanism action of microwave EMF pulses should cause local disturbances or damage (microdamage), which, accumulating,
result in effects opposite to thermal
influence. Obviously, at a certain value of PPMav it is possible compensate for the increase in the speed of propagation of the excitation wave by the accumulation of microdamages. If the heat generated is not disrupts the normal functioning of the object, then such a state
object could be considered boundary for the separation of observation-

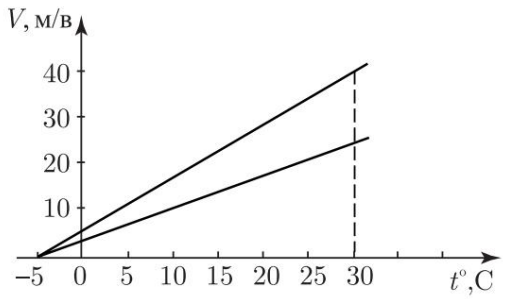

Rice. 2.01. Dependence of the speed of propagation of the excitation wave on temperature

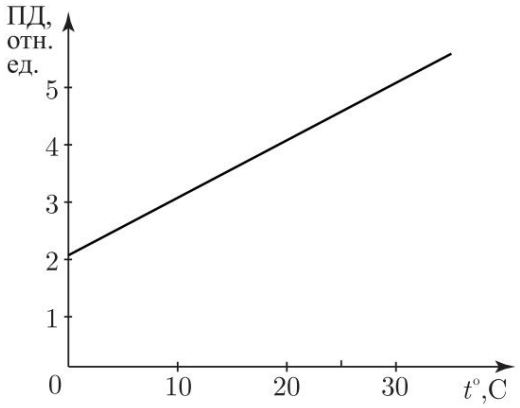

Rice. 2.02. Dependence of action potential amplitude on temperature

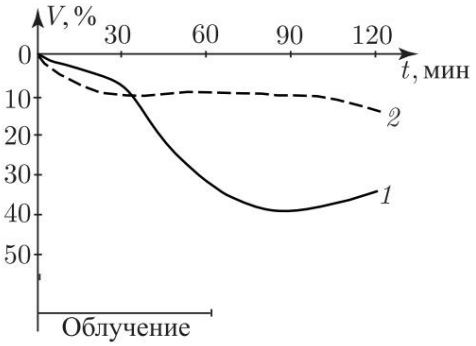

Rice. 2.03. Change in the speed of propagation of the excitation wave at pulsed microwave irradiation

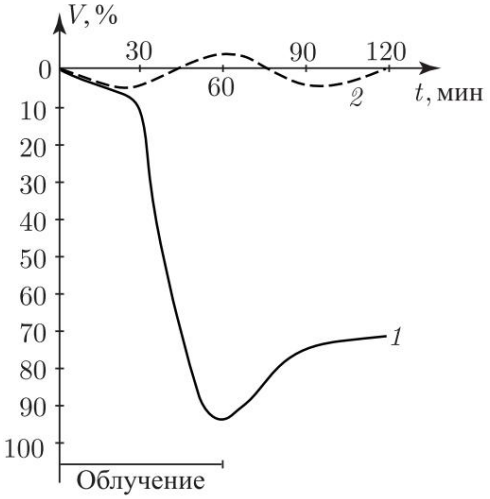

Rice. 2.04. Change in the amplitude of the action potential during pulse microwave irradiation

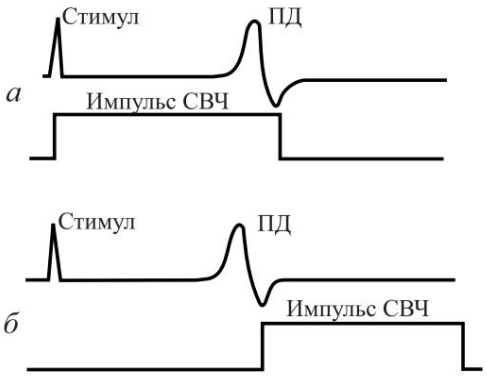

Rice. 2.05. Phased irradiation of a nerve preparation with pulses Microwave: a) irradiation during the latent period; b) irradiation in the post-latency period

possible effects on non-thermal (ano-mal) and combined, or combined, in contrast to purely heat-fishing

Dynamics of relative phases and absolute refractoriness were studied using the paired stimulation method [26].

Irradiation was also carried out at pulse repetition rate 20 Hz. Stimulation was carried out synchronously in periodic mode series with two pulses in a series, the interval between which is regulated

roared. During 30 minutes of irradiation, the time of absolute refractoriness increased by 95%, the duration of the relative refractory phase - by 210%. With non-synchronous irradiation, the pulse repetition rate was 17 Hz. The time of absolute refractoriness also increased by 95%, the duration of the phase

relative refractoriness increased by 125% (Fig. 2.06).

Irradiation of a preparation of an isolated frog heart. With synchronous irradiation, the phase of development of the QRS complex was exposed to EMF; with asynchronous irradiation, the drugs were irradiated with a repetition rate

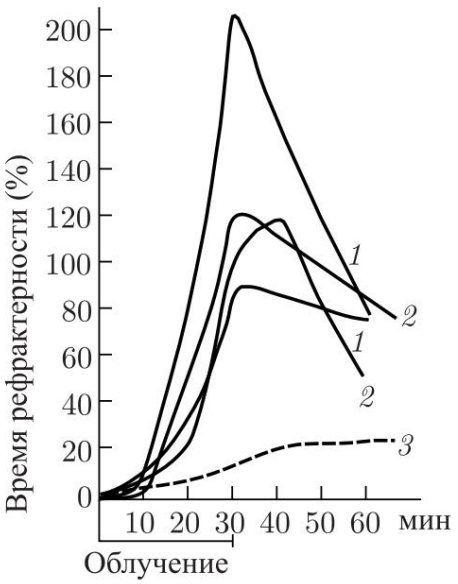

Rice. 2.06. Changes in the refractoriness phases of the nerve preparation frogs at pulsed microwave irradiation. *1* - phase changes absolute and relative refractoriness of the nerve preparation frogs with synchronous irradiation during the latent period (pulse repetition rate Microwave and stimulus - 20 Hz); *2* — the same with non-synchronous irradiation with microwave pulses (frequency stimulus sequence - 20 Hz, pulse repetition rate microwave — 17 Hz); *3* — control

microwave pulses close to the contraction frequency.

It is known that with increasing temperature the speed of propagation increases excitation waves in the cardiac muscle [27, 28]. In [29] it is shown that that when a whole frog preparation is irradiated with microwave EMF pulses with PPMav = 10 mW/cm2 observed decrease in heart rate and growth of the *P–Q* interval during irradiation in the Q-tooth developmental phase. At the former parameters of the EMF pulses of the SWF The time shift of these impulses into the phases of the cardiac cycle, characterized by an isoline, did not lead to visible changes. If irradiation was carried out without synchronization with the cardiac cycle, then the hit microwave EMF pulse in the phases of development of P-, R- and T-waves caused instantaneous short-term abrupt increase in the cardiac cycle. And finally, irradiation with continuous microwave EMF with the same value PPMsr did not lead to any noticeable changes in cardiac activities. According to B.N. Veprintsev, with an increase in temperature by 10°C, the speed of propagation of the excitation wave in the heart muscle increases by 1.8 ÷ 1.9 times, similar values are given and other authors.

During the control, by the end of the 30th minute, the cardiac cycle increased by an average of 6%, the *P-Q* interval remained stable. When the microwave radiation pulse is synchronized with the development phase of the QRS complex, shifts are observed 10-15 minutes after the start of irradiation in both parameters. By the end of the 30th minute, the magnitude of the cardiac cycle

increases by an average of 30%, the *P–Q* interval increases by an average of 130%. In this case, a transformation of the rhythm is observed. Experiencing the drug ends with sinus node blockade or conduction blockade ways. The time of experiencing objects can be reduced on average to 17 minutes, if the drug is in the direction “sinus node - ventricle” placed parallel to the electric vector of the microwave EMF.

With non-synchronous irradiation with pulses lasting 30 ms and peak power 220 W (PPMI = 1 W/cm2) changes in magnitude cardiac cycle and *P–Q* interval remained within control limits [29].

Irradiation of a preparation of an immobilized frog. During the first 30 min in the control there is a monotonous increase in the period of cardiac contractions by 8-9% with a simultaneous increase in the interval 3-4% on *P-Q .*

Under conditions of non-synchronous irradiation with a microwave pulse duration of 30 ms (irradiation of the cardiac cycle phases is random) and PPMav = = 10 mW/cm2 , a stabilizing effect of irradiation on the size of the cardiac cycle was noted when irradiated with a lower energy density.
Irradiation with PPMav = 10 mW/cm2 leads to a decrease in the value cardiocycle. At the same time, a greater decrease in the *P–Q* interval is observed when objects with a higher energy density are irradiated.

Against the background of a gradual decrease in both the magnitude of the cardiocycle and and the *P–Q* interval , a sharp (jump-like) increase in both values is observed when a microwave pulse accidentally hits the phases active state of the drug - in the zone of “vulnerability” before *the QRS* complex, in the phase of atrial systole (P wave) and in the phase of the last parts of ventricular systole (T wave). On average, the amplitude of such “jumps” amounted to +8%.

In the synchronous exposure mode (irradiation was carried out in the area “vulnerability” of the QRS complex), a microwave radiation pulse was triggered command pulse generated by a phase biosynchronizer from the R-wave of an object’s ECG [30]. Average Energy Density 10 mW/cm2. In Fig. 2.07 shows a graph of relative changes cardiac cycle values for one of the drugs.

The first profound disturbance in cardiac activity was registered at the 31st minute of irradiation in the form of sinoatrial blockade, which on the electrogram was expressed as a complete “failure” of one cardiac complex of both the atrial and ventricular parts. To that

time as a result of slowing down the sinoatrial conduction period heart rate increased by 45%.

The next blockade was observed at the 32nd minute. The lack of activity lasted longer than after the first blockade. Third blockade was noted at the 35th minute, lack of drug activity lasted longer than after the second blockade.

The subsequent blockade took place in the 37th minute, the absence activity lasted 20 minutes, after which, at the 57th minute, the last activation of the drug, and then after 30 s - stop. In those

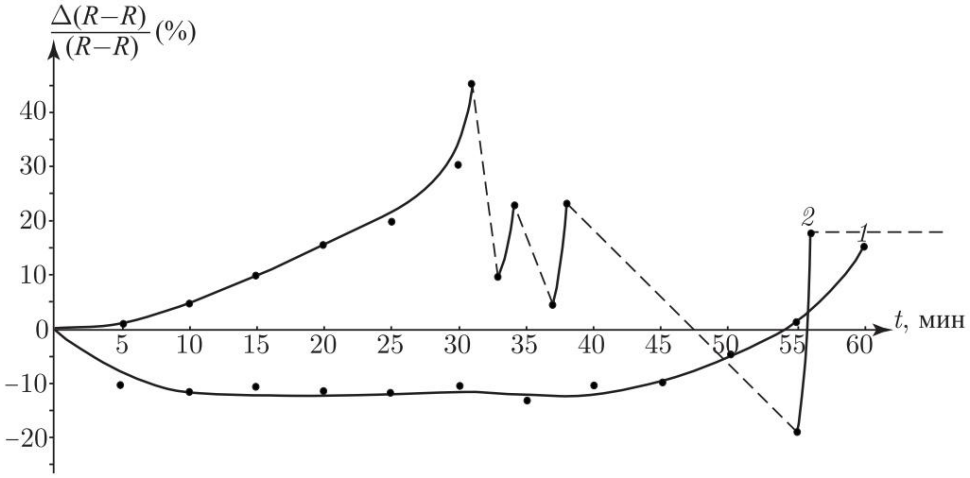

Rice. 2.07. Relative change in the magnitude of the cardiac cycle of a whole frog. *1* - control; *2* — synchronous irradiation with microwave pulses into the zone "vulnerabilities" of the QRS complex

over the next 35 minutes, no cardiac recovery was observed activities.

The spread of the onset of the first blockade in time for various objects was observed within the range of 26–41 minutes. Described phases observed violations for different objects varied in time within the range of 3–7 minutes [29].

Irradiation of a preparation of the innervated frog sartorius muscle. Irradiation of the drugs was carried out with PPMav = 12 mW/cm2 at a microwave pulse repetition rate of 1 Hz with a duration of 8 ms. When stimulating control drugs with a frequency of 1 Hz at a Ringer's solution temperature of 15–17°C, pH 7.5–7.7, the muscle almost stops contracting, and at the 8-9th minute - completely muscle adhesions disappear on the oscilloscope screen.

Irradiation of the drug with microwave pulses synchronously with stimulation removes the block of myoneural transmission up to exposures equal to 40 min. After cessation of irradiation, decline in muscle activity occurs within 1–2 minutes.

The selected microwave pulse duration (8 ms) corresponds to the total time of excitation along the nerve, through synaptic formation and partial propagation of the excitation wave along muscle fibers. Thus, the microwave pulse "captures" active state of the drug at all levels. A phase shift of the microwave pulse by 50% relative to the stimulus leads to blocking myoneural transmission at the 20th minute [11].

Thus, the contradictions mentioned above can be formulate as follows:

— recorded heating of an object when irradiated by pulses Microwave EMF does not correspond to the functional state, determined by the amount of energy absorbed and converted into heat.

— the energy of microwave EMF pulses absorbed by the object leads to to changes in recorded parameters that are opposite to those under thermal influence.

Formulated in this way, the identified contradictions between the magnitude of the absorbed energy of microwave EMF pulses and the observed shifts in the functioning of the object allow us to put forward main theses for searching for evidence of the proposed hypothesis mechanism of action of pulsed EMF microwave:

1) The energy of microwave EMF pulses partially absorbed by the object converted into heat, partially transformed into another, not yet identified, type of energy.

2) This type of energy leads to such a disruption in the functioning of the object that the course of the temperature dependences of the main parameters reflecting the functional state of the object does not coincide with those under thermal action.

3) Starting from a certain value of the energy of microwave EMF pulses absorbed by the object, the course of the temperature dependences of the main object parameters can change sign. The angle of inclination of these dependences to the x-axis reflects the contribution to the observed effect each type of energy - heat and unknown.

4) The development of the effect is preceded by a certain period of time, presumably necessary for the accumulation of local changes (possibly violations) caused by the presence of an action in the object an as yet unknown type of energy, representing part of the transformed energy of microwave EMF pulses (presumably this is mechanical vibrations).

The listed points, naturally, cannot fully characterize the actually existing mechanism of the specific pulsed effect of microwave EMF, the subtleties of the action of this mechanism during irradiation of biological objects of various organizations. But even in this form, these points help determine the main search paths this mechanism, the direction in setting up experiments to identify it.

It would probably be logical to put forward the requirement that the observed effects take place at comparable values of PPMav. Comparing the results obtained in experiments with those listed objects, it can be argued that there is a fulfillment of the put forward conditions and that the theses proposed above are universal, at least for objects that are cellular and tissue structures. On the possibility of the existence of non-thermal The effects of pulsed microwave EMFs have been indicated by many authors. Assuming that when a biological object is exposed to microwave EMF pulses, a summation of local changes occurs, and more pronounced at a high pulse repetition rate, Kamensky [24] came to the conclusion that this is explained by the small interpulse interval. At lower pulse repetition rates, the interpulse

the interval increases, which, according to Kamensky, reduces the level summation of local changes in an object. All listed here experiments do require some period of time to the beginning of the development of visible changes, and it would be more correct call this period of time not the time of summation of local changes, but the time of accumulation of microdamages (microviolations).

The term “microdamage” allows us to more fully characterize state of the object, since the effects then recorded are actually are anomalies. The possibility of summation of some local disturbances is also indicated in [12]. The time given in [25] necessary for the beginning of the development of visible changes in the functioning of an object coincides with that in [22] with an accuracy of minutes.

2.2. Ultrasound analogues of abnormal bioeffects of pulsed EMF microwave

In light of the proposed hypothesis of the mechanism of the specific action of pulsed microwave EMFs, it would be advisable to compare the results of the action of this factor and ultrasonic vibrations on the same and the same biological objects. It also seems necessary comparison and quantitative assessment of the corresponding quantities characterizing mechanical vibrations in the medium and responsible for the occurrence of the observed effects. Comparison of the results of experiments on the effects of microwave EMF and ultrasonic (US) vibrations on a nerve preparation leads to the idea of the possibility of comparing these results and, therefore, to a certain extent, the adequacy of the mechanisms of biological action. Thus, Frey et al. [31–35] found that exposure to a series of very weak doses of ultrasonic oscillations, the following at intervals of several minutes, leads to paralysis of the limbs frogs (quoted from [34]). This means that the accumulation of violations when exposed to ultrasonic vibrations, which separately cause a reversible biological effect, leads to irreversible damage.

According to Coronini and Lassman [36, 37], irradiation with ultrasonic oscillations loosens nervous tissue. According to [22], during the first 20-30 minutes of irradiation with microwave EMF pulses, visible changes No. In the next 20 ÷ 30 minutes, the values of the observed parameters the spread of excitation changed sharply, which ultimately led to block the spread of excitation.

A very similar picture occurs when irradiating an immobilized frogs by microwave EMF pulses [11]. When an impulse hits one From the ECG waves, an abrupt change in the value of the subsequent cardiac cycle is observed. If the pulse hits one again does not occur from the active phases of the cardiocycle, then the ECG is restored. If the hit occurs over several cardiac cycles, then the value of the cardiac cycle after a sudden increase

remains at a new level. With a repeated series of hits, the value
the cardiocycle is growing. The picture develops before the onset of a block of the conduction pathways or before the onset of blockade of the sinus node.

The following comparison is interesting here. As in experiments on in the nerve preparation and in the frog heart specimen, visible disturbances occur only when the preparations are irradiated at moments of active
their states (latent period for the nerve preparation and waves P, Q, T - for the heart preparation), that is, at moments characterized by redistribution of ionic currents through membranes.

It can be assumed that the main functional disorders
states of objects occur as a result of the influence of excited mechanical vibrations on the channels during their active state, which leads to a change in the conditions for the conduction of ions by them.
Analogues of this phenomenon occur in many areas of research.
and practices - this is the so-called capillary effect of ultrasound. Leman, Becker and Jenicke [38] established experimentally the passage
chlorine ions through the skin of a frog when irradiated with ultrasonic vibrations. To change the active transport of ions through the skin of a frog under Sarvazyan and Pashovkin also indicated the influence of ultrasound [39]. Assume that in the case of irradiation of an object with microwave EMF pulses the field itself interacts with the ions is hardly possible, since when
At carrier frequencies of the order of 109 Hz, the ion mass is too large to he could keep up with the periods of the field, that is, he could oscillate in time with the changes in the field. This is indicated in [40].
A qualitatively similar picture can be obtained by comparing the results effects of pulsed EMF microwave and ultrasonic oscillations on bacterial and animal cells. Jung [41] showed that during hemolysis, the membrane of erythrocytes destroyed by ultrasonic vibrations has numerous holes. According to Barth, Erlhof and Streibl [42], hemolysis of erythrocytes is a consequence of the cavitation effect of pulsed ultrasonic oscillations. The results of irradiation can be compared with these data.
suspensions of E. *coli* with bacteriophage T-5, given by Fraser (USA).
When the suspension was irradiated, he observed cell lysis and infection bacteriophage. Irradiation mode: pulsed, intensity:
240 mW/g. It is interesting that the extensive material reviewed on the effects of microwave EMF on erythrocytes contains only information about the results of exposure to continuous microwave EMF radiation. At the same time, nowhere There is no mention of hemolysis of red blood cells. Impact information
No pulsed microwave EMFs on erythrocytes were detected. Failed also detect data on pulsed exposure to microwave EMF
to microorganisms. According to Theisman and Wallhäuser [43], Houseman, Köhler and Koch [44, 45], the effect of ultrasonic vibrations on bacteria is mainly mechanical, heating has
of secondary importance. It is extremely interesting to compare the results of exposure of brain tissue to ultrasound oscillations and EMF.
Microwave. The works [46, 47] show the destruction of brain tissue in single

with powerful ultrasound pulses. Starting at some point in time (less than 1 s) in the observed effect of ultrasonic vibrations on the tissue begins to be introduced by the cavitation effect of ultrasonic vibrations, that is, mechanical damage.

Thus, with a pulse duration of ultrasonic oscillations equal to 10ÿ3 s, the intensity required to destroy brain tissue is a value of the order of 104 W/cm2. According to Fraser, for inactivation brain of small animals, they used EMF irradiation with a pulse intensity of 1 MW/kg, which led to an increase in temperature about 100ÿÿ/s. To change the functioning of the neuromuscular the drug is indicated by Kazarinov, Sharov, Putvinsky [48]. Under the influence of microwave EMF pulses with a power of 1 MW and a duration of 10 ns in the millimeter range they showed excitation of the neuromuscular drug without noticeable heating. At the same time, Schmitz and Hoffman [49] indicate that stimulation of the frog's nerves by sound or heat is impossible without tissue damage. Work [48] shows also a significant acceleration of the transport of sodium ions through the skin frogs in the Using apparatus. It should also be noted that there are interesting results of the reaction of biological objects to turning on and off the microwave EMF [50].

Analyzing the data presented here, we can come to the following conclusions:

1. Effects observed during irradiation of biological objects different levels of organization by microwave EMF pulses cannot be explained by the assessment of the total heating of the object within the framework of the concept of the specific action of the electromagnetic field.

2. Dynamics of development of the observed effects when acting on the object of microwave EMF pulses and cavitation ultrasonic oscillations has similar character.

3. One can raise the question about the role of the acoustic factor in the formation study of the biological effects of pulsed microwave EMFs.

2.3. Hypothetical sound field picture

In accordance with the hypothesis put forward here, the process of converting the microwave EMF pulse power absorbed by an object into the power of mechanical vibrations and heat can be represented in the form following diagram:

$$P_n \longrightarrow k_1 P_n \longrightarrow k_2 P_n \begin{cases} \nearrow k_3 Q_1 \\ \searrow k_4 Q_2 \end{cases}$$

where: Pn is the power of the microwave EMF pulse incident on the object; k1Pn — microwave EMF power absorbed by the object; k2Pn —thermal pulse power; k3Q1 — power spent on heating the object;

k4Q2 is the power consumed to excite mechanical vibrations.

The value of k1Pn is determined by many parameters - geometry and the size of the object, electrical conductivity and dielectric properties, orientation of the object in the microwave field, etc. Biological object when it is in the microwave EMF action zone, it is distinguished by the heterogeneity of its structural organization and physical and chemical properties, and the problem of determining the internal field is in the general case unsolvable. Therefore, this value must be determined in each specific case separately, and, as a rule, exact solutions of this problem are possible obtain only for bodies of the simplest configuration [51]. Here you can just note that the value of the coefficient can vary from 1 to values of the order of 10ÿ3. In the general case, the range of values of the coefficient k1 can be much wider, however, in those considered here experiments, the specified framework can be considered appropriate real conditions. The coefficient k2 is the conversion indicator absorbed energy of microwave EMF into thermal and in its value may be close to 1. Frequency range of mechanical vibrations will be determined by the spectrum of oscillations, starting from the repetition frequency thermal impulses and ending with frequencies determined by subunits, the size of which can be found from the relation [52–54]

$$f_{time} = \frac{0,66}{2r} \quad [kHz],$$

where r is the radius of spherical particles in cm (the relationship is valid for gas bubbles).

Depending on the geometry of the object, its physical and chemical properties, it will be spent on excitation of mechanical vibrations a certain part of the energy of the thermal impulse. Rest energy thermal impulse will be released in the form of heat. According to [55], there is gas cavitation, which is the vibration of small bubbles gas in the form of stable cavities. In this case, the bubbles may oscillate only if there are inhomogeneities in the object with resonant frequencies equal to the resonant frequencies of the bubbles. However not only the presence of bubbles of dissolved gas in a biological object can cause high-frequency mechanical hesitation. The cells themselves, subcellular units and even individual molecules can be considered as sources of mechanical vibrations. Thus, the coefficient k4 is associated with the geometry and dimensions of the object, its structural organization and physico-chemical properties.

Let us consider the possible nature of mechanical vibrations excited in objects. As is known, in pure liquids only longitudinal vibrations can exist. Real biological objects when irradiated with microwave EMF pulses should be characterized by the presence of not only longitudinal mechanical vibrations, but

and transverse, or shear, due to their heterogeneity. Because the
the absorption coefficient of shear waves is very high, ÿt = 105ÿe, where
ÿt is the shear wave absorption coefficient, ÿe is the
absorption of longitudinal waves [56], one can expect that the greatest
It is these waves that have the intensity. That shear
waves are decisive in the destruction of living cells and macromolecules when they are irradiated by sound fields, Hughes points out
and Nyborg [57]. They came to the conclusion that the main reason for the destruction of cells and large molecules at vibration amplitudes lying
Below the cavitation threshold, there are pulsating bubbles. Mechanism
They associated the resulting destruction with high shear stresses that arise near such bubbles [55].

The considered types of possible mechanical vibrations in a complex heterogeneous medium give only a general idea of the nature
transformation of incident electromagnetic energy. From the moment
mechanical vibrations are excited in such a system, it can be considered as a certain limited volume in which
elastic vibrations of various modes. Therefore, to such a system
you can apply all the methods and techniques for studying its characteristics,
used in the practice of ultrasound research. Since biological objects are heterogeneous systems, it is necessary to take into account the possible localization of microwave EMF energy at the interface
two environments For example, membranes of cellular structures are characterized by low electrical conductivity and low dielectric constant. Since the magnitude of the electric field vector
in the membrane exceeds that in solution by = 30 times [58], where ÿe is $\frac{eh}{ÿl}$
dielectric constant of the electrolyte, ÿl - dielectric
lipid permeability, then in this case the localization of field energy
in a membrane can be 103 times higher than in a homogeneous medium.

2.4. Generation of elastic waves during rapid heating

Until some time, the problem of generating acoustic disturbances in a substance as a result of rapid heating of its surface
or allocated local volume represented an independent
interest and was considered without specifying the heat source and, accordingly, with arbitrary assumptions regarding the nature
thermal field distribution. In the case of excitation of elastic
waves caused by the absorption of pulsed energy from electromagnetic fields, it is necessary to take into account the peculiarities of the interaction of the latter with the substance and the properties of the substance itself. Obviously the solution tasks in general form due to the multifactorial nature of the input parameters extremely difficult, and therefore it is advisable to limit ourselves to a fairly simple consideration of this problem, given in [59].

The interested reader can find a more in-depth consideration in the literature [60–63].

However, in the cited works the problem of the occurrence of acoustic disturbances during the entire period of action of the heating agent is considered.
impulse ÿti. And naturally, in the expression for the conversion coefficient of the incident (or absorbed) energy, in this case
electromagnetic, in acoustic there is precisely duration
of the entire heating pulse. Secondly, in the mentioned works
surface heating is considered, while during irradiation
The object is instantly heated by microwave pulses of the entire volume
provided that the penetration depth of microwave energy is equal to or greater than the maximum size of the object. As a rule, this condition is always
feasible in experiment, unless we are talking about irradiation
large laboratory animals. And finally, acoustic disturbance occurs immediately when the microwave field is turned on, i.e. at the moment of increase in absorbed electromagnetic energy, which corresponds to the front
Microwave pulse ÿf. The same displacement, but in antiphase, occurs
when the microwave field is turned off. Thus, the object is formed
a thermal pulse with a duration equal to the duration of the microwave pulse, and fronts close to the front and fall of the microwave pulse (see.
rice. 1.02). When irradiating biological objects with microwave pulses
pressure jump in the absorbing volume, in the presence of heterogeneity
environment, leads to the formation of a bodily antenna - limited
volume playing the role of a resonator with a quality factor determined
viscoelastic properties of the absorbing medium.

Since matter has a finite speed of propagation
interaction (speed of sound C) and some density ÿ, then when
sufficiently rapid heating, when the duration of the rising front
The microwave pulse is small, i.e. the rate of “pumping” of electromagnetic energy is high compared to heat dissipation, shear stress
will lead to the generation of mechanical vibrations with a frequency
determined by the linear dimensions of the body antenna. At the end
irradiating pulse, mechanical vibrations are excited by the rear
front (fall) of the pulse - ÿc in antiphase with oscillations excited by the leading edge (rise) of the pulse ÿph. That's why
when the pulse duration changes, both the suppression of excited oscillations and their amplification due to interference should take place. The same effect will take place when excitation of mechanical
oscillations in periodic short pulses. For closed people
volumes further study of the sound field pattern in each
In a particular case, it should be carried out in accordance with ordinary acoustic laws. It is essential that all closed volumes
are resonators and, therefore, under a certain mode
modulation of EMF, the amplitude of mechanical vibrations in them can be
orders, in accordance with the quality factor of a particular resonator,

exceed the amplitude of a single pulse of arbitrary duration
burdens.

2.5. Experiment

In order to confirm the main theses proposed here
Based on the hypothesis, a series of experiments was carried out on the
effects of pulsed microwave EMFs on various objects. Irradiation was carried
out in a rectangular waveguide with a cross-section of 31 × 240 mm2, pulse power
72 W, PPMi = 2 W/cm2.

A bimorph crystal, used in the heads of piezoelectric pickups, was chosen
as a receiver of the expected mechanical vibrations. Mechanical vibrations
converted
crystal into an electrical signal, amplified and recorded on
oscilloscope screen.

Any model objects can be used
polar liquids. In our experiments we used aqueous
NaCl solutions and ethyl alcohol. Ethyl alcohol at a radiation frequency of
2375 MHz (wavelength 12.6 cm) has at 20°C: ÿ = 5.5
and ÿ = 7.8 [3], a one-molar aqueous solution of NaCl at a close frequency
3 GHz (wavelength 10 cm) has at the same temperature: ÿ = 67.4
and ÿ = 13.1 [64]. All reference data necessary for calculation,
are given in table. 2.1.

Table 2.1

Absorber	C, m · sÿ1 ÿ, gradÿ1 ÿ,	kg · m3	Sÿ1 J/kg · city	a, mÿ1
Ethyl alcohol 1.2 103 3.7 10ÿ4 1.48 103	789	2.39 · 103	166	
Water	6.9 10ÿ5	1000	4,189 · 103	100

The conversion of electromagnetic energy into mechanical energy in
alcohol is almost two orders of magnitude more efficient than in water. In this regard
ethyl alcohol was widely used in the experiments described
in order to increase the sensitivity of energy conversion methods
excited mechanical vibrations into an electrical signal.

The block diagram of the experimental setup is shown in Fig. 2.08.
The first series of experiments was carried out in a 1 M NaCl solution.
Using this solution, the hypothesis itself about the excitation of mechanical
vibrations in an object when irradiated with microwave EMF pulses was tested,
a technique for measuring the parameters of mechanical vibrations has been developed.

Results of experiments on irradiation of a 1 M NaCl solution.
Test tube with internal diameter 7 mm, wall thickness 1 mm
and 100 mm long is inserted into a hole in the wide wall of the wave-water in
the center plane. In order to increase concentration
fields in the test tube, the latter is located in the beyond waveguide

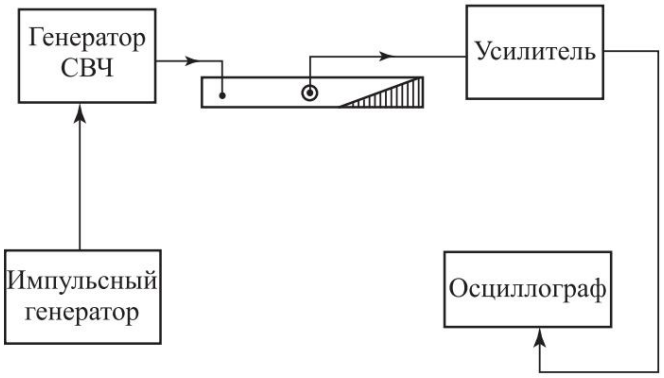

Rice. 2.08. Block diagram of an experimental setup for recording mechanical vibrations excited in liquids by microwave EMF pulses

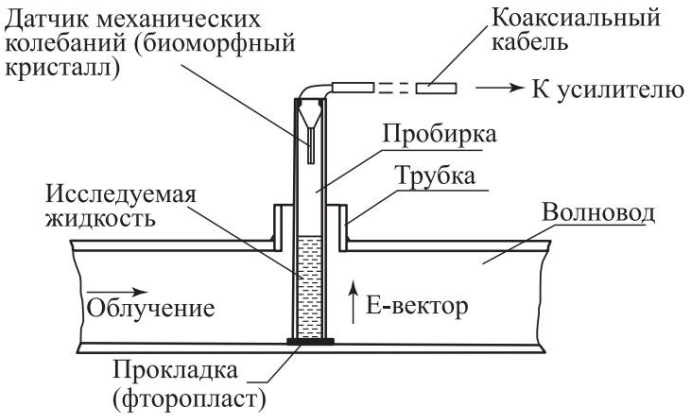

Rice. 2.09. Layout of the test tube with the test liquid

(Fig. 2.09). A bimorph crystal is introduced into the test tube from above, which held in a test tube using two elastic conductors soldered to the crystal. Conductors simultaneously serve as current conductors buses to which a coaxial cable is soldered, connecting the crystal to the amplifier input. Excited through elastic conductors inside the object, mechanical vibrations are transmitted to the crystal from test tube walls. This was done for the purpose of minimal damping irradiated object. Although this crystal is intended for recording torsional vibrations, nevertheless, the electrical signal removed from the crystal turned out to be sufficient for registration.

In order to identify the artifact, the action of the pulses was checked Microwave EMF on a crystal placed in a waveguide on a dry test tube in the waveguide, onto the test tube with the crystal. Since the microwave voltage induced on the crystal and then detected on the input circuits of the amplifier, the entire system was checked - test tube-crystal-amplifier - at applying rectangular pulses directly to the crystal from generator G5-54. In none of these cases were any fluctuations recorded on the oscilloscope screen. Along with the it turned out that the use of selective amplification equipment can lead to an artifact.

To minimize the influence of sound vibrations on the crystal due to the possible ponderomotive effect of microwave EMF [51], the test tube with the sensor is installed on a bearing made of absorbent material. From the outside, the entire waveguide is covered with a thick layer of porous rubber. The height of the solution column in the test tube varied from 30 to 50 mm, pulse repetition rate - within 10 ÷ 104 Hz, pulse duration is 10ÿ5–10ÿ3 s. For all three columns solution (height 30, 40 and 50 mm), mechanical vibrations were recorded on the oscilloscope screen. Using the marks on the screen were the periods of mechanical vibrations were determined (Table 2.2). Taking advantage relations L = and c = ÿf, it $\frac{no}{4}$ [65], where L is the column height, ÿ is the wavelength is possible to obtain the values of the speed of sound in the solution for three values of the height of the liquid column (Table 2.3). Taking into account the measurement error of the period (up to 10%) and the height of the liquid column (up to 3%) The obtained data are in good agreement with those presented in the literature.

Table 2.2

Dependence of the frequency of excited waves in a 1 M NaCl solution mechanical vibrations from the height of the liquid column

Pole height liquid, mm	Mechanical period oscillations, ÿs	Mechanical frequency oscillations, kHz
30	80 ÷ 100	12 ÷ 10
40	100 ÷ 120	10 ÷ 8
50	140 ÷ 160	7 ÷ 6

Table 2.3

Calculated values of the speed of sound in liquid based on data measuring the frequency of excited mechanical vibrations

Wavelength, cm	Mechanical frequency oscillations, sÿ1	Calculated value speed of sound, cm/s
12	$\frac{1}{0{,}8 \cdot 10ÿ4}$	1,44 · 105
16	$\frac{1}{1{,}1 \cdot 10ÿ4\ 1}$	1,45 · 105
20	$\frac{}{1{,}4 \cdot 10ÿ4}$	1,42 · 105

In Fig. Figure 2.10 shows an oscillogram of excited mechanical oscillations for one of the pulse repetition frequencies. As the duration of the microwave EMF pulses increases, mechanical vibrations excited by the leading and trailing edges of the thermal pulse are clearly observed on the oscilloscope screen (Fig. 2.11). When it changes duration of the microwave EMF pulse and with increasing frequency of their traces

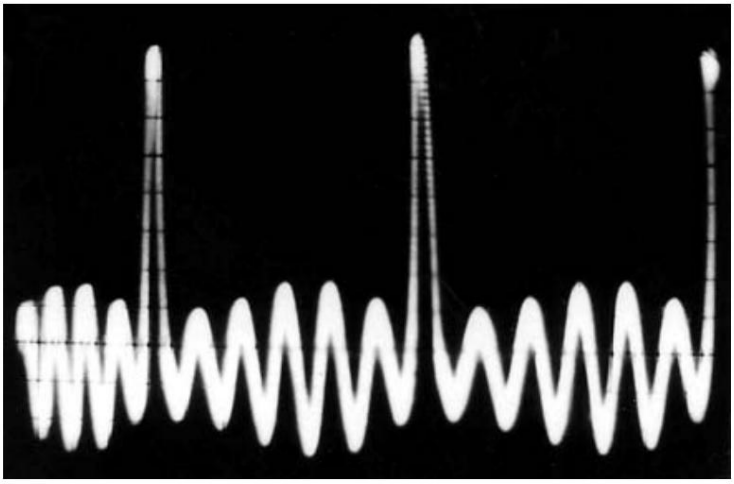

Rice. 2.10. Oscillogram of excited mechanical vibrations at action of a short pulse of microwave EMF

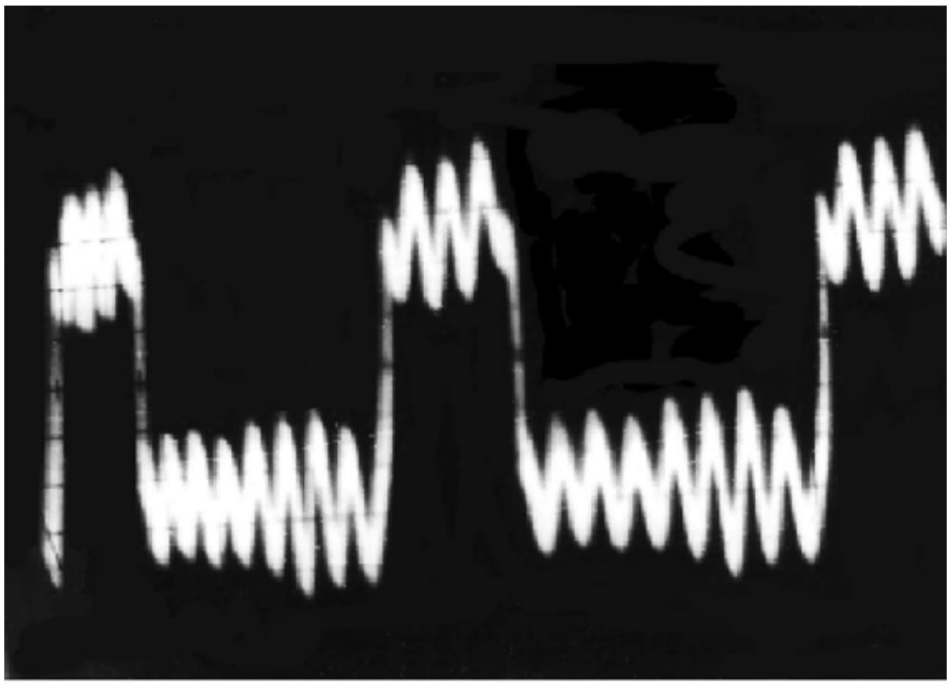

Rice. 2.11. Oscillogram of excited mechanical vibrations at action of a wide pulse of microwave EMF

In this case, an interference pattern is clearly observed, due to the phase relationships of mechanical vibrations excited
leading and trailing edges of the thermal pulse. With duration
pulse (the same for their repetition frequency), sufficient for normal
attenuation of excited mechanical oscillations both from
the leading and trailing edges of the thermal pulse, interference is not observed. As the pulse duration decreases
the interference pattern becomes clearer. With duration
pulse less than half the period of excited mechanical

oscillations, the latter are observed only from the trailing edge
thermal impulse. From this point on, the interference
the picture is observed with increasing pulse repetition rate.
An oscillogram of the interference of excited mechanical oscillations (the
oscillations are in antiphase) is shown in Fig. 2.12.

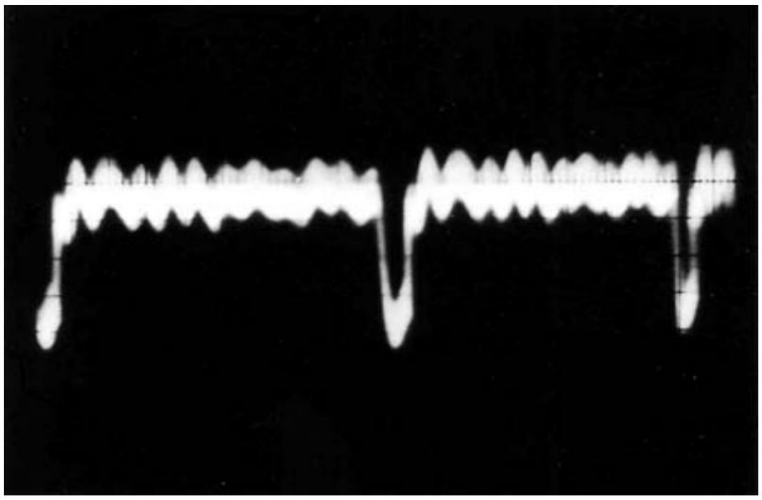

Rice. 2.12. Suppression of excited mechanical vibrations

After working out the methodological questions, a second
a series of experiments on NaCl solution in spherical cones
made of glass with a diameter of 30, 20 and 10 mm. In cones with a diameter of 20
and 10 mm, it was not possible to register mechanical vibrations due to
significantly lower value of the internal field. However, by ear
vibrations are perceived. In a cone with a diameter of 30 mm, mechanical
vibrations were recorded using the same crystal.
The frequency of excited mechanical vibrations is about 9 kHz. It was of
interest to determine the dependence of the amplitude of excited
mechanical vibrations in the solution due to pulse power. To
to avoid heating the sample, the data were obtained by irradiation at a
repetition frequency of 10 ÷ 20 Hz with a pulse duration of 10 ÷ 20 ÿs.
In Fig. Figure 2.13 shows a graph of this dependence. Power loss,

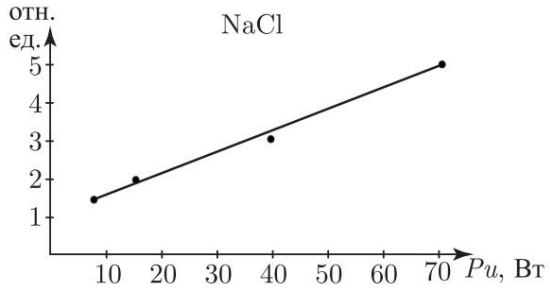

Rice. 2.13. Amplitude dependence of excited mechanical vibrations
on the microwave EMF pulse power for a 1 M NaCl solution

or field inside the object, was determined by the rate of temperature growth solution. At F = 500 Hz and pulse duration 100 ÿs, the increase temperature for 1 min was 6°C with a sample volume of about 2 cm3, that is, for NaCl - 0.1 deg/s. Power loss in electrolyte is determined by the known relation

$$w = \frac{\ddot{y}E2}{2} v, \text{ or } w = cm \frac{\ddot{y}T}{\ddot{y}t}.$$

For a given duty cycle equal to 20, the power loss per pulse in terms of the volume of solution was 8.4 W/cm3. Addiction amplitudes of excited mechanical vibrations depending on duration Microwave EMF pulses are shown in Fig. 2.14. Highs and lows the amplitudes of excited mechanical vibrations, starting from a certain value of the pulse duration, follow with periodicity, corresponding to the period of these oscillations. At moments corresponding to the maximum amplitude of oscillations, clear high pitch of a resonating column of liquid. At moments corresponding to the minimum amplitude, a low tone is heard.

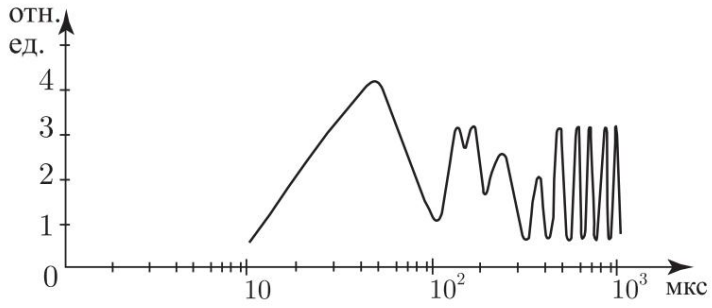

Rice. 2.14. Amplitude dependence of excited mechanical vibrations on the duration of the microwave EMF pulse for a 1 M NaCl solution

2.6. Results of experiments on irradiation of clean liquids

The irradiation of pure liquids was of interest not only from the point of view of confirming the hypothesis put forward if there is mechanical vibrations in them, but also from the point of view of the presence of such vibrations in a homogeneous medium. For this purpose, a series was created experiments on the effects of pulsed microwave EMFs on alkalis, alcohols, organic acids, solvents. It was also interesting identify the presence of excited mechanical vibrations in polar and non-polar liquids.

The results of these experiments are summarized in table. 2.4. Given In this table, the values of the speed of sound obtained in the experiment and the reference values are in good agreement. The amplitude values of excited mechanical vibrations are given in Table. 2.4, —

averaged values, and the measured values of these values for
of the same test tube could differ by 4–5 times, depending
on the degree of contact of the elastic conductors of the crystal with the side wall
test tubes

Table 2.4

Amplitude-frequency characteristics of various liquids

ÿ n/p	An object	Height table-bull liquid come on cm	Period fur- nothing- ski of coleba, mx	Speed sound, 105 cm/s		Amplitude of coleba, μV
				measured meaning	reference	
1.	NaOH, 1 M	4	65	-	-	14
2.	KON, 1 M	4	65	-	-	14
3.	Butyl alcohol 4.8		170	1,13	1,27	470
4.	Ethyl alcohol	4,1	140	1,15	1,18	400
5.	Glycerin	4	80	2,0	1,92	120
6.	Diethylene Glycol	4	100	1,6	1,58	350
7.	Acetone	3,7	150	1,15	1,19	30
8.	Dichloroethane	3,2	120	1,06	1,03	15
9.	Acetic acid 3.8		120	1,26	1,15	50
10.	Oleic acid	4,5	130	1,34	1,33	15
11.	Benzene	4,2	120	1,4	1,32	8
12.	Nitrobenzene	3,8	110	1,37	1,47	210
13.	Cyclohexanone	4	115	1,4	1,44	15
14.	Cyclohexane	4	120	1,23	1,28	10
15.	Threonine, 0.01 M 3.2		120	1,2	-	13
16.	Oil capacitor	4,5	120	1,5	1,42	15
17.	Chloroform	4	-	-	-	15
18.	D-glucose, 1 M 3.7		100	1,48	-	25

Average value of power flux density in ethyl alcohol based on the measured
value ÿT /ÿt = 0.03 deg/s at F = 500 Hz
and ÿi = 100 ÿs, that is, with the same parameters as for a 1 M solution
NaCl turns out to be significantly less. Despite this, the amplitude

excited mechanical vibrations are more than an order of magnitude higher than for a NaCl solution. Amplitude dependence of excited mechanical vibrations from the duration of the microwave EMF pulse for ethyl alcohol is represented by the graph in Fig. 2.15. Qualitatively the picture repeats a similar dependence obtained for 1 M NaCl solution. The same dependences were obtained for a 1 M solution NaCl and ethyl alcohol at different heights of liquid columns.
With a decrease in the height of the liquid column, the first maximum of the oscillation amplitude is observed at a shorter duration of the EMF pulse Microwave, and this value of the pulse duration always corresponds to the half-cycle of mechanical oscillations.

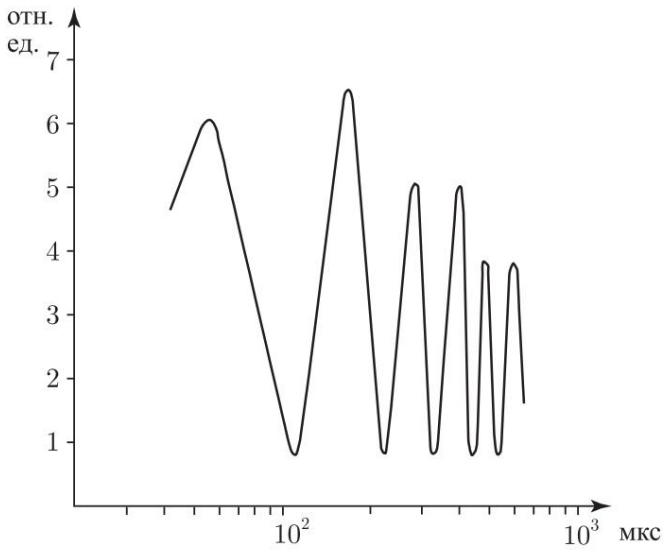

Rice. 2.15. Amplitude dependence of excited mechanical vibrations on the duration of the microwave EMF pulse for ethyl alcohol

The second method for determining the frequency of excited mechanical vibrations was tested using ethyl alcohol. When irradiating a test tube an electrodynamic emitter was turned on simultaneously with the sample, powered by an audio frequency generator. At close frequencies excited mechanical vibrations and a sound signal on the screen The oscilloscope shows zero beats (Fig. 2.16). Thus, with a column height of ethyl alcohol equal to 5 cm (ÿ = 20 cm), zero beats are observed at a sound signal frequency of 5.1 kHz. Hence, the speed of sound in ethyl alcohol will be equal to 1.2 105 cm /s at a reference value of 1.18 × 105 cm/s.

Just as for the NaCl solution, for alcohol there is a linear dependence of the amplitude of excited mechanical vibrations on microwave EMF pulse power.

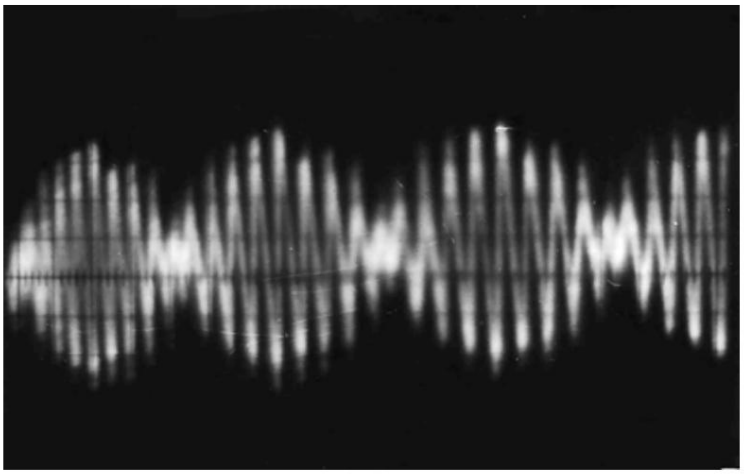

Rice. 2.16. Oscillogram of zero beats excited in ethyl alcohol mechanical vibrations and acoustic sinusoidal signal

Excitation of mechanical vibrations by both pulse fronts Microwave [59, 66] leads to the fact that we actually observe the summation of two damped oscillations having the same frequency and shifted in phase by ÿ + ÿi, where T is the period of natural oscillations of the mechanical system, ÿti is the duration of the microwave pulse. Obviously, the amplitude of the resulting oscillation Aÿ will depend on ÿ as follows:

$$A\ddot{y} = A2_{1} + A2_{2} + 2A1A2\cos\ddot{y} + \ddot{y}\ddot{y}, \qquad \frac{2p}{T}$$

where A1 = A0eÿÿt and A2 = A0eÿÿ(tÿtÿ) are the amplitudes of damped oscillations. Naturally, the consideration is carried out only for t>ÿ, since otherwise only oscillations from the leading edge are observed. Thus, Aÿ is maximum and equal to A1 + A2 = and is minimal, i.e. equal to $\frac{2n+1}{2}T$, where n = 0, 1, 2, ..., with mi

2 A1 ÿ A2, with ÿÿ = nT. Considering that in the oscillatory systems we are considering, the measured quality factor was of the order of 100, and the maximum pulse duration did not exceed several T, the attenuation can be neglected and considered A1 = A2 = A0. Therefore, by changing the pulse duration, you can vary the amplitude excited oscillations from a single microwave pulse ranging from $\frac{2n+1}{2}$2A0 at ÿÿ = T until oscillations are completely suppressed at ÿÿ = nT.

2 The minimum value of ÿi is determined by the energy required for excitation of mechanical vibrations in the system.

2.7. Excited registration system mechanical vibrations based on piezoceramic sensor with longitudinal piezoelectric effect

In order to increase the accuracy of measurements of the amplitude of excited mechanical vibrations and refinement of the vibration mode, a system for recording these vibrations was developed based on a piezoceramic sensor with a longitudinal piezoelectric effect. Sensor represents is a disk with a diameter of 20 mm made of barium titanate. Disc thickness - 0.25 mm. The resonant frequency of the sensor, determined by the relation $f_{res} = [kHz] \cdot [67]$, where d is the thickness of the sensor in mm, about 9 MHz. At frequencies far from resonant, the nonlinearity of the amplitude-frequency response is within ±5 dB. The sensitivity of the sensor is 10ÿ6 V dyn ÿ1 cm2 . In Fig. 2.17 is given schematic representation of a system for recording excited mechanical vibrations on a rectangular waveguide and fixation of a test tube with liquid. To amplify an alternating electrical signal, taken from the sensor, a transistor amplifier with a band was developed 20 ÷ 3 106 Hz . The measured value of the amplitude of the electrical alternating signal, proportional to the amplitude of the mechanical vibrations excited in ethyl alcohol, was 20 mV.

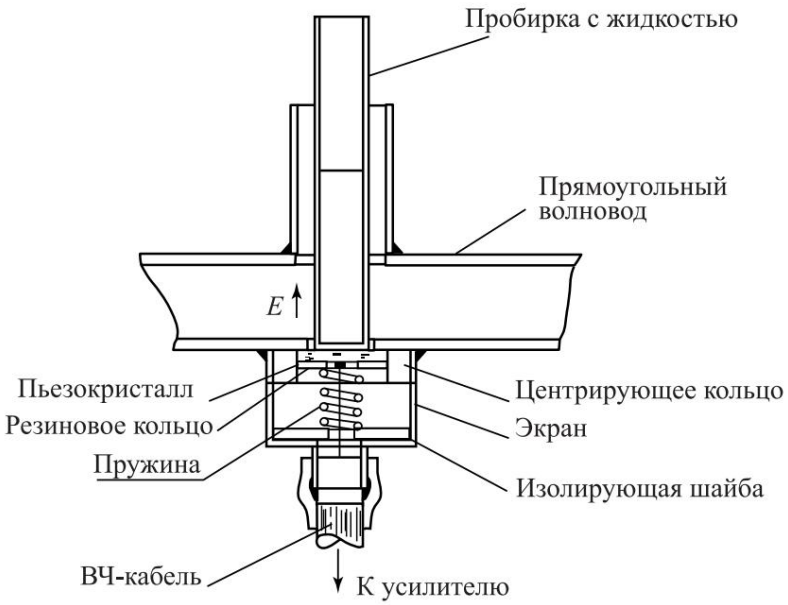

Rice. 2.17. Scheme for recording excited mechanical vibrations using a piezoceramic sensor

Thus, the value of variable sound pressure reaches 105 dyn/cm2, which makes it possible to determine the intensity
vibrations according to the known relationship [53, 68]

$$J = \frac{p2}{2ÿc} \quad ÿ = 10ÿ2 \text{ W/cm2} .$$

The use of a piezoceramic sensor with a longitudinal piezoelectric effect, which works like a piston when an alternating load is applied perpendicular to its plane, allows us to state that

In the experiments described, plane longitudinal waves are excited in liquids.

In all experiments, an increase in the amplitude of excited mechanical vibrations is observed as the repetition rate of microwave EMF pulses approaches the resonant frequency of the liquid column,
determined by its height. The quality factor of a liquid column as a resonant system reaches 220.

2.8. Discussion of the obtained experimental data

The experimental material obtained allows us to express
some considerations in favor of the hypothesis considered here.

The main result should be considered the widespread excitation of high-intensity mechanical vibrations. The most important

fact - excitation of mechanical vibrations by both the leading and trailing edges of the thermal pulse. This indicates the possibility of a high rate of thermal energy dissipation at inhomogeneities.

The amplitude of excited mechanical vibrations depends in a complex way on the physical, mechanical and chemical properties of the object.
Such properties include viscosity, elasticity, dielectric constant, electrical conductivity, etc.

Noteworthy is the fact that the smallest amplitude
possess mechanical vibrations excited in non-polar liquids, the greatest are alcohols. This circumstance allows us to outline
ways to search for the entire chain of subtle mechanisms for converting absorbed microwave energy in complex biological objects.

In [69] there are references to data from other authors who
studied the effect of ultrasound with intensities of 10ÿ2 W/cm2
and lower on neuromuscular characteristics. At the same time, there are stable subtle functional changes in the voiced system.
There are also links to works in which ultrasound with an intensity of 10ÿ3 W/cm2 was used. In these works, the exposure time varies from 0.5 to 5 minutes.
Comparison of the obtained values
intensity of excited mechanical vibrations and applied
in experiments on exposure to ultrasound allows us to talk about

their biological significance. An intensity of the same order, that is, 10ÿ3 W/cm2, is the pain threshold for human hearing. The generation of mechanical oscillations by

both fronts of the thermal pulse and the interference of these oscillations make it possible to get closer to understanding the inconsistency of experimental data that occurs in the literature. Rice. 2.12 and graphs in Fig. 2.14, 2.15 show that at certain values of the microwave EMF pulse duration, the amplitudes of mechanical vibrations excited by both fronts of the thermal pulse can be in antiphase. If these oscillations play a certain role in the formation of the bioeffects of pulsed microwave fields, it becomes clear that under the same experimental conditions on the same object, different results can be obtained if the durations of the microwave EMF pulses were different. In this sense, there is also a correlation with the work of Kamensky [24], when he observed an increase in the effect at a high repetition rate of microwave EMF pulses and a low PPM. Kamensky at the same time put forward the assumption of a more pronounced nature of the summation of local changes at a high repetition rate of field pulses. Indeed, in this mode, the process of generating mechanical vibrations, simultaneously with an increase in their amplitude from damping, approaches continuous, that is, it becomes more energy-intensive. Accordingly, the degree of influence of these vibrations on the object increases.

Chapter 3

PHASE SYNCHRONISM AND PERIODIC BIOLOGICAL STRUCTURES 1)

In many works related to the study of biological effects of non-ionizing radiation (electromagnetic radiation (EMI), ultrasound (US), vibration) at low doses [70–73], the results experiments are often associated with traditional ideas about resonance, mechanisms of resonant energy absorption at microstructural levels are proposed. However, despite the clearly resonant nature of the impact of vibration on various biological objects, the authors of these works come to the conclusion that the observed the effects manifest themselves due to the presence of certain structural and biological features at the molecular level, and the presence of characteristic frequencies corresponds to a different type of resonance of a living cell, for example, arising from surface vibrations. In this case it is indicated on the possibility of the existence of enhancing mechanisms in living cells. It is obvious that the conclusions reached by the authors of these works dictated by the discrepancy between the observed frequency dependencies classical concepts of resonance.

On the other hand, there are effects under the action of impulses non-ionizing radiation of non-thermogenic levels in the phase of the most active state of the object during rhythmic biological processes.

The mechanism of the biological action of ultra-low doses is considered on the basis of some general patterns that occur during the interaction of various physical factors with biological systems, and is conditionally limited from above by frequencies of the order 3 109 Hz - approximately up to these values of the EMR carrier frequency, some effects identical to those realized using other non-ionizing radiation.

The similarity of the effects observed in this case can be explained by the excitation of mechanical vibrations as a result of the release biological structures of the envelope of pulsed modulated radiation. However, under the influence of the noted physical factors of non-thermogenic levels, the wavelength of mechanical vibrations on several orders of magnitude larger than the size of a biological object, and their intensity is significantly less than known biologically significant quantities In this case, the effects are observed either at sufficiently low frequencies - about 102 ÷ 104 Hz, or with pulse modulation

---

1) Materials are published for the first time.

significantly higher frequency external acting field
low frequencies. In an attempt to elucidate possible mechanisms for this
researchers propose a mechanism of resonant interaction
energy absorption at microstructural levels [70–73].

Thus, in [73] it was shown that the maximum change in the fluorescence of probes embedded in shadow membranes observed in the experiment
erythrocytes, occurs at pulse repetition rate modulation
EMI (at a carrier frequency of 800 MHz), equal to 55 ÷ 60 Hz in the absence of heating. There is a frequency-dependent vibration effect
on actomyosin [71], manifested in a sharp increase in ATPase
actomyosin activity at a frequency of 200 Hz at acceleration 2. At g
this is the intensity of a sinusoidal plane wave, determined from
known ratio:

$$J = p2(2\ddot{y}c)\ \ddot{y}1 \qquad \text{(I.14)}$$

is estimated at 3 × 10ÿ3 W cm ÿ2. The sound pressure value of excited pulses measured using a piezoelectric transducer
The EMR of mechanical vibrations in a suspension of erythrocyte ghosts [71] averaged 500 dynes cm ÿ2. In this case, the calculated value of the intensity of excited mechanical vibrations is 10ÿ7 W cm ÿ2
at a frequency of 104 Hz. Average power flux density
(PPM) EMR was 5 mW cm ÿ2 with a pulse PPM equal to
2 W cm ÿ2. In [71], it was experimentally shown that for object sizes of the order of 1 ÷ 10 µm, effects are observed at frequencies of the order
102 ÷ 103 Hz. The work of Doering and Frey [74] indicates that when
the action of vibration pulses with a frequency of about 102 Hz in a certain phase of the cardiocycle of a guinea pig heart preparation is observed
changes in the magnitude of the cardiac cycle with sound pressure amplitude
50 mbar, which corresponds to an intensity of the order of 10ÿ9 W cm ÿ2.

Thus, we can distinguish at least three main
moment when exposed to non-ionizing radiation on biological structures that cannot be explained by existing concepts
about possible ways of interaction with biological objects:

1) Frequency-dependent resonance effects are observed when the ratio of the wavelength of the influencing factor to the size of the biological object is equal to several orders of magnitude.

2) Phase-dependent effects are observed under the action of pulses of non-ionizing radiation in certain phases of periodic
biological process characterized by the greatest activity
object.

3) Levels of intensity of the influencing factor on several
orders of magnitude below those of biological significance.

A prerequisite for searching for the mechanism of non-resonance effects
The information signal to biological structures was provided by the results of studies of the processes of generation of mechanical vibrations
in liquid media by EMR pulses and the proposed hypothesis about the possibility

the possible predominant role of these oscillations in the formation of specific effects of non-ionizing radiation. From this point of view mechanism of biological action of pulsed-modulated microwaves fields, ultrasonic fields (US), laser radiation [75] and vibration can be considered as a single one [66].

3.1. Periodic structures

There is a wide range of different devices and devices Microwave for amplification and generation of electromagnetic oscillations containing non-resonant broadband oscillatory systems, the basis of which is the phenomenon (principle) of phase matching [74], implemented using so-called slow-down structures (ZS), which are periodic structures of various types [76, 77].

In the presence of two wave processes, such as electronic flux and microwave electromagnetic field, their interaction is possible at similar propagation velocities. This condition is feasible in the case of using a transmission line with a delay, i.e. in the presence of ZS. Thus, phase matching ensures long-term interaction of two wave processes. At the same time, if wave processes are of the same nature and have close values of speeds, then with their parallel movement at points equal phase, the wave amplitude increases [78].

Involving the basic concepts of this principle to explain the mechanisms of the biological action of non-ionizing radiation of non-thermal doses allows us to identify signs of similarity of some technical and biological structures, the presence of which allows us to say about the fundamental possibility of implementing the principle of phase synchronism by some biological structures. Thus it is possible assume the presence of a certain range of biological structures, capable of playing the role of not only primary converters of absorbed energy of non-ionizing radiation into an information signal, but also to carry out its non-resonant amplification.

Thus, for the implementation of phase synchronism by biological structures, the latter must have periodicity. In order for continuous oscillations to arise and be maintained in a microwave generator device, the electron flow must constantly slow down, giving off its energy to the resonator system of the generator device. An analogue of this process in a biological system there must be a traveling acoustic displacement wave, attenuating in the periodic system and thus giving off its energy to it.

Many studies have shown that when irradiating limited macrovolumes of some substances, EMR pulses excite longitudinal mechanical vibrations in the medium. The same happens when irradiation of the head of an animal or a person with EMR pulses, and

the frequencies of excited mechanical vibrations are determined by the speed of sound in the medium and the size of the head and lie in the region of sound and ultrasonic frequencies [12, 79–82]. In this case, the wavelength of mechanical vibrations excited in macrovolumes is commensurate with the size of the irradiated objects, and the very nature of the excitation of these vibrations is resonant. Analyzing the references given here to work on the study of non-ionizing radiation of non-thermal doses at cellular and subcellular structures, as well as data from a large number of other works, we come to the unequivocal conclusion that it is these structures are decisive in the formation of observables effects associated with impaired functioning as individual cellular (subcellular) structures and biological structures in general.

The periodicity of biological structure must be formed in space in such a way as to provide the possibility of multiple interactions of shear waves in its individual sections each other and thus simulate the spread of two individual wave processes at a given moment in time. Wherein the presence of a traveling wave regime becomes fundamentally important, which is ensured by the finite amount of attenuation of mechanical fluctuations in biological systems. In Fig. Figure 3.01 shows fragments of some technical microwave systems that implement the principle phase synchronism when electromagnetic radiation propagates in them waves, and their possible biological analogues, having one common property - periodicity.

Small transverse dimensions of cellular and subcellular structures do not allow to attract as a dominant influence factor possible modes of longitudinal and transverse mechanical oscillations excited in a medium by non-ionizing radiation or introduced directly into the medium using a mechanical vibrator.

Let us consider the interface between the cell membrane and the extracellular space. Since the interface between these two media curved, the pressures in both environments are different. The condition for thermodynamic equilibrium of such a system is given by Laplace's formula [83] as

$$p1 - p2 = \sigma(R\sigma 1_{1} + R\sigma 1_{2}),$$

where σ is the surface tension coefficient, p1 and p2 are the quantities pressure on both sides of the membranes, R1 and R2 are the main radii of curvature at a given point on the surface. When mechanical vibrations are excited in a medium, the surface force will act on the membrane. tension. By this, the surface of the membrane is removed from the equilibrium state, and a movement occurs in it, propagating along the entire surface in the form of waves. If the wavelength small compared to the depth of the layer in the equilibrium state or

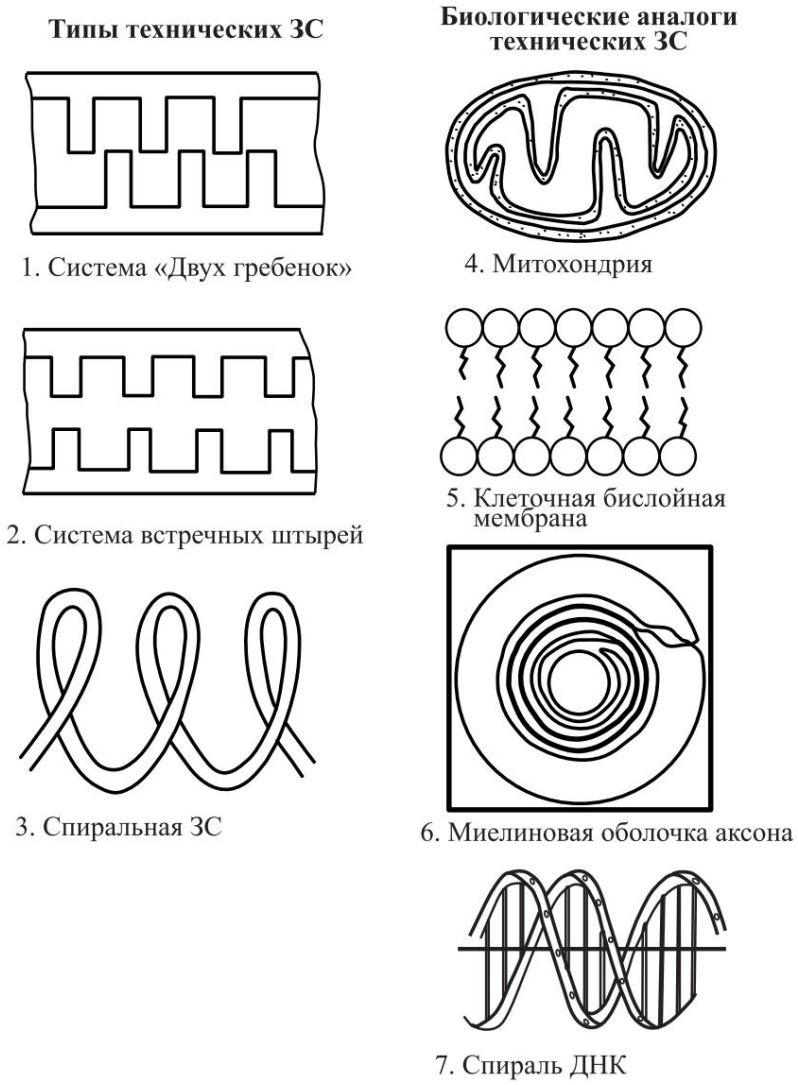

Rice. 3.01. Schematic representation of technical ES and their biological "analogs"

is commensurate with it, then in this layer the trajectories of individual particles of the layer in the traveling wave are circles. For such waves, the dispersion relation approximately has the following form [83, 84]:

$$2o = g\,k + no^{\,1\,3\,k}$$

Phase velocity of wave propagation of the ion equation: $v_f = \frac{ÿÿ}{ÿk}$ can be found from the dispersion

$$(^{l}\cdot) 15$$

Solving this equation for wave number k , we obtain: + 12ÿ2ÿÿÿ1

$$v_f = 0{,}5(\ g\ l^{\,2})(2p\ g\ l^{\,1} + a\ (\ )\ 2p^{\,3}{}_{pÿ1}\ l\ 3)\ ÿ1/2 \qquad (^{l}\cdot) 16$$

Where a —surface tension coefficient, ÿ - wavelength,

g — free fall acceleration, ÿ – density.

Since we have determined that phase synchronism in a biological periodic structure when a wave circulates along the structure is possible only if there is a traveling wave, it is necessary consider the case of short waves, i.e. those for which the condition ÿ>ÿ is satisfied, where ÿ is the wave amplitude, ÿ is the wavelength. In this case, we can neglect the influence of the gravity field and

$$ÿ2 = nrÿ1\ k3\ . \qquad (I.17)$$

Waves that satisfy this condition are called capillary. Phase velocity of capillary waves found using the equation (I.15), is determined by the expression:

$$vÿ = 1.5[2pa(ar)^{ÿ1}]\ ÿ1/2 \qquad (I.18)$$

According to [85], the surface tension coefficient of biological membranes is of the order of 10ÿ2 dynes cm ÿ1. At a lipid layer density of about 0.8 g cm ÿ3, using the given expression for frequency of 104 Hz, the wavelength will be only 9 microns. In this case, it is necessary to take into account that the given value of surface tension is given for the erythrocyte membrane. The lack of data on the value of surface tension for other cells does not allow us to more accurately determine wavelength calculation. Moreover, consideration of models of spherical volume, which includes cells, under exposure conditions external forces on them, given in various works [83, 85, 86], does not allow, in principle, a strict assessment of the possible length waves of a wave process propagating along the cell membrane. This is due to both the lack of data on the rigidity of the cell membrane, and with various assumptions when considering one or another spherical model. However, the wavelength obtained here for lipid membranes, the order of magnitude suggests the possibility of realizing phase synchrony by periodic biological structures, especially multilayer ones. In Fig. 3.02 schematically depicts the regions of capillary energy localization

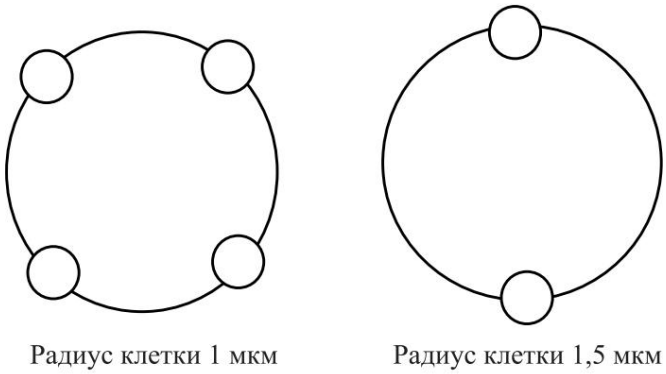

Rice. 3.02. Scheme of formation of capillary energy localization regions waves on a spiral biological structure

waves at a frequency of 104 Hz with a wavelength of 9 ÿm and cell radii of 1 and 1.5 µm. It is easy to see that with the number of layers in the membrane 12 ÷ 100 and a cell radius of 1 µm amplitudes of waves with equal phase in the marked areas will be summed up every second wave run
next layer, i.e. from 6 to 40 times, which corresponds to the gain in power from 36 to 1600 times. With a cell radius of 1.5 µm, at Under the same wave parameters, two localization regions will exist energy, and the summation of amplitudes will occur every times, i.e. the power gain in these areas will be from (12)2 to (100)2 or from 144 to 10,000 times.

In large nerves, the myelin sheath can reach 2-3 microns thickness and be formed by 200 turns of the spiral.

When irradiating homogeneous liquids in test tubes with pulses EMR at the resonance frequency of a liquid column, close in its electrical parameters to biological objects (0.15 M solution KCl), the measured amplitude of variable sound pressure was 3 × 103 dynes cm ÿ2, at frequencies far from resonance - 2 × × 10ÿ2 dynes cm ÿ2. The intensity of excited mechanical vibrations, calculated from the measured amplitude value at frequencies, far from resonance is 1.3 × 10ÿ8 W cm ÿ2. With volume liquid equal to 1 cm3, and a surface area equal to 10 cm2, the volumetric acoustic power density will be 1.3 × 10ÿ7 W cm ÿ3. With a loss power of 6 W cm ÿ3, the conversion coefficient of electromagnetic energy into acoustic energy is 2 10ÿ8 (by power). At the resonance frequency of the liquid column (5.9 kHz, 0.15 M KCl solution) the measured quality factor is 15. If, under these conditions, a multilayer membrane is irradiated with a number layers N = 102, then at the resonance frequency of the liquid column the total the pressure amplitude amplification factor is determined by the relation Kus = N · Q = 102 · 15 = 1.5 · 103, where N is the number of membrane layers, Q is the quality factor of the system. In terms of power, the gain will be (1.5 · 103)2. At the resonance frequency, the volumetric acoustic energy density is 1.3 × 10ÿ7 × 2.25 × 106 = 0.3 W cmÿ3 with an equivalent conversion coefficient equal to 5 × 10ÿ2.

The assessment of the parameters of mechanical vibrations, excited or introduced from the outside, shows that the presence of periodicity in biological structures can lead to an “intensification” of the biological effect of low-dose non-ionizing radiation to values comparable and even exceeding the strength characteristics of a biological object. Thus, with a value of Young’s modulus equal to biological objects 103 ÷ 105 dyn cm ÿ2, calculated value on the amplitudes of variable sound pressure at the resonance frequency reaches 106 dynes cm ÿ2, which should lead to delamination or rupture of the layers of the myelin sheath and, as a result, disruption

cell functioning. In this case, it is necessary to take into account the quality factor a system used to fix a biological object.

Works [2, 66] noted the effects of the biological action of pulsed EMR that occur when an object is heated by tenths degrees, and explained by the possible occurrence of microdamages. Fundamentally important are the noted unidirectionality and qualitative similarity of effects under the action of pulsed EMR and low doses of ultrasound.

If we set the minimum value of Young's modulus Emin = pres. = = 103 dynes cm2 , where pres. — magnitude of the amplitude of variable pressure at the resonance frequency of the system, necessary for the beginning of the development of the effect, then for the case of excitation of mechanical vibrations by EMR pulses, the minimum value of the electromagnetic field power in impulse can be determined from the relation

$$\text{pyrez.} = \frac{\text{paresis}}{\text{cut}} = \frac{\text{Jarez.} \cdot S}{\text{cut}} = \frac{p2_{\text{cut.}}}{2\text{pc}} \cdot \frac{S \cdot 10\ddot{y}7}{\text{cut}} = 6.2 \cdot 10\ddot{y}5 \text{ W}, \qquad \text{(I.19)}$$

where is the cut. is the volumetric density of acoustic energy at the resonance frequency, S is the surface area of the irradiated volume (for the case under consideration, S = 10 cm2), nres. — equivalent coefficient converting the electromagnetic energy of a microwave pulse into acoustic energy at the resonance frequency. With a volume of medium equal to 1 cm3, the volumetric The absorbed power density per pulse will be 62 ÿW cm ÿ3. Taking into account the data from [58], the minimum EMR power in a pulse can be in the order of magnitude 10ÿ8 W.

The principle of phase matching can be most clearly demonstrated using the example of a spiral structure. When excited wave process, an acoustic wave will begin to propagate in a spiral by an external force. Since the process of generating mechanical oscillations can last for a certain period of time necessary for the pressure wave to reach the end of the spiral, the wave the process will take place at all its points. Due to the fact that the radius each subsequent turn of the spiral is less than the previous one, oscillations in the radial section of the spiral have different instantaneous phases on every turn. With a sufficiently large aspect ratio spirals to the length of the propagating wave on some radial components of the spiral, the phases of oscillations will be presented as follows: in general form:

$$\begin{aligned} \ddot{y}2 &= \ddot{y}1 + 2\ddot{y}n \text{ m, n } \ddot{y} \text{ N,} \\ \ddot{y}k &= \ddot{y}1 + 2\ddot{y}m \text{ m>n,} \end{aligned} \qquad \text{(I.20)}$$

where ÿ1, ÿ2, ÿk are the instantaneous phases of oscillations at different turns spiral along the radius of the spiral. That is, the phase shift between oscillations by several turns in the radial direction can become equal 2ÿn, where n is a positive integer depending on the turn number (the quantitative dependence of n on the turn number will be displayed below).

In this case, the oscillations will become in-phase, i.e., the spiral turns along these radii will oscillate in phase, which will lead to a proportional increase in the amplitude of these oscillations in the selected radial directions, and localized regions will appear on the spiral
energy of capillary waves.

If the energy of the total vibration exceeds
the binding energy of the spiral turns, its delamination will occur, which in case of elastic deformation will disappear after the action ceases excited mechanical vibrations. If the energy of the total vibration is sufficiently large, a rapid, almost instantaneous, rupture of the spiral turns is possible.

It should be noted that phase matching in the application
to the biological structure is somewhat different from its classical representation.

Considered as a spiral GL, the multilayer lipid membrane does not slow down one wave process
relative to another, and the shift of instantaneous values of the oscillation phases on each subsequent turn of the spiral relative to the previous one
counting different values of linear velocities of propagation of oscillations on turns, thereby simulating deceleration. Process described
summation of amplitudes on the turns of the myelin sheath of the axon at points equal phases can be represented in the form of amplification of excited
acting non-ionizing radiation of capillary waves, and itself
myelin sheath - as a biological amplifier.

3.2. Mathematical model of propagation capillary wave in spiral biological structures

It is possible to propose a mathematical model for the propagation of a capillary wave along a spiral to the center, with the spiral itself acting as a slowing system that reduces the length by K times
waves ÿ. The mathematical model under consideration is based on
principle of phase synchronism. Equation of a spiral resting on
circle (Fig. 3.03) of radius ÿ0, looks like this in polar coordinates

$$ÿ = ÿ0 + aÿ, \tag{I.21}$$

where ÿ is the rotation angle, a is the coefficient. Let us determine the coefficient a from the boundary conditions:

$$\begin{aligned} ÿ &= 0ÿÿ = ÿ0 \\ ÿ &= 2ÿ\ ÿÿ = ÿ0 + S \\ ÿ &= 2ÿn\ ÿÿ = ÿ0 + nS \\ ÿ &= ÿ0 + aÿ \end{aligned} \qquad ÿ\ a = S(2ÿ) \tag{I.22}$$

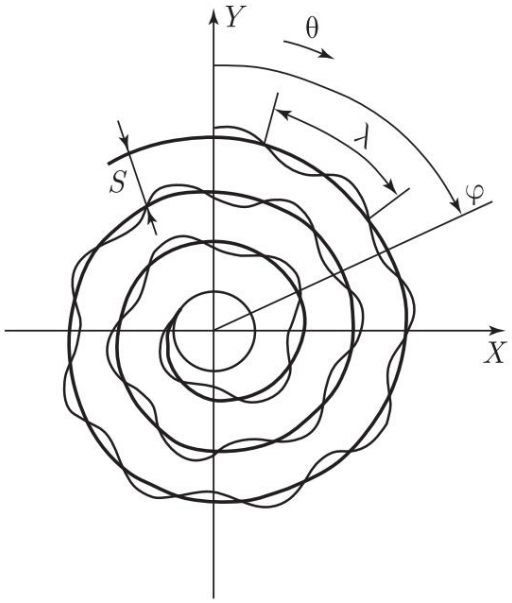

Rice. 3.03. Scheme of summation of vibration amplitudes with equal phase of a capillary wave in the radial directions of a spiral structure

$$\ddot{y} = \ddot{y}0 + S\ddot{y}(2\ddot{y}) \qquad \ddot{y}1 \quad \text{— equation of a spiral with initial radius } \ddot{y}0. \tag{I.23}$$

Length of the spiral element from the beginning to rotation through an angle ÿ:

$$\ddot{y}l = \int_0^{\ddot{y}} [(dx/d\ddot{y})^2 + (dy/d\ddot{y})\,2]\,1/2\,d\ddot{y}. \tag{I.24}$$

Passing to a rectangular coordinate system and differentiating in accordance with (I.24), we obtain:

$$\begin{aligned} \ddot{y}\ x &= \ddot{y}\cos\ddot{y} = \ddot{y}0 + 2\ddot{y}\ \frac{S\ddot{y}}{}\ \cos\ddot{y}, \\ \ddot{y}\ y &= \ddot{y}\sin\ddot{y} = \ddot{y}0 + \ddot{y}\ 2\ddot{y}\ \frac{S\ddot{y}}{}\ \sin\ddot{y}, \end{aligned} \tag{I.25}$$

$$\frac{dx}{d\ddot{y}}^2 + \frac{of}{d\ddot{y}}^2 = \frac{S}{2\,p}^2 + p2_0 + \frac{\ddot{y}0S}{Pi}\ \ddot{y} + \frac{S\ddot{y}}{2\,p}^2. \tag{I.26}$$

We will carry out integration starting from a circle with radius ÿ0, i.e. from ÿ to 0:

$$\ddot{y}l = \int_0^{\ddot{y}} \frac{S}{2\,p}^2 + p2_0 + \frac{\ddot{y}0S}{Pi}\ \ddot{y} + \frac{S}{2\,p}^2 i2^{1/2}\ d\ddot{y}. \tag{I.27}$$

Using [88] we get:

$$\ddot{y}l = \frac{S}{2p}\ddot{y}\frac{\ddot{y}+\frac{2pr0}{S}\ddot{y}+\frac{2pr0}{S}^{2}+1}{2}^{1/2}+$$

$$-\frac{1}{}\ln\ddot{y}++\ddot{y}+\frac{2pr0}{S}\frac{2pr0}{S}^{2}+1^{1/2}$$

$$\frac{\frac{2pr0}{S}\frac{2pr0}{S}^{2}+1^{1/2}}{2}\frac{1}{2}\ln\frac{2pr0}{S}+\frac{2pr0}{S}^{2}+1\ 1/2\ \ddot{y}\ddot{y}. \quad (I.28)$$

In lipid membranes S ÿ 100 ÷ 200 ÿA, ÿ0 ÿ 10ÿ4 cm, hence

$$\ddot{y}\frac{2pr0}{S}1,\quad \ddot{y}\ddot{y}+\frac{2pr0}{S}1. \quad (I.29)$$

Taking into account assumptions (I.16), we obtain the length of the spiral element:

$$\ddot{y}l(\ddot{y}) = \frac{S}{4p}\ddot{y}2+\frac{4pr0}{S}\ddot{y}+\ln 2\ddot{y}+\frac{4pr0}{S}\ddot{y}\ln\frac{4pr0}{S} \quad (I.30)$$

If we assume that the surface wave propagates in a spiral,
then the instantaneous phase of the wave, depending on the angle of rotation in the direction of propagation, will be determined by the expression:

$$\ddot{y}\ddot{y}\ddot{y} = 2\ddot{y}l(\ddot{y})\ddot{y}\ddot{y}1\ \ddot{y}\ ;\ \ddot{y}\ddot{y} = v\ddot{y}f^{\ddot{y}1} \quad (I.31)$$

where ÿÿ is the wavelength in the spiral, vÿ is the phase velocity of wave propagation along the spiral to the center is defined as the ratio
the length of the segment connecting the beginning and end of the spiral, by time
the wave travels the full path along the spiral: vÿ = r/ÿ = nSvpadl $\ddot{y}1_{s}$,
where n is the number of turns of the spiral, S is the pitch of the spiral (thickness of the turn), vpad is the speed of the incident wave, ls is the total length of the spiral, r is spiral radius. Summarizing the above, we can conclude:

$$\ddot{y}\ddot{y}\ddot{y} = 2\ddot{y}l(\ddot{y})\ddot{y}\ddot{y}1\ \ddot{y}\quad \ddot{y}\quad \ddot{y}\ddot{y}\ddot{y} = 2\ddot{y}l(\ddot{y})v\ddot{y}1$$

$$\ddot{y}z = vff^{\ddot{y}1}\quad vf = nSvpadl\ f_{s}^{\ddot{y}1} \quad (I.32)$$

Thus, the instantaneous phase of the wave is:

$$\ddot{y}\ddot{y}\ddot{y}(\ddot{y}) = 2\ddot{y}flsl(\ddot{y})(nSvpad)\ \ddot{y}1, \quad (I.33)$$

where ls = l(2ÿn) is the total length of the spiral. Focusing on Expression for the instantaneous phase of a wave propagating in a spiral, it is possible to determine the places where the instantaneous phases of the wave coincide at different turns in radial directions. If a certain level is entered

phase coincidence, causing deformation (deflection) of the spiral turn, determined by Hooke's law [87]

$$Pkr \ddot{y} E \frac{h2}{R2}. \quad (I.34)$$

where h is the thickness of the plate, E is Young's modulus, R is the bending radius, Pcr is the critical value of the external load, beyond which small changes in the shape of the shell spontaneously increase, then you can count the number of phase coincidences for each degree of angle rotation of the spiral. Based on Hooke's law, elastic deformations turn into plastic ones if the deflection is so great that irreversibly changes the structure of a substance. This is possible with action forces causing pressure greater than Young's modulus E.

$$Ppl = p E. \quad (I.35)$$

Delamination of the spiral layers due to stretching will occur when the number of phase coincidences in each radial direction is greater than a certain number, which is determined by the attenuation of the wave in system.

A program has been compiled that simulates the propagation of a surface wave in a spiral. During the execution of the program, the number of phase coincidences along the radial directions of the spiral is calculated at specified gradual intervals of rotation. Amplitudes bends of turns in different directions are added to the opposite sign, the resulting deformation, if it exceeds a given the number of phase incursions causes delamination of the spiral turns, up to rupture. Attenuation in the system is taken into account when estimating the resulting deformation in the form of a specified number of phase incursions. The result of program execution is graphs of the dependence of the resulting deformation of the spiral turns depending on the angle of rotation in the range from 0ÿ to 360ÿ.

In a real biological spiral structure, nearby layers interact with each other. That is, layer I is affected by a force from sides of layer II, on layer II - from sides I and III, etc. (Fig. 3.04). Connection between layers can be characterized linearly to a first approximation using the coupling coefficient K = Kst so that the layer deformation according to the law f(ÿ) was transmitted to neighboring layers with a coefficient k, i.e. these layers underwent deformation k · f(ÿ).

Let us analyze the instantaneous state of the spiral in the radial direction, taking into account the connection between the layers. AI functions $_{g}$ (ÿ), AII_{g} (i), ..., AN_{g} (ÿ) will characterize the bending amplitudes of layers from I to N at the presence of a connection between the turns of the spiral. AI (ÿ), ..., AN (ÿ) - amplitudes bending of the spiral turns without taking into account the connection between them.

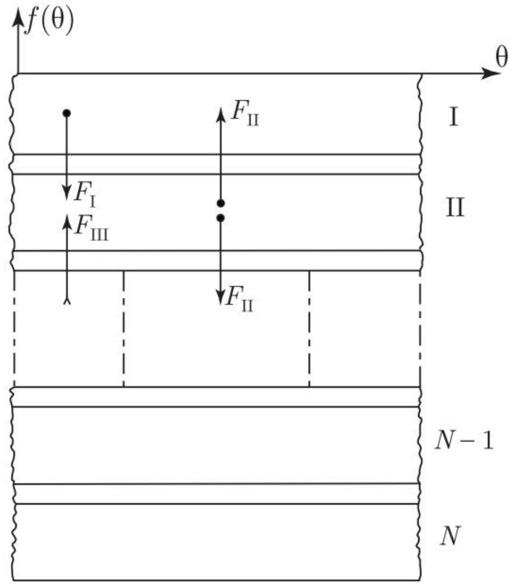

Rice. 3.04. Interaction of individual turns of a spiral structure in the presence of a capillary wave

$$\begin{aligned} A_I^g(\ddot{y}) &= A_I(\ddot{y}) + kA_{II}(\ddot{y}), \ddot{y} \\ A_{II}^g(\ddot{y}) &= A_{II}(\ddot{y}) + kA_I(\ddot{y}) + kA_{II}(\ddot{y}), \\ &\vdots \\ A_{N\ddot{y}1}^g(\ddot{y}) &= A_{N\ddot{y}1}(\ddot{y}) + kA_{N\ddot{y}2}(\ddot{y}) + kA_N(\ddot{y}), \\ A_N^g(\ddot{y}) &= A_N(\ddot{y}) + kA_{N\ddot{y}1}(\ddot{y}). \end{aligned} \qquad (I.36)$$

The total stress along the radius of the spiral has the form:

$$\sum_{i=1}^{N} A_i^g = A_I^g + A_{II}^g + \ldots + A_{N\ddot{y}1}^g + A_N^g \qquad (I.37)$$

where we get:

$$\sum_{i=1}^{N} A_i^g = \sum_{i=1}^{N} A_i(\ddot{y}) + 2\sum_{i=2}^{N\ddot{y}1} kA_i(\ddot{y}) + k[A_I(\ddot{y}) + A_N(\ddot{y})]; \qquad (I.38)$$

simplifying, we have:

$$\sum_{i=1}^{N} A_i^g = (k+1)[A_I(\ddot{y}) + A_N(\ddot{y})] + (2k+1)\sum_{i=2}^{N\ddot{y}1} A_i(\ddot{y}). \qquad (I.39)$$

From formula (I.39) it is clear that the linear connection between the layers introduces additional bending of the layers, which is characterized only quantitatively. In this case, the qualitative deformation is described by the wave propagation equation and the conditions of phase matching in the spiral.

3.3. Experimental data

Previously obtained results on the effects of pulsed EMR for isolated preparations of the tibial-sciatic nerve [2, 22, 26] frogs indicate that the irradiation of drugs is synchronous in the post-latency period does not lead to registered disturbances in the functioning of objects. However, when irradiated synchronously during the latent period 20 ÷ 30 minutes after the start of irradiation a decrease in excitation conduction speed and amplitude begins (see Chapter 2). Increasing the frequency of stimulation and, accordingly, the frequency repetition of EMR pulses from 20 to 100 Hz led to an increase the temperature of the object and the typical manifestation of the thermal effect - an increase in the speed of excitation and the amplitude of the action potential. According to the experiment, the calculated value of the absorbed by the object pulse power is 300 ÿW, which allows in this particular case to estimate the intensity of excited capillary waves taking into account phase matching of 1.5 × 10ÿ5 W cm ÿ2. The amplitude of the sound pressure will be 6 × 103 dynes cm ÿ2, i.e., at moments of hyperpolarization, the total amplitude of the pressure acting on the membrane will exceed the compressive force. However, the resulting value of the sound pressure amplitude is less than the compressive strength, which, apparently, can be explained by the need for sufficient long irradiation time (20 ÷ 30 minutes) to begin development effect. A similar picture occurs when drugs are irradiated. isolated frog heart, however, the lack of sufficient experimental data does not allow for at least a rough assessment effective value of the intensity of excited mechanical hesitation. Sounding an isolated specimen of a marine heart pigs by pulses of low-frequency vibration with pressure amplitude up to 40 dynes cm ÿ2 (sound intensity 10ÿ9 W cm ÿ2) at a certain phase of the cardiac cycle also led to an increase in the cardiac cycle, as and when irradiated with EMR pulses [1, 10, 26, 29].

Experimental verification of the considered amplification principle the effect of non-ionizing radiation on biological periodic structures was carried out on slices of the hippocampus of a guinea pig under irradiation with pulsed EMR with a carrier frequency of 2375 MHz and separately when exposed to acoustic vibrations introduced into the washing solution. The cuvette in which the drug was located and through which the solution flowed had the shape of a cone. The height of the liquid column was 45 mm. Irradiation was carried out with a standard microwave irradiator from the medical device "Luch-3". The device itself after modernization was used in the experiment in the pulsed radiation mode.

Sections of guinea pig hippocampus with a thickness of 400 ÷ 600 μm were incubated in a solution saturated with 4% carbagene. Speed the flow rate was 4 ml/min at a solution temperature of 37 ÿC. Acoustic vibrations were introduced into the solution using a vibrator,

in which a headphone is used, to the membrane of which
a metal rod with a diameter of 1.5 mm is soldered. On the other end
The rod is soldered with a brass disk with a diameter of 15 mm. A piezoceramic
sensor is built into the bottom of the cuvette. The cuvette is surrounded by a
thermostatic jacket. The resonances of the cuvette were determined by the excitation method
in a solution of mechanical vibrations by microwave pulses. The signal from the piezoceramic
sensor, after amplification, was recorded on the screen
oscilloscope. Intense mechanical vibrations were excited at
microwave radiation modulation frequencies equal to 1.2 and 4.2 kHz. Wherein
in meander mode, i.e., with a duty cycle of two, the signal from the piezo-ceramic
sensor was an undamped sinusoidal process of excitation of mechanical vibrations.

Irradiation of drugs was carried out at a pulse repetition rate
1.2 kHz with a pulse duration of 80 ÿs. Irradiation duration is 1 minute. Increase in
the temperature of the drug during irradiation
was 3.4 ÿC. The drugs were sounded at a frequency of 4.2 kHz
within three minutes. Amplitude of mechanical vibrations in solution,
recorded by a piezoceramic sensor, was installed in three
times greater than the amplitude of mechanical vibrations excited in the solution by
microwave pulses. Subsequent microstructural analysis of irradiated and sonicated
hippocampal slices was carried out.
using an electron microscope Tesla BS-500. Analyzed
the state of the myelin sheath of the axons of hippocampal nerve cells.
In the photographs provided, localized areas of dissection of the myelin sheath are
clearly visible. Analysis of control sections
showed the presence of qualitatively similar myelin sheath dissections
in about 10% of cases. However, the number of bundle regions is not
exceeded 1 ÷ 2, and the width and length of the delaminations were significantly
less. Based on the given mathematical apparatus that describes the propagation of
an acoustic wave along a spiral structure, a program was developed for calculating
the total incursions of oscillation phases along the radial components for a spiral
structure with geometric parameters determined from electronic data

microscopy. Four photographs out of 20 were selected for calculation -
three photographs of the sounded preparations and one of the irradiated one. Selection
photographs from the total number were taken from the conditions of the greatest
availability of measuring the geometric dimensions of objects with the smallest
measurement error. Precise definition of geometric
dimensions of the spiral structure of the axon according to the photographs obtained
impossible due to the presence of a number of methodological errors,
present when measuring the linear dimensions of slices. So, for example, due to
the irregular shapes of the sections in the photographs, the diameter
model spiral was taken equal to the arithmetic mean between
largest and smallest cut sizes.

Calculation of pressure values based on the radial components of the spiral
was carried out every 10ÿ. The initial phase of the wave process, propagating

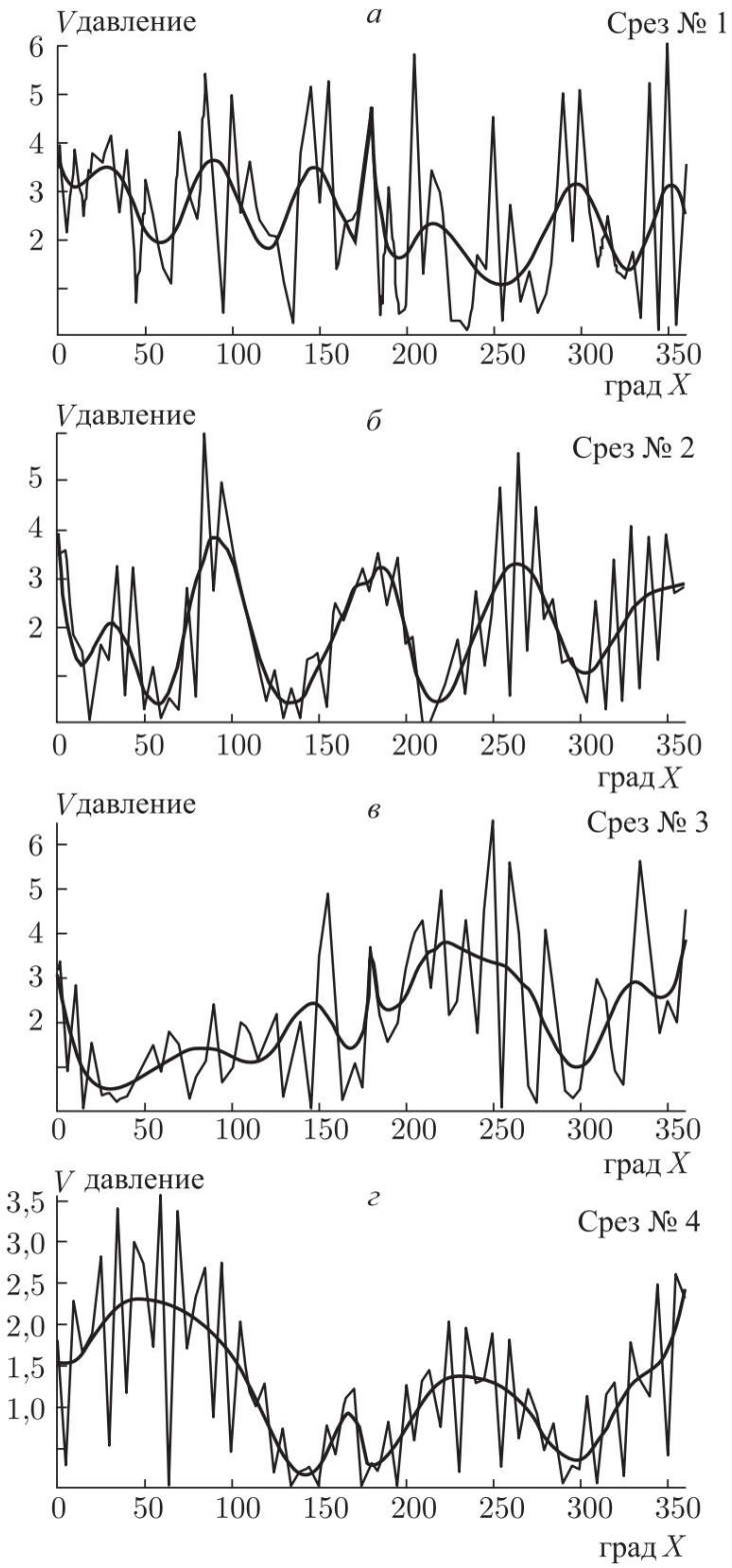

Rice. 3.05. Graphs of pressure distribution on a spiral structure

traveling along the spiral, taken arbitrarily, the length of the acoustic capillary wave was determined from the dispersion equation
(I.4) for the resonant frequencies of the cell. In Fig. 3.05 *(a–d)* are given graphs of pressure distribution on models of spiral structures, calculated from data obtained from photographs. The amplitude of the vibrator oscillations was 2 × 10ÿ4 cm. The calculated amplitude value sound pressure equal to 6 105 dyne cm ÿ 2, sound intensity - 1.2 10ÿ1 W cm ÿ2 . Calculated values of sound pressure amplitude mechanical vibrations excited by EMR pulses is equal to 6 × × 104 dynes cm2 , sound intensity - 1.2 10ÿ3 W cm ÿ 2.

3.4. The discussion of the results

The correlation between the main provisions of the considered model and experimental results was assessed by comparing the obtained
photographs (Fig. 3.06 *(a* –d)) and graphs according to the following criteria:

1) counting the number of areas of dissection of the axon's myelin sheath and areas of maximum sound pressure on the spiral;
2) comparison of the length of the areas of dissection of the myelin sheath of the axon and the width of the areas of maximum sound pressure on the spiral;
3) comparison of the width of the areas of myelin sheath dissection axon and the amplitude of the areas of sound pressure maxima on spirals.

Analysis of the obtained photographs of sections of myelin sheaths of axons and graphs of sound pressure distribution on the spiral model showed a fairly satisfactory agreement between the calculated and experimental data. Comparison of the parameters of the original and the model, characterizing the areas of dissection of the myelin sheath and the area of maximum sound pressure on the graphs, and their quantities required

introduction of a conditional minimum sound pressure level in relative units, leading to dissection of the myelin sheath
(fulfillment of the pmin E condition). For this purpose, a photograph of the irradiated preparation was used (section No. 4) in the presence of two areas of delamination. On the graph constructed using data from slice No. 4, minimum conventional sound pressure level in relative units accepted as 1.0. In accordance with this methodological approach this level was introduced on all charts, and the number of highs on each graph was determined by the excess of sound pressure over him. At the same time, according to the data of slice No. 1, four areas of maximum sound pressure, which corresponds to four areas of dissection of the myelin sheath of the axon, for slice No. 2 - four areas on the model with four areas on the photo, for slice No. 3 - four areas on the model compared to five areas in the original and for slice No. 4 - two areas each.

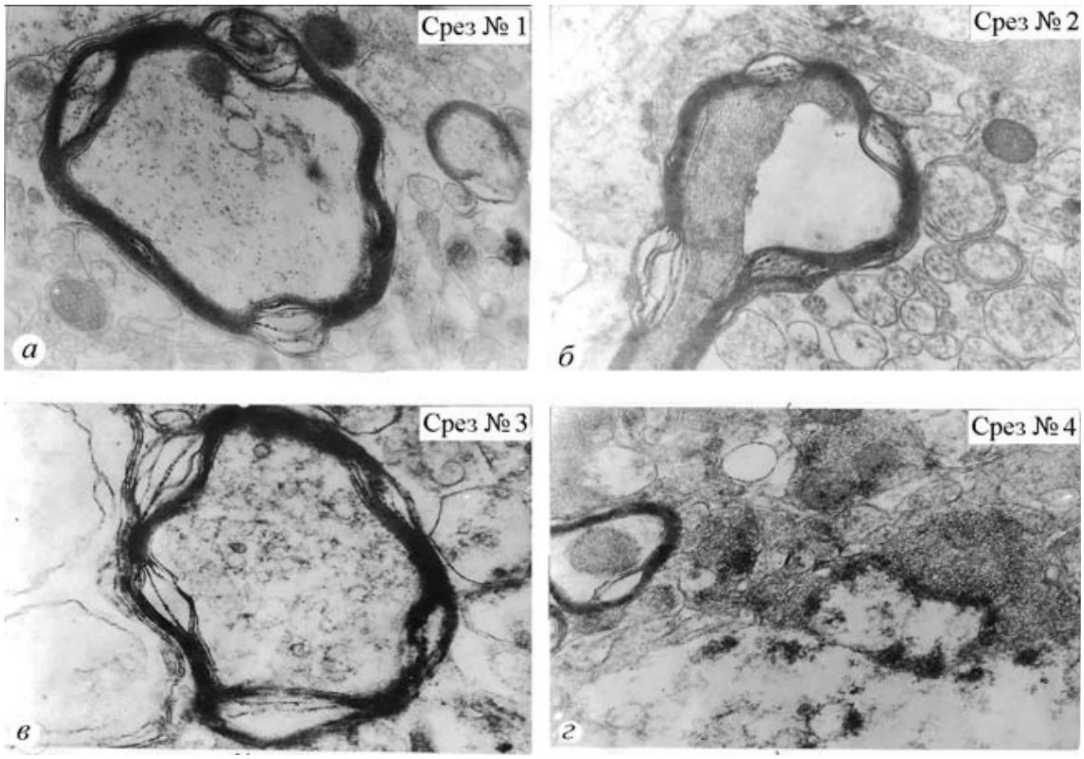

Rice. 3.06. Areas of dissection of the myelin sheath of the axon (method electron microscopy)

Thus, in randomly selected photographs the number areas of dissection on the myelin sheaths of axons and the number of sound pressure maxima on the graphs of the spiral structure model coincide to within one. Correlation between the parameters of the areas of object delamination and the areas of sound pressure maxima on the model was determined by measuring the linear dimensions of the areas stratification - length and width, and areas of maximum sound pressure - width and height of areas of maximum. Discrepancy between model and object according to measurement data for the length of delamination areas averaged 36.4% - 15.6, 29.1 and 64.7%, respectively for sections in photographs 1 ÷ 3, length of the width of the delamination areas - 17.5% (30, 4 and 15.2%, respectively). The degree of discrepancy between the results obtained on the object and on the model obviously significantly depends on the change in the selected conditional sound pressure level, accepted as the minimum required for myelin debranching shells. On the other hand, the method for comparing the results obtained by measuring the linear dimensions of the areas of myelin dissection axon sheaths in photographs leads to measurement error up to ±20% due to the different quality of delamination areas on different objects and even on the same shell. Discrepancy between calculated and experimental data on the number of delaminations can also be attributed to the arbitrariness of the choice of phases.

For the given model of the spiral structure, we considered
free boundary, i.e. the interaction of the turns with the external environment was not taken into account. In real conditions, the axon of a hippocampal nerve cell surrounded by microformations. The varying degrees of connection of these formations with the myelin sheath of the axon cannot but influence the picture
sound pressure distribution in a real spiral structure. However, taking this influence into account is very difficult due to the random
distribution of microformations around the axon, as well as differences
in the characteristics of the micro-formations themselves, such as, for example, dielectric constant and conductivity. These characteristics
influence, first of all, the degree of localization of the electromagnetic field
Microwaves at the boundaries of microformations in the case of irradiation of an object, which can significantly influence the sound pressure distribution pattern. When excited in a medium of mechanical vibrations
A certain role in the distribution of sound pressure is played by the ratio of the acoustic resistance of the myelin sheath and surrounding microformations. The degree of severity of the observed effects is determined by two more important points.

1. Orientation of the plane of the myelin helix relative to the electric vector when exposed to microwave or front EMF pulses
an incident ultrasonic wave, or the front of sound vibrations of a vibrator.

2. The frequencies of the microwave EMF pulses and the vibrator in the described studies are taken equal to the resonance frequencies of a specific cell and not can be considered optimal. The choice of these frequencies was dictated by the desire to enhance the effect of excited mechanical vibrations
and mechanical vibrations of the vibrator due to the quality factor of the cuvette as resonator.

Thus, in a real situation, a spiral structure like
and any other, is connected with the structures surrounding it, which leads
to the presence of a non-uniformly fixed border. At the same time, good
The correlation between the number of dissections on the myelin sheaths and the number of sound pressure maxima obtained on the calculated graphs indicates the possibility of using the considered model to explain
mechanism of action of ultra-low doses of non-ionizing radiation on
biological structures.

3.5. Proposed mechanism of interaction non-ionizing radiation with periodic biological structure

In well-known works, direct and reverse piezoelectric effects were experimentally discovered in the model structure of purple membranes - periodic deformation generates a difference in it
potentials, and the electronic excitation energy is transformed

to mechanical. When stimulating the axons of the crab and squid with electric current impulses and further propagating the potential actions (AP), according to Tasaki et al., transverse and longitudinal displacements of axon fibers were recorded in objects. Levin et al. note that lateral movement in the form of sound waves are caused by a change in transmembrane potential - when depolarization of the membrane, straightening of the axon bend occurs, with hyperpolarization - increased bending. From this we can conclude, that depolarization of the membrane is accompanied by its compression, hyperpolarization - by stretching. Spreading along the nerve fiber structural changes detected by optical methods are localized in the peripheral part of the axon - the membrane - and the sheath [Cohen, Levin], and the displacement propagates along the axon synchronously with the AP. The analyzed results, by analogy with the data, obtained on purple membranes [Ketis], suggest that the axon displacements observed in [Tasaki et al.] propagation of PD are a manifestation of the inverse piezoelectric effect and are associated with voltage-dependent deformation of the membrane [Levin, Ma-lev, etc.].

Mechanical movements when electrical voltage is applied are also observed in hair cells. Thus, with hyperpolarization of isolated outer hair cells of a guinea pig the latter lengthen, and with depolarization they shorten [88]. It is known that the permeability of the membrane can be changed either by deforming its external mechanical force, or by changing the applied tension to her. Since when absorbing pulsed energy non-ionizing radiation in a biological object are excited mechanical vibrations, then the latter can be considered as a force that deforms the membrane and leads to a change its permeability or by blocking channels for Na+ ions at the moment of depolarization, or potassium channels at the moment of hyperpolarization. Mechanotransduction of hair cells is considered in [89]. and the concept of a mechanosensitive ion channel was introduced. According to [89] stretching bilayer lipid membranes increases their conductivity in proportion to deformation, and the mechanosensitivity of these membranes in a model system can be realized by incorporation of synthetic ion channels formed by the antibiotic gramicidin A. According to [89] and research results passive transport of ions in biomembranes, the concept of an elementary mechanosensitive center (EMC) as an ionic channel with fluctuating conductivity together with the associated part of the cell membrane [89].

It is known that in the physiological range of changes in the transmembrane potential, electrostrictive changes in the thickness of natural membranes amount to tenths of an angstrom. Thus, with a potential difference of 0.1 V, the relative change in membrane thickness

NA is 0.2%, i.e. about 0.2 ÿA. However, according to Levin et al., when a nerve impulse propagates along the axon of a crab or squid, the transverse displacement of the axon is 20 ÷ 40 ÿA. If we assume that the resulting membrane deformation will spread along the myelin sheath, then, as a result of phase synchronism, the total deformation along the radial component increases in proportion to the number of myelin turns. Thus, with a number of turns of the order of 2 × 102, the displacement of the axon will be 40 ÿA, which coincides with the experimentally obtained result [Levin et al.]. It is also noted that the relaxation of mechanical displacement of the axon is 10 ÷ 20 ms. If we use the value of the capillary wave speed (see section 3.1) and take the axon radius of the order of 10ÿ4 ÷ 1.5 × × 10ÿ4 cm, then with the number of myelin layers up to 2 102 the total travel time of the deformation wave along the spiral structure will be, under certain assumptions, from 20 to 50 ms, i.e. it will be commensurate with the relaxation time. This circumstance allows an explanation for the large amplitude of the radial displacement of the axon due to phase synchronism and, no less important, allows us to consider the relaxation time as the time of establishment of a quasi-static field pattern. At a potential difference of 0.1 V, a compressive force of about 104 dynes cmÿ2 acts on the membrane , which will change when the membrane is excited.

Considering that, with respect to force, the membrane behaves as a linear system, and introducing the concept of EMC, it can be assumed that the action of an external force on the membrane at the moment of depolarization will lead to blocking of Na+ channels, which should be expressed in a decrease in the positive phase of AP. This circumstance, in turn, should lead to blocking of channels for K+ ions and to a decrease in the negative half-wave of the AP.

According to [89], Young's modulus for biological membranes is of the order of 103 ÷ 105 dyn cm ÿ2. Consequently, when the external force is within 104 dyne cm ÿ2, structural changes in the membrane should begin. Taking into account the value Kÿ ÿ 103 obtained in section 3.2, we can determine the minimum required value of the sound pressure amplitude of excited mechanical vibrations to block the EMC of 10 dynes cm ÿ2, for structural changes - 102 dynes cm ÿ2 (intensity values, respectively, 10 ÿ10 and 10ÿ8 W cm ÿ2). It should be noted here that according to [Levin, Cohen], when a nerve impulse propagates synchronously with it, structural changes localized in the peripheral part of the axon spread along the nerve fiber. However, since the drug functions normally, it can be assumed that the structural changes that occur during PD are transient and completely reversible. Structural changes, presumably arising under the action of an external force exceeding the compressive force, will have to be either slowly passing, i.e. accumulate over time and lead to partial

Rice. 3.07. Scheme for converting the absorbed energy of a non-ionizing radiation

disruption of the functioning of the membrane, or irreversible - with large values of external force. Under the action of a periodic external force due to phase synchronism in the presence of a periodic structure, it is possible to sum up both negative and positive half-periods of oscillations, which will lead to both compression, and to membrane stretching; the prevalence of one or another process may lead to different results depending on the time relationship between the phases of the PD and the phases of the summed oscillation. Thus, the mechanism of action of non-ionizing radiation may be associated with blocking the conduction of excitation,

and with violations of the mechanical integrity of membranes. Exactly a similar effect on biological structures can be realized using very weak doses of pulsed ultrasound, leading to paralysis frog limbs [31–35].

The mechanism of the biological action of non-ionizing pulsed radiation and vibration considered here can be represented diagram (see Fig. 3.07).

Basic provisions of the mechanism model considered here biological effects of non-ionizing radiation were published in a report at the symposium “Mechanisms of biological action electromagnetic radiation", Pushchino, 1987 [92]. Electron microscopy data were obtained by senior engineer P.V. Mashkin.

in the laboratory of neuronal ultrastructure of the Institute of Biophysics of the USSR Academy of Sciences. Mathematical model of the spiral structure and program for calculating the total phase incursions were developed by a junior researcher at the Microwave Irradiation Service of the Institute of Biophysics of the USSR Academy of Sciences, Candidate of Sciences. physics and mathematics Sciences Koltun S.V.

Chapter 4

PSYCHOPHYSICAL STUDIES AND PHYSICAL MODELS

Introduction

An example of the impact of pulsed microwave radiation on the human body is the auditory effect, often called “radio sound” in the literature - the response of a biological system to
an instantaneous change in the magnitude of emitted electromagnetic energy, manifested in a person’s objective perception of these changes. This perception is expressed in the appearance of an auditory sensation when a person’s head is irradiated with electromagnetic pulses
microwave energy. This phenomenon was noticed when persons servicing radar stations operating in pulsed
mode, accidentally found themselves in the coverage area of the radiating antenna. It was noted that people experience sounds of very different colors.

The American researcher A. Frey [93|] was the first to study this phenomenon and reproduced it in laboratory conditions.
radio sound effect. He also put forward some assumptions regarding the possible mechanism of this phenomenon. Attempt
J. Lin [63] undertook to explain the mechanism of the appearance of radio sound almost a decade and a half later. The interpretation of radio sound he proposed was developed under the influence of earlier works
Foster and Finch [19], as well as White [21], who showed that
when irradiating certain liquids, in particular 0.15 M solution
KCl, microwave pulses excite mechanical vibrations of sound
frequencies. J. Lin developed the thermoelastic concept of radio sound, based on the assumption that when a person’s head is irradiated
as a result of the absorption of electromagnetic energy by brain tissue
rapid expansion of these tissues occurs - thermoelastic shock,
which excites mechanical vibrations. These fluctuations lead
to the emergence of sound sensations in a person. Work by J. Lin
is theoretical in nature and is mainly devoted to the completed
using a computer to calculate the distribution of sound pressure amplitude inside a spherical model with infinite quality factor and acoustic and electrical parameters in values approaching those for brain tissue. However, experimental work
confirming the theoretical consideration of the issues raised
in the book by J. Lin, at that time it was not.

Despite the large amount of accumulated phenomenological data, for a long time not a single one has been put forward
a holistic, consistent concept regarding the emergence
radio sound effect. Much of the research on this effect
theirs were carried out on volunteers. Based on analysis and synthesis
the entire volume of psychophysical, electrophysiological, biochemical experiments, theoretical works devoted to excitation
mechanical vibrations in the medium when absorbing an EMF pulse, physical measurements in various materials, own results
on the study of the parameters of mechanical vibrations excited by microwave pulses in cylindrical and spherical liquids
resonators and audiometry of hearing thresholds by bone conduction
a new concept of the formation of auditory sensation is proposed. The essence
it lies in the assumption of the existence of a complex oscillatory system responsible for the perception of radio sound, which
consists of at least two low-Q circuits with a coupling coefficient between them above the critical one. This approach
made it possible to explain the complex spectral composition of the perceived
auditory sensation, the shape of threshold curves of radio sound, as well as
Some features in bone conduction audiograms that
were obtained by recording auditory thresholds using non-
previously used methodology.

Based on the proposed concept, a two-circuit resonant electrical model has been developed and built, which has functional analogues in the original. Model experiments show the identity of the threshold curves of the effect and the amplitude-frequency response (AFC) of the model in the pulsed excitation mode. Shown

the uniform nature of the so-called “types” of radio sound, manifesting themselves differently at different pulse durations, which is unambiguous
confirmed by spectrograms and explained by redistribution
spectral components of mechanical vibrations when the pulse duration changes.

In a full-scale experiment, zero beats of an acoustic tone signal with radio sound were detected in the frequency range below 8 kHz,
previously not registered by anyone, but the need for existence
which followed from model experiments.

The experiment shows the possibility of modeling radio sound
acoustic analogues by directly exciting the tissue of the skull with a bone vibrator.

The fact that the proposed concept not only explained the well-known literature data on radio sound, but also made it possible to predict a fundamentally important effect, which then received experimental confirmation, as well as an unconditional dependence

frequency-threshold curve of radio sound depending on the shape of the threshold curve
bone conduction indicate sufficient completeness of compliance
the proposed model to the phenomenon under study.

It has been shown, therefore, that regardless of the form of manifestation
effect, the mechanism of radio sound is associated with the physical processes of absorption
of EMR energy in the tissues of the head and excitation of mechanical vibrations in them, and
the emergence of an auditory sensation occurs
due to the conduction of these vibrations along the bone to the receptor apparatus
the organ of hearing.

Some essential principles of physical modeling
radio sound are applicable to explain other effects of the biological action of EMR. Method and
data of audiometry of hearing thresholds according to
bone conduction have independent significance and can be
used for early diagnosis of diseases of the auditory system.

Over the past 50 years (the first work is dated 1957), in works on the study of radio sound,
two main and fundamentally different views have emerged on the possible mechanism of this

phenomenon. The first assumed the presence of direct action
electromagnetic energy on brain structures and nerve formations,
i.e., in essence, a mechanism was proposed associated with the processing of incoming
information into a certain signal, a spectral characteristic
which is partially accessible to human perception in the form of a distorted auditory sensation.
The second explanation for radio sound was associated
with the presence of such a factor as expansion of the tissues of the skull of the head
humans due to the absorption of electromagnetic energy and the release of heat. This
expansion of the tissues of the skull should have led to
to the excitation of elastic mechanical vibrations and their perception as
bone conduction count. However, neither the first nor the second approaches
were not able to fully explain some fundamental
questions that remain unresolved to this day. The thermo-elastic theory of radio sound,
proposed by J. Lin, is also not
was able to answer the question why, for example, the auditory sensation,
arising due to the generation of elastic vibrations does not correspond
dominant frequency spectrum of the transmitted signal.

4.1. History and development of effect research the radio sound

Psychophysical experiments with people. First message
that pulse-modulated electromagnetic radiation
can cause auditory sensations in humans dates back to 1956
[94]. Employees of the radar station noted the appearance of sound sensations if they were
near the emitting
antenna, while there were no acoustic sources nearby.
The radar station operated at a carrier frequency of 1.3 GHz. The antenna emitted rectangular
radio pulses with a duration of 2 ÿs,
power 500 kW and repetition frequency 600 Hz. Sound observed
at a distance of 1.5 ÷ 2 m from the radiating horn. With the help of a cylinder

drical (ÿ/4 in diameter) screen, it was found that the most
the sensitive area of the head is the zone near the point located in the middle
and slightly above the conventional line connecting
ear and eye. It is noted that the sound was felt enriched with high
frequencies and had almost no fundamental, i.e. 600 Hz. Two people,
those who had a high-frequency hearing limit (HFHL) near 5 kHz perceived the signal
significantly worse than those with auditory sensitivity
which extended to at least 15 kHz.

The beginning of systematic research into the discovered phenomenon laid down the technical note by A. Frey [93]. The experiments used two generators with carrier frequencies of 1.31 and 2.982 GHz.
The first generator emitted rectangular radio pulses with a duration of 6 ÿs with a frequency of 244 Hz, the second - 1 ÿs, 400 Hz. Subjects
were located at a distance of 6 m from the radiating antenna. Ears at
this was closed with special plugs, which made it possible to reduce
ambient noise level up to 40 ÷ 50 dB above the absolute threshold
hearing (AHL), equal to 0.0002 dyne cm ÿ2. 8 people took part in the experiments. The buzzing nature of the sound was felt by all faces.
The sensation arose without a noticeable latent period, immediately after the generator was turned on or a person entered the irradiation zone.
When ambient noise is reduced, subjectively perceived loudness
radio sound increased. For all subjects, the sound source seemed
localized at a short distance behind the head, regardless
on their orientation relative to the emitter. When determining threshold values, average flux densities were obtained
power (PPMsr) - for a generator with a carrier frequency of 1.31 GHz -
0.4 mW cm ÿ2, for a generator operating at a frequency of 2.982 GHz, -
2 mW cm ÿ2. When multiplying these values by the duty cycle, we get
pulse power flux density (PPMD) - 266.8 mW cm ÿ2
and 5 W · cmÿ2, respectively. A parameter that makes sense is used
amount of energy transferred during the pulse action through
unit area, is the energy flux density (EFD). In this
in the case of PPE = 1.6 and 5 ÿJ · cmÿ2.

Air and bone conduction audiograms were taken from the volunteers who participated in the experiment. Moreover, volunteers with different types of hearing impairments and with various pathologies were selected. The results of the experiments and audiograms of volunteers allowed us to come to the following conclusions:

1) to perceive radio sound, it is necessary for a person to perceive an acoustic signal with a frequency above 5 kHz through bone
conductivity;

2) to perceive radio sound there is no need for the ability
sound perception due to air conduction.

Thus, the first conclusion actually predetermined the search
in further work on the mechanism of the occurrence of radio sound as a consequence of the physiological characteristics of human hearing. Absolutely

After this, it was natural to direct efforts to search for the point of application of the influence of the electromagnetic field, which, as follows from the conclusions made in [95], most likely it should have been be in the area of the hearing organ. At the same time, it became possible in principle to consider some other structures as possible pulse-modulated converters Microwave fields in the auditory sensation.

In the following works [95, 96], A. Frey established the dependence perception of radio sound depending on the carrier frequency and modulation mode.

Using the method of shielding various areas of the head, it was established that the effect is not a consequence of the action of EMF on the filling or tooth crowns. Direct action was also excluded on the eardrum, since the presence and quality of the effect is not depended on the position of the subjects relative to the emitter. The possibility of interaction of EMF with neural complexes is put by the author of [95, 96] is questioned due to the absence of any other sensory effects.

The experimental results also showed that the level of perception correlates with peak power rather than average level power.

Experimental data and constructed calculated curves [95] the depth of penetration of radiation into brain tissue depending on carrier frequencies allowed the author of this work to determine that the most sensitive region to microwave radiation, from the point of view formation of the auditory image is the temporo-auricular region. Since calculations have shown that the absorbed energy of the microwave field can affect the cortical sections, A. Frey came to the following conclusions relative to the possible point of application of the microwave field as exciter of radio sound (or as the initial substance that triggers radio sound perception mechanism):

1) The eardrum cannot be the causative agent, since persons suffering from otosclerosis experienced a subjective feeling sound when irradiated with microwave pulses.

2) The causative agent of the auditory sensation when the human head is irradiated with microwave pulses may be the cochlea of the organ of hearing, but there is no experimental data confirming this assumption.

3) A direct effect of the microwave field on the brain is possible. However, A. Frey himself immediately posed the question: “If such a possibility exists in principle, then why doesn’t the pulsed microwave field manifest itself in other objective sensations?”

Irradiation with a pulse repetition rate equal to or less 100 Hz, perceived as separate buzzing clicks, with At higher frequencies the sound merged. This work points out for the first time dependence of the subjective assessment of the emerging auditory image on pulse repetition rates. A. Frey could not explain the results their research in terms of the presence of any mechanism,

however, his other works allow us to make some observations on this occasion.

It is known that with increasing carrier frequency, the depth of penetration of radiation into brain tissue decreases, and the threshold level of peak power required for the formation of radio sound. It is obvious that the radiation levels used in the work [96], turned out to be insufficient for the formation of perception of radio sound. The same conclusion can apparently be reached based on that all subjects required multiple irradiations to create the sensation of radio sound.

A. Frey pointed out the different nature of perceived sounds in their works [95–97]. During irradiation, all subjects It was noted that radio sound manifests itself in the form of buzzing and hissing. A. Frey notes that the subjective assessment of the subjects indicates the high-frequency nature of the perceived radio sound. And the perception of radio sound itself manifests itself better in the carrier range 0.3 ÷ 3 GHz.

Psychophysical experiments on human perception of radio sound were also carried out by A. Guy et al. [82] at carrier frequency 2450 MHz with pulse durations from 0.5 to 32 ÿs.

V.V. Tyazhelov et al. [98, 100] conducted a large series of psychophysical studies in which they succeeded, along with a variety techniques aimed at elucidating the characteristics of the subject under consideration phenomena, to introduce previously absent in this kind of experiments element of objectivity. The same experimental material was used in works [99–102] with the only difference being what is done in them an attempt to interpret the results and formulate on this basis hypotheses of the possible mechanism of the phenomenon.

The experiments used a generator with a carrier frequency 800 MHz and maximum pulse power of 500 W. The duration of the pulses varied within 5 ÷ 150 ÿs, repetition frequency - from 50 to 20,000 Hz. For all subjects (18 people)

The high-frequency hearing limit was previously determined. Level ambient noise in the room where the experiments were carried out was estimated at 40 ÷ 60 dB above the ABL.

None of the subjects whose HFGS was below 10 kHz heard radio sound with a pulse duration of 10–30 ÿs. Of the 15 observers with HFGS above 10 kHz, only one was unable to hear radio sound with such modulation. Everyone who heard radio sound at pulse duration 10–30 ÿs (in this case, the PPM on the surface head exceeded 0.5 W cm ÿ2), a polytonal character was noted sound sensation at repetition rates up to 8 kHz and monotonal at repetition rates above 10 kHz. In all cases, the sound source seemed to be in the head.

In the experiments, the threshold characteristics of radio sound were measured depending on the repetition frequency and pulse duration.

With an increase in the pulse repetition rate from 6 to 8 kHz, a decrease in volume was observed (an increase in the sensitivity threshold), while while the sound became more monotonal, although still contained at least three components. Observers with HFGS below 15 kHz in the zone of increasing threshold, they completely lost the ability to perceive radio sound at the applied PPM (ÿ 1 W cm ÿ2), while while observers with HFGS 17 kHz had only slight rise in threshold (ÿ 0.3 W cm ÿ2) (Fig. 4.01). Except Moreover, it was noted that the former were unable to distinguish signals with a repetition rate of 5 and 10 kHz. Subjects with a wider auditory range noted that the apparent pitch for 5 kHz higher than for 10 kHz. For various pulse repetition rates, the duration of which in this series of experiments was 10 ÿs, thresholds expressed in PES vary from 2 ÿJ cm ÿ2 and mostly up to 10 ÿJ cm ÿ2. Single pulses begin to be heard at PES ÿ 45 ÿJ cm ÿ2.

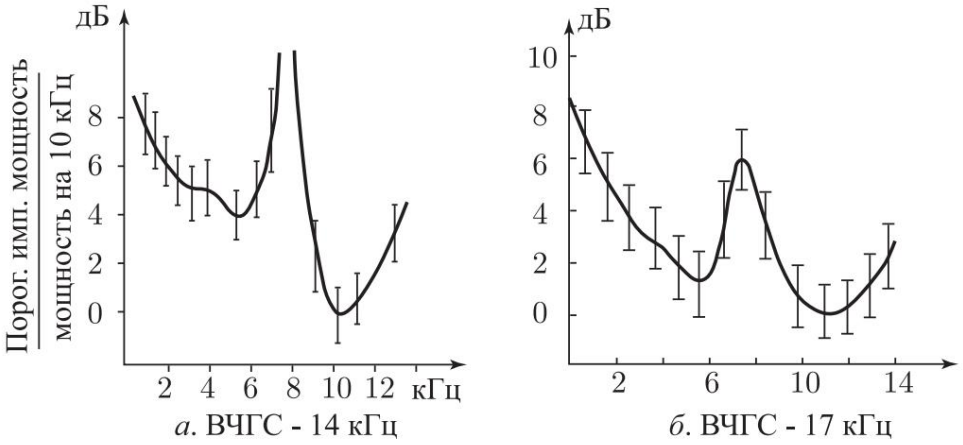

Rice. 4.01. Threshold curves of radio sound effect depending on frequency pulse sequences with a duration of 10–40 ÿs: *a* — HFGS 14 kHz; *b* — VCHGS 17 kHz

A complex threshold characteristic was also discovered for the dependence on the pulse duration at a constant peak amplitude (Fig. 4.02). When the pulse duration changes from From 5 to 50 ÿs, the volume of the perceived radio sound increased, then at durations from 70 to 100 ÿs the sound decreased to full disappearance, reappeared and increased at longer durations. Moreover, as the pulse duration approaches the value 110 ÿs, some subjects noted a sharp change in character sensations - abrupt decrease in pitch and movement the apparent source of sound from the head to the outside. It turned out that even people who had HFGS below 10 kHz and were not able to perceive radio sound at short pulse durations heard it at large. For other observers with a smooth decrease pulse durations from 100 to 60 ÿs, a kind of

“frequency locking effect” [100, 102], which consisted in the simultaneous perception of both high-frequency and low-frequency (i.e., manifesting itself at long durations) radio sound - with a duration of less than 50 ÿs, the latter disappeared. Break in irradiation for

2 ÷ 4 s also led to the disappearance of low-frequency in the perception the radio sound.

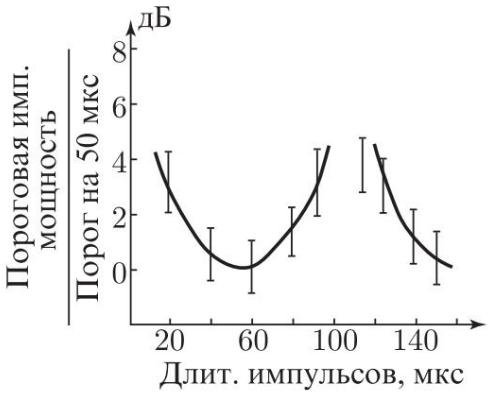

Rice. 4.02. Threshold curve of the effect of radio sound depending on on the pulse duration at a repetition frequency of 800 Hz

The most important characteristic of the phenomenon under study is from the point of view of the possibility of its subsequent interpretation for the purposes of searching for the most optimal modulation mode, and from the point in terms of searching for a possible mechanism, the frequency range perceived radio sound. Knowledge of this characteristic allowed to narrow down the search and make it more targeted. Exactly this The problem is primarily addressed in work [14], in which the method zero beats, it was possible to determine the boundaries of the frequency range perceived radio sound under the experimental conditions in which it was usually studied.

Analysis of previous works showed that the nature of the perceived According to subjective assessment, radio sound does not correspond to the pulse repetition rate. This circumstance primarily gave rise to attitude towards radio sound as a phenomenon that has a physiological basis.

The term “physiological” means specific the effect of the electromagnetic field only on biological objects, and the term “physical” means the interaction of electromagnetic fields with matter in general.

At the same time, none of the works showed any the integral mechanism of this phenomenon, in which the physiological characteristics of any of the structures identified in [95] were manifested would be clear and unambiguous. However, by the time the work was completed [5] Information about the results of research has already appeared in the press, which actually represented the first attempt to understand the process of formation of the auditory sensation in humans during irradiation with pulses Microwave not from the point of view of physiology, but from the point of view of physics. And although priority in this direction belongs to the work [21], published in 1963, however, only 12 years later, researchers were an attempt has been made to consider the effect of radio sound from the perspective physics.

Let us return to work [5], which describes the following experiment. Simultaneously with irradiation of the subject’s head with microwave pulses

the electrodynamic emitter, powered by the generator, was turned on sound frequencies. The idea of the experiment was that if frequency of field pulse repetition and frequency of sound vibrations the subject should hear zero beats. However, this did not happen. At any pulse repetition rate from 0.8 kHz and above zero beats were recorded only if the frequency acoustic signal was above 8 kHz and corresponded to the overtone microwave pulse repetition rate. In table 4.1 provides values microwave pulse repetition frequencies and acoustic signal frequencies, at of which zero beats were recorded.

Table 4.1

Values of repetition frequencies of microwave pulses and tone signals, corresponding to the presence of zero beats according to subjective assessment subjects (crosses indicate the moments when beats)

Repetition frequency pulses, microwave, kHz	Tone frequency, kHz													
	1	2	3	4	5	6	7	8	9	10	11	12	13	14
1								+ +	+ +	+ + +				
2								+ +				+		+
3									+			+		
4								+				+		
5										+				
6												+		
7														
8								+						
9									+					
10										+				
11											+			
12												+		
13													+	
14														+

The data presented in the table allowed us to come to the conclusion that that the lower limit of perceived radio sound lies in the region 8 kHz and extends to HFGS. For a clearer fixation of zero beats, observers were given the opportunity to adjust the amplitude

amplitude and phase of the acoustic signal in such a way that complete suppression of the sound sensation occurs. It should be noted that these The data were obtained at microwave pulse durations of 5–10 ÿs.

Thus, the authors of this work concluded that it is possible to perceive radio sound only for frequencies starting from 8 kHz and higher. The manifestation of lower-frequency radio sound is considered as fundamentally different from the usual “high-frequency radio sound" phenomenon, at least another type of it, which is not less than 20 dB is suppressed by high frequencies and is felt only in the minimum manifestation of the latter.

From the theory of J. Lin [63], who considered the human head as resonator and connecting the frequency of excited mechanical vibrations with the size of the head, it followed that with increasing size head, the resonance would have to shift, which should have led to a change in the frequency of the perceived radio sound. For check this assumption, the subjects were immersed in a container with water a solution of table salt with acoustic and electrical parameters close to those in tissues. At the same time, it was assumed that due to an increase in the effective radius of the head, due to equality of these parameters, the resonance frequency should decrease and the subject will perceive lower frequency radio sound. However, this could not be discovered. With pulse duration less than 50 µs there was a decrease in volume proportional to degree of immersion of the head in water. With increasing duration pulses over 50 µs, even partial immersion in water led to to loss of sensation of sound.

Works [101, 102] considered the possibility of the existence of two types of radio sound - “high-frequency” and “low-frequency” based on the results obtained earlier [5]. The possibility of the existence of “two types of radio sound” was considered as a consequence of the presence of two mechanisms leading to the formation various auditory sensations. One is low-frequency, interpreted as a result of thermal expansion of tissues when absorbing an impulse electromagnetic microwave energy (in accordance with thermoelastic concept of J. Lin), high-frequency - as a result of action the same impulse on neural structures - parametric synchronization. However, these works did not receive further development, and the mechanism for excitation of one or another type of radio sound remains on level of assumptions.

In work [103], the authors attempted to reproduce the results of psychoacoustic studies [104, 105] based on subjective comparison of two pulse sequences with different modes modulation, replacing the test sound signal with a microwave signal. However obtain the same result as in psychoacoustic studies, the authors couldn't. There were obvious methodological errors in the work, which could have been the reason for the failure. In particular, the conclusion that

that the frequency of audible radio sound lies within 4.8 ± 0.8 kHz,
made from a flawed premise and contradicts both the classic work
one of the authors [93] and other works [5, 98]. Based on this
However, it is concluded that the structure that detects EMF is the outer hair cells of the organ of Corti.

In conclusion, it must be added that there are a number of works on
study of behavioral reactions of laboratory animals to MI
EMR [106, 113]. They confirm in various independent ways the assumption that in animals, just like in humans,
Pulsed microwave EMF can cause auditory sensations.

Methods and instruments for excitation and recording of mechanical vibrations in liquid media by microwave pulses. Spherical
volumes when mechanical vibrations are excited in them have
the whole spectrum of frequencies [114]. In this regard, to simplify the assessment of the results obtained and to identify the dependence of the parameters of mechanical vibrations excited in the liquid on the parameters of the pulse
microwave sequence, a test tube with liquid placed in the action zone of pulsed EMR was chosen as the simplest model.
In this case, the column of liquid filling the test tube has the properties of a quarter-wave resonator with a certain quality factor.

The simplicity and clarity of such a system, as well as complete equivalence with the theoretical model of J. Lin in terms of basic formal
signs allowed us to consider her as adequate physical
model for studying the effect of radio sound.

To record mechanical vibrations excited in a liquid, piezoceramic transducers with a sensitivity of 10ÿ6 V dynÿ1 cm2 in the frequency range 40 ÷ 2 104 Hz with an uneven amplitude-frequency characteristic of ±5 dB were used. Calibration

sensors was carried out using the pistonphone method [115].

Flasks and plastics were used as spherical resonators.
woven balls filled with ethanol.

For irradiation of large volumes of liquid (up to 3 l) they used
irradiators in the form of an open end of a rectangular waveguide with a cross-section of 10 × 72 mm2 and a rectangular horn with an aperture of 90 × 120 mm2, used at 2375 MHz with 140 and 20 W cm ÿ2 PPP,
respectively. The source of microwave oscillations was the developed
previously pulsed microwave generators based on a laboratory generator
GS-6 and medical device for microwave therapy “Luch-58-1”
[116–118]. Maximum output power per pulse at frequency
800 MHz was 120 W, at a frequency of 2375 MHz - 500 W.

Registration of mechanical vibrations excited in spherical glass resonators is carried out using switched on
into the wall of the flask of piezoceramic transducers.

Vibrations can also be recorded using an autonomous
a piezoelectric receiver on which a resonator with liquid is directly installed. Plates are also installed on the same receiver

stick spherical resonators. In Fig. 4.03 provides a section design of an autonomous piezoelectric receiver.

In Fig. 4.04 and 4.05 show methods of irradiating spherical models, in Fig. 4.06 is given block diagram of experiments on excitation and recording of mechanical vibrations.

The photo shows the hardware complex for studying the characteristics of mechanical vibrations excited in spherical models. In the foreground is the modernized generator “Luch-58-1M”,

on the table (from left to right) is a spherical flask with a radio-absorbing liquid, installed on a self-contained piezoelectric receiver, behind which a microwave adapter with a ferrite decoupling valve is installed.

Next is the rectangular generator pulses for modulating microwave radiation, millivoltmeter, oscilloscopes and frequency meter.

Irradiation of large spherical resonators at a carrier frequency of the order of 0.9 GHz showed that as a result of diffraction

a parasitic signal is induced on the piezoceramic transducer Microwave, which makes it practically impossible to register mechanical hesitation. To carry out the experiment at these frequencies, the EMR was

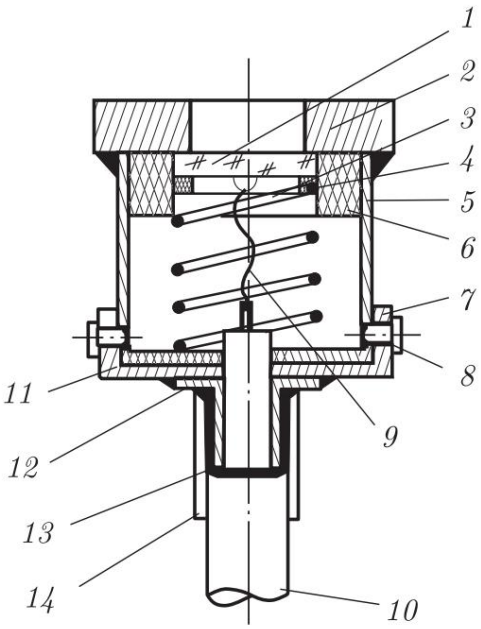

Rice. 4.03. Section of the design of an autonomous piezoreceiver: *1* - piezoelectric transducer, *2* — base (brass), *3* - pressure spring, *4* - insulating washer (textolite thickness 0.15 ÷ 0.2 mm), *5* - body (brass), *6* — centering washer (textolite), *7* — removable cover (brass), *8* — peg (brass), *9* - flexible conductor, *10* - cable, *11* - insulating gasket (textolite 0.5 mm thick), *12* - glass, *13* - cable screen, *14* - tube (polyvinyl chloride)

a method has been developed for exciting mechanical vibrations in glass spherical resonators using a microwave applicator with a diameter of 13–15 mm, immersed in ethanol through the neck of the flask.

In all cases, when irradiating spherical resonators, it is necessary to apply all measures that reduce mechanical vibration of the resonator from external sources. It is advisable to conduct experiments in screened, soundproofed rooms. A set of these measures allows you to work in conditions of a significant reduction in impulse microwave power (sometimes up to several units of watt) and register signals taken from the plates of the piezoelectric transducer about 10ÿ5–10ÿ4 V.

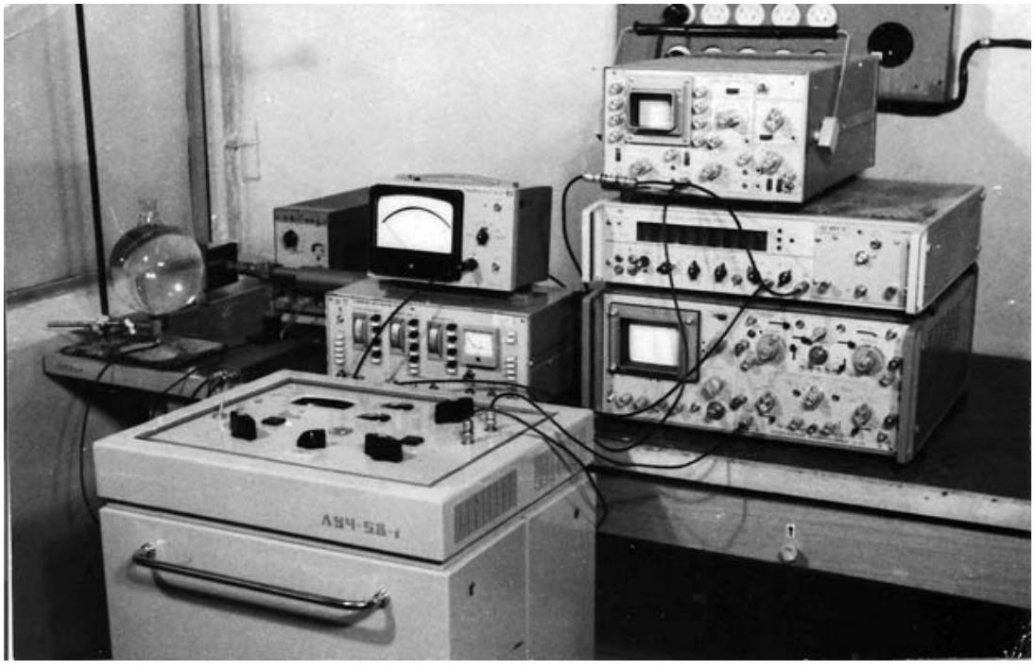

Photo. Hardware complex for studying excited spheres
mechanical vibrations

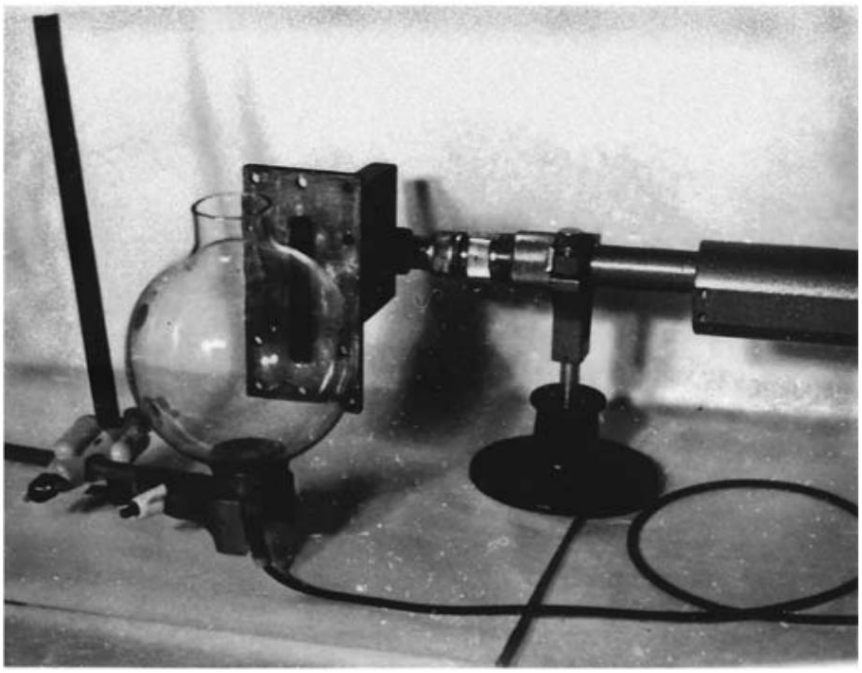

Rice. 4.04. Irradiation of a sphere by a rectangular waveguide with a cross-section
10 × 70 mm2

In Fig. Figure 4.07 shows a diagram of an experiment on excitation of mechanical vibrations in a spherical glass resonator using applicator operating at a frequency of 915 MHz, with registration of these

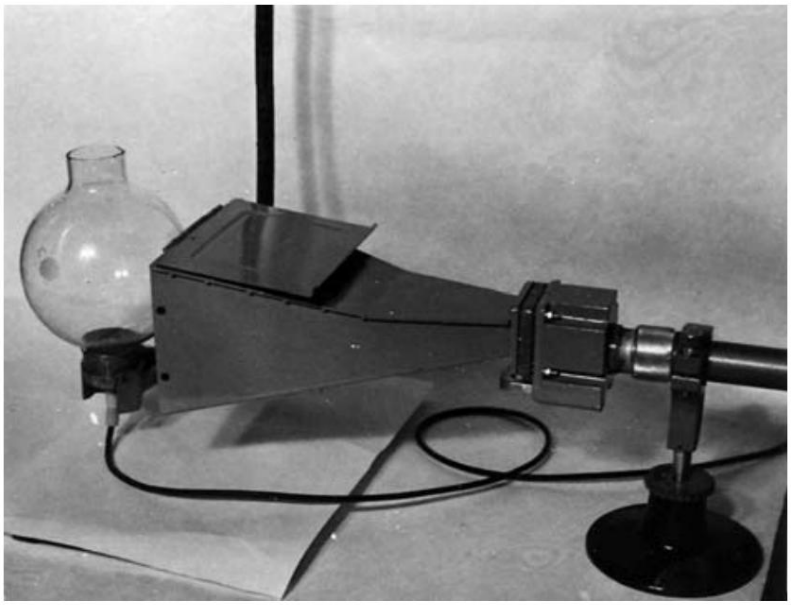

Rice. 4.05. Irradiation of a sphere with a rectangular horn with a cross section of 90 × 120 mm2

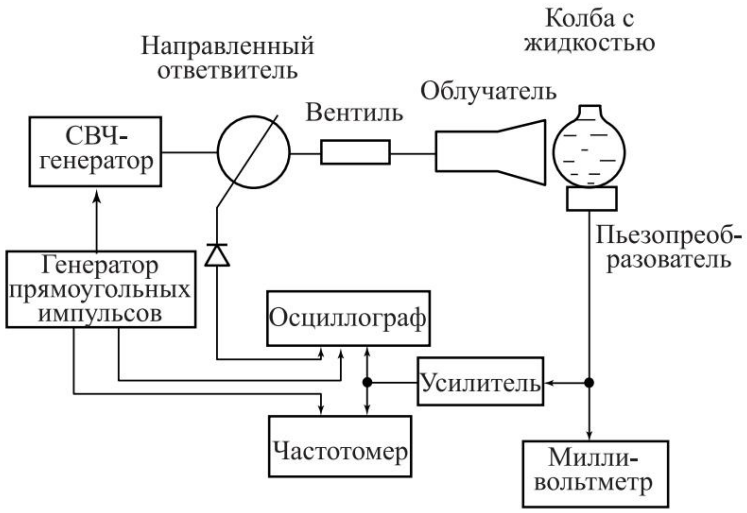

Rice. 4.06. Block diagram of an experiment on excitation of mechanical vibrations in liquid spherical models: *1* - microwave generator, *2* - square-wave pulse generator, *3* - oscilloscope, *4* - frequency meter, *5* - amplifier, *6* - millivoltmeter, *7* - piezoelectric transducer, *8* - flask with liquid, *9* - feed, *10* - valve, *11* - directional coupler

vibrations using a glued piezoceramic transformer
calf.

As a rule, amplification of weak signals against a background of noise is carried out using resonant amplifiers. In this case, this could be all the more justified due to the rather narrow frequency band
excited mechanical vibrations during experiments with a limited set of resonators. However, experience with microwave generators
shows that even when operating at a closed load under conditions

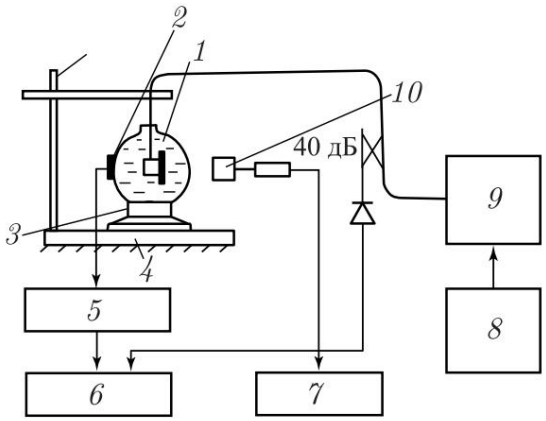

Rice. 4.07. Excitation of mechanical vibrations by EMR pulses in a glass spherical resonator using a microwave applicator: *1* - spherical resonator, *2* - piezoceramic sensor, *3* - plastic bottom, *4* - rubber gasket, *5* - amplifier, *6* - oscilloscope, *7* - wattmeter, *8* - rectangular pulse generator, *9* - microwave generator, *10* - frame

shielded rooms [116] in pulsed radiation mode
a negligible induced potential from EMR on the input circuits of selective amplification equipment is enough to excite it
at frequencies close to those recorded.

To test the possibility of using amplification equipment with selective properties, a V6-9 selective microvoltmeter was used in the experiment. As a source
rectangular pulses generator G5-54 was used. Preliminarily to the input of a selective microvoltmeter directly from the output
generator G5-54 supplied rectangular pulses with a duration
about 5–25 ÿs and a repetition rate of about 100 Hz. In Fig. 4.08
shows one of the oscillograms of the output signal of the selective microphone

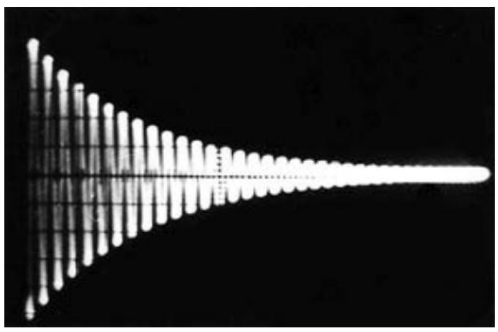

Rice. 4.08. Artifact of excited mechanical vibrations when applied to input of the selective amplifier of a short rectangular pulse from the G5-54 generator (V6-9 selective microvoltmeter)

level voltmeter when it is excited by rectangular pulses from
generator G5-54 in the tuning band 1–20 kHz. Then turned on
microwave generator, loaded it onto an open emitter with a cross-section
10 × 72 mm2 and installed in close proximity to it

spherical resonator with ethanol. With the previous parameters of the pulse sequence, the pulse modulation mode was carried out
EMI at a carrier frequency of 2375 MHz. Selective microvoltmeter
located in an area with intensity within acceptable levels
irradiation - about 30–50 ÿW cm ÿ2.

In Fig. 4.09 shows an oscillogram of the output signal of a selective microvoltmeter when the input of the device is open. Comparison
The oscillogram clearly shows the possibility of an artifact when using selective amplification equipment
even under acceptable operating conditions.

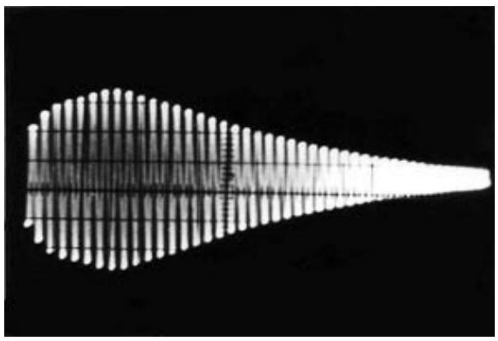

Rice. 4.09. Artifact of excited mechanical vibrations by a short induced microwave pulse with selective amplification (selective microvolt meter V6-9)

The next stage of checking the possibility of an artifact occurrence was recording the output signal of a selective microvoltmeter
when connecting a signal from the converter to its input. Oscillations
excited in a test tube with ethanol according to the scheme shown in Fig. 2.17, using EMR at a frequency of 800 MHz. Pulse power at input
into the waveguide - 70–75 W. The measured EMR intensity in the area
where the selective microvoltmeter is located is within 10 ÿW cm ÿ2.
Frequency of excited mechanical vibrations in ethanol and frequency
the settings of the selective microvoltmeter were somewhat upset
relative to each other in order to ensure the possibility of observing zero beats between the signal taken from the converter,
and excited in a selective microvoltmeter due to the induced
on the EMI input circuits and detected in the device. In Fig. 4.10
The oscillogram of such a body is shown.

For undistorted amplification of the video pulse generated on
amplifier input circuits, amplifier bandwidth
is determined by the known relation fÿ = 1/ÿÿ, where ÿÿ is the pulse duration. The applied values of ÿi in experiments on
exposure to any model or biological EMR systems
in the decimeter range are practically limited from below by the value
10ÿ6 s, i.e. the value of fÿ should be of the order of 1-3 MHz. The input impedance of the amplifier when working with piezoceramic converters is

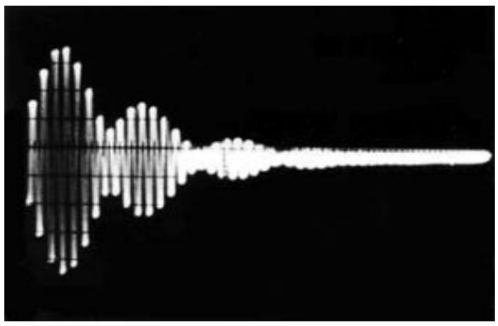

Rice. 4.10. Artifact of communication frequency beats during selective amplification of an induced microwave pulse together with an electrical signal taken from a piezo-ceramic transducer (selective amplifier V6-9)

telami is ÿ 105 Ohm. Amplifier output amplitude
can be set within 0.1–1.0 V. Therefore, the coefficient value
gain can be determined within 500 ÷ 1000, which is quite
is enough to observe the signal on the oscilloscope screen and carry out any measurements.

Schematic diagram of the developed amplifier with close
The described parameters are shown in Fig. 4.11.

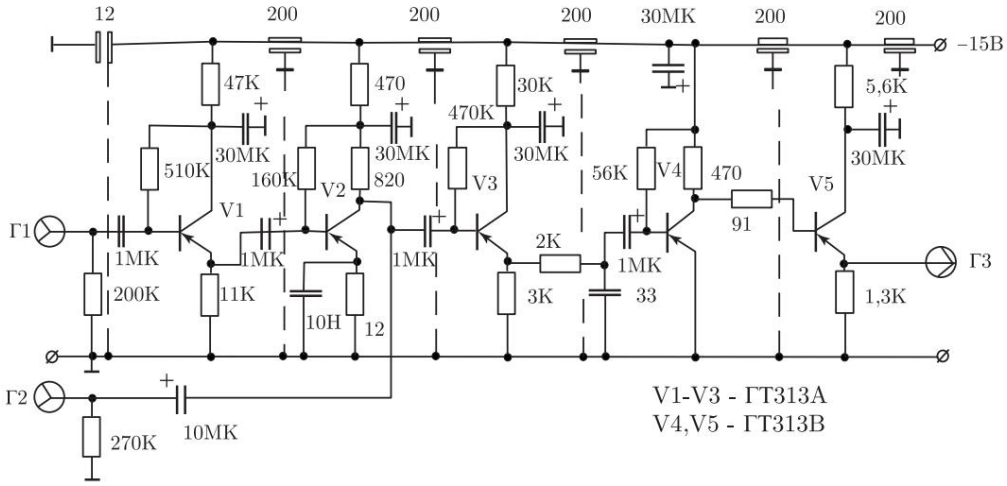

Rice. 4.11. Schematic diagram of a broadband amplifier

Due to the operation of the amplifier under pulsed microwave conditions fields in order to increase its noise immunity and reduce the tendency resistance to self-excitation, the installation of the amplifier is sectioned, the housing and cover have an electrical connection along the entire connector line contact and made of brass. The power bus is laid using block containers installed on transverse screens. A photograph of the amplifier installation with the cover removed is shown in Fig. 4.12.

The amplifier has three CP-50 type connectors, with which it is connected to a piezoceramic transducer and an oscilloscope.

In order not to install a special switch when switching from work with a small signal to a large one, connectors G1, G2, G3 (see Fig. 4.11)

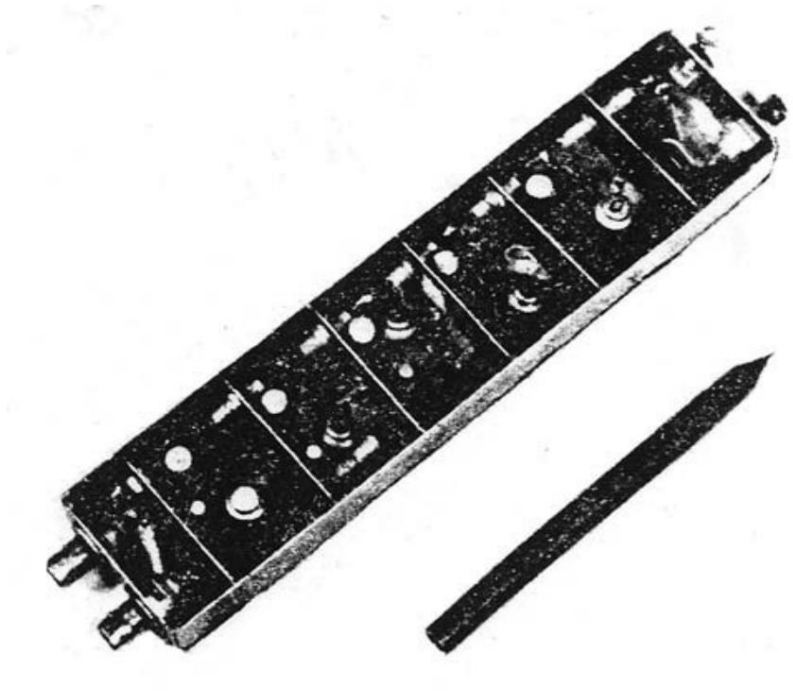

Rice. 4.12. Amplifier design (view with cover removed)

allow operation with the following gain values with different cable rearrangements:

G1 ÿ G3, Ku = 500
G1 ÿ G2, Ku = 37
G2 ÿ G3, Ku = 13.

The arrows indicate the direction of the signal from input to output, Ku is the gain.

The developed amplifier was tested under the same conditions as the selective microvoltmeter. In this case, beats were observed in a test tube with incomplete filling. If the height of the liquid column and the height of the air column are selected so that their frequencies are close or multiples, then when mechanical vibrations are excited in such a system, beats can be obtained.

Test tubes of the same diameter with a height of 50 and 60 mm were used. The height of the liquid column in both cases was 40 mm. In this way, two systems of resonators were obtained - liquid with a height of 40 mm and air with a height of 10 mm, and liquid with a height of 40 mm and air with a height of 20 mm. Accordingly, the frequency of mechanical oscillations excited in the liquid in both cases is unchanged, and the frequency of oscillations of the air resonator should change by half. This circumstance should appear when recording beats and indicate the absence of an artifact.

In Fig. 4.13 and 4.14 show oscillograms of communication frequency beats for both systems. To illustrate the shorter beating process, the oscillogram in Fig. 4.13 was obtained at a higher scanning speed of the oscilloscope beam. It should be noted that when recording beats in the described system of resonators, to obtain the recorded amplitude of the beat signal, the transducer was located inside the test tube in an air resonator due to the weak effect of the air column on the liquid column. A bimorph crystal was used as a converter [66].

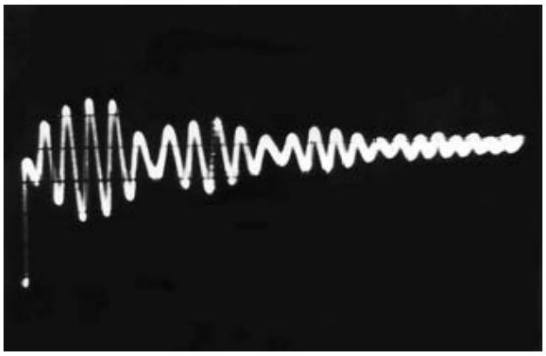

Rice. 4.13. Communication frequency beats: liquid column height - 40 mm; air column height - 10 mm

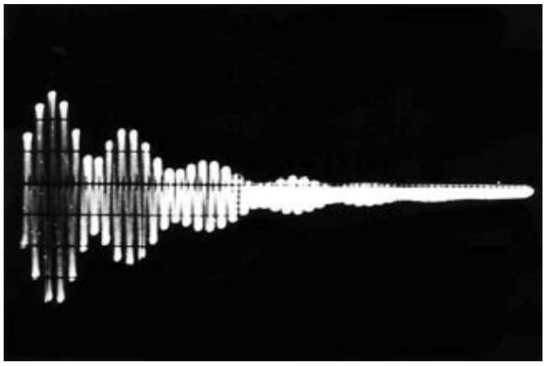

Rice. 4.14. Communication frequency beats: liquid column height - 40 mm; air column height - 20 mm

It is advisable to conduct experiments using physical models in shielded rooms with sound insulation, especially when working with open emitters [117]. In Fig. Figure 4.15 shows a diagram of the arrangement of equipment in such a room. In Fig. For comparison, Fig. 4.16 shows an oscillogram of the beats of communication frequencies when a test tube

with ethanol is irradiated according to the diagram in Fig. 2.17 when excitation of resonant oscillations and their registration using the developed amplifier. The second signal is realized using an acoustic electrodynamic head, the radiation axis of which is directed towards the test tube. The mixer is a piezoceramic

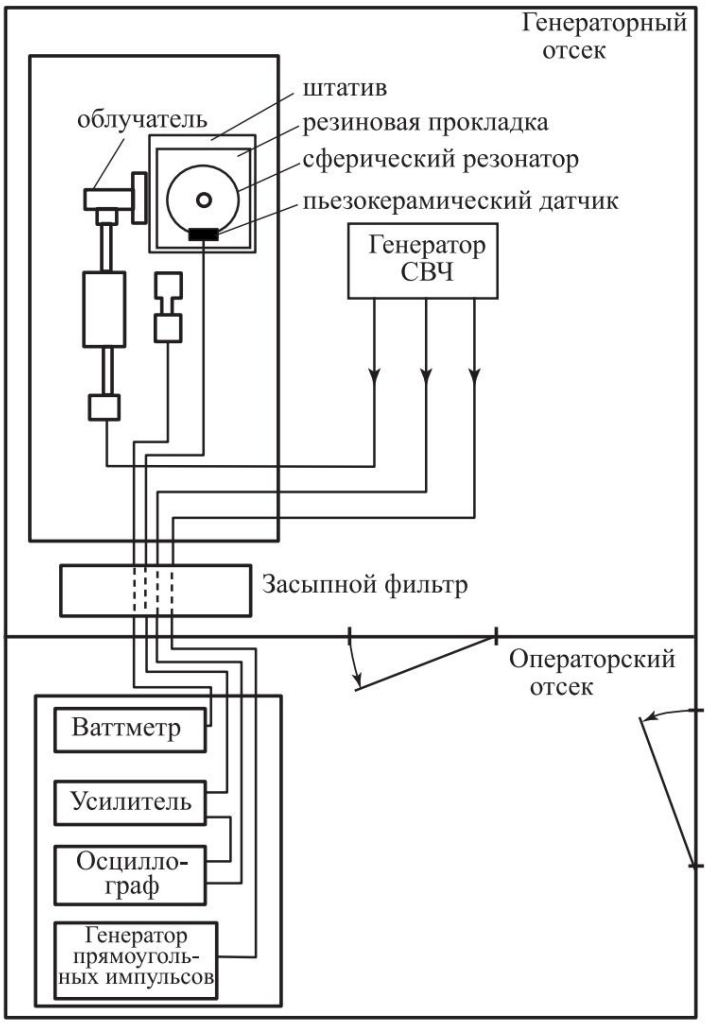

Rice. 4.15. Layout of equipment in a shielded room

ski converter. Thus, it can be considered that the application broadband amplifier and operation in a shielded room ensure correct setup of experiments.

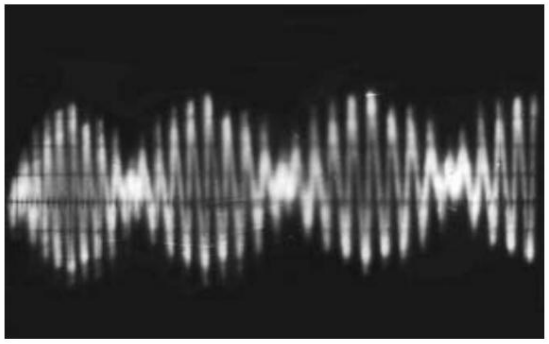

Rice. 4.16. Beating of mechanical vibrations excited in a test tube EMR pulses with an acoustic signal

4.2. Excitation of mechanical vibrations in limited volumes pulsed EMR

4.2.1. Single-circuit resonant models. According with the concept of J. Lin, according to which the human head, when exciting mechanical vibrations in tissues, is considered as an acoustic resonator with a resonance frequency determined by the speed of sound in the tissues of the skull and the radius of the head (single-circuit model), as of irradiated volumes of liquids, single-circuit systems were used in the experiments.

Cylindrical model. Used as a resonator test tube with NaCl solution [119], which is a quarter-wave resonator due to the presence of a free liquid surface and the fixed bottom of the test tube. The height of the liquid column in a test tube varied from 30 to 50 mm.

Table 4.2

Height column liquids, mm	Period mechanical hesitation, mx	Frequency mechanical hesitation, kHz	Length waves, mm	Calculated average meaning speed sound in water cm · sy1
30	80 ÷ 100	12 ÷ 10	120	1,44 · 105
40	100 ÷ 120	10 ÷ 8	160	1,45 · 105
50	140 ÷ 160	7 ÷ 6	200	1,42 · 105

For all three liquid columns (30, 40 and 50 mm) on the screen mechanical vibrations were recorded on the oscilloscope. By using marks on the oscilloscope screen, the periods of mechanical oscillations were determined (Table 4.2). Using the relation L = [1], where $\frac{no}{4}$ L is the height of the liquid column, ÿ is the wavelength and C = ÿf, you can obtain approximate values of the speed of sound in liquid for all three cases. A more rigorous expression for L is given in [65].

Taking into account the errors in measuring the period of mechanical vibrations (up to 10%) and the height of the liquid column (up to 3%), the obtained data are in good agreement with those reported in the literature. Similar data were obtained for ethanol.

When the pulse repetition rate changes, the EMR amplitude mechanical vibrations excited in the liquid are maximum at fi = fr/n, where fi is the EMI pulse tracking frequency, fr is frequency of mechanical resonance of a liquid column, n = 1, 2, 3, ..., and the higher, the smaller n, and is minimal for values of fi equal to $\frac{2fy}{2n+1}$. At a pulse repetition rate sufficient for attenuation

excited mechanical vibrations in a liquid in the time intervals between pulses, when the duration of microwave pulses changes
The amplitude of excited mechanical vibrations changes periodically. Frequency of occurrence of amplitude maxima (minimums) mechanical vibrations is equal to 1/f, where f is the frequency of excited in a fluid of mechanical vibrations. In Fig. 4.17 provides experimental

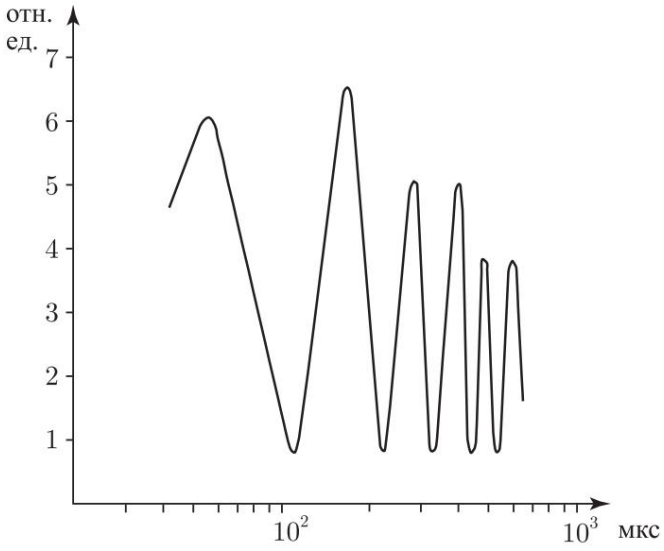

Rice. 4.17. Dependence of the amplitude of excited mechanical vibrations on microwave pulse duration

mental dependence of the amplitude of excited mechanical vibrations in a liquid column on the duration of EMR pulses [120].
With pulse duration ÿ and T /4 oscillations from the leading edge are not distinguishable on the oscillogram, but only the total periodic process is visible (see Fig. 2.10). It is important that in those moments when the duration of the pulses is such that the amplitude of the excited resonant oscillations decreases (at ÿi = nT), clearly
a lower tone corresponding to the frequency is perceived “by ear” impulse following. The perception of low-frequency oscillations begins with the repetition rate of EMR pulses, at which
individual clicks. Tone corresponding to its own resonant vibrations of the system, is perceived “by ear”, starting from the frequency pulse repetitions of the order of 250 ÷ 300 Hz. In Fig. 4.18 is given an oscillogram of excited mechanical vibrations corresponding to a perceived low-frequency tone.

Possibility of direct aural perception and visual observation on the oscilloscope screen of excited oscillations
in a liquid when a test tube is irradiated with pulsed microwave EMR, allows us to make the assumption that radio sound is also caused conversion of incident EMF energy into mechanical energy vibrations in the absorbing substance. From this point of view, the object

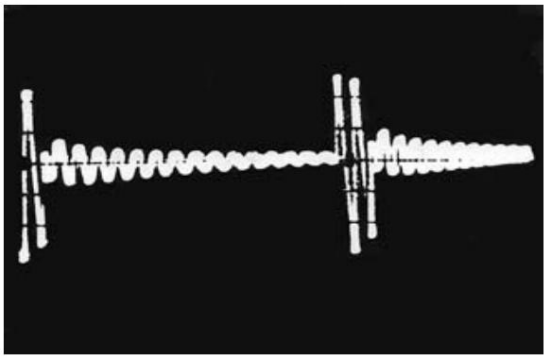

Rice. 4.18. Oscillogram of mechanical vibrations excited in a test tube at a low repetition rate of EMR pulses with a duration equal to nT

in which the research was carried out can be considered as a physical model in relation to the study of radio sound, and the results model experiments interpreted in application to this phenomenon.

The results of the work considered here on radio sound and the generation of mechanical vibrations allow us to express some considerations. The dependence shown in Fig. 4.17, completely coincides with the theoretically calculated by J. Lin, which confirms

a formal analogy of our models. The fundamental difference between the results obtained on this physical model and the results J. Lina [121] is to identify the frequency dependence of the amplitude of mechanical vibrations, which puts our model much closer to the real situation, since the dependence of the radio sound effect on pulse repetition rate has been noted by many studies [5, 97, 108, 122, 123]. It is important that such a dependence was obtained both during objective registration on the oscilloscope screen, and during subjective perception “by ear”.

Particularly interesting and important is the result consisting in the possibility of perceiving “by ear” a low-frequency tone corresponding to the pulse repetition rate, at moments when, at pulse duration ÿi = nT (n = 1, 2, ...), vibrations corresponding

resonant frequency of the model, are suppressed and only generation takes place packs of oscillations from the leading edge (Fig. 4.18). This result allows us to consider the so-called low-frequency type of radio sound, described in [5, 104], as perceived by the hearing organ the first harmonic of mechanical vibrations excited inside skull while simultaneously suppressing more intense resonant oscillations with a pulse duration equal to their period. For length 2n + 1 equal to $\frac{}{2}$ T, is perceived by high-frequency pulses a tone corresponding to the resonant frequency of excited vibrations.

The data obtained from the model make it possible to explain the dependence threshold for the perception of radio sound on the pulse duration obtained

in a full-scale experiment [5] and shown in Fig. 4.02. If we proceed from the value of the frequency of excited mechanical oscillations of 8 kHz, then with a pulse duration equal to half the period, i.e. 60 ÿs, a minimum threshold is naturally observed. With a pulse duration equal to the period of excited mechanical oscillations, i.e. 120 ÿs, there is a complete suppression of the perception of a high-frequency tone and the appearance, against the background of this suppression, of a lower-frequency tone of height corresponding to the pulse repetition frequency, as can be assumed based on Fig. 4.18.

Thus, a fairly simple and visual system made it possible to answer complex questions regarding the mechanism of radio sound, which gives the right to consider the object itself on which the research was carried out as a physical model of radio sound.

The hypothesis about “two types” of radio sound, due to physiological characteristics, still remains at the level of speculation. At the same time, the microphonic potential of the cochlea occurs when the basilar membrane is mechanically displaced [124]. Experiments on recording the MPU of guinea pigs showed that this potential arose when the hearing aid was exposed to both an acoustic signal due to air conduction, and excitation of mechanical vibrations of the skull bones using a radiating piezocrystal due to bone conduction, and under the action of a microwave pulse [125]. Moreover, regardless of the nature of the influencing factor and the type of conductivity, the shape of the microphone potential is approximately the same in general in all cases, i.e., in all three cases there was a mechanical displacement of the basilar membrane.

The presence of microphone potentials during mechanical action on the bones of the skull and during microwave irradiation, taking into account the results of irradiation of liquid media with microwave pulses, speaks in favor of a single mechanism for the occurrence of auditory sensation in all described cases. However, the described model does not explain in any way the complex spectral

composition of the excited sound stimulus [126–129], the polytonal nature of radio sound in the frequency range of 8 kHz, as well as the quantitative relationships on the threshold curves [5, 100] and, moreover, the dependence - similarity of the shape of the threshold curves of radio sound from the subjects’ own HFGS [5, 98]. **Spherical models of the radio sound effect.** At the second stage of studying the role of mechanical vibrations excited by microwave pulses in the formation of sound

sensations in persons exposed to irradiation, models that were more responsive to this task were used [130]. Since the human head, to a first approximation, can be represented as a spherical shell filled with a substance with certain mechanical properties [131, 121], glass and plastic spheres were used as a model,

filled with the same liquids as the test tubes in the first series of experiments. Experiments were carried out with

glass spherical flasks with a diameter of 105, 120 and 185 mm and a plastic sphere with a diameter of 120 mm, which were filled with ethyl alcohol. In some cases, other models were used to compare results, as will be discussed at the appropriate place. It is known that the subjectively perceived loudness of radio sound has a logarithmic dependence on the pulse PPM [97]. In a similar way, the amplitude of the N1 response in

the auditory nerve and the amplitude of the MPU, recorded in the round window of the cochlea of guinea pigs, depend on the PES [80, 132]. It was also shown in [125] that the dependence on PPE in its pure form occurs only up to a certain pulse duration (30 ÿs), and at longer durations, the amplitude of responses in the brain stem depends only on PPE. Summarizing these experimental data, we can come to the conclusion that the subjective loudness of radio sound, as well as the threshold of sensation and the amplitude of EP in the auditory pathways, have a logarithmic dependence on PES. Moreover, this is true only for pulse durations not greater than a certain maximum, which, as can be seen from the graph in Fig. 4.17, should be equal to half the period of excited oscillations. It is known that the organ of hearing is a logarithmic device, so it is quite logical to assume that the factor leading to the appearance of an auditory sensation or electrical response in the auditory pathways should linearly depend on the PES or on the PPM at a constant pulse duration. In [133], a linear dependence of sound pressure in spheres of various diameters on the incident PPM was theoretically predicted. No experimental confirmation of this result has been found in the literature, despite its fundamental nature.

In Fig. 4.19 shows graphs of the experimentally obtained dependences of the amplitude of excited mechanical oscillations on the output pulse power of the generator and, accordingly, the calculated PPM. Dependence *1* was taken for a resonant frequency of 11.8 kHz of a sphere with a diameter of 105 mm at a pulse duration of 20 ÿs. Dependence *2* was taken for a resonant frequency of 2.6 kHz of the same sphere with a pulse duration of 80 ÿs. The pulse power was calculated from the measured average and duty cycle. The maximum voltage values of the electrical signal taken from the piezoelectric sensor, measured with a voltmeter, are respectively equal to ÿ240 mV for dependence *1* with an amplifier gain equal to Kÿ = 500, and 43 mV for dependence *2* with Kÿ = 37. As can be seen from the given data graphs, the amplitude of mechanical vibrations excited in spherical volumes linearly depends on the PPM (PPE).

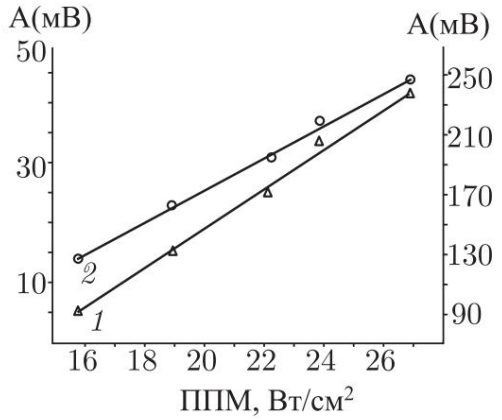

Rice. 4.19. Dependence of the amplitude of mechanical vibrations excited in a sphere with a diameter of 105 mm, from PPM: *1* - for a resonant frequency of 11.8 kHz (y-axis on the right); *2* - for resonant frequency 2.6 kHz (ordinate axis on the left)

Since in the experiments the geometric dimensions of the model objects were commensurate with the wavelength of the radiation used (ÿ = 12.6 cm), it seemed important to experimentally study the nature of local field inhomogeneities inside volumes. The possibility of the occurrence of such inhomogeneities due to focusing was justified in a number of works [134–137], and J. Lin used the condition focusing EMF in your model.

In the “thermoelastic” concept of J. Lin [121, 138], this moment is considered as fundamental and determining the modes of excited mechanical vibrations. And although the results obtained in an experiment on excitation of mechanical vibrations in a test tube with liquid [119], showed that the vibration modes are classical acoustic picture [139], the case of irradiation of a sphere with dimensions comparable to the wavelength needed verification.

To create areas of absorption of electromagnetic energy with different volumes and sphere geometries inside a liquid sphere was irradiated in two ways - with a rectangular waveguide with a cross-section 10 × 72 mm2 and a rectangular horn 90 × 120 mm2.

The distribution of absorbed electromagnetic energy in a spherical volume was determined by measuring the temperature of the liquid inside the sphere and using the probe method based on the magnitude of the microwave voltage induced on it, followed by its detection.

Registration of the frequencies of excited mechanical vibrations in a sphere with a diameter of 105 mm showed that (with an error within 1-2%) frequencies of excited oscillations when irradiating a sphere with a waveguide and the speaker coincide. Special definition of the field pattern inside liquid was not carried out, but it is quite obvious that during irradiation under conditions of equality of power input to the irradiator the horn and waveguide must form different absorption regions electromagnetic energy - both in shape (due to different geometry of the end of the irradiator) and in size (due to different PPM).

Comparing the obtained results of excitation of mechanical oscillations by microwave pulses with equal conditions for their excitation using a laser [75], it can be assumed that the dimensions of the energy absorption region can be decisive only if the medium is semi-infinite, i.e. e. at least there is no reflected

acoustic wave. If the medium is limited (the case we are considering), then the frequency of excited mechanical vibrations will be determined by the dimensions and geometry of the bounding volume, and the the region of energy absorption can only be considered as a source of external disturbance having a wide spectrum of frequencies. About, that when spheres are irradiated by various irradiators, absorbing areas different in size and shape, he says fact that in the case of irradiation of a sphere with a waveguide having a smaller cross-section compared to the horn and, accordingly, a significantly larger MRP value, amplitude of recorded mechanical vibrations was significantly higher. The fact that when a limited volume is irradiated by various irradiators, the resonance frequency of the volume is determined only by its size, is indicated in [132, 140].

The temperature distribution was measured during irradiation spheres with diameters of 105 and 185 mm and a cylinder with a diameter of 185 and height 65 mm, filled with ethyl alcohol and 1 M NaCl solution. Time irradiation varied from 15 s to 5 min. Temperature measurement was carried out immediately after turning off the field at three points: in the layer liquid located directly in front of the emitter, at the center and point diametrically opposite to the first. To avoid error associated with temperature equalization throughout the volume measurement time (ÿ 10 s), the procedure was repeated three times so that Each time the sequence of temperature measurements at the selected points was different. It turned out that the uneven heating across diameter of the spherical volume is of the order of 2.5ÿ, and The greatest heating occurs near the emitter and decreases as moving away from him. Thus, the experiments did not reveal concentrations of electromagnetic energy in the center of the spheres - the so-called “hot spots” mentioned in the work of J. Lin [121].

Measuring the distribution of the electromagnetic field strength inside the liquid filling the sphere showed that the field maximum close to the emitter and decreases exponentially as moving away from him. Since the relative change in the electromagnetic field strength was measured, the disturbance introduced by the probe was neglected. The amplitude values of the detected pulses when the antenna is located at the wall of the bulb adjacent to the emitter, in the center of the bulb and at the wall, as far as possible from emitter, the ratio is 1: 0.5: 0.2.

The absence of concentration of electromagnetic energy in the liquid spheres used was confirmed by an experiment with different methods excitation of mechanical vibrations in a cylinder with a diameter of 185 mm

and height 65 mm. In the first case, the emitter was located on the side of the cylinder. In the second case, irradiation was carried out from above, i.e., focusing conditions were excluded. There were no significant differences in the parameters of the excited mechanical vibrations, i.e., in both cases the same vibration modes were excited if the EMF parameters coincided. The same picture occurred when a cylinder with a liquid with a diameter of 60 mm and a height of 200 mm was irradiated from above and from

the side by various irradiators and at different frequencies (915 and 2375 MHz). In all cases, the frequencies (modes) of excited mechanical vibrations corresponded to the calculated ones. The measured temperature distribution over the volume of the cylindrical model also did not allow us to identify any characteristic temperature rise associated with the value of the model radius or the dielectric constant of liquids.

The experimental data obtained make it possible to exclude the condition of concentration of electromagnetic energy as necessary for excitation of mechanical vibrations in a closed volume by microwave pulses. In accordance with this, it does not seem necessary to consider the center of the sphere as a source of mechanical vibrations excited in the liquid. The location of an antinode or pressure node in the center of the sphere depends on the degree of connection of the sphere with the external environment, i.e., on the boundary conditions.

Thus, in these experiments, as well as in work [141], carried out on the heads of animals, no predominant concentration of electromagnetic energy was found in the center of the irradiated objects. In Fig. Figure 4.20 (1–4) shows the distribution of pressure amplitudes in glass spherical flasks filled with

ethanol, obtained using acoustic probes. Acoustic probes (Fig. 4.21) are a hollow glass tube, open at the top. The lower end of the tube is expanded. A piezo-electric transducer with a diameter of 10 ÷ 12 mm is attached to the end of the tube using glue. The coaxial cable connecting the converter to the amplifier is routed through a glass tube. The sound field pattern is determined by measuring the amplitude of excited mechanical vibrations along the diameter of the bulb from the base of the neck to the bottom. The measurements were carried out in a flask with a diameter of 105 mm with a step of 5 mm. The graphs are plotted for four frequencies of excited mechanical vibrations - 3; 6; 8.5; 11.3 kHz. The results obtained are in good agreement with calculations for the wavelengths of mechanical vibrations excited in the flask. So, for a frequency of 6.1 kHz at a speed of sound in ethanol equal to 1.18 × 105 cm s ÿ1, the wavelength is 20 cm, i.e., half the wave should fit in the flask. The resulting graphs show that, regardless of the irradiation method, in the center of the flask there can be an antinode,

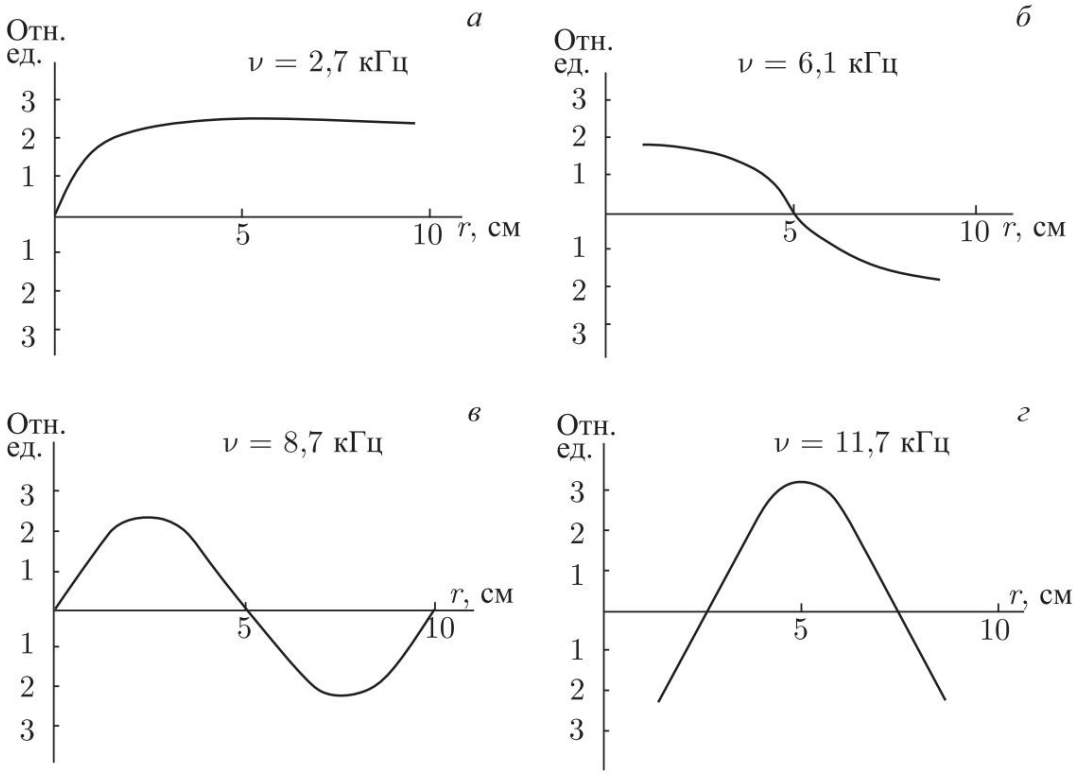

Rice. 4.20. Amplitude dependences of acoustic pressure in spherical flasks with ethanol for different frequencies: *1* - f = 2.7 kHz; *2* - f = 6.1 kHz; *3* — f = 8.7 kGc; *4* — f = 11.7 kGc

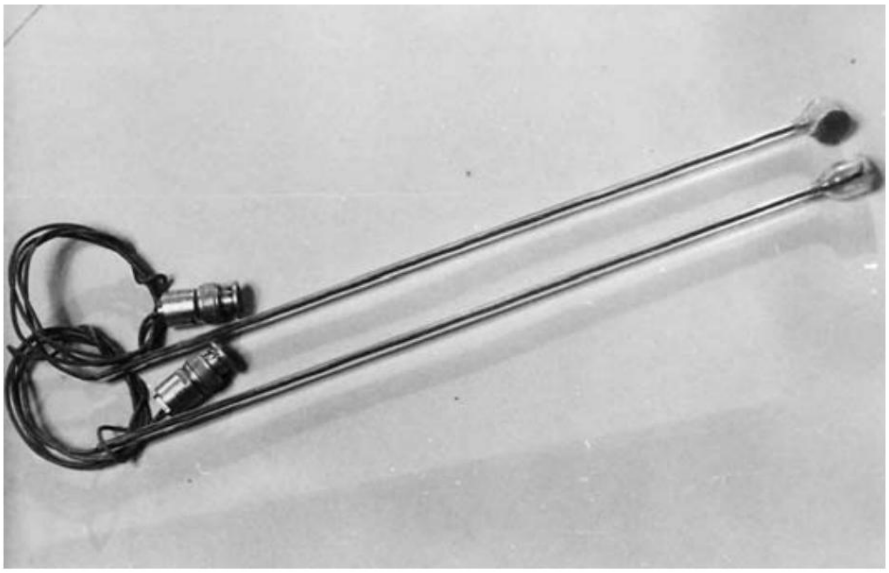

Rice. 4.21. Acoustic probes

and the pressure unit. The validity of this conclusion is indirectly confirmed in [133, 142].

To calculate the maximum pressure occurring in a liquid
when it absorbs pulsed electromagnetic energy, we use the expressions obtained by L. Garney [59]:

$$Pc_{max} = \frac{C\ddot{y}Io}{2JS}\ (1\ \ddot{y}\ e\ddot{y}\ddot{y}C\ddot{y}\ddot{y}\ ) \qquad (I.40)$$

for a free border and

$$Pz_{max} = \frac{C\ddot{y}Io}{2JS}\ (1\ \ddot{y}\ e\ddot{y}\ddot{y}C\ddot{y}\ddot{y}/2\ ) \qquad (I.41)$$

for a fixed boundary, where the notations are the same as in the expressions Chapter 2. Since both extreme cases are mathematical
idealization, and real physical objects can be attributed to one or another only with varying degrees of accuracy, calculations
it is advisable to produce according to both formulas, thereby obtaining boundary values. If we denote the expressions for Io in the formula (I.40) as Kÿ, and in formula (I.41) - Kÿ, then, accordingly:

$$Pc_{max} = KcIo \text{ and } P\ddot{y}_{max} = KzIo.$$

For alcohol under the conditions under consideration and ÿi = 20 ÿs - Kÿ =
= 9.1 dyn · Wÿ1, Kz = 8.0 dyn · Wÿ1. Simultaneous use
CGS and SI units is explained by the fact that for convenience in calculations when dimension [Io] = W cm ÿ2 we need to obtain the dimension [Pmax] in dyn cmÿ2. In the vast majority of PPM experiments
taking into account 50% reflection ranged from 15 to 70 W cm ÿ2. Consequently, the pressure arising inside the spheres filled with alcohol should reach values ranging from 120 to
650 dyne cm ÿ2. These values are calculated similarly for aqueous solutions of NaCl, based on the acoustic and electrical characteristics close to the brain substance [143]. For a concentration of 0.125 M, at
which ÿ = 63 mÿ1 [143], Ks = 1.0 dyn W ÿ1, and Kz = 0.73 dyn W ÿ1,
and for the same PPMs, the pressure values will be in the range from 10 to 70 dynes cm ÿ2. These values are in good agreement
with our own experimental data. Indeed, the signals had amplitudes of tens to hundreds of millivolts and up to 1 ÷ 2 V in some cases. Taking into account the sensitivity of the recording system
(10ÿ5 V dyne ÿ1 cm2) resonance characteristics of spheres and Kÿ = 37 or 500 depending on the amplitude of mechanical vibrations and type
recording device, a fairly good match is obtained
in orders of magnitude. Let's demonstrate this with a specific example:
related to the experiment to determine the dependence of the amplitude of excited mechanical vibrations on the PPM. When irradiating a glass flask with a diameter of 105 mm at the natural frequency
resonance 11.8 kHz at Kÿ = 500, ÿÿ = 20 ÿs and measured incident PPMi = 26.8 W cm ÿ2, the voltmeter readings were 240 mV.
The voltage amplitude across the sensor is therefore 1344 μV
and pressure - 1344 dyne cm ÿ2, and taking into account the quality factor (ÿ 10) the pressure

from a single pulse should be about 130 dynes cm ÿ2. For a resonant frequency of 2.6 kHz from the same example - Ku = 37, voltage
according to the voltmeter - 43 mV, we find that the pressure on the sensor at the same The PPM and quality factor will be an order of magnitude lower, which is in good agreement with J. Lin's data calculated for a single pulse.

When determining the resonant frequencies of specific spherical volumes, we proceeded from preliminary calculations using formulas for spherical resonators [116] and a Helmholtz resonator [53].

Calculation using the formula for a Helmholtz resonator:

$$fp = \frac{C}{2ÿ}\sqrt{S/lV},$$

where fp is the resonant frequency, C is the speed of sound in the medium filling the resonator, S is the cross-sectional area of the throat, l is the height of the throat, V is the volume of the resonating medium having the lowest frequency value,
for a sphere with a diameter of 105 mm, a neck height of 20 mm and a diameter of 30 mm, filled with ethyl alcohol, gives a value of the order of 1.4 kHz. In the experiment, the minimum frequency for the flask at different fillings
throat (from the level of the sphere to the cut of the throat) changed accordingly from 1735 to 913 Hz, which does indicate a strong dependence
resonance properties on the degree of filling of the neck of the flask.

As stated earlier, the amplitude of excited mechanical
oscillations are maximum at a pulse duration equal to half
period of oscillation of a given frequency. However, the limits within which the pulse duration can be varied are determined by the achievement of the meander mode. Based on the above conditions, the initial pulse duration (about 400 ÿs) and the range were selected

searching for a low resonant frequency. For a sphere with a diameter of 105 mm the resonant frequency was 1238 Hz. With an increase in the repetition rate of microwave pulses at the moment of occurrence of mechanical oscillations in the sphere, both the frequency of exciting pulses and the frequency of excited oscillations were recorded by a frequency meter. Data
of this experiment are summarized in table. 4.3. It is important that fluctuations
arose not only in the case of equality of frequencies, but also when
the pulse repetition frequency was equal to the resonant subharmonic
sphere frequencies. Dependence of the amplitude of excited mechanical
oscillations from the pulse repetition rate equal to the numbers of subharmonics are shown in Fig. 4.22.

Comparison of the obtained data with data on determining the resonant frequencies of mechanical vibrations in ideal spherical
resonators shows that the presence of a non-harmonic range of frequencies,
registered in the experiment is the result of the discrepancy between the model under consideration and the ideal resonator. Presence of a throat in the flask
leads to the formation of a complex system of coupled resonators -
cylindrical and spherical - with varying degrees of connection, depending on the level of liquid in the neck of the flask. It should be noted that when

Table 4.3

The frequencies of excited mechanical vibrations at various parameters of microwave pulses

Frequency trace- niya im- pulsov EMI, Hz	Frequency excited- fur- nic hesitation, Hz	Duration- ness impulses EMI, ÿs	Frequency trace- niya im- pulsov EMI, Hz	Frequency excited- fur- nic hesitation, Hz	Duration- ness impulses EMI, ÿs
23	1238	400	8270	8270	
24	1238	Same	9030	9030	25
			9190	9190	
			9310	18620	
54	1238	—»—	9640	19280	
56	1238	—»—	10050	10050	
			10700	10700	
80	1238	—»—	11020	11020	
95	1238	—»—	11140	22280	
			11220	11220	
177	1238		11490	11980	
206	1238		11820	11820	
			12030	12030	
619	1238		12900	12900	
1238	1238		13100	26200	
1710	3420	300	13130	52520	
1750	5250	100	14070	28140	
2280	6840		14650	29300	
2625	5250		14660	29320	
2925	5850		16670	16670	
3160	6320		16940	16940	
3420	3420	70	17170	17170	
4460	4460		19280	19280	
4600	4600		19810	19810	
5250	5250		20040	20040	15
5850	5850		20450	20450	
5920	5920		20960	20960	
6320	6320	50	21340	21340	
6410	6410		21930	21930	
6610	6610		22280	22280	
6840	6840		22440	22440	
7290	7290	40	22980	22980	
7410	7410		23120	23120	
7560	7560		25380	25380	
8060	8060				

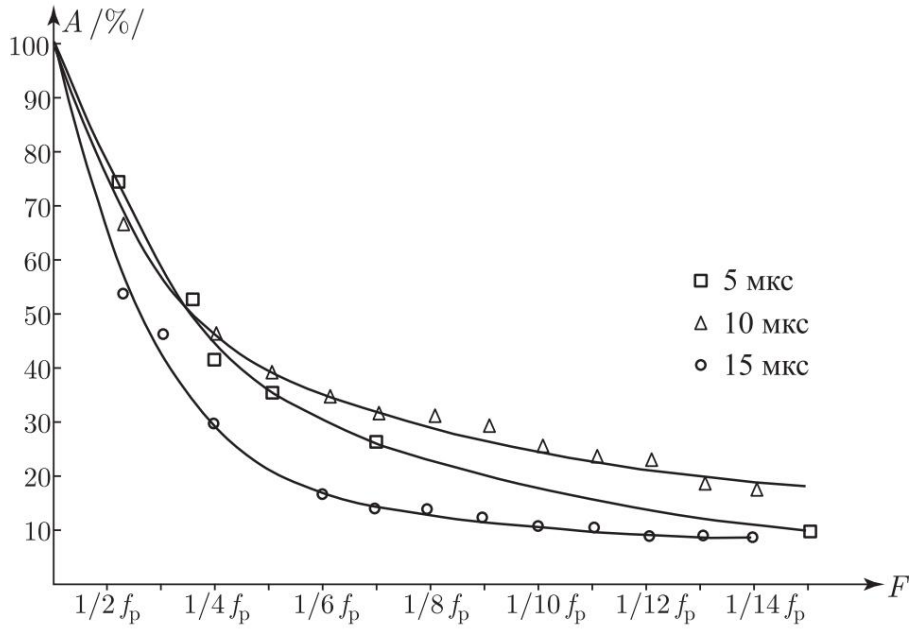

Rice. 4.22. Dependence of the amplitude of excited mechanical vibrations on the pulse repetition rate: *1* - 5 µs, *2* - 10 µs, *3* - 15 µs. Pulse repetition frequency fi = fÿ/n, where n is the frequency subharmonic number resonance

extrapolation of the obtained experimental data to the full-scale radio sound effect must be taken into account more complex geometry human head and the presence of inhomogeneities. It is obvious that in real conditions, this should lead to an even denser range of frequencies, the perception of which should be limited above the high-frequency the hearing limit of each individual. In Fig. 4.23 shows oscillograms of excited mechanical vibrations in a spherical resonator, demonstrating the transformation of the frequency of these oscillations when changing the duration of EMR pulses.

The results obtained suggest that the factors determining the range of mechanical vibrations excited in the sphere (human head) and recorded (perceived by the organ of hearing) are, first of all, the duration of microwave pulses and their repetition frequency. This explains the reason why the subjects experienced a sensation of sound that was higher in frequency than the repetition frequency pulses in early work on radio sound, in which experimenters used short pulses to modulate microwave radiation.

Thus, we can come to the conclusion that the excitation mechanism both low-frequency and high-frequency mechanical vibrations have a single physical nature associated with absorption electromagnetic energy from head tissue or working fluid, and manifests itself in one form or another depending on the parameters external influence. The formation of an auditory image in humans goes the same way as normal sound is perceived with defects

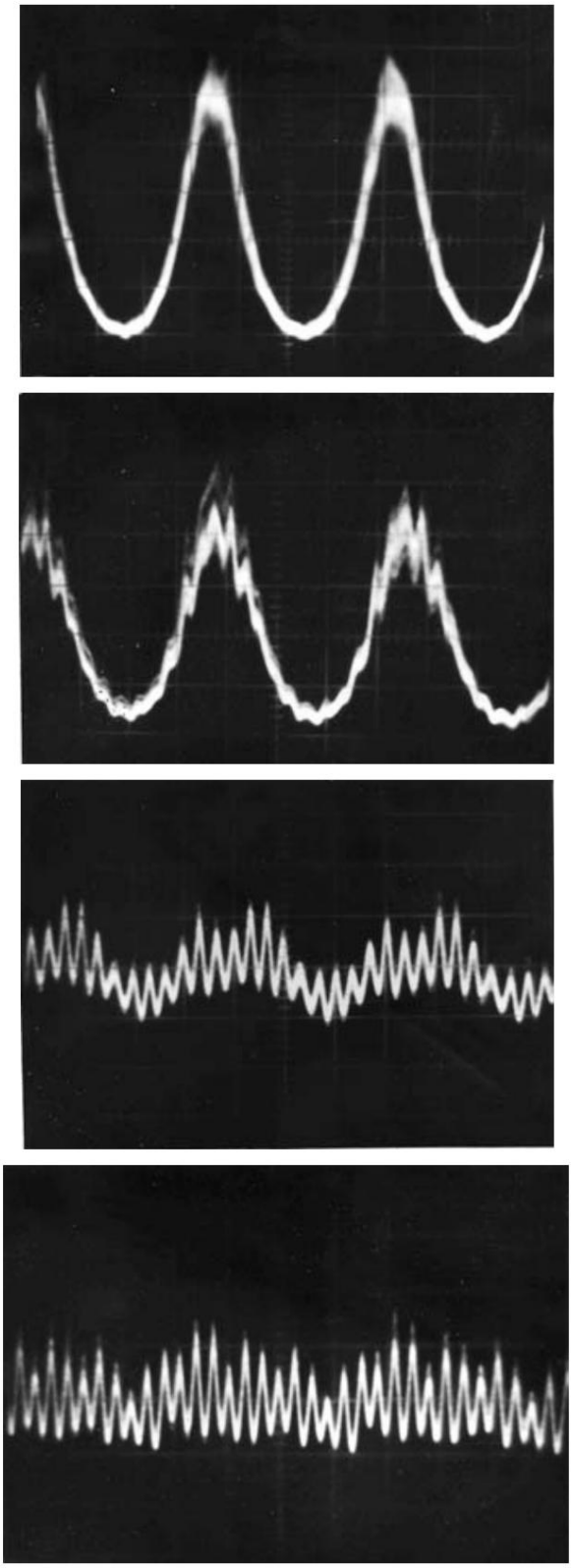

Rice. 4.23. Change in the frequency of excited mechanical vibrations in ethanol with a change in the duration of the microwave pulse. *1–4* —reducing the duration of the microwave pulse. Oscillograms obtained at the same speed oscilloscope beam sweep

middle ear (otosclerosis) or as under water, i.e. through bone conductivity.

The question of the possible value of the frequency and quality factor of the mechanical resonance of the head as an acoustic resonator when mechanical vibrations are excited in its tissues by pulses up to the present time remains open. The ratios C/2a and 1.44C/2a given in the works of J. Lin to determine possible values mechanical resonance frequencies of heads cover a range of frequencies of the order of 7.5–10.8 kHz for a sound speed of 1.44 105 cm s ÿ 1 and a = 9 cm, where a is the radius of the head. On the radio sound threshold curve the indicated range is often limited below by the area of maximum sensitivity threshold, above - minimum. That is, if we move on to a curve equal to the volume of radio sound and consider it as the amplitude-frequency response (AFC) of some resonant system, then these areas will have diametrically opposite properties - minimum and maximum coefficients signal transmission. Such inconsistency does not allow us to accept such a wide range of possible frequencies of mechanical head resonance. On the other hand, a wide range of mechanical vibrations excited in spherical resonators with a high quality factor (about 300-500), allows you to determine any of frequencies as the main one and compare with one or another characteristic frequency on the radio sound threshold curve. Based on data [52, 116], it can be assumed that the quality factor of the head as an acoustic the resonator should be low.

4.2.2. The human head is like a multimode acoustic resonator.

Bone-tissue audiometry in a wide frequency range.

The problem of determining the resonant characteristics of the human head stems from the need to introduce into the thermoelastic concept the final value of the mechanical quality factor and experimentally find the value of the resonant frequency of the head as an acoustic resonator or show the possibility of the existence of a multimode system.

The author of the thermoelastic model himself, apparently, proceeded from his own general ideas regarding the resonant properties of the head, although there are theoretical ones on this issue [145–148, 132], as well as experimental works [149, 150]. A serious disadvantage of both is their remoteness from the real object.

In theoretical works, models are considered as as a rule, spherical shells of varying degrees of rigidity, filled with liquid, and in experimental resonance characteristics studied on dry turtles. There are also audiometric studies in which the detected resonances made sense to some anomalies in the speed of sound wave propagation (deviation from linear dependence) [151, 152], but they were carried out at frequencies

not exceeding 4 kHz. The work [153] was carried out on animals and not can claim generality, since it was carried out under unusual conditions.

It was natural to assume that the resonant characteristics of the head should influence the perception of sound through bone conduction. In any case, one could assume the presence of some features in the bone conduction audiogram

at the frequency(s) of mechanical resonance of the observer's head. The need to conduct such studies was dictated by the fact that analysis of the literature on bone tissue audiometry did not give the desired information. Much of the research is limited by frequency, not exceeding 5-6 kHz [149, 151–156], or dedicated to the ultrasonic range [157, 158]. The same jobs where one way or another the range of interest to us is presented (4–12 kHz) [159–166], not could provide the necessary information, since traditionally bone-tissue audiograms were taken at points spaced apart either by an octave, or by a value not less than 1–2 kHz, in conditions asymmetrical supply of sound to the mastoid. We need was to have a threshold curve for the frequency range 4–12 kHz taken with a step of no more than 200 Hz. This condition was dictated by the fact that on the threshold curve of radio sound (see Fig. 4.01) the slope of the threshold in the region frequencies 6–8 kHz reaches 60 ÷ 90 dB· octÿ1.

Today there is practically no uniform methodology audiometry of bone conduction thresholds, no GOST and advanced specialized equipment. Most often, in clinical settings, airborne audiometry units are used, and special vibrators are used as a sound emitter. structures, appropriately calibrated [154, 155, 159–161, 163].

The sound emitter was an acoustic vibrator is used, which is a battery of piezocrystals made of Rochelle salt, enclosed in duralumin a cup with a diameter of 30 and a height of 50 mm and filled with epoxy resin. The amplitude-frequency characteristics of this emitter, shown in Fig. 4.24, filmed

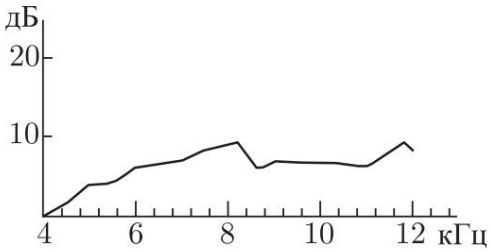

Rice. 4.24. Frequency response of bone phone

on acoustic control equipment from Brühl and Kjer (measuring microphone type 4145, measuring amplifier type 2606) in an anechoic box with an input voltage of 1.5 V.

All audiometric measurements were performed inside a cubic room with a side of 2.8 m. In addition to the subject, only the operator was in the room. The walls of the room are lined with foam concrete, The floor is covered with foam rubber mats. Ambient level

noise, measured using the MKE-2A measuring microphone, is not
exceeded 25 dB relative to the APS. The GS-100I generator was used as a source of
alternating audio frequency voltage
with high stability of the output voltage amplitude (about
1 ÷ 2%) over the entire range of frequencies used. The output voltage was controlled by the
operator using a VZ-33 voltmeter, frequency -
using a frequency meter ChZ-34. The sound emitter was applied with its flat bottom to the
subject's forehead at a point located in the sagittal plane and 1–2 cm from the border of the
hairline,
and was fixed in this position with a rubber belt for the entire procedure. At the same time,
the pressing force was maximum, at which
the subjects did not experience any unpleasant sensations, which, according to the data
[161], leads to increased stability of results. To avoid
fatigue of the subject, the procedure for measuring thresholds did not continue
more than 30 minutes, and repeated measurements were carried out no earlier than after
2–3 days. To prevent over-the-air listening and influence
extraneous noise, the subject's ears were covered with noise-protection
headphones type VTSNIIOT-2M (NP 45 × 7), the damping ability of which in the frequency
range 1–8 kHz is within
22–45 dB.

The subject was seated in a chair in a comfortable position. In the left hand
he had a push-button breaker, and with his right hand he could freely
manipulate the output voltage regulator of the sound generator. With the breaker open, the
operator set the frequency
output signal, monitoring it using a frequency meter. Then the subject
slowly increased the output voltage from zero level (the regulator in the extreme position)
until the appearance of auditory
Feel. At the same time, for greater reliability of recording the presence of sound [169], he
closed and opened the breaker,
pressing the button and releasing it. At the moment of feeling
sound, the subject gave a signal to the operator, who recorded the voltmeter readings and
adjusted the frequency of the output signal of the generator, after which the procedure was
repeated. Thus, in one
session, 41 points were taken in the range from 4 to 12 kHz with a step of 200 Hz.
A total of 6 men aged from 22 to
35 years, 5 of which did not have any significant deviations
from normal hearing, and one subject had a noticeable decrease
sensitivity in the frequency range above 8 kHz.

The audiograms of the subjects were constructed based on 3–5 trials after
preliminary averaging at each point and taking into account the characteristics of the bone
phone. In Fig. 4.25 all 6 audiograms are presented
under numbers corresponding to the numbers assigned
to the test subjects.

Even with the most superficial examination, it can be noted that
Each audiogram is highly individual. It follows that it is impossible to build a general audiogram
for

“average” subject, since in this case the characteristic features are inevitably leveled out,

belonging to each audiogram separately. This circumstance Apparently, this is one of the main reasons for the “smoothness” of the vast majority of audiograms cited in the literature. Interesting,

that in work [149] the authors especially note the uniqueness of the resonant characteristics of dry skulls. With another On the other hand, despite their individuality, all audiograms have an unconditional similarity, such as similarity of shape. The similarity lies in the presence alternating rises and falls in sensitivity, and the position of extreme mov on the frequency axis and their relative The magnitude makes each audiogram different from the others. About similarities and the differences between individual audiograms can be judged from Fig. 4.25, in which, for greater clarity, zones of increase and decrease in The sensitivity horns are highlighted with oblique shading, and the lines connecting the corresponding features are indicated in lowercase letters.

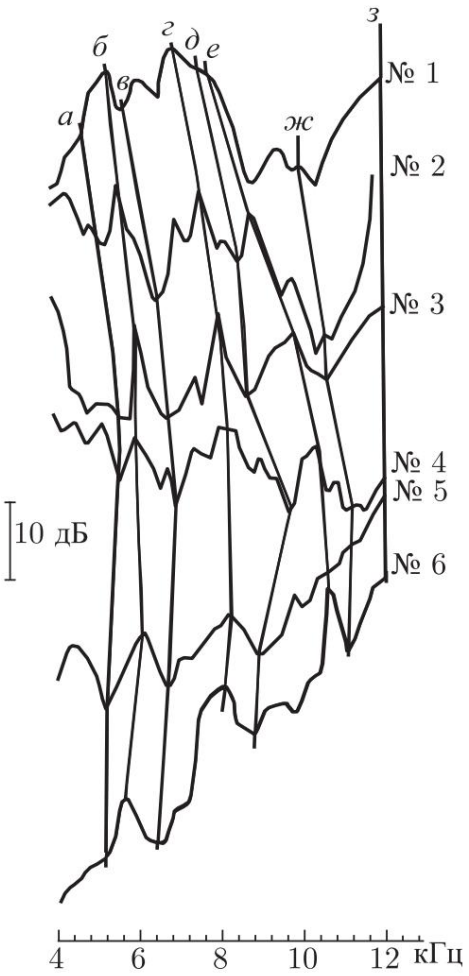

Rice. 4.25. Bone tissue human audiograms

A detailed analysis of the above figure, apparently, can give interesting information for specialists in the field of physiology and pathology of hearing. The most important thing is that audiograms have view of resonance-like curves with highlighted areas of increase and decreased sensitivity. This gives us reason to believe that and the appearance of the radio sound threshold curve (see Fig. 4.01) is largely degree is due to the sensitivity characteristics of the bone conduction, which, in turn, is most likely formed by the resonant properties of the bones of the skull and head as a whole.

In any case, the threshold rise (up to 20 dB), observed at all audiograms in the zone “c”–“d” with a maximum along the line *“d”* in the area 7–8.5 kHz, and a significant reduction in the threshold (up to 35 dB) in the “e”–“z” zone with the minimum line *“zh”* at frequencies of 10–11 kHz correlate very well with similar features on the radio sound threshold curve.

The main conclusion that can be drawn from experiments on audiometry of hearing thresholds by bone conduction, is that that the human head can be considered as a multimode resonance

torus, this is manifested in the nature of audiograms recorded using
the minimum possible frequency step. It is obvious that the features
in the perception of sounds by bone conduction also influence
nature of perception of radio sound.

4.3. Double-circuit resonant model of radio sound

The concept of a two-circuit resonant model. For analysis
threshold curve of radio sound and attempts to describe it by physical
characteristics of the anatomical structures of the head and their interactions during the
excitation of mechanical vibrations, we will use the terms and categories of quadripoles and
operate
with a mirror image of the radio sound threshold curve - curve
equal to the volume of radio sound, i.e. we will operate with a certain frequency response
resonant system.

As can be seen from Fig. 4.01, the frequency response of such a system has two frequencies
maximum, which may correspond to mechanical resonance
cranial tissue, which occurs at a pulse repetition rate
equal to the natural frequency and subharmonic. Moreover, the maximum corresponding to the
low pulse repetition rate breaks up into two less pronounced maxima, which appear at

pulse repetition frequencies equal to subharmonics. Basically,
a single oscillatory signal can have an amplitude-frequency characteristic that qualitatively
coincides with the threshold curve of radio sound
circuit. When applying external disturbance pulses to such a circuit
damped oscillations will be excited in it. However, you can immediately
postulate the following:

1) When applying pulses to a single oscillatory circuit
external disturbances in the circuit excite shock oscillations
with a frequency close to the natural frequency of the circuit.

2) The frequency response of a single circuit has one maximum at its own resonance
frequency with gentle slopes in both directions from this frequency. Qualitative coincidence of
the frequency response of a single circuit with shock
excitation and a curve equal to the volume of radio sound is explained
interference between damped oscillations excited
external impulses.

On the other hand, analysis of the graphs given in [5] shows (see Fig. 4.01 and 4.02) that
if we take the resonance frequency
frequency value is 10–11 kHz, then the maximum threshold on the curve of the dependence of
this value on the pulse duration should correspond to a pulse duration equal to the period of
the excited
mechanical vibrations, i.e. 90–100 ÿs. However, from these graphs
it can be seen that the threshold maximum is shifted to 120 μs, i.e. it corresponds to
frequency of excited oscillations close to 8 kHz.

The same can be said about the minimum threshold on this curve, corresponding to a
pulse duration close to 60 ÿs and equal to half

due to a period of excited mechanical vibrations. In the same time
the minimum threshold region on the radio sound threshold curve corresponds to a pulse repetition frequency of 10.5 kHz, which naturally leads to the assumption of the presence of resonance at this frequency.

Correspondence of resonant frequencies of single-circuit radio sound models to the range of possible values of mechanical resonance of the head
(see section 4.2) creates certain conveniences when setting up an experiment. Analysis of the amplitude dependences of the sound pressure of mechanical vibrations excited in a liquid by EMR pulses showed that
that at a resonance frequency of a liquid column equal to 10 kHz, the ratio of sound pressure amplitudes at pulse repetition frequencies,
equal to 5 and 10 kHz, in the model experiment it is significantly more,
than the length of the same frequency values on the radio sound threshold curve.
In this case, the frequency of 5 kHz is considered as a subharmonic due to the monotonal nature of the auditory sensation in a full-scale experiment
at a frequency of 10 kHz and highlighting the first harmonic of the repetition frequency pulses, also equal to 10 kHz, in model experiments. Steep
(up to several hundred dB octÿ1) decrease in sound pressure amplitude
at a pulse repetition frequency of 7.5–8 kHz, in the model
The experiment can be explained by the presence of a high quality factor of the single-circuit models used in the model experiment. Availability
can hardly have such a quality factor in a full-scale experiment
place, at least due to the large values of viscosity and attenuation
in the tissues of the head compared with those for working fluids.

To determine the quality factor of the head as an acoustic resonator, let's move on to a curve equal to the volume of radio sound and apply
a well-known technique for determining the quality factor of a resonant circuit. Let us use the well-known expression for the amplitude of steady-state
oscillations in the resonant circuit:

$$X = \frac{K}{Is} = \frac{F}{\sqrt{f^2 \cdot f_p^2/Q2 + (f_p^2 \ddot{y} f\,2)2}}.$$

where K is the signal transmission coefficient at frequency f, Ko is the signal transmission coefficient at frequency fÿ, F is the disturbing force. We get expression for the quality factor of the circuit near the resonance frequency:

$$Q2 = \frac{1 \ddot{y} X2\, f^2}{X2\,(1 \ddot{y} f^{2)2}}.$$

From the condition F = 1 with Xmax = 1 for f = fÿ, and at the point f = fp,
fp = 1. From the radio sound threshold curve for points fp = 5.5 kHz
and f = 1 kHz (selected arbitrarily) the amplitude of oscillations in this
point is 5.4 dB less than at point f = fÿ, i.e. X = 0.53. Wherein
f = 0.18 (fÿ = 1). Substituting the values of these quantities into the expression for quality factor of the circuit, we obtain the value of this quantity for the first
contour, close to 2. The same result can be reached by re-

using data on sound pressure amplitude attenuation
acoustic wave in brain tissue [171]. For comparison, we point out that
the value of the quality factor given in [33] for the head of a dolphin, both for
oscillatory system with lumped parameters is
2–3, which is in good agreement with the results obtained. With another
side, the slope of the threshold increase on the radio sound threshold curve
in the frequency range 7.5–8 kHz is 60–90 dB octÿ1, which indicates a high
quality factor of the resonant system under consideration, which also cannot be
achieved for a single-circuit resonator at
specified quality factor. The authors come to similar conclusions
work [58|.

If we assume that the threshold curve of radio sound is the result of pulsed
excitation of a single-circuit system, then it is not difficult
show that in this case the difference in amplitudes at the fundamental frequency,
equal to 10 kHz, and at the subharmonic frequency (respectively 5 kHz) not
should exceed 2 dB, whereas on the radio sound threshold curve
the corresponding points differ by more than 4 dB.

However, the main circumstance that does not fit
within the framework of a single-circuit resonant model, which generally
describes the phenomenon of radio sound well, are the results of experiments
by audiometry of auditory thresholds by bone conduction of sounds.
On all audiograms in the frequency range 7–8.4 kHz there is a rise
threshold by 5–25 dB relative to the threshold at 9–10 kHz and by approximately
5–10 dB relative to 5.5–6.5 kHz. Explain threshold rise
on audiograms in the same frequency range as at the threshold
radio sound curve, within the framework of a single-circuit resonant model is not
seems possible. In order to eliminate these contradictions, it is necessary to
state not only the formal similarity
threshold curves in Fig. 4.01 and audiograms of hearing thresholds according to
bone conduction in Fig. 4.25, but also to assume that both of them characterize
the resonant properties of the system that perceives
bone sound, and radio sound, actually being the double-hump of an frequency-
frequency mechanical resonator. At the same time, one cannot ignore the data
work [152] on direct recording of mechanical vibrations inside
heads of dead animals when irradiated with EMR pulses, where
it was shown that the head, in this experimental setup, is
monofrequency resonator with a resonant frequency corresponding
resonator with free boundaries - fÿ = C/2a.

Consider a system of two coupled oscillatory circuits,
having equal natural frequencies. It is known that the shape of the AFC single
circuit is determined by its quality factor, the shape
The frequency response of connected circuits is also a coupling coefficient. In Fig. 4.26
[170] provides a family of frequency response characteristics of two connected circuits with equal
quality factor and different values of the coupling coefficient. As seen
from the figure, with a strong connection, i.e., with K>Kcr, the frequency response has two
frequency maximums, called communication frequencies.

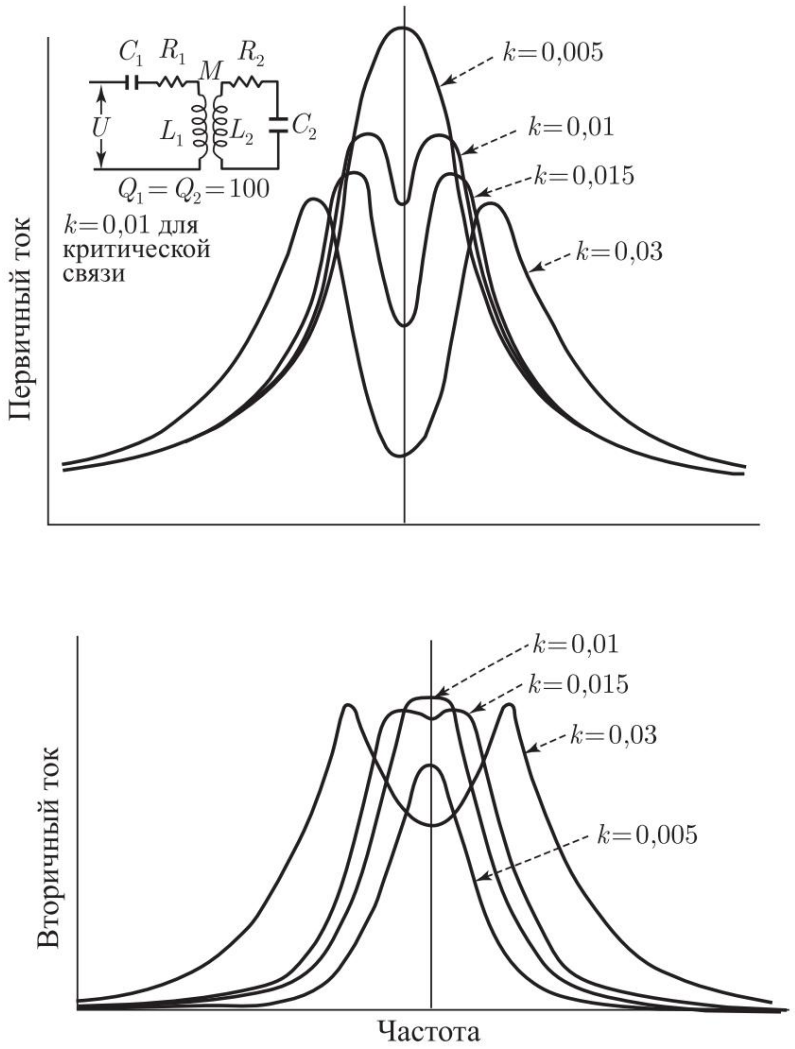

Rice. 4.26. Frequency response family of two connected circuits with different coupling coefficient (borrowed from [170])

If we excite a system of two connected circuits with a degree connection, above critical, with a short pulse, then in this system short damped oscillations will occur with two different frequencies close to the communication frequencies. As a result of transient processes In such a system, beats also occur, which last even after removal of external excitation.

Thus, the frequency spectrum of oscillations generated by a system of two coupled circuits when excited by a short rectangular pulse is significantly richer compared to a single outline

When the connection is equal to the critical one, the dual-circuit bandwidth systems are more than three times wider than a single circuit with equal quality factor, i.e. ÿf2ÿ = 3.1fp/Q, where fÿ and Q are the resonance frequency and quality factor of a single circuit. With further increase coupling coefficient “dip” at the resonance frequency increases

and the resulting double-humped curve is characterized by
two passbands, i.e. the total passband
frequencies are even wider. The main advantage of a dual-circuit system
in this case, the quality factor increases with the expansion of the band
transmission, which helps to increase the steepness of the frequency response slopes.

A qualitative comparison of the frequency response of a two-circuit system with a coupling coefficient K>Kcr with the threshold curve of radio sound leads to to the assumption of the possibility of the existence of a real two-circuit system. However, this comparison allows us to make
and the following conclusion. Symmetry of frequency response shape relative to frequency resonance is due to the equality of the quality factors of both circuits and their resonant frequencies. This means that the asymmetry of the radio sound threshold curve, interpreted as the frequency response of a double-circuit oscillatory system, is the result of the presence of two connected circuits with different quality factors and different values of resonant frequencies [170]. In this
connection, it is necessary to take into account some properties of circuits with low quality factor.

To prove the existence of a two-circuit system that explains the effect of radio sound, the assessment of the quality factor of both circuits has
of paramount importance.

This concerns, first of all, determining the value of the coupling coefficient. We will evaluate this characteristic based on information
about the amplitude-frequency properties of the periphery of the hearing organs and the threshold curve of radio sound.

It is first necessary to consider the possibility of
or another structure of the human head to play the role of an equivalent second circuit. The resonant model is taken as the first circuit
J. Lin with resonance frequency fp = C/2a, where C is the speed of sound
in brain tissue, a is the radius of the head. It can be immediately noted that due to similar impedance values of biological tissues, any structure,
chosen as the second resonator will be quite strong
connected to the first resonator. However, this situation leads to a paradox - it is impossible to allocate a smaller volume within a certain volume
with a sound speed value equal to or close to the same value
for a larger volume that has the same frequency as it. Wherein
it is assumed that the densities of matter in both volumes are close or
equal to each other.

A way out of this situation can be found if we assume the presence inside the skull of a structure that meets one of the following conditions:

1) the speed of sound in the structure is different from the speed of sound for other brain tissues due to the presence of certain specifics of the selected structure;

2) the speed of sound in the structure is different from the speed of sound for the remaining volume so that the ratio C/2a for the selected structure

has the same numerical value as for the entire volume absorbing electromagnetic energy as a whole.

Analysis of the literature data shows that at least three anatomical structures of the skull can be identified as a structure that meets one of the requirements - the cochlea, the frontal sinuses and the mastoid. The snail is characterized by a variable elastic modulus along its length. Considering that the speed of sound is determined by the relation C = (where ÿ is the elastic modulus, ÿ is

$$\sqrt{\frac{m}{r}}$$

density) and that the compliance of the cochlea membrane (the reciprocal of the elastic modulus) along its length varies 100–1000 times [172], it is possible, within the rather small size of the cochlea of the hearing organ (length about 35 mm), to obtain points with the speed of sound, sharply different from the value of the same value for brain tissue. If we consider certain air cavities as the second resonator (in air the speed of sound is almost 4 times less than for biological tissues - 0.33 × 105 cm s ÿ1), then at equal resonant frequencies of the head of an adult and the air cavity the radius of the cavity will be approximately 2.2 cm, which is close to the size of both the frontal sinuses and the mastoid [173]. Let us consider the cochlea as a possible second resonator that takes part in the formation of the auditory sensation when the human head is irradiated with microwave pulses. From modern ideas about the amplitude-frequency properties of the cochlea of the hearing organ it follows that when

applying a monofrequency signal to it, the displacement localization point
has a characteristic frequency, and the response of the displacement localization point itself allows us to imagine it as an oscillatory circuit. Ideas about the processes of pressure wave propagation in the cochlea of the hearing organ are

quite fully covered in numerous literature. In this case, we will be interested in the postulate of the modern theory of hearing - each point of the cochlea of the hearing organ, when excited by alternating pressure, is equivalent to an oscillatory circuit and has an frequency response similar to the frequency response of a single circuit. Using this position, we can consider the cochlea of the hearing organ with displacement localization points having characteristic frequencies f1 and f2 as a second oscillatory circuit that takes part in the formation of the auditory image when the human head is irradiated with microwave pulses. At close values of the impedances of the tissues of the skull and cochlea of the hearing organ (the impedances of the tissues of biological objects differ by 8 ÷ 12%) [174, 175], the pressure wave excited by a microwave pulse in the tissues of the skull will reach the cochlea without much distortion. Thus, we can assume that the tissues of the skull, which together represent the first resonator, and the region of the cochlea of the hearing organ, which responds to a periodic pressure wave as the second resonator, are quite strongly connected.

If this is so, then in accordance with physical laws that have
place in a double-circuit resonant system, the total frequency response is also
should look like a two-humped curve.

Since the cochlea of the organ of hearing is the last link that transmits and forms a displacement with certain amplitude-frequency properties, i.e., the location of the points for collecting information, we assume in the case of excitation of shock acoustics in the tissues of the skull
waves, the presence of two points of localization of displacements. In this case we get maximum signal transmission at communication frequencies f1 and f2 arising
at two points of localization of displacements, and the minimum signal transmission coefficient at the excitation frequency of the cochlea fp, i.e. at the frequency
shock vibrations excited in the tissues of the skull.

According to [113], the quality factor of the amplitude-frequency characteristics of the cochlear septum changes within 1–6 when the observation point moves from the apical to the basal part of the cochlea.
If we accept the range of possible values proposed in [121]
head resonance frequency, then by plotting a linear dependence
quality factor of the points of localization of displacements from frequency, we obtain that equivalent cochlear contour in this frequency range
will have a quality factor of about 2.5.

The conditions for the existence of two maxima in the frequency response of connected circuits, their position on the frequency axis and amplitude are determined by the quality factor of the circuits and the coupling coefficient. Position of the maxima on the frequency axis is determined by the relation

$$f1,\ 2/fp = 1 \pm K\ 1\ \ddot{y}\ \left(\frac{K2_{Cr}}{2K2}\left(\frac{Q1}{Q2} + \frac{Q2}{Q1}\right)\right)^{1/2\ddot{y}1/2}$$

where K is the actual coupling coefficient, Kcr is the critical coupling coefficient, determined by the relation $Kcr = \frac{1}{\sqrt{Q1 \cdot Q2}}$, Q1 and Q2 - quality factor of the circuits. At low quality factors

$$\ddot{y}\ K \quad \frac{fp\ fp\ f1 = ,\ f2 = \ddot{y}1 + K\ \ddot{y}1}{}$$

With values of f1 = 5.5 kHz, f2 = 11.3 kHz and fÿ = 7.4 kHz, obtained from the radio sound threshold curve, the value of the coefficient
connections are close to 0.6. Having determined the value of Kcr (Kcr = 0.46), we obtain condition K>Kcr. The given estimate of the quality factors of the circuits
and their coupling coefficient is possible only under certain assumptions and reflects the formal side of the phenomena necessary for
demonstration of the methodological approach to the study proposed here
the mechanism of these phenomena. Lack of fully formed
ideas about the mechanisms of hearing does not allow for a complete
calculation of equivalent parameters of such circuits. Thus, according to modern concepts, the elasticity of the main membrane along its length can vary within 102–103, which leads to a change in speed

sound from 10 to 30 times. But it is this value that determines the impedance
cochlea and, accordingly, the coefficient of its connection with other tissue structures. On the other hand, for small values of quality factor of equivalent circuits, the change in these values is several
times practically does not lead to a significant change in relations
coupling frequencies to the resonance frequency.

Previously, we considered the conditions that a certain
structure included in the total volume of cranial tissue in order to
it could play the role of a second resonator.

Therefore, it is quite possible to assume that a certain cavity or formation can serve as the second resonant circuit
inside the skull with a density different from the density of the main
mass of tissue. Since the speed of sound values for different biological tissues differ by no more than 10 ÷ 15%, it remains
assume that the second resonator can act
any air cavity inside the skull. In this case, its radius is from
conditions fÿ = C/2a should be on the order of 2–3 cm. Thus
Thus, the frontal sinuses or mastoid can be considered as the second resonator, and the cochlea can be assigned the role of receiver of the resulting
acoustic signal. Considering that the attenuation of sound in air
less than in tissues, which will lead to a higher quality factor of the second
resonator, the asymmetry of frequency amplitudes will also become clearer
maxima on the threshold curve of radio sound relative to the resonance frequency. With a higher quality factor of the second resonator, the amplitude of the low-frequency maximum is always less than that of the high-frequency one [170].

Since the cochlea is the organ of hearing
is the last structure that carries out mechanical
frequency selection, then it is its parameters that
will ultimately determine the nature of the excited
auditory image. Therefore, the choice of the second

there is no equivalent circuit
principled.

A qualitatively close analogue of the threshold
curve can be obtained by parallel connection of
two resonant oscillatory circuits -

parallel and serial.
In Fig. 4.27 shows the frequency response of these
circuits and the total frequency response of the two systems
these contours. However, in the original we
could not find a structure capable
react to an external signal in a similar way, and we
do not consider this option for forming the frequency response.

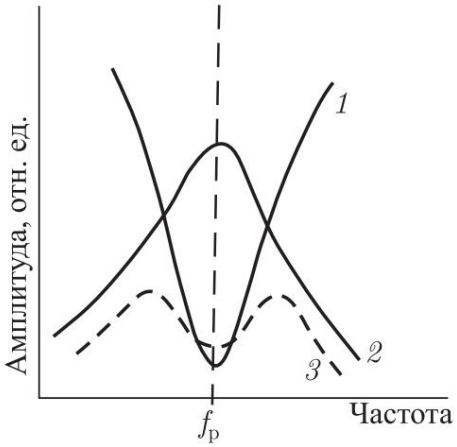

Rice. 4.27. Frequency response of parallel and serial resonant circuits connected in parallel, and their total frequency response. *1* — frequency response of the sequence -
body resonant circuit;
2 — frequency response of a parallel resonant circuit; *3* — total frequency response

In connection with the small values of the quality factor of the first and second circuits, it is necessary to consider one more issue regarding the resonant circuits. It is known [176, 177] that the resonance frequency of a single contour is determined by the ratio:

$$fp = fo\ 1 \ddot{y} \frac{1}{4Q2}$$

From this relationship it follows that the lower the quality factor of the circuit, the greater will be the difference between the resonance frequency and the frequency of the circuit's own oscillations. Substituting here the values of quality factors contours of the considered model, equal to 1.8 and 2.5, we obtain the value detuning for each of the circuits from the calculated value:

ÿf = 0.96 - for the first circuit;

ÿf = 0.98 - for the second circuit.

Since the detuning of the primary circuit is greater, and its quality factor less than that of the second circuit, the low-frequency maximum on the threshold curve of radio sound is significantly less [170].

Justification for the choice of model structure. So, using the two-circuit resonant model, we can quite fully describe radio sound threshold curve. However, the system itself oscillatory circuits with a coupling coefficient greater than critical does not reflect the entire mechanism of radio sound formation.

Above we have already considered the issue concerning the direct impact of microwave radiation on neural structures. Conclusions, made as a result of this consideration, allow us to limit ourselves to the frequency-selective properties of the physical model, adequate to those for the peripheral hearing organs. According to [176, 178] main contribution to ensuring frequency selection of signals on the periphery of the auditory system is contributed by the mechanisms of the cochlea.

Thus, the physical two-circuit model is based on the following provisions reflecting the individual mechanisms of the entire effect of radio sound as a whole:

1) radio sound is based on the resonant excitation of acoustic vibrations in brain tissue due to their thermoelastic expansion when absorbing the energy of a microwave radiation pulse (thermoelastic concept of J. Lin);

2) the amplitude-frequency characteristics of the perceived radio sound are determined by the amplitude-frequency characteristics of the periphery of the auditory system and the resonant properties of the anatomical head structures.

Based on these provisions, we will try to formulate the main requirements that the physical model must meet.

The choice of a model of any object or phenomenon is based on a certain number of provisions characterizing this object [179].

We will try to identify those of them, taking into account which will allow us to develop

a physical model that reflects the original as much as possible, i.e., a full-scale experiment on radio sound. Let us accept the following provisions.

1. The ability to use different elements when constructing different elements of the model.

2. Adequacy of terms for describing the object and model.

3. High degree of materiality of as many as possible
common properties of the model and the original.

4. Logical correspondence of elements and relations of the element model
there and the relations of the original.

From modern ideas about the amphibious organ of hearing [172, 180–182] it follows that when a monofrequency signal is applied to it, the resonance curve at the point of displacement localization has a sharply asymmetric shape relative to the resonance frequency. According to [183, 184], cited in [172], the amplitude-frequency characteristic has
slope towards high frequencies 90 ÷ 150 dB octÿ1 for
characteristic frequencies 5–7 kHz, slope of characteristics rise
in the low-frequency region is about 6 dB oct ÿ1, and near resonance it reaches 12 dB oct ÿ1. If the signal frequency in question
is limiting, then, apparently, there is a steep decline in the resonance curve
towards high frequencies can be considered as high-frequency
border.

In [172] it is indicated that the quality factor of the oscillatory system that forms the exciting effect on the neuron in question is
is equal to 7–10 and, according to experimental data [112], the considered
The slope of the amplitude-frequency characteristic decreases monotonically with increasing characteristic frequency.

The change in the steepness of the declines towards high frequencies when the characteristic frequency changes is also indicated in [143], and
here the range of these changes lies within 60–245 dB· octÿ1.

Thus, the aggravation of the frequency response occurs both in the cochlea and and in the mechanism of formation of the excitatory effect on the neuron. Additional aggravation of the frequency response also occurs with strong coupling
contours. By the way, in technical devices, a system of connected circuits makes it possible to resolve the contradiction that arises during transmission
of a certain frequency band, - the presence of a high slope slope, i.e.
high quality factor with wide bandwidth.

Since these exacerbation mechanisms perform the same
The same function, without affecting other parameters of the signal, in the model can be limited to one functional block for sharpening the frequency response. An exception will be the block that forms the decline in the upper limit of the frequency response, which should provide the ability to smoothly set the cutoff frequency of the upper limit of the range of the transmitted signal.

Rise and fall of tissue temperature during pulsed irradiation
human head, i.e. the formation of thermal pulse fronts,
cannot occur in times equal to the duration of the front
and trailing edges of the irradiating pulse, due to the finite value

heat capacity of fabric. Meanwhile, the amplitude of the excited ones in the circuit oscillations strongly depend on the parameters of the exciting pulse. In this regard, the model must also contain a block that performs function of tightening the fronts of the pulse exciting oscillations in models ie integrator.

Finally, in order for the radio sound model to allow setting up an experiment to identify the band of human-perceivable frequencies using the zero beat method, it should contain the following main functional blocks, reflecting the mechanisms of the entire phenomenon generally:

1) A system of connected oscillatory circuits with a coefficient connections above critical; 2) Integrator; 3) Frequency response aggravation system; 4) Low pass filter with adjustable upper cutoff frequency (LPF); 5) Low-pass filter with frequency response of the middle ear; 6) Device output signal indication.

The listed points allow us to present the model only in a general form. To specify it, it is necessary to move on to possible technical implementations. Based on the provisions included in the physical model of radio sound, it is easy to come to the conclusion that in order for this model to be as close as possible to the original, the oscillatory circuits must have geometric similarity with the anatomical structure original. However, this can lead to significant complications when constructing such a model and is unlikely to be justified. Selection of the necessary parameters of the spherical model under such conditions exposure presents known difficulties. Therefore spherical It is advisable to replace the model with an electric one while maintaining the transfer function in order to obtain the basic laws and making sure that the premises are correct, move on to the spherical liquid model.

Thus, as a physical electrical model there was a system of two connected radio circuits containing capacitance and inductance was selected. Losses in a real system are represented by a series resonant circuit having at frequency resonance minimum resistance.

Technical implementation of an electric two-circuit model. In accordance with the model structure described above, consider its technical implementation, primarily the system of connected contours. In models of the cochlea [172], each point of the main membrane simulated by an independent circuit. In the first models, excitation circuits were carried out in parallel. The model was simple however, some of its disadvantages, associated with the need to use low-Q circuits, forced researchers to look for new structural diagrams of models. The most widespread models are in the form of long heterogeneous lines, consisting of either from individual links and called chain links, or representing a heterogeneous line built on elements

with distributed parameters. As a rule, all models take into account not only the frequency-selective properties of the original, but also the losses that are inevitably present in the original and are caused by the dissipation of part of the energy of the pressure wave as it propagates along the cochlea.

Models of the cochlea, the characteristics of these models and their mathematical apparatus are given in [172], where you can find the main starting points that form the basis of a particular model. Our task of selecting and implementing the main link of the radio sound model is significantly simplified, since in accordance with the possible mechanism of formation of an auditory image when irradiating a person's head with microwave pulses, we need to simulate just one point of the main membrane and its connection with the first resonator. Analysis of electrical circuits of cochlea models showed that the traditional circuit of a sequential resonant circuit as a separate link is not optimal in the case of modeling the excitation of one point of the cochlea of the hearing organ. Therefore, a system of two parallel resonant circuits with capacitive coupling, tuned to the resonance frequency determined from the radio sound threshold curve, was chosen. A serial resonant circuit is tuned to the same frequency, simulating losses during the propagation of a pressure wave in the cochlea and connected in parallel to the first two circuits. The contours were calculated in accordance with the quality factors of the cochlea and skull tissues. In Fig. Figure 4.28 shows a diagram of a two-circuit model for implementing an frequency response that qualitatively coincides with the threshold curve of radio sound, taking into account losses in the cochlea, in Fig. 4.29 shows the frequency response of this circuit in the shock excitation mode with pulses of 15 ÿs duration for two different upper limits of the low-pass filter1 cutoff - 14 kHz (A) and 17 kHz (B) and in the tone signal mode (B). To demonstrate the analogy with the results of full-

scale experiments, graphs A and B show the radio sound volume level curves in dotted lines. Quantitative coincidence of the frequency response of the system of two connected circuits with the threshold curve of radio sound is achieved by using a sharpening circuit.

From the literature data it follows that the equivalent quality factor of the resonance curves of individual points of the main membrane of the cochlea is very low - on the order of unity. At the same time, psychoacoustic studies indicate a very high selectivity of the human and mammalian hearing organ. The exacerbation hypotheses, based on the nature of the physical mechanisms, are divided into two groups. The first includes hypotheses about the mechanical nature of the process of exacerbation of frequency characteristics, which assume the linear nature of the exacerbation. The second group of hypotheses explains the process of sharpening resonance curves by information processing mechanisms in a neural network. These hypotheses use ideas about both the linear and nonlinear nature of the processes of signal transmission through nerve elements. The principle common to all hypotheses is aggravation through comparison.

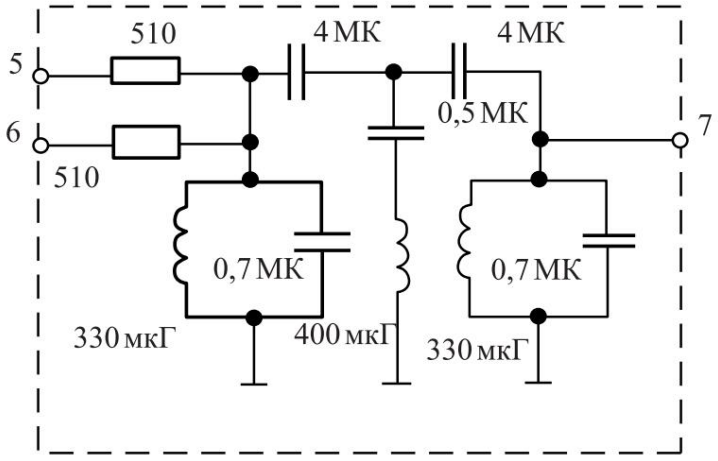

Rice. 4.28. Schematic diagram of a system of connected circuits

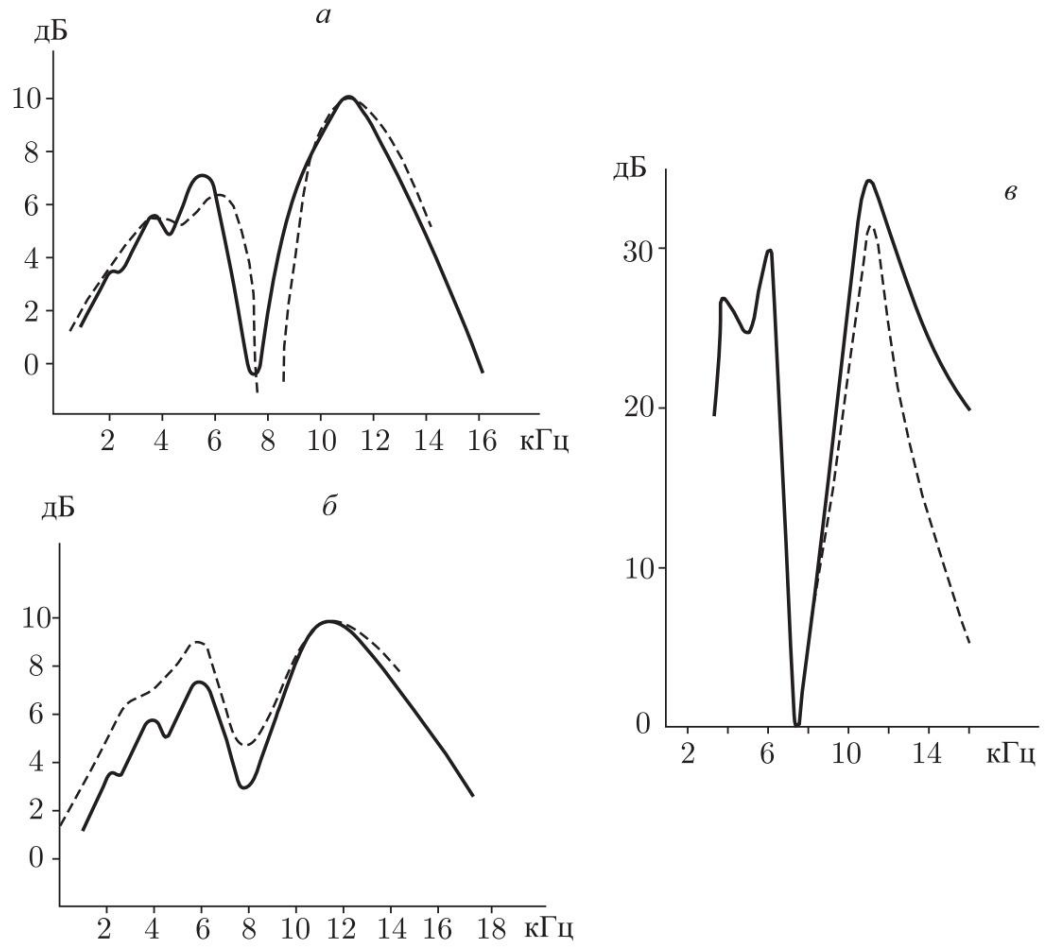

Rice. 4.29. Frequency response of a two-circuit resonant model: *a, b* - shock excitation mode, *c* - tone signal mode. *1* - cutoff frequency 17 kHz, *2* - cutoff frequency 14 kHz

vibration intensities of neighboring points of the main membrane [176, 185]. Since the model considered here uses only one point of the main membrane, exacerbation may not occur.

those of comparison, but absolutely: i.e., to sharpen the frequency response of the model in this case, you can abandon the traditional method of sharpening by using circuits for separating the second, third, etc. difference in signals from neighboring points of the main membrane. From these two points it follows that in our model the sharpening of the frequency response should be linear, implemented using any narrow-band device with parameters determined by the radio sound threshold curve. Sharpening the frequency response of a two-circuit circuit to values that determine the steepness of the slopes of the points of localization of cochlear displacements and the slopes of the threshold curve of radio sound is achieved by using two functional blocks. The first of them (Fig. 4.30) is a rejection filter tuned to the resonance frequency, and contains an operational amplifier with a double T-bridge in the feedback circuit. Using this block, it is possible to increase the slope of the frequency peaks of the frequency response model near the resonance frequency to the required value. The sharpening of the slope of the frequency response towards higher frequencies is achieved by using a low-pass filter (LPF1) with a variable upper limit of the cutoff frequency. Low-pass filter1 consists of 6 identical cells connected in series. The attenuation provided by one cell at the set cutoff frequency in the range of 7–20 kHz is 12 dB/oct.

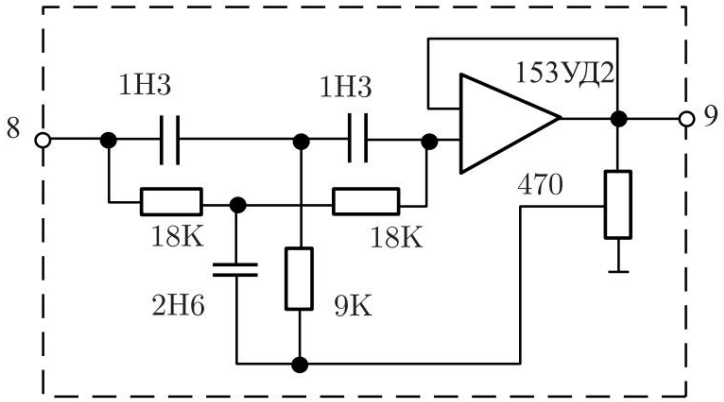

Rice. 4.30. Schematic diagram of the double-circuit frequency response amplification system models

In Fig. Figure 4.31 shows a schematic diagram of one LPF1 cell. The functional block for forming the required frequency spectrum when a rectangular pulse is applied to its input consists of several series-connected integrating chains with a time constant much greater than 5 ÷ 25 ÿs. To match this block with the low input impedance of a two-circuit system, a field-effect transistor repeater is connected at its input (Fig. 4.32). To ensure the coordination of the model with the source of the tone signal in order to apply the zero beat method, the model is equipped with a block that simulates the frequency response of the auditory tract at the level of the middle ear (Fig. 4.33). This block is built on the basis of the mo-

Delhi Flanagan [185] for the middle ear and is a filter
low pass (LPF2) with a cutoff frequency of 4 kHz. Indication
The output signal of the model is displayed on the oscilloscope screen.
Listening is provided by the 4GD-8E emitter after preliminary amplification of the signal in terms of power.

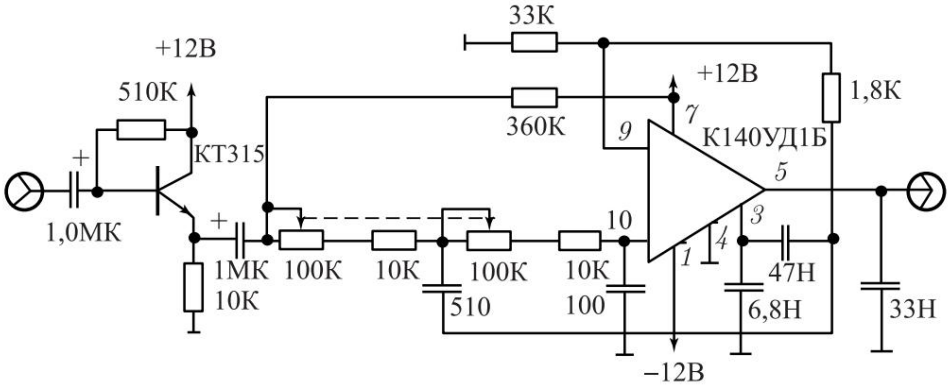

Rice. 4.31. Schematic diagram of the LPF1 cell (block for regulation upper limit of the frequency range)

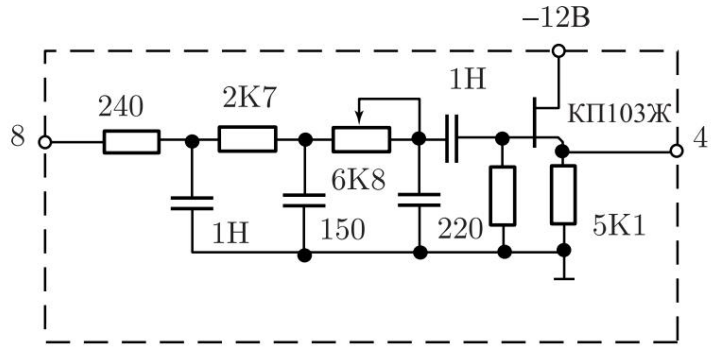

Rice. 4.32. Schematic diagram of the model integration block

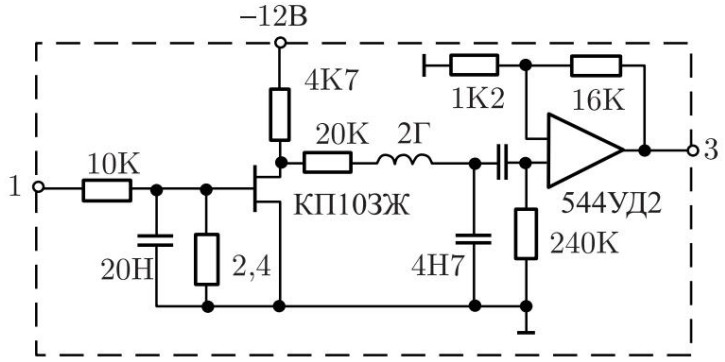

Rice. 4.33. Schematic diagram of the middle ear model (LPF2)

Experimental testing of a double-circuit resonant model. In Fig. Figure 4.34 shows a block diagram of the electrical model.

Rice. 4.34. Block diagram of the electrical model: *1* - low-pass filter (LPF2), *2* - integrating circuit, *3* - double-circuit resonant system, *4* — aggravation system, *5* — low-pass filter (LPF1), *6* — amplifier power, *7* - oscilloscope, *8* - electrodynamic emitter

The fully assembled electric model was tested in modes exposure to a tone signal in the frequency range 1 ÷ 18 kHz and a pulse sequence in the range 1–18 kHz with a duration pulses within 5–25 ÿs. Separately at repetition frequency pulses of 800 Hz and pulse durations of 100–140 ÿs were tested the possibility of obtaining an analogy of the “low-frequency type” of radio sound. The maximum slope of the high-frequency region reaches 72 dB/oct, which is within the measured values for

steepness of resonant curves of localization points of cochlear displacements [172]. The output signal of the electric model in shock mode excitation was assessed on the oscilloscope screen scale and by auditory perception. Just as in the natural experiment, it was noted complex signal composition in the frequency range 1–7 kHz. At the same time on the screen oscilloscope observed a signal containing both a frequency equal to frequency of exciting pulses (in the form of an envelope), and frequency, allocated frequency response circuits. “Aurally” the observed signal is equivalent to the auditory sensation in full-scale experiments on radio sound - subjectively perceived as a high-frequency “ringing” and “buzzing”. Thus, in the frequency range up to 7–8 kHz, the output signal The model has a polytonal character. Signal suppression at frequency resonance (resonance frequency is chosen equal to 7.4 kHz) - about 40 dB.

In the frequency range 8–18 kHz there is a monotonal character observed output signal. On the oscilloscope screen at the same time a smooth change in the frequency of the sinusoidal signal is observed synchronously with the change in the repetition rate of the exciting pulses. In a subjective assessment “by ear” when listening to the output signal of the model there is also a smooth change in the output frequency - signal with a change in the frequency of exciting pulses. So Thus, the monotonality of the signal in the frequency range above 8–10 kHz and here it emphasizes the similarity between the original and the model.

In Fig. 4.35 shows spectrograms of the model's output signal, obtained experimentally when the model is excited
rectangular pulses. To select components of a complex signal, a selective microvoltmeter V6-9 and a voltmeter VZ-33 were used
and frequency meter ChZ-34. The obtained experimental material allows one to objectively observe changes in the spectral composition of the signal.
In Fig. 4.35 *(1–4)* shows the spectra of repetition frequencies in the pre-resonance region *((1)* - 1 kHz), the first coupling frequency *((2)* - 5.5 kHz), resonance frequency *((3)* - 7.4 kHz) and second communication frequency *((4)* - 11 kHz). In this case, the duration of the pulses exciting the model
is the same everywhere and equal to 15 ÿs.

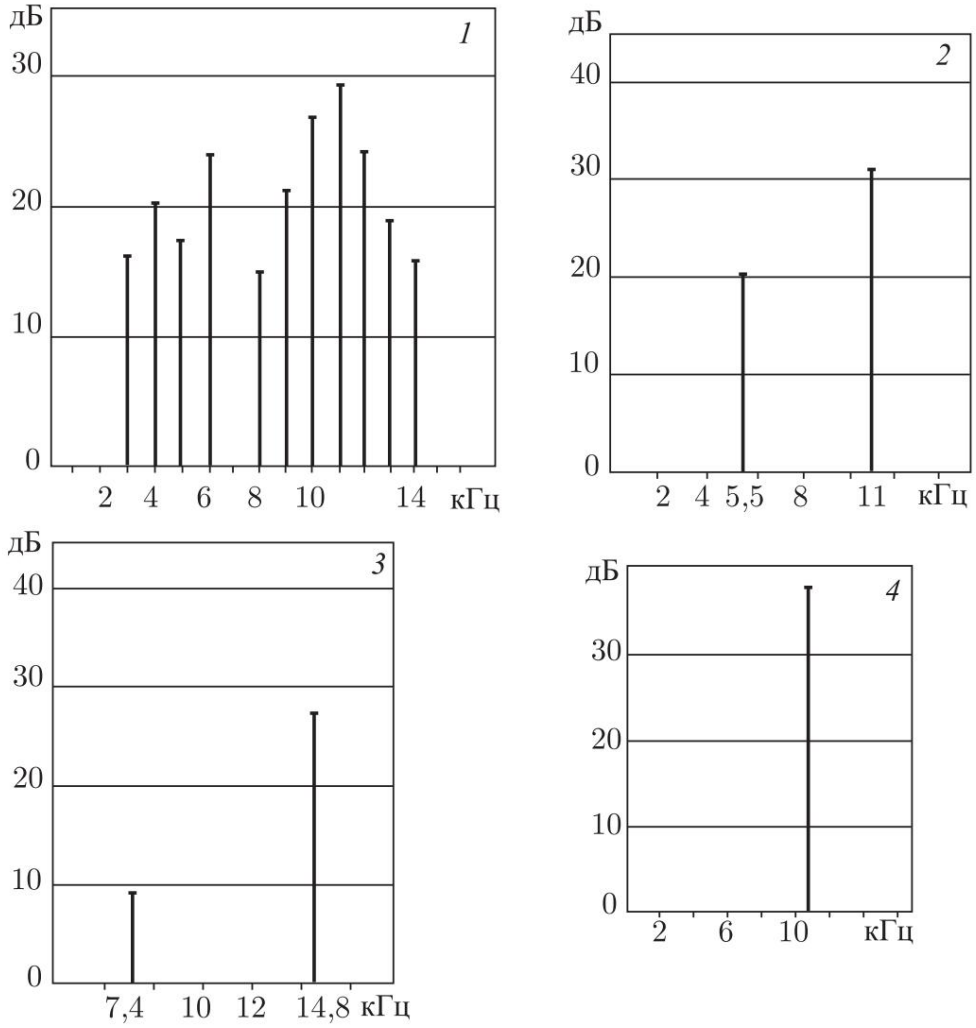

Rice. 4.35. Spectra of the output signal of the two-circuit electrical model at different pulse repetition rates. Pulse duration 15 ÿs.
1 — 1 kHz; *2* — 5.5 kGc, *3* — 7.4 kGc; *4* — 11 kHz

Analysis of these spectrograms allows us to understand some of the features of radio sound noted by subjects in a full-scale experiment.
The spectra presented here clearly demonstrate sufficient

complex nature of the recorded signal (noted in the field experiment). Signal spectrum in Fig. 4.35 allows us to understand the subjects' subjective assessment of pitch at microwave pulse repetition rates of the order of 5-5.5 kHz. Due to the lower value of the threshold at frequencies of 10-11 kHz, the second harmonic of the repetition frequency is perceived by humans significantly better than the first (the difference in the threshold levels at 5.5 and 11.0 kHz on the threshold curve is 4 dB), which was noted in situ experiment. At a pulse repetition frequency equal to the system resonance frequency, a sharp decrease in the amplitude of the recorded signal is also noted (the region of increased threshold values). Moreover, in a full-scale experiment, a subject with a high-frequency hearing limit (over 14 kHz) perceives a complex signal consisting of two frequencies - 7.4 and 14.8 kHz. At the same time, due to the lower threshold value at 14.8 kHz compared to the frequency of 7.4 kHz (minimum up to 6 dB on the radio sound threshold curve), the subject subjectively perceives a higher frequency signal.

At pulse repetition frequencies lying above the second communication frequency of the system, the signal becomes monotonal, its physical spectrum corresponds to the first harmonic of the pulse repetition frequency, which in a full-scale experiment leads to the correspondence of the pitch of the perceived radio sound to the microwave pulse repetition frequency.

As mentioned above, already on the first physical single-circuit models, the possibility of obtaining analogues of both "types" of radio sound - low-frequency and high-frequency by changing the duration of the microwave pulse - was demonstrated. In Fig. Figure 4.36 *(a* and b) shows the spectra of the output signal of the electrical model when it is excited by rectangular pulses of different durations at the same repetition frequency. A comparison of these spectra clearly shows that the low-frequency sensation that arises in natural experiments with pulse durations of the order of 100-140 ÿs is explained by the redistribution of the intensities of the spectral components of mechanical vibrations, and not by the manifestation of some other mechanism of action of EMR, different from that observed during the action of short pulses [186]. It was of interest to compare the data from a full-scale experiment, obtained by subjective assessment, and the signal at the output of the model using the zero-beat method. For this purpose, by analogy with the full-scale experiment, a tone signal was applied to the input of the model simultaneously with the exciting pulses. In this experiment, unlike the full-scale one,

beats were observed not only at the frequencies of the tone signal, which are overtones of the pulse repetition rate, but also at a frequency equal to the pulse repetition rate up to 100 Hz. It is noted that at a given higher frequency of the tone signal, the value of the beat frequency amplitude (intensity)

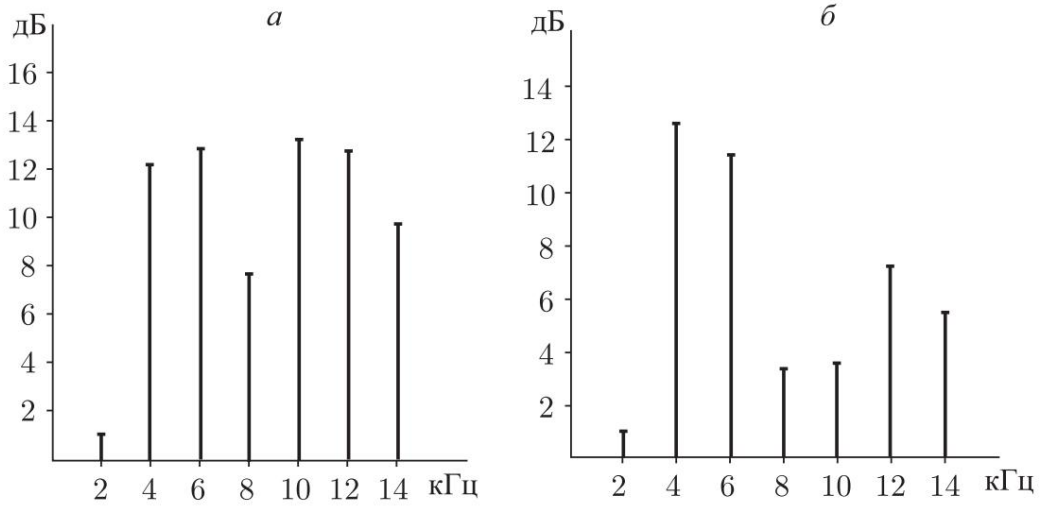

Rice. 4.36. Spectra of the output signal of the two-circuit electrical model for two pulse durations. Pulse repetition rate 2 kHz: *a* — pulse duration 15 ÿs, *b* — pulse duration 135 µs

increases in proportion to the increase in the repetition rate of exciting impulses.

The noted distinctive feature of the model requires clarification, since as one of the main issues concerning the phenomenon of radio sound is the absence of zero beats between the first harmonic frequency repetition of microwave pulses and the frequency of a tonal acoustic signal in full-scale experiments in the pulse repetition frequency band 1–7 kHz. To explain this discrepancy, let us turn to some physiological characteristics of hearing. Schouten [187–189] suggested that the perception of the height of periodic sounds with a missing first harmonic can be explained using a mechanism for measuring the period of oscillation of a sound wave. According to Schouten's hypothesis, the auditory system should be considered not as a purely spectral, but as a spectral-temporal analyzer, in which, along with the Fourier series expansion, the analysis is carried out temporary form of exciting oscillations. Sound matching the first harmonic not contained in the signal, Schouten called residual. Schouten's hypothesis is supported by neurophysiological observations up to frequencies of the order of 3-5 kHz [125]. In Fig. 4.37 some forms of sound wave signals are presented, perception whose pitches cannot be explained from the point of view of spectral analysis, since they do not contain a component with a frequency corresponding to the height of the perceived tone [125]. From point of view perception, all three types of signals have the same height, despite the fact that the spectra of these sounds are significantly different from each other. It was experimentally shown that in the first case *(A)* the height corresponds to the pulse repetition rate 1/Toi [190], in the second *(B)* - modulation frequency 1/Tom [191], in the third *(C)* -

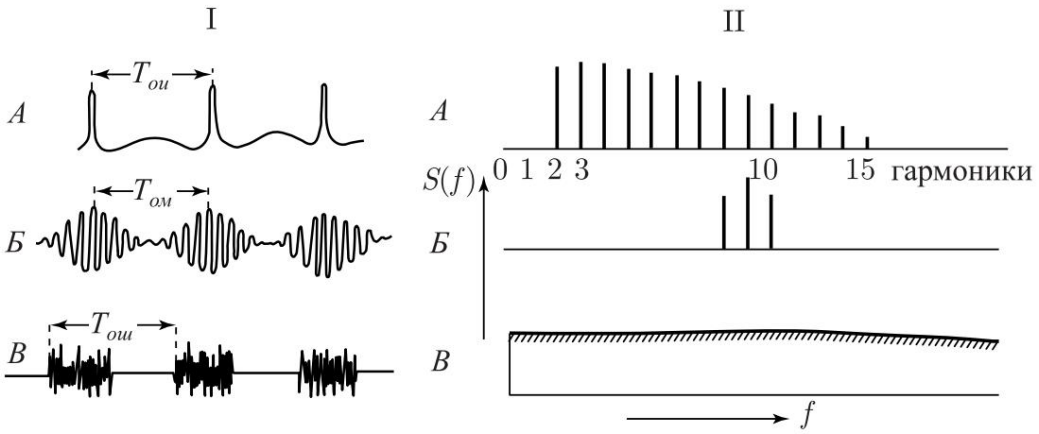

Rice. 4.37. Sound waveforms (borrowed from [124])

noise interruption frequency 1/Tosh [192]. At the same time, the physical spectra these sounds do not contain components corresponding to the indicated frequencies. The main property that determines the perception of their height is are periodic changes in the amplitude of the sound wave. Comparison of oscillograms of mechanical vibrations excited in a liquid by microwave pulses (see Fig. 2.11) and damped vibrations on output of an electrical model excited by voltage pulses (Fig. 4.38), with those given here from [125] in Fig. 4.37 shows that in this case, their spectral characteristics are close and also not contain the first harmonic. However, as already mentioned, unlike In a full-scale experiment, the model makes it possible to register the missing component (pulse repetition frequency) using the beat method.

If we were talking about the perception of an ordinary acoustic signal, one could immediately assume the presence of an artifact in the experiment on the electric model, since in this case beating is required should have taken place. And although the concept of our model assumes the absence of structures responsible for signal processing in the formation of the radio sound effect, however, an unambiguous conclusion cannot be drawn here. In this regard, it seems to us possible the following interpretation of the results obtained.

The proposed two-circuit resonant model quite fully reflects the structural structure of hearing and, in accordance with existing analogues, identifies the first harmonic that is missing in the signal, without thereby contradicting physiological and neurophysiological data. If this is so, then the absence of residual sound in the frequency range 1–7 kHz in a full-scale experiment, noted subjects can apparently be explained by the following reasons:

1) insufficient attention of the subjects during the experiment to detect the presence of beats at low frequencies;

2) high noise level in the room where the full-scale was carried out experiment;

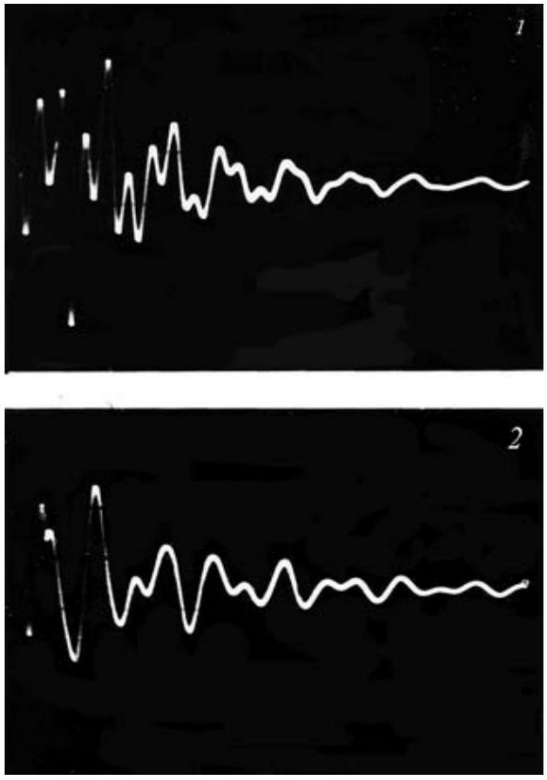

Rice. 4.38. Oscillogram of the response of a two-circuit electrical model to single pulse of different durations: *1* - pulse duration 50 ÿs; *2* — pulse duration 100 ÿs. Sweep speed 200 µs/cm

3) low amplitude of the beat frequency signal at the average level at low microwave pulse repetition rates;

4) the discrepancy between the transfer functions in the model and in the full-scale experiment when the model and the original are excited by an external impulse, which as a result should lead to different the spectral composition of the signal entering the recording system. This situation is in principle possible if the critical band original is less than the value f ÿ F (where f is the frequency of the resonant oscillations, F - modulation frequency), and in the model - more.

According to [5], the noise level in the room where the full-scale experiment was carried out was 40 dB at a frequency of 1 kHz. At the same time, according to according to J. Lin [121], at close values of energy density in an impulse, the displacement of human head tissue is of the order of 10ÿ11 cm, which provides a pressure of the order of 10ÿ2 dyne cm ÿ2 at the signal frequency 1 kHz, i.e. comparable to the pressure caused by the noise level.

An attempt to eliminate residual sound (when receiving “by ear”) in the model by changing the spectral composition of the signal by varying the parameters of the integrating unit did not lead to tangible results. Since in all other respects the model describes the full-scale experiment, then taking into account the comparability of the noise level in the room and subjectively perceived in a natural experiment auditory

sensations, and physiological characteristics of the spectrotemporal
analysis of signals by hearing mechanisms, we came to the conclusion that residual sound in the frequency range 1–7 kHz in a full-scale experiment
must be present. Thus, the need arose to conduct a full-scale experiment either with a reduced level of external noise or with an increase in the microwave energy density in the pulse.
In addition, from the considered two-circuit model it followed that
when the head tissue is exposed to another external physical factor that can lead to the excitation of pressure waves, it must
a similar auditory sensation is formed, i.e. this model
should “work” when stimulating the bones and soft tissues of the skull
an ordinary acoustic signal of the same shape and intensity that
and pressure waves excited by microwave pulses. The results are as follows
checks could already be considered conclusive in favor of
one concept or another.

Obtained using an electric two-circuit model of radio sound
the results determined the need for experimental verification
the following provisions.

1. The frequency of the mechanical resonance of the head, as a single circuit of a double-circuit resonant system, must be in the region
maximum threshold on the radio sound threshold curve, i.e. in the area
7.5–8 kHz, and at a speed of sound in tissues of the order of 1.44 105 cm s ÿ 1
and a head radius of about 9 cm is determined by the ratio C/2a.
In this case, the quality factor of the head as a resonator is estimated by the value about 2.

2. Zero beats in a full-scale experiment between the first harmonic of the EMR pulse repetition rate and tonal acoustic
signal must be observed over the entire audio frequency range.

3. When excitation of bone tissue formations of the skull by bone
vibrator and simultaneous stimulation with an acoustic tonal signal by air conduction, analogues should take place
radio sound by auditory perception.

4.4. Experimental testing of the working hypothesis

Spectral analysis of spherical models of radio sound. Of practical interest is the spectral analysis of excited
mechanical vibrations in spherical resonators with low quality factor. Glass models were used as spherical models
round-bottomed flasks with a diameter of 105 and 120 mm, lined on the outside porous rubber 10 mm thick, and a plastic sphere with a diameter
120 mm with a shell thickness of about 1 mm. In all working models
ethanol served as the liquid.

Registration of mechanical vibrations excited in glass models was carried out using piezoceramic transducers with a diameter of 20 and a thickness of 0.5 mm, glued into the wall

flasks. The plastic sphere was installed on an autonomous piezoelectric ceramic receiver. Irradiation was carried out using an open end rectangular waveguide with a cross section of 10 × 72 mm2 at the carrier frequency 2375 MHz, pulse power - up to 500 W. Frequency Spectra excited mechanical vibrations were recorded using spectrum analyzer SKCh-26 with a bandwidth of 20 kHz.

In Fig. 4.39–4.41 show recordings of the spectra of mechanical vibrations excited in a liquid by pulsed EMF. On all spec-

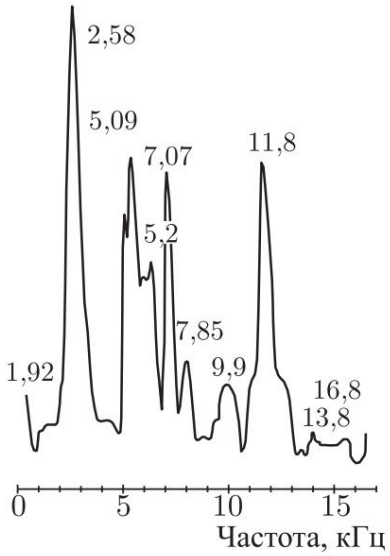

Rice. 4.39. Spectrum of mechanical vibrations excited in a glass sphere with a diameter of 105 mm. Pulse repetition frequency - 100 Hz, duration - 10 ÿs

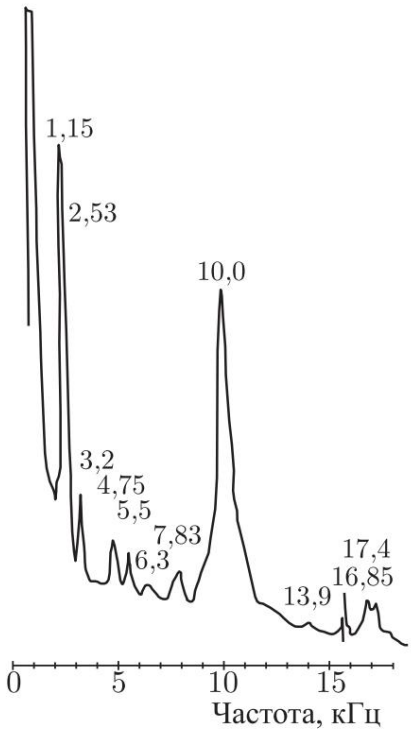

Rice. 4.40. Spectrum of mechanical vibrations excited in a glass sphere with a diameter of 120 mm. Pulse repetition frequency - 100 Hz, duration - 10 ÿs

fucking the frequency corresponding to the first mode is clearly visible oscillations of the sphere, with free boundaries fÿ = C/2a [63, 133], where C is the speed of sound in the liquid, a is the radius of the sphere, as well as others frequencies that can apparently be identified as modes vibrations, fmn, corresponding to a sphere with fixed boundaries, where m is the mode (type) of vibrations, n is the overtone number [114]. Except Moreover, in spheres with a throat, the frequency corresponding to the Helmholtz resonator fH = where C is the speed is clearly visible $\frac{C}{2p}$ sound in the substance filling the resonator, V is the volume of the resonator, l and S are the height and area of the resonator throat [53], as well as the frequency, close in value to the frequency of oscillations of a liquid column as

quarter-wave resonator Fÿ/4 = C/8a
[52]. The presence of other frequencies is more
difficult to identify, but they may well be
overtones of the frequencies described above. It is forbidden
completely exclude the possibility of the existence of shell
resonances [131, 142].

In table 4.4 shows all the data on the frequencies
excited in the spheres and gives them
presumptive identification, as well as
calculated value of the quality factor of a mechanical
resonator Q for a frequency corresponding to C/2a.
From the table it follows that
there are no exact quantitative matches of
experimental data for a real object and a specific
mathematical model,
but it is quite possible to establish a qualitative similarity
Maybe.

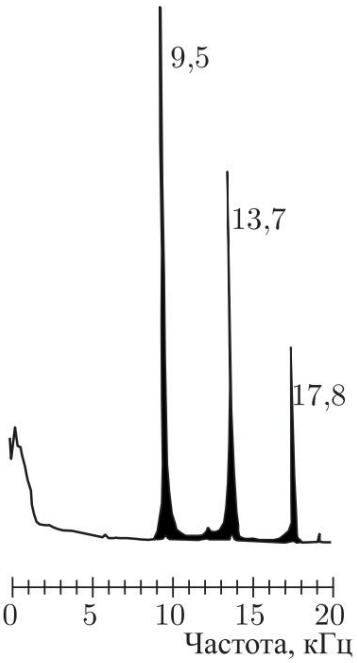

Rice. 4.41. Spectrum of
mechanical vibrations,
excited in a plastic sphere with a
diameter of 120 mm. Pulse
repetition frequency - 75 Hz,
duration - 10 µs

Comparison of the spectra of excited mechanical
vibrations of glass flasks with a neck with the
spectrum of vibrations excited in a plastic sphere that
does not have a hole allows us to conclude

that frequencies below the frequency

fÿ = C/2a, are uniquely determined by the presence
of a throat, that is, they represent
frequencies of the Helmholtz resonator and quarter-
wave resonator, and their overtones. In this sense, frequency fp = C/2a
is basic for our models. It is reasonable to believe that this is how it is
made, for example, in [131, 149], that the real prototype is
the head is closest to a closed model with the same boundary conditions over the
entire surface, that is, to a plastic sphere
no holes. This also follows from the fact that the content
the skull is under some excess pressure and therefore
the existence of any “vents” similar to the throat in our
models seems unlikely. Based on this, all dependencies important from the point of view of the
analogy with radio sound were removed for
fundamental frequency.

In Fig. Figure 4.42 shows the dependence of the amplitude of the fundamental frequency
vibrations (10 kHz) in a glass sphere with a diameter of 120 mm (spectrum
in Fig. 4.40) on the repetition rate of pulses with a duration of 10 ÿs.
In Fig. Figure 4.43 shows the dependence of the amplitude of the fundamental frequency
(11.8 kHz) mechanical vibrations in a spherical flask with a diameter
105 mm (spectrum see Fig. 4.39) from the pulse duration at
their repetition frequency is 1.7 kHz. Vibration spectra corresponding
The maxima and minima of the amplitude of the fundamental frequency, at durations
of 40, 80, 120 and 160 ÿs, are shown in Fig. 4.44. These spectra

Machine Translated by Google

Table 4.4 [illegible]

Spherical [illegible]	diameter, mm	Sphere [illegible] three		Helmholtz [illegible]			Quarter-[illegible] liquids	Sphere [illegible]			[illegible] frequency
			[illegible]	fH	[illegible]	IV	[illegible]	f11	f21	f22	fp 2a
[illegible]	105	experience riment	11,8	1,95			2,58	16,8	7,07 7,85	–	19
		Calculation	11,4	1,75			2,86	[illegible]			
[illegible]	120	experience riment	10	1,15			2,53	[illegible]		16,85 17,4	
		Calculation	10	1,43			2,3	[illegible]			
[illegible] sphere	120	experience riment	9,	–			–	[illegible]			78
		Calculation	10	–			–	[illegible]			

spherical

are a good demonstration that in the low-Q area
a whole set of mechanical vibration frequencies are excited, multiples
EMR pulse repetition rate. At the same time, the intensity of that
or another of the components, their relative values are determined
pulse duration and are redistributed when it changes.

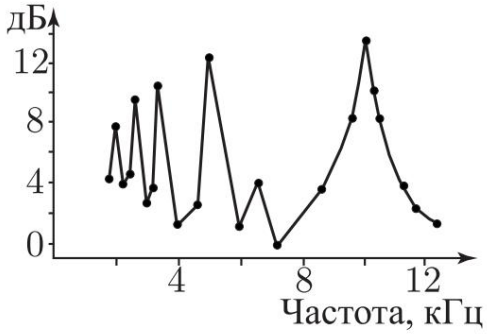

Rice. 4.42. Amplitude dependence
mechanical vibrations main
frequency (10 kHz) in a glass sphere with
a diameter of 120 mm from the frequency
pulse duration

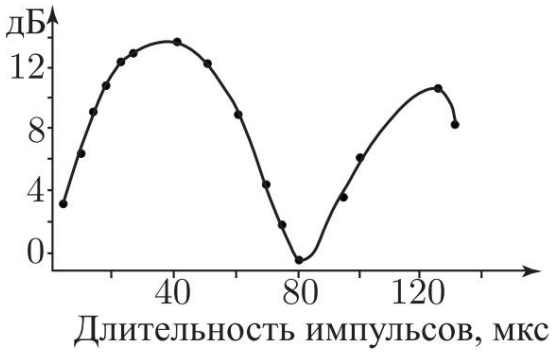

Rice. 4.43. Amplitude dependence
mechanical vibrations main
frequency (11.8 kHz) in a glass sphere with a
diameter of 105 mm from the pulse duration at a
repetition rate of 1.7 kHz

10 µs

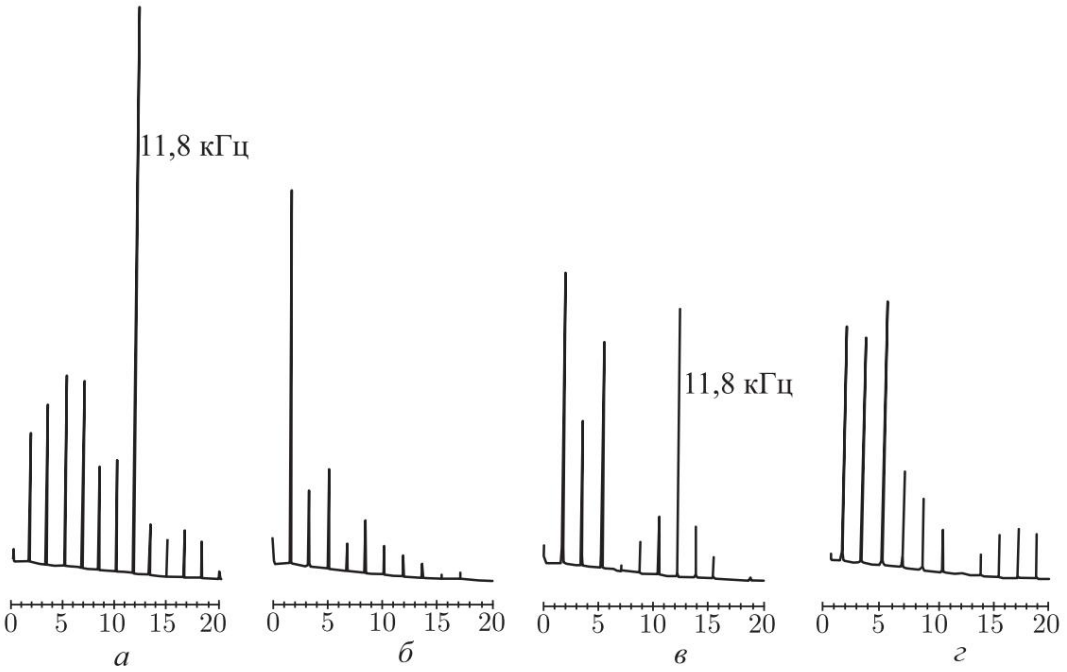

Rice. 4.44. Spectra of mechanical vibrations in a sphere with a diameter of 105 mm at
pulse repetition rate 1.7 kHz, corresponding to the maximums *(a* -
duration 40 ÿs, *c* — 120 ÿs) and minima *(b* — duration 80 ÿs,
d - 160 ÿs) amplitude of the fundamental frequency in Fig. 4.43

Natural experiment. As already mentioned, the results obtained on a two-circuit electrical model indicated the need to perceive low frequencies (below 8 kHz) in full-scale
experiment on irradiating the human head with microwave pulses. The reasons why the subjects had not previously noted beats on
pulse repetition frequencies in the pre-resonance region, could be
how high the noise level in the room where the experiment was carried out, and insufficient microwave pulse power. Therefore we were
An experiment was carried out to identify beats in the frequency range 1–7 kHz in conditions of significantly lower noise levels - about 20-25 dB
regarding APS [14]. Carrier frequency - 0.8 GHz. For irradiation
An exciter (a section of a rectangular waveguide) with a cross section of 150 × 270 mm2 was used, the microwave pulse power was 120 W.
Thus, the energy flux density in the pulse was
0.6 W cm ÿ2. The parietal region of the head, which has the lowest threshold value, was irradiated, as in previous experiments.
to excite the auditory sensation. Microwave pulse duration
selected within 25 µs. A tone signal was given to the subject
through TDS-8 headphones from the GS-100I generator. Repetition frequency microwave pulses were set in the range of 1–7 kHz. The change in the tonal acoustic signal was also in the range of 1–7 kHz.
The pulse repetition rate and tone signal frequency were controlled using ChZ-34 frequency meters.

In order to minimize possible harmful effects on the subjects, the search for beats was carried out only at a few points specific to
each subject, in which, during preliminary listening
radio sound was perceived most clearly. After determining such a point and fixing the frequency, headphones were put on, through which
an acoustic signal was given. Its intensity and frequency were selected blindly by the subjects themselves until clearly distinguishable
beats. For the first subject these frequencies were: 3.58; 4.21;
5.23 and 6.99 kHz. For the second subject, the frequencies at which the search for zero beats was carried out had values of 4.01, 5.33 and 6.99 kHz. The third subject noted beats with repetition frequencies
pulses 3.80, 4.74, 4.97 kHz.

In order to check the presence of a possible artifact consisting
in the probability of excitation of mechanical vibrations in metallic
details of headphones when they are brought into the irradiation zone, experiment was also carried out in conditions where the headphones were taken out of the area exposure at arm's length. Beats were recorded
at the same frequencies as in the first case. Feeling of beating
headphones placed on the head disappeared as soon as the subject removed his head from the irradiation zone.

Based on the data from the natural experiment, the following conclusion can be made. Firstly, the conclusion about the need to have
zero beats with microwave pulse repetition rates in the region

below 8 kHz, resulting from data obtained on a dual-circuit
electric model. Secondly, the detected beats expand
possibilities of practical use of radio sound. Thirdly, the frequencies at which zero beats are detected correspond to areas of low threshold values, which explains the lack of their perception

at the energy densities used in our experiments and previously
Microwave in the high threshold region, i.e. at frequencies of the order of 1-3 kHz. That the fact that the proposed model made it possible to assume the existence of zero beats at frequencies of the pre-resonance region and to detect
them in a full-scale experiment, allows us to come to the conclusion about the correctness of the double-circuit resonant model and its structure.

Acoustic analogues of radio sound. In the experiment, when irradiating spherical and cylindrical models filled with liquid,
it has been shown that excitation of both low-frequency and high-frequency oscillations is achieved by changing the duration
microwave pulses.

The double-circuit resonant model, despite the great analogy with the original, did not completely remove the question of the possibility
the effects of microwaves on signal processing structures following the receptors, i.e., there is a need to exclude the direct influence of pulsed microwave radiation on neural structures.

Since in a full-scale experiment such a situation is physically
impossible, the microwave pulse as the exciter of the pressure wave was replaced by an acoustic signal representing periodic series
damped oscillations with a frequency in a series equal to f = C/2a, and the frequency of their sendings in the range of microwave pulse repetition rates, i.e.
within the range of 1–17 kHz [79].

The experiments were carried out under the same conditions as audiometry of thresholds for bone conduction of sound, but instead of anti-noise headphones, ordinary TDS-8 type headphones were worn,
with the help of which the tone signal was heard. To the bone
telephone, located in the same way as in the previous one
experiment, an electrical signal was supplied, generated by a specially designed electronic unit. The block was
shock excitation circuit with a natural frequency of about 8 kHz
and a quality factor of about 2. The circuit was started by rectangular pulses. The repetition frequency of the series changed
by changing the pulse repetition rate from the generator
G5-54. Such an acoustic signal should excite in the bones of the skull
mechanical vibrations similar to those due to thermal expansion
head tissues that absorb microwave pulses.

When subjects simultaneously listen to signals from
bone telephone and ordinary telephones, the repetition frequency of shock-excited acoustic vibrations was set equal to an integer number of kilohertz in the range of 1–14. Tone frequency

could vary throughout the entire audio range. To the subject first

a signal from the bone phone was presented, and then he himself selected intensity and frequency of the tone sound signal supplied to regular phones. A total of 4 people participated in the experiments.

The developed technique of simultaneous exposure to two acoustic signals through bone and air conduction made it possible, first of all, to show the possibility of the presence of beats between these two signals. We have not found similar works in the literature. Secondly, the presence of beats, if they are registered by the subjects, could explain the effect of radio sound at the level of the mechanisms of the inner ear. True, one could assume that it is possible that excited pressure waves directly influence signal encoding structures. However, I. A. Vartanyan and E. M. Tsirulnikov [193] note that when focused ultrasound acts on the structures of the midbrain of a frog, no changes in the microphone potentials of the sacculus are observed up to intensities of the order of 240 W cm ÿ2. Moreover, electrical responses to sound were recorded before, during and after exposure to focused ultrasound in the zone of those structures of the center from which electrical reactions to sound stimulation were removed. According to the same authors cell activation is possible at ultrasound intensities of the order of 900 W cm ÿ2 in the center of the focal region, and for certain structures. The intensity value for excitation of receptors in the auditory labyrinth of animals and humans is less than 1 W cm ÿ2, to excite the auditory nerve endings in conditions of damage hydrodynamic system of the labyrinth or destruction of receptor cells – 80–120 W cm ÿ2 [193]. Since in a full-scale experiment the order of magnitude of the pressure wave is estimated to be 10ÿ2 dynes cm ÿ2, then the question is about the direct initiation of electrical activity brain structures can be removed by mechanical vibrations.

In preliminary experiments it was established that the sound subjectively perceived from the bone telephone is similar in its main manifestations to radio sound. If the pulse duration less than 30 μs, then at a repetition rate below 8 kHz the perceived the sound is polytonal with a predominance of high-frequency components, but monotonal at a repetition frequency from 8 kHz to HFGS. When the pulse duration increases to 65-70 ÿs, the subjectively felt the volume of the polytonal sound increases, then decreases as with a duration of about 120-130 ÿs, sound is perceived as a tone with a frequency corresponding to the pulse repetition rate (compare from fig. 4.02). A further increase in the pulse duration leads to a repetition of the situation with a period of 130 ÿs.

All subjects, while simultaneously listening to signals from bone phone and regular phones, beats were noted at frequencies of the tone signal, as equal to the repetition frequency of the series shock-excited oscillations, and multiples of it, but less than HFGS.

The obtained result gives reason to believe that in experiments by recording beats between radio sound and tonal acoustic the first signal was perceived by the “mixer” thanks to the bone carried out, although it cannot be considered evidence of this. Significant difference between the obtained result and the natural experiment with radio sound is that the beats in a full-scale experiment in [5] were recorded only for the tone frequency acoustic signal above 8 kHz, whereas in experiments on bone conduction of sound, beats were recorded at lower frequencies.

Thus, it is shown that between the tonal acoustic signal supplied through the air and the acoustic signal in the form of series shock vibrations supplied by bone-tissue conduction, beats can be recorded provided that the tone frequency signal is equal to the pulse repetition frequency or one of the overtones of this frequency, less than the HFGS, but without a lower limit.

Radio sound as a physical phenomenon. The concept of a double-circuit resonant system proposed by the author to explain the sensory acoustic effect of microwaves was confirmed in the considered electrical model. Dual-circuit output signal resonant model with natural frequencies of the circuits close to the resonant frequency determined from the radio sound threshold curve, almost identical to this curve. At the same time, they agree well the obtained values of communication frequencies of the electrical model with each other with the values of frequency maxima on the radio sound threshold curve. The question of choosing one or another anatomical structure as the second equivalent circuit should apparently be connected to the first turn, with the ability to provide strong communication between the circuits, i.e., the condition of proximity of numerical values must be ensured impedances of the anatomical structures under consideration. From this point vision, frontal sinuses or mastoid, although they satisfy one of requirements, namely, they have a calculated value of the natural oscillation frequency close to the natural oscillation frequency of the first equivalent circuit, but do not provide the impedance value, close to the value of soft tissue impedance. Indeed, if impedance of soft tissues (ÿC)t ÿ 1.5 105 g cm ÿ2 s ÿ1, then the impedance air cavity (ÿC) ÿ 3.4 g cm ÿ2 s ÿ1. Impedance ratio close to 103. This means that to obtain the same intensity vibrations in the air cavity, as well as in soft tissues, are necessary increase the excitation amplitude by more than three orders of magnitude, i.e. from of soft tissues, only one thousandth passes into the air cavity part of the total supplied mechanical energy. Therefore, the connection between such contours is obviously extremely small. Availability weak connection between the contours does not provide the possibility of obtaining a double-humped curve and, accordingly, the possibility of obtaining complex frequency signal at the output of such a system. However, if

the connection is close to critical, in the second circuit there may be two
frequency maxima at one frequency maximum (at frequency
resonance) in the primary circuit. A similar situation can be realized
in a model experiment when test tubes were irradiated with microwave pulses,
partially filled with liquid. If you choose the height of the column
liquid and the height of the air column with similar values of resonant frequencies
and excite shock mechanical vibrations in the liquid, then we obtain a model of a
two-circuit system with weak coupling.
Moreover, depending on the location of the collection of mechanical vibrations (in
the air or liquid column), the picture of excited mechanical
vibrations will have different forms. Subjective assessment of the day off
The signal from the electrical model by the subjects “by ear” coincides with that in
a full-scale experiment. As in the natural experiment, with
pulse duration close to the period of excited oscillations,
the presence of a low-frequency tone is noted, a high-frequency tone is noted when
I'm depressed about this. At pulse durations equal to or less
half of the period, the low-frequency tone is suppressed and the high-frequency
polytonal nature of oscillations is noted in the pre-resonance
areas. Audiometry of bone-tissue conduction, as in the mode
excitation of mechanical vibrations by a tone signal, and with the help of shock
mechanical vibrations, showed a good coincidence of the obtained threshold
curves with the threshold curve of radio sound.
The last circumstance, as well as implementation using models
analogues of “low- and high-frequency” types of radio sound allow
consider that the mechanism of radio sound is entirely determined by the mechanisms
organ of hearing. Setting up a full-scale experiment at a lower level
noise in the room using anti-noise headphones made it possible to detect the presence of zero
beats in the frequency range 1 ÷ 7 kHz
radio sound threshold curve. Moreover, the pulse repetition rate
Microwave frequencies at which zero beats with a tone signal were observed correspond to
frequencies at which low values were observed
bone-tissue conduction threshold and radiosound threshold curve. From these
same curves it follows that to identify zero beats
at lower pulse repetition rates it is necessary to increase the power in the pulse in
proportion to the increase in the threshold. This
shows good agreement with the two-circuit resonant model
full-scale experiment. Identity of the threshold curves of radiosound and bone-
tissue conduction in the mechanical shock mode
oscillations of the end-to-end frequency response of the double-circuit resonant
model allows us to say that the appearance of these curves is a consequence of
the physical processes taking place in the double-circuit resonant system,
and not the physiological characteristics of biological structures.

Thus, we can assume that the sensory acoustic effect of microwaves is a
physical phenomenon associated with the absorption of microwave electromagnetic
energy in tissues on the way to the receptor apparatus. The mechanism of this
effect is associated with excitation in tissue

the head of mechanical vibrations due to thermoelastic expansion when absorbing the energy of the EMR pulse and conducting these vibrations into the cochlea through the bone conduction. Formation of the same spectrum The auditory sensation perceived by a person is associated with the interaction of anatomical structures representing a system of oscillatory circuits, with a connection above the critical one. Amplitude-frequency the properties of a real two-circuit system are determined to a greater extent degree cochlea of the organ of hearing, presumably the second equivalent circuit. The fact that in the observed effect the frequency resonance of a double-circuit resonant system strongly depends on the acoustic properties of bone tissue, indicating the dependence of the value this frequency from the speed of sound in that part of the skull where The emitting telephone is located.

The obtained experimental material also allows us to clearly define as the main frequency of the mechanical resonance of the head as an acoustic low-Q resonator the frequency determined by the ratio C/2a.

4.5. Information communication channel

Selection of irradiation pulse parameters. The results of studies of the conditions for excitation of mechanical vibrations in various objects, including biological ones, allow us to state some considerations and determine the boundaries within which it is possible to vary the parameters of the microwave EMF pulse, realizing the information link. This is the pulse repetition rate and their duration, as well as impulse power. These parameters are used to determine PPM value and the required output power of the microwave generator. The pulse repetition rate is mainly determined by the experimental conditions, and in accordance with the data of psychoacoustic studies the upper limit frequency can reach 20 kHz. Lower the frequency threshold can be determined by a value of 1 Hz - this is the same low repetition rate of microwave pulses, known from the wide variety of published materials on this topic. What already indicated in clause 1.1.6 (part I), for a real radio pulse (pack microwave oscillations) the time of establishment and decay of oscillations is determined by the relation tset ÿ= tsp = (100 ÿ 150) f ÿ1, where f is the oscillation frequency Microwave. At f ÿ 109 Hz tset = ÿf = 102 10ÿ9 s = 10ÿ7 s. That is, the fronts Microwave pulses must be no shorter than 0.1 ÿs. Duration of im- 2n + 1 pulse is selected in accordance with the expression ÿi = 2 according to refined graphs $\frac{\quad}{\quad}$ T or 2.14) for each specific case (object). The energy of the front and decay of the pulse is converted into the energy of mechanical vibrations excited by the fronts of the thermal pulse. Microwave - Eph ÿ 0.5ÿf · Pi and Ec ÿ 0.5ÿc(Pi ÿ ÿPi) - see fig. 1.10 and 1.11.

Therefore, increasing the pulse duration makes no sense - according to
At the end of ÿph, the process of pumping microwave energy becomes stationary.
The minimum limit value ÿi must satisfy the condition
ÿ and T /4, where T is the period of excited mechanical vibrations.

The minimum “technical” pulse duration can be
determined from expression (1.13)

$$ÿti = 10ÿf = 1.0\ \mu s$$

The frequencies of excited mechanical vibrations observed in the works cited here are determined by a value of the order of 104 Hz.
From here we can write:

$$10ÿ6 \quad \text{what} \quad 10ÿ5\ c.$$

Analysis of the graph of changes in the conductivity of phospholipid membranes (Fig. 1.02) shows that the front of the increase in conductivity, proportional to the increase in temperature in the channel, can be estimated at a value of the order of 40 ÿs, the time of temperature decline - at a value of the order of 100 ÿs.
Thus, the formation of thermal pulse fronts in this case allows us to assume the excitation of mechanical oscillations. On the other hand, the minimum duration of the front and fall
thermal impulse should provide excitation of mechanical
oscillations with energy sufficient for the occurrence and summation
microdamages in a biological object. If equal to or exceeding this
energy of the Young's modulus of an object, one can expect the manifestation effect. For biological structures with periodicity,
the effect can manifest itself at a microwave pulse power of the order of a few microwatts (the “amplification” of the amplitude of capillary waves on the myelin sheath can reach 106). When irradiating suspensions in test tubes, an increase in the power of excited mechanical vibrations
proportional to Q2, where Q is the quality factor of the resonator. In the cases considered here, the oscillation power increases by ÿ 5 × 104 times.

Reasoning regarding the choice of the duration of the front and decline
impulses are consistent as long as ÿf (ÿc) tdis, i.e. until those
as long as the duration of the front and fall is much less than the time of dissipation of thermal energy. On the other hand, with decreasing ÿph (ÿc)
at a constant value of Pi, the energy of the pulse front decreases
and, accordingly, the amplitude of excited mechanical vibrations,
and at ÿph ÿ 0, A0 ÿ 0. With increasing ÿph (ÿc), the energy pumping time increases
Microwave and, accordingly, despite the increase in the value of ÿph · Pi, A0
begins to fall , because ÿf (ÿc) ÿ tdis. With further increase in duration
pulse rise and fall, A0 ÿ 0. In Fig. Figure 4.45 shows the hypothetical course of the curve depending on the amplitude of excited mechanical
fluctuations depending on the duration of the front (fall) of the thermal pulse.

Bandwidth. The equivalent value of the bandwidth of a biological object as a receiver of information in pulse mode can be determined using the well-known expression

2ÿf = $\frac{2}{\text{what}}$. However, unlike radio technical systems for biological information objects are the rise and fall of microwave pulses, leading to the formation of a thermal pulse, the fronts of which excite mechanical vibrations. Thus, in order to transfer undistorted information in this case to the calculated formula you need to enter a value duration of the front (fall) of the modulating pulse, i.e.

$$2\ddot{y}f = \ddot{y}\ddot{y} \quad \frac{2}{\text{—}}$$

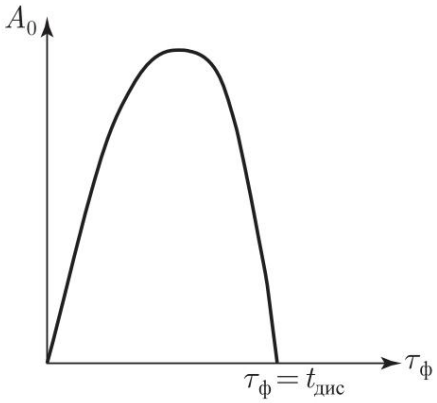

Rice. 4.45. Hypothetical image of the dependence of the amplitude of excited mechanical oscillations on the duration of the front (decay)

Taking on average ÿf = 10ÿ6, we obtain the value of double bandwidth transmission equal to 2 106 Hz . In fact, the bandwidth in this case is practically unlimited due to the small value quality factor of biological structures (Q = 1.5 ÷ 3). That is, in the decimeter wavelength range, a biological object can be considered as aperiodic structure (2ÿf = Q in fact, because $\frac{f}{\text{—}}$ ÿ (6.6 ÿ 3.3) 108 Hz). In the very the same effects during irradiation of biological objects are observed at different carrier frequencies, differing by hundreds and thousands of megahertz. Assume the existence of structures or systems capable of directly responding to microwave EMF, it is not necessary due to their large mass, which does not allow them to follow the periods fields with a carrier frequency of ~ 109 Hz. One thing remains to be assumed - excitation of mechanical vibrations during the formation of thermal impulse in a biological object is the only possible function of converting microwave pulses into an information signal. And in this sense, a biological object can be considered as direct conversion receiver with conversion factor k = F1/F2, where F1 is the pulse repetition rate, F2 is the frequency excited mechanical vibrations. Coefficient k is always less than 1 except for the case when the first harmonic of the pulse is isolated sequences, i.e. when F1 = F2.

Energy of excited mechanical vibrations. The energy of excited mechanical vibrations can be estimated by the expression Em = = 10ÿ8 · 0.5Pi · ÿf, where 10ÿ8 is the energy conversion coefficient Microwave EMF into mechanical, 0.5 · Pi · ÿf - front (fall) energy microwave pulse. At Pi ÿ 75 ÷ 500 W and ÿph ÿ (0.1 ÷ 10) 10ÿ6 s

Em = 2.5 10ÿ11 J.

Taking into account the possible amplification (ÿ 106) of power by a periodic structure due to the presence of phase matching

$$Emmax ÿ 2.5 10ÿ5 J = 25 ÿJ .$$

When energy is transferred through a single area during the pulse action

$$Emmax ÿ 0.7 \cdot 10ÿ7 J \cdot cmÿ2 = 7 ÿJ \cdot cmÿ2 .$$

When irradiating cell suspensions in test tubes, the energy of excited mechanical vibrations increases in proportion to the square of the quality factor of the test tube as a resonator. As was shown above, the quality factor of such a test tube with liquid can reach 200. In this case, the energy of mechanical vibrations excited by microwave pulses at the resonance frequency will be in the order of magnitude

$$Em ÿ 1.5 10ÿ7 4 104 J cm ÿ 2 = 6 mJ cm ÿ 2 .$$

Thus, the block diagram of the information communication channel can be presented in the following form (Fig. 4.46):

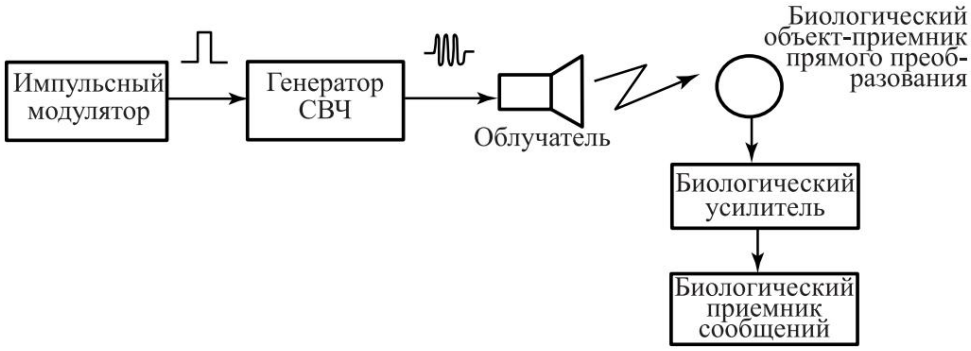

Rice. 4.46. Structure of the information communication channel

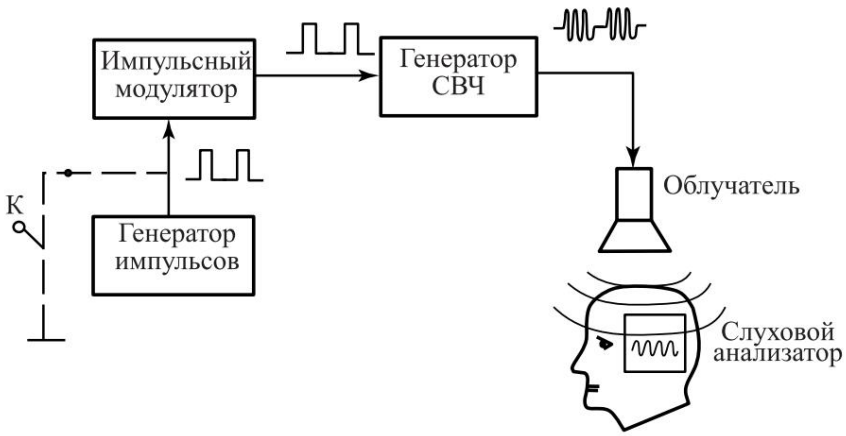

Rice. 4.47. Information communication channel in psychophysical research

The structure of the information communication channel can be especially striking be represented by direct reception of pulsed EMF
Microwave irradiation of the human head (Fig. 4.47). The formation of thermal impulses leads to the excitation of mechanical vibrations in the bone and tissue formations of the human head and through them
conduction of the hearing organ into the cochlea leads to the appearance of an auditory image.

If in this case the modulating pulse generator is started using key K (shown in the dotted line in the figure), then it is possible to transmit code information (Morse code) and directly

selection of the useful signal in the auditory analyzer.

Part II

TECHNICAL SUPPORT FOR SOFTWARE EXPERIMENTS

BIOEFFECTS OF MICROWAVE

Introduction

The study of the effects of low- and medium-power microwave radiation on biological objects is currently attracting everyone more experimenters.

Of greatest interest is the non-thermal effect of modulated microwave fields. The ability to manipulate the output power of generators makes it possible to study small dynamic shifts in biological objects by the accumulation method, provides irradiation at certain moments of the functioning of objects, allows study the kinetics of parameters. However, as mentioned above, work in this direction is hampered by the lack of necessary equipment, primarily due to the lack of microwave generators with wide possibilities for varying the parameters of the irradiating field.

A large number of existing generator devices are adapted for solving purely technical problems and does not satisfy the requirements of a biological experiment. In particular, band generators signals of early releases (GS-6, G3-20, G3-23, GSS-12, etc., see [194, 195]) have an output power level not exceeding units watt. There are completely no modulation devices for these generators that provide modulation over a wide range of the spectrum, including infra-low frequencies. Powerful generators from a number of technical devices, for example, transmitters, generator devices radar stations (radars), etc., have very limited capabilities for changing their parameters.

However, not only the lack of generators and modulators for them explains the difficulty, and often the impossibility, of setting up an experiment on the effects of microwaves on biological objects. One of the central tasks in an experiment on the bioeffects of microwaves is the transfer energy of electromagnetic vibrations to an object. The task, it would seem, long ago solved for technical purposes and, at first glance, not presenting a serious obstacle. However, here a whole a set of new tasks, since the configuration of the object and its dimensions vary widely, which entails inconsistency ratio of the cross-section of the irradiation zone of the object itself. This, in turn, leads to variations in the amount of absorbed power. Therefore, ongoing monitoring of the value is necessary absorbed power. During irradiation, the object can be very significantly heat up due to the absorbed microwave power, which also entails a change in some of its parameters, registration which is often necessary. Finally, and this is the most important thing, it is necessary to carry out permanent registration of bioelectric information, which in itself presents certain difficulties.
In this case, the situation is aggravated by the fact that many classical methods for recording bioelectrical information are not applicable when irradiation of objects with a microwave field. In some cases, microwave power

generator can reach hundreds of watts per pulse to provide
necessary EMP, especially for studies of EMF exposure
Microwave on the whole organism. So, to ensure more or less
uniform field distribution when irradiating small animals
The waveguide cross-section can reach 400 ÷ 500 cm2. The same cross-
section of the irradiator is required when studying the auditory effects of microwaves.
Naturally, the use of such high powers requires the development of special
methods for retrieving useful information in order to
eliminating the possibility of an artifact.

Modern waveguide technology used in such experiments has very
limited capabilities in this regard.
plan [196, 197], since the introduction of any sensors and devices
Receiving information into the irradiation zone leads to a violation of the specified
field patterns due to the introduction of reactivity. In addition, there is
problem of reliability of registered information [191].

The use of such devices in a biophysical experiment is not
makes it possible to achieve any significant coefficient of use of
electromagnetic energy in biological research
objects with small transverse dimensions. On the other hand, in the
conditions of using waveguide systems as irradiators of biological objects
in the decimeter and centimeter ranges, synchronous control and analysis
of the functional state of the object are connected
with certain technical difficulties [196, 197]. They can come here
be attributed to the large transverse dimensions of the waveguides and,
as a consequence, high power to ensure the required flux density
power (PPM). In this case, as a rule, removal devices and systems
biological information have a fairly large geometric
length and, being in the irradiation zone, not only become
source of interference, but can also lead to artifacts.

The need to use high-power microwave generators
requires experiments to be carried out in shielded rooms, which
associated with large capital investments and the availability of appropriate
areas [196]. At the same time, the question of safety arises
experimenter, associated with the need to ensure working
PPM zone not exceeding the maximum permissible values [198].

Synchronous recording of information is especially necessary when
short-term, rapidly passing functional states of a biological object occur
during phased pulse irradiation
EMR, such as abrupt changes in the magnitude of the cardiac cycle
when irradiating heart preparations or the whole organism in certain
phases of the cardiac cycle.

Studying the subtle mechanisms of interaction of EMFs with biological
structures in a modern biophysical experiment requires
involving not only electrophysiological research methods,
already mastered to some extent, but also optical, spectral,
polarographic, etc. Many experimental studies

are associated with the need to measure current values of pH, pO2, pK and some other parameters of culture media during perfusion object directly in the process of irradiation with microwave EMR. Enough The effect of this factor on cell suspensions is being widely studied according to various object parameters such as electrophoretic mobility, temperature dependence of membrane permeability. How As a rule, such studies are carried out in a duct along a closed cycle for the purpose of measuring the values of the studied parameters outside the zone irradiation of the object. This simplifies the process of irradiating objects and allows one to use classical research methods. Very promising for solving many problems in biophysical experiments may turn out to be transmission lines based on microstrip lines (MSL).

The modern element base of radio engineering devices in the decimeter and centimeter ranges allows us to move on to the development of a fundamentally new generation of microwave irradiators based on lines. MPLs are printed circuit boards manufactured using mesaplanar technology using photolithography based on foil-coated dielectric material. Currently exists a large number of types of MPL, which are modifications the following main types:

1) asymmetrical strip line (NSL);
2) coupled asymmetrical strip line (CSNL);
3) symmetric strip line (SPL);
4) coupled symmetric strip line (SSL);
5) symmetrical slot line (SSL);
6) asymmetrical slot line (ASL);
7) coplanar line (CL);
8) dielectric waveguides (DV);
9) shielded strip lines of the above types.

For each type of line there is a more or less complete theory that allows you to calculate the main transmission characteristics electromagnetic energy depending on the design features of the MPL, as well as determine the geometric dimensions and shapes such lines for solving specific electrodynamic problems [199].

In electromagnetobiology, the main technical task is is the problem of the most complete transfer of electromagnetic energy from the generator to the object. This problem is solved by pairing the characteristic impedances of the absorbing object and the supply line. From this position, the issues of designing irradiators for biological objects based on microwave micropaths should be resolved [200].

The fundamental possibility of using MPLs as irradiating devices opens up broad prospects for reducing the output power of microwave generators and, accordingly, eliminating the use of expensive shielded rooms. In these conditions

development and application become possible and expedient
miniature microwave generators based on semiconductors, taking into account all requirements for such experiments. In this plan
analysis of the possibilities of using MPLs as irradiators of biological objects is not just an independent technical task
to ensure biophysical experiment at the modern level.
Theoretical assessment of the parameters of the irradiating zone and integral MPL parameters with their subsequent adjustment in a real experiment is the basis for the development of microwave microgenerators for
biophysical research.

The use of microwave micropaths as irradiators of biological objects allows us to solve another problem. It is known
that a biophysical experiment on the effects of microwaves is based on already which has become a traditional scheme: microwave generator - feeder-matching device - irradiator - object. The introduction of MPL into the circuit of a microwave autogenerator as an oscillatory system makes it possible to exclude given diagram of intermediate stages and implement the experiment according to the “microwave generator - object” scheme, which will not only simplify the technology experiment, but will also provide docking with analytical instruments,
for example, with optical microscopes, spectral equipment
etc. Such a solution dramatically expands the capabilities of biophysical experiment. However, another scheme is possible that allows us to solve using microwave microgenerators for tasks in a biophysical experiment - “microwave generator is a biological object.” The arrows in this case mean that in operating mode some parameters
microwave autogenerator will be determined by the parameters of the biological object in the presence of a strong connection between the oscillatory system and the active nonlinear element. It is this quality that will allow us to determine the functional

state of a biological object. This is a fundamentally new aspect
in the use of microwave radiation in a biophysical experiment, simultaneously both as an actively influencing physical factor and as
method of monitoring the functioning of a biological object not only
when exposed to microwave radiation itself, but also to other physical or chemical factors.

A preliminary experimental study of the functional state of biological objects under the influence of microwaves according to the traditional scheme using MPL is not only a search for ways
interaction of EMF with biological objects, but also the possibility of obtaining information to determine technical parameters
microwave microgenerators.

The choice of a specific MPL design can be made based on
analysis of its properties when paired, on the one hand, with biological objects, on the other hand, with a nonlinear element of a self-oscillator. This approach will allow us to assess energy performance
self-generator as a technical device and at the same time reveal

the possibility of implementing one or another class of biological tasks using MPL.

The task of creating microwave microgenerators using MPLs in itself is not new [78]. These devices are widely application in satellite equipment, their main area of application is communications and telemetry. The requirements for such devices primarily address stability issues carrier frequency. Therefore, microwave generators based on semiconductor base are built according to the frequency multiplication circuit of the self-oscillator and contain 6 ÷ 8 cascades. Load with constant parameters significantly simplifies the technical solution of issues and allows operation these devices in optimal mode. On the other hand, the constancy of the load parameters and the generator output power level, and, accordingly, the mode of the output stages makes them unnecessary current coordination or determination of power absorbed in the load. In a biological experiment, these questions are reversed - one of the main tasks is the correct measurement of absorbed in the power object. Requirements for high frequency stability carrier in the decimeter and centimeter ranges in this case are presented only in certain cases.

These circumstances allow us to choose as the main scheme microwave generator on an MPL oscillator circuit. The inability to work in optimal mode in the presence of strong variability in the parameters of biological objects leads to the need inclusion of microwave nodes in the microgenerator circuit to protect the transistor from the action of a wave reflected from the object, etc. At the same time, the question arises about the need to regulate the output power level, the solution of which, in the presence of a semiconductor generator element, is more complicated compared to microwave tube generators [200].

In terms of the issues considered, the development of the fundamentals of the theory of calculation and design of microwave microgenerators on MPL for biological research is the first stage.

The most optimal microwave microirradiator in terms of its interface with a microscope, fluorimeter, as well as with other optical instruments is an irradiator based on (SSHL). It's simple in production [199], easy to use and does not require the development of additional optical devices. However, these conveniences are not possible be implemented due to the insufficiently developed theory of constructing lines of this kind [203], as well as due to the difficulties of measuring microwave frequencies parameters [204].

One of the methods for monitoring the condition of microscopic biological objects in laboratory conditions is visual control using a microscope. When irradiating a biological object, located under the lens, the question arises about supplying electromagnetic energy to an object located near metallic parts of the microscope that change the structure of the supplied field

and significantly distort the expected field distribution in the object. In addition, the location in close proximity to the emitting element of the researcher must comply with accepted

PPM standards [198]. Accurate control of absorbed power is also necessary.

The most easily calculated and having a simple design along with wide capabilities is a shielded symmetrical strip line (ESPL). From a safety point of view, the use of an ESPL as an irradiator with localization

fields in a closed volume can be considered a better option.
At the same time, finding an object inside the ESPL requires the use of
long focal length lenses.

Research at the cellular and molecular levels under the influence of non-ionizing radiation requires the development of special
microelectrode technology and recording devices capable of
function normally in the microwave irradiation zone, ion-selective
electrodes, dosing devices and samplers. Works in this
areas showed that the intensity of excited mechanical vibrations is sufficient for their recording by piezoceramic sensors with a sensitivity of 10ÿ6 V dyn ÿ 1 cm2. At UPM values

of the order of 10 ÷ 100 mW g ÿ1, usually occurring in biophysical
experiment, the amplitude of the sound variable pressure will be
a value of the order of 10 ÷ 103 dyn. With the above-mentioned sensitivity of the piezoceramic transducer, the amplitude of the alternating electrical signal on its plates will reach 1 mV. However
to achieve such sensitivity it is necessary to use piezoceramic transducers with a diameter of 30 ÷ 50 mm, which causes
certain difficulties when docking them with irradiators. That's why
in some cases you have to make a compromise and a few
increase the dimensions of the irradiator. For example, the use of piezoelectric sensors in model experiments on the study of auditory
microwave effects made it possible to largely abandon experiments on
people and arrive at spherical models while simultaneously obtaining objective information.
Numerous literature have described
Microwave resonators as systems for concentration and localization of EMF
in limited volumes, in a variety of configurations. As a rule, these are cylindrical or cubic formations, diameter, height
and the method of excitation of which determines the type of wave in the resonator and energy distribution throughout the volume. An analysis of the literature shows that the uniform distribution of energy in the resonator is almost
impossible for any one vibration mode or for one type
waves. Quite good distribution of microwave energy evenly
throughout the entire volume can be achieved only in multimode resonators [40]. An example of the use of such resonators is
electronic microwave ovens for heating food products.

The use of resonators with high field inhomogeneity in biological research with high heterogeneity of the biological objects themselves will not allow an unambiguous interpretation of the obtained results.
information and will introduce errors in quantitative estimates of the observed effects. Irradiation of biological objects in multi-mode resonators, due to the presence of a wide range of active

electromagnetic oscillations, can lead to the formation of a whole
a number of different effects, complexly interconnected in a biological system. The integral response is practically not
provides information about the functional state of the object.

It should also be noted that when designing resonators
Microwave in the frequency range 460 ÷ 2450 MHz, the dimensions of structures are commensurate with the wavelength. Reduce the size of the resonator
possible using a decelerating structure (SS).

One of the valuable properties of GS is its superficial nature.
wave propagation, which makes it possible to use such
systems as sensitive elements of converters of physical quantities. Thus, the use of GS in the resonator will allow
solve several issues at once - significantly reduce the size
resonator, increase field uniformity and PPM. Constructive
features of ES and distribution of electromagnetic energy in them
allow you to choose a cylindrical resonator with a spiral GS as an irradiator for biological objects. This design
allows you to solve a wide range of biological problems both in single microvolumes and in a duct.

This section discusses the problem of technical support for experiments on the bioeffects of microwaves, including
methods and instruments capable of solving a wide range of biological
tasks. Considering that the industry does not produce the necessary
instruments described in the experiments, this chapter provides detailed
description of methods for modifying serial domestic and foreign ones
laboratory measuring microwave generators and medical devices for microwave therapy as one of the most accessible
ways to create devices in laboratories that can provide research into the bioeffects of microwaves. Calculation and designs are described
and assembly technology for some types of transmission lines used
as irradiators of biological objects. Fixation issues considered
various biological objects, methods for collecting useful information. Several examples present hardware complexes for staging biophysical and electrophysiological experiments in laboratory and shielded rooms. Issues briefly discussed

shielding of equipment during experiments.

Chapter 1

LONG LINES

In the previous section, free electromagnetic waves propagating in the space between the transmitting and receiving antennas were considered. In addition to free waves, there are guided waves that propagate along artificially constructed

guide systems, which, first of all, include
long lines.

The simplest long line, called two-wire, consists of
two parallel wires of the same diameter, separated by a dielectric. Coaxial lines are often used, in which one
a wire is located inside another, and the space between the wires
usually filled with a solid dielectric.

The long line refers to electrical circuits with distributed parameters. If one of the geometric dimensions of the circuit (in this case, length l) is equal to or greater than the wavelength of the current
oscillations, such a circuit should be considered as a system with inductance, capacitance, active resistance and active conductivity distributed along its length. Virtually distributed

the nature of the line parameters is taken into account if l ÿ/4.

This chapter discusses the basic properties, characteristics and applications of long lines. The main attention is paid to the following issues:

1. *What are the main parameters that characterize a long line, what is its equivalent circuit?*
2. *How does the process of energy propagation along the line proceed?*
3. *What are the features of running, standing and mixed* modes? *waves in lines?*
4. *What determines the input resistance of the line?*
5. *What coefficients characterize the reflection of waves in the lines?*
6. *Which devices use long lines?*

1.1. Equivalent circuit and main parameters of long lines

Main parameters. The electrical circuit of a line of length l is shown in Fig. 1.01, a. A generator is connected to points *1–1 ,* EMF E
which varies according to a sinusoidal law. In the general case , the internal resistance Zi of the generator is complex. Resistance
Load Zn is connected to points *2–2.*

The long line equivalent circuit (Fig. 1.01, b) is
series connection of many elementary sections *(cells)* of length dx, each of which has some inductance
L1 dx, capacitance C1 dx, active resistance R1 dx and active conductivity G1 dx, where L1, C1, R1, G1 are parameters related to unit of line length and called *primary* (or linear).
If these parameters have the same value in any section
line, the line is called *homogeneous.*

For lines used in radio devices, usually
the following inequalities are valid: ÿL1 R1, ÿC1 G1, where ÿ is the angular generator frequency. Such lines are called *lossless lines.* Scheme
lossless line replacement is shown in Fig. 1.01. As we see,
this circuit is a series connection of n links
electrical low-pass filters at n ÿ ÿ.

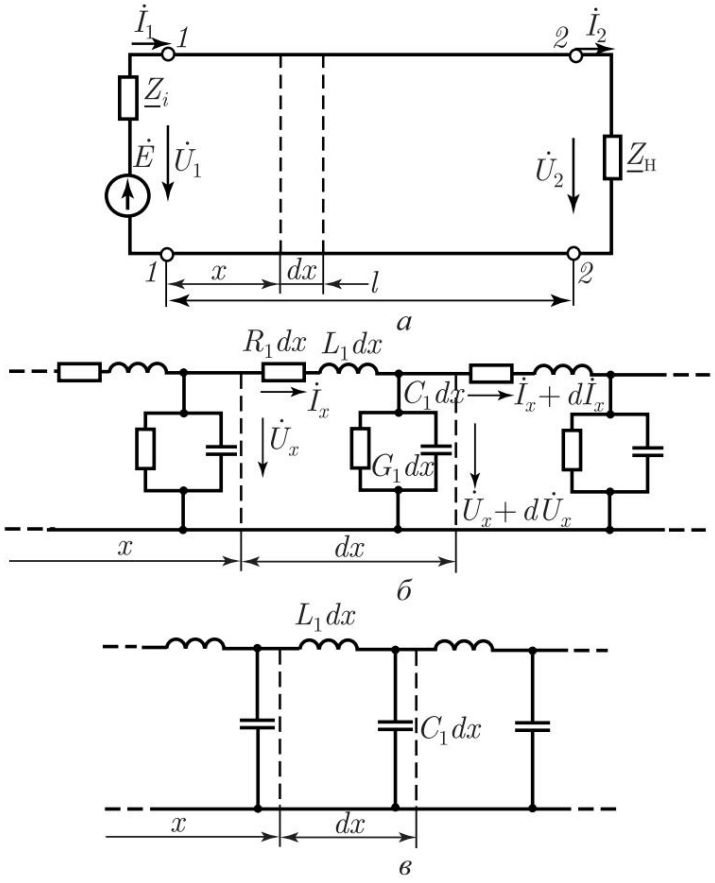

Rice. 1.01. Long line and its equivalent circuits

Primary parameters depend on line constructions and
dielectric properties between wires. In a two-wire line with an air dielectric, the linear inductance, ÿH/m, and capacitance,
pF/m:

$$L1 \text{ ÿ } 0{,}92 \lg(a/r),\ C1 \text{ ÿ } 12{,}1/\lg(a/r), \qquad \text{(II.1)}$$

where a is the distance between the centers of the line wires, r is the radius of the wire (Fig. 1.02, a).

In coaxial line

$$L1 \ddot{y} 0{,}46 \lg(D/d),\ C1 \ddot{y} 24{,}1\ddot{y}r/\lg(D/d), \qquad \text{(II.2)}$$

where ÿr = ÿa/ÿ0 is the relative dielectric constant of the medium filling the space between the wires of the line; D and d are the diameters of the wires (Fig. 1.02,). *b*

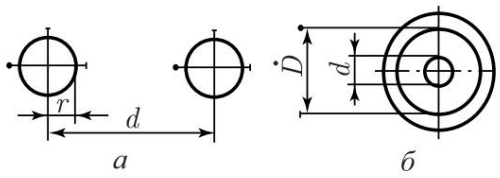

Rice. 1.02. Cross-section of wires of overhead and coaxial lines

Using the equivalent circuit of a homogeneous line (see Fig. 1.01,) *b* you can create equations for current and voltage in any section, acting at any time. Let us select an elementary section on the line t lines x dx , located at a distance la, and determine the difference in voltages and currents at the beginning and end of this section: x from its beginning

$$IN_x - (IN_x + d\,In_x) = -d\,IN_x = I_x R_1\,dx + I_x \ddot{y}L\,j_1\,dx.$$
$$I_x - (I_x + d\,I_x) = -d\,I_x = IN_x G_1\,dx + In_x \ddot{y}C\,j_1\,dx.$$

From these expressions we obtain second-order linear differential equations with constant coefficients, called *telegraph equations*

$$2d\,IN_x/dx^2 = \underline{\text{WITH}}\,1\underline{Y}\,\underline{1U}_x; \quad 2d\,I_x/dx^2 = \underline{\text{From}}_1\,\underline{\text{AND}}\,\underline{1I}_x. \qquad \text{(II.3)}$$

Where $\underline{Z1} + j\,\bar{y}\underline{L}$ is the complex resistance of the series 1 dx Y ÿC + j branch of the section; 1 linen branch of this site. Equations (II.3) make it possible to explore various modes $\underline{\bar{R}}_1$ $\underline{\bar{G}}_1$ — complex conductivity of parallel

work of long lines.

The solution to (II.3) in the special case when a lossless line is considered is the following expressions:

$$Ux = U\ddot{y}\,1\cos\ddot{y}x + j\,I1Zc\sin\ddot{y}x,$$
$$Ix = I1\cos\ddot{y}x \ddot{y} (jU\ddot{y}\,1\sin\ddot{y}x)/Zc, \qquad \text{(II.4)}$$

where $U\ddot{y}1$ i I1 - voltage and current at the beginning of the line; x - coordinate distance measured from the beginning of the line.

In many cases, the voltage values Uÿ are known 2 and current I2
at the end of the line. Then (II.4) take the following form (provided
that the coordinate y = l ÿ x is measured from the end of the line):

$$U_{ÿ\ and} = U_ÿ 2 \cos ÿy + j\, I2Zc \text{ without } ÿy,$$

$$Iy = I2 \cos ÿy + (jUÿ\ 2 \sin ÿy)/Zc. \qquad \text{(II.5)}$$

Equations (II.4) and (II.5) include quantities ÿ and Zc, called
respectively, *the phase coefficient* (wave number) and *wave*
line resistance. These quantities can be expressed through the primary parameters L1 and C1:

$$ÿ = ÿ\ L1C1\ ;\ Zc = L1/C1\ . \qquad \text{(II.6)}$$

Secondary parameters. The phase coefficient and characteristic impedance are called secondary line parameters. As will be shown later, coefficient ÿ characterizes the change in voltage phase
or current per unit line length.

The characteristic impedance of the line has the same meaning as the characteristic impedance of the electric filter, which follows from
analogies between the equivalent circuit of the elementary section of the dx line and the circuit (LPF). However, in a lossless line, unlike a filter, this resistance does not depend on frequency, therefore, if the line load
is the active resistance Rÿ = Zc, it will be matched to
all frequencies.

Let's find the wave impedances of the overhead two-wire and coaxial lines by substituting the values of L1 and C1 into the formula for Zc
from (II.1) and (II.2). After calculations we get: for an overhead line
Zc ÿ 276 log(a/r) Ohm; for coaxial line with solid dielectric
Zc ÿ [138 lg(D/d)]/ ÿÿr ÿÿ.

In addition to the phase coefficient and wave impedance, the secondary parameters of lines include *the speed of energy propagation*
and attenuation coefficient.

1.2. Distribution of energy in a line without loss. Running waves

Formation of traveling waves. Let us assume that a generator is connected to a homogeneous lossless line of infinite length
constant voltage Uÿ (Fig. 1.03, a). At the time of connection
Capacitance C begins to charge 1 elementary section *1* through inductance L
1. The voltage across the capacitance increases gradually, so
due to the influence of self-induction emf arising in L 1, charge current
grows smoothly. At time t1, capacity C 1 charges up to
voltage u = Uÿ.

Simultaneously with the process of charging capacity C 1 its discharge occurs
through inductance L 2 and capacity C 1 of the second elementary section.
Capacity C gradually charges, and the associated decrease
2 voltages on capacitance C 1 is compensated by the source Uÿ. Through

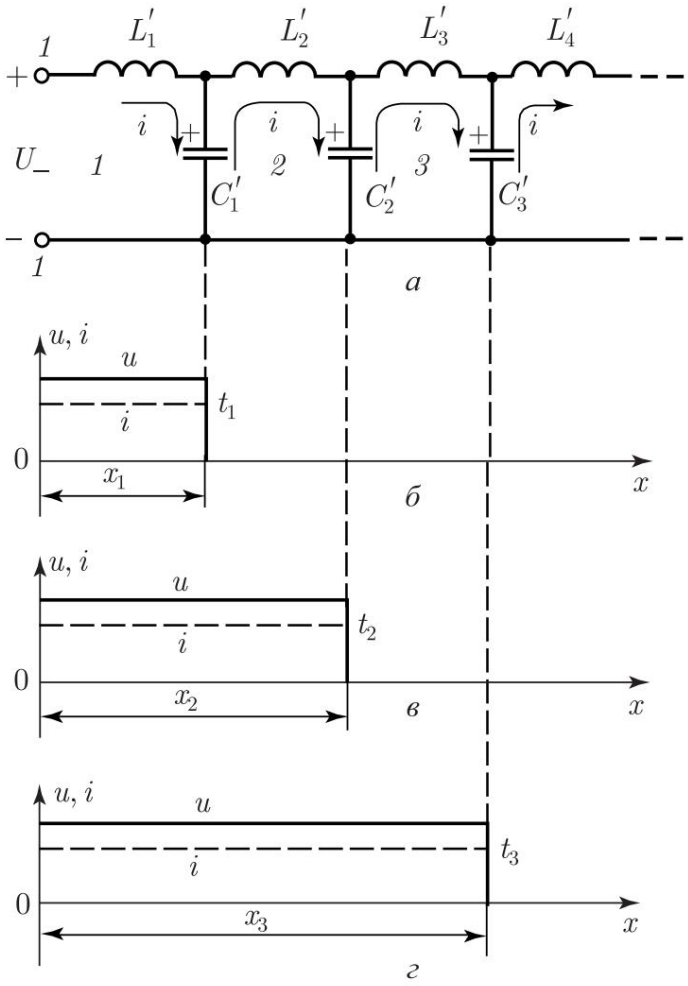

Rice. 1.03. Propagation of DC voltage along a line

capacity C 1 equal but oppositely directed currents pass,
therefore the resulting current in capacitance C ₁ = 0. Therefore, it is possible
assume that the generator current charges capacitance C2 via inductance
L and L 2. Capacitance charge C₂ ends at time t2.

1 At the same time, capacitance C is charged 3 through inductance L 1,
L 2, L ₃ etc.

As a result of this process of charging the capacitances of elementary sections in the line, a current and voltage wave is created, called *a traveling wave.*
As it propagates, a constant current is established in the line
and tension. The described process is illustrated in Fig. 1.03, b, c, d.

The current in any section of the line is the same and is determined by the ratio of the voltage Uÿ to the characteristic impedance Zc of the line. That's why,
if the line is loaded with resistance Rÿ = Zc, a current equal to the current in the line will pass through it. It follows that in a consistent
line, all supplied active power is absorbed by the load.
This does not happen if Rÿ = Zc.

Let, for example, Rÿ = 100 Ohm, Zc = 50 Ohm, Uÿ = 50 V. Then the current in the line i = 50/50 = 1 A, and the current in the load in = 50/100 = 0.5 A. The remaining 0 .5 A creates a traveling wave in the line, the power of which is equal to the difference between the power supplied by the generator and the power absorbed by the load. This wave propagates from the load to the generator and is therefore called *reflected* in contrast to *the incident* wave propagating from the generator to the load. The reflected wave can be considered as a process of alternate charging of the capacitances of elementary sections of the line, occurring in the direction from the end of the line to its beginning.

Let's consider how the voltage and current will change in a matched line of length l = ÿ/2 if the generator voltage changes according to the sinusoidal law u = Um sin ÿt (Fig. 1.04, a). According to the same law, the current at the beginning of the line i = u/Zc = (Um sin ÿt)/Zc = = Im sin ÿt will change. When the generator is turned on,

the voltage and current in the line are zero. During the period of time ÿt1 = T /8, the voltage at the line input will increase from 0 to 0.7Um, and the current - from 0 to 0.7I (indeed, i = Im sin ÿt = Im sin(2ÿt/T) = Im sin(2ÿT/8T) = Im sin(2ÿ/8) = = Im sin 45ÿ = Im ÿ 2 /2 ÿ 0.7Im. In this case, a traveling current wave will appear in the line, propagating with speed v. During the time ÿt1 the wave will reach. line sections x1 = vT/8 = ÿ/8, where vT = ÿ. At time t1, the current in the line will be distributed as follows: at the line input i ÿ 0.7Im, in sections x x1, current i = 0 (Fig. 1.04 , b, curve 1). After a period of time ÿt2 = 2ÿt1 = T /4, when the voltage at the line input becomes equal to Um, the current wave

reaches the cross section x2 = = ÿ/4; the current at the line input at the same time i = Im (Fig. 1.04, b, curve 2).

Using similar reasoning, it can be shown that at time t3, the current at the line input will decrease to 0.7Im and the current wave will spread to cross section x3. By time t4, the current wave reaches the end of the line, and the current at its input will become zero (Fig. 1.04, b, curves 3, 4). Simultaneously with the current wave, a voltage wave propagates along the line, and these waves are in phase (voltage wave graphs are not shown in Fig. 1.04). Let us pay attention to the

uneven distribution of current along the line, which is explained by the time delay of the traveling wave, which is greater the further the section under consideration is from the beginning of the line. To do this, let’s compare the graphs of current changes over time in line sections x = 0, x1, x2, x3, x4 (Fig. 1.04, b). A comparison shows that if in the line section x = 0 changes in current over time begin at t = 0, then in the section x = x1 = ÿ/8 at t = t1 = T /8, in the section x = x2 = ÿ/4 at t = t2 = T /4, etc. **Equations of traveling waves of voltage and current in a**

lossless line. Let the instantaneous value of the generator voltage u1 = = Um1 sin ÿt. Then in an arbitrary section of the line located at a distance x from its beginning, the voltage ux will lag by

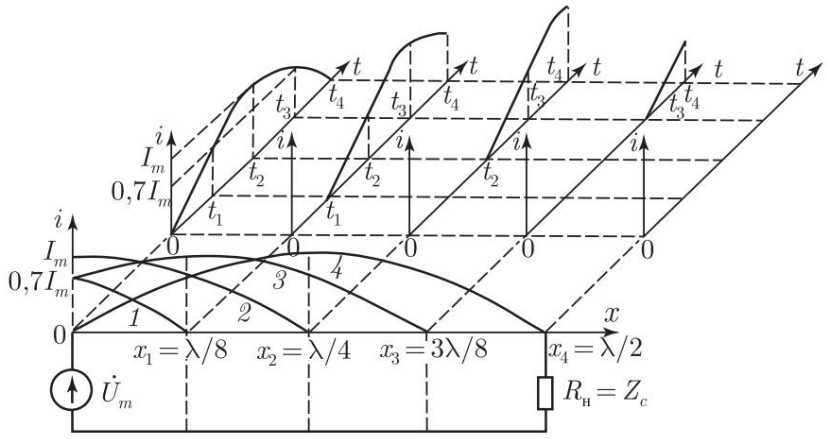

Rice. 1.04. Diagrams explaining the propagation of a current wave in a line

time tx = x/v, so we can write ux = Umx sin ÿ(t ÿ tx) =
= Umx sin(ÿt ÿ ÿtx) = Umx sin[(ÿt) ÿ (ÿx/v)].

Let's consider the ratio ÿ/v. Angular frequency ÿ shows at
how many radians or degrees per second does the phase of the oscillation change?
in section x of the line, and the speed v is the distance it moves
wave during this time. Therefore, dividing ÿ by v, we obtain a number indicating the change in wave phase per unit length
line, i.e. phase coefficient ÿ. Considering that ÿ = 2ÿf, and v = ÿt,
we get the phase coefficient, rad/s

$$ÿ = ÿ/v = 2ÿf /ÿf = 2ÿ/ÿ. \quad (II.7)$$

Since we are considering a lossless line, the voltage and current amplitudes in all sections are the same, therefore, it is possible
write down

$$ux = Um1 \sin[ÿt ÿ (ÿx)/v] = U1m \sin(ÿt ÿ ÿx). \quad (II.8)$$

A similar expression is obtained for the current:

$$ix = [Um1 \sin(ÿt ÿ ÿx)]/Zc. \quad (II.9)$$

Relations (II.8), (II.9) are equations of traveling waves
in a lossless line. As can be seen from these equations, current and voltage
are functions of two variables: time and distance coordinates, which to a certain extent complicates the analysis of the operation of circuits with distributed parameters compared to circuits with concentrated
parameters.

Using the equations of traveling waves, it is possible to construct the distribution of current and voltage along the line for different moments in time (Fig. 1.05, a). From the figure it can be seen that the wave seems to be moving
along the line at a certain speed. From (II.6) taking into account (II.7) the speed

$$v = 1/\sqrt{L1C1}. \quad (II.10)$$

Substituting into (II.10) the values of L1 and C1 from (II.1) of an overhead two-wire line and carrying out calculations, we obtain that v ÿ 3 108 m/s, i.e. the speed of propagation of a traveling wave is close to the speed c0 of light in a vacuum. Substitution in (II.10) values L1 and C1 (II.2) coaxial line with a solid dielectric gives: v1 ÿ v/ÿÿr = c0/ ÿÿr . Because ÿr > 1, we find that the speed of propagation of traveling waves in such line is less than c0, so the oscillation wavelength is less ÿ0. This conclusion is valid for any line whose wires are located in a real environment.

Traveling wave equations for a line with losses. In a line with losses, part of the energy of traveling waves is irreversibly converted in the wires into other types: thermal, radiation energy, etc. Therefore the amplitude of the voltage and current of the wave gradually decreases (attenuates) as the wave propagates. It can be shown that the damping occurs according to the exponential law (Fig. 1.05). For a line with losses, the traveling wave equations

$$u_x = U_{m1}e^{ÿÿx}(\sin ÿt ÿ ÿx),$$
$$i_x = [U_{m1}e^{ÿÿx}(\sin ÿt ÿ ÿx)]/Z_c, \qquad \text{(II.11)}$$

where ÿ is *the attenuation coefficient,* characterizing the decrease in voltage or current amplitudes per unit line length.

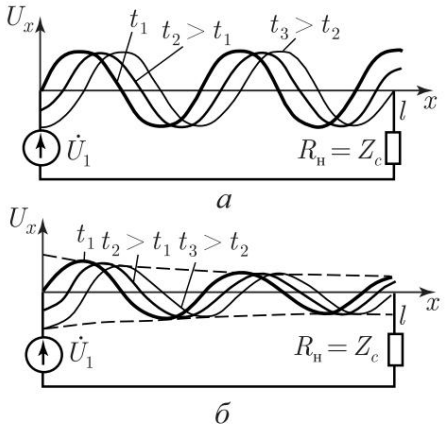

Rice. 1.05. Traveling waves in ideal and real lines

When taking into account the primary parameters of the line, the attenuation coefficient, dB/m

$$ÿ \approx 8{,}7R\sqrt{C1/L1}, \qquad \text{(II.12)}$$

where $R_1 = R1/2 ÿ 0.04ÿf/r$ - active resistance, Ohm, one meter of copper wire with radius r, mm, at frequency f, MHz.

Thus, the coefficients ÿ and ÿ included in equations (II.11) characterize changes in the amplitude and phase of traveling waves propagating along a line. These coefficients are components of a complex quantity called *the propagation coefficient* ÿ = ÿ + jÿ.

Lossless line input impedance. Let's move on to consider one of the important characteristics of the line - input resistance, which is understood as the ratio Zin = Uÿ 1/ I1. In line without
losses loaded with resistance Rÿ = Zc, input resistance
active and equal to the load resistance, i.e.

$$Z_{vh} = R_{vh} = Z_c = R_n. \qquad \text{(II.13)}$$

The active nature of the input impedance means that instantaneous
the voltage and current values at the input of a line of any length are the same
in phase, as can be seen from the comparison of (II.8) and (II.9). In this case, all active power supplied to the line input is absorbed by the load,
which means there are no reflected waves in the line.

Application of electromagnetic field theory to the analysis of the process of energy propagation along a line. Let there be an ideal
two-wire line of length l = ÿ, and the dielectric separating
wires are also perfect. The line is matched, so traveling waves of voltage and current propagate in it. For some arbitrary time t1, the waves are distributed in the line as shown in

Fig. 1.06.

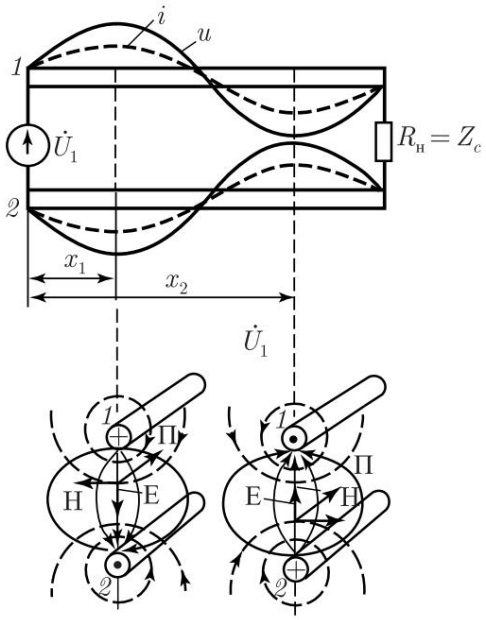

Rice. 1.06. Electromagnetic field of traveling waves

Since there is an alternating voltage between the wires of the line associated with an electric field, and an alternating current associated with a magnetic field passes through the wires, we can assume that along
a traveling electromagnetic wave propagates along the line. Let's highlight
in the section lines x1 and x2, corresponding to the voltage amplitudes
and current, and determine the direction of the Poynting vector in these sections
(for the positive direction of the current we will take the direction from the generator

torus to the load on the line section with positive amplitudes
voltage and current).

As follows from Fig. 1.06, in the selected sections the vector ÿ has
the same direction (to the load), despite the fact that the currents
in these sections are identical and directed towards each other. Consequently, a traveling
electromagnetic wave transfers energy from
generator to load; line wires form a channel guiding
energy flow.

The traveling wave mode is the most preferable and expedient when transferring energy
from the generator to the load, but
and requiring maximum effort for its implementation.
Let us also consider possible modes of wave propagation along guide structures encountered
in practice.

1.3. Standing waves in a lossless line

Formation of standing waves. If all the energy of the incident wave
is reflected from the end of the line and is completely returned to the generator,
two traveling waves with the same amplitude arise, propagating along the line towards each
other at the same speed.

As a result of the addition (interference) of these waves, *hundred*
cellular waves.

Standing waves arise at idle speed (Zÿ = ÿ), short
short circuit (Zn = 0) or when the line is loaded with reactance, i.e. in those cases when
irreversible
energy conversion.

Standing waves at idle. Let's consider the idle speed of the line. Since the load resistance
Zÿ = ÿ, the current at the end of the line is equal to
zero, which is possible if in the section x = l (or y = 0) the incident currents
and reflected waves are identical, but shifted in phase by an angle of 180ÿ.
The current being zero means that at the end of the line the magnetic energy
field of the incident electromagnetic wave is converted into its energy
electric field, resulting in the electric intensity
fields and voltage double. From this we can conclude: the voltages of the incident and reflected
waves at the end of the line have the same
phase. Thus, the voltage is reflected from the end of the open circuit
lines without changing phase, and the current upon reflection changes phase by
the opposite.

In Fig. 1.07, *and* there are diagrams showing the distribution of instantaneous voltage
values of the falling voltage (continuous
line), reflected (dashed line) and standing (thick line)
waves in the line at times t0 ...t6, separated by intervals
T /8. The directions of wave movement are indicated by arrows. The origin of the coordinates of
the diagrams is combined with the end of the line, since it is in this
cross section at any time it is known that the voltage drop
and reflected waves have the same phase.

From an examination of the diagrams it follows that the oscillation obtained as a result of the addition of the running voltages of the incident and reflected waves does not move along the line. This *is a standing voltage wave.* Similarly, we can show the formation of *a standing current wave.*
You just need to remember that the phases of the incident and reflected currents the waves at the end of the line are opposite. Distribution of voltage and current of standing waves along a line for fixed moments of time
t0 ...t6 passing through T /8 is shown in Fig. 1.07, b.

Level of standing waves. These equations can be obtained from (II.5) after substituting I2 = 0 and a number of transformations

$$uy = 2Umpad \cos ÿy \sin ÿt,\ iy = [2Umpad \sin ÿy \sin(ÿt + 90ÿ)]/Zc, \quad \text{(II.14)}$$

where Umpad is the voltage amplitude of the incident wave at the end of the line.

In (II.14), the expressions 2Umpad cos ÿy and (2Umpad sin ÿy)/Zc represent the amplitudes of voltage Umc and current Imc, respectively standing waves. The amplitude distribution along the line is shown in rice. 1.07, in.

The properties of h and h waves. From Fig. 1.07, as well as from the considered of the diagrams shown in Fig. 1.07, a, b, c, follows:

1. In any section of the line, voltage and current vary time according to a sinusoidal law, and the phase shift angle between them 90ÿ. At times t2, t6, corresponding to the maximum voltage, the current in the line is zero, at maximum current at times t0, t4 the voltage in the line is zero (Fig. 1.07, b). Can show that at times t2, t6 the average energy of the electric field at each quarter-wave segment of the line is maximum, and the magnetic field energy is zero. At times t0, t4, on the contrary, a maximum of the average magnetic field energy is observed; the energy of the electric field is zero. In the intervals between the indicated moments of time, a mutual transformation of the energies of the electric and magnetic fields occurs, and the sum of these energies remains constant (the exception is the end of the line, where all energy is concentrated in the electric field). Let us recall that similar energy processes occur at resonance in an ideal oscillatory circuit.

2. In line sections y = 0, y2 = ÿ/2, y4 = ÿ, i.e. at distances from the end of the line, multiples of ÿ/2, maximum voltage amplitude, and the current is zero. Such sections are called *stress antinodes and current nodes.* In sections y1 = ÿ/4, y3 = 3ÿ/4, y5 = 5ÿ/4, i.e. distances from the end of the line that are multiples of an odd number ÿ/4, on the contrary, the voltage is zero and the current is maximum. These sections are called *voltage nodes and current antinodes.*

3. The voltage phase in all sections of the line is the same, therefore maximum or zero voltage values are obtained in one

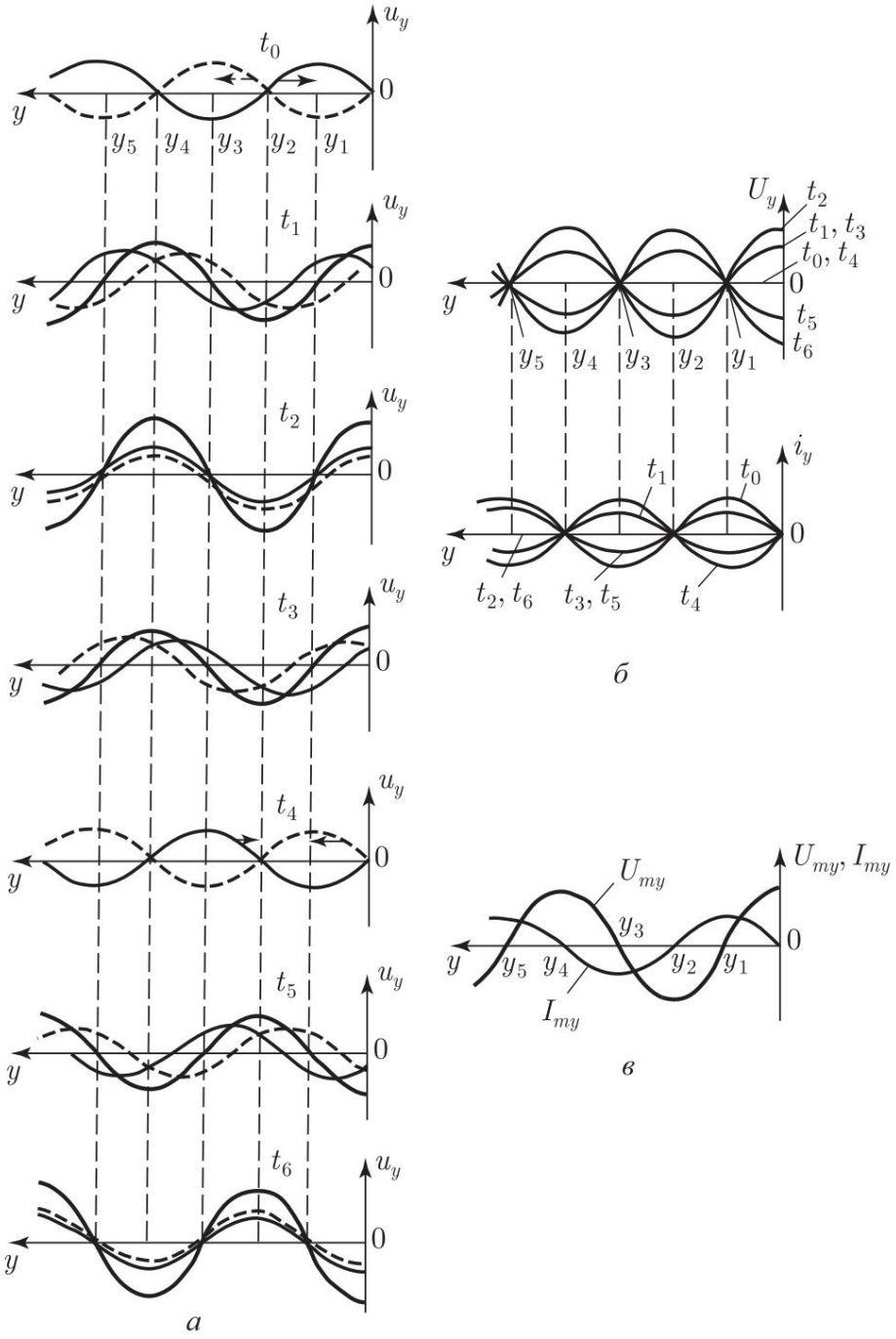

Rice. 1.07. Standing waves in an open line

and the same moments in time. However, the voltage maxima in different
sections are different due to changes in the stress amplitude along
lines. The same conclusion is true for the current in the line.

4. The characteristic impedance of the line is equal to the ratio of the voltage amplitudes Ump and current Imp at the antinodes. To make sure of this,
Let us substitute the values cos my = 1 into the expressions for the amplitudes Umÿ and Imc

and sin my = 1. We get Ump = 2Umpad, Imp = 2Umpad/Zc, from where Zc = = Ump/Imp.

Input with resistance. Open line without losses has a reactance input impedance

$$X_{in.x} = \ddot{y} Z_c \operatorname{ctg} \ddot{y} y. \qquad \text{(II.15)}$$

Dependence of the input resistance on the y coordinate (or, otherwise speaking, from the length of the line) is illustrated using Fig. 1.08. From an examination of this figure it is clear that when the length changes, the input The line resistance can be capacitive or inductive and varies from 0 to ÿ. If the line length is odd number ÿ/4, its input resistance is zero, if even - then infinite.

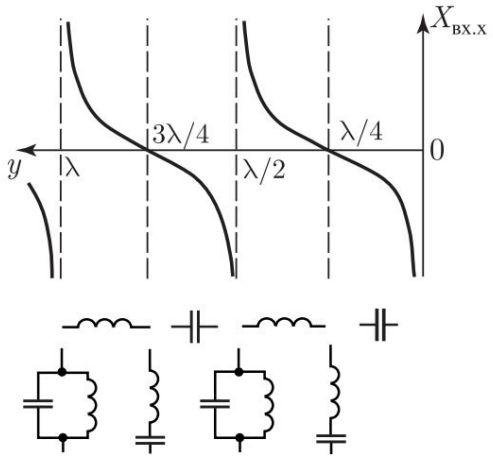

Rice. 1.08. Dependence of input resistance on line length

Let's consider how the input resistance of a line of length l = ÿ/4 will change when the generator frequency f changes. Let the frequency decrease f1 < f. This means that the wavelength of the generator oscillations has increased to the value ÿ1 > ÿ, therefore, we can write ÿ1/4 > ÿ/4 or l<ÿ1/4. Thus, at a lower generator frequency the relationship between l and ÿ/4 is violated , therefore, as can be seen from Fig. 1.08, the line input impedance becomes capacitive. Similarly, it can be shown that if f2 > f, then ÿ2 < ÿ and l > ÿ/4. In this case the input resistance is inductive. As we see, the nature of the dependence input resistance versus frequency is the same as that of series outline.

Note that at a fixed frequency of the generator, the input resistance is determined by the length of the line. So, with a decrease in length y < ÿ/4 the input resistance becomes capacitive, and as ÿ/2 > y > ÿ/4 increases, it becomes inductive.

The frequency dependence of the input resistance of an open line of length ÿ/2 is the same as that of a parallel circuit: for f1 < f it is inductive, when f2 > f it is capacitive.

If we take into account that the nature of the energy processes in quarter-wave segments of the line is the same as in an oscillatory circuit, we can draw a conclusion: sections of an open line, the length of which is a multiple of ÿ/4, equivalent to ideal serial or parallel
circuit tuned to resonance. In this regard, the line having
a length that is a multiple of ÿ/4 is called *resonant.*

The input impedance of a lossy line contains, in addition to the reactive component, an active component, which depends on the frequency and length lines. Therefore, resonant segments of real open lines
are equivalent to real oscillatory circuits that have active
losses.

Standing waves in a short-circuited line. Because in such
line Zÿ = 0, voltage U2 = 0 and energy is completely reflected from
end, forming reflected waves of current and voltage. In this case, the phase The incident current wave coincides with the phase of the reflected one, and the phases of the incident and reflected voltage waves are opposite. As a result The addition of incident and reflected waves produces standing waves.

Equations of standing waves for a line short circuit:

$$uy = 2Imÿÿÿ Zc \sin ÿy \sin(ÿt + 90ÿ);$$
$$iy = 2Imÿÿÿ \cos ÿy \sin ÿt, \qquad \text{(II.16)}$$

where Impad is the current amplitude of the incident wave at the end of the line; 2ImpadZc sin ÿy is the amplitude of the standing wave voltage;
2Impad cos ÿy is the amplitude of the standing wave current.

Analysis (II.16) shows that at the end of the short-circuited line
there is a current antinode and a voltage node (Fig. 1.09, a). From the comparison of Fig. 1.09, *a* and 1.07, *c* it is clear that the amplitude change curves voltage and current along open and short-circuited lines
shifted by ÿ/4.

Input short circuit impedance

$$Xvx.k = Zc \operatorname{tg} ÿy \qquad \text{(II.17)}$$

has a reactive nature and depends on the line length and frequency
(Fig. 1.09, b). Resonant line segments with lengths that are a multiple of odd number ÿ/4, have an infinitely large input resistance and are equivalent to an ideal parallel circuit; with a line length that is multiple
no even number ÿ/4, the input resistance is zero and the line
is equivalent to an ideal series circuit.

Standing waves in a line loaded with reactance. In such a line, all the energy entering the load is completely
is reflected from it and returned to the generator, resulting in
standing waves disappear.

The amplitudes of voltage and current of standing waves are distributed along lines according to a sinusoidal (cosine) law, however, antinodes and voltage (current) nodes are shifted by a distance l relative to

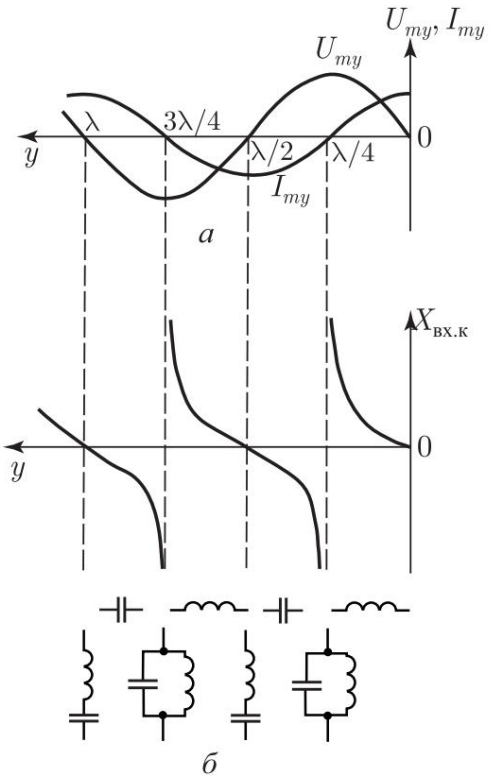

Rice. 1.09. Distribution of amplitudes of standing waves and dependence on the length of its input resistance

sections spaced from the end of the line by nÿ/4, where n is an integer. This shift depends on the magnitude and nature of the load reactance. For example in Fig. Figure 1.10 shows the distribution

of voltage and current amplitudes in a line loaded with an ideal capacitor. As can be seen from this figure, due to the shift of nodes and antinodes of standing waves, the amplitudes of voltage and current in the load decreased compared to their values at the antinodes; in addition, the length of the resonant line segments decreased by l .

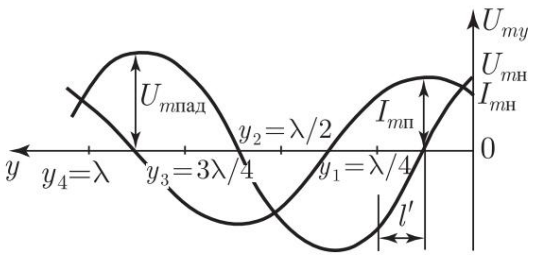

Rice. 1.10. Distribution of amplitudes of standing waves in a line with a capacitive load

1.4. Mixed waves in a lossless line

Coefficients characterizing wave reflection. As is known, electromagnetic energy transferred by an incident wave can completely irreversibly transform in the load if its resistance is active and equal to the characteristic impedance of the line. If these resistances are unequal, only part of the energy is converted in the load; the remaining part is returned to the generator, forming reflected waves, the amplitude of which is less than the amplitude of the incident waves.

When the incident and reflected waves are added in the line, mixed waves, which can be considered as the sum of traveling and standing waves.

For ease of analysis of line operation in mixed wave mode the concepts of the coefficients of traveling and standing waves are introduced, as well as about the reflection coefficient.

The traveling wave coefficient kb is the lesser of the ratio Rÿ/Zc or Zc/Rÿ, and the standing wave coefficient kc is the larger one. Therefore kb = 1/kc, and kb 1, kc 1.

The reflection coefficient is the ratio of complex voltage amplitudes of the reflected waves Uÿ mpad, i.e. and falling Uÿ

car

ÿ = Uÿ moÿÿ/Uÿmÿÿÿ = ÿejÿ.

The modulus of the reflection coefficient ÿ shows what part the amplitude of the reflected wave is from the amplitude of the incident one, and the argument ÿ is the phase shift angle between the voltages of these waves. The reflection coefficient through the current ratio ÿ = ÿ nus" Coefficient Imotr/Impad. Sign "mi- shows that the phase shift between the incident and reflected currents waves are equal in magnitude and opposite in sign to the angle ÿ.

It can be shown that the reflection coefficient is related to the load resistance and the characteristic impedance of the line:

$$\underline{ÿ} = ÿÿjÿ = (Zÿ ÿ \underline{Zc})/(Zÿ + Zc). \quad \text{(II.18)}$$

Substituting in (II.18) $Z\underline{ÿ} = Zc$, which corresponds to the traveling wave mode, we obtain: ÿejÿ = 0, whence ÿ = 0, ÿ = 0. Therefore, in this mode there are no reflected waves.

In the case of an open line ($Zÿ = \underline{ÿ}$) we obtain ÿ = 1, ÿ = 0, i.e. the voltage wave is completely reflected from the end without changing phase lines.

For a short-circuited line (Zÿ = 0) ÿ = ÿ1, ÿ = 180ÿ. This means that the voltage wave is completely reflected from the end of the line and changes the phase by 180ÿ.

Line operation mode at Rÿ < Zc. Substituting Rÿ into (II.18), we find that the reflection coefficient is negative and in absolute value greater than zero. Therefore, the voltage (current) is partially reflected from the load, and the phase of the reflected voltage wave opposite to the falling phase (current is reflected without changing phase).

As a result of the addition of incident and reflected waves,
mixed waves.

For a graphical illustration of the mode under consideration, it is convenient
take advantage of the distribution of effective voltage values
and current (Fig. 1.11, a).

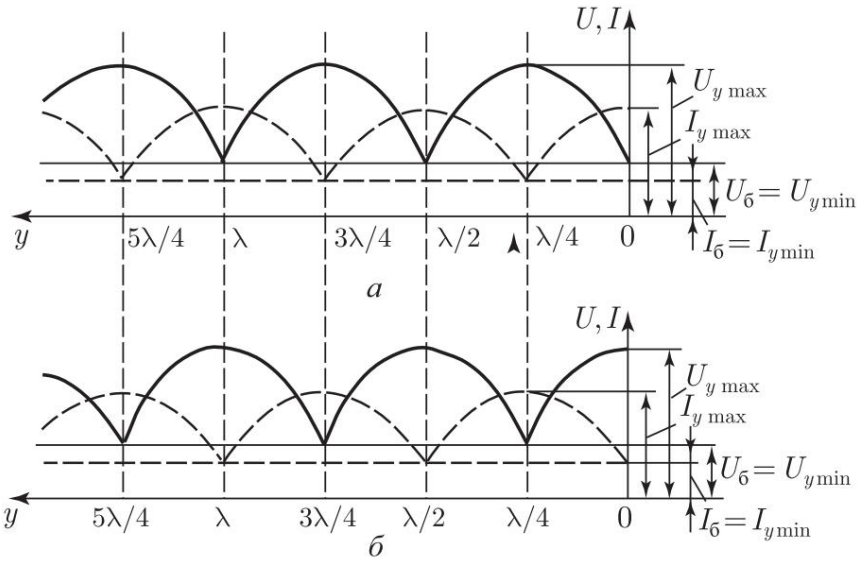

Rice. 1.11. Distribution of effective values of voltage and current in the line
with mixed waves

Mathematical analysis [200] shows that at the end of the line there is a maximum current
and a minimum voltage equal to the effective value of the traveling wave voltage. In this case,
Iy max = Im2/ ÿ 2, and Uy min = Im2Zckb/ ÿ 2 where Im2 is the current amplitude at the end
= =

lines; kb = Rÿ/Zc. In the section y1 = ÿ/4, the voltage Uy max = = Im2Zc/ ÿ 2
maximum, and the current Ib = Iy min is small and Im2kb/ ÿ 2 - mini becomes
equal to the effective value of the traveling wave current.
Comparing expressions for maximum and minimum values
voltage and current, we get

$$U_{y\min}/U_{y\max} = I_{y\min}/I_{y\max} = k_b. \qquad \text{(II.19)}$$

In all sections of the line located at a distance that is a multiple of
ÿ/4 from its end, voltage and current are in phase, so these
the cross sections are resonant. Series resonance is observed in cross sections corresponding
to an even number ÿ/4, and parallel resonance - to an odd number.

The reflection coefficient modulus is related to the running coefficients
cabbage soup and standing waves dependence

$$ÿ = (1 ÿ kÿ)/(1 + kÿ)=(k_c ÿ 1)/(1 + k_c). \qquad \text{(II.20)}$$

Line operating mode at Rÿ > Zc. In this case the coefficient
reflection is positive, so the phase of the incident and reflected

the voltage waves are the same, but the phases of the current waves are opposite. Mixed waves formed in the line are characterized by the presence of a maximum voltage at the load and a minimum current in it
(Fig. 1.11, b). At a distance of ÿ/4 from the end of the line, the voltage is minimal and the current is maximum. Relations (II.19) and (II.20) remain
fair, but kb = Zc/Rÿ, kc = Rÿ/Zc.

Operating mode of a line loaded with complex resistance. Mixed waves occur in a line if it is loaded
complex resistance of arbitrary value. The reflection coefficient module can take any values ranging from
ÿ1 to +1, and the argument is from 0 to 360ÿ depending on the ratio
between the active and reactive components of the load resistance. Therefore, the voltage and current in the load have some intermediate values, and the resonant sections of the line are shifted relative to
sections spaced from the end of the line at a distance multiple of ÿ/4.

In a line with mixed waves, the input impedance is complex, and its active and reactive components depend on both
line length and frequency.

In resonant sections, the input resistance is active: with series resonance Rin = Zc/kc, and with parallel resonance Rin = Zckc.

If the line is loaded with active resistance and has a length that is a multiple of an odd number ÿ/4, then

$$R_{vx} = Z_c^2 / R_ÿ. \qquad \text{(II.21)}$$

Chapter 2

WAVEGUIDES AND VOLUME RESONATORS

2.1. Sewerage, radiation and absorption microwave electromagnetic energy

Each surface separating two media with different electrical properties has the property of directing electromagnetic waves. This surface may be the boundary between a conductor and a dielectric, or between two different dielectrics with markedly different dielectric constants. The effect of coupled wave propagation (coupled electromagnetic waves are waves propagating along certain devices) is observed in open metal wires, shielded metal wires, coaxial lines,

hollow metal pipes and dielectric rods. All these
devices are radio waveguides, since they set the direction of wave propagation. The term "waveguide" is used only
to hollow metal pipes and dielectric rods. The most widely used are hollow metal pipes of various types.
cross section. Waveguides also include strip lines (Fig. 2.01). Application of coaxial and open two-wire

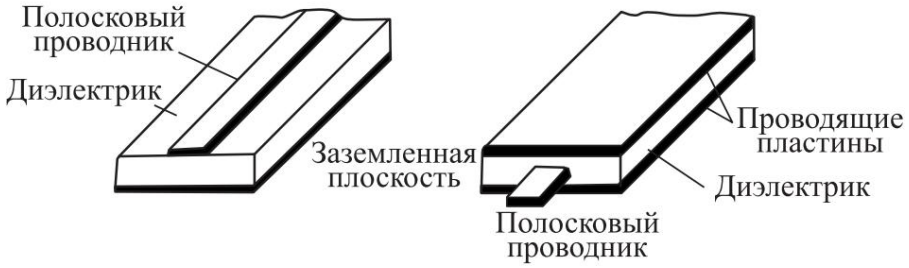

Rice. 2.01. Strip lines

lines in the microwave range has a number of limitations, first of all,
associated with radiation losses and electrical breakdown. Waveguides have a number of advantages over coaxial ones
and two-wire lines. Transferable electromagnetic energy
enclosed inside the waveguide. Modern technology makes it possible to produce light, cheap and mechanically strong waveguides. Since there is no central conductor inside the waveguide, the

breakdown strength of the waveguide. The losses in the walls of the waveguide are smaller, than losses in coaxial cable. The disadvantages of waveguides include a narrow bandwidth. Cross section dimensions
waveguide are proportional to the wavelength corresponding to the operating
waveguide frequency. Nowadays they are widely used
strip or tape lines. These electromagnetic energy transmission lines are small in size and have a very large bandwidth
transmission and although they are not shielded transmission lines,
like waveguides, the radiation from them is small.

As the frequency of electromagnetic energy transmitted over long lines increases, thermal losses in them and radiation losses
are increasing. Therefore, in the decimeter wave range, two-wire
overhead lines are replaced by coaxial ones, in which radiation
there is no energy.

For the transmission of electromagnetic energy in centimeters or more
in the shortwave range, waveguides are used that represent
are hollow metal pipes or dielectric rods (the latter are used less frequently). Typically metal waveguides have
rectangular or round cross-section. Inner walls of the waveguide
carefully polished and coated with a layer of silver, which allows
increase their conductivity and reduce losses.

Waveguides have a number of advantages over coaxial lines.
Due to the absence of an internal wire and the insulators supporting it in waveguides, there are fewer losses. In addition, with the same cross-sectional dimensions, it is possible to transmit

more energy than a coaxial line. One of the disadvantages
waveguides, as will be shown later, is the impossibility of transmitting wave energy of any length through them.

It should be noted that waveguides serve not only to transmit electromagnetic energy. A number of elements are built on their basis
electrical circuits, for example oscillatory systems called
volumetric resonators, filters, etc.

2.1.1. Transmission of electromagnetic energy through a waveguide

Possibility of energy transmission through a waveguide. Let's pretend that
there is a matched two-wire line.

Let us consider the types of waves propagating along waveguides. The simplest type of electromagnetic wave propagating in free space is a plane transverse wave, which

denote TEM (the letter T is the initial letter of the English word trans-verse - “transverse”, E and M are the initial letters of the words electric and mag-netik, that is, “electric” and “magnetic”). In the TEM wave the power
lines of electric and magnetic fields are located in transverse
planes perpendicular to the direction of wave propagation.
In any electromagnetic wave, electric and magnetic fields
change in time and space according to a sinusoidal law.

Changes in electric and magnetic fields in a propagating,
or “traveling” electromagnetic wave coincide in phase, that is
the increase in one field corresponds to the increase in the other, and they reach their maximum amplitudes simultaneously (Fig. 2.02). If on the way
propagation of an electromagnetic wave, media with different properties are encountered, then at the interface between these media the tension
electric and magnetic fields must satisfy the so-called boundary conditions. If we neglect losses, then at the border
metal with air, the electric field is always perpendicular, and the magnetic field is parallel to the metal surface.

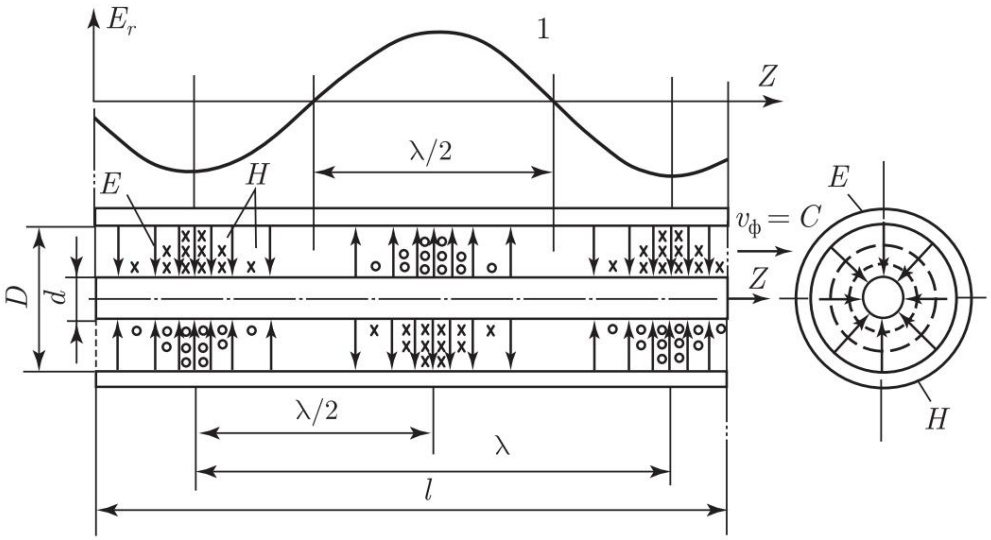

Rice. 2.02. Picture of the field of a “traveling” electromagnetic wave in a coaxial line (distribution of electric field strength along the line for
fixed point in time t): d —diameter of the central conductor; D— inner diameter of outer conductor

How does an electromagnetic wave propagate in a waveguide, and, accordingly, what will be the distribution of electric and magnetic
field components in different sections of the waveguide? For an answer
Consider a quarter-wavelength two-wire line, short-circuited at the end and excited at the resonant frequency. At the entrance
at the end of the line the voltage is maximum and the current is minimum, that is
the input resistance of such a line is high (Fig. 2.03). Applicable
a number of such short-circuited lines as supports
for the transmission line. Since the input resistances of quarter-wave lines are large, they can be considered as insulators, and the conditions for energy transfer along a two-wire line will remain
unchanged. If a two-wire line is fixed at the top and bottom
(Fig. 2.04) with such quarter-wave lines, then in this case
the conditions for transmitting energy over a two-wire line will not change. Moreover, when these quarter-wave lines approach each other, right up to their
contact with each other, they will not change the total resistance

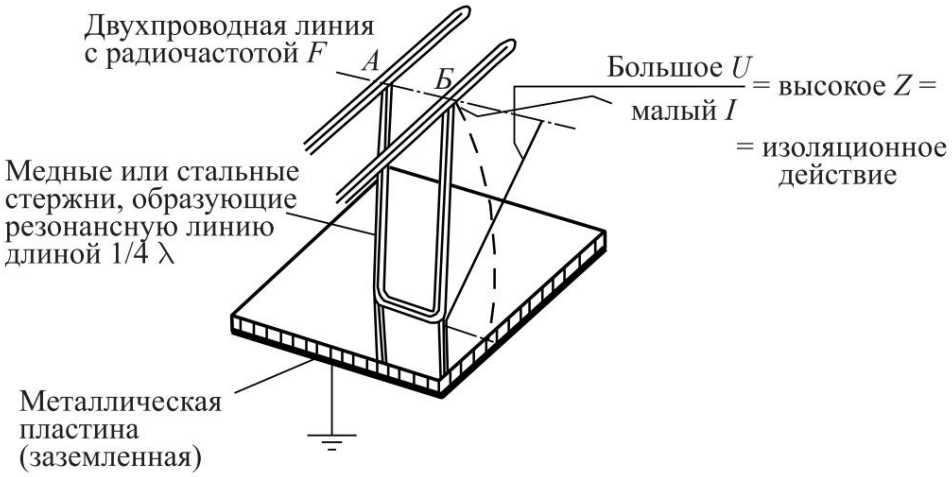

Rice. 2.03. Metal insulator

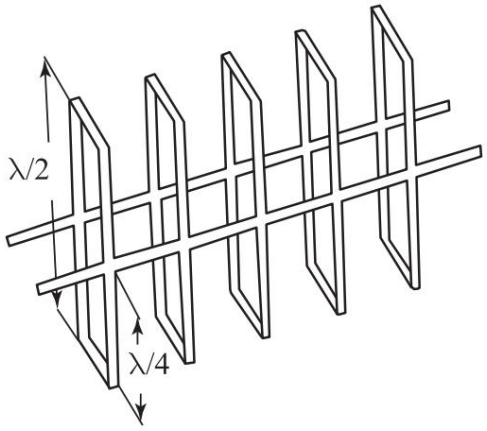

Rice. 2.04. Support of a two-wire line on two metal insulators

performance of a two-wire line, and energy losses during transmission will be reduced. But when the quarter-wave lines come into contact with each other, we will get a closed box, that is, a waveguide, inside which all the energy will propagate. One of the walls of the waveguide, namely the one formed by segments of short-circuiting lines, turned out to be wide and equal to ÿ/2. If you now begin to increase the wavelength (reduce the excitation frequency of the waveguide) so much that half of the wave no longer fits on the wide wall, then the insulator turns out to be shorter than a quarter of the wave and begins to shunt the current in the line. When the length of the short-circuited line is equal to 3/16 ÿ, it turns out to be equivalent to inductance, and the propagation of energy along the waveguide stops, that is, with a waveguide width of the order of 0.38 ÿ, the attenuation of electromagnetic waves increases sharply. The frequency at which sharp attenuation occurs is called critical, and electromagnetic waves with a frequency below the critical one (for a given waveguide) cannot propagate along the waveguide.

Let us now consider the narrow side of the waveguide. It is formed by short-circuiting jumpers of quarter-wave lines. If length
jumper is small compared to the length of the line, then its inductance
per unit length can be neglected compared to the same quantity
for line. Thus, the distance between the segments of the short-circuited quarter-wave line is not critical. Therefore the size is narrow
the waveguide wall is not critical in terms of transmitted frequencies,
and determines the breakdown strength of the waveguide. In practice size
wide wall of the waveguide for reliable operation is selected equal to
0.7, the size of the narrow wall is within 0.2–0.5 wavelengths in air.

Let us consider the process of excitation and propagation of energy in a waveguide. To understand this mechanism, it is necessary to know the field pattern in the waveguide, that is, the shape and magnitude of the electric and magnetic fields inside the waveguide. To do this, let's return to the example of a two-wire transmission line with metal insulators on both sides.
Let's close the two-wire line at both ends and put it in the center
excite from a generator. As a result of reflections from the ends of the line
standing waves of current and voltage will be established in it. Standing waves
will also be established in metal insulators. If the arrows
designate electric current lines, then the density of location
These arrows give us a picture of the field strength. It is natural that
The density of the arrows corresponds to the amplitude of the electric field, determined by its sinusoidal shape. If along
line fits an integer number of half-waves, then the number of voltage maxima, marked by areas with a denser arrangement
arrow, will be equal to the number of half-waves (Fig. 2.05). Every half wave, the electric lines change direction in accordance with the periodic law of changes in field strength. Therefore, through
every half wave the direction of the arrows in Fig. 2.05 is also changing.
Since the location of electrical lines (E-lines) and magnetic
lines (H-lines) in an electromagnetic wave are mutually perpendicular
and the lines must be closed, then in a two-wire transmission line
H-lines form closed loops perpendicular to E-lines.
When moving to a solid waveguide, the pattern of the arrangement of H-lines
will have the form shown in Fig. 2.06. In both examples given, the distribution
of electric and magnetic lines is for simplicity.
paintings of the second type of field lines were excluded. In reality, the E- and H-lines exist simultaneously. If we mentally cut
rectangular waveguide in a plane perpendicular to the direction
energy propagation, then we obtain a complete picture of the field in the section of the waveguide (naturally, in the section where the field is different from zero).
By designating with arrows the E-lines and dots and crosses the cross-section of the arrows indicating the H-lines, you can show the full picture of the field (Fig. 2.07).

First of all, we note that transverse
electromagnetic waves like TEM. Such a wave exists, for example

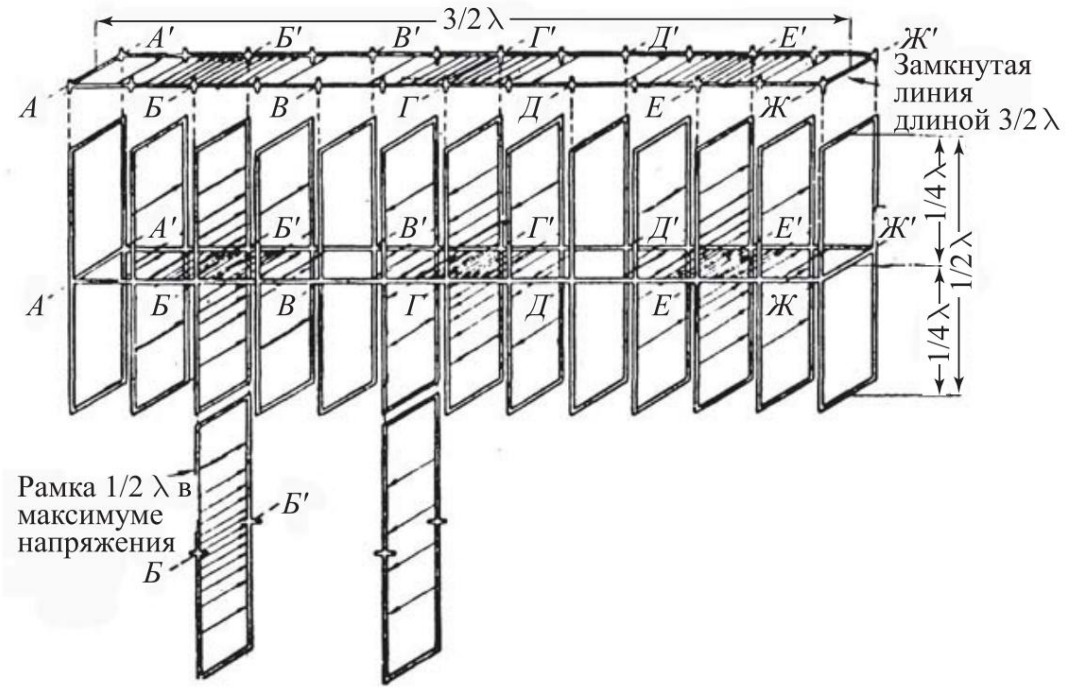

Rice. 2.05. Voltage distribution in a short-circuited line mounted on half-wave frames made of conductive material (schematic representation). *A–Zh, A–Zh* - sections of a short-circuited line, spaced from each other friend at a distance equal to ÿ/4

measures, in a ribbon line (Fig. 2.08, a). If we neglect the edge effect, then the fields between the tapes can be considered uniform; vector E is perpendicular and H is parallel to the inner surface of the tapes, Moreover, both vectors do not have a longitudinal component, i.e. they are in a plane perpendicular to the direction of propagation waves P. This, as is known, is a sign of the TEM wave. Now let's join close to the line are conducting planes, which are shown in the figure outside the line. In the resulting waveguide (Fig. 2.08) the boundary conditions for the TEM wave are no longer met: electrical power the lines merge with the side walls, and the magnetic lines are perpendicular im.

Boundary conditions will be satisfied if the structure changes fields. As applied to metal waveguides, these changes are reduced to the formation of either *transverse electric waves* TE, *otherwise called magnetic* H, *or transverse magnetic waves* TM, *otherwise called electric* E.

In H(TE) waves, the electric field remains transverse (hence the name transverse electric wave TE), but becomes uneven, and the magnetic field H has, in addition to the transverse component, a longitudinal one (hence the second name of the wave - magnetic H). One of the waves of this type is shown in Fig. 2.08, b: electric power lines are completely located in the transverse plane

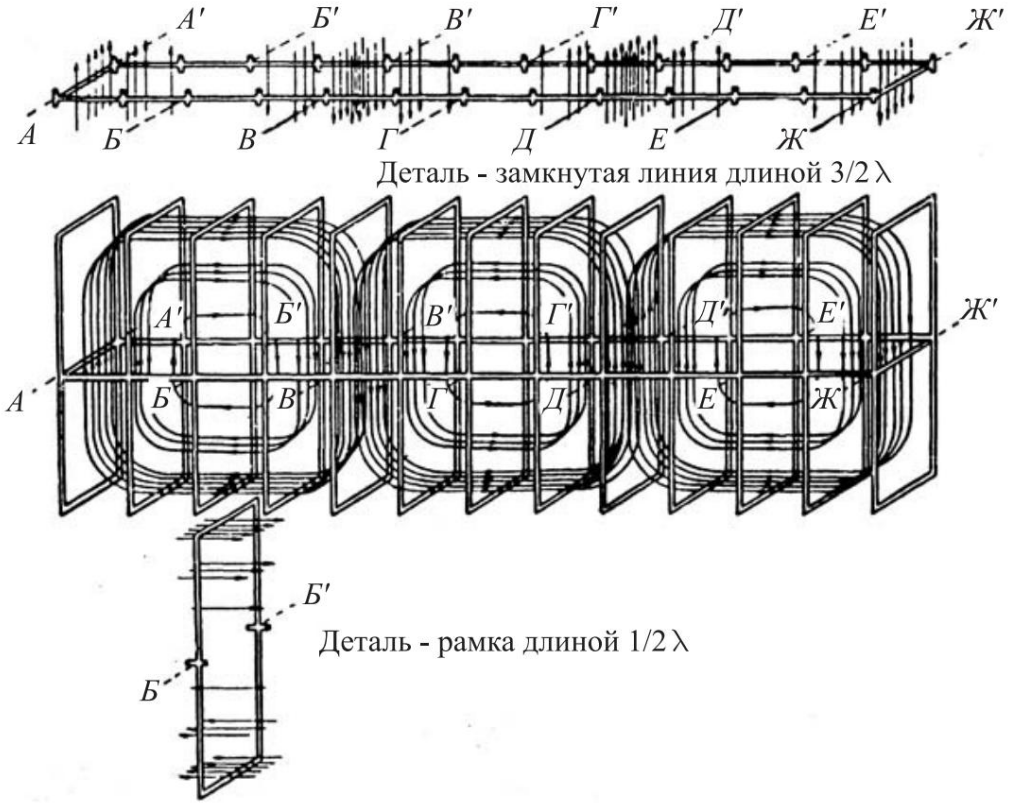

Rice. 2.06. Magnetic flux distribution in a closed line 3/2 ÿ long, mounted on metal frames 1/2 ÿ long (schematic illustration). *A–Zh, A–Zh* - sections of a short-circuited line, spaced from each other at a distance equal to ÿ/4

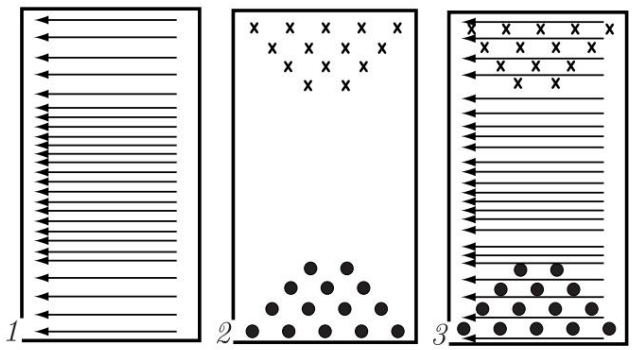

Rice. 2.07. View from the end of the waveguide: distribution of H- and E-lines: *1* - E-lines; *2* - H-lines; *3* - E- and H-lines

bones are perpendicular to the upper and lower walls of the waveguide, but there are none on the side walls, i.e. the field is uneven; the magnetic field lines closed inside the waveguide along its side walls, so a longitudinal component appeared in the magnetic field, parallel to the direction of propagation of the P wave. In E(TM) waves, the magnetic field is completely in the transverse plane (hence the name transverse magnetic TM

waves),

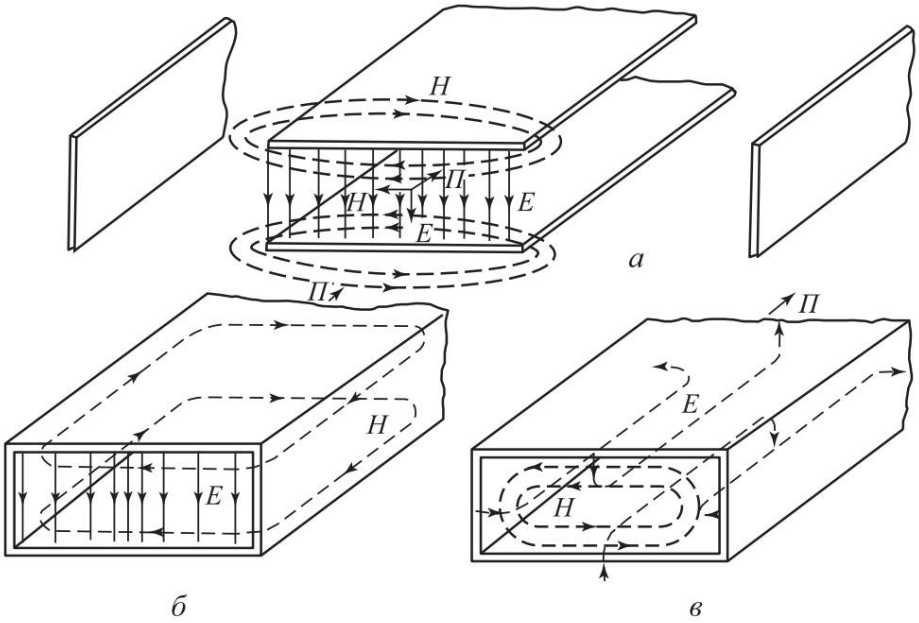

Rice. 2.08. Waves: *a* - TEM; *b* - *H* (TE); *c* - *E* (TM)

and the electric field has, in addition to the transverse component, a longitudinal component (hence the second name of the wave - electric E). An example of the E(TM) wave is the wave depicted in rice. 2.08, c: here the magnetic field lines are closed inside the waveguide and remain in the transverse plane, and the electric field lines partially located parallel to the direction of wave P, in addition they begin and end on the same wall of the waveguide under right angle. As we see, the waves H and E in the waveguide satisfy boundary conditions: field lines E approach any wall at right angles, and the H fields are parallel to them near the walls.

To the letters H(TE) and E(TM) the indices “m” and “n” are added, for example Hmn or TEmn, Emn or TMmn. For a rectangular waveguide the index “m” means the number of standing half-waves that fit on the wide side a of the cross section, and “n” is the number of standing half-waves, located on the narrow side b. For a circular waveguide m is the number field maxima on the semicircle, and n on the radius.

When the field intensity along one dimension does not change, then the corresponding digit will be zero. In round waveguides the first the figure shows the number of complete field changes (whole waves) according to waveguide circumference, the second digit is the number of half-waves of change fields that fit on the diameter (Fig. 2.09).

The electric field is located entirely in the transverse plane and, since it is directly proportional to the voltage, is maximum in sections *1* and *5* and is equal to zero in section 3. Magnetic lines the fields are closed around the displacement currents. Transverse component magnetic field is maximum in sections *1* and *5* and is equal to zero in section 3, i.e. it is in phase with the electric field strength

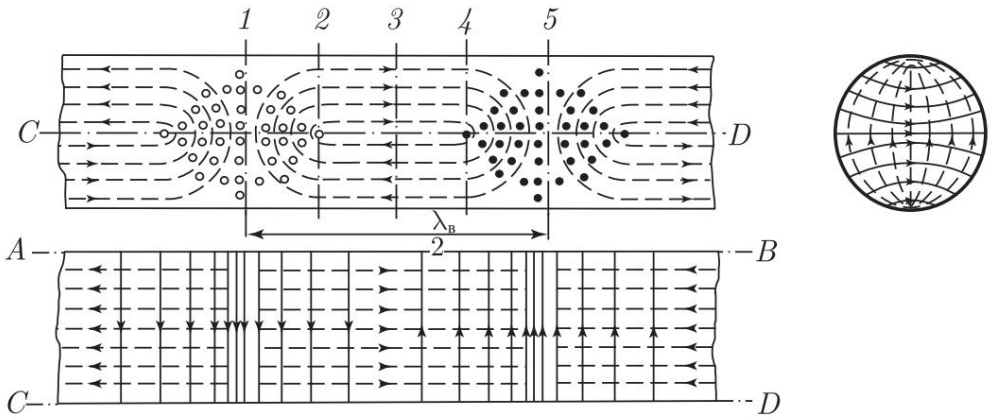

Rice. 2.09. Distribution of electric and magnetic fields in a round waveguide

and longitudinal current, which determines the transverse magnetic field. The longitudinal component of the magnetic field has a maximum in section *3* and is equal to zero in sections *1* and 5, i.e., it is in phase with the transverse current. In sections *2* and *4,* the electric and magnetic fields have intermediate values. Let us consider the field distribution shown in Fig. 2.07 and 2.10. In Fig. 2.07 it is clear that the electric

field is perpendicular to the wide wall of the waveguide, that is, the electric field is transverse, and the waves are TE-type. To determine the indices, consider Fig. 2.10. As can be seen, the electric field intensity does not change along the smaller waveguide cross-section. So there is no change in field along this direction and the first digit must be zero. Along the wide wall of the waveguide, the intensity of the electric field varies from zero at one wall to a maximum in the center and again to zero at the other wall. Thus, along the wide wall of the waveguide, the field distribution has the form of half a sinusoid, that is, half of the wave fits. Therefore, the type of wave shown in Fig. 2.10, designated TE01. In Fig. Figure 2.11 shows six of the possible types of waves in rectangular and circular waveguides. The same method can be used to consider other types of waveguides and the types of waves propagating in them. In previous examples, we considered waveguides closed at both ends in order to obtain standing waves, since with such an energy distribution along the length of the waveguide, it is easier to consider the picture of the field of electromagnetic waves. If we use a waveguide loaded in such a way that there are no reflections in it, then there are no standing waves along the waveguide and energy transfer occurs. The picture of the field in the waveguide during energy transfer can be depicted by shifting the maxima of the E-lines and

H-lines until they merge, that is, until the phases of the current and voltage coincide. Moving along the waveguide a new field pattern at a speed close to the speed of light will display the energy transfer in the waveguide as in a transmission line.

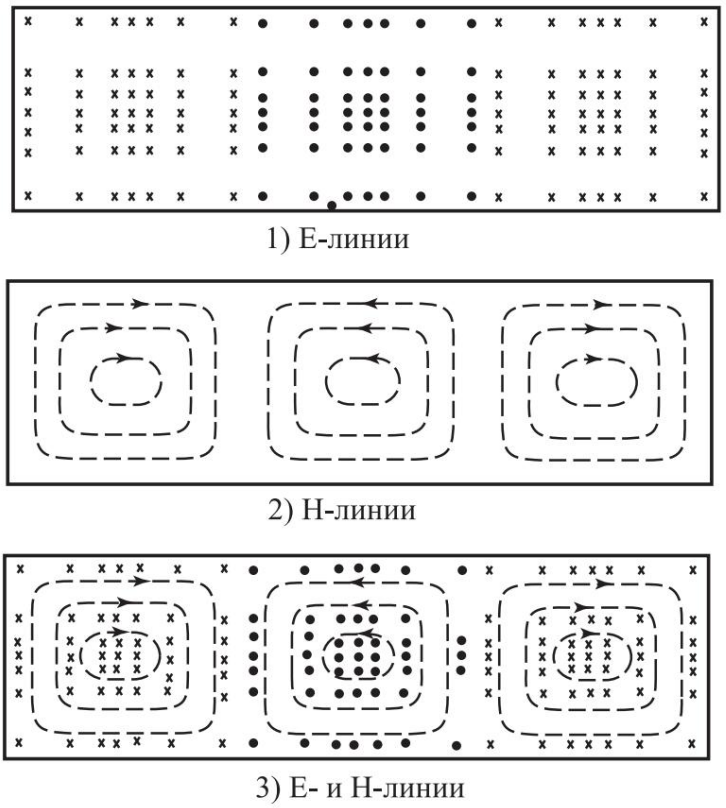

Rice. 2.10. Side view of the waveguide: E- and H-line distribution

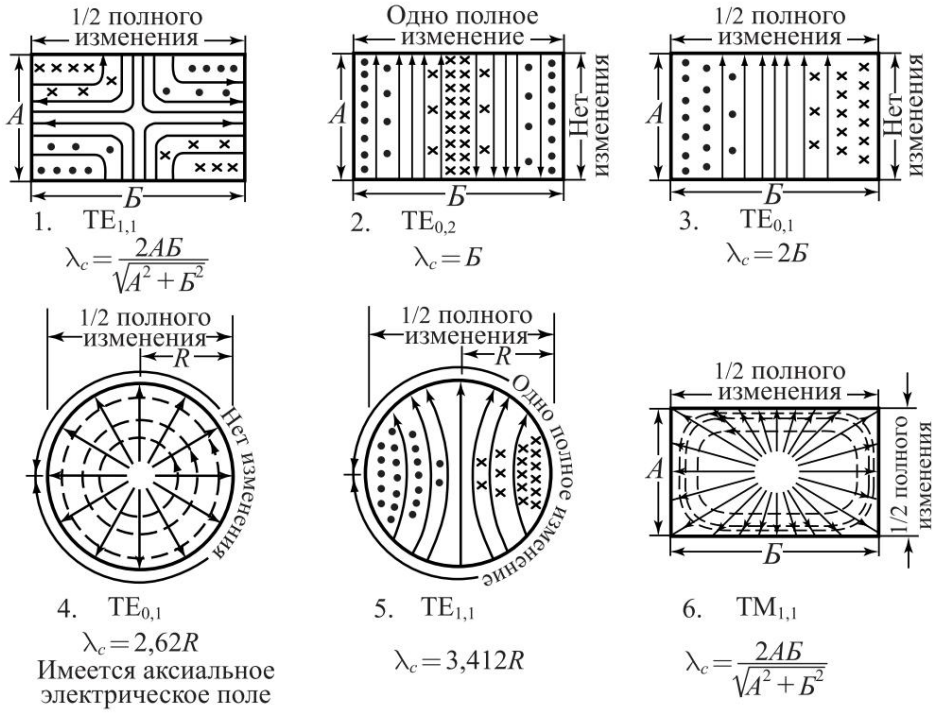

Rice. 2.11. Possible types of waves in rectangular and round waveguides: - - - - electric lines; ×•×• magnetic lines; ÿc —critical wavelength

As mentioned above, there is a certain limiting, or critical, wavelength of electromagnetic oscillations of measurement in free space, at which the propagation of a wave of this type

in the waveguide is terminated. The relationship between the wavelength in the waveguide ÿÿ, wavelength in free space ÿ and critical length
wave ÿcr is described by the known relation:

$$ÿv = \frac{l}{\sqrt{1 ÿ (l/lkr)2}} > l,$$

valid for waveguides with any cross-sectional shape.
From this relationship it is clear that as the operating wavelength ÿ approaches the critical one, the wavelength in the waveguide increases sharply. If ÿ/ÿcr > 1, then this type of wave cannot propagate in the waveguide. For this type of wave, this waveguide becomes prohibitive.
This property of waveguides is used in surveillance devices
behind the object inside the waveguide during its irradiation. In the simplest In this case, the transient waveguide is a hollow metal tube with a diameter much smaller than the wavelength. If the waveguide
filled with a dielectric with a relative dielectric constant
ÿ, then the wavelength in the waveguide is determined by the relation:

$$ÿvd = \frac{l}{ÿ\sqrt{ÿ (l/lkr)2}}$$

The value of the critical wavelength is related to the shape of the waveguide, its transverse dimensions and wave type. For a rectangular waveguide with any type of waves Hmn and Emn, where m and n are positive integers
numbers or zero, the critical wavelength is determined by the relation:

$$ÿkr = \frac{2}{\sqrt{\frac{m2}{a2} + \frac{n2}{b2}}}$$

where a is the wide wall of the waveguide, b is the narrow wall. Expression for ÿcr is maximum when n = 0 and m = 1, that is, for wave TE10 (H10),
and equal

$$ÿÿÿ = 2a.$$

If a<ÿ< 2a, then only
one wave type H10. Therefore, the H10 type wave is called the main one, and all other types of waves are higher. On the other hand, as ÿ approaches ÿcr , losses in the waveguide sharply increase, the minimum of which is occurs at a = 0.7.

Since the wavelength in the waveguide is different from the wavelength in the air, even if the waveguide is also filled with air,
then it is obvious that the speed of energy propagation inside the waveguide will differ from the speed of energy propagation in free

space. The basic law of physics states that energy cannot travel faster than the speed of light. We'll be back
to the formula for the wavelength in the waveguide ÿw. By definition, length
wave is the distance over which the phase of the electromagnetic field changes by 360ÿ, or, in other words, the wavelength
is the distance over which a certain phase of the electromagnetic field moves during one period T. Since ÿÿ > ÿ, then
speed of movement of the phase of the electromagnetic field along the waveguide with air or vacuum filling vf should be greater
speed of light c. The speed of energy propagation along the wave-water is called the group velocity vgr and is always less than the speed
Sveta. The phase velocity vf is related to ÿv by the relation vph = ÿv/T, where T = l/f. From here

$$v\ddot{y} = \ddot{y}\ddot{y} \cdot f = 2\ddot{y} \quad \frac{\ddot{y}\ddot{y} \cdot \ddot{y}}{} = \frac{oh}{b}.$$

where ÿ = 2 p is the phase constant of the wave, ÿ is the angular frequency.
ÿv

From these relations it is clear that with shortening of the wavelength ÿÿ vf decreases . In transmission lines with a TEM wave, the phase and group velocities are equal to the speed of light in the medium filling the line.
In the case of a waveguide

$$vf \cdot vgr = \ddot{y}\ddot{y} \quad \frac{C2}{}.$$

In practice, the wavelength in the waveguide is usually 1.5-2 times greater than in free space. This must be taken into account when calculating
waveguides according to formulas that include wavelength.

We need to consider one more issue concerning the specifics of energy propagation in guiding structures. Until now
For now, we simply stated that, for example, the TEM wave propagates in free space or in guiding structures
only a certain type, Emn- and Hmn-waves propagate
in waveguide systems, that the apparent wavelength in the waveguide
longer than the wavelength in free space. Let's now consider
these points in detail and we will find out the reasons that distinguish the conditions for the propagation of the energy of electromagnetic oscillations in the guides
structures. Consider a rectangular coordinate system in which
E- and H-lines of the electromagnetic field, represented by vectors E
and H are located along the x and y axes , respectively (Fig. 2.12). Let the guided wave propagate along the Z axis. The energy of the electromagnetic wave is characterized by the Umov–Poynting vector associated
with the vectors of electric E and magnetic H fields as follows:
(II.22):

$$\ddot{y}\ddot{y}P = [\ddot{y}\ddot{y}E \qquad \text{(II.22)}$$

and ÿÿH The relation between is satisfied at any point
ÿÿH], ÿÿP ÿÿE
space for any wave structure. There are two options

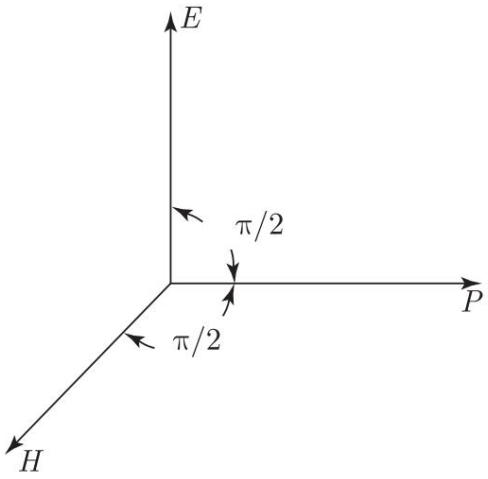

Rice. 2.12. E- and H-lines of the electromagnetic field in a rectangular system coordinates

energy distribution - parallel to the Z axis, that is, in a straight line (Fig. 2.13, a), and distribution along a broken line while maintaining translational movement along the Z axis (Fig. 2.13, b). In the first case

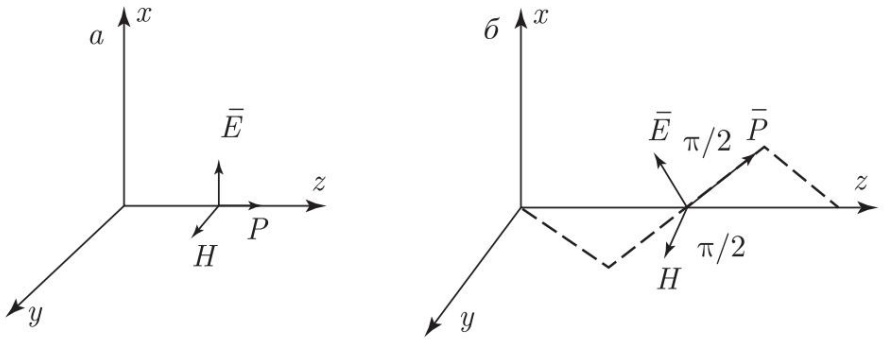

Figs. 2.13. Energy dissipation options: *a* — parallel to the Z axis; *b* — translationally along the Z axis

according to the relationship, the vectors E and H are in a plane perpendicular to the Z axis, that is, a TEM wave occurs. In the second case, these same vectors are in planes not perpendicular to the Z axis, or at least one of the intensity vectors electromagnetic field (E or H) must have a direction not perpendicular to the Z axis (Fig. 2.14, 2.15). Therefore, either vector E or vector H must have a longitudinal component, then there is a second case corresponding to waves of type E or H. Obviously, that in the second case the simultaneous existence of both types of waves. Let us consider under what conditions certain or other types of waves. As is known, in a homogeneous medium waves propagate rectilinearly. Bending of the wave propagation path is possible in a heterogeneous environment. But the propagation of the wave along a broken line in a homogeneous environment is possible if this environment is surrounded by another environment

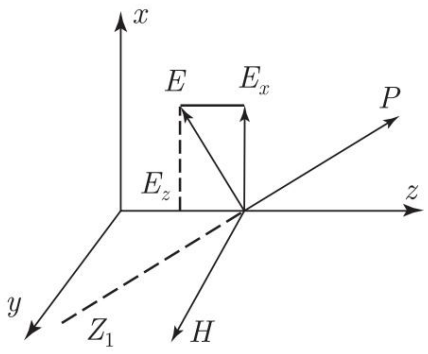

Rice. 2.14. To the description of the classification of guided waves. Vector E has a component along the Z axis Ez

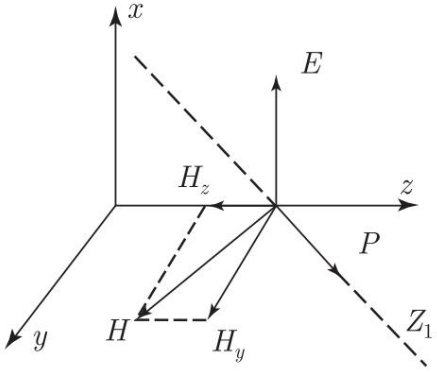

Rice. 2.15. To the description of the classification of guided waves. Vector H has a component along the Z axis Hz

and waves are reflected at their interface. Hence,
For the TEM wave to propagate, the medium must be not only homogeneous, but also infinite. Therefore, TEM waves propagate in free space. However, TEM waves can propagate
not only in free space, that is, the condition of boundlessness
environment is not always mandatory. Examples of guides
structures in which the TEM wave propagates can serve
asymmetrical strip and coaxial lines. In the first case
the absence of side walls eliminates the reflection of electromagnetic
waves, in the second - the presence of conduction current in the internal conductor provides the condition for the propagation of energy along the line.
However, according to general considerations, the existence of any types of waves is possible in any shielded line. If there is
some homogeneous medium bordering another medium, and at the border
section there is a reflection of an electromagnetic wave, then in such
waves of type E or H will propagate in the medium . It follows that
that waves of type E or H are possible in hollow metal pipes,
in coaxial lines, in dielectric rods, between two
parallel plates. The concept of propagation of electromagnetic waves presented here is called the Brillouin concept.
Based on it, it is possible to explain the relationship between the velocities vf, vgr and C.
The speed of propagation of TEM wave energy along the Z axis and the speed
The energy propagations of E and H waves along the broken line are identical. But since the projection of the broken line onto the Z axis is less than the broken line itself, and the speed propagation along the broken line is equal to C, then the propagation speed
energy (group velocity) along the Z axis of waves E and H will be less
the speed of TEM waves, that is, less than the speed of light. Ratio of group velocity of energy propagation along the Z axis vgr for waves E
and H to the TEM wave speed along the broken line is equal to:

$$\frac{v_{gr}}{v_{TEM}} = \cos\ddot{y},$$

where ÿ is the angle between the Z axis and the broken line.

Let us choose some direction of the broken line Z1, forming with the Z axis angle ÿ (Fig. 2.16). The wave front at each point of the line Z is perpendicular to

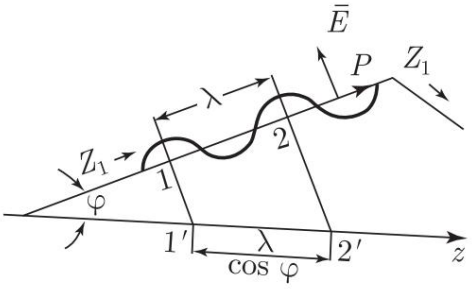

Rice. 2.16. To explain the differences in phase velocities of E, H and TEM waves

is aligned with the corresponding segment of line Z1. Vectors E and H are located in planes perpendicular to the Z1 axis. Umov–Poynting vector directed along the Z1 axis. In the direction of the Z1 axis , phase and group speeds are equal

$$v_{gr} = v_f = \ddot{y}\ddot{y}\ddot{y} \quad \frac{1}{\text{——}}$$

But since vÿ = ÿ/T, and a wave with length ÿÿ = ÿ/ cos ÿ propagates along the Z axis , then the phase velocity on the Z axis, that is, along the guiding structure (waveguide) will be equal to:

$$v_{fv} = \frac{\ddot{y}v}{T} = \frac{l}{T \cdot \cos\ddot{y}} = \frac{v_{TEM}}{\cos\ddot{y}}.$$

From this relationship it is clear that the phase velocity along the Z axis, then is along the guide structure, greater than the TEM wave speed, then there is more speed of light.

It is necessary to consider one more quantity characterizing the transmission lines. Knowledge of this value is necessary not only to present a general picture of the propagation of energy along the guide structures, but also for practical calculations of the sizes of these structures,
coordination of guide structures with each other, with the generator and with load. This quantity is called characteristic impedance lines and is determined by the ratio of voltage to current in it in the mode traveling wave. Since in microwave transmission lines, unlike long lines, voltage and current vary across the cross section, then the concept of wave resistance in this case is conditional character. Therefore, for a lossless medium, the characteristic impedance Z can be written as:

$$Z = \frac{\text{AND}}{H} = \frac{\overline{m}}{e}$$

what follows from the solution of equations representing the dependence between the components of field vectors in a three-dimensional coordinate system [205] for the case Ez = Hz = 0, that is, for the case of transverse electromagnetic waves. If we substitute the values ÿ0 and ÿ0 into this relation , then for free space the value of wave resistance Z0 will be equal to:

$$Z0 = \sqrt{\frac{m0}{e0}} = \sqrt{\frac{4ÿ\ 10ÿ7\ [G/m]}{\frac{1}{4p \cdot 9 \cdot 109}\ [F/m]}} = 120ÿ\ ÿ\ 377\ ÿ.$$

The characteristic impedance of the guide structures is not determined only by parameters ÿ and ÿ, but also by constructive ones, since the latter determine the conditions for the propagation of the energy of electromagnetic vibrations in these structures. Characteristic impedance [206] for waveguide with a uniform cross section for all types of TE waves is determined is given by the relation:

$$ZTE = Z0(ÿÿ/ÿ)\ \sqrt{\frac{m}{e}}$$

and for all types of TM waves as

$$ZTM = Z0(ÿ/ÿÿ)\ \sqrt{\frac{m}{e}}$$

For practical calculations, you can use the given forms - llamas

The resulting formulas show that the waveguide impedance for *H* waves is always greater, and for *E* waves it is always less, than the characteristic impedance of free space.

These formulas also make it possible to verify that the wave waveguide resistance Zÿ for waves *H* and E, in contrast to the waveguide free space resistance Z0 for the TEM wave, depends on frequency, and if the wavelength is greater than the critical one (ÿ>ÿcr), then Zÿ is expressed as an imaginary number. Indeed, if ÿ>ÿcr, then there is no energy transfer from the generator to the load, between transverse components of the electric and magnetic fields, a shift appears in phase by 90ÿ, and this is a sign of the reactive nature of the wave impedance Zÿ = Eÿ p/Hÿ p.

The analogy between a two-wire line and a waveguide allows assert that if the waveguide is not matched with the load, then the waves reflected from the load, therefore in the longitudinal direction of the waveguide standing waves arise.

Obviously, based on the analogy between a waveguide and a two-wire line, concepts such as coefficient reflections, traveling wave ratio and standing wave ratio, one should only, moving from the waveguide to the equivalent line, have keeping in mind that the line is assumed to be located in the middle of a wide waveguide walls, where the voltage amplitude is maximum and longitudinal

The current current has the highest density. Their relationship is determined characteristic impedance of the equivalent line Zÿ.

For the H10 wave , this resistance is slightly different from the waveguide waveguide resistance Zÿ, calculated from the transverse components of the electric and magnetic fields of H10 type waves:

$$\text{с}_V = \frac{etc}{2a} Z\ddot{y} = \frac{etc}{2a} \cdot \frac{377}{1 \ddot{y} \left(\frac{l}{\ddot{y}kr}\right)^2} \qquad \text{(II.23)}$$

If a = 2b then $Z_V = 0{,}79Z\ddot{y}$.

The described field distribution in waveguides is consistent with the boundary conditions on a perfectly conducting surface, which can be count (with some approximation) the inner walls of the waveguide. The electric field lines are perpendicular to the inner surface of the waveguide and do not merge with it anywhere, and the lines of the magnetic field fields are parallel to this surface. At any point in the waveguide, power the lines of electric and magnetic fields are mutually perpendicular.

2.2. Selecting the wave type and transverse dimensions waveguide cross sections

Centimeter wave transmission lines most often use rectangular waveguides excited at the H10 wave. This is guided by the following considerations. In any section of the waveguide Only one type of wave must propagate. In the presence of they do not interfere with two or more types of waves, and since the waveguide The wavelength ÿw is different for these types of waves, then changes in the amplitude of oscillations occur in the longitudinal direction. Changes are amplified at the slightest inconstancy of the generator frequency. Them This disrupts the matching of the waveguide with the load and decreases power supplied to the load.

In a waveguide, a wave of one type is most easily excited when this type is the lowest. Then it is possible to set the transverse dimensions of the waveguide such that for only one lowest type of wave the working length ÿ was less than the critical ÿcr. This solution, except In addition, it allows the use of waveguides with minimal transverse section. In a rectangular waveguide, electric waves with a zero index (E01 or E10), its lowest wave type, are not possible is H10, and for a circular waveguide it is wave H11.

When appearing in a circular waveguide excited at wave H11 (see Fig. 2.09), bends or deformations of the field, the waves can rotate relative to the axis of the waveguide. The resulting change in polarization waves will disrupt the matching of the waveguide with the load. Rectangular waveguides are free from this drawback, since they have polarization closely related to the cross-sectional shape; for example, with wave H10

electric field lines are always perpendicular to the wide
waveguide walls. This is why rectangular waveguides are
the main type of waveguide transmission lines. They get excited like
usually on wave H10.

Let's move on to choosing the cross-sectional dimensions of such a waveguide.
In order for the operating wavelength ÿ to be less than the critical
ÿcr, size a, according to the formula ÿcr = 2a, must be greater than 0.5ÿ.
At the same time, in order to exclude the nearest wave types H20 and H11,
you need to set the size a<ÿ (since ÿcr = a for H20) and b < ÿ/2
(to exclude H11). The choice of side a is also influenced by the desire
reduce energy losses in the waveguide.

Until now it was assumed that the inner surface of the waveguides
has ideal conductivity and attenuation in the waveguide occurs
only at ÿ>ÿcr and for the same reason as in reactances (energy is reflected).
In real waveguides, attenuation is also observed at ÿ<ÿcr, but its nature is
different: here it is electromagnetic
energy is converted into heat. This is reflected in the structure of the fields: due to the finite conductivity of the walls of the waveguide, the electric field is not strictly perpendicular to the walls, but has a certain
albeit a very small, longitudinal component. It matches
energy spent on heating the metal surface of the waveguide,
the energy reaching the load decreases accordingly.

An increase in frequency affects heat losses in two ways: the surface
effect, which causes an increase in losses, increases, and it decreases
the number of reflections from the narrow walls of the waveguide (see Fig. 2.16),
which reduces losses. The attenuation increases especially sharply when, decreasing,
frequency f approaches critical fcr. In such conditions with
given the waveguide cross-sectional dimensions there must exist
the optimal frequency at which attenuation is minimal. It changes very
slightly when the frequency deviates from the optimal
within large limits. Thanks to this, the waveguide can transmit
no noticeable distortion (with almost constant attenuation) wide
frequency spectrum. Between the optimal fopt and critical fcr frequencies
there is a dependency

$$\text{ÿcr fopt} = \text{ÿ } 3 \text{ fcr or ÿopt} = \text{ÿ } 3 \frac{}{} = \frac{2a}{\text{ÿ } 3}$$

Typically, to reduce the dimensions of the waveguide, size a is chosen
somewhat smaller: a ÿ 0.71ÿopt. This satisfies the required inequality 0.5ÿ<a<ÿ.

A decrease in the narrow wall b is prevented by a decrease in the limit
power of transmitted waves Padd due to increased tension
electric field, which can cause breakdown between wide
between the walls of the waveguide.

So, the size b should not be too small to avoid a breakdown, but not more than 0.5ÿ to exclude the H11 wave. Usually b ÿ 0.5a = 0.36ÿ is chosen. When connecting the waveguide to standard feeders with

a characteristic impedance of 50 or 75 Ohms, the characteristic impedance of the waveguide must be equal to the characteristic impedance of the feeder. Otherwise, most of the energy supplied to the waveguide will be reflected back to the generator. The characteristic impedance of the waveguide is determined by the dimensions of the walls, and to implement a standard (50 or 75 Ohm) impedance, the size of the narrow wall must be small. In this case, the waveguide turns out to be “flat”, which does not always fit into the experimental conditions. On the other hand, the desire to bring the characteristic impedance of the waveguide closer to the characteristic impedance of free space (377 Ohms) leads to a large cross-section of the waveguide. In this case, the waveguide and feeder line are matched through a Chebyshev step junction, which has a wave impedance of 50 or 75 Ohms at the input, and a resistance of 377 Ohms at the output. A complete calculation of step transitions is given in [207]. The attenuation coefficient of a rectangular waveguide at wave H10 is determined by the formula

$$a = \frac{\sqrt{\frac{pfma}{c}}\ 1 + \frac{2b}{a}\left(\frac{l}{2a}\right)^2}{377b\sqrt{1 - \left(\frac{l}{2a}\right)^2}} \text{ nep/m} \qquad \text{(II.24)}$$

where ÿa is the magnetic permeability of the waveguide walls, G/m; ÿ is the specific conductivity of the inner surface, f is the frequency of transmitted waves, $\frac{1}{\text{ohm} \cdot \text{m}}$; Hz. For copper ÿa = ÿ0 = 4ÿ · 10ÿ7 gn/m. The quantities a, b and ÿ are expressed in meters.

Round waveguides are usually used when there are moving and stationary parts in the antenna-feeder system, for example, with a rotating antenna. In order to keep the nature of the field unchanged when moving from a fixed section of a waveguide system to a moving one and vice versa, it is desirable that the fields in the waveguide have axial symmetry. Wave E01 in round waveguides has these properties . Due to the axial symmetry of the fields, this wave is used more often than H11, despite the fact that the latter type of wave is inferior and can be obtained in a waveguide of smaller diameter: when transmitting the H11 wave, the diameter is D > ÿ/1.71, and when transmitting the E01 wave, D > ÿ /1.31. Among other types of waves, the H01 wave in a circular waveguide deserves special attention . The electric field of this wave is in the transverse plane and does not change along the perimeter, i.e., it is depicted by circles centered on the axis of the waveguide (Fig. 2.17, a, b), about which

says index m = 0. Since n = 1, the field at the radius has one
maximum.

The displacement current (Fig. 2.17, d), as is known, reaches a maximum at the moment when the electric field intensity passes through
zero value (section *e–f),* and is equal to zero when this field passes through a maximum (sections *c–d, g–l).* Bias currents cause
magnetic field, the lines of which cover the currents that excite them.
Comparing Fig. 2.17, *b* and 2.17, d, you can see that the transverse
component of the magnetic field is in phase with the electric one
field, as in all H-type waves. In Fig. 2.17, *c* shows the electric field lines in the transverse plane of the waveguide and the projection of the magnetic field lines onto this plane.

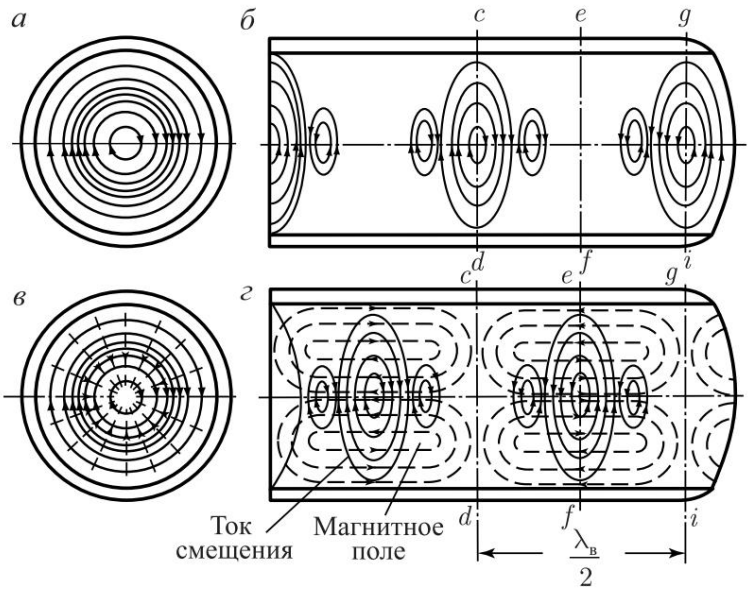

Rice. 2.17. Distribution of H01 wave fields in a circular waveguide: a, *b* — electric field; *c* - electric and magnetic fields; *g* - displacement currents and magnetic field

The longitudinal component of the magnetic field is adjacent to the walls of the waveguide. This means that on the surface of the waveguide there must be a transverse conduction current. This current is directed in the opposite direction compared to the bias current present inside a given section of the waveguide.
If there were no conduction current and it did not balance the displacement current, then the magnetic field would exist in the walls of the waveguide and beyond its limits, and this contradicts the boundary conditions on an ideal
conductive surface.

As the wavelength ÿ decreases , the magnetic field lines shorten in the longitudinal direction and the longitudinal component of the magnetic field weakens near the walls of the waveguide. As a result, the current
conductivity and the losses caused by it become smaller. Especially
Losses are significantly reduced at the highest radio frequencies.

Advantages and disadvantages of waveguides. Let's compare a metal waveguide with a coaxial line, as the most commonly used transmission line.

The advantages of waveguides are as follows. There is no internal wire in the waveguide, and therefore losses due to conduction currents in it are minimal; in addition, losses are reduced due to the fact that the conducting surface of the waveguide is large (the cross section of the waveguide is relatively big).

In a waveguide, as in a coaxial line, electromagnetic waves concentrated between conducting surfaces, and therefore losses no for radiation.

There is no dielectric filling in the waveguide and, therefore, Indeed, there are no dielectric losses in it.

Maximum power of high-frequency vibrations transmitted along the waveguide, significantly more than in a coaxial line. This is explained by the fact that the waveguide does not have an internal wire, which reduces the distance between the conducting surfaces, from which depends on the permissible voltage in the transmission line, and therefore and transmitted power.

The waveguide has great mechanical strength.

The disadvantages of a waveguide include:

— the presence of a critical wavelength at a given cross section;

Waveguide Research Institute;

- complexity of production, since the inner surface of the walls The waveguide must be carefully polished and coated with a highly conductive metal (usually the inner walls are silvered);

— the possibility of propagation of unwanted types of waves.

Metal waveguides are used over the entire centimeter wave range, and rigid coaxial lines are used only on waves longer than 10 cm. On decimeter waves, and even more so on meter scales, the use of waveguides as a transmission line is impractical, since for this their dimensions must be excessive great. In the millimeter wave range, dielectric waveguides and mirror waveguides successfully compete with metal waveguides. and single wire lines.

2.3. Volumetric resonators

A volume r esonator is called an oscillating system in the form of a cavity limited on the inside of a metal highly conductive surface. For the first time, volumetric resonators theoretically and practically studied by M. S. Neumann (1937). It is also necessary to note the works of V. I. Bunimovich, G. V. Kisunko, N.N. Krylov and other Soviet scientists in this field.

Volumetric resonators are used in the ultra-high frequency range. Of these, the most widely used are waveguide, coaxial and toroidal resonators.

Waveguide resonators. Such resonators can be considered as a waveguide, limited in length and closed on all sides
walls, the inner surface of which has high conductivity
bridge.

In Fig. Figure 2.18 shows a rectangular cavity resonator built on the basis of a rectangular waveguide. The resonator is excited
a pin that serves as a continuation of the internal wire of the coaxial line connecting the exciter to the resonator.

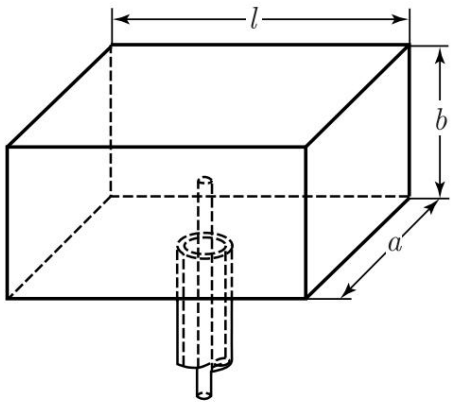

Rice. 2.18. Excitation circuit of a volumetric resonator having the shape
parallelepiped

Fields and waves in a cavity resonator are distributed differently than
in the waveguide. If the resonator length satisfies the condition l/2 = ÿÿ/4,
then during the movement from the pin to the side wall and back the field
change their phase by 180ÿ; at the moment of reflection of the wave, electric
the field additionally changes the phase by 180ÿ. As a result, *in volume*
standing waves are installed in the resonator with an antinode of the electric field and a magnetic node near the pin and the antinode
magnetic field and an electric node on the side walls.

If we divide the electric field strength by the magnetic field strength at the pin, it turns out that the input resistance of this resonator is very high. Such resistance is typical

for a parallel circuit tuned to resonance. It's obvious that
parallel resonance can be obtained not only at l = ÿÿ/2, but
and at l = ÿc, ÿc, 2ÿc, .. ., i.e. at $\frac{3}{2}$

$$l = p\,\frac{ÿv}{2}$$

where p is any integer.

A large number of resonant frequencies in a cavity resonator is a natural phenomenon. This is typical for all systems with distributed
permanent.

Note that for any value of p, the exciting pin must be located in the place of the resonator where the electric field is maximum and the magnetic field is zero.

Let's find the resonant wavelength of a rectangular volumetric resonator. The wavelength in the waveguide is

$$ÿv = \frac{l}{\sqrt{1 - \left(\frac{l}{ÿkr}\right)^2}} = \frac{1}{\sqrt{\left(\frac{1}{l}\right)^2 - \left(\frac{1}{ÿkr}\right)^2}}$$

where

$$ÿ = \frac{1}{\sqrt{\left(\frac{1}{ÿv}\right)^2 + \left(\frac{1}{ÿkr}\right)^2}}$$

Let us substitute into this formula the values of ÿÿ, corresponding to the resonance condition l = pÿÿ/2, and then the wavelength in free space ÿ will correspond to the resonant wavelength of the volumetric resonator:

$$ÿ0 = \frac{1}{\sqrt{\left(\frac{p}{2l}\right)^2 + \left(\frac{1}{ÿkr}\right)^2}}$$

Keeping in mind that for a rectangular waveguide

$$ÿkr = \frac{2}{\sqrt{\left(\frac{m}{a}\right)^2 + \left(\frac{n}{b}\right)^2}}$$

we get

$$ÿ0 = \frac{1}{\sqrt{\left(\frac{p}{2l}\right)^2 + \left(\frac{m}{a}\right)^2 + \left(\frac{n}{b}\right)^2}}$$

Finally

$$ÿ0 = \frac{2}{\sqrt{\left(\frac{m}{a}\right)^2 + \left(\frac{n}{b}\right)^2 + \left(\frac{p}{l}\right)^2}} \qquad \text{(II.25)}$$

Waves in a cavity resonator are designated by the letters Hmnp or Emnp. For a rectangular cavity resonator, m is the number of standing half-waves on side a, n is the number of standing half-waves on side b, and p is the number of standing half-waves along the length of the resonator l.

For a cylindrical resonator, m is the number of field maxima along the semicircle, n is the number of field maxima along the radius

(as in a circular waveguide) and p is the number of field maxima along the length resonator.

Let's compare the fields H10 in a rectangular waveguide (Fig. 2.19, a) and H101 in a rectangular cavity resonator (Fig. 2.19, b). The boundary conditions are the same in both cases. Since n = 0, then along the side
b the electric field does not change and its field lines are parallel to this side of the resonator. The indices m = 1 and p = 1 mean that
in the resonator, the electric field strength in the middle of the sides is a
and l is maximum and equal to zero at the edges. Magnetic lines are perpendicular to electric lines of force and, closing near the walls
resonator, are located parallel to the walls, as required
border conditions.

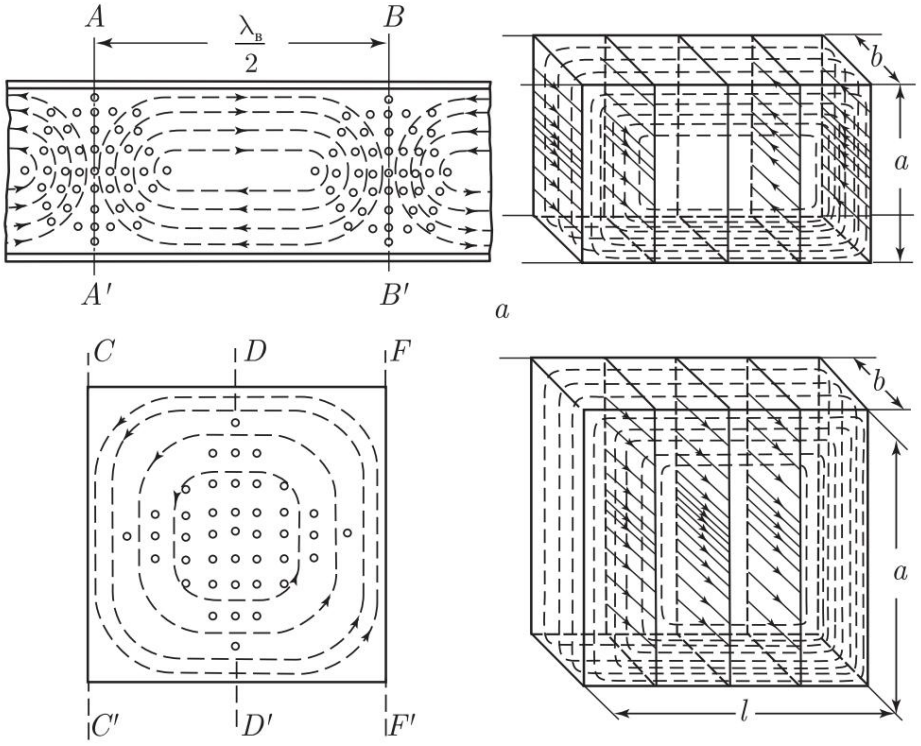

Rice. 2.19. Mutual arrangement of electric and magnetic fields in a rectangular waveguide (wave H10) and in a rectangular cavity resonator (wave H101)

Comparing the fields in the waveguide and in the resonator, we notice significant differences between them: in the waveguide the transverse component
magnetic field and the electric field, which is also transverse, are in phase (see sections AA BB); in the resonator between these components, judging by the differences in the fields in the cross section DD relative to fields in sections CC and FF there is a shift by ÿÿ/4.

This reflects the physical essence of phenomena. Along the axis of the waveguide, coordinated with the load, traveling waves propagate, for them
characteristic phase coincidence of electric and magnetic fields in
time and space. In a volumetric resonator there are standing

waves, which are characterized by a shift between the electric and magnetic fields by a quarter of a period in time and by ÿÿ/4 in space.

Shown in Fig. 2.20 wave H102 differs in that along a narrow side b of the cross section there are no standing waves along the wide one standing half-wave is placed on side a and along the length of the resonator l two standing half-waves are stacked, with electrical power the lines are in the transverse plane.

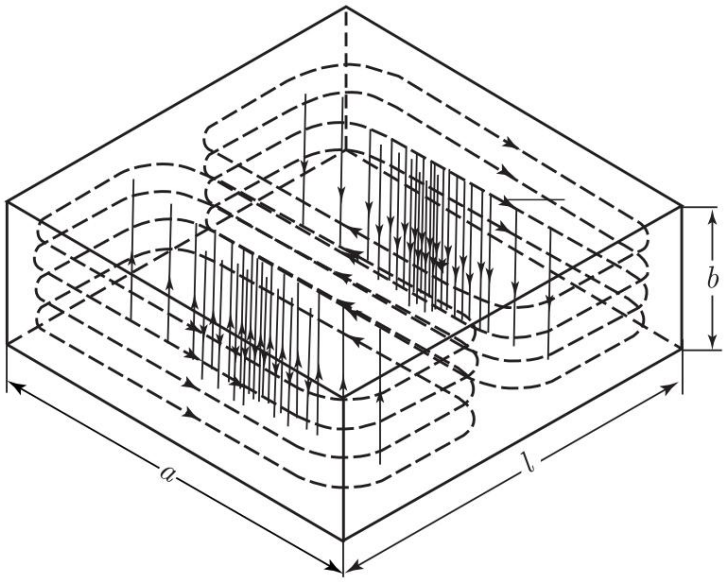

Rice. 2.20. Electric and magnetic fields of wave H102 in a rectangular resonator

In Fig. Figure 2.21 shows for comparison the H01 wave in a circular waveguide and the H011 wave in a cylindrical resonator. When excited H01 waves in a circular waveguide, the electric field lines are completely located in the transverse plane and have the shape of concentric circles with center on the waveguide axis (m = 0); there is a radius one maximum (n = 1); magnetic field lines span the lines electric field. The fields in a cylindrical resonator are distributed similarly at H011, since in this case the indices m and n for the waveguide and the resonator coincide. However, there are differences: in the waveguide, the maxima of the electric field E and the transverse component of the magnetic field Hn coincide, but in the resonator they are shifted of ÿv/4.

Toroidal and coaxial resonators. *Toroidal resonators* (Fig. 2.22) differ from waveguide resonators in being more complex cross-sectional profile. In the middle part *c–d, e–f* distance between the walls of the toroidal resonator is smaller than at the edges, where the cross section is round (Fig. 2.22, a) or rectangular (Fig. 2.22, b) shape.

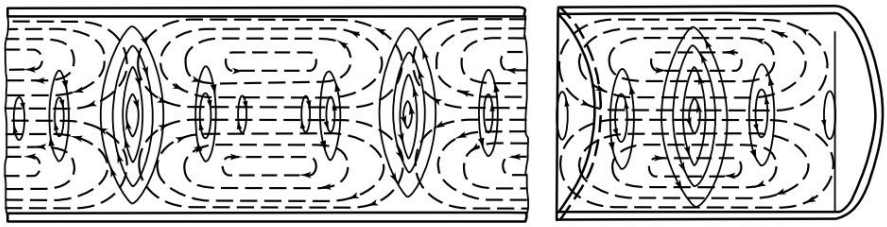

Rice. 2.21. Electric and magnetic fields of H01 wave in a circular waveguide and H011 waves in a cylindrical resonator

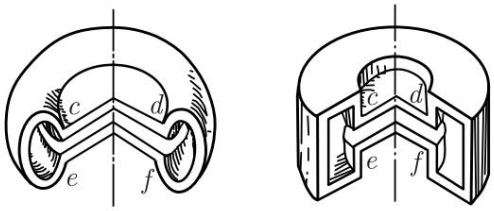

a *б*

Rice. 2.22. Toroidal resonators round *(a)* and rectangular *(b)* sections

An example of the use of toroidal resonators is ultrahigh frequency electronic devices (for example, klystrons), in which the electron tube and the oscillatory circuit are structurally united. Electron flow passing through holes in close located on the walls of the resonator (the holes are not shown in Fig. 2.22), excites electromagnetic oscillations in its cavity. Small the distance between the walls makes it possible to reduce the time of flight of electrons in the resonator, and this is very important when generating and amplifying ultrahigh frequency oscillations.

The shape of the resonator profile determines the structure of the excited electromagnetic fields (Fig. 2.23). The electric field is basically is concentrated in the inner part of the resonator, where the distance between the walls is small, i.e. this part of the resonator is predominantly capacitive in nature, and the peripheral part, where mainly located magnetic field, equivalent to inductance. Consequently, a toroidal resonator, with some approximation, is represented as a circuit with lumped constants. If the walls of the resonator in the section *c–c, e–f* are made flexible and, for example, brought closer together, then The resonator capacitance will increase and its natural frequency will decrease.

Coaxial resonators (Fig. 2.24) are a coaxial line, the ends of which are short-circuited, open or closed to capacitance. In most cases, in such resonators the TEM wave is excited.

In the resonator shown in Fig. 2.24, a, section *ab–cd* is a circular waveguide. Since the TEM wave cannot propagate in it, the electromagnetic field exists only in the area line *ef–ab,* which at one end *(ef)* is short-circuited, and at the other

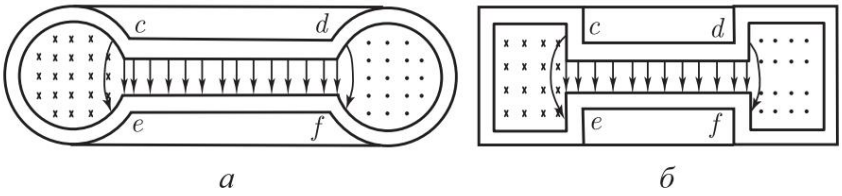

Rice. 2.23. Electric and magnetic fields in toroidal resonators of round *(a)* and rectangular *(b)* cross-sections

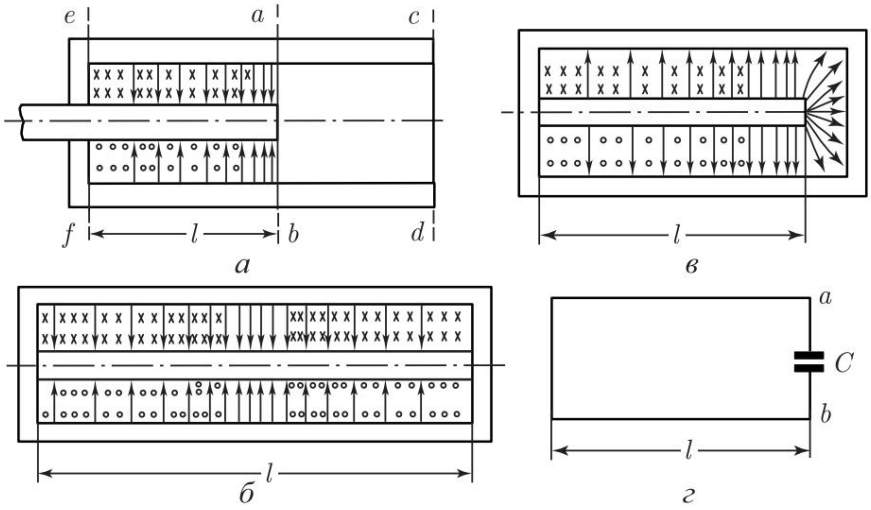

Rice. 2.24. Coaxial resonators: *a* - quarter-wave; *b* - half-wave; *c* - loaded on a container; *g* - equivalent circuit

gogo *(ab)* is open. Obviously, such a line operates in the mode standing waves (typical of resonators) with a magnetic antinode field and the electric node at the short-circuited end and the antinode electric field and a magnetic node at the open end. For this The resonator length l must be equal to an odd number ÿ/4.

If the coaxial resonator is short-circuited at both ends, then its length l should be equal to an even number ÿ/4. An example of this is the half-wave resonator shown in rice. 2.24, b.

In the ultrahigh frequency range, coaxial resonators are used, which are short-circuited at one end and short-circuited at the other. at the end they have a gap between the inner wire and the transverse jumper of the outer wire (Fig. 2.24, c). This gap concentrates electric field, which is equivalent to closing a line of length l to equivalent capacity C (Fig. 2.24, d). Input conductance (between points a, b) of such a resonator is determined by the expression

$$Y_{in} = j\ddot{y}C + \frac{1}{jZ_{in}\,tg\,\frac{2\pi l}{\lambda}} = j\,\frac{530\,l\,[m]}{C\,[pf]}\cdot\frac{1}{Z\ddot{y}}\,ctg\,\frac{2\pi l}{\lambda}$$

For a resonant wave ÿ0, the conductivity Yin = 0. Consequently,

$$\frac{530l0\ [m]}{C\ [pf]} \cdot \frac{1}{Z\ddot{y}}\ ctg\ \frac{2p}{}\ l = 0.\ \ddot{y}0 \qquad (II.26)$$

Advantages and disadvantages of cavity resonators. Now let's consider the question of the quality factor of cavity resonators. Quality factor
The oscillatory circuit after obvious transformations can be represented by the formula:

$$Q = \frac{\ddot{y}L}{R} = \frac{2\ddot{y}fLI2\ m}{RI2_m} = 2p\ \frac{\frac{LI2_m}{2}}{T\ \frac{I2\ mR}{2}} = 2p\ \frac{Wx}{WR}.$$

where Wx is the reactive energy stored in the circuit;

WR - energy spent to compensate for active losses in the circuit for one period.

The energy Wx stored in the cavity resonator is proportional to its volume, and the active losses in the resonator WR are proportional to the length of its inner surface in the direction of the current.

Therefore, they strive to give the volumetric resonator such a shape (according to capabilities round off sharp corners and avoid flattened structures) so that it has maximum volume with minimum
area of the internal walls. Cylindrical resonators are different
higher quality factor than rectangular ones: in them the volume ratio
to the surface above.

It is necessary to distinguish between the quality factor of unloaded Q and loaded Qn of resonators. When calculating Qn , not only active losses WR inside the resonator, but also energy W R coming from resonator into a load for one oscillation period:

$$Qn = 2\ddot{y}\ \frac{Wx}{WR + W_R} = \frac{1}{\frac{WR}{2\ddot{y}Wx} + \frac{IN_R}{2\ddot{y}Wx}} = \frac{1}{\frac{1}{Q} + \frac{1}{Q}} = \frac{QQ}{Q + Q}.$$

where $Q = 2\ddot{y}\ \frac{Wx}{R}$ is the quality factor corresponding to the energy received - W into the load. The quality factor of the loaded resonator is obviously less quality factor of an unloaded one.

No dielectric and radiation losses, low losses
on conduction currents (cross section of the conducting surface
great) determine a very high quality factor of the volumetric resonators. The latter reaches tens of thousands. The second advantage
The main advantage of volumetric resonators is the rigidity of their design.

The disadvantages of cavity resonators include small limits
changes in the resonant wavelength and the presence of multiple resonant
frequency

The indicated advantages of cavity resonators are especially significant in the shortest wavelength part of the ultrahigh frequency range,

where conventional oscillatory circuits cannot be practically used
used.

2.4. Types of metal waveguides

Hollow metal waveguides are not the only type
waveguide transmission lines. For example, in microminiature equipment for centimeter waves, *strip (plane-parallel) waveguides* have been used in the form of a strip conductor separated from a metal flat screen by a thin layer of dielectric (Fig. 2.25).

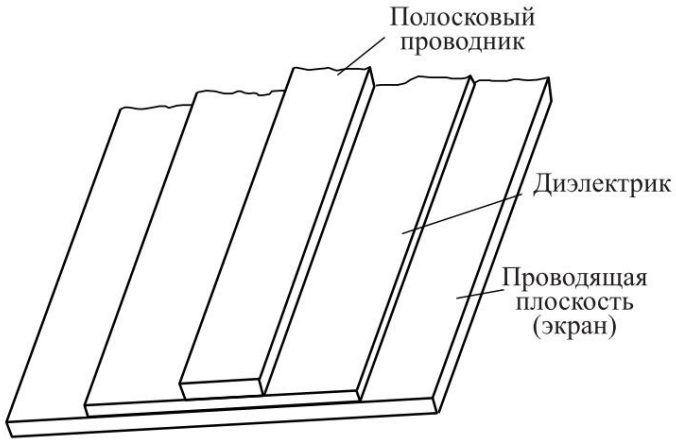

Rice. 2.25. Strip waveguide

Polystyrene is usually used as a dielectric, and the strip
(copper, silver) is applied to the dielectric using the printed circuit method.
The influence of the screen on the electromagnetic field of the propagated wave can be taken into account by the mirror image of the strip, and then the line
becomes two-wire symmetrical. This gives reason to believe
that a wave similar in type propagates in a strip waveguide
to the transverse TEM. Hence the following advantages of such lines
transmissions: broadband, ease of manufacture, low weight and dimensions. Disadvantages:
significant losses in the dielectric and partially on
radiation, as well as a small permissible propagating power
our waves.

Strip lines are used as transmission lines and elements of feeder units in meter, decimeter and centimeter wave equipment.

The width of the metal base must be at least 5 ... 6a,
the distance between adjacent conductors is at least 3 ... 4a. Manufactured by etching from single-sided or double-sided
sheet foil materials - foil fiberglass SF-2 (ÿ = 6, tan ÿ = 25 10ÿ3 at a frequency of 106 Hz), foil fluoroplastic FF-4 (ÿ = 2, tan ÿ = 3 10ÿ4 at a frequency of 1010 Hz),

foil fluoroplastic with fiberglass FAF-4D SKL (ÿ = 2.5;

tg ÿ = 8 10ÿ4 at a frequency of 106 Hz), foil sheet material FLAN (ÿ from 2.8 to 16 depending on the brand, tg ÿ = 15 × × 10ÿ4 at a frequency of 1010 Hz). The use of double-sided foil materials allows the use of foil on one side of the board as a metal base (ground), and on the other - for obtaining a strip pattern of the required configuration.

Strip lines are also produced using the thin film method. technology on ceramic substrates (polycor) with ÿ = 9.6 and tan ÿ = 1 × × 10ÿ4 at a frequency of 1010 Hz.

Cross-sectional dimensions of strip lines with zÿ = 75 Ohm and zÿ = 50 Ohm, made of various materials, are given in Fig. 2.26. Dependence of zÿ and ÿeff of a strip line made of material FAF-4D SKL 1 mm thick from strip conductor width a shown in Fig. 2.27. For practical calculations you can use the formulas given below for various types of strip lines (Table 2.1).

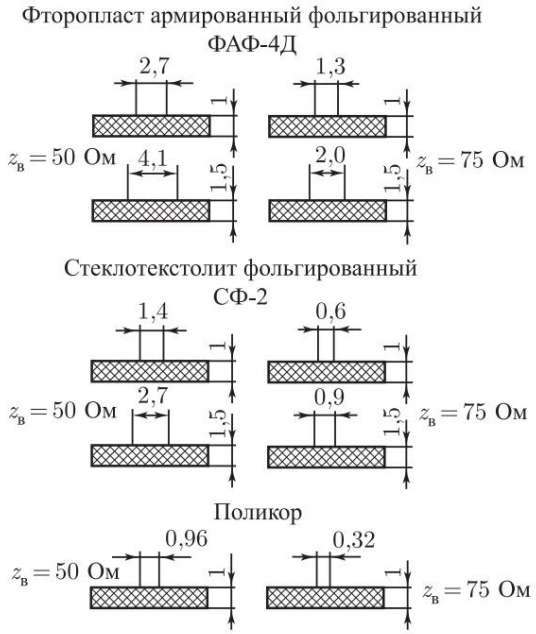

Rice. 2.26. Strip lines

In Fig. 2.28–2.30 shows graphs of the dependence of the wave impedance of various strip lines on the transverse dimensions these lines.

There are waveguides that are designed to transmit millimeter waves. During the transition from centimeter waves to millimeter waves the transverse dimensions of hollow waveguides become very small. Such waveguides can no longer be produced by conventional pipe drawing. Here Electrolytic methods are used, and only the outer surface of the waveguides is machined.

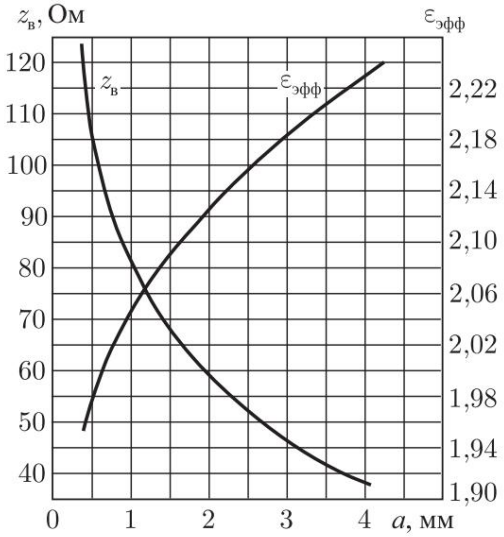

Rice. 2.27. Dependence of zb and ÿeff on the strip line width (FAF-4D SKL)

Table 2.1

Transmission line type	Characteristic impedance, Z0, Ohm	Notes
Shielded symmetrical strip line	60 ln(8b/ÿw) ÿÿÿ (w/b) 1	at (w/b) 1, Z0 ÿ ÿ 15ÿ2 [(ÿw/2b) + ln 2]
Asymmetrical strip line with air gap	120ÿ{2 + (w/b) + + (t/ÿb) × [1 + ln(1 + + 2b/t)]}ÿ1 ÿÿÿÿÿÿÿÿ t final but small	at wb for an infinitely thin strip ÿÿ Z0 = 120ÿ{(w/b) + + (2/ ÿ) × [1 + ln(1 + + ÿw/2b)]}ÿ1
Asymmetrical strip line with solid dielectric	104 /3 ÿÿ [7 + 8,83(w/b)] ÿÿÿ w>b ÿ t w	

At millimeter waves, the current penetration depth is very small. The smaller the roughness of the conductive layer should be, since they lengthen the path along the walls of the waveguide and increase its surface resistance, for example, the finish of the processing of the inner surface of the waveguide for ÿ = 3 mm should be about 0.0001 mm. Due to the small depth of current immersion and the perimeter of the cross-section of the waveguide, losses in them at millimeter waves are tens to hundreds of times greater than in waveguides in the centimeter range. The exception is *round waveguides excited at wave* H01: they are characterized by a decrease in attenuation with increasing frequency. Such

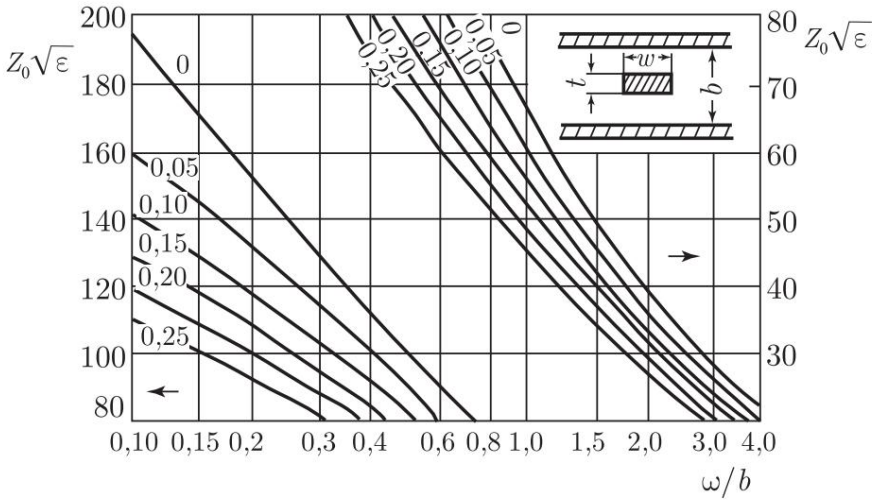

Rice. 2.28. Characteristic impedance of shielded symmetrical stripline lines

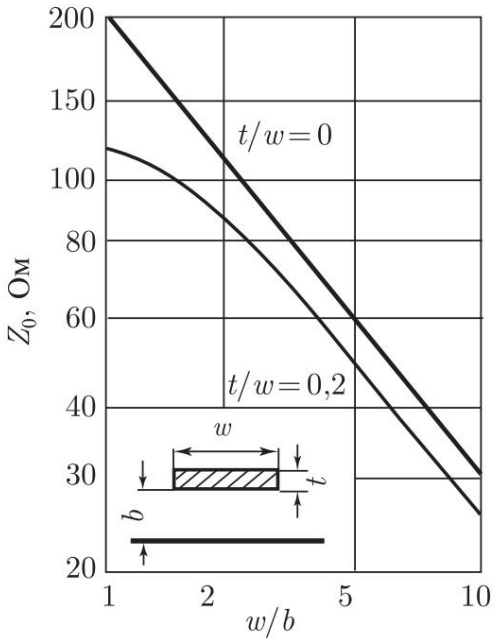

Rice. 2.29. Characteristic impedance of an asymmetrical strip line

waveguides have great prospects for use in long-distance
co-band communication lines.

The manufacture of such waveguides is associated with great difficulties. To ensure minimal losses in the waveguide, the diameter of the waveguide is chosen
c 25–50 mm, i.e. significantly b longer than required by the critical length
waves type H01. Then, along with the H01 wave , a
many other types of waves. The probability of the appearance of spurious waves increases as the shape of the waveguide deviates from an ideal cylinder. Any
The inhomogeneity of the waveguide line generates spurious waves. Especially
significant heterogeneity can be observed at the junction of individual sections
waveguide, in places of bends with a small radius of curvature, at different

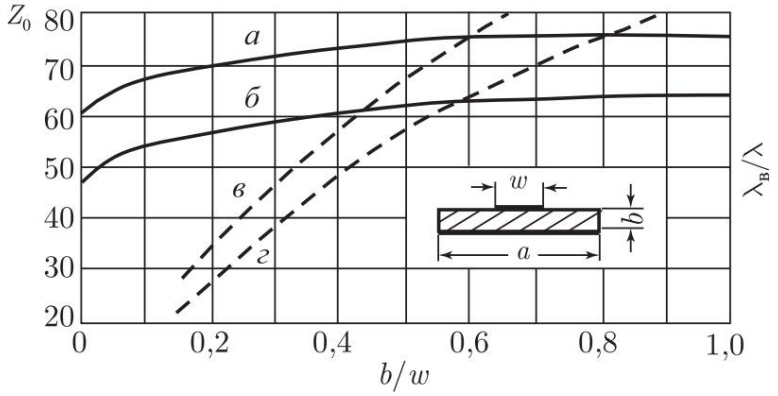

Rice. 2.30. Characteristics of an asymmetrical strip line with a solid dielectric: characteristic impedance; wavelength in the line at a > 3w; *a* and *c* - fiberglass impregnated with Teflon, ÿ = 2.65; *b* and *d* - glass fabric with silicone impregnation, ÿ = 4.18

line deformations, etc. Therefore, such waveguides are subject to very stringent requirements regarding manufacturing accuracy.

To improve the filtration of spurious waves , *round waveguides with a dielectric absorbing film,* as well as spiral ones, have recently begun to be used . Filtration using a dielectric film deposited on the inner surface of a circular waveguide is based on the fact that this film does not introduce attenuation into the H01 wave, since the electric field of the H01 wave does not have a longitudinal component, and other waves that have a longitudinal component of the electric field, are intensively absorbed by the film.

Spiral waveguides are a cylindrical spiral of copper wire placed in a casing made of dielectric. Waves in spiral waveguides are filtered as follows. The longitudinal current in the parasitic waves is interrupted by the turns of the spiral, and therefore these waves penetrate into the dielectric casing and are absorbed by it, while the H01 wave , due to its structure, causes only transverse currents in the waveguide, which are transmitted with low losses.

2.5. Dielectric waveguides

Dielectric waveguides are dielectric rods or tubes of round or rectangular cross-section in which electromagnetic waves are excited.

The fundamental possibility of propagation of electromagnetic waves along a dielectric rod follows from the analogy between it and a metal waveguide of the same shape. The analogy is that in a dielectric rod there is a dielectric-air boundary surface, on which the propagation conditions change sharply. On this surface the waves are reflected and refracted (Fig. 2.31, a), and the reflected waves propagate inside the rod, and the refracted ones - in the air. The presence of waves not only inside, but also outside the rod affects the structure of the electromagnetic field. In dielectric waveguides it is usually

mixed waves of type HE11 are used (see Fig. 2.31, b). They
differ from H11 waves in that, along with the longitudinal component
magnetic field contain a longitudinal component of the electric
fields

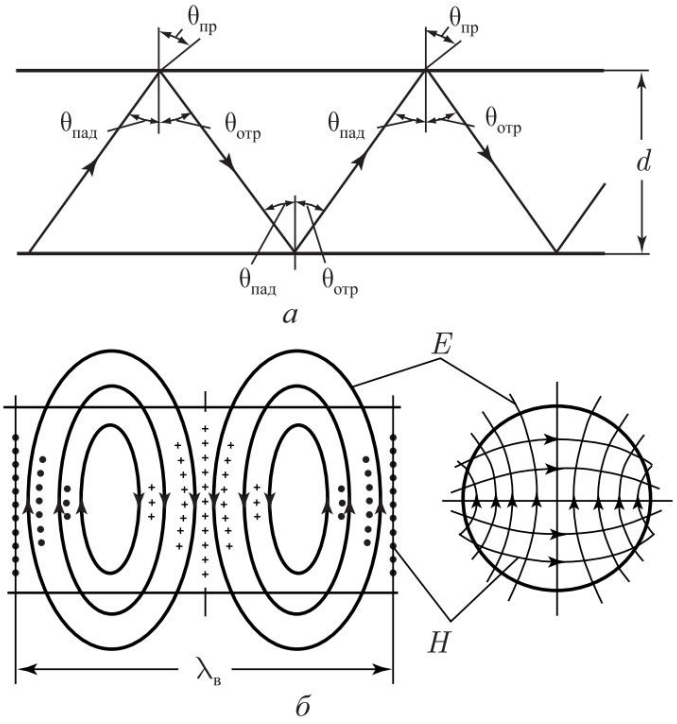

Rice. 2.31. Distribution of electromagnetic waves in a dielectric rod:
a - reflection and refraction of waves; *b* - distribution of electric and magnetic fields

If the diameter of the rod d is significantly less than the wavelength in free space ÿ, then electromagnetic waves mainly propagate in air and their phase speed is close to the speed of light

c = $\frac{1}{\sqrt{ÿÿ0ÿ0}}$. At the same time, the waves according to the structure of the electric and magnetic fields are similar to transverse electric fields H11, and since energy losses in air are disproportionately less than in a dielectric, the attenuation
waves are minimal. As d increases compared to
with ÿ electromagnetic fields are increasingly concentrated in the rod
and the conditions for wave propagation are increasingly approaching the conditions
propagation in an unlimited medium with dielectric constant ÿa. This means that the wave attenuation increases, and the phase
the speed decreases to v = 1/ $\sqrt{ÿÿ0ÿ0}$, accordingly the wavelength $\overline{\quad\quad}$
in the waveguide decreases from ÿ to ÿÿ = ÿ/ÿÿ/ÿ0 .

When excited and received, waves transmitted along a dielectric waveguide propagate both inside the rod and around
him. In Fig. Figure 2.32 shows a diagram of excitation and reception of waves at
using a dielectric waveguide.

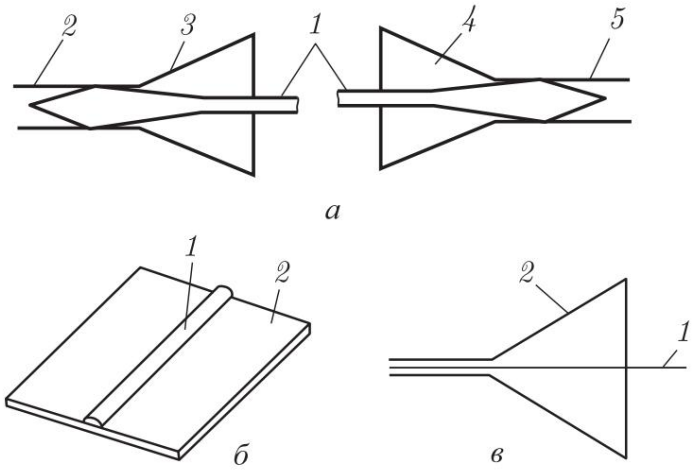

Rice. 2.32. Transmission line using dielectric rod

Dielectric rod *1* is inserted into metal waveguides 2, 5, which end in horns 3, 4. Wave H11 propagates in waveguide *2 ,* which in rod *1* transforms into wave HE11

due to the similarity of the structure of these fields. At the receiving end, reverse transformations occur. Dimensions of transmitting *3* and receiving *4*
horns are selected taking into account the concentration of electromagnetic energy in the radial direction.

Dielectric waveguides have an advantage over metal ones in that they do not require high manufacturing precision and create less attenuation for millimeter waves. At centimeter waves, the use of dielectric waveguides is impractical; they are not

give a gain in attenuation; due to the air environment involved
in transmission, the radius of dielectric waveguides is larger; Attaching the dielectric rod is difficult.

2.6. Transmission lines

2.6.1. Characteristics of transmission lines. *Linear capacity* Cpog — capacitance per unit line length.

Linear inductance Lpog - inductance per unit length
lines.

Characteristic impedance zÿ is a parameter that determines the ratio relationship between the amplitudes of the incident voltage and current waves:

$$Ipad = Upad/zv.$$

Characteristic impedance depends on the shape and size of the conductors in the cross section of the line, degree of filling of the cross section
insulation and its relative dielectric constant ÿ.

The relationship between characteristic impedance and linear capacitance and inductance

$$zv = \sqrt{Lpog/Cpog}\ .$$

The characteristic impedance (Ohm) of an overhead line can be determined through its linear capacitance

$$z\ddot{y} = 3300/$$

Cpog.v, where Cpog.v is the linear capacity of the air line, pf/m.

The characteristic impedance of a line filled with a dielectric is

$$z\ddot{y} = 3300/\ \ddot{y}\bar{\ddot{y}}\ \ddot{y}\ddot{y}.\ddot{y} \text{ or } z\ddot{y} = 3300\ddot{y}\ddot{y}\ /\ddot{y}\ddot{y}.\ddot{y},\ \bar{}$$

where Cpog.d is the linear capacitance of the line filled with a dielectric, pF/m.

The wavelength shortening factor n is a parameter showing how many times the wavelength in the line ÿd is less than the wavelength ÿ0 in free space (n = ÿ0/ÿd). For shielded lines completely filled with dielectric,

$$n = \ddot{y}\bar{\ddot{y}}.$$

For shielded lines with incomplete dielectric filling and unshielded lines

$$n = \ddot{y}\ddot{y}\overline{\text{eff}},$$

where ÿeff is the effective dielectric constant, equal to the ratio of the linear capacitances of a line with a dielectric and a line of the same cross-section, but without a dielectric.

For example, the wavelength in a coaxial cable filled with a dielectric with ÿ = 2.3 at a frequency of 50 MHz (ÿ0 = 6 m)

$$\ddot{y}\ddot{y} = \ddot{y}0/\ \ddot{y}\bar{\ddot{y}} = 6/\ 2.3\ \overline{=}\ \overline{6}/1.52 = 3.95 \text{ m}.$$

Linear attenuation ÿ is a decrease in voltage, current or wave power per unit line length. Usually expressed in decibels per meter or kilometer (dB/m or dB/km). Total attenuation in a line of length l

$$N = \ddot{y}l.$$

The attenuation can be expressed in neper (Hn) using the relation

$$1 \text{ Np} = 8.68 \text{ dB}.$$

Line efficiency (efficiency) ÿd = P2/P1,

where P1, P2 are the powers at the input and output of the lines. The efficiency of a line can be determined in terms of the total attenuation of the line

$$\ddot{y}d = e^{-\frac{2\ddot{y}l}{8,68}}$$

where ÿl is in dB, e is the base of natural logarithms (e = 2.72).

The dependence of the line efficiency on its total attenuation ÿl is shown in Fig. 2.33.

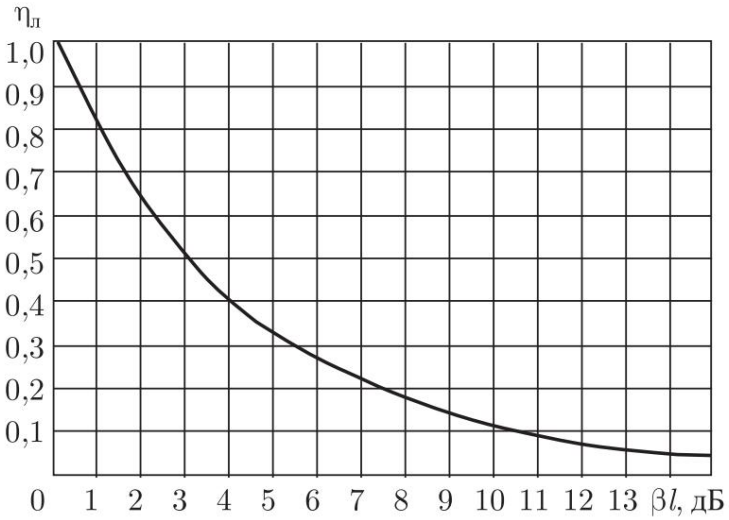

Fig. 2.33

Using the relationship between the characteristic impedance of a line and its linear capacitance, it is possible to determine the characteristic impedance and shortening factor of a transmission line, for example, a coaxial cable of an unknown brand.

Example. Determine the characteristic impedance and shortening coefficient of a coaxial cable of an unknown brand. 1. Measure the diameter of the inner conductor d1 and the diameter along insulation d2 (Fig. 2.34)

d1 = 0.72 mm; d2 = 4.6 mm.

2. We measure the capacitance C between the inner and outer conductors of a cable segment, the length l of which should be no more than 0.05ÿ, where ÿ is the wavelength corresponding to the selected measurement frequency. The free end of the cable segment must be open (idle). We choose the frequency f = 10 MHz, ÿ = 300/10 = 30 m), with l = 0.05ÿ = 0.05 × 30 = 1.5 m. The measured capacitance is C = 100 pF. 3. Linear capacity

$$C_{pog.d} = C/l = 100/1.5 = 67 \text{ pF/m}.$$

4. We calculate the linear capacitance of a cylindrical air capacitor having the same cross-section as the coaxial cable. Capacitance of the capacitor, pF, length l, m,

$$C = 24.1l/\lg \frac{D}{d}$$

Linear capacity

$$C_{pog.v} = 24,\ 1/\ \lg \frac{D}{d} =$$

$$= 24,1/\ \lg 0,72\ \frac{4,6}{} = 24.l/(\lg 6.35) = 24.1/0.804 = 30\ pF/m.$$

5. Dielectric constant of cable insulation

$$ÿ = C_{pog.d}/C_{pog.v} = 67/30 = 2.3.$$

6. Characteristic impedance

$$z_v = 3300/\ ÿÿ\ \overline{C_{pog.v}} = 3300/\ 2.3\ 30 = \overline{75\ Ohm}\ .$$

2.6.2. Transmission line designs and parameters

Radio frequency cable is a flexible coaxial cable (Fig. 2.34), consisting of a copper inner conductor 1,

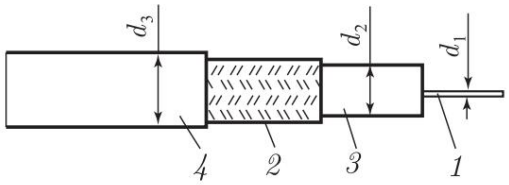

Rice. 2.34. Flexible coaxial cable

outer conductor 2, braided from copper wires, polyethylene insulation 3 and protective sheath 4 made of polyethylene or polyvinyl chloride. The conventional name of the cable consists of the letters RK (radio frequency cable); numbers indicating the nominal impedance, Ohm; numbers indicating the diameter of the insulation, mm, separating the inner and outer conductors; numbers indicating the serial number of the development. Example of a symbol: RK 75-4-15 (radio frequency cable with a characteristic impedance of 75 Ohms, internal insulation diameter 4 mm). The design and electrical parameters of radio frequency cables are given in Table. 2.2. In Fig. Figure 2.35 shows the dependence on frequency and power (curves 3, 4) for the most common cables. Curves 1 and 3 refer to cables RK 75-4-11, RK 75-4-12,

RK 75-4-15, RK 75-4-16, curves 2 and 4 - to cables RK 75-9-12, RK 75-9-13.

Machine Translated by Google

Table 7.2

RF

Brand	Called,	Cpog, pF/	n	Size d1, m		d3, m	Minimum permissible	Temperature	Weight, kg
RK-1-12	75					yyy	yyy ...		5,4
	RC-2-11yyy								14,7
									34
									63
RK-4-12	35								63
RK-4-15	35								72
RK-9-12	50								72
									189
									172
									5,8
RK-2-13	50								24,6
									50
	RK-3-12y								141
									134
									178
RK-9-12	20				0,3				213

yy Double. Screen.

yyy Conductor.

Insulation.

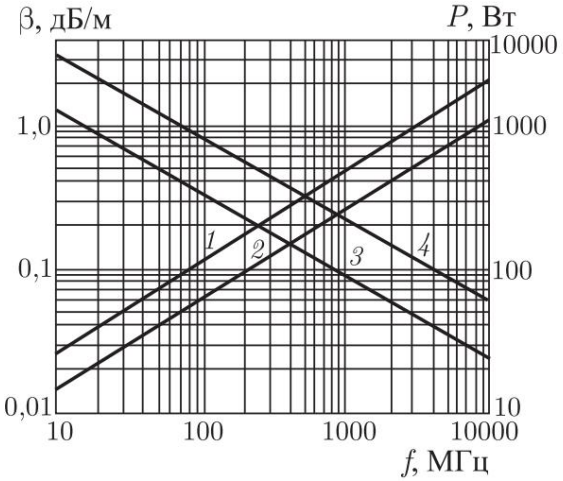

Rice. 2.35. Dependence on the frequency of linear attenuation (curves *1,* 2) and the maximum permissible transmitted power (curves *3,* 4) for the most common cables. Curves *1* and *3* refer to cables RK 75-4-11, RK 75-4-12, RK 75-4-15, RK 75-4-16, curves *2* and *4* - to cables RK 75-9-12, RK 75-9-13

Cross sections of *rigid transmission lines* of various designs are shown in Fig. 2.36. Wave impedances of these lines, Ohm:

coaxial (concentric) line (Fig. 2.36, a)

$$z\ddot{y} = 138 \lg D/d;$$

coaxial line with eccentricity (displacement) of internal conductor (Fig. 2.36, b)

$$zv = 138 \lg d \quad \frac{D}{} \text{ ÿ } 1{,}75 \quad \frac{\text{It is}}{D}^{2} \qquad \text{at } e/d < 0.3;$$

coaxial line with a spiral inner conductor made of tapes (Fig. 2.36, c)

$$z\ddot{y} = z\ddot{y}0k \text{ at } \ddot{y}S\ S,$$

where zÿ0 is the characteristic impedance of a coaxial line with a smooth internal conductor with diameter d and internal screen diameter D, determined by the formula $z\ddot{y}0 = 138 \log k\frac{D}{d}$ correction factor, taking into account the spiral design of the inner conductor:

$$k = \frac{\sqrt{2{,}1q2\ d2\ 1\ \ddot{y}\ \frac{d}{D}^{2}}}{\lg \frac{D}{d}}.$$

where q is the number of turns per 1 cm of length;

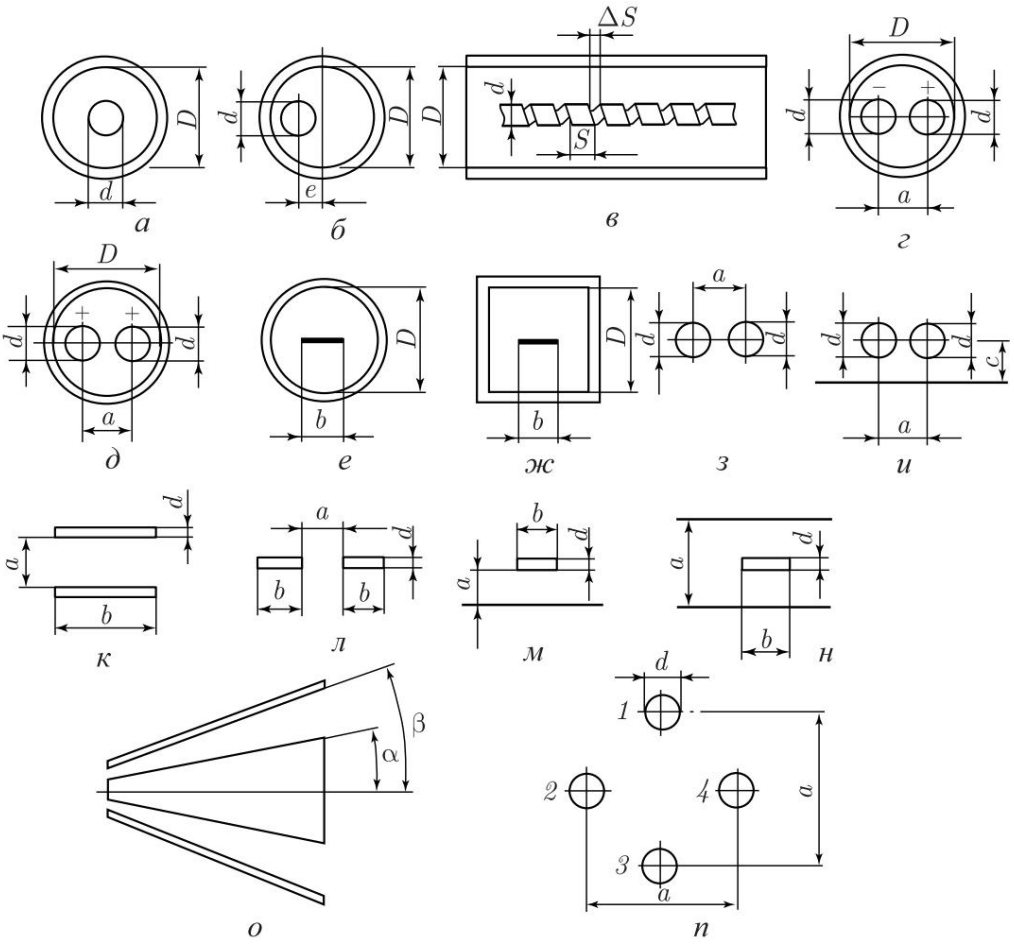

Rice. 2.36. Cross sections of various rigid transmission lines designs

two-wire line in a cylindrical screen (Fig. 2.36, d) in antiphase excitation mode (voltage applied between internal conductors, the screen is grounded)

$$zv = 276 \lg \frac{2a}{d} \frac{D2 ÿ a2}{D2 + a2} \qquad ÿÿÿ\ D/d > 4\ ÿ\ d/a > (1 ÿ 2d/D);$$

two-wire line in a cylindrical screen (Fig. 2.36, e) in the common-mode excitation mode (voltage is applied between parallel-connected internal conductors and the screen)

$$zv = 69 \lg \frac{1}{8\,da} \frac{D4 ÿ a4}{D2} \qquad \text{at } D/d\ 1 \text{ and } D/a\ 1;$$

tape in a cylindrical screen (Fig. 2.36, e)

$$zc = 138 \lg(2d/b) \text{ at } D/b\ 1,$$

$$zÿ = 6{,}5ÿ2 / \frac{ÿ\ ÿ\ \frac{4}{ÿlg\ ÿ\ 1 ÿ \frac{b}{D}}\ ÿ\ ÿ}{} \qquad \text{at } D/b\ ÿ\ 1;$$

tape in a screen with a square section (Fig. 2.36, g) zÿ = 138

log(2.16D/b) at D/b 1,

$$z\ddot{y} = 6{,}5\ddot{y}2 \,/\, \ddot{y}\,\ddot{y}\,\ddot{y}\lg\frac{3{,}06}{1\,\ddot{y}\,\frac{b}{d}}\,\ddot{y}\,\ddot{y}\,\ddot{y}\,\ddot{y}$$ at D/b ÿ 1;

two-wire unshielded line (Fig. 2.36, h)

$$z\ddot{y} = 276 \lg ; d \frac{2a}{}$$

two-wire unshielded line above the plane (Fig. 2.36, i)

$$zv = 276 \lg \frac{2a}{d\left(1 + \left(\frac{a}{2c}\right)^2\right)}$$

strip line with conductors located one above the other (Fig. 2.36, j),

zc = 377a/a + b for db and a/b < 3;

strip line with adjacent conductors (Fig. 2.36, l)

b $z\ddot{y} = 257/\lg 4 + 8\frac{}{a}$ for db and b/a > 1,

$zc = 276 \lg 4 + 4a\frac{}{b}$ at db ÿ b/a < 1;

strip conductor above the plane (Fig. 2.36, m) zÿ = 138 lg 3.5a

$\frac{}{b}$;

strip conductor between planes (Fig. 2.36, n) b zÿ = 150/ 0.69 + 1.6

$\frac{}{a}$ at db and a/b < 1;

conical line (Fig. 2.36, o)

$$z\ddot{y} = \lg \operatorname{tg} \frac{\ddot{y}}{2} / \operatorname{tg} \frac{a}{2}$$

A two-wire line (Fig. 2.36, h) is usually used as a transmission line with a characteristic impedance of 200 Ohms and higher. To obtain lower wave impedances, a four-wire line is used (Fig. 2.36, p). The characteristic impedance of such a line can be determined from the graphs in Fig. 2.37. Curve 1 corresponds to the case when one wire is pairwise connected conductors 1–3, the other wire is pairwise connected conductors 2–4, and curve 2 corresponds to the case of pairwise connection of conductors 1–2 and 3–4. The conductors are connected at the beginning and end of the line.

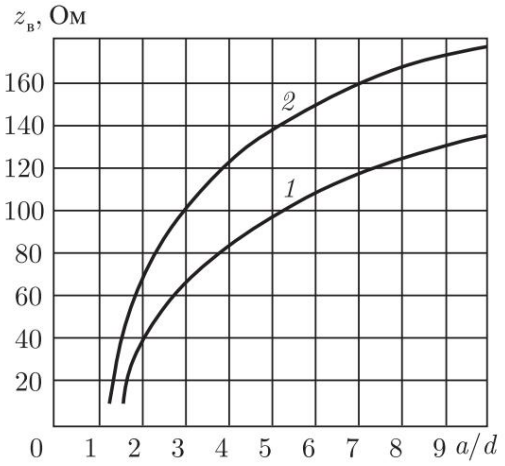

Fig. 2.37

The characteristic impedance of shielded lines filled with a dielectric can be determined by dividing z in the corresponding overhead line by ÿÿ .

The wavelength shortening factor n in an air coaxial line with a spiral inner conductor is numerically equal to
correction factor k, taking into account the spiral structure
conductor in the formula for z in lines of this type given above.

Chapter 3

MICROWAVE GENERATORS WITH BROADBAND MODULATION

3.1. Features of the design of microwave generators UHF

Some of the characteristic features of microwave oscillations in the decimeter range discussed above allow us to move on to a more detailed study of them in order to answer some specific questions,
in particular, how a microwave generator is built, what it has in common with generators of lower frequencies, how it differs, what nonlinear elements it is based on, what its oscillatory vibrations are
systems, etc. This is necessary not only from a general point of view
acquaintance with microwave technology. Without this it will be difficult to understand why, for example, some modulator circuits, usually used in electronics, are not applicable to UHF microwave generators,
what are the backup capabilities of a particular lamp mode, what
is limiting when deciding on the frequency range
modulating signal, etc.

Let us consider an oscillatory circuit consisting of a concentrated
capacitance C and lumped inductance L. When operating at relatively low frequencies, real values of capacitance and inductance make it possible to obtain fairly high quality factors

and selectivity. However, as the wavelength shortens, these contours
become inconvenient for use as oscillatory systems. As the wavelength shortens, their inherent

at ultra-high frequencies disadvantages:

- low quality factor associated with large radiation losses, losses during the passage of conduction currents through the contacts
and along the conductors, losses due to currents induced in the surrounding
conductors and losses due to dielectric hysteresis in insulators;

— significant stray fields creating unwanted connections
and additional losses in surrounding conductors;

— low standard of resonant frequencies.

Since the power losses in the oscillatory system of the generator
is determined by the expression [208]:

$$P_{loss} = \frac{1}{2} \cdot \frac{U^2 \ddot{y} C}{Q_0}$$

where U is the voltage amplitude in the oscillatory system, C is the capacitance oscillatory system, Q0 is the unloaded quality factor, ÿ is the circular frequency, then with increasing operating frequency it is necessary to increase quality factor of the oscillatory system to reduce power losses.

In Fig. 3.01 shows a gradual transition from an oscillatory circuit with lumped parameters L and C to a non-radiating oscillatory system with distributed parameters, called hollow resonator. Currently, the hollow resonator is the main one the shape of the oscillatory system of UHF microwave generators, as it provides high quality factor, the possibility of smooth adjustment of the frequency of generated oscillations, has sufficient compactness and mechanical rigidity. To other advantages hollow resonator we will return after we consider generator lamps used in microwaves.

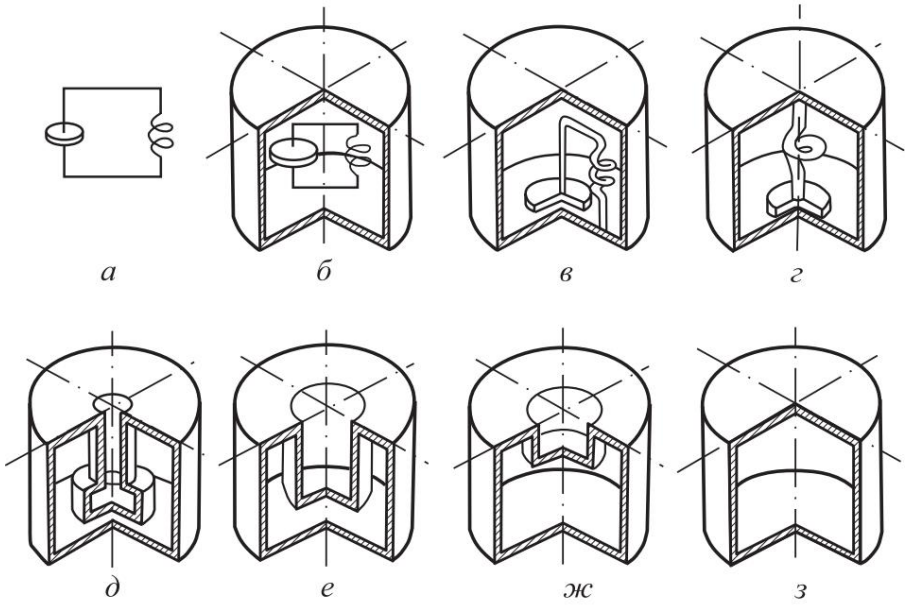

Rice. 3.01. Transition from an oscillatory circuit with lumped parameters to an oscillatory system with distributed parameters: *a* - LC circuit; b, *h* - cylindrical vibrator; c, *d* - cylindrical vibrator with concentrated capacitance and inductance; *d*–*g* — transition to cylindrical voter

To operate in the microwave range, the generator lamp must satisfy do the following:

- have a minimum value of lead inductance;

— at a given rated power it is possible to provide less, that is, to have as much as possible neck ratio Ea nom/Jm max, cathode emission;

— have a minimum resistance value for high-frequency energy losses.

Reducing the wavelength of oscillations generated by the lamp is possible both by reducing the interelectrode capacitances and by reducing lead inductances. Reduction of interelectrode capacities can be obtained either by increasing the distance between the electrodes, or by reducing their area. However this will lead to an increase in the time of flight of electrons and a decrease in cathode emissions. Both will entail a decrease in useful power taken from the generator. To reduce high-frequency losses, it is necessary to reduce the amount of dielectric fittings in the lamp to a minimum. These and many other requirements are for the first time were implemented in lamps of a fundamentally new design, developed by a group of Soviet specialists under the leadership of academician N.D. Devyatkov in 1938. In Fig. 3.02 shows the design

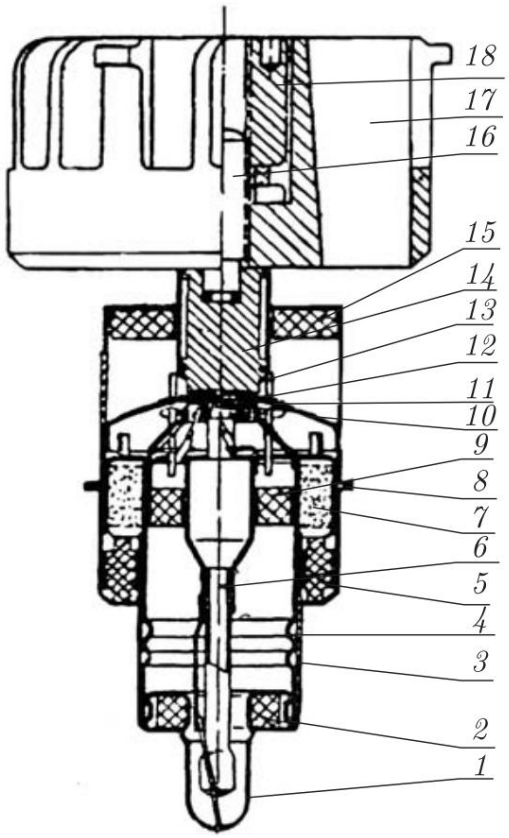

Rice. 3.02. Section of the design of a metal-ceramic lamp: *1* - cap filament output; *2* — ceramic washer of the base; *3* — external cathode tube; *4* - internal corrugated cathode tube; *5* - ceramic insulator between the cathode and grid cylinders; *6* - plug; *7* - ring with layer getter; *8* — grid cylinder (grid output); *9* - ceramic cathode insulator; *10* — heater; *11* - cathode; *12* - mesh; *13* — pins communications; *14* - anode; *15* - ceramic insulator between the anode and the mesh cylinder; *16* — anode bolt for attaching the radiator; *17* — radiator; *18* - radiator mounting nut

modern metal-ceramic lamp (MCL) of domestic production. Let us now return again to the designs of hollow resonators.
As you can see, the only correct solution for connecting the lamp and a hollow resonator is their direct connection as two coaxial systems (Fig. 3.03). The lamp thus becomes

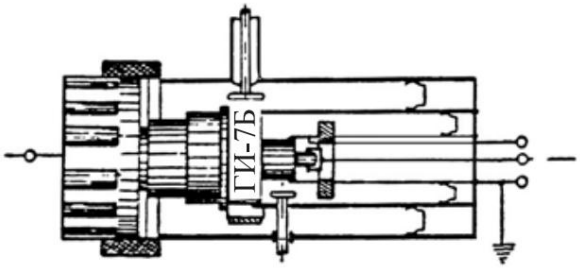

Rice. 3.03. Docking a metal-ceramic lamp with a hollow resonator

part of a hollow resonator. Such a system allows you to implement everything higher requirements for the creation of a self-oscillating system Microwave with high performance. On the other side,
The operation of various types of microwave tube generators has shown that the most convenient option is a double-circuit circuit generator This scheme allows for optimal communication generator with a load, setting to the desired wavelength, adjusting the feedback value. Moreover, taking advantage of the opportunity direct docking of SCLs with oscillatory systems, it is possible get the most technologically advanced design. Since at the same time the question arises of supplying voltage and insulation to the lamp metal structure of oscillatory systems, then the most appropriate is a design with zero potential of oscillatory systems. In Fig. Figure 3.04 shows a cross-section of the double-circuit design

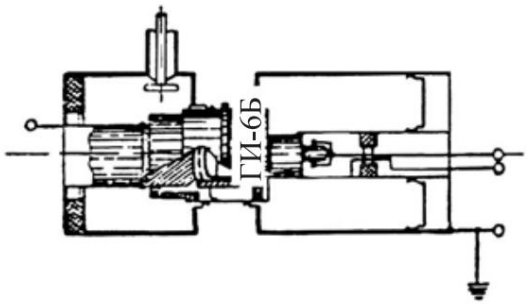

Rice. 3.04. Cross-section of the design of a double-circuit microwave generator with zero potential of all elements

Microwave generator with zero potential of all elements of hollow resonators. This design implements a generator circuit with a grounded grid, which, in addition to some additional positive
properties, on the one hand, predetermines the range of possible circuit designs wideband modulator solutions, on the other hand. Generators,

built according to this type are divided into two classes: generators with a grounded cathode and generators with an insulated cathode. Generators, built according to other schemes may also have an isolated or grounded cathode. Therefore, the division of generators introduced here with a grounded grid into two classes is formal and serves just for the convenience of considering some points later, limiting the use of one or another modulator circuit.

A microwave generator can be built to operate on a fixed frequency As a rule, this is a specialized generator operating for the same type of load with the same degree of coupling output oscillatory circuit with load. An example of such a generator is the Volna-2 therapeutic device [209] for microwave therapy, which is a self-oscillator operating at a frequency of 460 MHz. However, in research work it is impossible to be satisfied with such a scheme, since the operating conditions microwave generator are determined here by many factors - various the volume of the object and its cross section, varying degrees connection between the generator and the load, which is largely determined the ratio of the areas of the irradiating zone and the object, different depths of field penetration in the object, etc. All this leads to a more complicated design of the microwave generator, primarily the resonator systems. One of the requirements for such generators is is the presence of restructuring of oscillatory systems in a wide frequency range. Smooth frequency tuning across the range is realized by introducing pistons into cylindrical (coaxial) hollow resonators. For the case of circuits with distributed inductances, what are homogeneous coaxial lines, short-circuited at the end, their length is related to the input inductance by the ratio [208]:

$$L_{ÿÿ} = \mathrm{tg}\,\frac{Z0}{oh}\,ml,$$

where Z0 is the wave resistance of the line, l is its length to the short-circuiting piston. Hence, the change in the length of the short-circuit homogeneous coaxial line leads to a change in its input inductance, which in turn leads to a change in frequency generated oscillations. Examples of such designs are generators of the LMS series, covering the wavelength range 9 ÷ 16 cm, 18 ÷ 33 cm and 30 ÷ 100 cm, laboratory measuring generators of types GS-6, GSS-12, GSS-15. In Fig. 3.05 shows equivalent circuits generators with grounded grid and grounded and isolated cathodes. As can be seen from the given equivalent and constructive microwave generator circuits, for their normal operation it is necessary to separate MCL electrodes are separated from each other by constant voltage. The supply of power to the SCL electrodes necessitates disruption continuity of metal shells of hollow resonators serving oscillatory systems. Violations of their integrity also require

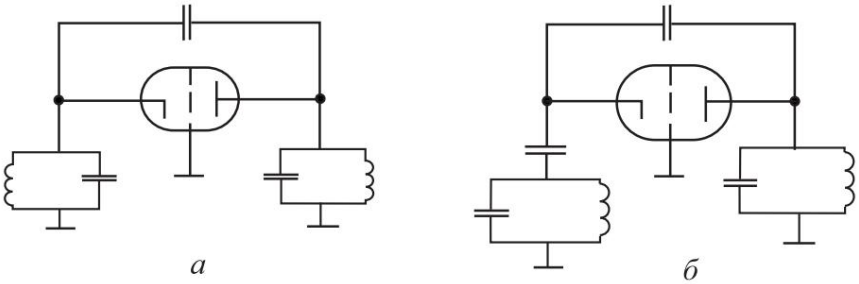

Rice. 3.05. Equivalent circuits of microwave generators based on metal-ceramic triode with a grounded grid: *a* - with a grounded cathode; *b* - with isolated cathode

conditions for modulating the output power of generators, since, as it can be seen from these diagrams that the modulating signal must be supplied either to the anode or cathode of the MCL. As a result, leakage conditions are created energy of high-frequency oscillations from the internal cavities of the resonators into the external space, which not only affects the normal operation of the generator as a whole, but also poses a threat to human health, especially at high power output levels generator Elimination of these undesirable phenomena is carried out by blocking the power wires using block capacitors or other blocking elements. Moreover, along with the use of block capacitors, when developing designs for microwave generators, the connection they try to install power wires at the points where the nodes are located voltage. If the power cord runs along a line along which the intensity of the high-frequency electric field is zero, then no electromotive force is induced in it. Because constructively It is convenient to build microwave generators in the decimeter range using MCLs using a parallel circuit excitation circuit, then in these In circuits, the anode and cathode of the MCL are under a significant high-frequency potential relative to the screen, and the power wires of these electrodes require careful blocking. In Fig. 3.06 shown high-frequency blocking circuit for MCL cathodes of microwave generators GS-6 and GSS-12, operating in the range 0.15 ÷ 1.0 GHz. In Fig. 3.07 options for the arrangement of block capacitors in a single-cycle UHF microwave generator made on MCL according to the scheme with a grounded grid. Blocking schemes shown in rice. 3.07, are used mainly when the generator operates in a wide range frequency band. When the generator operates at a fixed frequency and especially in high-power generators instead of block capacitors (or in addition to them) it is possible to use quarter-wave blocking elements consisting of sections of coaxial or radial lines (Fig. 3.08). The operation of such a blocking element is based on the fact that a segment of the coaxial line *ab,* short-circuited at its upper end (Fig. 3.09), formed by the intermediate and internal cylinders, has a very high input resistance at its lower end. Therefore, the line segment *bv* formed by

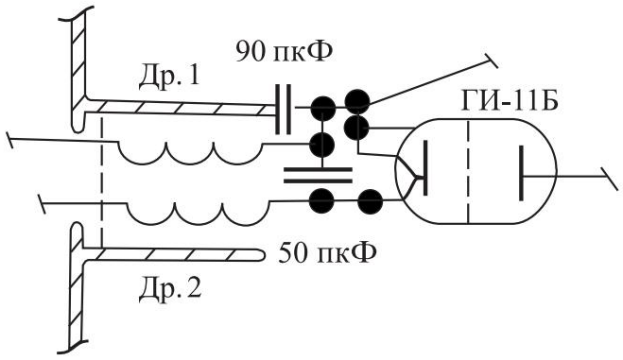

Rice. 3.06. Blocking the cathode of a metal-ceramic lamp in GS-6 generators and GSS-12: Dr. 1, Dr. 2 - blocking chokes, 90 pF - cathode block capacitor, 50 pF - shunt capacitor. GI-11B - generator lamp. Bold dots are the junction points of the generator lamp and block containers and resonator

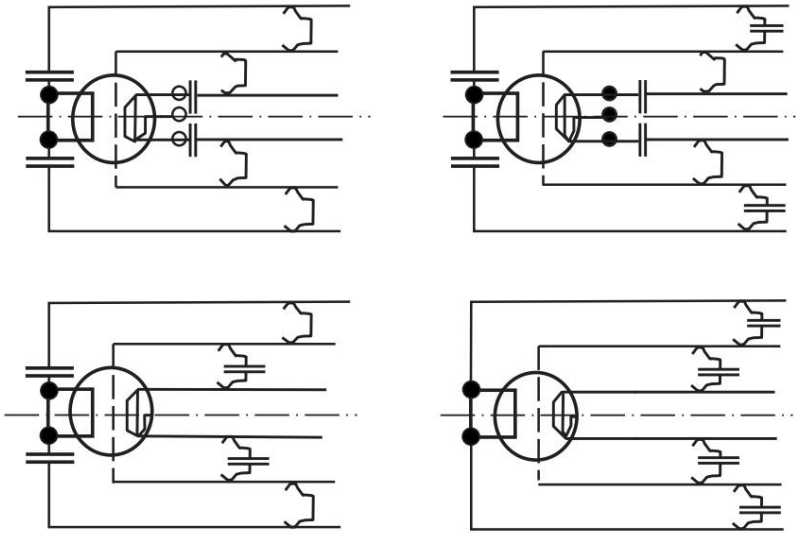

Rice. 3.07. Options for the location of block capacities in a single-cycle generator

Microwave

intermediate and outer cylinders, loaded at its lower end with very high resistance, that is, practically open. As a result, it has a very low input impedance, i.e. represents a short circuit for high frequency currents at its top end. If the amplitude of the high-frequency current in the circuit is its cross section, where a block capacitor with a capacitance Cbl is connected, is equal to I, then the amplitude of the high frequency voltage on the block capacitor is equal to

$$U = \frac{I}{\ddot{y}Cbl}.$$

The capacitor must withstand the combined effect of this high frequency voltage and the direct voltage generated by the power source. Power circuits with which communication is created through block capacitor can be considered as some lines with dis-

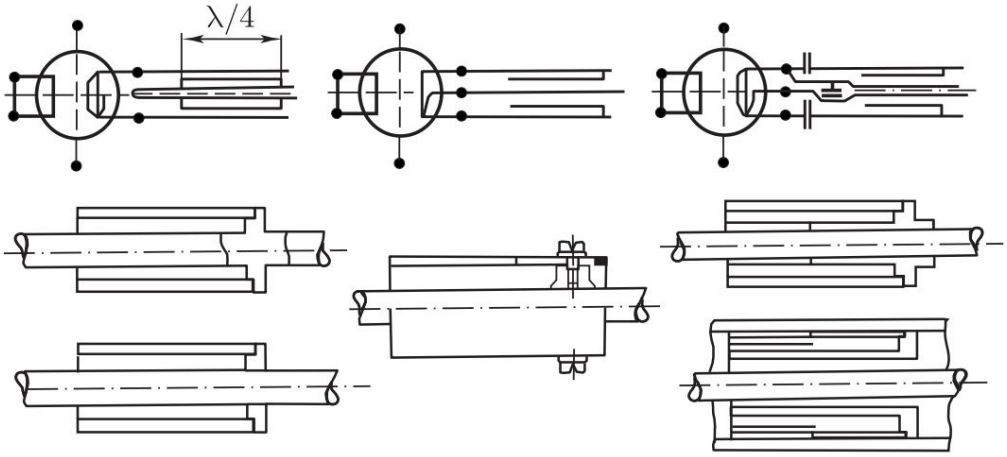

Rice. 3.08. Examples of using quarter-wave blockers elements and their designs

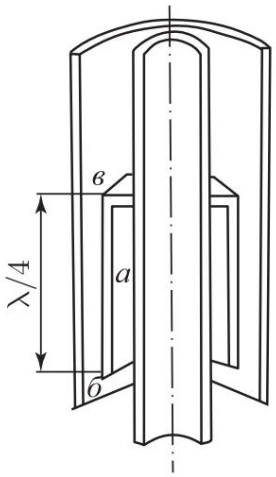

Rice. 3.09. Short-circuited interlock element

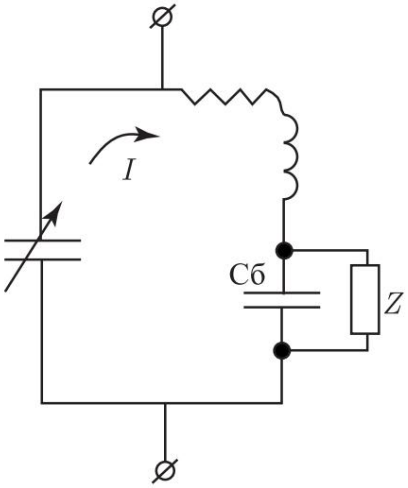

Rice. 3.10. Equivalent circuit diagram of a circuit with a block capacitor loaded on the complex resistance of the power circuit (description in the text)

limited constants, the input resistance of which has complex nature. This input resistance Z turns out to be connected in parallel with the block capacitor so that the equivalent The circuit diagram with a block capacitor can be reduced to the form shown in Fig. 3.10. When working in a wide range of waves the Z value can vary within wide limits. Under certain conditions, this value may turn out to be so small that it will lead to to the breakdown of oscillations. On the other hand, a block capacitor is limiting element in determining the upper limit of the frequency range of the modulating signal during modulation in the MCL anode circuit. A detailed calculation of the structural elements of microwave generators in the decimeter range can be found in the literature [208, 210], description the elements themselves - in [211].

3.2. Construction of modulated oscillators UHF for biological experiment

The considered way of constructing wide-range modulated microwave generators can be effectively used in conditions research laboratories and in the development of serial equipment and, naturally, it is advisable before the advent of industrial designs.

At present, the bioeffects of microwaves in various parts of this range have not been well studied. Therefore the presence in generators the possibility of smooth frequency tuning over the range may be considered appropriate at this stage. Only if available large amount of information, it will obviously be possible to identify separate narrow ranges or fixed frequencies with universality in terms of their use for solving a wide range of biological problems. This circumstance naturally makes it easier the task of developing generator devices, increases their reliability and durability, reduces cost. The microwave generator is thus is the basis of the complex of technical support for biological experiment. In table 3.1 provides data on UHF generators that have the highest output power among models of this class and which served as base models in the development of powerful modulated microwave generators for biological experiment.

3.2.1. Basic requirements for generator sets devices. Requirements for microwave generator devices for their possible use in an experiment to study the influence of continuous and modulated electromagnetic fields on biological structures are based on the specific conditions of irradiation of biological objects, their size and orientation in the electromagnetic field, are determined by the boundaries of the values of relaxation periods of biochemical reactions, the degree of severity of the effect from the shape of the envelope electromagnetic field, etc. Requirements for modulation capabilities generators turn out to be quite wide: in repetition frequency from approximately 10ÿ3 Hz (synchronization of oscillatory biochemical reactions) up to tens of kilohertz (studies of quasi-acoustic perceptions of EMF, etc.). At the same time, in order to ensure a small average level of power incident on the object, lower limit of duration It is advisable to choose a pulse of about 10ÿ6 s. At the same time for When studying the effect of EMF on various self-oscillating and conducting systems, it is necessary to ensure the duration of the field pulses, equal to seconds and even minutes. Availability of functional blocks, providing a change in EMF power with an analog signal (linear modulation), would allow the implementation of complex types of amplitude modulation. The frequency bandwidth of such a block can be

Table 3.1

Brand (Type) Technical		Output power, mW	Frequency range, MHz	Frequency accuracy, %	Modulation: internal imp.	external		
GS-120		0,5	200	1,5	+ — —			
	(GZ-37A)	0,6	1000	0,5	+			
G4-121			8200		+ —			
	(GZ-76A)	0,5	1000	0,01	+			
G4-128			3200		+ —			
G4-144			900	1	+			
GS-6			960	1,5	+			
GSS-12			1600		+			
GSS-15A			1600		+			
GSS-15B		0,5	2000		+			
		0,3	2600	1	+			
EMG-1274/2 (Hungary)		2	2600	1	+			
EMG-1275		2	2600	1	+			
DDR-541		5	3000	–	— — — ?			
		3	1700	–	— — — ?			
LMS-522		3	3200	–	– – – –			

determined by order of magnitude 10ÿ2 ÷ 104 Hz. At the same time, it should taken into account in a number of experiments the need for replacement in order to reducing the average radiation dose of the microwave field, varying according to linear law, pulse sequences with envelope
linear signal.

Indications of a significant dependence of the depth of development of the effect on the shape of the irritating signal (see, for example, [5]), on the other hand on the other hand, require the presentation of fairly stringent requirements for the linearity of the dependence of the generator output power level on the control signal. The undoubted presence, although quite smooth,
dependence of bioeffects on carrier frequency (see, for example, [212])
puts forward the requirement for the maximum possible width of the tuning range of such generators with the possibility of covering the entire area
minimum effect thresholds for small and medium-sized animals.

Typically, a biophysical experiment deals with objects whose cross-sectional area does not exceed several tens
square centimeters. Only in a limited number of experiments is it necessary to irradiate objects with a cross section of 0.5 m2. Since in this
In this case, the depth of the object is usually sufficient for absorption
almost the entire radiation power that penetrated inside the object,
It is advisable to limit the average power flux density of the irradiating field to 10 mW/cm2. This is necessary both to prevent the development of thermal overloads of the object [213], and from the point of
in terms of hygienic requirements for equipment, since the power reflected from the object, as a rule, is dissipated in the surrounding
space. If the irradiation device does not allow significant
power losses from the generator to the object, it is enough to require,
so that the maximum average power of the generator is 50 W.
For local irradiation, this value makes it possible to obtain an average power flux density (PPMD) over an area of about 100 cm2
up to 500 mW/cm2. Application of local irradiation of animal organs
fields with high intensity allows to reduce thermal
overload the body as a whole and get clearer results
in the experiment. In pulse mode, optimal can be considered
setting the pulse power level equal to the power in the mode
continuous generation. It is necessary to take into account that in certain experiments (for example, when studying the effect of radio sound)
the required pulse power can reach 500 W or more.
Even this brief analysis of the conditions for setting up a biophysical experiment allows us to determine the basic technical requirements,
which UHF generators must satisfy
in relation to studies of the effect of EMF on biological objects
ects:

1) frequency range 0.3 ÷ 1 GHz;
2) frequency stability - no worse than 0.1%;

3) maximum output power - not less than 50 W. Must the possibility of obtaining pulse power up to 500 W;

4) linear modulation of output power by an external signal with a modulation depth of at least 80% in the frequency band 0 ÷ 104 Hz;

5) nonlinear distortion coefficient - no more than 10%;

6) pulse repetition frequency - 0 ÷ 105 Hz;

7) pulse duration - 10ÿ6 ÷ 102 s.

3.2.2. Basic principles of constructing generator devices. The advanced technical requirements for generator sets UHF devices for setting up an experiment on effects of EMF on various biological structures and comparison these requirements with the technical data of serial devices of this the same class show that it is not fully satisfied at least at least one requirement is the need for a high level output power. The overwhelming number of generators do not provide fully or partially possible wide manipulation output power level. Parameters such as frequency range, stability and frequency setting error are in accordance with the technical requirements put forward. So Thus, the task of technical support, first of all, comes down to to two points:

— creation of powerful wide-range generators in the decimeter range;

— creation of broadband manipulators for linear and impulse control of generator output power.

Analysis of technical characteristics of laboratory measuring instruments microwave generators and medical devices for microwave therapy allows you to choose ways and principles for constructing UHF generators in research laboratories. Creation of the required generator devices in research conditions laboratories is most optimally carried out on the basis of elements of existing measuring generators of the required range. Below the developed designs of powerful microwave generators are described, for in which the most common types of measuring generators in the decimeter range are selected as basic models, and their technical data are given. Methods of linear and pulse modulation of microwave tube generators in a wide frequency range. The fundamental principles developed by the author are described. circuits of linear and pulse modulators and their characteristics.

It must be remembered that it is preferable to work at frequencies specially allocated for scientific research and specified in the relevant documents. These issues, as well as issues related to permissible radiation standards, are discussed below.

As already indicated, in laboratory practice the most common range generators are currently GS-6,

LMS-551, 522, 541, GSS-12, GSS-15, etc. These generators use metal-ceramic lamps (MCL) of types GI-11B, GI-12B, which, in order to increase their service life, are used in the mode reduced anode voltage and anode current [214]. According to their own passport data for these lamps when choosing a higher voltage the anode supply (and accordingly the anode current) can be supplied to the load in the considered range up to 35-40 W of continuous power and up to 100 W per pulse, which is very close to the required parameters. Therefore, modification of the power supply in the specified generators at the same time with a slight increase in the connection between the grid and anode circuits allows, in principle, to solve the problem of obtaining from them the required power.

The question of the required amount of output power can be considered, on the one hand, based on the possibilities of obtaining it on existing basic models of microwave generators, on the other hand, from the point of view of ensuring a field with maximum uniformity on an area determined by the transverse dimensions of objects. Wherein it is necessary to take into account that the PPM average for most objects is not leading to their heating, ranges from 10 ÷ 100 mW/cm2. The above generators cover the wavelength range from 10 up to 200 cm with smooth frequency adjustment, output power for certain types of generators it reaches 3 W. Detailed description, technical characteristics of these generators and circuit diagrams (except for the LMS series) are given in [194, 195]. As already indicated, Using standard MCLs, the output power of generators of the indicated types can be increased by an order of magnitude or more, mainly for by increasing the anode voltage and current of the SCL. Replacing the standard one An MCL with a more powerful one, for example GI-6B, GI-7B, opens up the possibility of increasing the output power by two orders of magnitude or higher. In view of the fact that the installation dimensions of the GI-7B and GI-6B lamps are larger than for GI-11B and GI-12B lamps, it is necessary to introduce changes to the resonator system of the generator, which, naturally, complicates and increases the cost design. Thus, two ways to increase generator output power:

— increase in anode voltage and anode current of a standard MCL and the degree of positive feedback;

— replacement of the standard SCL with a more powerful one and modification of the structural elements of the resonator system.

The limitation in this case is imposed on the value of the anode voltage of the generator lamp, which should not exceed maximum permissible values for a locked lamp (for GI-12B - 0.8 kV, for GI-7B - 2 kV). One of the points that contributes to increasing the output power of the generator, serves as removal from the circuits anode or cathode of MCL current-limiting resistors or introduction into one of these rheostat circuits with its output to the front panel generator So, for example, in generators of types GS-6, GSS-12 in the circuit

MCL cathode (standard version) has a resistor connected to it
Voltage is simultaneously released to control the MCL current
external signal [194].

Practice (see below) has shown that the design of sliding
and crimp contacts, used in serial generators, remains
acceptable up to a load power of about 200 W in continuous
and up to 500 W in pulse mode.

3.3. Modulating devices

As already noted, at this stage of research there arises
the need to modulate microwave generators with linear and pulsed
signal. It is obvious that the creation of a single universal
devices for modulation could hardly be considered appropriate. At the same
time, various solutions for resonator designs
microwave generator systems, methods of supplying power to MCL electrodes
allow modulation modes to be implemented for each
type of microwave generator based on unified principles for constructing
modulating devices. There are two main types of microwave generators on
MCL:

— generators with a grounded SCL cathode;
— generators with an insulated SCL cathode.

In the first case, manipulation of the generator output power
is possible only in the anode circuit of the SCL, in the second - both in the anode circuit and
and in the cathode circuit. The choice of a particular modulator is also determined
parameters of the modulating signal, primarily its frequency
characteristic. One of the simplest methods of linear anode modulation is to
include a generator lamp in the anode circuit
controlled by an external signal of variable resistance, which can be an electron vacuum tube.
Basic
the difficulty in this case will be the “decoupling” of control circuits from
changing in time with the modulating high voltage signal
on the anode of the generator lamp.

One of the main requirements for the linear modulation mode is to ensure
a modulation depth close to
to 100%. In turn, the presence of almost 100% modulation depth
imposes very strict requirements when choosing a manager
element, or more precisely, the requirements for the modulation characteristics
of the control element. It is appropriate to say a few things here
words about modulation of microwave generators using magnetrons. These devices
designed primarily for operation in pulse mode
modulation with short pulses or in continuous generation mode with a
correspondingly reduced output power. Linear modulation in continuous
magnetrons is possible at
a small section of the current-voltage characteristic of the magnetron, determined

divided by the quantities Uapore and Uarab , and Uapor = (0.7 ÷ 0.8) · Uarab . This means that in this case the possible modulation depth is not exceeds 20% [215]. Let us use some considerations to assessments of the quality of reproduction of the modulating signal given in [215]. For this purpose, dynamic and static modulation characteristics are used. Dynamic characteristics represent dependence of the modulation coefficient on the magnitude of the modulating voltage m = ÿ(Uÿ), their nature does not depend on the type of implementation modulation. Static modulation characteristics for tube generators represent the dependence of the amplitude of the first harmonic anode current Ian and current in the circuit Ik on the magnitude of the changing voltage for this type of modulation. Using static modulation characteristics, it is possible to determine the current values for the carrier frequency and maximum power modes, the permissible undistorted modulation coefficient in the linear section modulation characteristics m = ÿia/Ian and the required amplitude modulating voltage Uÿ. Convenient introduce the concept of static modulation characteristics and power modulation coefficient as a ratio

$$mp = ÿP/Pÿ,$$

where ÿP is the power increment, Pÿ is power in carrier frequency mode. In this case, static modulation the characteristic represents the dependence of the change in oscillatory power in the load on the magnitude of the changing when modulating voltage.

In Fig. 3.11 presents static power modulation characteristic for anode modulation of the generator Microwave. For linear (undistorted) modulation, the course of this characteristic should correspond to the quadratic law - the curve must correspond to a parabola, since P ÿ I2. The relationship between the coefficients volume of modulation by power and current or voltage is given by:

$$mp = \frac{ÿP}{Pÿ} = \frac{0{,}5ÿI2\ aRa}{0.5IaÿRa} = \frac{ÿI2_a}{I2_{Tuning}} = m2$$

or

$$m = ÿ\overline{mp}\ .$$

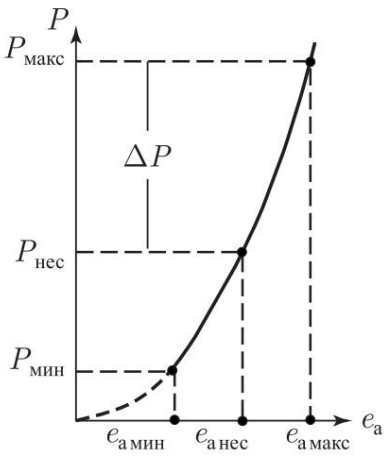

Rice. 3.11. Static mo- power dulation characteristic for anode modulation of the microwave generator (along the absolute axis ciss deferred values voltages, along the ordinate axis - power values ness). ea carried - voltage in carrier mode; ea max, ea min - maximum noe and minimum value voltage; Pnes - power in carrier mode; Pmax, Pmin - max maximum and minimum power values; ÿP — power increment

From here it is easy to determine the maximum permissible coefficient undistorted modulation according to the characteristics taken for the generator Microwave. Thus, the control element must have a large linear section on the control characteristic.

3.3.1. Linear modulators. Consideration of circuits of linear mo- Let's start with the simplest dulators, described in [215].

Linear modulator without conversion using an electronic vacuum tube. The circuit of a linear modulator without converting the modulating signal is shown in Fig. 3.12. Control operating point

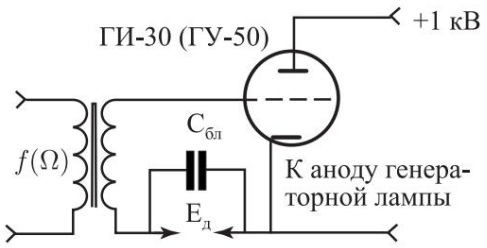

Rice. 3.12. Linear modulator without modulating signal conversion

element is installed using a bias source E Using a low-frequency transformer, the control circuit is "decoupled" from the high anode voltage of the generator lamps. Can be used as a control element modulator tetrode GI-30 or pentode GU-50. These lamps have high electrical strength, sufficient dissipation power on the anodes. At an anode supply voltage of 1 kV, the value bias source voltage is about ÿ60 V, the amplitude of the modulating signal on the lamp grids is about 120 V. The measured nonlinear distortion factor is 10%, the bandwidth when using conventional low-frequency lamp transformers radio receivers lie in the audio range. At the same time, secondary The transformer winding serves as the input winding. The voltage drop across fully unlocked control lamps is 120 ÷ 150 V. Thus Thus, using a low-frequency transformer as The separating element does not allow modulation with an infra-low-frequency signal.

Linear modulator with signal conversion using electron vacuum tubes. Expansion of the modulation band towards infra-low frequencies can be achieved by transferring the modulating signal at a subcarrier frequency and then separating it in the control circuit of the control element using an amplitude detector. In this case, there is a need for preliminary linear modulation of the subcarrier frequency generator signal. So Thus, the external signal is amplified and fed to a submodulator, which modulates the amplitude of the signal of the subcarrier frequency generator, which is fed to a passive amplitude detector, inductively coupled

List of components for a linear modulator with a subcarrier

Resistors:

R1 — 330 k
R2 - 510 k, 0.5 W
R3 - 470.1 W
R4 - 560, 0.5 W
R5 - 150 k
R6 — 150 ÿ
R7 — 510 ÿ
R8 - 1 k, 0.25 W
R9 - 1.0, 0.5 W
R10 - 22 k
R11 - 150 k
R12 - 910 k, 0.5 W
R13 - 47 k, 4 W
R14 - 11 k
R15 - 47 k, 1 W
R16 - 47 k, 4 W
R17 - 22 k, 0.5 W
R18 - 470, 2 W
R19, R20 - 510 k, 0.25 W
R21 - 510 k, 0.5 W
R22 - 510 k
R23 - 8.2 k, 0.5 W
R24 - 5.1 k, 0.5 W
R25 - 10 k
R26 - 100 k, 0.5 W
R27 - 10 k
R28 - 15 k, 0.5 W
R29, R30 — 100
R31, R32 - 20 k, 2 W
R33–R35 - 20 k

Lamps:

V1 — 6H2P
V2 — 6ÿ3ÿ
V3 — 6P14P
V4 — 6C6B
V5 — GI-30
V6 — GI-30

Capacitors:

C1 — K50 —12
C2 — 20.0 100 KE-1
C3 — 0.05 KBG-I
C4 — 30 KTK
C5 — 6 —25 PDA-2
C6 — 24 KTK
C7 — 39 KTK
C8 — 60 TSI
C9 - 6 -25 KPK-2
C10 — 2700 MBM
C11 — 0.1 MBM
C12–C13 — 0.05 MBM
C14 — 100 TSI
C15 — 2.0 × 100 KE-1

Diodes:

V7–V9 — D2ÿ
V10 — D226 V

connected with a resonant amplifier circuit. In Fig. 3.13 is given
schematic diagram of a linear modulator with transfer of a modulating signal at
a subcarrier frequency. To provide
the greatest modulation depth possible is necessary so that the generator
subcarrier frequency worked in soft excitation mode. The linear modulator uses
a three-point generator with an inductive
connection (the right half of lamp V2 according to the diagram). On the left (according to the diagram)
Half of the V2 lamp is assembled with a submodulator according to the
absorption circuit. The modulating signal, amplified in cascade on the V1 lamp, is fed to
submodulator control grid. At the same time, depending on am-

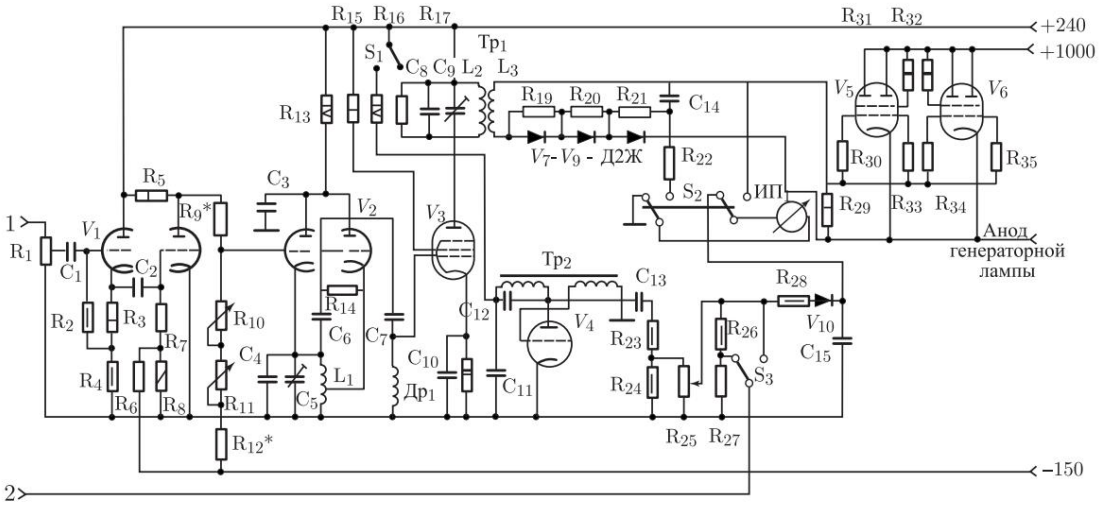

Rice. 3.13. Schematic diagram of a linear modulator with modulating signal transfer at a subcarrier frequency

amplitude of the modulating signal, the pass resistance of the lamp changes, which leads to proportional shunting of the L1C4C5 circuit of the subcarrier generator and to the same change in the amplitude of oscillations of the subcarrier frequency. In Fig. 3.14 shows the family

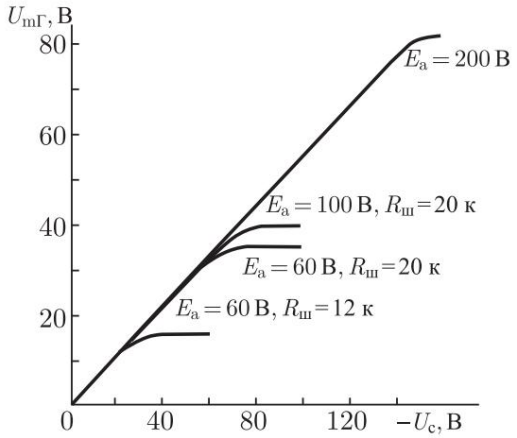

Rice. 3.14. A family of static modulation characteristics of a linear modulator's subcarrier frequency generator. The abscissa axis shows the voltage values on the control grid of the modulator tube, the ordinate axis shows the voltage amplitude on the subcarrier generator circuit

modulation characteristics of the subcarrier frequency generator. As can be seen from the graphs, this simple modulation method allows you to obtain a modulation depth of up to 97–99% with high linearity of the modulation characteristic. The modulated subcarrier signal is amplified by a resonant amplifier on tube V3 and isolated in circuit L2C8C9. The inductance L2 of the resonant amplifier circuit and the coupling inductance L3 form a high-frequency isolation transformer.

In the developed modulator, the subcarrier frequency is 7.5 MHz. For convenience, the modulator is supplemented with a calibrator on a V4 lamp.

The modulator bandwidth from below is determined by the constants time of the amplifier circuits and is 0.05 Hz, on top - by the type of lamps, installation capacitance, connecting cable capacitance and capacitance relative to the housing of the power transformer feeding the lamp filaments GI-30. In this modulator circuit, the maximum frequency of the amplified signal at level 0.7 is equal to 104 Hz. Generator circuit coil L1 subcarrier is wound on a frame with a diameter of 30 mm and a length of 50 mm with a forced pitch of 1 mm, number of turns 18, tap from the 7th turn, counting from the grounded end, wire PEV-0.8. Circuit coil L2 resonant amplifier is wound on the same frame, number of turns 12, wire PEV-0.8. Communication coil L3 is wound on a frame with a diameter of 38 mm long 54 mm wire PEV-0.8 and put on the coil frame resonant amplifier circuit. High frequency choke wound on a frame with a diameter of 11 mm, a length of 14 mm, wire PEV-0.16.

Pulse modulators. When developing the ones discussed below pulse modulators, the task was to create extremely simple and cheap devices that provide pulse modulation microwave generators within a wide range and available for repetition in research laboratories. At the same time, these The devices were subject to all the requirements that are usually presented when developing serial equipment. The traditional principles and circuit solutions of pulse modulation used in magnetron generators are not considered here - these are devices with strictly fixed modulation parameters or, at best, with their variation within very narrow limits. These devices are enough widely described in numerous literature.

Cathode pulse switch. In microwave generators operating on MCL and having an insulated cathode output MCL, most simply carry out pulse modulation by introducing a cathode into the circuit transistor switch. The initial locked state of the MCL is ensured by applying a positive locking voltage to the cathode.

If the overall power of the standard power transformer is sufficient, this voltage can be obtained using a divider connected to the anode power source circuit. Otherwise In this case, you will need to install an additional power source.

In Fig. Figure 3.15 shows a schematic diagram of a pulse transistor switch in relation to microwave generators that have an insulated cathode of the generator lamp, with a voltage at the anode of the MCL up to 1 kV.

In Fig. 3.16 shows a schematic diagram of a powerful pulse modulator in relation to microwave generators with voltage at the anode MCL up to 2 kV. It should be noted that with such delivery methods voltage to the transistor collector, the saturation voltage of the unlocked transistor exceeds the rated value and leads to a decrease pulse power. Power conservation possible when powered

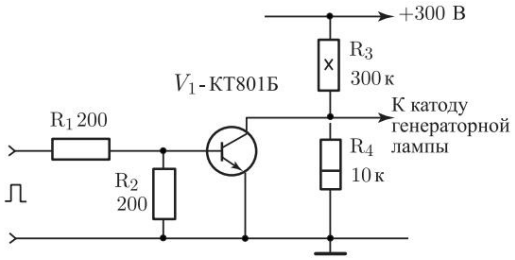

Rice. 3.15. Wideband Pulse Cathode Modulator

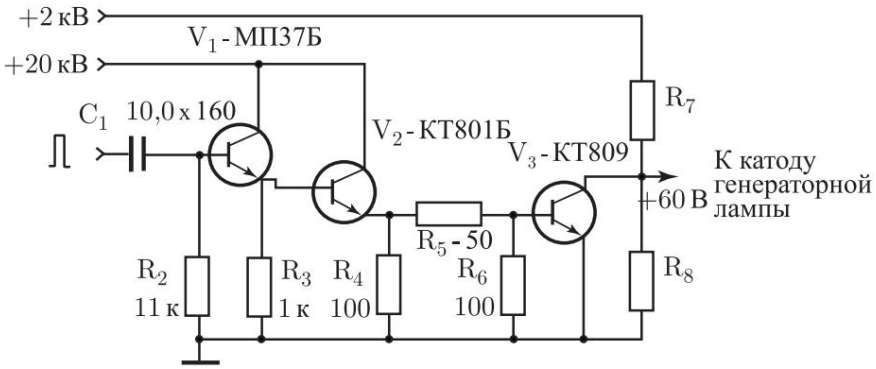

Rice. 3.16. Powerful broadband pulse cathode modulator

MCL cathode and transistor switch from a separate power source with a current that provides the rated value of the saturation voltage this type of transistor. Developed transistor pulse modulators provide modulation by pulses with a repetition frequency of 0 ÷ 105 Hz with a pulse duration of up to 5 10ÿ6 s. Maximum The pulse duration is determined by the permissible power scattering on the transistor and the time constant of the input circuit. The amplitude of the input pulses is 2 ÷ 3 V.

Anode pulse switch. In microwave generators that do not have isolated output of the MCL cathode, it is possible to carry out a pulse modulation in the anode circuit. The simplest anode pulse circuit a normally closed transistor switch can serve as a modulator, connected in series to the power supply circuit of the MCL anode. In Fig. 3.17 A diagram of an anode pulse modulator is given. Low frequency the isolation transformer is assembled on a core made of ÿ 15 plates, package thickness 18 mm. The primary winding contains 500 turns of PEV-0.16 wire, the secondary winding contains 50 turns of PEV-0.5 wire. For the type of transistor used, the maximum permissible source voltage anode supply is 1 kV. The modulator provides current in a pulse up to 1 A at any duty cycle. Pulse repetition frequency - 0 ÷ 105 Hz, pulse duration - 10ÿ3 ÷ 5 10ÿ6 s . If you need to work with pulses of a different duration, you need to change transformer inductance. The area of the transistor radiator is about 100 cm2.

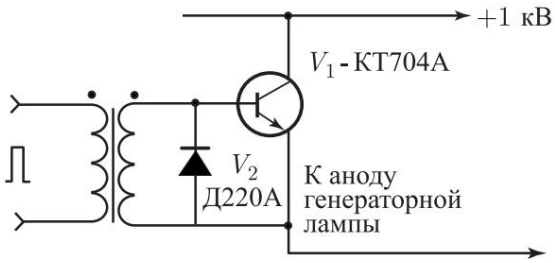

Rice. 3.17. Wideband anode pulse modulator with voltage at the anode of a metal-ceramic lamp up to 1 kV

Experience with pulse modulators has shown that in order to ensure modulation by short pulses with steep edges, it is advisable to locate these devices inside the housing of the microwave generator, and choose the minimum length of wires in the switching circuits.

3.4. Tube microwave generators for the frequency range 150 ÷ 1600 MHz with wideband modulation

The requirements discussed above for modulated microwave generators used in biophysical experiments allow us to divide the class of these devices into two subclasses: - with a pulse power of up to 50 W; - with pulse power up to 500 W. This division is conditional, but it allows you to navigate in determining the scope of work when developing a generator to obtain the required power.

In microwave generators of the GS-6, GSS-12, LMS-551 and LMS-541 types, an increase in output power is mainly achieved by increasing the supply voltage of the MCL anode. The permissible anode voltage for the GI-12B type lamps used in these generators is 0.8 kV, which can be obtained by modifying the standard electronic stabilizer (in the LMS-551 type generator - by modifying the rectifier). By increasing the anode voltage in these generators, the output power can be increased to 20 ÷ 30 W. A further increase in the power of generators of the GS-6 and GSS-12 types is possible both in pulsed mode and in continuous generation mode by increasing the anode current of the MCL. Generators of both types have a DC-isolated output of the MCL cathode, the circuit of which includes a resistance for switching the output power and limiting the anode current [205]. In pulse modulation mode, this resistance is replaced by the switch resistance (infinity - zero), which allows you to obtain pulse power at individual points in the frequency range up to 80 W. In this case, the pulse current of the MCL is within 200 mA,

MCL blocking voltage is ÿ(+14) V, minimum pulse duration is about 10ÿ6 s.
Generator with output power up to 500 W
in pulse developed on the basis of one of the LMS series microwave generators overlapping wavelength range 30 ÷ 100 cm. The main point in this design is the translation of the oscillatory system
generator to a lamp type GI-7B, delivering to the load in continuous mode, oscillatory power up to 200 W (forced mode).
Below are specific diagrams of the developed microwave generators.

3.4.1. The base model is GS-6. Laboratory measuring
generator type GS-6 covers the range of 33 ÷ 200 cm in length
waves and develops maximum power at a 75-ohm load
3 W. Structurally, the GS-6 generator is distinguished by an isolated output of the generator lamp cathode in order to ensure the possibility modulation. At the same time, the cathode of the GI-12B generator lamp includes current limiting resistance. The anode supply is stabilized. Increasing generator power includes replacing the lamp
on GI-11B, increasing the anode supply to 800 V by completely
unlocking the stabilizer pass-through lamp using the regulating resistance and removal of current-limiting resistance in the cathode circuit when operating in pulse mode. Changes made
allow you to obtain an output power per pulse of up to 80 W and up to 24 W continuous operation. If the generator must
time to use in continuous generation mode, it is necessary to install a fan to cool the lamp or limit
lower output power. The standard modulator is assembled on a lamp 6P3S, the cathode of which includes resistances R9 and R10, as well as shunt resistance R12 (hereinafter [194]). Eye-catching
at these resistances the signal is applied to the cathode of the generator lamp. Thus, the GS-6 generator carries out a grid pulse modulation. In the absence of an alternating signal at resistors R9 and R10, due to the flow of the anode current of the 6P3S lamp, a constant positive potential is released, which closes the generator lamp, thereby preventing generation from occurring. Preservation of this modulator circuit would be possible if it were not required increase in power, which in this case is possible due to
decreasing the value of resistances R9 and R10. However, this led would lead to an increase in the anode current of the modulation lamp and its exit from building. Thus, the modulator must provide maximum possible pulse current and reliable locking of the generator lamp in pause. An electronic circuit was chosen as such a modulator.
transistor switch shown in Fig. 3.15. In order to increase
input resistance of the pulse modulator input signal to
the transistor switch is fed through a lamp installed on the standard panel. The complete circuit of the pulse modulator of the GS-6 generator is shown in Fig. 3.18. In position “1” of switch P1 from the divider R4R5 a positive voltage is applied to the cathode of the generator lamp

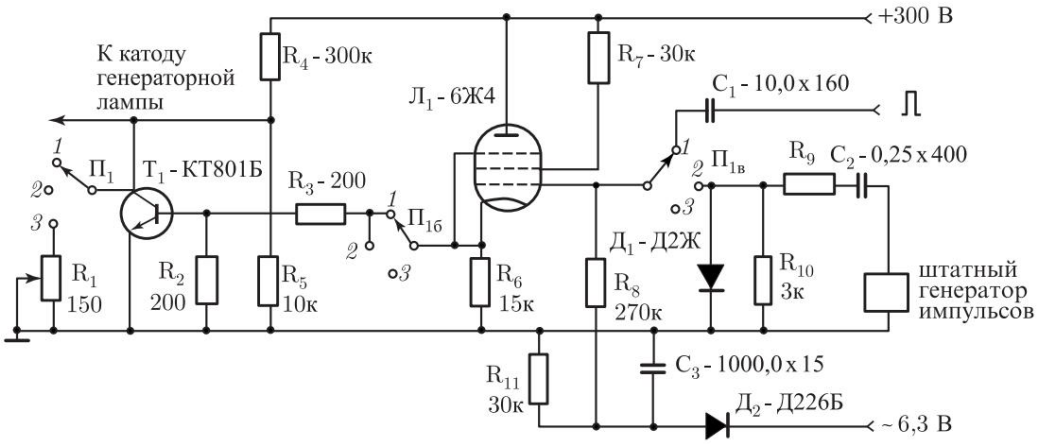

Rice. 3.18. Schematic diagram of a broadband pulse cathode microwave generator modulator, developed on the basis of the GS-6 laboratory measuring generator

voltage of about 10 V - the lamp is locked and microwave oscillations are generated absent. The 6P3S lamp was replaced with a 6Zh4 lamp. In the initial state, the lamp is locked along the first grid with negative voltage, removed from the rectifier connected to the filament winding. Entrance capacitive modulator. When a positive pulse is applied to the input polarity, the modulator lamp is unlocked, the potential at the cathode increases, transistor T1, unlocking, bypasses the divider R4R5, and the generator the lamp unlocks. In this case, a microwave radio pulse is generated. In position “2” of switch P1, a standard pulse generator is connected to the lamp input. The switch used in the modulator is regular Into the circuit of a standard output power meter a resistance of the order of several tens of kilo-ohms is switched on in series. The device is installed on the front panel of the generator for monitoring the anode current of the generator lamp. The duration of the modulating pulses is 5 · 10ÿ6 ÷ 5 · 10ÿ3 s. Position “3” of switch P1 is used to ensure continuous generation mode. In this case, resistance R12 is connected to the cathode of the generator lamp, which was shunted by resistances R9 and R10. After replacing the modulator (resistance R1 in Fig. 3.18), the value of this resistance is reduced and designed as an additional organ control with its placement on the front panel of the generator. This measure allows you to control the anode current of the generator lamps, and therefore the output power of the generator in mode continuous generation. In order to expand the possibilities of manipulating microwave power, connector (similar to those available on LMS series generators) and toggle switch to connect the linear modulator described above. At frequency pulse repetitions up to 40 kHz modulation depth is maintained for level 100%.

3.4.2. The base model is GSS-12. The GSS-12 type generator covers the range of 30 ÷ 100 cm in wavelengths and makes it possible to obtain
75-ohm load power up to 1 W. Qualitatively, the design of the resonator system is similar to that for the GS-6 generator. Circuit
solutions for individual components of the GSS-12 generator differ in many ways parameters from the GS-6 generator units. Therefore, the amount of refinement of this the generator is significantly larger. The operation of previously modified generators has shown that a generator with a linear modulator located within the generator is safer and more convenient. Therefore, in volume
The work included the development of a linear modulator mounted inside the casing. In addition, the GSS-12 generator was the first
which allowed for both local and remote
control from a separate remote control. New development required
components such as stabilizer, rectifier, power meter.
System for switching irradiation modes and ensuring the possibility
remote control required the introduction of additional controls. Electronic protection has been introduced in the GSS-12 generator
MCL for current. The developed generator allows for four modes of irradiation of objects: 1) continuous generation mode,
2) linear modulation mode, 3) pulse modulation mode, 4) linear-pulse modulation mode.

The development of a microwave generator based on the GSS-12 generator includes the following positions:

1) replacement of the generator lamp;
2) installation of a fan for blowing the radiator of the generator room lamps;
3) installation of a generator lamp radiator;
4) introduction of a broadband linear modulator with transfer
frequency of the modulating signal at the subcarrier frequency into the anode circuit generator lamp;
5) introduction of a broadband pulse modulator into the cathode circuit yes generator lamp;
6) introduction of a smooth auto-bias regulator into the cathode circuit of the generator lamp;
7) introduction of smooth regulation of the generator anode current lamps;
8) introduction of relay switching of the anode voltage of the generator lamp;
9) introduction of electronic current protection for the generator lamp with start-stop mode;
10) switching of the anode voltage stabilizer of the generator lamps in order to obtain a forced mode;
11) replacing selenium rectifier columns with diodes;
12) setting the device control switch from local to remote;
13) installation of a generator lamp anode current device;

14) installation of a reversible engine RD-09 to control the connection of the generator resonator with the load both at local and remote control;

15) elimination of the DC bridge in the output meter power;

16) installation of a connector for monitoring the shape of the field envelope;

17) the device is equipped with a remote control.

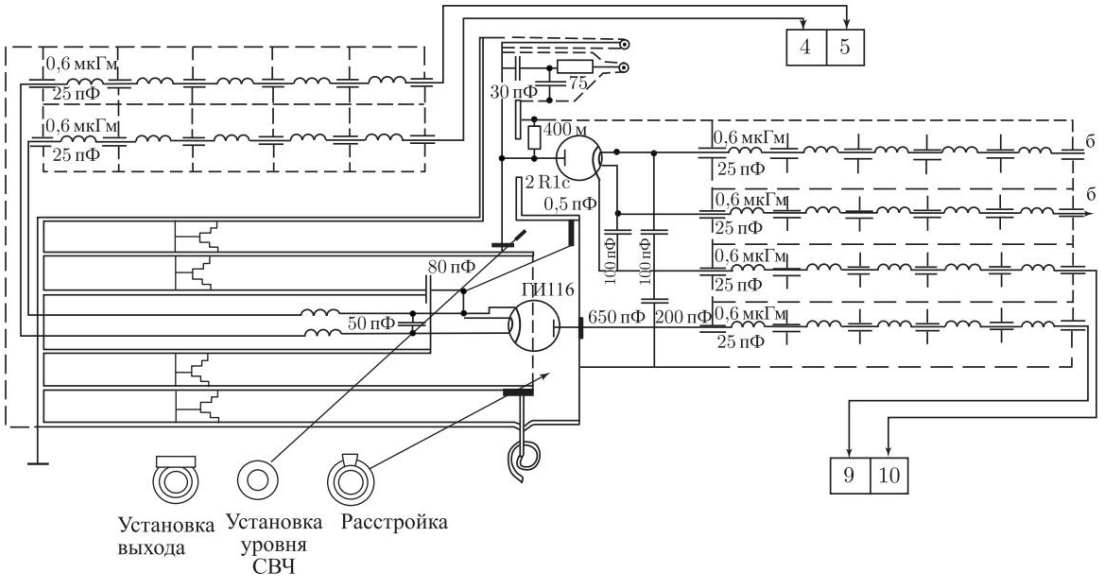

Rice. 3.19. Schematic diagram of a microwave generator developed on the basis laboratory measuring generator GSS-12 *(a–g):* a) - self-oscillator Microwave; b) — power supply; c) - pulse modulator; d) - stabilizer tension; e) — operating mode switch; e) - linear modulator; g) — remote control (RC)

a) Autogenerator microwave

Technical characteristics of the developed microwave generator:

Operating frequency range 0.15 ÷ 1.0 GHz.

Linear frequency range modulating signal Modulation depth 5 10ÿ2 ÷ 104 Hz . 95 ÷ 97%.

Parameters of the pulse modulating signal:

a) pulse duration b) pulse repetition frequency 10ÿ1 ÷ 10ÿ5 s, up to 5 · 104 Hz.

Output power at a load of 75 Ohms:

a) in continuous generation mode b) in pulse modulation mode up to 30 W, up to 50 W.

The indicated output power values correspond to the forced mode with the anode voltage stabilizer turned off

Modulating signal amplitude:

a) in linear modulation mode b) in pulse modulation mode 0.3 V, 8 V.

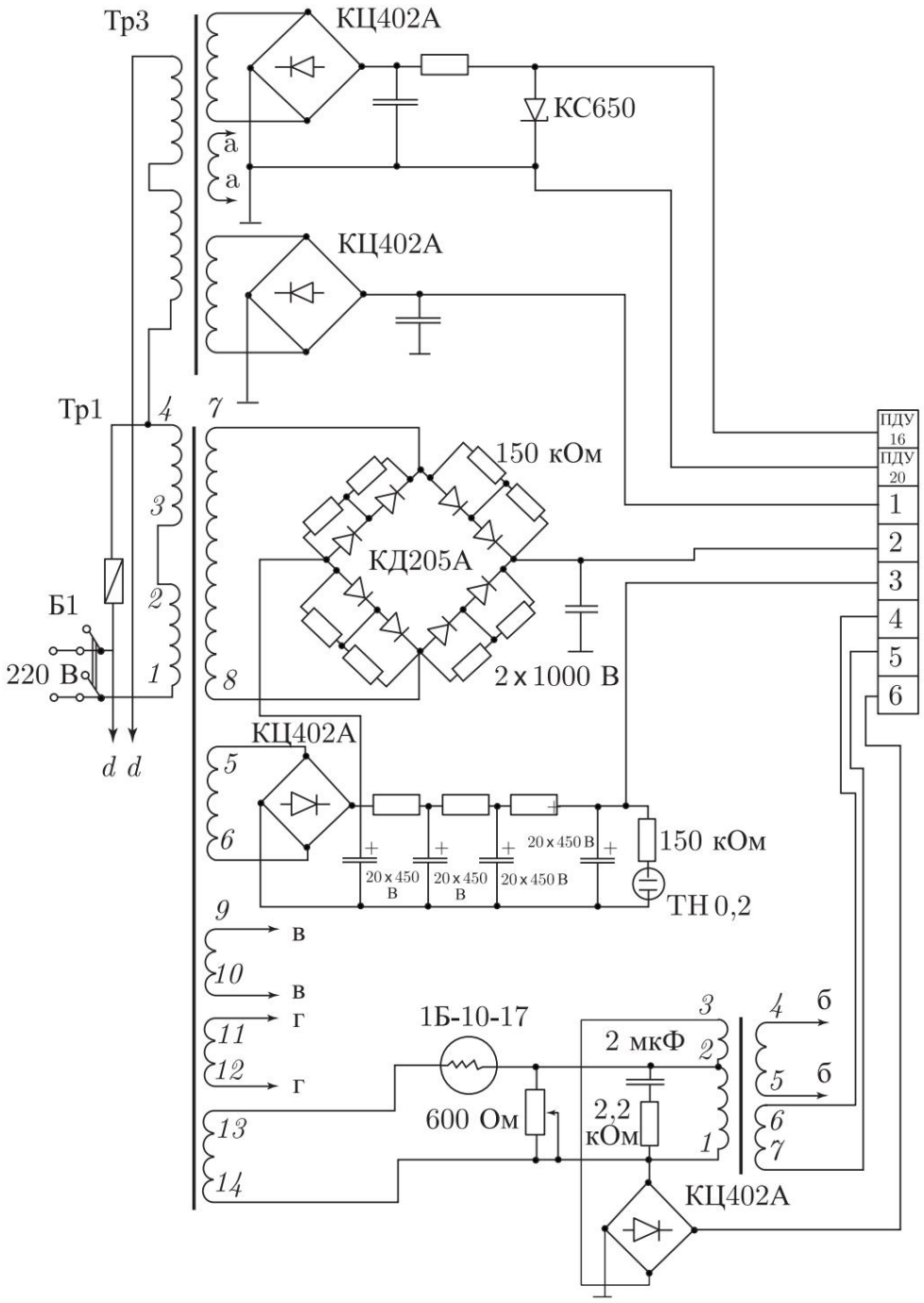

b) Power supply

Complete circuit diagram of a generator-based microwave generator GSS-12 shown in fig. 3.19.

3.4.3. The basic model is GSS-15 A. The GSS-15A type generator (new designation G4-8) covers the range of 1.0 ÷ 1.6 GHz and allows you to get up to 1 W of power at a 75 Ohm load in the standard version. The generator is assembled on a GI-12B lamp according to a circuit with a grounded grid and an insulated cathode. Scope of work - increasing output

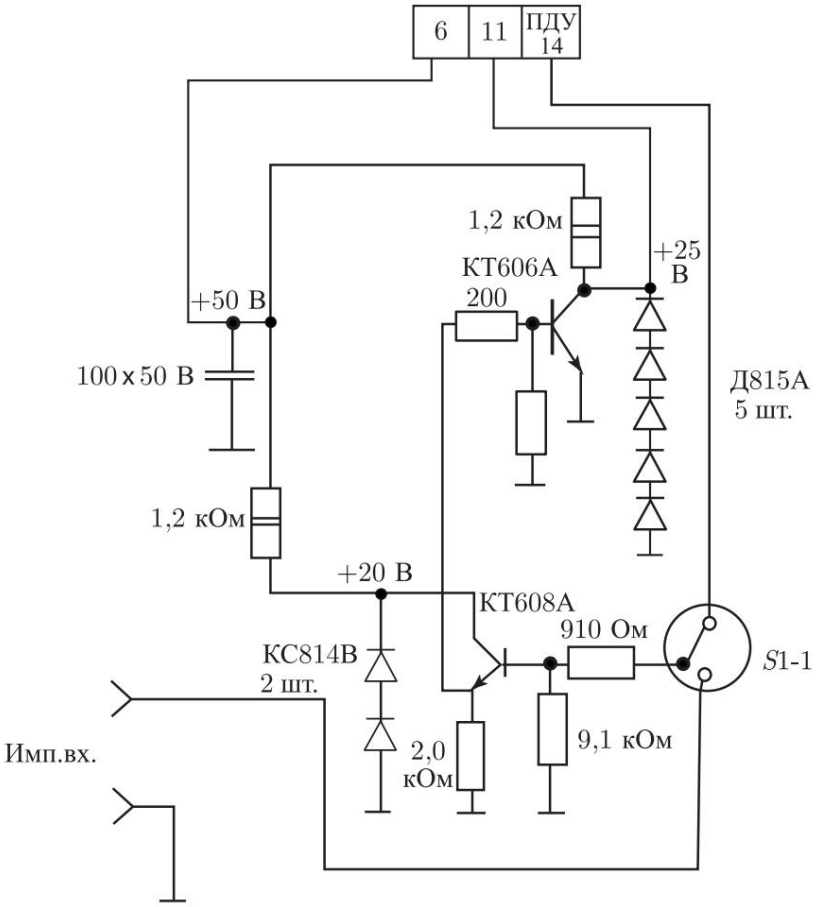

c) Pulse modulator

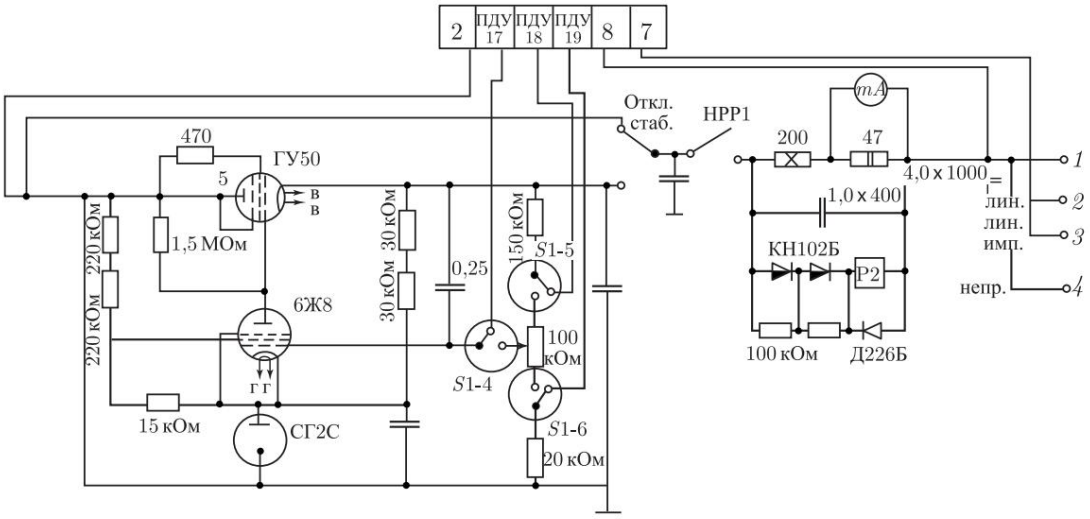

d) Voltage stabilizer

high power of the generator, providing pulsed and continuous operating modes, local and remote control of the generator, ensuring protection of the main components of the generator and the thermal regime of the generator MCL. In order to avoid duplication of management bodies,

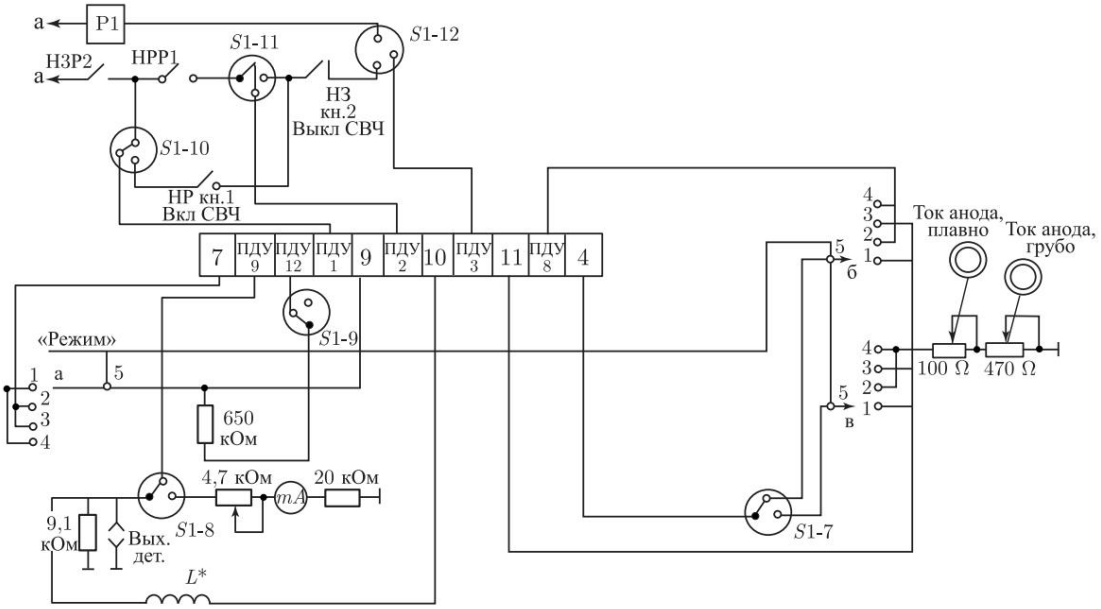

e) Operating mode switch

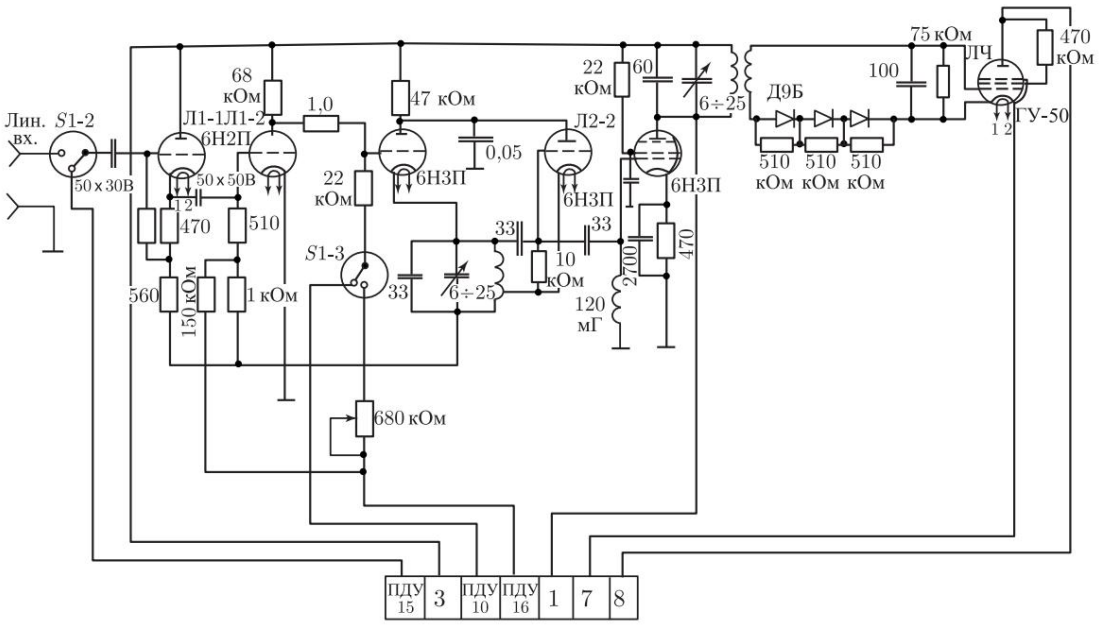

e) Linear modulator

In addition (as is done in the GSS-12 model), some of the controls are located directly on the remote control. For local control, the remote control is connected to the generator with a short (1 m) cable; for remote control, a longer cable is used.

The scope of work for modification includes the following items: 1) removal of all units and systems of standard design, except for transformers and the resonant system;

2) installation of a fan for blowing the generator MCL; 3) manufacturing a new power supply;

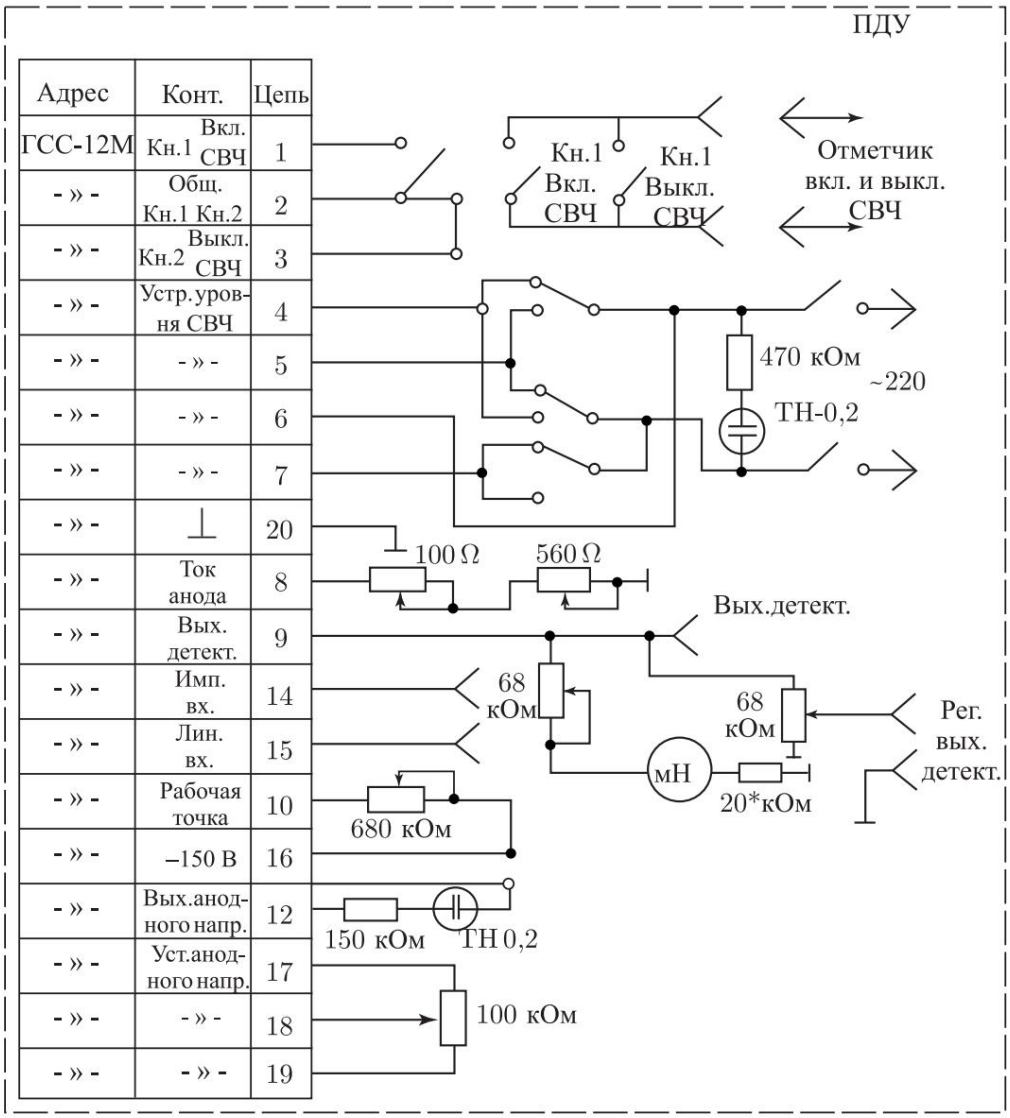

g) Remote control (RC)

4) Installation of the radiator on the MCL anode with a groove in the bottom of the radiator;
5) installation of a pulse modulator in the cathode circuit of the MCL;
6) installation of a smooth power regulator in the MCL cathode circuit;
7) installation of relay switching of the anode voltage of the MCL;
8) installation of a thermal protection unit with start-stop mode;
9) complete set of remote control generator.

Completing the specified scope of work will ensure the following technical characteristics of the device:

Operating frequency range 1.0 ÷ 1.6 GHz.

Pulse modulation mode:

a) pulse duration b) pulse repetition frequency 1 ÷ 10ÿ5 s, 0 ÷ 2 104 Hz .

Output power at a load of 75 Ohms:

a) in continuous generation mode 10 W,

b) in pulse modulation mode, 18 W per pulse.

The amplitude of the modulating signal is 2 ÷ 4 V.

Power supply 220 V, 50 Hz.

MKL ventilation system using a VN-2 fan shown in Fig. 3.20. The schematic diagram of the developed microwave generator is shown in Fig. 3.21.

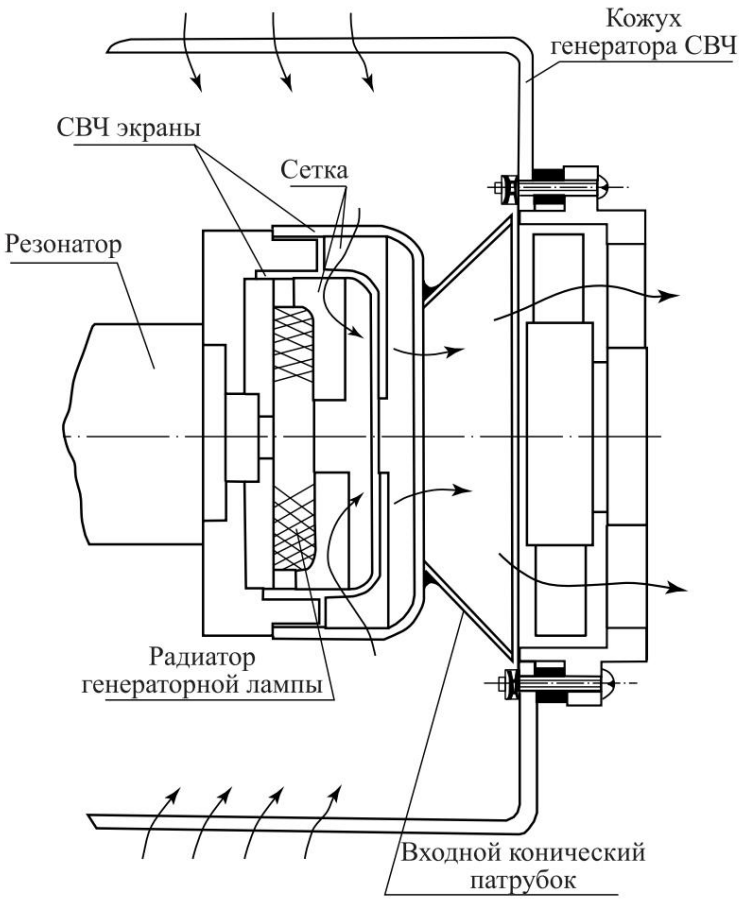

Rice. 3.20. Cooling system for a generator lamp in a microwave generator, developed on the basis of a laboratory measuring generator GSS-15A

As a note, it can be noted that with individual copies of GI-11B lamps it was possible to obtain a power almost twice as high as that indicated here.

3.4.4. Generators of the LMS series. Three generators of this series The wavelength range 9 ÷ 100 cm smoothly overlaps. The output power at a 75-ohm load at certain points in the range reaches magnitude 5 W. Without changing the design of the resonator system pulse modulation on the SCL grid is not possible (except for the model LMS-522, wavelength range 9 ÷ 16 cm). Power supply for MCL generators series LMS is carried out from a rectifier assembled according to a full-wave circuit, the anode voltage is in the range of 400 ÷ 1200 V.

In its standard version, the rectifier provides a current of up to 100 mA.

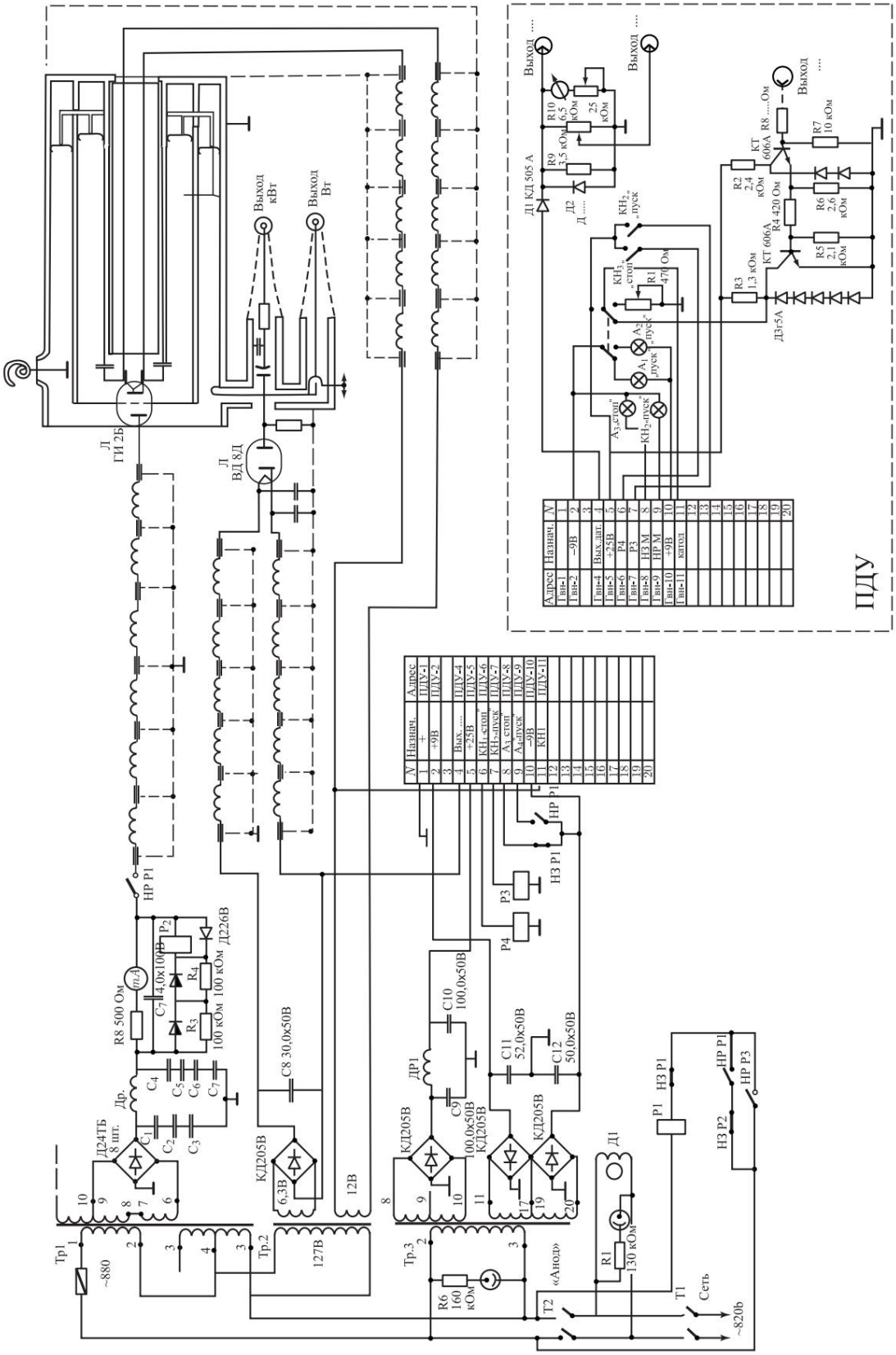

Rice. 3.21. Schematic diagram of a microwave generator developed on the basis of the GSS-15A laboratory measuring generator

The basic model is LMS-541. The scope of work to finalize this model is primarily associated with an increase in source voltage anode power supply of MCL and installation of a powerful fan for blowing MCL. These measures are necessary to increase power output.
An increase in the supply voltage of the MCL anode is achieved by changing the rectifier circuit from full-wave to bridge, which allows you to get up to 850 V at the SCL anode. When modifying the block power supply, it is necessary to replace heated kenotrons with semiconductor diodes. The LMS-541 generator has a dual-circuit resonator system with separate adjustment of the anode-grid and cathode-grid circuits. Therefore, the possibility of landing the anode radiator SCL is excluded and with increased power it is necessary to install a more efficient fan. For a new fan a commutator DC motor MA-40A was used on voltage 24 V at current 2 A. When powering the motor with voltage 15 The number of revolutions per minute of the fan impeller is about 5000. The engine is powered from a separate rectifier mounted on the generator chassis. In Fig. 3.22 shows the design a fan that ensures normal thermal conditions of the MKL.

In continuous mode at a voltage at the MCL anode of 600 V, the output power of the generator was 25 ± 2 W over the entire range (18 ÷ 33 cm). In pulse mode with voltage at the anode of the MCL 800 V pulse power reaches 40 W. Baseband signal in linear modulation mode - 10 kHz with a modulation depth of up to 95% using an external linear modulator with transfer of a modulating signal on a subcarrier, in a pulsed mode - 100 kHz, using a pulse anode switch minimum pulse duration 10 μs. If necessary implementation of shorter pulses and linear-pulse mode modulation requires modification of the cathode-grid circuit in order to insulation of the MCL cathode for direct current.

The basic model is LMS-551. Modification of the generator includes increasing the anode voltage of the SCL to 800 V by transferring the full-wave rectifier circuit to the bridge circuit, replacing the heating kenotrons on semiconductor diodes. In this model, the anode is SCL The standard version is equipped with a radiator. The MCL is blown high-performance fan. In continuous generation mode and in pulsed mode, the achieved power is 36 W per load 75 Ohm. The use of an external linear modulator with transfer of the modulating signal on the subcarrier provides the bandwidth modulation within 5 10ÿ2 ÷ 104 Hz with modulation depth up to 95%. In pulse modulation mode in the anode circuit, the minimum pulse duration - 25 ÿs.

The base model is LMS-551 V. In the generators described above, the maximum possible output power has been achieved, which The GI-11B lamp [214] is capable of outputting with this power supply method.

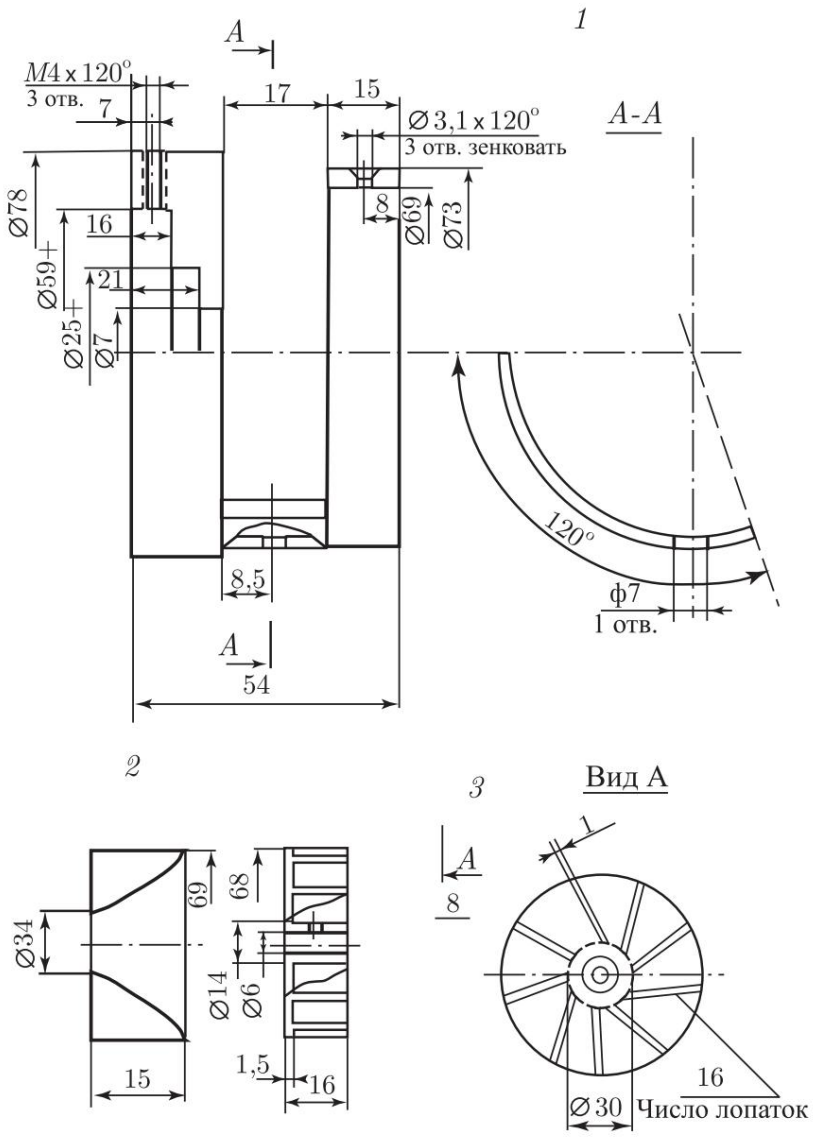

Rice. 3.22. Design of a fan for cooling a generator lamp in a microwave generator, developed on the basis of the LMS-541 measuring generator: *1* - housing, *2* - inlet nozzle, *3* - impeller

To further increase the power, it is necessary to replace the generator lamp with the next, more powerful standard size. The LMS-551 V generator was chosen as the base model for creating a powerful (up to 500 W in a pulse and up to 200 W in a continuous mode) generator, since its resonator system has fairly large dimensions and is most suitable for installing a larger lamp. A GI-7B metal-ceramic triode is used as a generator lamp. The seats in the coaxial oscillatory system of the generator have been increased to the required dimensions. In order to provide the possibility of pulse modulation to the cathode, the output of the latter is structurally carried out according to the circuit in Fig. 3.23. In the LMS-551 V generator using two quarter-wave filters

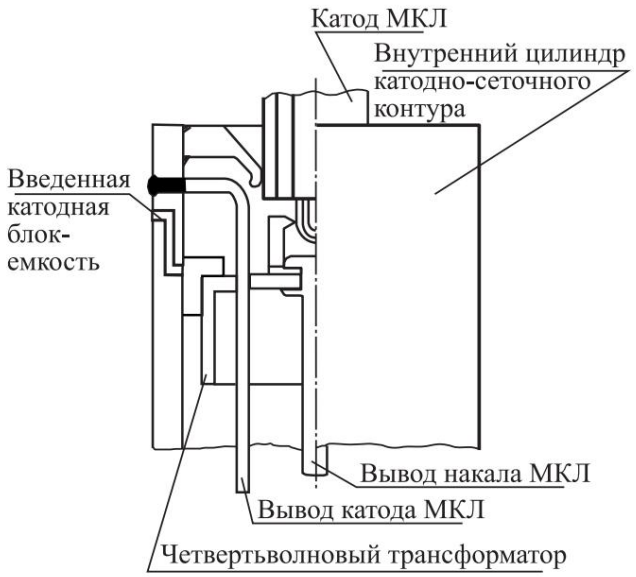

Rice. 3.23. Insulation of the cathode of a metal-ceramic lamp by constant component in a microwave generator developed on the basis of a measuring generator LMS-551V

in the cathode circuit of the MCL, stable generation is ensured in the range wavelengths 30 ÷ 70 cm. A new power supply is installed in the generator with an output voltage of 2 kV to power the MCL anode and a current of 0.3 A (in a pulse - up to 1 A). The power supply is supplemented with an electronic voltage regulator for smooth regulation of the anode voltage MCL, thermal protection, triggered by accidental increase anode current of the MCL above normal, and blocking circuits that remove anode voltage of the MCL during a short-term shutdown of the industrial network. Re-activation is possible only by the experimenter. The thermal regime of the generator lamp is ensured by greater performance (up to 30 m3/h) of the fan by changing its designs while maintaining the standard engine. In pulse mode A damping resistance is introduced into the fan motor power supply circuit and the fan operates at reduced speed, ensuring productivity is about 10 m3/h. Impeller and volute dimensions the fans are the same as for the LMS-541 generator. The exception is the housing size and the ejection hole dimensions. air.

To provide pulse mode with modulation by short pulses, the generator is supplemented with a pulse modulator according to the circuit in Fig. 3.16. The pulse modulator is triggered by rectangular pulses of positive polarity with an amplitude of 3 V, width pulses vary from 3 10ÿ6 s to 10ÿ3 s. Achieved power at a matched load of 75 Ohms in continuous generation mode in the range of 30–70 cm - 220 W, in pulse mode - 550 W.

In Fig. 3.24 shows the electrical diagram of the power supply, protection and regulation of the generator current. Docking this generator

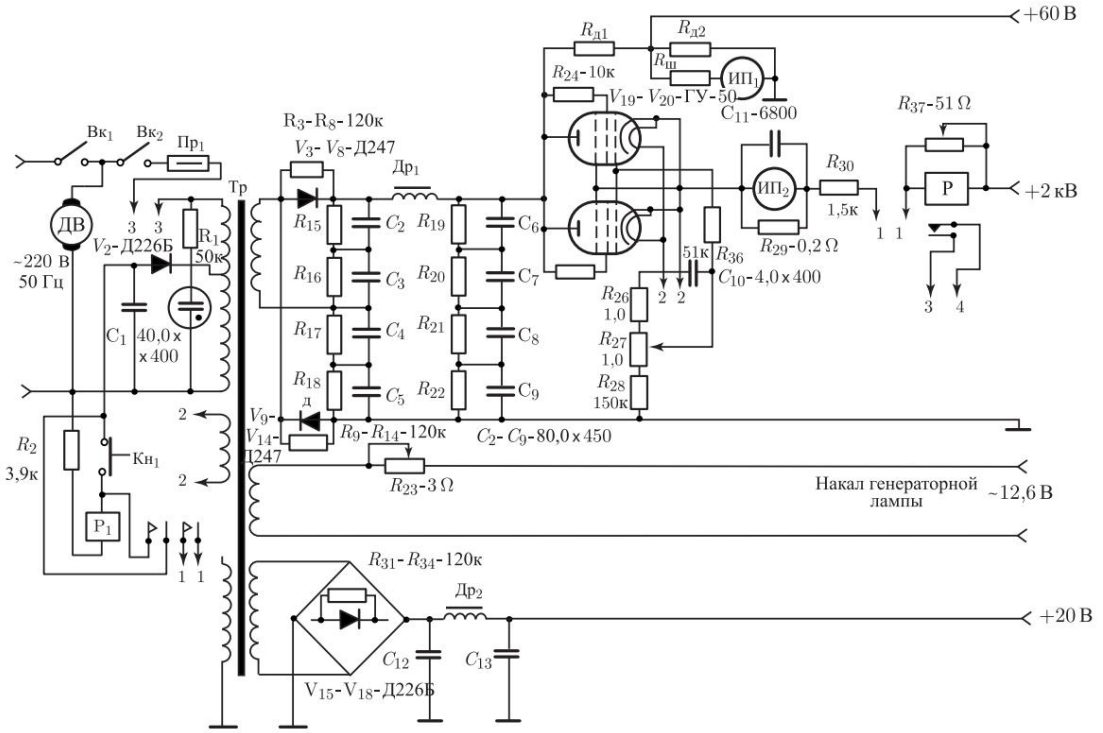

Rice. 3.24. Electrical circuit of the power supply, protection and current regulation generator lamp

with linear modulator provides 5 × linear modulation bandwidth
× 10ÿ2 ÷ 104 Hz with modulation depth up to 95%. Level of nonlinear distortion in linear modulation mode for series generators The LMS along the entire tract averages 5%, reaching 10 ÷ 12% only on selected areas in the wavelength range 9 ÷ 100 cm.

In Fig. 3.25 shows the experimental static modulation characteristics of the power of generators of the LMS series in the wavelength range 18 ÷ 100 cm, taken at several points in the frequency range.

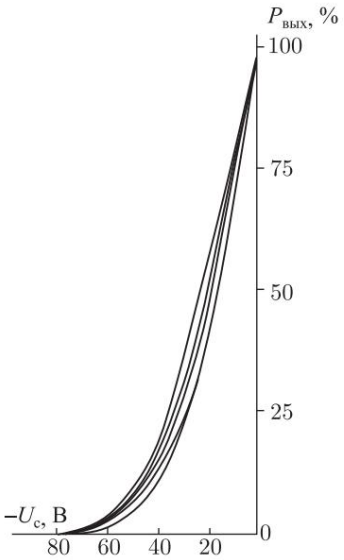

Rice. 3.25. Family static modulation characteristics by powers in dia- wavelength range 18 ÷ 100 cm for several points along range

3.5. Magnetron and tube microwave generators for fixed frequencies with broadband pulse modulation

Among the devices that are of interest for the development of generators based on them Microwave for a biological experiment, we can include medical devices for micro-

wave therapy operating at frequencies of 460 MHz and 2375 MHz (see table 3.2). The fairly high output power level of these

Table 3.2

Medical device data for microwave therapy

Device type	Day off Power, W	Frequency, MHz	Modulation	
			internal	external
"Luch-3"	20	2375 ± 2%	-	-
"Luch-58-1"	150 ± 45	2375± 50	-	-
"Volna-2"	100 ± 30	460 ± 1%	-	-
"Chamomile"	14,3	460	-	-

devices makes it possible to obtain high values of the MRP in the case of using rectangular waveguides or strip lines as irradiators. However, the absence of modulators in these devices is not allows them to be widely used in biophysical and physiological experiments. Thus, the development of microwave generators for biological

experiments require, first of all, the presence of blocks that provide pulse modulation mode with wide variability parameters of the modulating signal. In this case, it is necessary to take into account what devices such as “Luch-3” and “Luch-58-1” represent magnetron generators with a grounded “plus” of the power source [216, 217]. Standard pulse circuits described in the literature modulators for magnetron generators [210] in this case are not suitable due to the technical difficulty of ensuring variability parameters of the modulating pulse. On the other hand, non-compliance with the requirements for such modulating parameters pulse, as the steepness of the fronts, leads to the appearance of parasitic oscillations in the magnetron [206, 215]. Checking the operation of these devices in normal mode (continuous generation) showed that due to insufficient overall power of the anode transformer and low capacity of the smoothing filter, parasitic amplitude modulation of output power with modulation index, exceeding 0.2, which, in turn, leads to the emergence parasitic oscillations in the magnetron.

Thus, the development of microwave generators at wavelength 12.6 cm (2375 MHz) based medical devices for microwave therapy is actually an independent and quite a technically complex task.

The Romashka and Volna-2 devices operating at the frequency 460 MHz, are tube oscillators with resonator circuit designs, and both devices use the circuit

with an insulated cathode [211, 218]. This allows you to dramatically reduce scope of work on the development of microwave generators for biological research.

Below is a description of the developed microwave generators based on mentioned medical devices for microwave therapy.

3.5.1. Magnetron generators at a frequency of 2375 MHz with wideband pulse modulation. Magnetron is microwave self-oscillator with a grounded anode. This design feature simplifies the solution of the problem of broadband pulse modulation of magnetron generators. In Fig. 3.26 shows a simplified electrical circuit for powering a magnetron generator used in medical devices “Luch-3” and “Luch-58-1” [216, 217, 219] with the inclusion of an electronic key magnetron anode in the power supply gap for providing broadband pulse modulation mode.

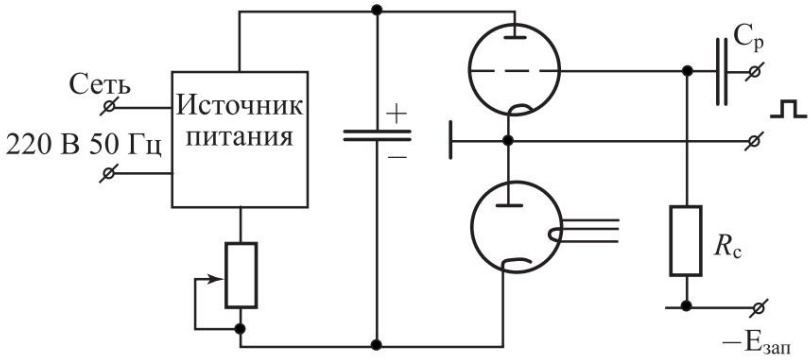

Rice. 3.26. Simplified magnetron power supply circuit in broadband mode pulse modulation

With this method of switching the anode supply of the magnetron The control signal is supplied to the grid of the electron tube relative to its grounded cathode. Thus, there is no need to transfer the modulating signal at the subcarrier frequency when while maintaining a wide band.

Below is a description and schematic diagrams of magnetron generators for biological research, created on the basis of medical devices for microwave therapy “Luch-3” and “Luch-58-1”.

Basic model "Luch-3". The device "Luch-3" is microwave self-oscillator with output power up to 20 W. The frequency of the generated electromagnetic oscillations is 2375 MHz. Adjustment generator output power is achieved by changing the current magnetron anode.

The development of a generator based on the Luch-3 model aims to:

- improved filtration of the rectified anode voltage thereby increasing the filter capacity and introducing a choke into the filter;

— installation of the modulator and submodulator power supply;

— introduction of an electronic switch for switching the magnetron anode circuit in order to implement pulse modulation mode in a wide frequency range;

— introduction of a submodulator, providing amplification of the control pulse signal to the value necessary for compensation locking voltage on the control grid of the electronic key;

— introducing switching circuits to transfer the generator from a pulse mode to a continuous oscillation mode;

— installation of a fan for blowing the modulation lamp and magnetron.

A modulator tetrode was chosen as an electronic key GI-30, which has sufficient electrical strength and power dissipation at the anodes. The turn-off voltage in a triode connection at an anode voltage of 1600 V is about ÿ100 V. The electronic switch is controlled by a submodulator assembled on transistors. The submodulator represents two normal

unlocked key with galvanic connection. The sub-modulator is also galvanically connected to the modulating tube. Modulation tube anodes are connected to the power supply up to resistor R35 (see the data sheet of the Luch-3 device) through a chain of resistances that allows stepwise change the generator output power in pulse mode. To prevent the occurrence of parasitic generation in the circuit anodes and grids of the GI-30 lamp include resistors with a resistance of 200 Om.

In the initial state, the GI-30 lamp is locked with negative voltage removed from the collector of transistor V2 (see Fig. 3.27, a). When a rectangular pulse of positive polarity is applied to the base of transistor V1, transistor V1 is turned off and, as a result of galvanic coupling, transistor V2 is turned off. In this case, the potential of the GI-30 lamp grids relative to the cathode becomes equal to zero and to the magnetron supply voltage is supplied. For a time equal to the duration of the unlocking pulse, the magnetron generates high-frequency fluctuations. A complete circuit diagram of the modulator is shown at rice. 3.27, a. In Fig. 3.27, *b* shows the network connection diagram microwave generator together with a modulation unit.

The modulator and submodulator are designed as a separate unit, connected to the Luch-3 device using three connectors. For two The connector supplies the supply voltage to the anode circuit of the magnetron, which is removed from the filter capacitance C2 of the device. The third connector supplies power supply voltage 220 V, 50 Hz. To be able to translate device "Luch-3" from pulse mode to continuous mode, the "plus" supply voltage of the anode circuit of the magnetron is supplied to the connector through toggle switch The second position of the toggle switch is used to supply this the same voltage across resistor R35, and thus is restored normal mode of the device. The switching toggle switch is installed on the front panel of the Luch-3 device above the control button; connectors -

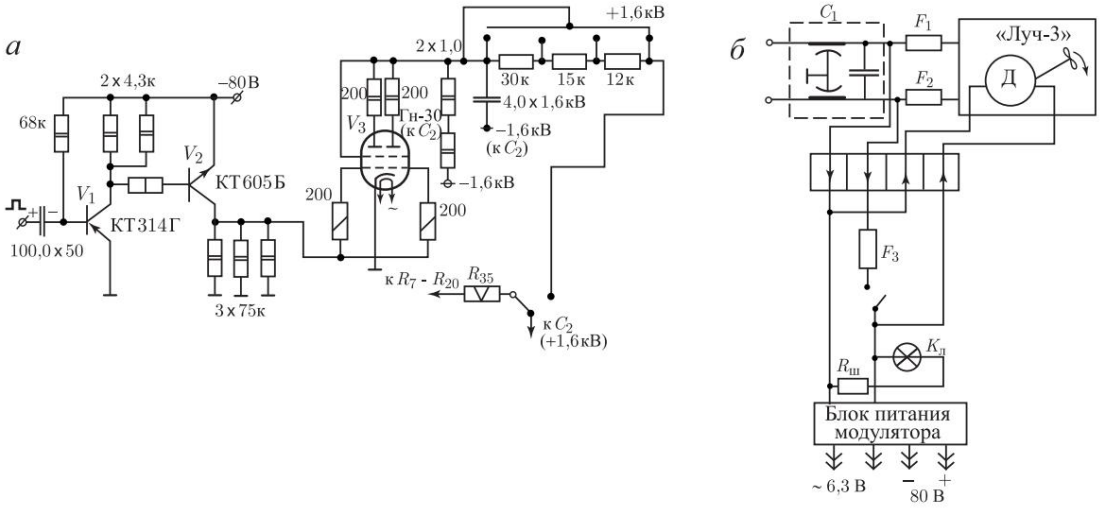

Rice. 3.27. Microwave generator with a wide modulating signal band, developed on the basis of the Luch-3 device: *a* - schematic diagram of the unit modulation; *b* - connection diagram to a 220 V industrial network

on the back panel. On the front panel of the modulation block there is toggle switch for turning on the fan (type VN-2) and the power supply of the modulator and submodulator. A fan is necessary to cool the cylinder of the modulation lamp and the magnetron, since in pulsed mode a significantly larger current flows through the magnetron than in the continuous generation. The fan is mounted on the cover of the device, on in which the hole for the fan casing is pre-selected.

The modulation block has the same installation dimensions as itself apparatus, and is placed on the apparatus body from above so that the flow air, directed by a fan, blew on the modulation lamp below. The bottom of the modulation unit housing and the top cover are equipped with perforated for air flow. On the back of the unit modulation there are mating connectors for connecting to the device using three connecting cables. On the front panel the modulation block also contains control neon lamps, signaling the on state of the fan and power supply, modulator and submodulator, connector for supplying modulating pulses and a switch to set the output power level.

The generator parameters are as follows:

— pulse amplitude, V — pulse duration, s — pulse repetition rate, Hz — power control limits in pulse, W - average initial magnetron current in absence of impulses, A

$5 \cdot 10^{-6} \div 50 \cdot 10^{-3}$;
$0 \div 5 \cdot 10^{3}$;
$10 \div 100$;
$3 \cdot 10^{-3}$.

It should be noted that at certain ratios of pulse duration and their repetition frequency at long durations pulses, the amplitude of the pulses decreases towards the end of the pulse

up to 50% of the initial value. In addition, it is possible to excite parasitic oscillations in the magnetron, especially if the load is bad coordinated with the generator. It is advisable to install a valve between the generator and the load. The generator output must be switched on coupler with detector section for observing pulse shapes on the oscilloscope screen.

The basic model is “Luch-58-1”. The device "Luch-58-1" presents is a self-oscillator operating at a frequency of 2375 MHz and providing power up to 150 W at a load of 75 Ohms. Output adjustment power is carried out by changing the anode current of the magnetron. A distinctive feature is a decrease in the supply voltage of the magnetron filament with an increase in the output power and its complete shutdown at the last stages of output power regulation. The main development points are the same as for the device "Luch-3", however due to the significantly higher output power and higher values of magnetron anode voltage and current the amount of work is much greater.

Two parallel keys are used as an electronic key. included GI-30 lamps, another same lamp is used in the output stage of the submodulator with a grounded anode, which allows the number of stages to be reduced to a minimum. The first stage is a normally locked lamp switch V1 with rheostatic-capacitive coupling with the second stage. Second stage of the submodulator is a normally unlocked lamp switch V2 and is galvanically connected to the modulator - two parallel connected modulator tetrodes GI-30 (V3 and V4), included triodes. The initial state of the modulator is locked. When fed to the grid lamp V1 square pulse positive polarity lamp V1 unlocks and locks the lamp with a negative pulse from the anode V2. In this case, the potential difference in the “grid-cathode” section of lamps V3 and V4 becomes zero and current begins to flow through the magnetron. In this case, the magnetron generates a microwave radio pulse. At the end of the pulse, lamp V1 is closed, the potential at its anode increases and lamp V2, unlocking, locks lamps V3 and V4. The current through the magnetron stops, which leads to disruption of microwave oscillations. In order to increase power in the pulse and reducing the parasitic modulation index that occurs in the standard version of the device "Luch-58-1", filter C4C5 (see data sheet apparatus "Luch-58-1") is supplemented by two capacitors with a capacity of 2 μF with an operating voltage of 4 kV, connected in parallel between “plus” and “minus” of the magnetron power supply. Capacitors C6 and C7 are excluded from the circuit in order to implement short microwave pulses. As a result, after turning off the modulating tubes, the current through the magnetron stops abruptly, which allows you to get a steep decline in the voltage pulse at the anode of the magnetron. For a smooth decline voltages on newly installed tanks are shunted three series-connected resistances MLT-1.0-2.0.

When the anode voltage of the magnetron increases to 3 kV, a breakdown is observed between the magnetron cathode and the primary winding of transformer T2, since these voltages are brought to one contact
bar Therefore, pin No. 22 of the winding of transformer T2 should
disconnect from the common contact strip. Into the vacant nest
an insulating stand with a height of 25 ÷ 30 mm is mounted, on which
winding terminal No. 22 and the wire feeding the magnetron filament are attached
and under high voltage (3 kV).

The magnetron filament power supply mode in pulse mode should
have autonomy, since in this case it depends on the well-
sti. Therefore, resistance taps R15 are unsoldered from biscuits S4.2
switch S4 (upper biscuit in the switch) and are mounted on
newly installed switch with an equal number of switchings.
This measure allows you to regulate the heating mode of the magnetron independently from the position of switch S4, which determines the output level
generator power. To control the filament voltage of the magnetron
the generator is equipped with an additional measuring device installed on the front panel.

In order to eliminate the problem of “decoupling” the high voltage supplying the magnetron from the control signal, the cathodes of the modulator
lamps are connected to the body, and the anodes are connected to the “ÿ” of device P1. Since in this case there is no need to control the network voltage (which is necessary when using the Luch-58-1 device
for its intended purpose) and taking into account that when connected to the circuit
magnetron power supply, the “ÿ” pin of device P1 is high
voltage relative to the housing (network), switch S1 and circuit V1R1R2 are excluded from the circuit. Thus, device P1 performs
functions of the magnetron anode current meter and the presence of microwave oscillation generation.

The power supply of the modulator and submodulator provides the following current voltages and currents:

- U1 = ÿ12 V, 5 mA - grid shut-off voltage of the first lamp - ÿÿ V1;
- U2 = +300 V, 30 mA — supply voltage of the anode of lamp V1;
- U3 = ÿ600 V, 100 mA — supply voltage of the anode of lamp V2;
- U4 = 12.6 V, 4 A — supply voltage of the incandescent circuits of lamps V2, V3, V4;
- U5 = 6.3 V, 1 A — supply voltage of the lamp V1 filament circuit (it is possible to power the filament circuits of all lamps with a voltage of 6.3 V at a current of 9 A).

The power supply of the modulator and submodulator is turned on
stepwise. When switch S3 is turned on , the “compensator” from terminals No. 17–19 of the network winding of transformer T2 through the half-wave rectifier V1C1 (Fig. 3.28, a) supplies voltage to relay K1,
which with its contacts closes the power circuit of the primary winding
network transformer of the lamp power supply V1 ÷ V4. At the same time, on

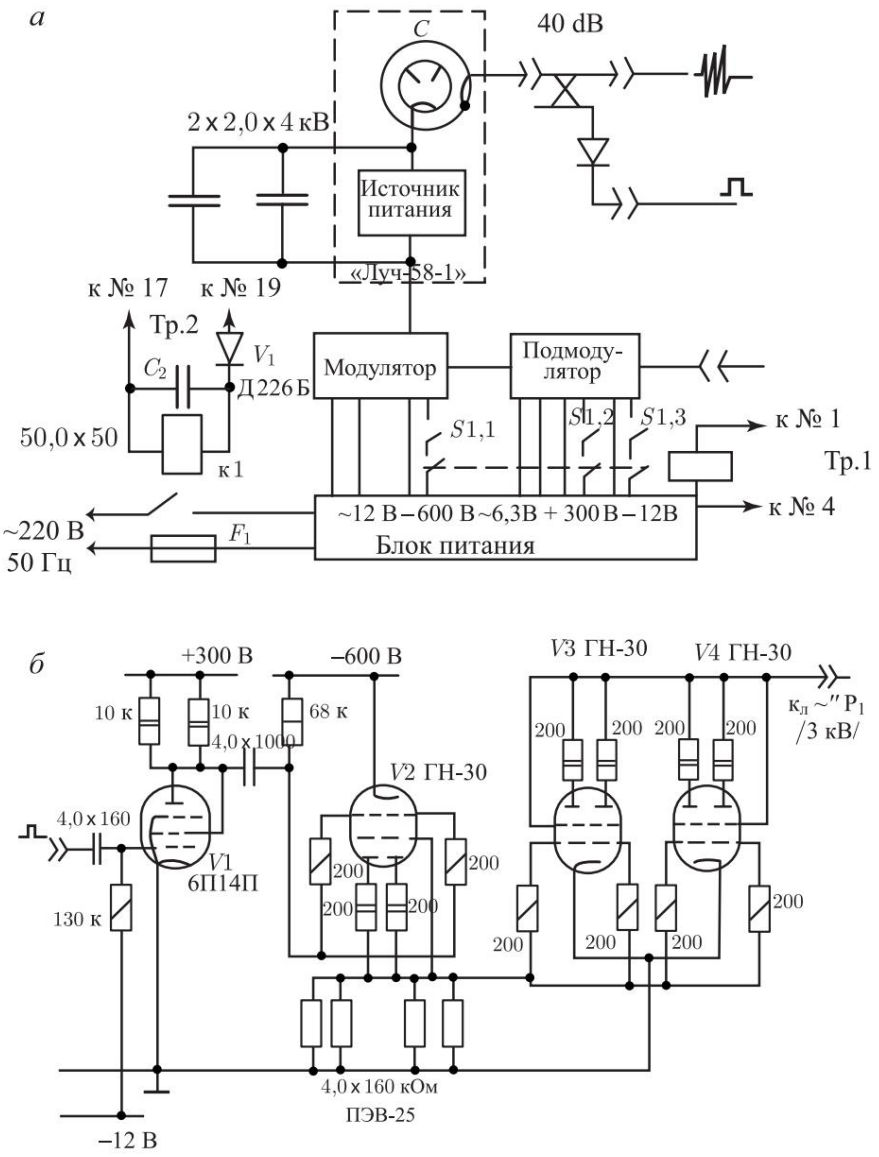

Rice. 3.28. Microwave generator with a wide modulating signal band, developed on the basis of the Luch-58-1 device: *a* - block diagram; *b* - fundamental modulation block diagram

The modulation unit is supplied with only the supply voltage to the filament circuits. After 1–5 minutes required to warm up the lamps, the automation unit of the "Luch-58-1" device will operate and when switch S4 is turned on voltage will be applied to the primary winding of transformer T1 127 V. Relay K2 is connected to Nos. 1 and 4 of the primary winding of transformer T1 , which provides, when activated by its contacts, readiness of supply voltages ÿ600 V, +300 V and ÿ12 V, which are supplied to the modulation block. If the generator is used in pulse mode, toggle switch S1 is turned on. In this case, until the input of the submodulator is trigger pulses are supplied, microwave generation is absent. If the generator used in continuous generation mode, toggle switch S1 is not turned on

and modulating valves V3 and V4 are unlocked. At the same time, through the magnetron current flows and microwave oscillations are generated. Toggle switch S1 is installed in place of the standard toggle switch S1. Also installed on the front panel connector for connecting the cable from the pulse generator.

During the development of the generator, it became clear that current control of the envelope shape in pulse modulation mode is necessary. For this purpose, an omnidirectional coupler was introduced into the generator (a coaxial system from the D4-4 attenuator was used) with attenuation about 40 dB, the output of which is loaded onto the detector section. The voltage from the detector output is supplied to the connector installed on the front panel of the generator to observe the shape of the envelope on oscilloscope. Generator developed on the basis of the Luch-58-1 device The microwave has the following technical characteristics:

— carrier frequency — 2375 MHz;
magnetron anode supply voltage — maximum output 3 kV;
power value
in a pulse - 0.5 kW;
pulse duration - pulse repetition rate $1.5 \cdot 10^{-6} \div 10^{-2}$ s;
- amplitude of modulating pulses up to 50 kHz;
maximum 10 V;
— pulse polarity Since the positive.
magnetron voltage in the developed generator exceeds the standard value for the Luch-58-1 apparatus, it is necessary
carry out power measurements in continuous mode at all stages of power control. In Fig. 3.28, *and* a block diagram is given
developed generator, in Fig. 3.28, *b* - schematic diagram
modulation block. Relay K1 can be used as relay
MKU-48 for voltage 12 V. If you use the winding leads
No. 17–21, then you can use the MKU-48 relay for a voltage of 24 V.
A PE20 127 V relay was used as relay K2 . Modulation unit
and 2.0 × 4 kV tanks are located on the second floor of the device chassis "Luch-58-1", power supply - on the first floor.

3.5.2. Tube oscillators at a frequency of 460 MHz with wideband pulse modulation. These generators are based on medical devices for DCV therapy “Romashka” and “Volna-2” [209, 218]. Both devices are self-generating microwave oscillators, built according to a dual-circuit circuit using triode MCLs with isolated cathode. The latter circumstance makes it possible to use a transistor switch circuit in the MCL cathode circuit as a broadband modulator. In standard version in continuous generation mode output power (maximum) of the "Romashka" device - 14 W, apparatus "Volna-2" - 100 W. In Fig. 3.29 shows power supply diagrams SCL of these devices. Adjusting the output power in the device “Chamomile” is carried out using a resistor connected to the circuit

cathode of the MCL, in the Volna-2 apparatus - by changing the value of the anode voltage of the MCL.

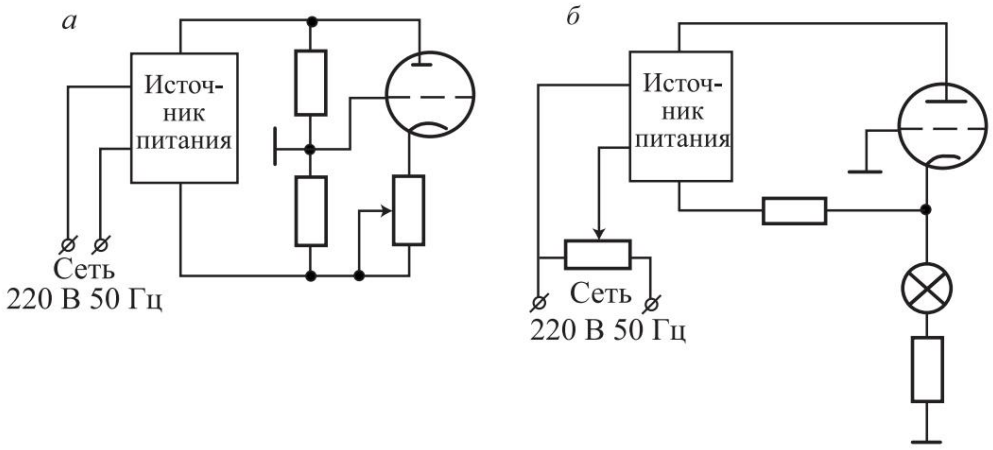

Rice. 3.29. Simplified power supply circuits for the generator lamp of medical devices: *a* - “Chamomile”; *b* - “Volna-2”

The basic model is “Chamomile”. The presence in the Romashka device of a voltage stabilizer in the power supply circuit of the MCL anode allows you to obtain more power in pulsed mode, compared to the standard mode, by increasing the supply voltage of the MCL anode. In this case, however, the voltage ripple at the anode of the MCL increases significantly at long pulse durations. To implement the pulse mode, you must first complete the following points (items are indicated according to the passport of the Romashka

device): 1. In accordance with the procedure for disassembling the device (see the technical description and operating instructions for the Romashka device, p. 30), disassemble the body of the device to access to

details. 2. Unsolder resistors R11, R12 from the housing. 3. Unsolder resistor R14 from the minus bus of the MCL anode power supply. 4. Solder the MCL to the minus bus of the anode power supply

variable resistor PPZ-680 Ohm.

5. Mount a transistor switch on a fiberglass board (npn type transistor with a collector current of at least 0.2 A and a cutoff frequency of at least 1 MHz), the initial state is locked. 6. Remove the power meter.

7. Drill a hole with a diameter of 3 mm in

the side wall of the case

power meter.

8. Solder a mon-

tazhnoy wire and pass through the hole. 9.

Assemble the power meter and mount it on site. 10. On the

front panel (on the side of the handle for carrying the device), drill two holes for installing small-sized connectors

SR-50 - one next to the power meter, the second - closer to the high-
network switch.

11. To the connector located next to the power meter,
solder the wire step 8.

12. Near the connector mounted near the power switch,
install the circuit board of the transistor switch and solder the decoupling capacitor (“plus” to the connector) between the connector and the base
transistor.

13. Mount the P2K switch on the front panel - one
a button with a fixed pressed state, with the help of which you can switch between operating modes - pulse and continuous.

After completing steps 1–13, assemble the circuit according to Fig. 3.30. Having completed the installation, unsolder the black wire going from the insulating stand

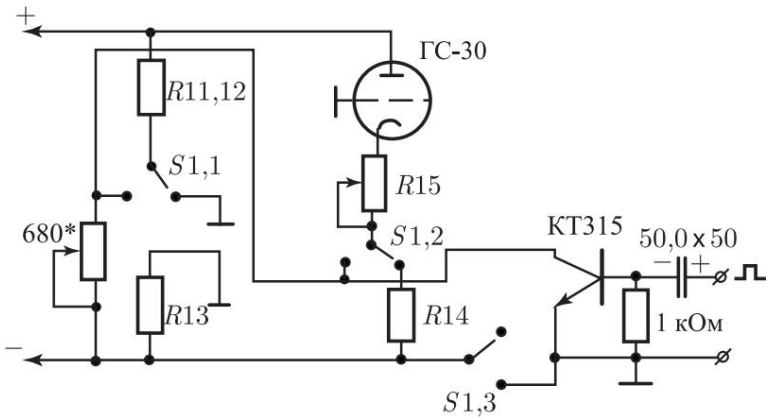

Rice. 3.30. Microwave generator with a wide modulating signal band, developed on the basis of the Romashka apparatus (switch in the mode position continuous generation - normal mode)

to the SCL anode, and connect a laboratory milliammeter into the gap.
Turn on the device according to the instructions, having previously set switch S1 to the “pulse mode” position. Use the slider of the divider potentiometer to set the resistance value at which

the current through the measuring device will become zero. This position corresponds to complete locking of the SCL, and the generation of oscillations
There is no microwave. Turn off the device, solder the MCL anode wire
in place. Connect a square pulse generator of positive polarity and an oscilloscope to the connectors. Turn on the device and
gradually increasing the amplitude of the pulses to 2 ÷ 3 V, observe
on the oscilloscope screen the field envelope. In this case, the device must be loaded to the equivalent load, according to the recommendations given
in the technical description.

It is advisable to carry out the transfer from pulse mode to continuous mode and vice versa when the device is turned off in order to avoid burning the contacts of the P2K switch.

The pulse generator has the following parameters:

1. Carrier frequency 460 MHz.
2. Maximum pulse power:
   a) when the MCL anode is powered with a stabilized voltage 16 W;
   b) when the MCL anode is powered with an unstabilized voltage, removed from the anode of the 6S41S lamp, 3. 22 W.
Pulse duration 4. Pulse repetition $0.5 \cdot 10^{-6} \div 15 \cdot 10^{-3}$ s.
frequency 5. Triggering pulse amplitude 6. up to $5 \cdot 10^{5}$ Hz.
Pulse polarity **Basic model "Volna-2".** In the Volna-2 within 5 V.
device, wideband pulse modulation positive.
is carried out using a cathode

transistor switch. Circuit design of power and control circuits currents and voltages allows you to transfer this device to a pulse mode without any alterations inside the device itself apparatus. The modulator is located inside a small housing, one the walls of which are made of insulating material (plexiglass, textolite). Three pairs of instrument plugs are mounted on this wall so that so that they can enter the nests "I ", "Ia" and "Ua" located on side wall of the device. To switch the device to pulse mode the following operations must be performed:

1. Connect the "ÿ" socket on the "Ua" connector to the "ÿ" socket of the connector «I_g».
2. Remove the short-circuit plug from socket "I". 3.$_g$ ».
Remove the short-circuit plug from socket "Ia".
4. Connect the "+" socket of connector "Ia" to the collector of the transistor CT 908 A.
5. Place a 20 kOhm resistor into the gap in connector "Ia" .
6. Connect the "+" socket of the "Ua" connector through a 300 kOhm resistor with socket "+" of connector "Ia".
7. Connect the base of the KT908A transistor through a 5 Ohm resistor to the emitter of the KT604B transistor.
8. Connect the emitter of the KT908A transistor to the "ÿ" socket of the connector «Ua» or «Ig».

These operations make it possible to implement the wideband pulse modulation scheme shown in Fig. 3.31. On the modulator body an instrument connector is installed to connect the cable from the device modulation. All of the above operations are performed by printed installation on foil-coated getinax (fiberglass). In the appropriate places, the instrument plugs are fastened with nuts and then soldered. When the transistor is off, the voltage drop is on the 20 kOhm resistor should be equal to +60 V ÷ 120 V (relative to body). If the MCL does not close completely, it is necessary increase the resistance of this resistor so that it completely

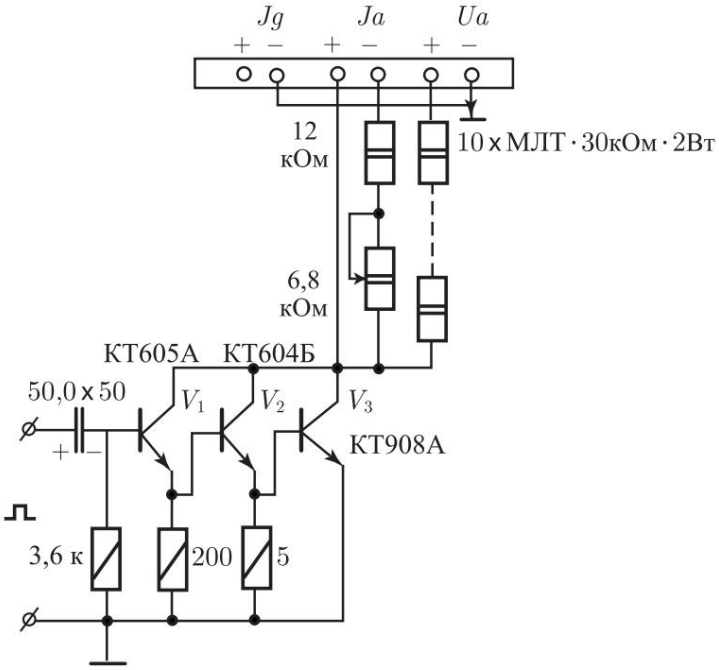

Rice. 3.31. Wideband pulse modulator for the Volna-2 device

the current through the MCL was reduced. In order to reduce the parasitic index amplitude modulation is additionally included in the standard filter
RC cell . The modulator transistor KT908A is mounted on a radiator with an area of 100 ÷ 150 cm2. Generator Specifications
in pulse mode the following:

1. Pulse repetition rate 2. Pulse	50 kHz.
duration 3. Pulse power 4.	10ÿ5 ÷ 10ÿ2 s.
Spurious amplitude	150 W.
modulation index	0,05.

3.6. Transistor microwave generators

Currently, intermediate and output stages of low- and medium-power microwave transmitting devices are often performed at
transistors [78]. Sufficiently developed summation methods now
power make it possible to create semiconductor transmitters with an output power of up to several kilowatts and higher in the long-wave part
Microwave range.

3.6.1. Features of high-power microwave transistors. When using powerful transistors in the microwave range, a number of difficulties arise,
due to physical restrictions on the maximum voltage between the electrodes of the transistor and the maximum density
emitter current. The frequency properties of amplification transistors are characterized by the value of the maximum amplification frequency fy max, at exceeding which the transistor power gain
KP in small signal mode becomes less than 3 dB.

The limiting factor is the effect of compression,
when, at high injection levels, the current of minority charge carriers is pushed to the edge of the emitter and therefore its density is determined not by the entire area of the emitter, but only by its part located
near the perimeter. Since there is a limiting value of density
emitter current, the excess of which leads to destruction of the device,
The pushback effect limits the power of the transistor.

If you create multi-emitter transistors, the emitter of which
performed in the form of a large number of parallel-connected cells, then
it is possible to significantly increase the ratio of the emitter perimeter to its
total area. This in turn allows you to increase the current,
practically without increasing the capacitance of the transitions, and, therefore, increase the power while simultaneously increasing the cutoff frequency.

3.6.2. Analysis of the operation of transistor power amplifiers (THUMP) MICROWAVE. When analyzing the operation of TUM, the static characteristics of transistors are used (Fig. 3.32). Convenient analytical dependencies are obtained by linear approximation (dotted line).
The parameters of the approximated characteristics are the slope
S, shear stress E (Fig. 3.32, a), as well as line slope
critical mode Scr. Optimal in terms of output power (according to
gain) and efficiency at low frequencies is
critical mode. Significant gain drop at this frequency
range occurs only in overvoltage mode. In the range
microwave, where, as a rule, operating frequencies are close to the cutoff frequency
transistor fgr, the gain decreases noticeably even in the undervoltage
mode. In Fig. 3.32, *b* area of significant power gain
bounded on the left by line A, called the boundary line. The line of critical mode B is also depicted there .
The steepness of the boundary mode line Sgr is less than the steepness of the critical mode line Sccr and can be estimated by the formula

$$Sgr = 15Pout/E2\ k\ ,$$

where Pout, W is the output power, and Ek, V is the collector supply voltage of the transistor in typical operating mode.

In the region of high and ultra-high frequencies when analyzing the operation of TUM it is necessary to take into account inertial phenomena associated with the final
the time of movement of carriers, as well as the capacitance of pn junctions and the inductance of transistor terminals.

3.6.3. Practical implementation of matching and correcting circuits. TUM design elements. Transistor amplifiers
From a design point of view, microwaves in most cases are hybrid devices:
a transistor is an attached element;
input and output matching circuits and power circuits are performed according to
film technology on dielectric substrates.

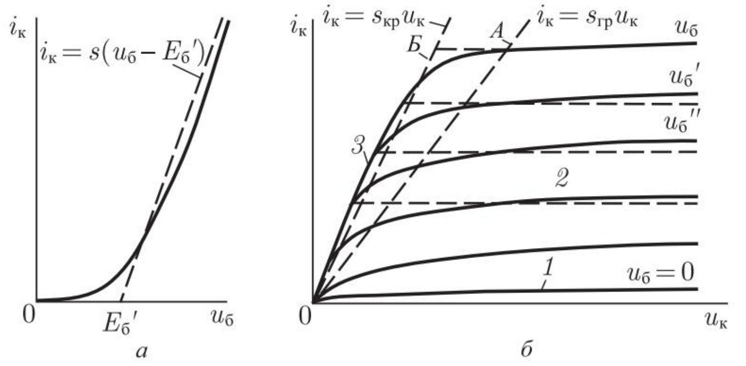

Rice. 3.32. Static characteristics of the transistor: *1* - cut-off region; *2* - active area; *3* - saturation region

When making electrical circuits, TUM is the most convenient The type of feeder path is microstrip line (MSL). However, the frequency range in which it is advisable to use MPL is limited. Typically, MPLs are not recommended for use at frequencies below 100 MHz, since sections of microwave circuits become too long. The use of MPL at high frequencies is accompanied by increasing losses and increasing the possibility of excitation in the line waves of higher types. Therefore the operating frequency should be lower critical frequency of the transverse electric wave of the lowest order:

f<fÿÿ = 75/(h ÿÿ ÿ 1),

where h is expressed in mm; f - in GHz. The wavelength in the line, and consequently, the dimensions of many elements of microwave circuits are determined effective dielectric constant ÿeff:

ÿÿ = ÿ/ÿÿÿFF ,

ÿeff = 2 (e + 1)/ + (e ÿ 1)/2 1 + 10h/IN ÿ1/2

When creating TUM schemes, the lumped elements of the calculated circuits can be replaced by distributed ones, which are segments of MPL of a certain length with a certain characteristic impedance, and they can be made using film technology in a planar design. However, the use of concentrated reactive elements allows in some cases to significantly compact the installation scheme. We can assume that inductive coils and capacitors have the properties of elements with lumped parameters if they dimensions are small compared to the wavelength in the line [are no more than (0.05 ÷ 0.1)ÿl]. Lumped inductances perform in the form of a coil of MPL (Fig. 3.33, a), in the form of a round and square spiral coil (Fig. 3.33, b, c) or in the form of a segment of MPL with a large wave resistance (Fig. 3.33, d).

Options for performing a concentrated container are shown in
rice. 3.33, d, f, and the capacitance (Fig. 3.33, d) is included in the line
parallel.

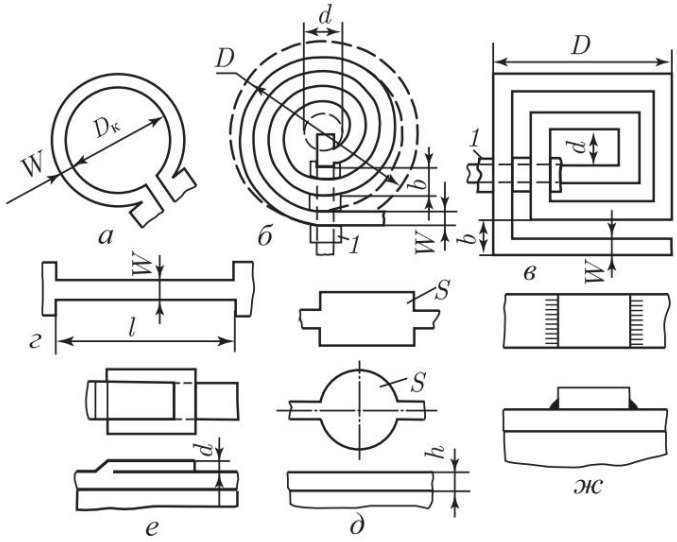

Rice. 3.33. Designs of lumped inductances *(a–d),* capacitances *(d–g): 1* — insulating gasket

In some cases, especially in the long-wavelength part of the microwave range,
microcapacitors are used (Fig. 3.33, g), having
the shape of a rectangular parallelepiped, two opposite sides of which are metallized and
tinned. With increasing working
frequency, the technological difficulties of manufacturing elements with lumped parameters
increase and losses in them increase. Therefore, the scope of application of such elements is
currently limited
frequencies 2–3 GHz. Formulas for calculating lumped parameters
elements are summarized in table. 3.3.

Configurations of the most commonly used distributed
elements and their equivalent circuits without taking into account parasitic parameters such
as edge capacitances of line segments, various types of inhomogeneities (angles, abrupt
changes in the width of conductors
etc.) are presented in table. 3.4. Formulas for calculation are also given here
their parameters.

Note that in real circuits with distributed elements
equivalent capacitances and inductances depend on frequency. All this
causes deviations in the frequency characteristics of circuits from the calculated ones,
and these deviations are determined by the number of elements of the original circuit,
type of frequency response, electrical lengths of the segments used. For circuits with distributed
elements with the Chebyshev form of the frequency response of the original circuit, it is
recommended to limit the maximum electrical lengths used

Table 3.3

Lumped parameters elements	Calculation formulas 1)
Turn inductance, nH (see Fig. 3.33, a)	L = 0,2ÿDÿ[2,3 lg(4Dÿ/W) ÿ 0,5]
Dimension D and inductance, nH, of a round spiral coil (see Fig. 3.33, b)	D = d + (2N ÿ 1)b + 2W; L = [5(D + d) 2 N2]/(15D ÿ 7d)
Dimension D and inductance, nH, of a square spiral coil (see Fig. 3.33, c)	D = d + (2N ÿ 1)b + 2W; L = (6(D + d) 2 N2]/(15D ÿ 7d)
Inductance of an MSL segment with a high wave resistance, nG (see Fig. 3.33, d)	L = 0,2l[ln(8h/W)+(0,177W) 2 /h2]; W/h 2; L = 0,628l/{0,5W/h + 0,9 + +0,318 ln[W/(2h) + 0,94]}; W/h > 2
Capacitance of the extended section of the MPL, pF (see Fig. 3.33, d)	C = 0,884 · 10ÿ2 ÿS/h
Capacitance of the film capacitor, pF (see Fig. 3.33, e)	C = 0,884 · 10ÿ2 ÿS/d

segments at the central frequency of the operating range with a value calculated from the ratio, rad:

$$ÿÿÿ \max 2ÿ/5 ÿ 0.5(ÿÿ ÿ ÿÿ)/(\sqrt{ÿÿÿÿÿ}) ÿ 0.15n,$$

where n is the number of reactive elements. When

moving from the original circuits with lumped elements to circuits with a distributed structure, the number of calculated relationships becomes less than the number of characteristics to be determined. This explains a certain freedom in choosing parameters and makes it possible to satisfy additional technological or design requirements.

At the technical design stage, it is advisable to use a computer to optimize the frequency characteristics of the amplifier. In this case, the problem is usually set of the so-called parametric synthesis, i.e., the optimal choice of numerical values of the parameters of matching or correcting circuits. The maximum reflection coefficients at the input and output of the amplifier in the frequency band under consideration are used as the target function to be minimized. When synthesizing circuits, restrictions are usually imposed on the maximum structurally feasible values of wave impedances: 10 Z0 100–150, Ohm.

1) All dimensions in mm; N is the number of turns; b is the spiral pitch.

Table 3.4

Distributed view th element	Options for an equivalent circuit with lumped elements and formulas for their calculation	
þël p/4 (l ÿl/8)	$L = \frac{\sin ÿel}{oh} Z0;$ $C = \frac{tg(ÿÿÿ/2)}{Z0oh}$	$L = \frac{tg(ÿÿÿ/2)}{oh} Z0;$ $C = \frac{\sin ÿel}{Z0oh}$
i p/4 (l ÿl/8)	$L = \frac{8 people}{p2o} Z0;$ $C = \frac{tel}{2ÿZ0}$	$L = \frac{tg ÿÿÿ}{oh} Z0$ ÿÿÿ ÿÿÿ ÿ /10? L 3.33Z0l ÿÿeff , (at l in m) nG
þël p/4 (l ÿl/8)	$L = ; \frac{ÿelZ0}{2ÿ}$ $C = \frac{8ÿel}{ÿ2ÿZ0}$	$C = \frac{tg ÿÿÿ}{Z0oh}$ ÿÿÿ ÿÿÿ < ÿ/10; C ÿ 3,33 · 103 $\frac{l}{Z0}$ × ×ÿÿÿÿÿ , pF
z02 Z01 thel1; ÿÿÿ2 p/4	$L = \frac{\sin ÿÿÿ2}{oh} Z02 + \frac{tg(ÿÿÿ1/2)}{oh} Z01;$ $C = + ÿZ02 \frac{tg(ÿÿÿ2/2)}{ÿZ01} \frac{\sin ÿÿÿ1}{ÿZ01}$	
thel1; ÿÿÿ2 p/4	$L = \frac{8ÿel2}{p2o} Z02;$ $C = + 2ÿZ02 \frac{thël2}{ÿZ01} \frac{tg ÿÿÿ1}{ÿZ01}$	

In Fig. Figure 3.34 shows a schematic diagram *(a)* of a broadband TUM in the decimeter wavelength range and an example of its constructive implementation (b). Amplifiers made according to this circuit provide a gain of 7–10 dB with an efficiency of over 45% within a band of approximately ±20% of the center frequency. Containers C1 and C9 separating, container C6 - blocking. Chokes L2 and L3 provide direct current mode. Length of the segment forming inductance L2, equal to a quarter of the wavelength at medium frequency range. Inductance L3, in addition, compensates for the average frequency range influence the output capacitance of the transistor. Entrance the amplifier circuit (C2 + C3; L1; C4 + C5; Lin) is corrective two-section low-pass filter type circuit. Output circuit L4; C8 + C7 - two-element low-pass filter with limited bandwidth.
Structurally, capacitances C2, C7 and all inductances are made of microstrip line segments. Possibility of changing inductances and capacitances by connecting the appropriate jumpers allows you to configure the amplifier. Tanks C1, C3, C4, C5, C6, C8, C9 —

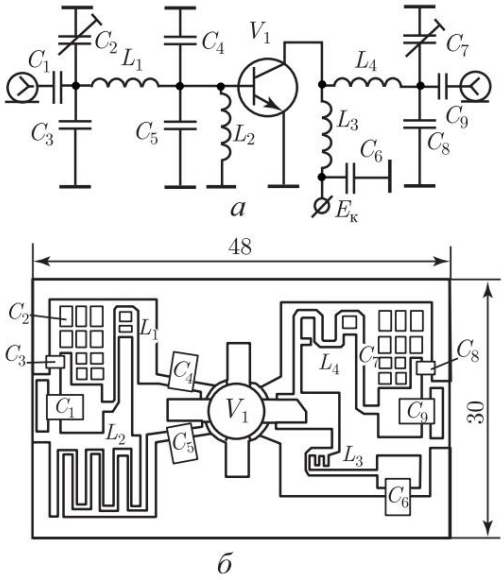

Rice. 3.34. Schematic diagram of TUM of the decimeter length range
wave) and its topology (b)

focused. The entire amplifier is made of 22XC ceramic board
or polycor, its size is 48 × 30 × 1, transistor - KT913B.

Removing from the one shown in Fig. 3.34 circuits TUM input and output filters and by introducing positive feedback, TUM can switch to the oscillation generation mode and thus implement microwave self-generator. Trimmer capacitor C7, by extending the rotor handle and bringing it to the front panel of the generator, it will be possible adjust the generator mode within small limits at different loads. By introducing a detector section based on microstrip lines, it will be possible to determine the optimal matching mode generator and load according to the maximum reading of the measuring device. Pulse modulation of microwave oscillations is carried out using an emitter follower connected in series with a self-generator. A schematic diagram of a microwave self-oscillator with a pulse modulator is shown in Fig. 3.35.

To control the magnitude of the collector current (microwave power), an ammeter P1 with a total deviation current of 1 A is introduced into the circuit. The numbering of the circuit elements corresponds to that in Fig. 3.34. Denominations and numbering of new elements are set after configuration self-oscillator and modulator.

A transistor can be used as a pulse switch KT815 or KT817, radiator area is about 10 cm2. Toggle switch SA1 select the generation mode. When the toggle switch is closed, the generator switches to continuous generation mode. Any low-power microwave diode can be used as VD1. Shown in Fig. 3.34 the TUM circuit can be switched to self-oscillator mode by also entering

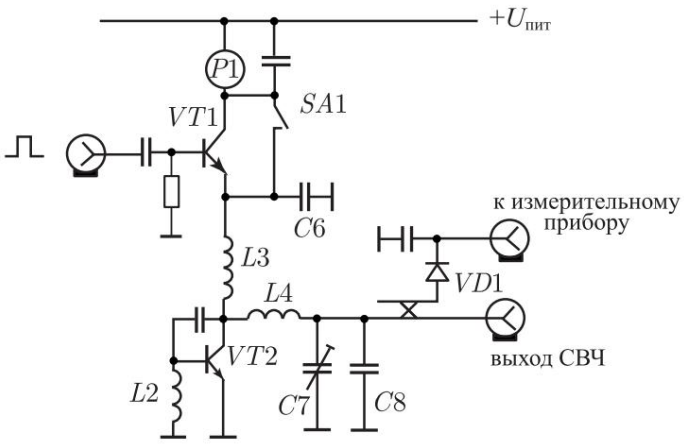

Rice. 3.35. Microwave oscillator with pulse modulation

positive feedback with correction of strip filter elements and selective circuits.

Chapter 4

CONDITIONS FOR IRRADIATION OF BIOLOGICAL OBJECTS

A biophysical experiment involving the irradiation of small objects, the area of which does not exceed tens of square centimeters, does not require the creation of electromagnetic fields in significant volumes. Therefore, in this case it is not necessary to use for irradiation various irradiating devices (mirrors, lenses, horn), forming quasi-plane electromagnetic waves with a significant cross-sectional area. Moreover, localization energy of the irradiating field over an area comparable to the cross-sectional area of the object, makes it possible to reduce the required power generator devices.

The method of irradiating small objects by placing them in a regular transmission line, or more precisely, to that part of it that is occupied by the electromagnetic line passing through energy [1, 3, 58, 73, 91]. Additional winnings in this In this case, there is also the presence of significant shielding of the experimenter and measuring equipment from unwanted irradiation by fields Microwave. However, the use of transmission line waves for irradiation has a number of disadvantages. The main one is the difference between the structure of the incident wave and the structure of the free space wave. This applies both to amplitude unevenness along the wave front, and to a violation of the relationship between the vectors of electrical and magnetic fields. In addition, the presence of inhomogeneities in the line often leads to an additional change in the structure of the falling on the object of the wave, which significantly depends on the frequency, which can be the cause of erroneous conclusions about the frequency properties of that or other object. The reason for this is the higher types of waves that arise on inhomogeneities. As a rule, this is not observed when irradiation of an object in free space due to the significant attenuation due to reflections. The presence of standing waves in the line, which arise during reflections of the main type of wave, also violates as the relationship between the components of electric and magnetic fields, which in principle can change the picture of the development of effects, so and the overall amplitude of the wave incident on the object. General requirement to irradiate biological objects in transmission lines, such thus are:

— the correct choice of the type of transmission line that provides
proximity of the field structure over sufficient areas to the field structure
free space;

— ease of determining the power flux density at the point where the object is located using integral parameters in the line (total power in the line, standing wave coefficients in sections of the line);

— correct selection of parameters of line elements to ensure acceptable uncertainty in the assessment of the force acting on the object
fields

One of the most important issues when irradiating biological
objects is to ensure the possibility of obtaining information
about the functional state of the object during irradiation ("under the beam"). Changes that occur in an object can be either long-term in nature, manifested in long-term consequences, or quickly

changing, disappearing with the cessation of irradiation. An example of the latter is work devoted to the effects of microwave EMF
onto membranes [58]. Therefore, in addition to the above requirements, the irradiation device must contain a removal system
information. Also important, from the point of view of the degree of severity of the observed effect, is the orientation of the object relative to the vectors
fields, that is, issues of fixing an object in the irradiation zone also have
of paramount importance.

The observed biological effect of microwaves ultimately depends on the magnitude of the field inside the object. Can usually be calculated
the magnitude of the field inside the transmission line. So, if the irradiator is
waveguide with a TE10 wave, then the power flux density (PPD) in the traveling wave mode is determined by the relation:

$$ÿÿÿ\ ÿ = \frac{P}{0.5(a \times b)}$$

where a and b are the transverse dimensions of the waveguide.

However, this dependence does not take into account the properties of the object that lead to to reflections and disruption of the field pattern in the waveguide. Hence,
there is a need, at a minimum, to measure the amount of reflected power.

We are dedicated to the consideration of these issues and their practical implementation.
puppy is the real head.

4.1. Selecting the type of transmission lines for irradiating small biological objects

In the technical literature (see, for example, [206]) it is quite widespread
and the devices for channeling microwave energy and irradiators are discussed in detail. The theory of their calculation, tabular data of constructive
parameters, data on electrical and mechanical strength, etc.
However, all information about these devices, about the types of waves that exist in them, is given from the point of view of their applicability in solving technical problems.
or other technical problems. We will try to evaluate these systems

from the point of view of their applicability in biological experiments, then
we will consider the criteria for selecting irradiators that best meet
certain requirements of a biological experiment. There will always be
There are special problems, the solution of which requires the presence of
any special irradiation conditions, for example, irradiation of biological objects in fields with a large intensity gradient or irradiation
the same objects from different sides using a rotating field.
In the vast majority of irradiation of biological objects, it is necessary to create conditions for uniform irradiation in free space
or, conversely, local irradiation of individual areas of the object.
Obviously, the choice of one or another transmission line as an irradiator
should be determined by the correspondence of the field picture in it to the task set.
This correspondence is the condition for optimizing the choice
irradiator.

Flat lines turn out to be the most satisfying to the above provisions. Of these, it is natural to highlight, first of all,
lines with the TEM wave, providing the relationship between the vectors
E and H equal to Z0 (Z0 = 377 Ohm). These include shielded strip lines, symmetric strip lines and asymmetric strip lines.

The field structure in the mentioned types of lines is quite close to the ratio of vectors E and H in free space, and the specific
the choice of one type or another depends on additional reasons.

Thus, a shielded strip line is preferable from the point
view of its complete shielding from external space and, therefore,
from the point of view of the absence of influence of the electromagnetic energy dissipated on inhomogeneities of the line on various elements of the measuring equipment and on the experimenter. However, if transverse
line dimensions are comparable to the wavelength, line inhomogeneities
(in particular, the irradiated object itself) can serve as sources
higher types of waves, which disrupts the structure of the field on the object in an almost indefinite way. Asymmetrical strip line
attractive due to its simplicity of manufacture, ease of access to the area
premises of the object.

The symmetrical stripline is an intermediate case
for the lines highlighted above.

One of the most widely used guiding structures is the rectangular waveguide. It satisfies all the requirements put forward above and imposed on the irradiator of biological objects, with the exception of one - in a rectangular waveguide

with the main wave TE10, according to Brillouin's concept, propagate
two TEM waves, and this is why the structure of the field differs from the structure fields in free space. Strip lines and rectangular
waveguides are characterized by high field uniformity in the middle part
cross section through which the main part of the propagating electromagnetic energy is transferred. However, when located in this
In the area of the object, the field pattern is naturally disrupted [206]. With another

On the other hand, the requirement to bring the irradiator field pattern closer to that for free space is dictated more by the desire to ensure ease of extrapolation of the results obtained in laboratory conditions to natural irradiation conditions. **4.2. Reflections in the irradiator with an object**

When energy propagates from the generator to the load, the incident electromagnetic wave undergoes reflections from inhomogeneities of various types. An inhomogeneity in the microwave EMF energy channel channel can be any section of it where the specified ratio of field vectors is violated. In such a section, the complex resistance will be different from the wave impedance of the path and, depending on what type of resistance it has, there will be a reflection of a current or voltage wave. As a heterogeneity, one can imagine a narrowing of the waveguide cross-section along a wide wall (capacitive reactance), or along a narrow wall (inductive reactance), or simultaneously along both walls (resonant circuit). These types of inhomogeneities are presented in Fig. 4.01. As a heterogeneous

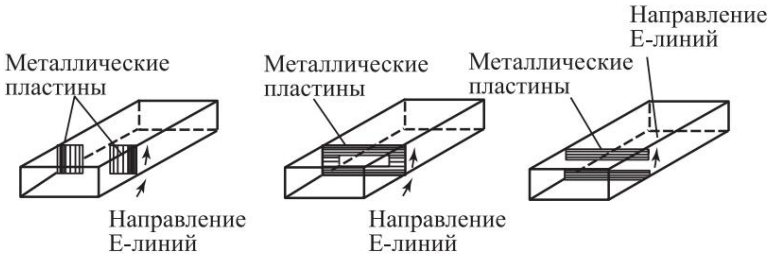

Rice. 4.01. Types of inhomogeneities in a rectangular waveguide

A coaxial-waveguide junction can also serve as a solution. Due to incomplete matching of the waveguide with the load, reflections also occur from the latter. Finally, the biological object itself with its fixation system inside the waveguide can serve as heterogeneity. Reflections from all inhomogeneities also represent electromagnetic waves with different phases. The resulting voltage distribution along the line, obtained by summing

When the voltage of the incident (Upad) and reflected (Uref) waves changes, it forms a standing wave. The reflected wave, reaching the generator in phase with the incident wave, increases the field strength at points spaced apart at a distance of ÿ/2 along the line. If the reflected wave reaches the generator in antiphase with the incident wave, then the total field strength at the same points decreases. The location of these points is usually uncertain. Therefore, a change in tension along the line introduces uncertainty into the determination of the field acting on the object. The ratio of the maximum value of the standing wave voltage Umax to the minimum Umin is called the voltage standing wave ratio (VSWR) and is determined by the relation

$$KCBH = K = \frac{Umax}{Umin} = \frac{Down + Up}{Downward \ddot{y} Downward}$$

The reciprocal of VSWR is called traveling wave ratio (KBVN). The VSWR value is related to the reflection coefficient as follows:

$$D = \frac{K \ddot{y} 1}{K + 1} \qquad K = \frac{1 + D}{1 \ddot{y} D.}$$

The voltage values Umax and Umin are read from the scale of the measuring device, the sensor of which is a crystal detector with a small antenna (probe). Because the detector is weak connected to the line in which electromagnetic energy propagates, and operates at low currents, that is, in a quadratic section current-voltage characteristic, then in practice the following formula is used to determine VSWR [220]:

$$K = \sqrt{Umax/Umin} .$$

To improve measurement accuracy, you must first remove the current-voltage characteristic of the detector, since the actual form of the characteristic is for different detectors and for different areas may differ significantly from quadratic. Details with methods for measuring quantities reflecting propagation conditions electromagnetic energy in transmission lines, you can get acquainted in [220]. Thus, in practice, in the transmission line used as an irradiator, there are always inhomogeneities that lead to the formation of standing waves in the line and difficult to eliminate uncertainty in the parameters of the field acting on the object.

In the simplest case, the irradiation device has three inhomogeneities that can create uncertainty in the determination parameters of the influencing field: the object itself, load and transition from the feed line to the standard transmission line. To determine the amplitudes of the incident and reflected waves in the high-frequency path (usually at the output of the microwave generator) a meter can be turned on backward wave, for example type P2-2, which makes it possible to take into account the reflected wave. Thus, to the requirements discussed above, presented to the irradiating device, it must obviously be one more added. Approximation of irradiation conditions in experiment to irradiation in free space, other things being equal the greater the ratio of the cross-sections of the object's transmission line, the better. At the same time, however, it must be remembered that with an increase in the cross-section of the transmission line to ensure a given value of PPM it is necessary to increase the output power value generator, which is not always possible and in any case impractical. The most optimal, apparently, should be considered the line transmission having a cross section at the point where the object is located with characteristic impedance equal to the impedance of the object. Besides,

it is desirable to minimize reflections from the load, which would lead to to increase the accuracy of determining the power in the line. As shown practice, excellent results can be obtained by using as load wedge made of plexiglass with beveled planes in horizontal and vertical planes and filled with NaCl solution. Different types of loads applied for absorption power at the end of lines are considered in [206]. As a second option for irradiating an object, the case can be considered when the cross sections of the transmission line and the object are close or equal to each other. In this case, almost all of the reflected power will be determined by the parameters of the object.

4.1. Registering object parameters synchronously with irradiation

4.1.1. Electrode system for recording electrophysiological information

The principle of constructing artifact-free electrodes. As indicated earlier, recording current information about the functional the state of a biological object during the entire experiment on exposure to microwave EMF is one of the central tasks. First It is also of interest to register electrophysiological information under conditions of irradiation of a biological object with an electromagnetic field. Therefore, it is necessary to consider the general requirements to a system for recording this information in these conditions. What already It was noted that it is practically impossible to eliminate inhomogeneities from the transmission line, that is, it is impossible to create an ideal traveling wave. Consequently, any orientation relative to the field vectors E and H any metal conductors is impossible without inducing microwave currents in them. This means that the use of traditional in biology, physiology, methods and devices for removing biological information is impossible without distorting the results obtained.

In this case, significant high-frequency potentials are induced on the supply electrodes, even if their position in the field is selected. These potentials distort the field directly at the point of contact with an object. On the other hand, penetrating the input circuits of amplifiers and when detected on them, they become sources of low-frequency interference to the object, which can significantly distort the picture of the effect being studied.

Frey's proposed coaxial electrode (US patent 3,540,434) although it significantly reduces the degree of interference amplification equipment does not solve the issue of distortion of the influencing EMF.

From general physical considerations it is clear that a decrease in the diffraction of the acting field on cylindrical formations, which

These electrodes can be achieved by increasing their volumetric resistance so that the total diameter of the cylinders is less than the thickness of the skin layer in its substance. At the same time, the cylinder begins to dissipate wave as a dielectric body, that is, significantly smaller compared to metal formations. Surface waves such
cylinders decay extremely quickly and as a result one can expect that electrodes are much smaller in diameter than the wavelength of the irradiating fields will distort the incident field near them significantly less
compared to metal electrodes. Transitions from such electrodes
standard metal wires must be removed from the area
action of a high-frequency field. It is advisable to install low-pass filters between high resistance connections and metal wires for
preventing high-frequency energy from reaching the latter.
The fulfillment of these conditions can be achieved by using thin dielectric tubes with a diameter of
2-3 mm filled with Ringer's solution.

Low-pass filters are formed by the same tubes, which play the role of internal conductors of coaxial absorption filters (a metal screen is installed on top of the tube).

The amount of attenuation in such filters at frequencies of the order of 1010 Hz is approximately 30 dB/cm.

Design of artifact-free electrodes. Several types of artifact-free electrodes have been developed that allow the removal of bioelectrical activity either by applying them to
object, and by implantation [221]. The general requirement for electrode designs is compliance with the condition < 1 S/m, where

— electrical conductivity of the substance used to contact the electrode with the object. These may include Ringer's solution, thin
metal films on a dielectric substrate and microwires
made of nichrome. Electrode designs based on application
thin silicone tubes filled with Ringer's solution are the simplest. To prevent liquid bubbles from bursting
air, it is advisable to insert a wick made of cotton fabric into the silicone tube. The tube itself is put on a tip that has
the shape of either a drawn glass tube (suction cup electrode) or
various types of cups tightly filled with cotton wool (applied electrode). The same design can be made with microwire.
These electrodes are convenient for recording bioelectrical activity from the surface of the object.

For implantable electrodes, a design that is more suitable having a tip in the form of a thin glass or ceramic
a rod coated with a thin film of platinum followed by coating with a dielectric. For the effective electromagnetic field in the band
frequencies 10 MHz ÷ 3 GHz surface resistance of metal
film should lie within 1 ÷ 5 kOhm, related to the area
its surface. For all electrode designs, the connection diameter

body tubes are selected on the order of 1–3 mm. In Fig. 4.02 shown sections of the described electrode designs.

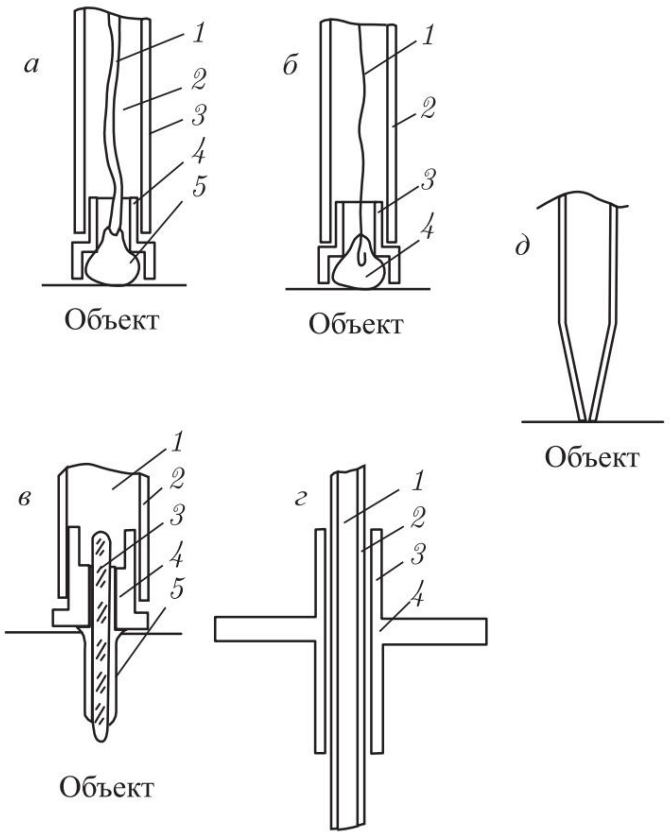

Rice. 4.02. Sections of designs of artifact-free electrodes: a) *1* - wick, *2* - electrolyte, *3* - dielectric, *4* - housing, *5* - cotton wool; b) *1* - microwire, *2* - dielectric, *3* - body, *4* - cotton wool; c) *1* - electrolyte, *2* - dielectric, *3* - platinized glass rod, *4* - body, *5* - protective coating; d) *1* - electrolyte, *2* - dielectric, *3* - metal tube, *4* - screen (FNC); e) suction electrode

System for supplying bioelectric activity potential to recording equipment. As already stated, to avoid possible interference when an object is irradiated with an electromagnetic field Microwave, the transition to metal electrodes must be removed from irradiation zones. Depending on the type of object and irradiation conditions The length of low-pass filters can reach tens of centimeters. Transitions “liquid-metal” are combined with a system for filling tubes with liquid into one unit, which is located inside the screen. The number of liquid-metal transitions is determined by the number of electrodes. The metal electrode is made of silver or silver chloride wires with a diameter of about 0.3 mm and a length of 15 ÷ 20 mm. Inside screen, a plexiglass strip is installed, in the body of which holes are drilled for attaching metal electrodes. On this same fittings are attached to the strip with glue for connecting to low-pass filters and nozzles for rubber bulbs with a diameter of 40 mm, used for

filling the electrode system with conductive liquid. The screen has a connector for connecting metal electrodes with recording equipment via a cable. The screen itself is attached to the waveguide by soldering using rigid rods. As practice has shown, it is most convenient to mount the screen against the narrow wall of the waveguide, since in this case the output of tubes with liquid introduces minimal distortion into the field picture and, in addition, tubes with liquid can be enclosed in rigid tubular screens, which are soldered at their ends to the walls waveguide and screen. In Fig. Figure 4.03 shows a cross-section of the liquid-metal transition unit and a block diagram of the transfer of bio-electrical activity as a whole.

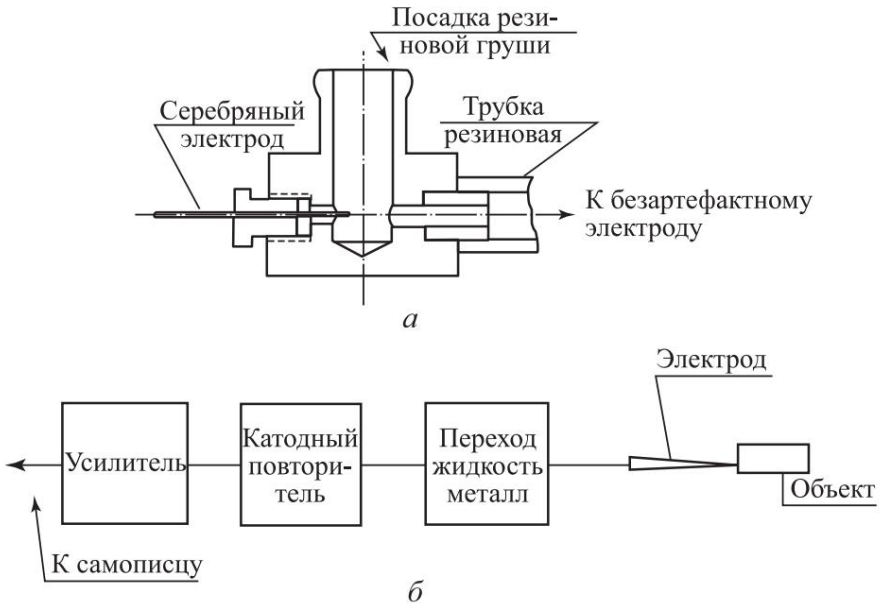

Rice. 4.03. Transfer of bioelectrical information synchronously with the irradiation of the object by EMF: *a* - section of the “liquid-metal” transition node; *b* - block diagram of the bioelectrical information transmission system

Due to its low intrinsic resistance, the electrode system can be connected directly to recording equipment via a cable. However, if necessary, cathode (emitter) followers can be placed inside the screen to match the electrode system with the recording equipment. The designed system was tested when recording electrograms in a field with a pulsed PPM of up to 2.5 W/cm2. When the sensitivity of biopotential amplifiers (4EEG-1 type

encephalograph) was up to 5 ÿV, the amplitude of the induced microwave pulses in the recording did not exceed the amplitude of the 4EEG-1 noise at any position of the electrodes in the field.

4.2. Methods for fixing biological objects during irradiation with microwave electromagnetic field

As mentioned above, the orientation of a biological object relative to the vectors E and H of the irradiating field plays a significant role role in the development of one or another observed microwave effect. It was shown in [222] that by changing the length of the preparation section tibial nerve of the frog, parallel to the electrical vector, you can change the severity of the effect, which consists in changing the speed of propagation of the excitation wave when irradiating the drug with microwave pulses.

In general, there can be three main orientations: orientation relative to the E vector - E-orientation, orientation relative to the H vector - H-orientation and orientation relative to directions of energy propagation - K-orientation. There will be Several specific methods of fixation of various preparations are considered.

Fixation of preparations in the form of thin long formations.

The large ratio of the length of the object to the diameter makes it especially clear to demonstrate the dependence of the magnitude of the studied parameters of the object on its orientation relative to the field vectors. As As an example, a specimen of the frog tibial nerve was chosen. For this object, changes in the speed of wave conduction were studied excitation and action potential amplitude. In Fig. 4.04 shown three ways to fix a nerve preparation relative to the E-vector. It was found that with an increase in the total length of sections of the nerve preparation parallel to the E-vector, the degree of severity increases effect (Fig. 4.05). At the same time, when the object is located perpendicular to the E-vector, changes in the studied parameters are comparable with changes in the control. In Fig. 4.06 provides a drawing chamber designs for the nerve preparation. The camera itself and the cover made of organic glass. The electrodes are molybdenum glass tubes drawn and sealed at the end with an outer diameter of 4 mm. On the side wall of the drawn part The tubes are cut. The electrodes are attached so that the cuts were facing upward. Bandages made of silicone tubular rubber serve as a seal when attaching electrodes to the chamber. Electrodes connected to an electrical stimulator using silicone tubes ESU-1 and biopotential amplifier UBP1-02. Due to the required length of the tubes is approximately 200 mm, which leads to the appearance of an additional resistance of 5 ÷ 10 kOhm between stimulator output and object, amplitude of stimulation pulses rises to 20 V. Ringer's solution is poured into the chamber so that the electrodes were covered with it, and with the help of rubber bulbs the entire system filled with solution. When filling the system, it is necessary to constantly

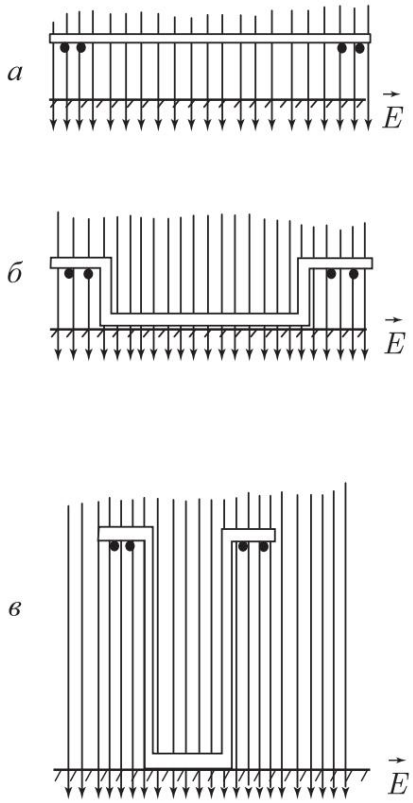

Rice. 4.04. Various methods of fixing the drug relative to the E-lines of the electromagnetic field. *A* - the drug is located perpendicular to the E-lines; *B* — the preparation is partially located perpendicular to the E-lines; *B* - the preparation is almost completely parallel to the E-lines

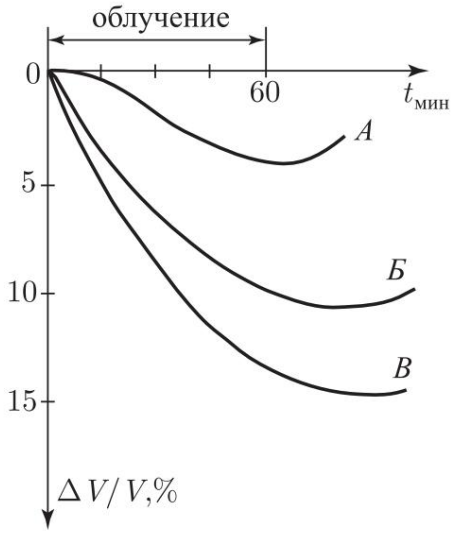

Rice. 4.05. Values of excitation wave conduction velocity corresponding to three methods of fixation of a frog nerve preparation

add a solution to the chamber so that air does not get into the tubes, which will lead to a sharp increase in the resistance of the electrode system and, as a rule, to disruption of the system. After filling all

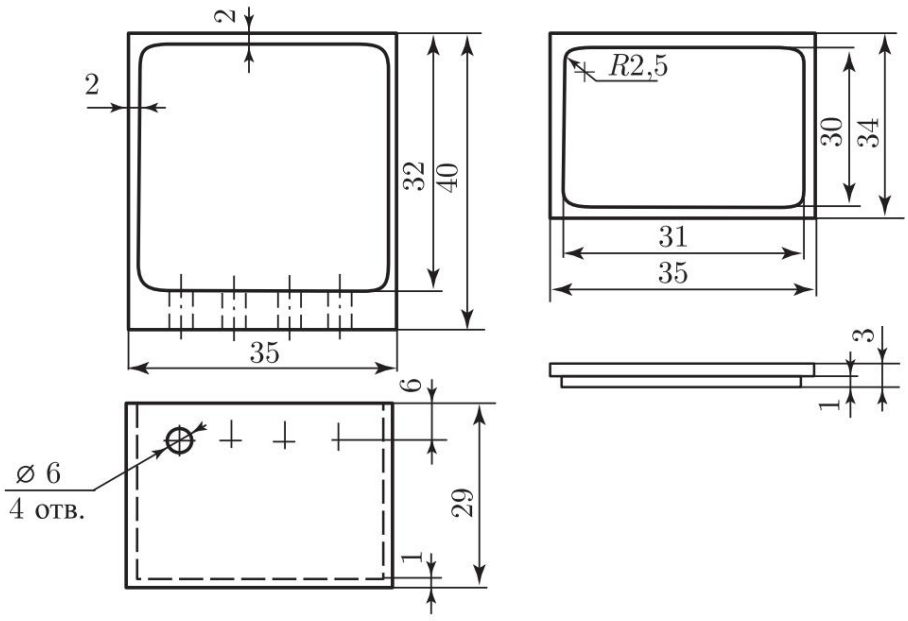

Rice. 4.06. Design of a chamber for fixation of a frog nerve preparation

Four tubes of Ringer's solution are removed from the chamber. All that remains is a thin layer - a few drops at the bottom to feed the drug. Then
The drug is placed on the cuts on the electrodes and the presence of stimulation and response is checked. The chamber is tightly closed with a lid, which
Provides air humidification inside the chamber. After this the camera
with the drug ready for use. The camera fits into a rectangular
waveguide with a narrow wall height of 31 mm and an H10 waveform.
Method of isolation of frog nerve preparation and methods of treatment
described with it [223, 224].

Fixation of preparations with a small ratio of the lengths of two characteristic dimensions. As an example, a preparation of an isolated frog heart with a ratio of the longitudinal to transverse axis of the order of 1.5 ÷ 1.7 was chosen. For this object, changes in the rhythm of contractions were studied, in particular, changes in the *P-Q* interval and the magnitude
cardiocycle. These changes were observed on the electrogram of the drug, recorded using suction electrodes. Camera design
and its dimensions are shown in Fig. 4.07. The chamber is an open bath made of organic glass, with thickening of the side walls
reinforced with silicone rubber sealing sleeves
suction electrodes. Four legs are glued to the bottom of the chamber
made of plexiglass, with the help of which the camera is held on a special table made of foam plastic. The table is mounted on plexiglass bushings
to the hatch located on the side wall of the waveguide (wave-water cross-section 150 × 240 mm2). Rubber tubes pass through the same hatch,
connecting the chamber electrodes to the potential removal system.
The chamber is filled with Ringer's solution, and using pears one by one
all three channels are filled with solution with constant addition of solution

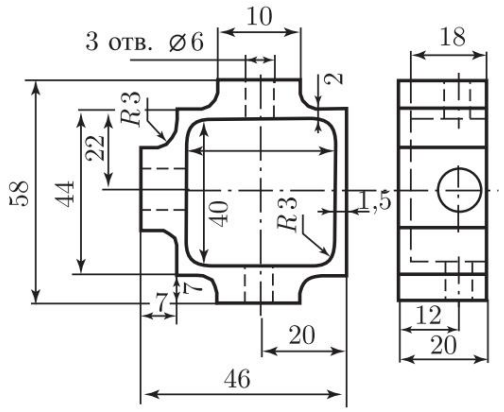

Rice. 4.07. Design of the chamber for fixing the isolated drug
frog hearts

Ringer into the chamber to prevent air from entering the system. A drug
the heart is transferred into the chamber, carefully brought in without injury
to the electrodes. Then lightly press the pear and the atrium area
The drug is brought close to the suction electrode. The bulb is released and the drug is sucked to the electrode. Same procedure
is also carried out with two other electrodes, to one of which the ventricle is attached, to the other, indifferent, the lateral side
heart drug. Excess Ringer's solution is aspirated from the cuvette.
syringe. The drug should be almost completely in solution.
In Fig. Figure 4.08 shows a cross-section of the entire assembly of fixation and abduction system.

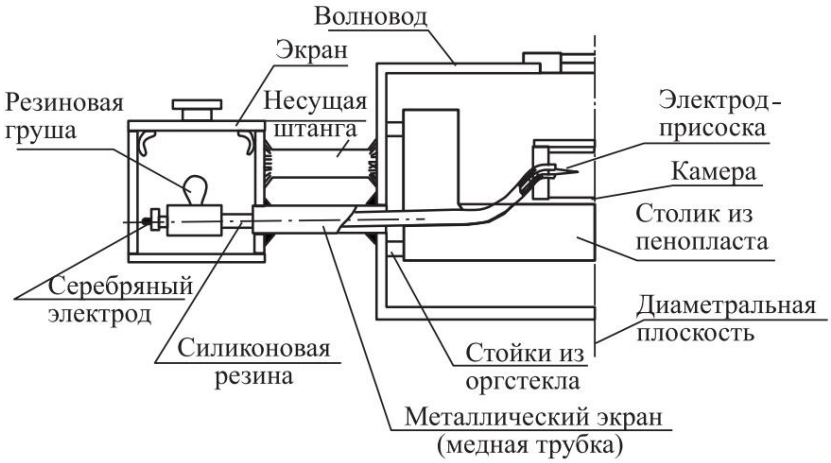

Rice. 4.08. Schematic representation of the drug fixation and removal system assembly (irradiation of drugs in a rectangular waveguide)

In studies conducted on the effects of pulsed fields
A specimen of a frog heart showed that the degree of manifestation of the observed effects depends on the orientation of the object in the microwave field. If experimental conditions require stabilization of the object's temperature, then through the side wall of the waveguide and through copper tubular screens

the same silicone tubes are inserted and connected to the chamber,
in which the object is located. The second ends of the silicone tubes are connected to the thermostat.

Fixation of small laboratory animals. Since the range
medical and biological tasks when irradiating whole animals are very
is wide, only some fixation methods will be considered here
animals in a microwave field in closed irradiators and removal methods
biopotentials.

Free warm-blooded fixation. The rat or mouse is placed in a perforated box with a lid made of plexiglass.
It is necessary that the animal sits quite tightly in the box and does not
could change poses. To remove biopotentials from an animal, you can use cup
electrodes and the removal system described above. In this case, the animal (rat)
is given anesthesia, since
Due to its high activity as a result of constant movements, useful information turns out to be masked by a spurious signal.
Although the use of cup electrodes ensures reliable recording of an ECG from an animal, placing them on the animal's paws
and fastening with rubber bands is not very convenient. With the aim of
To eliminate the inconvenience in working with these electrodes, a special chamber for warm-blooded animals was developed with built-in
chambers with three electrode pads made of filters
made of porous glass. In the side walls of the chamber, at the level of the electrodes
Plexiglas tubes were mounted on glue, onto which rubber tubes were put for connection to the filling system.
The bottom of the chamber is filled with Ringer's solution and using rubber
pears, each channel is sequentially filled with Ringer's solution,
which is sucked into the system through the pores in the glass. At the end
This procedure removes excess Ringer's solution from the chamber, the chamber dried. The anesthetized animal is placed in a chamber so that
the front and one hind paws were placed on the electrodes. This design for ECG recording was tested in a waveguide with a cross-section
150 × 270 mm2 when irradiating an animal with pulses up to
500 W. The design of the chamber is shown in Fig. 4.09.

Rigid fixation of a cold-blooded one. When taking an ECG, the animal must be immobilized. The frog can be immobilized by destroying
spinal cord. After this, the frog is placed on a foam table with its belly up, its legs are secured using U-shaped staples.
made of polystyrene foam. A small portal is installed above the chest, on which two discharge suction electrodes are attached, the third
indifferent, attached above the hind leg. The areas of skin under the electrodes are carefully cut out. After this, the electrodes and the entire system
filled with Ringer's solution and suctioned to the animal's body
using the method described above. Irradiation is carried out in a rectangular waveguide with a cross section of 150 × 270 mm2. In Fig. 4.10 shown schematically the location of the animal on the table, in Fig. 4.11 - ECG of a frog,

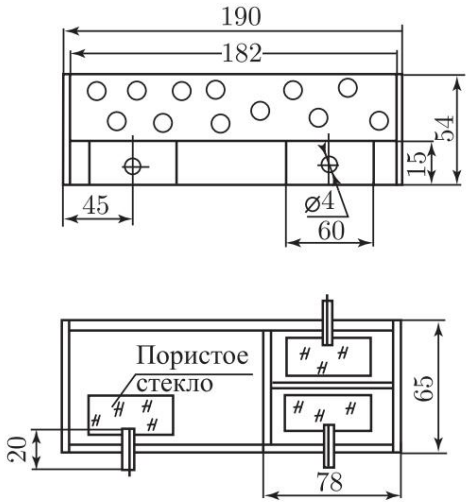

Rice. 4.09. Perforated box with pads-electrodes made of porous glass for ECG recording in rats

registered in the described way. The methodology for recording a frog's ECG under conditions of microwave field irradiation is described in detail in [225].

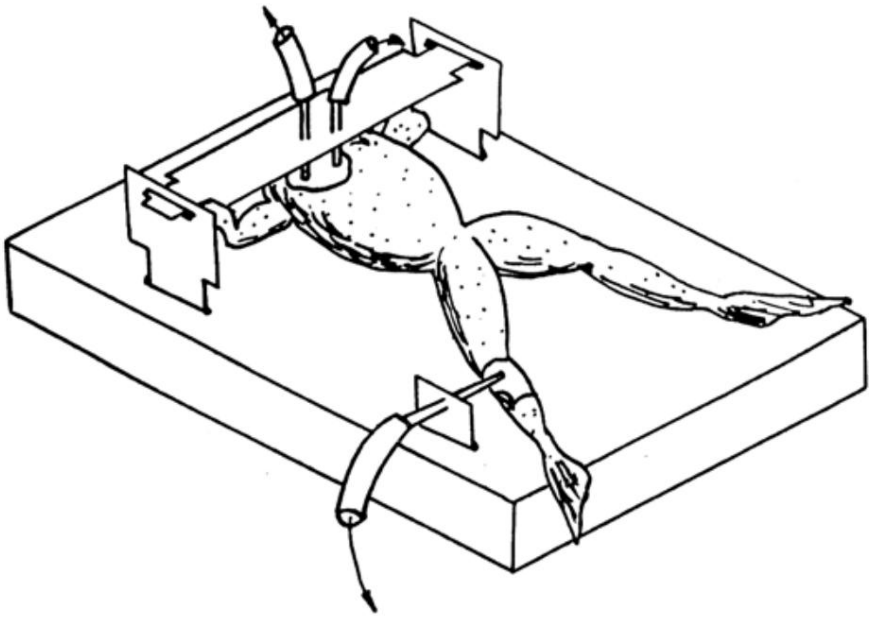

Rice. 4.10. Position of the frog on the foam table during ECG lead

Fixation of liquid biological media. Of well-known scientific and practical interest is the effect of the energy of electromagnetic vibrations on cellular structures, homogenates, and aqueous solutions of various chemical compounds. In this case, irradiation can be carried out by placing a test tube with liquid (or a coverslip with a thin layer of liquid) in a rectangular waveguide. In the diametrical plane of the wide wall of the waveguide, a beyond-limit wave-

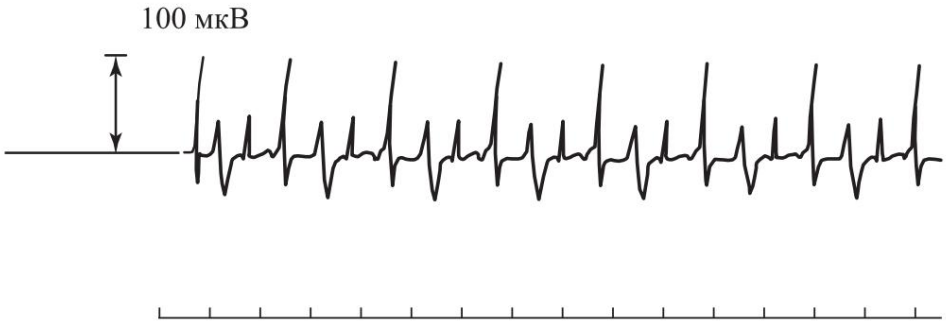

Rice. 4.11. Sample ECG recording of a frog under EMF irradiation conditions (PPMI = 1.8 W/cm2)

water with a height of 60 ÷ 80 mm, into which the test tube is lowered (Fig. 4.12). The test tube with liquid turns out to be parallel to the E-vector,

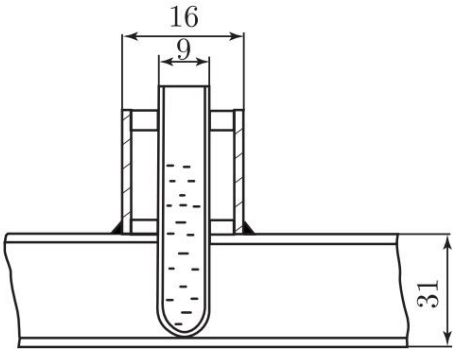

Rice. 4.12. Irradiation of cell suspensions in a rectangular waveguide (explanation in the text)

the field in it is maximum and can be equal to the field in the waveguide. Thus, with a pulse power of 72 W and a duty cycle of 20 in a test tube with a 1 M NaCl solution of 1.5 cm3, the rate of temperature increase was 0.1 deg/s. The waveguide cross-section is 31 × 240 mm2. The outer diameter of the test tube is 9 mm, the height is 120 mm, the inner diameter of the transient waveguide (copper tube) is 14 mm.

Chapter 5

ELEMENT MANUFACTURING TECHNOLOGY WAVEGUIDE TECHNOLOGY IN CONDITIONS RESEARCH LABORATORIES

As can be seen from the material discussed above, irradiation of a biological object with microwave EMF is quite complex.
task when it comes to recording useful information during
irradiation. In addition, supply directly to the transmission line
With all the additions listed above, in order to create certain irradiation conditions, the line itself turns into a measuring complex. Due to the inability to purchase such

complex of an industrial design, the task of its manufacture arises
in a research laboratory setting. In this regard, any experience
on the creation of such complexes should be viewed only positively. Therefore, it may be considered appropriate to present here
a small practical material on creating irradiators and the necessary additions to them in a laboratory setting.

5.1. General principles of manufacturing technology elements of waveguide technology

As already mentioned, when transmitting microwave energy through internal
currents flow to the (outer) surfaces of the guide structure, and the higher the frequency of oscillations of the electromagnetic field, the less
the depth of penetration of microwave current into the conductor. This means that the conductivity of the conductor must be very high in order to reduce thermal
losses and attenuation in the transmission line. From this point of view, the most acceptable materials are copper or brass. Because the
according to the considerations discussed above, in a laboratory setting, a rectangular waveguide can be considered the optimal irradiator, then
making it from copper, especially for operation in the decimeter range, will lead to the creation of a very heavy device that does not have sufficient rigidity. Therefore, it is preferable to manufacture
waveguide made of brass. Advantages: accessibility and lower cost
compared to copper, cost, sufficient mechanical strength,
greater rigidity compared to copper construction, which allows the original dimensions to be maintained during operation
and configuration, and accordingly the specified parameters. Because the
the length of such an irradiator is small compared to a conventional line
transmission, then the attenuation of energy as it propagates along the waveguide is negligible. Therefore, the need to silver the internal

waveguide surfaces disappears. The brass parts of the waveguide are attached to each other using flame soldering using POS grade solders. The most suitable flux is 30% phosphoric acid or active flux. The use of this flux does not require preliminary preparation of the metal surface for soldering - mechanical cleaning, degreasing, etc. The flux gives good fluidity to the solder and ensures reliable adhesion. Since it is necessary to solve a wide range of biological problems using the irradiator, it is advisable to make it collapsible - consisting of several sections connected to each other with bolts. If necessary, one of the sections can be replaced with a new one. In general, a rectangular waveguide can be divided into three sections - exciter, measurement and load. With the help of an exciter, a transition is made from the supply coaxial cable to a rectangular waveguide with simultaneous matching of the generator with the waveguide. The measuring section contains devices for fixing the object in the microwave field, devices for retrieving useful information, stimulation, powering the object, observation, etc. The ends of the walls of the sections are inserted into the flanges and the seams are soldered. The load is used to absorb energy propagating in the waveguide in order to create a traveling wave regime. The load is a wedge-shaped box made of sheet organic glass 3 ÷ 4 mm thick, glued with dichloroethane or formaldehyde and filled with a NaCl solution at the rate of 50 g per 1 liter of distilled water.

The technology for assembling the sections is as follows: the lower wide wall is inserted alternately into the flanges installed vertically, then two side walls, then the upper wide wall is mounted. The walls are tightened with wire bandages. The section assembled in this way is ready for soldering. First, the longitudinal seams are soldered, then the section is placed vertically and the joint between the flange and the side walls is soldered. After this, the section is placed on the second flange and the second joint is soldered. If the order of soldering the seams is violated, the section will suffer from heating, or the seams will burst due to expansion when heated. During soldering, you must ensure that the tin does not flow inside. After soldering, a thorough washing of the assembled structure in running warm water with alkali is necessary. After washing using files and sandpaper, it is necessary to remove any remaining tin from the surfaces and keep the finished section in running warm water for 30–40 minutes to remove any remaining flux. The next operation is to increase the electrical conductivity of the waveguide walls by removing oxides from the surfaces of parts using nitric acid. Following all safety rules when working with acids, each section is treated in 50% nitric acid in special baths for 5–10 s. After this, the sections are washed in a bath of running water and passivated in chromium. Then rinse in warm running water for 40–60 minutes. Ready

the upper sections are dried and painted (except for the internal planes and ends flanges). During assembly, gaskets are inserted between the flanges of the sections made of sheet lead 1 ÷ 1.5 mm thick to prevent leakage
energy from the waveguide. The coaxial-waveguide junction must be
installed on the waveguide at a distance ÿÿ/4 from the end of the waveguide, so that the wave reflected from the end would be in phase with the wave propagating towards the object and the load. This improves matching
waveguide with generator. In practice, the coaxial-waveguide junction is installed at a distance from the end, somewhat less
ÿÿ/4, due to the fact that during the manufacture of the waveguide it is impossible to accurately maintain all dimensions obtained by calculation. For accurate
exciter settings, a trimming capacitance is introduced into the quarter-wave section, allowing you to increase the equivalent length of this
section and thereby tune it into resonance. Technology issues
The manufacture of microwave units is considered in [206].

5.2. Development of an irradiation complex

The following components can be roughly introduced into the concept of "irradiation complex": 1) irradiator; 2) matching device; 3) agreed
load; 4) object fixation device; 5) useful removal system
information.

Let us consider a practical solution to the problem of creating such a complex to support experiments on biological
microwave effects. It is more expedient to have any one type of irradiator (measuring section), with the help of which it would be possible
carry out irradiation of various biological objects, that is, solve a certain range of biological problems. Therefore, first
it is necessary to define this range of tasks. The most difficult, from the point of view technical support, are electrophysiological
research under conditions of microwave EMF irradiation. As an example
Let us highlight several problems of interest to physiologists,
engaged in research into the biological effects of microwaves:

1. Study of the dynamics of time and amplitude parameters
isolated self-oscillating systems.
2. Study of the conditions for the functioning of excitable structures.
3. Study of the rhythm of heart contractions of the entire organ-
nizma.

Once the biological task has been set, it is necessary to consider a number of issues that allow us to proceed to the development of the complex,
namely:

1. Selection of an object and the conditions for its experience.
2. Determination of the method of fixing the object in the irradiation zone.
3. Determining the type of useful information taken from the object,
and systems for collecting this information.

4. Calculation of the geometric dimensions of the irradiator for a given length waves in free space.

Let's consider an irradiator with an irradiation frequency of 0.8 GHz (ÿ = 37.5 cm). As objects we will choose a preparation of an isolated frog heart, a preparation of a frog tibial nerve, a whole frog and a whole rat. The choice of these objects is dictated, first of all, the degree of their knowledge, which will allow us to compare the applicability of new information retrieval systems with traditional ones. In addition, it is known that the nervous and cardiovascular systems are most susceptible to influence Microwave EMF, that is, the selected objects are of quite great interest from the point of view of obtaining information about the impact on them of this physical factor. The conditions have already been discussed above experiences of these objects and methods of fixing them in a rectangular waveguide. Therefore, we can proceed to determining the geometric dimensions of the irradiator. The required height of the side wall of the waveguide for placement of an animal in it and access to it is approximately 150 mm. In order for the main type to propagate in the waveguide waves H10, it is necessary that the wide wall of the waveguide is a value of 0.7ÿ, that is, approximately 260-270 mm. Then ÿcr = 2a = 2 × × 27 cm = 54 cm and the wavelength in the waveguide will be equal to

$$ÿv = \frac{I}{\sqrt{1 ÿ (l/lkr)2}} = \frac{37,5}{\sqrt{1 ÿ (37,5/54)^2}} = 54 \text{ cm},$$

that is, in this case ÿÿ = ÿcr. Characteristic impedance of a rectangular waveguide with a cross section of 150 × 270 mm2 with a wavelength ÿÿ = 54 cm determined from the relationship:

$$Z = Z0(ÿÿ/ÿ) ÿ/ÿ = 377 \cdot 37.5 \quad \frac{54}{\cdot} \quad \frac{15}{27} \; ÿ \; 300 \text{ Ohm}.$$

Matching a waveguide with such resistance with the output impedance of the generator (50 or 75 Ohms) can be done using resistance transformer. In practice it can be done in the form of a step transition. The solution to this problem can be found in [207]. Here are the design dimensions of the calculated step transition containing adjustment elements (Fig. 5.01) and having an input impedance of 75 Ohms.

The waveguide measuring section contains two hatches. Round, located on the upper wide wall of the waveguide, designed to place an object inside the waveguide. This hatch is used constantly and is therefore pressed against the waveguide using wing nuts The second hatch is rectangular, containing a table for fixing auxiliary devices and the object itself on it. From outside A shielded system for collecting bioelectrical information and low-pass filters are attached to the sides of this hatch (see Fig. 4.08, part II). This the hatch is mounted on the side, narrow wall of the waveguide and is dismantled

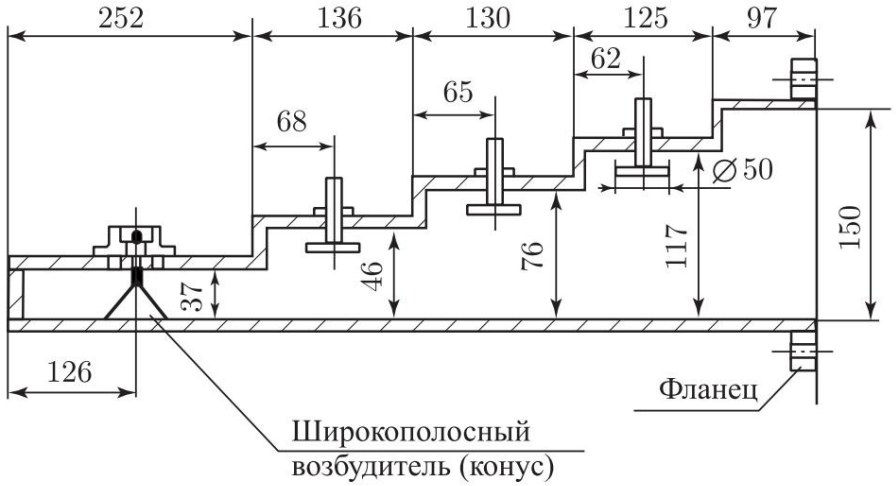

Rice. 5.01. Step transition for waveguide with large cross-section (150 × 270 mm 2)

rarely. For example, when working with rats, the table is removed, and a foam plastic plate 10–15 mm thick is placed on the bottom of the waveguide. The side hatch is secured with screws with a lead gasket.

To ensure a traveling wave mode in a waveguide, it is necessary to create conditions for energy absorption at the end of the line. To do this, a third section is introduced into the irradiator - a load, the description of which is given above. In Fig. 5.02 shows the dimensions of the load structure.

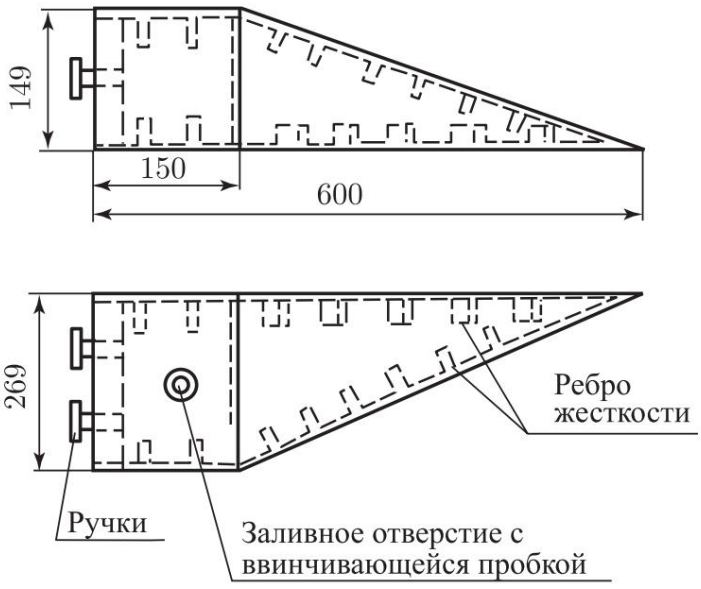

Rice. 5.02. Load design for 150 × 270 mm2 waveguide

The required load length is usually indicated in the literature as 3–5 ÿ. However, experience in working with loads of length ÿw shows that in a narrow frequency band (±10% of fres) the tuning of the waveguide makes it possible to achieve a KBVN value of no worse than 0.8, and at the design frequency - 0.9

and higher. In Fig. Figure 5.03 shows the appearance of a three-section rectangular waveguide with an operating wavelength ÿ = 37.5 cm. Together

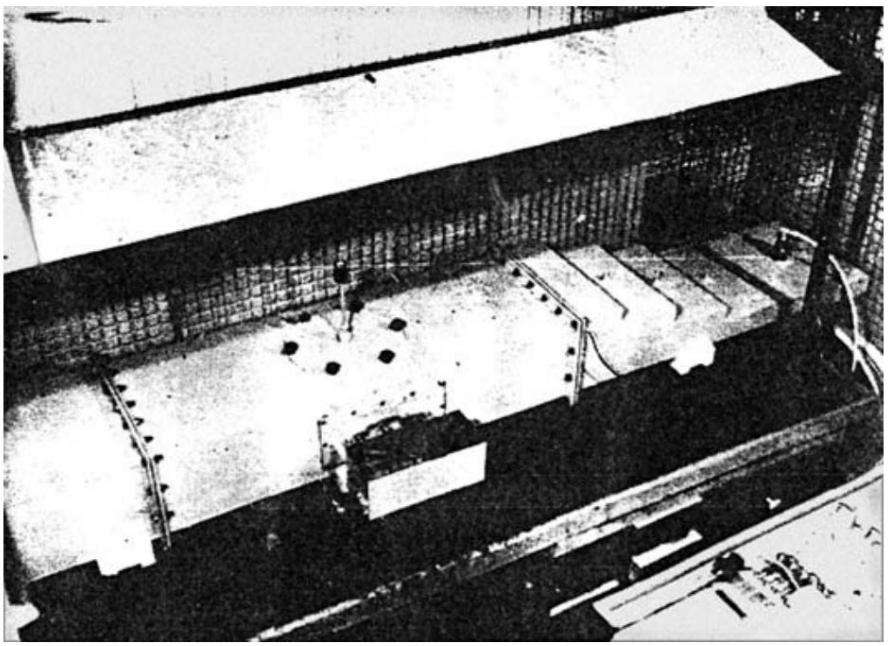

Rice. 5.03. External view of a rectangular three-section waveguide with a cross-section 150 × 270 mm2

with the developed generator based on the LMS-551V model with a pulse power of 500 W, the achieved DPP in the waveguide was 2.5 W/cm2. Obtaining such capacities is a serious technical challenge. Therefore, in order to reduce the required value output power of the microwave generator, it is desirable to minimize the operating cross-section of the waveguide at a given operating frequency. So, for irradiation of small objects (height up to 30 mm, in plan - not more than 50 × 50 mm2) it is possible to offer a version of a rectangular waveguide with an operating wavelength ÿ = 37.5 cm with a geometric cross-section 31 × 240 mm2. To ensure a PPMav value of 0.1 W/cm2, which, as a rule, is sufficient for observing many biological microwave effects, the power at the waveguide input is limited to about 4 W. If we switch to the pulse mode with equal PPMsr with a duty cycle of 10, then the required amount of power per input of the waveguide will be 40 W, which can be obtained practically using any modernized microwave generator operating on SCL type GI-11B or GI-12B. A flat waveguide does not require a matching step transition, that is, it is easier to manufacture.

The remote head of the biopotential amplifier is built into the screen containing the system for collecting bioelectrical information. UBP1-02, containing an input cathode follower. Both irradiation complexes have been used in experiments for many years with the above objects and many others. Efficiency

artefact-free electrode systems can be assessed by the appearance of the frog ECG (Fig. 4.11, part II).

When irradiating large animals (dogs), practical interest introduces a horn feed that allows for greater irradiation area. Installations containing such irradiators are described in [226]. The manufacturing technology of these devices is identical to the manufacturing technology of rectangular waveguides. In general, when When developing such an irradiator, it is convenient to construct a separate exciter in the form of a section of a rectangular waveguide with an H10 type wave and the horn itself, connected by bolts with a lead gasket on flange joint. The pathogen may in this case have a T-shaped execution. It is advisable to coordinate the output of the horn with the volume, walls which are made of radio-absorbing material (RPM), inside which the object is placed. This will significantly reduce radiation into free space. An example of such a design of an irradiator at a frequency of 0.8 GHz is shown in Fig. 5.04. When using foam concrete as a RPM in the structure, the achieved VSWR value = 1.15 (KBVN = 0.87). For operation in the frequency range 2000–3000 MHz The waveguide cross-section is 34 × 72 mm2. All other positions and the conditions described for a waveguide with a cross-section of 150 × 240 mm2 remain Precious.

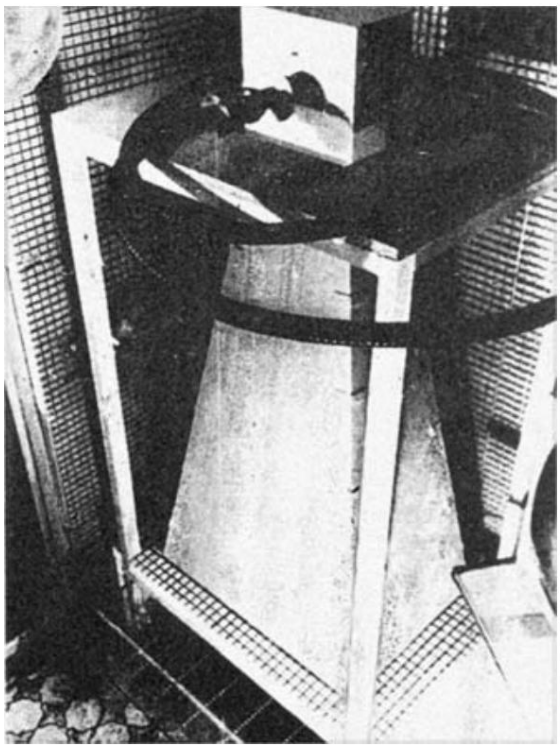

Rice. 5.04. Appearance of the horn feed with exciter and an irradiation chamber shielded using RPM

5.3. Methods for determining the power acting on biological object

The issues of determining the magnitude of the effective field inside an object are the most relevant and least developed in the world.
the current stage of setting up experiments on the bioeffects of microwaves.
There are calculation methods for determining the field inside an object for
some volumetric geometric shapes - spheres, ellipsoids,
cylinder, etc. However, this approach cannot cover everything in reality
existing situations in the experiment. On the other hand, this
modeling assumes the presence of structures with predetermined
parameters such as ÿ and ÿ - dielectric constant
and specific conductivity, and the model itself is usually isotropic
[227]. This method is convenient when working with phantoms and allows
get a general picture of the field distribution. There are also simple calculation methods for determining the field inside a transmission line;
finally, there are methods and instruments for direct measurement of incident,
reflected and absorbed powers [206]. However, all these methods are applicable either to some constant specific conditions
irradiation of objects with known and time-invariant object parameters, or for purely technical purposes. In conditions
constant change of objects, their configuration and volumes, frequency
fields or pulse parameters during pulsed irradiation, different
their orientation in the field, most of the methods described in the literature are either not applicable or do not have the necessary accuracy.
Depending on the task at hand, microwave technology uses
absorbing type wattmeters or transmitted power wattmeters. Many of them are based on a measurement method based
on converting microwave power into thermal energy. As
Converters use resistance wires, thermocouples, and thermistors. To measure high powers they are used
water calorimeters. Methods and instruments for measuring microwave power
described in the literature. When placing an object on a transmission line
part of the energy falling on it will be reflected, part will be absorbed. Depending on the ratio of the cross sections of the object
and the current irradiation zone, part of the energy will spread
further than the object along the line and be absorbed in the load. You can write down a relationship connecting all four components of the power of the electromagnetic field propagating in the line, in the form

$$Ppad = Rec. + Pch. + Proh.$$

Thus, knowing the amplitudes and phases of each of the components
This ratio allows us to determine with great accuracy the power absorbed by the object.
However, the implementation of this method is quite
complex and useful only for measuring absolute values

any parameter(s) of a specific object. On practice
It is easier to use the method of measuring transmitted power. If
The microwave path contains a directional coupler, then the power in the line
can be determined from the relation

$$Ppad = k\ A,$$

where k is the attenuation coefficient of the directional coupler, A is
readings of a wattmeter connected at the output of the directional coupler. Knowing the working cross section of the irradiation zone, it is possible to determine the average
power flux density value as

$$PPMsr = \frac{k \cdot A}{Sp}.$$

For rectangular waveguide $Sp = \frac{a \times b}{2}$ As directional
coupler, you can use a P2-2 impedance meter,
included in the gap between the generator and the irradiator. With this
In the method for determining PPMav it is necessary to ensure the mode in the line
traveling wave. The method considered, in addition, does not allow one to directly measure the field value inside the object itself. Therefore, recently the method of determining

specific absorbed power (SAP), which consists in determining the power per unit volume (or per unit weight) of an object.
Since the microwave EMF power absorbed by the object is converted
into heat, the method for determining SLM is reduced to measuring the growth rate object temperature:

$$UPM = \frac{IN}{IN} = \frac{cm\frac{\ddot{y}T}{\ddot{y}t}}{IN} = |C| \cdot \frac{\ddot{y}T}{\ddot{y}t} \quad [W/cm3\ ],$$

Where $\frac{\ddot{y}T}{\ddot{y}t}$ — numerical value of the measured temperature growth rate, degrees/ s; C —numerical value of the object's heat capacity, J/g×·
× deg, V is the volume of the object, cm3. It is more convenient to use the value measurements of UMP, expressed in W/kg. This is possible because for
most biological objects 1 cm3 ÿ 1 g. Thus, for
biological objects, we can write the following expression for
UPM:

$$UPM = 4200 \cdot \frac{\ddot{y}T}{\ddot{y}t} \quad [W/kg],$$

since the heat capacity of water is 4.2 J/g deg , which can also
be accepted for most biological objects. On practice
this measurement can be made using thermistors. Especially
Microthermistors MT-54 M are convenient for these purposes. Microthermistor
is included in one of the arms of the DC bridge powered by the element
volume with a voltage of 1.6 V, included in the diagonal of the bridge. To another diagonal included laboratory ampere-voltmeter. This method suffers, however, from the fact that measuring the rate of temperature rise directly

During the irradiation of an object, it is practically impossible due to
own heating of the thermosensitive element in the microwave field. Therefore, it seems
appropriate to develop indirect methods
determining the temperature of an object when it is irradiated with microwave EMF.

Chapter 6

EXAMPLES OF FORMATION OF HARDWARE COMPLEXES FOR STUDYING BIO-EFFECTS

Microwave

Let us consider several specific examples of organizing experiments to study the biological effect of microwaves on conductive and self-oscillating systems, and within the framework of this presentation Let's limit ourselves to the purely technical side of the issue.

Obviously, for most experiments the following devices and components are needed: a microwave generator, a modulator, an irradiator, a power meter, a system for recording useful information, a recorder for recording, a stimulator (pulse generator), an oscilloscope. In some cases, a synchronizer is also required.

6.1. Registration of the electrogram of the heart preparation frogs

The purpose of the technical support of the experiment is to register atrial and ventricular activity under the action of a pulsed field Microwave. The prepared frog heart is fixed in a cuvette made of plexiglass dimensions in plan 30 × 40 mm (or ÿ 30 ÷ 40 mm) and height 10 mm on suction cup electrodes located in the side walls cuvettes. An indifferent electrode is also located in the side wall. Electrodes using silicone tubes passed through side wall of the waveguide, connected to the filling system. Cuvette filled with Ringer's solution and using rubber tubes filled with this solution. The drug adheres to the electrodes using these pears. Registration of drug activity is carried out on cardiograph or electroencephalograph.

In Fig. Figure 6.01 shows a block diagram of the experiment. This circuit allows you to vary the parameters of microwave radio pulses, determine the power incident on an object and reflected from it in line, record the bioelectrical activity of the sinus node and ventricle simultaneously, observe the relative positions of microwave pulses and different phases on the oscilloscope screen electrograms relative to each other.

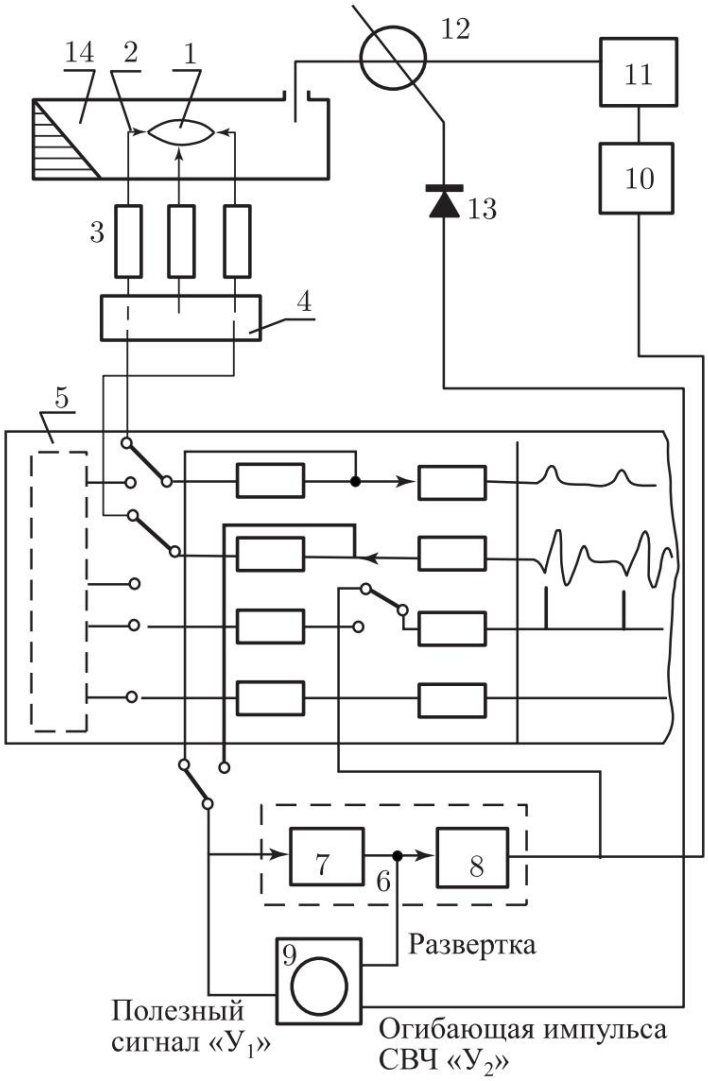

Rice. 6.01. Block diagram of an experiment to study the influence of EMF on rhythm of contractions of an isolated frog heart: *1* - object; *2* — suction electrode; *3* - filter; *4* - filling system; *5* — electroencephalograph; *6* - FBS-1; *7* - block for generating a clock pulse; *8* - block team formation; *9* — two-beam oscilloscope; *10* - modulator; *11* — microwave generator; *12* - directional coupler P2-2; *13* - detector section; *14* - rectangular waveguide 31/240 mm2

6.2. Registration of the heart electrogram as a whole frogs

The purpose of the technical support of the experiment is to record the electrogram of the heart of a whole frog under conditions of irradiation with microwave field pulses. The frog immobilized by a bloodless method is fixed on a foam table ventrally. The table together with the frog is located inside a rectangular waveguide. Majority electrophysiological studies of the heart of amphibians were carried out at its isolation from the body, when the chest is opened or by

insertion of electrodes into the chest. In this case, wires made of various metals were used as discharge electrodes.

Taking into account the above requirements, a method of abduction using artifact-free electrodes has been developed [221]. Registration is carried out on an electroencephalograph, the amplitude of the R-wave is about 150 ÿV. In Fig. Figure 6.02 shows a block diagram of the experiment. The block diagram allows you to carry out a controlled experiment using phase biosynchronizers FBS-1 [30].

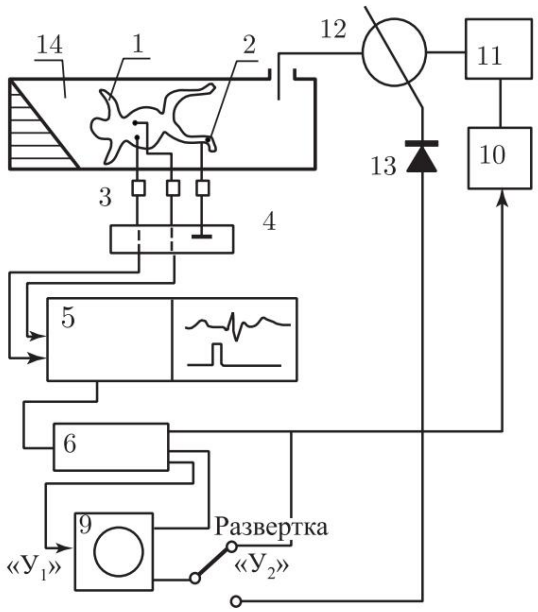

Rice. 6.02. Flow diagram of an experiment to study the influence of EMF on the parameters of the cardiac cycle of a whole frog. The symbols are the same as in Fig. 6.01

6.3. Registration of nerve conduction parameters impulse

The purpose of the technical support of the experiment is to register the parameters of excitation along the nerve trunk during irradiation microwave field pulses.

The prepared nerve is located in a rectangular cuvette made of plexiglass. There are various ways to orient the drug in the microwave field - perpendicular and parallel to the electric vector.

Depending on this, two types of cuvettes are used: small, with horizontal location of the drug, and deep, with a vertical location of the object (loop-shaped). Stimulation and abduction carried out using artifact-free electrodes. After filling the system with Ringer's solution, the nerve preparation is placed on the electrodes and electrical current is applied through the cuts on the electrodes. contact of the drug with the stimulator and the recorder. As an incentive

laboratory electrostimulator ESU-1 can be used.
The signal taken from the electrodes is amplified by a biopotential amplifier and recorded on the oscilloscope screen. The block diagram allows record the time (speed) of excitation by measuring the “artifact-response” interval (action potential) on the screen oscilloscope, action potential amplitude, relative and absolute refractoriness, excitability threshold. It is possible by introducing a delay between the stimulus and the modulation pulse, carry out various temporary location of the microwave pulse relative to the latent period, determine the magnitude of the incident and reflected power, length waves, PPM at the facility, etc. In Fig. 6.03 shows a block diagram experiment. The same block diagram is applicable when organizing experiments on the effects of microwave fields on synaptic transmission. On the picture shows a set of instruments that provide registration of parameters conduction of a nerve impulse.

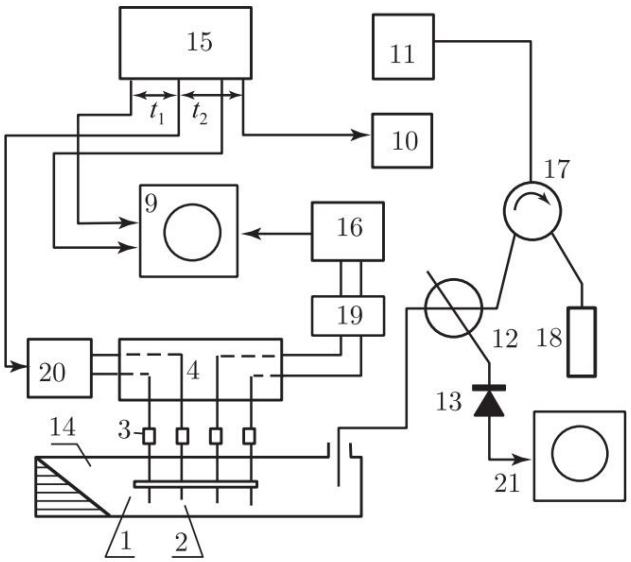

Rice. 6.03. Flow diagram of an experiment to study the effect of EMF on nerve and neuromuscular preparations of a frog. Legend: designations *1–14* cm, see Fig. 6.01; *15* — electrical stimulator ESU-1; *16* - biopotential amplifier UB1-02; *17* - circulator; *18* - load; *19* - external cathode follower; *20* - high-frequency attachment; *21* - oscillograph

6.4. Multi-purpose research facility moving cells in microwave fields

The impact of microwave radiation on cell suspensions under the condition shielding the irradiation zone from the surrounding space can be carry out both in small volumes - in test tubes, and in a duct.
Moreover, in order to localize the maximum impact of the microwave field on

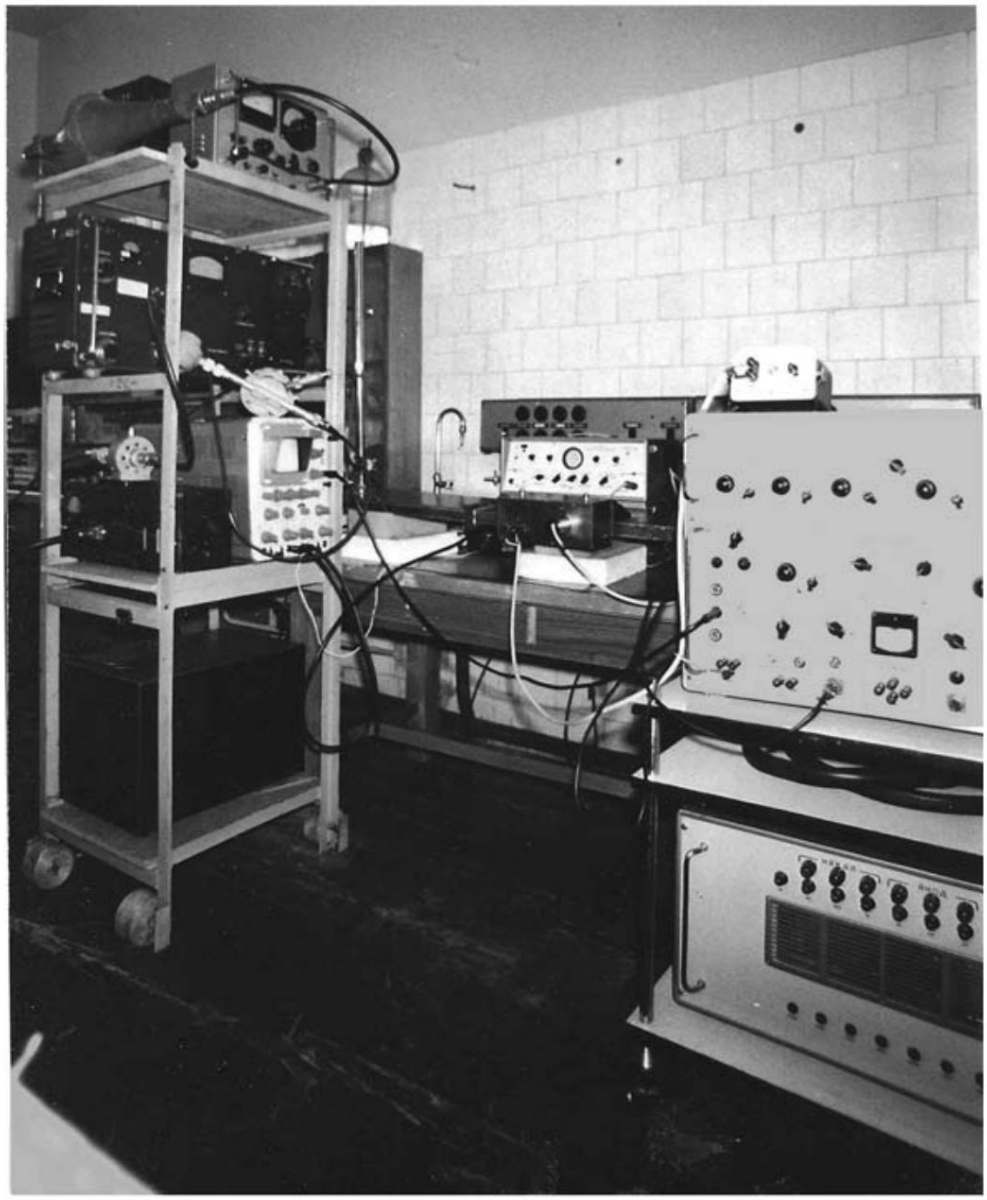

Photo. A set of instruments for studying the parameters of nerve impulse conduction during microwave irradiation. On the left in the figure there is (from top to bottom) an attenuator with an attenuation of 30 dB and a microwave power meter, an upgraded GS-6 generator, a wave meter and an oscilloscope. On the right is an electrical stimulator ESU-1. In the background you can see a waveguide with a screen in which pears are located for filling artifact-free electrodes with Ringer's solution and the remote head of the UBP biopotential amplifier; the amplifier itself is located behind the waveguide

the latter object must be located along the electric vector of the field in that part of it where it is uniform. Taking into

account the listed factors made it possible to develop some technical requirements when developing an installation for studying cell populations in suspension. Cell behavior is observed using optics synchronously with irradiation.

The presence of short-focus optical systems for observation required an increase in the operating frequency of radiation, i.e. a decrease transverse dimensions of the irradiator. In order to shield the irradiation zone and ensure the possibility of conducting research in a wide range frequency range, a shielded
strip line with internal cross-section 34 × 72 mm2. Running mode in the line is provided using an internal matched load, which is a parallel connection of ten resistors
(MLT type) with a total resistance of 75 Ohms and power dissipation 20 W (Fig. 6.04). The heat generated is removed naturally

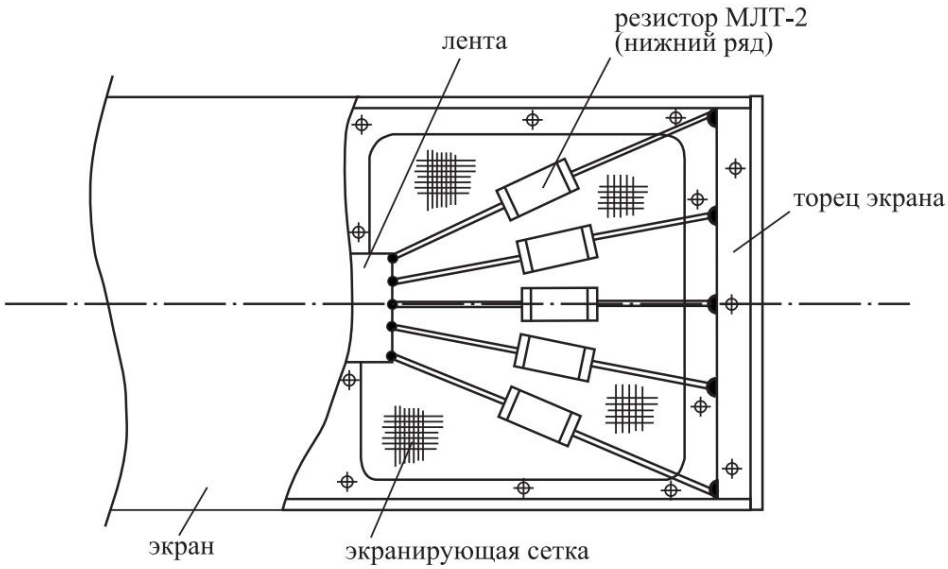

Rice. 6.04. Internal matched load (bottom row of resistors)

natural ventilation through rectangular hatches in wide walls screens covered with fine mesh brass mesh. Internal conductor, which is a brass strip with a cross section of 2 × 24 mm2
and providing a wave impedance of 75 Ohms for a given screen size, one end is attached to the high-frequency connector,
located on the end of the screen. To the other end of the tape MLT-2 resistors are soldered. In-screen ribbon supported
plexiglass pins. This design allows for high
traveling wave coefficient (TWC) value in a wide frequency range range - 500 ÷ 2400 MHz. In the diametrical plane of such an irradiator, the electric vector is directed perpendicular to the wide
screen and tape walls. In the upper wide wall there is a translucent waveguide for installing test tubes with suspension into the irradiator cells (Fig. 6.05).

In order to provide the possibility of studying the spectral characteristics of the cells themselves, as well as the properties of cell membranes using fluorescent probes, special mounting sockets for mounting optical systems are located on the side walls of the screen,

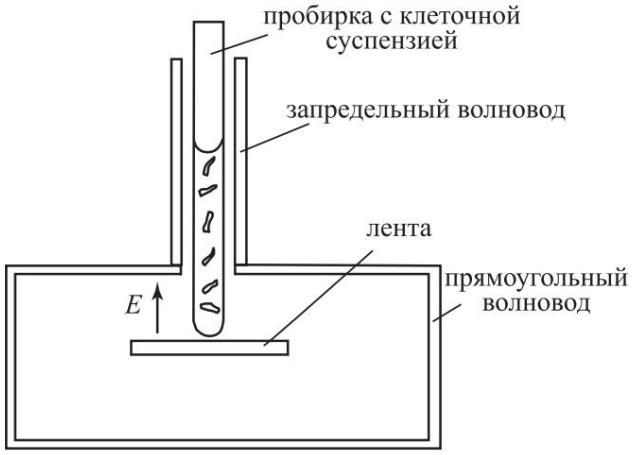

Rice. 6.05. Positioning the tube with cell suspension in the screened strip line

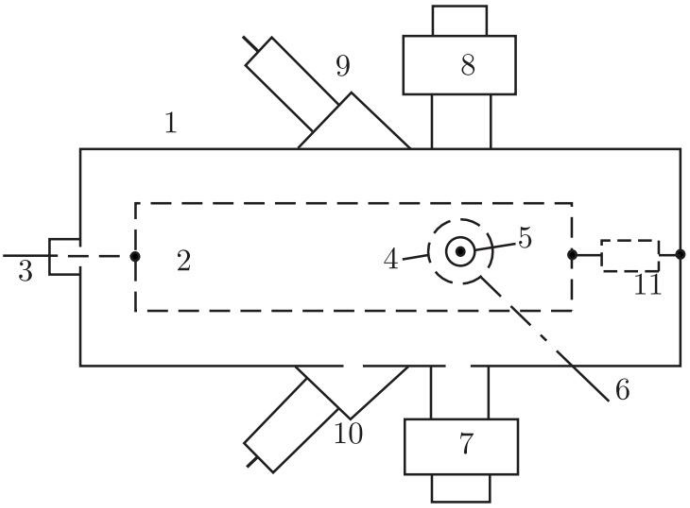

Rice. 6.06. Schematic diagram of a microwave irradiator with a strip waveguide and optical means for monitoring moving cells in an EMF: *1* - Waveguide screen; *2* - Strip waveguide; *3* — Cable and connector from the microwave generator; *4* — hole for installing a test tube with objects; *5* - Test tube; *6* — Transcendental waveguide; *7* - Microscope; *8* - Television transmitting tube; *9, 10* — Lighters; *11* — Load resistance (top view)

light sources and photodetectors (Fig. 6.06). The sockets are attached at an angle of 45ÿ to the longitudinal axis of the tape, and their optical axes form an angle of 90ÿ with each other and converge at the point through which the center line of the test tube passes vertically. The optical axis of two other mounting sockets passes through the same point, in which the lenses of an optical microscope are attached for direct visual observation of an object and film and photography, and a transmitting television tube for observation on a monitor screen (Fig. 6.07). The described irradiator can work with any microwave generator in the frequency range 500 ÷ 2500 MHz with an output impedance of 75 Ohms. When working

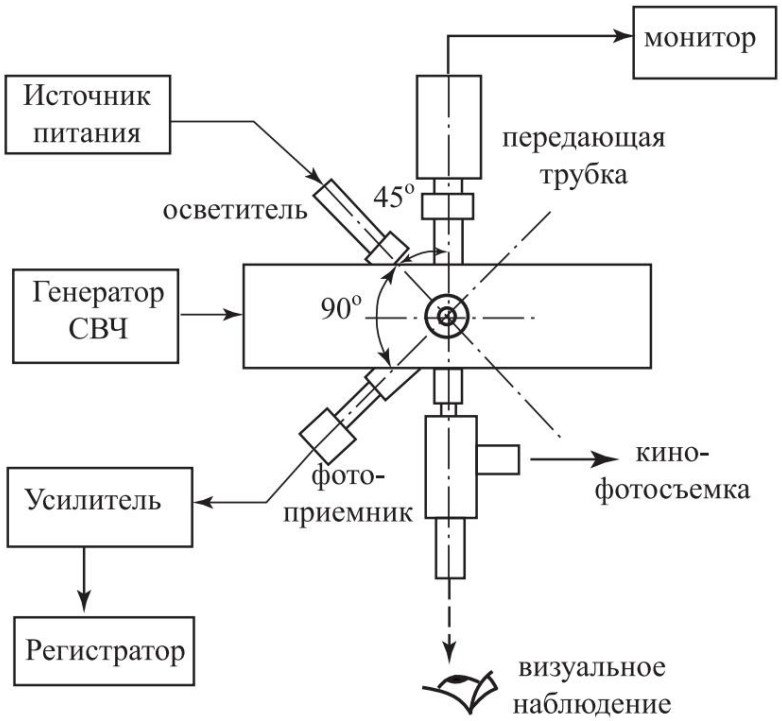

Rice. 6.07. Block diagram of a multipurpose cell research facility on microwave

in pulse mode, the average output power level should not exceed 20 W, i.e. the following condition must be met:

$$Psr = \frac{Pi}{Q}$$

where Pi is the power per pulse, Q is the duty cycle.

Technical characteristics of the installation:

1. The value of the traveling wave coefficient at a frequency of 2375 MHz is 0.8;
2. Maximum value of incident power in continuous irradiation mode, W - 20;
3. Carrier frequency range, MHz - 500 ÷ 2500;
4. Maximum average value of incident power in pulsed mode at a maximum duration of 100 ÿs, W - 20;
5. Wave impedance of the feed, Ohm - 75;
6. Sensitivity of the piezoelectric receiver, V dynÿ1 cm2 -10ÿ6 .

Features and requirements for the optical system. As it was noted above, short focal length microscope lenses are not possible insert into the cavity of the waveguide, and long-focus lenses placed on the outside (behind the mesh) do not provide the necessary resolution and, accordingly, sufficiently large increases in living microorganisms.

The installation uses a system of lenses in a plastic frame, installed in special holders between the object - a test tube with a culture of moving cells - and the side wall of the waveguide

(Fig. 6.08), which meets the requirements for irradiating biological objects without distorting the microwave field pattern.

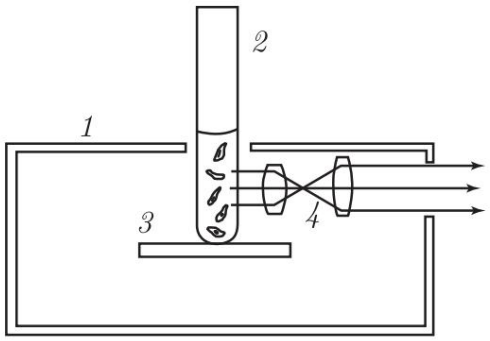

Rice. 6.08. Optical system for image output from a waveguide. *1* — waveguide wall, *2* — test tube with object, *3* — tape, *4* — optical system

The use of optical methods allows not only to significantly increase the total amount of information, but also to solve a wide range of problems. The latter include the study of excitation spectra using fluorimetry using fluorescent probes, energy indicators of microorganisms, cooperative interactions, etc.

Prefabricated lenses are installed in the cavity of the waveguide symmetrically on both sides of the object. The image from one lens falls on the eyepiece of the microscope, which performs an auxiliary function in the process of preparing the experiment itself, i.e., installing the object and observing it before turning on the microwave generator. An image of an object can be captured on film using a photo attachment (MNF-8) installed here and a Zorkiy type camera. The image of the object from another prefabricated lens is projected onto a television camera of the Volna-801 type and reproduced on the monitor screen, and, if necessary,

recorded on a video tape recorder. The use of a video system with image recording allows you to perform experiments on the effects of high-power microwave fields remotely or with an automatic programmer, without exposing the experimenter to accidental radiation. Providing high optical

resolution makes it possible to conduct high-quality morphological studies of cells and their behavior directly “under the beam”, conduct infrared spectroscopy of films with metal-containing proteins, etc.

Optical path lighting system. Illumination of moving cells inside the waveguide during microscopy and video recording of images is carried out using two light sources, allowing a beam of light to be supplied at an angle of 45 ÿ either from behind or from the front, creating a dark field effect. One light source (OI-18) is adjustable in brightness with a smooth regulator and is equipped with a special light

and a heat filter to prevent the occurrence of thermal convection in a test tube with cells. The second light source is powered by a special digital pulse generator, which creates the necessary shape fading flashes. The nature of stepwise attenuation of pulses light makes it possible to objectively record and, with fairly high accuracy, actively measure the speed and direction of movement floating cells during their irradiation with EMF. The structure of the instrument complex was developed jointly with Ph.D. Shvirst E.M.

6.5. Microslit microwave irradiator for biological objects

The emergence in recent years of new generation microwave technology micropaths (microstrip lines, slot antennas, lines on ferrite substrates, etc.) allows us to solve the problem of safe irradiation of a biological microobject for a researcher with minimal energy consumption combined with ease of manufacture irradiator and the possibility of docking with a whole complex of research equipment. In [228], the main principles of constructing an irradiator in the form of a two-wire strip lines, the structure of the field is determined in the quasi-static approximation, the main characteristics of line emission and absorption are outlined object of electromagnetic energy, the radius of the safe zone for the experimenter was calculated. The theoretical addition presented here makes it possible to more thoroughly elucidate the issues of matching the irradiator with the power supply device and the biological object, raised in [228], and to fully determine the design dimensions irradiator and consider the problems of connections with an optical microscope.

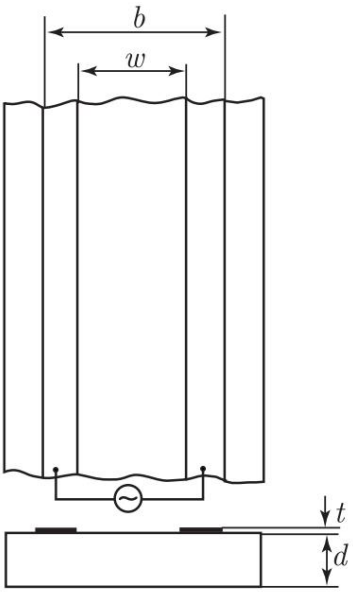

Rice. 6.09. Two-wire microstrip line

nia

The most optimal design of such an irradiator may be a design consisting of 2 conductive strips, sputtered or galvanically deposited per dielectric layer with a high value dielectric constant and small loss angle. From Fig. 6.09 it is clear that this design is similar to a slotted microstrip line. Rigorous theory shows [229], that there are areas in the slot line elliptical polarization of the magnetic field in a plane perpendicular to the surface of the dielectric substrate. Power magnetic field lines form closed loops with an interval of half a wavelength in the

control of energy propagation (the field pattern and current distribution in the slot line are shown in Fig. 6.10). Surface density

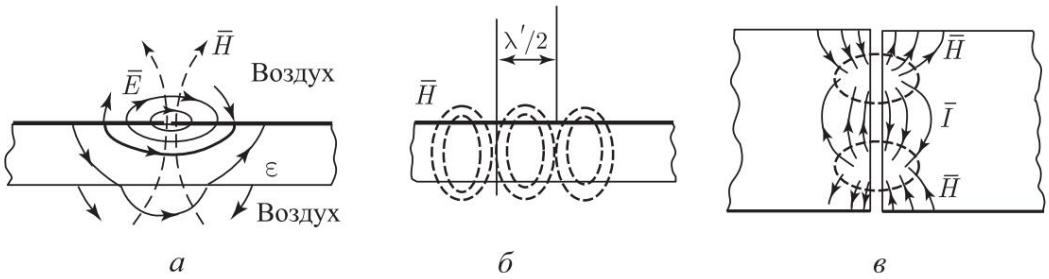

Rice. 6.10. Power lines of the electromagnetic field and surface current in the SSC

The current is greater at the edges of the slot and quickly decreases with distance from it. To minimize radiation into free space, materials with a high dielectric constant of the order of ÿr = 10 ÷ 20 are used as a substrate ; this leads to a significant decrease in the wavelength ÿ in the line compared to the wavelength ÿ in free space and ensures the concentration of field lines near the slot with insignificant radiation losses. For example, at a frequency of 3 GHz with a substrate dielectric constant ÿr = 16, the ratio ÿ /ÿ ÿ 0.38 and the microwave field at a distance of 25.4 mm from the center of the slit is attenuated by 28.4 dB, and at a distance of 33 mm - by 38. 6 dB compared to the slot field, i.e. more than a thousand times. At ÿr = 20 at a frequency of 3 GHz, the ratio ÿ /ÿ ÿ 0.33, and the microwave field decays sharply at a distance of 12.7 mm from the center of the slit. This allows the biological specimen to be positioned on a coverslip by placing it directly on the slit line. With a small glass thickness (0.25 mm), almost all electric field lines in this area will penetrate the object.

The possibilities of studying objects that have some anisotropy are interesting. This design of the irradiator makes it possible to arbitrarily orient the structure of an object relative to the transverse component of the electric field strength vector E. The longitudinal component of the vector E is an order of magnitude lower than the minimum value of the strength of the transverse component [230].

For minimal energy consumption and lightweight operation of the generator, it is necessary to ensure a traveling wave mode in the line. This is achieved by matching the supply and slot lines. The matching problem is complicated by the fact that the wave in the slot line, due to elliptical polarization, is different from the plane TEM wave; therefore, its characteristic impedance Z0 and phase velocity Vf are not constant, but vary with frequency. To a first approximation, the dispersion of the quasi-TEM slot line wave is determined by the relation [231]

$$h_{with} = k[(\ddot{y}r + 1)/2]\ 1/2, \qquad \text{(II.27)}$$

where h_{with} — real part of the longitudinal wave number; k = 2ÿ/ÿ0, ÿ0 — wavelength in free space. Therefore, the wave impedance Z0 is determined by the formula:

$$Z0 = 120\ddot{y}/[((\ddot{y}r + 1)/2)\ 1/2C0], \qquad \text{(II.28)}$$

where C0 is the linear slot capacity of the line. Relative wavelength in the slot line [229] taking into account (II.27):

$$\ddot{y}\ /\ddot{y} = [2/(\ddot{y}r + 1)]1/2, \qquad \text{(II.29)}$$

where ÿr is the dielectric constant of the substrate. From (II.29) we can obtain the value of the effective dielectric constant
homogeneous medium replaced by two different dielectric half-spaces, based on the fact that $\ddot{y}\ /\ddot{y} = \ddot{y}^{1/2}_{ef}$:

$$\ddot{y}eff = (\ddot{y}r + 1)/2. \qquad \text{(II.30)}$$

The field components on the air side of the slit can be calculated as functions of ÿ, ÿ and the distance from the slit r. Assuming ÿ/ÿ 1, then the electric voltage across the gap can be replaced by an equivalent linear source of magnetic current in the theory of a magnetic vibrator [228, 229]

$$H\ddot{y}_i = \frac{\ddot{y}2U\ddot{y}e\ddot{y}\ddot{y}r\ddot{y}\ l \sin \ddot{y}}{j\ddot{y}\ddot{y}04\ddot{y}r3}\ (1 + j\ddot{y}r\ddot{y}\ \ddot{y}\ \ddot{y}2\ r2\ ), \qquad \text{(II.31)}$$

or, taking Kc = (ÿ2 z + k2)1/2; ÿÿz = j2ÿ/ÿ; k = 2ÿ/ÿ,

$$H\ddot{y}_{with} = A \cdot H^{(1)}_0\ (kcr), \qquad \text{(II.32)}$$

Where $H^{(1)}_n(x)$ is the Hankel function of the first kind, nth order of argumint x.

Simple transformations lead to the definition of the relation stress along the trajectory of a semicircle of constant radius to the voltage directly applied to the slot [229]:

$$V\ (r)/V\ddot{y} = kcr|K(1)_1\ \ (kcr)|, \qquad \text{(II.33)}$$

Where $K(1)_1$ (x) is a modified Hankel function of the first kind, transfirst order from the argument x.

However, relation (II.33) can only be used on the distribution K(1) states r ÿ, otherwise, the value goes to infinity and the determination $_1$ (kcr) strives of the ratio V (r)/Vÿ has a significant error.

To determine the magnitude of voltage attenuation with air sides of the line at small distances r<ÿ to a first approximation you can use the static theory of slot field components

line described in [232]. Changes in the magnitude of the electric field vector will have the form: = (2U0/ÿÿ)[1 ÿ (2y/

$$Hey_{and}\ ÿ)\ 2]\ ÿ1/2 \qquad \text{along the OY axis (II.34)}$$

$$Ez_{and} = (2U0/ÿÿ)[1 + (2z/ÿ)\ 2]\ ÿ1/2 \qquad \text{along axes OZ.} \qquad \text{(II.35)}$$

The solution obtained by Kohn for formula (II.28) results in the main parameters of the slot line depending on its dimensions, the dielectric constant of the substrate and the frequency of the applied voltage [229]. The wave impedance Z0 is taken to be the ratio V 2/2P, where V = Ey dy is the peak voltage amplitude in the slot, and P is the average power flow of the electromagnetic wave. However, at a sufficiently long wavelength, the condition b/ÿ 1 will be satisfied, wave propagation in the line can be considered quasi-planar, and the feed can be calculated in a quasi-static approximation [228, 229]. For the TEM approximation, the slot line resistance can be estimated using the formula [14]:

$$Z0 = 591.7 \cdot [e_{ef}^{1/2}\ \ln(8b/po)]ÿ1\ ÿ. \qquad \text{(II.36)}$$

Taking into account formulas (II.29), (II.30), we can write Z0 in the form:

$$Z0 = 591.7(ÿ\ /ÿ)/\ \ln(8b/ÿÿ)\ ÿ. \qquad \text{(II.37)}$$

Formulas (II.36), (II.37) are quite accurate for the ratios b/ÿ > 3 and b/ÿ ÿ 0 [14]. It should also be

noted that determining the characteristic impedance through the average EMR power flow leads to some errors when developing transitions to microstrip and coaxial lines. An experimental study of a slot line shows [233] that to match a 50-ohm microstrip or coaxial line, a 75-ohm slot calculated using the above formula is required. **Determination of the design dimensions of the irradiator.** In accordance with [228] and the above theory of a microstrip slot line, an operating

microirradiator installation was manufactured. Taking into account the wide range of specific electrical conductivities of biological objects, the strong dependence of conductivity on temperature (for example, 0.1 M NaCl solution at T = 18 ÿC has a specific conductivity of 92.0 Sim g -equivÿ1 cm2 , and at T = 25 ÿÿ – 106.74 Sim g - equiv ÿ1 cm2 [234]); specific resistance of muscle tissue - 75–79 Ohm cm , brain - 670–1200 Ohm cm [235]), as well as the possibility of using different concentrations, the resistance of the slot line was taken equal to half of that given in [228] for mandatory shunting the resistance of the line resistance object, i.e.

Z0 = 150 Ohm.

The irradiator is made by electrolytic etching of FLAN-10 material, which has a dielectric constant of the substrate ÿr = 10.0 ± 0.5 and a dielectric loss tangent

tan ÿ = 1.5 10ÿ3 . The thickness of the plate is 2.0 mm, the coating is copper. The irradiator is a structure consisting of 2
conductive strips.

Based on the need to concentrate microwave energy near the slit, and on the other hand, the value of the minimum permissible window for sufficient illumination of the object, the slit width was chosen equal to ÿ = 3.6 mm. According to the formula b/ÿ = ÿ [8 exp(591.7/ÿ1/2 Z0)]ÿ1 found
ef
emitter width b = 7.6 mm. General view of the manufactured
the irradiator is shown in Fig. 6.11. The broadband transition from the coaxial cable to the feed (Fig. 6.11) is made according to data from [233] and provides a standing wave ratio (SWR) (the measurement slot is loaded with a matched load) of the order of 1.25 in the band
from 4 to 8 GHz, losses in the same range range from 0.8 to
1.2 dB [233]. Extrapolating the experimental curves to a lower frequency region, one can expect a significant reduction in losses (up to 0.5 dB) at frequencies around 1 GHz and an increase in SWR (up to 1.75).

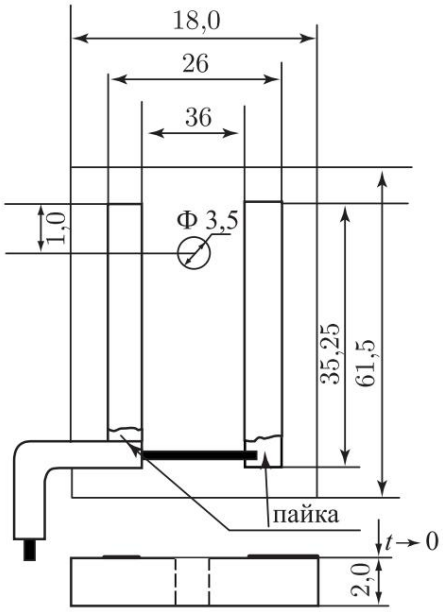

Rice. 6.11. Structural dimensions of the irradiator. Supply method
high frequency energy using semi-rigid cable

The most common type of functional testing
characteristics of biological objects with small linear dimensions is visual observation using an optical microscope.
Thus, the second main objective of this work is
analysis of the possibility of docking a microirradiator with a microscope. At often used in the study of a wide range of biological problems
optical microscope MBI-15. The device has 4 interchangeable lenses, a device for photography and filming, and an illuminator for observation.

object in transmitted and reflected light. Focal length to
15 mm.

At a distance l = 1 mm from the end of the line there is a through hole in the substrate with a diameter of 2 mm for observing the object through a microscope in transmitted light. At a distance from the feed along the OZ axis equal to the slit width, the magnitude of the E-vector of the static field will decrease
2.2 times, and at a distance of twice the width of the slit - 4.1 times.
In addition, static analysis does not take into account the slowdown effect
2.3 times, causing concentration of field lines near
slots, with a high-frequency signal [14]. Considering the structure of the field on the substrate side according to the results of [17] (the analysis is not given due to its bulkiness), we can draw a conclusion about the admissibility of fastening irradiator directly on the microscope stage (photo).

An object in the form of a drop with a volume V = 10 ÷ 50 μl is applied to cover glass and placed on the air side of the irradiator
above the hole. If it is necessary to observe a thin layer of an object
pressed on top with a second cover slip.

Experimental results. The main operating characteristics of the line were measured - wave impedance, running coefficient
waves (WW) in the modes of coordinated load and equivalent of a biological object, the magnitude of the PPM in the researcher's working area,
The correspondence of these characteristics to the calculated data obtained above, as well as in [13], was determined.

A block diagram of the installation for measuring performance characteristics is shown in Fig. 6.12. Used as a source of microwave oscillations
generator G4-5, carrier frequency is 915 MHz. A generator serves as a source of rectangular pulses for modulating microwave radiation
G5-54. Modulation parameters: pulse duration 100 ÿs, duty cycle Q = 2,
repetition frequency 1.65 kHz. Line SWR meter
type P3-35. The SWR was assessed using the readings of a B3-33 millivolt meter, the voltage to the input of which is supplied from the output of the detector meter. Controlling the shape of the high-frequency signal envelope
was carried out using an oscilloscope S1-55. Coaxial length
cable supplying power to the feed is selected equal to the length
waves in free space (lÿ = 328 mm).

Experimental determination of line impedance
was carried out in continuous operation of the microwave generator. Resistors with a resistance range from 100 to 200 Ohms were used as line loads. By the method of half division from the resonant
The dependence of the KBV on the resistance value of the resistors was found optimal load resistance R = 143 Ohm, which differs
from the calculated one by 4.6%. The BEF in an unloaded slit line mounted on the microscope stage is about 0.33. The experiment confirmed
the conclusion drawn from the analysis of the field on the substrate side is about the independence of the line operating mode from the height of the irradiator position above the microscope stage. The experiment also leads to the conclusion

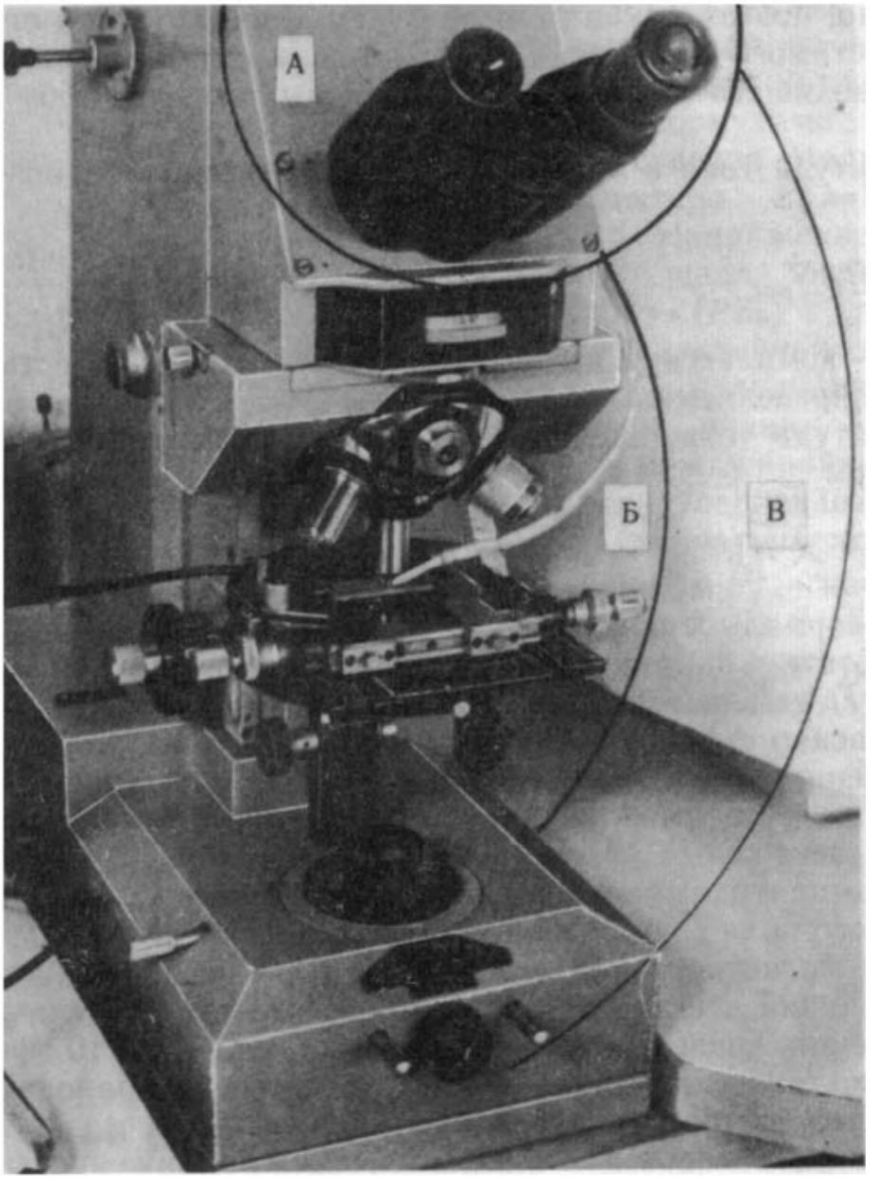

Photo. Microscope MBI-15 with installed micro-irradiator
and temperature sensor

about much greater field attenuation on the air side of the feed
if there is an object. At a distance of 4 mm from the slit the field weakens
more than 10 times. This distance is accepted as the minimum acceptable
for the lens.

The MPP in free space was determined by the method of induced current
in a frame made of bronze wire with a diameter of 4 mm; square,
limited by the contour of the frame, is 10 cm2. The frame is connected
through a high-frequency power divider to a Y2M-64 thermistor power meter.
The measurement was carried out for real
situations, i.e. in the presence of a drop of 0.15 M NaCl solution with a volume
10 µl placed on a coverslip over a hole in the substrate.

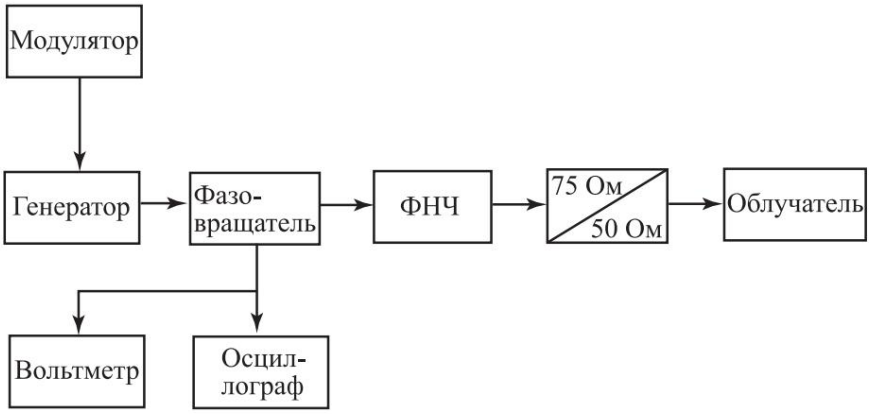

Rice. 6.12. Block diagram of a performance measurement setup
biological objects

With generator output power Pout = 1.2 W measured value
KBV = 0.46. PPM at the level of the researcher's eyes at the microscope
binocular (zone A, photo) no more than 3 ÿW cm ÿ2, in the area of the object
table within a radius of r = 8 cm from the irradiator (zone B, photo) no more
10 ÿW cm ÿ2. In the distant region (zone B, photo) the field decreases
proportionally to the square of the distance. Thus, we can conclude
on acceptable levels of PPM in the researcher's work area.

Energy characteristics of object irradiation. As
the main energy characteristic of the object irradiation is adopted
specific absorbed power (SAP), determined by speed
increase in the temperature of the irradiated material. At a given speed
temperature rise of the SPM can be found from the formula [235]:

$$SPM = 4.2\ \ddot{y}T / \ddot{y}t\ [W\ g\ \ddot{y}1], \qquad (II.38)$$

where ÿT is the absolute change in temperature during the observation time ÿt.
The object chosen was a 0.15 M NaCl solution, which has a high
specific conductivity. The instantaneous temperature is determined by an
MMT-54 thermal sensor coupled with a Shch-4313 digital voltmeter.
The sensor is mounted on the microscope lens (photo). The minimum
permissible distance of the sensor from the line can be determined from the formulas
modulus of the electric field vector, taking into account that the resistance of the sensor in the
range from 18 ÿC to 90 ÿC varies from 250 to 1700 Ohms. Knowing
field strength at the point where the sensor is placed can be determined
power released in the sensor by flowing current. At power
1.2 W generator at a distance of 3.5 mm from the heating temperature line
sensor does not exceed 0.2 ÿC, measurement accuracy 0.1 ÿC. This distance is accepted as
the minimum permissible with a generator power of up to
1 W.

Calibration was carried out by parallel thermostatic heating of the sensor
and a reference thermometer in the range from 18 ÿC to
90 ÿC in 0.5 ÿC. The resulting dependence of the readings of the device
coupled with the sensor is cut into three monotonic regions and approximated

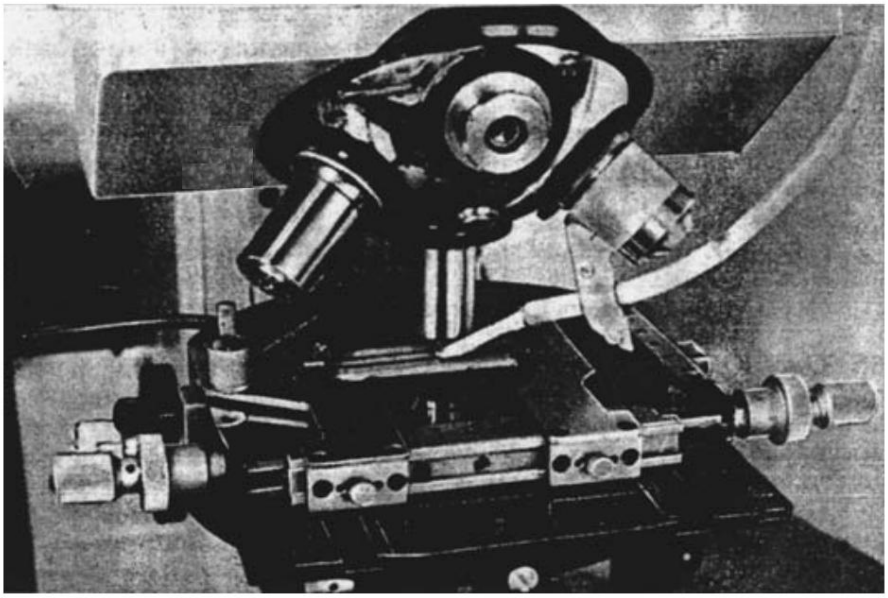

Photo. Installation of the irradiator on the microscope stage and a possible method of attaching the temperature sensor

simulated in each by a polynomial of the 5th degree. The approximated dependence is shown in Fig. 6.13. Below the figure are the coefficients of the polynomial and the approximation error for each part.

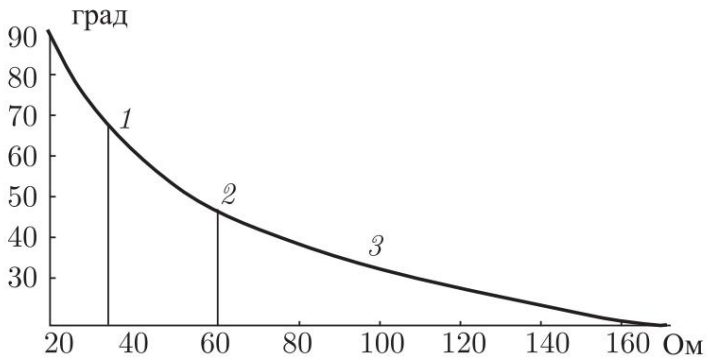

Rice. 6.13. Approximated temperature sensor characteristic

The dependence of the temperature increase on the irradiation time, as can be seen from Fig. 6.14, is linear only in the initial section, in a time interval of up to 10 s. In this area, the most reliable correspondence of the SLM to the rate of temperature increase.

Determination of temperature dependences for various volumes of the object was carried out by synchronously reading the temperature sensor readings and irradiation time intervals. The temperature sensor is immersed in a hemispherical drop of solution. Irradiation of the object began at a certain temperature and lasted up to 2 minutes. Time intervals were recorded with an electronic stopwatch; the used volumes of 10, 20, 30, 40 and 50 ÿl were collected using a PL-01-20 pipette. Measurements

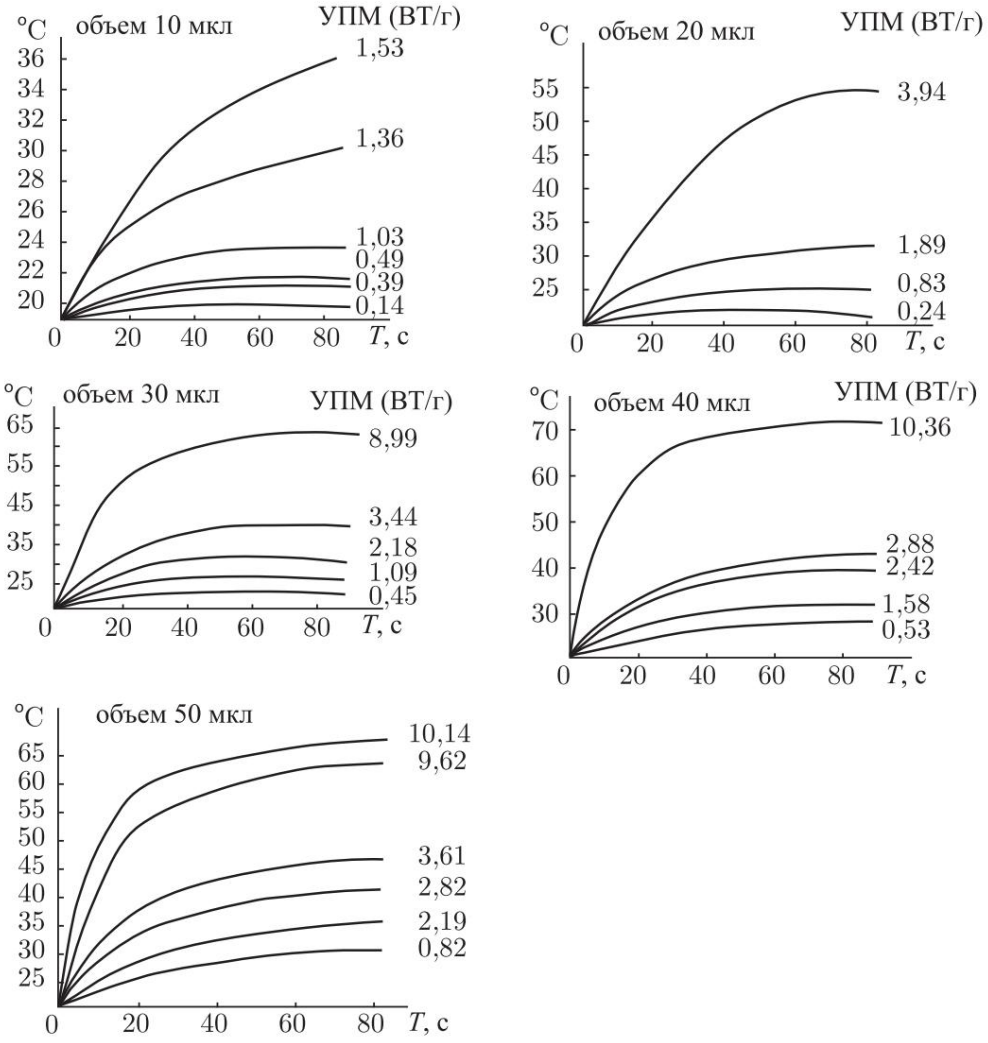

Rice. 6.14. Graphs of temperature growth in a biological model object from irradiation time

were carried out at different generator power levels within 0.1 ÷ 1.2 W.

When the volume of an object changes, its electrical conductivity and the degree of overlap of the electric and magnetic field lines change. The consequence of these changes is a variation in the matching of the line with the load (object), the power transfer coefficient to the load and the power absorbed by the object. So, with increasing As the solution volume increases, the BV in the line increases and the phase of the reflected signal changes. In this regard, the power received by the object (without taking into account radiation losses) was estimated through the reflection coefficient by power [236]:

$$\text{Kotrp} = \frac{1 - \text{KBV}}{1 + \text{KBV}2} . \qquad \text{(II.39)}$$

Where does the power in the object come from:

$$P0 = Pg(1 ÿ Kotrp), \quad \text{(II.40)}$$

where Pg is the power supplied by the generator.

Graphs of the taken dependences of the absolute temperature of the object on irradiation time at different powers in the object and volume are shown in Fig. 6.14. In parentheses, after the values of the SPM calculated according to formula (II.38), for each dependence the power is given in the object.

Experimental study of the operation of the irradiator with a real biological object. The functionality of the micro-slit irradiator was tested in an experiment on irradiation of protozoan microorganisms of the Tetrahymena species.

Irradiation was carried out according to the method described above, carrier frequency 915 KHz, pulse repetition rate 1.65 kHz, pulse duration 100 ÿs. The reaction of Tetrahymena was observed visually through the binocular of an MBI-15 optical microscope at various power levels and in 2 irradiation modes - continuous and pulse-modulated. The volume of a drop of the drug is 10 µl.

The value of the specific electrical conductivity of the Tetrahymena suspension is greater than the conductivity of a 0.15 M NaCl solution, as a result UPM in suspension with equal power and volume is much larger than in NaCl solution. Therefore, determining the amount of heating suspension encountered some difficulties, because suspension is enough heterogeneous, its total electrical conductivity varies from sample to sample, therefore the power released in the object also changes. The power supplied to the irradiator was controlled according to generator output power level.

The usual behavior of tetrahymena is manifested in chaotic movement in liquid without observing any preferential direction. When exposed to EMR, starting from a power level of 100 mW in pulsed mode and 70 mW in continuous mode, some large ciliates perform precessional movement around the contractile vacuole. The precession frequency is about 0.5 Hz. Further An increase in power leads to irreversible denaturation of cell protein as a result of heating. A qualitative study of the mechanism of precession (whether the cause of this movement was the heating of ciliates or there was a specific “non-thermal” microwave effect) was not carried out. The result of the experiment is a successful visual observation real biological object under EMF irradiation and characteristic change in the behavior of ciliates indicating the arrival microwave power into the suspension.

Conclusion. The developed microslit irradiator can be used to study the impact of EMR on various biological objects - cell suspensions, gels, fibers, tissue culture. Such an irradiator may turn out to be especially convenient

when studying the influence of EMR on an object with a pronounced electrical or magnetic anisotropy, because object can be easily orient relative to the field vectors. In addition, pairing irradiator with a microscope allows you to observe functional changes in the state of the object synchronously with irradiation, as it was shown in an experiment with tetrahymena. Big advantage the considered irradiation method is that there is no need using various shielding devices to protect researcher from exposure to non-ionizing radiation. At that At the same time, a high field concentration is achieved in the object and, as a consequence of this, energy costs for achieving the required value of UPM. If you use conditional coefficient of use of micro-slit emitter and currently used waveguide feeds for the ratio of UPM to pulse power (10 kW kg ÿ1/2 W for microslit feed and 5.6 kW kg ÿ1/75 W for waveguide irradiator), then the microslit irradiator turns out to be more effective more than 100 times.

6.6. Cylindrical microirradiators with spiral antennas

Widely used as rotating polarization antennas in the ranges of centimeter, decimeter and meter waves found spiral antennas emitting a field of approximately circular polarization in the direction of its axis.

Spiral antennas are divided into cylindrical, conical and flat.

A cylindrical helix antenna consists of several turns of wire spiral. Currents in the spiral are excited using a coaxial line, for whereby one end of the spiral is connected to the central conductor of the line. The outer conductor of the coaxial line (braided if it is a coaxial high-frequency cable) is connected to the metal screen that prevents the excitation of electrical currents on the outer surface of the coaxial power line and largely overwhelming the rear antenna lobe, as well as serving as a counterweight in relation to the spiral (Fig. 6.15).

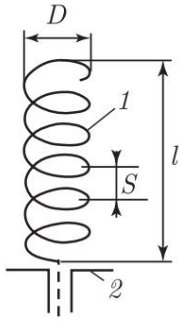

Rice. 6.15. Cylindrical spiral antenna: *1* — spiral; *2* — screen

When the line is connected to a high-frequency generator, a traveling wave of electric current is excited in the spiral. Therefore, a helical antenna can be classified as to the class of traveling wave antennas.

By choosing the appropriate coil diameter D ÿ0/3 and winding pitch S ÿ ÿ0/4, it is possible to ensure radiation of energy along the axis of the spiral (perpendicular to the screen) in the direction of motion of the traveling wave current, and in this direction the polarization of the electromagnetic wave in the far zone the antenna is close to circular.

The directivity coefficient of a helical antenna can be approximately determined by the formula

$$D ÿ 15(L/ÿ0)^2 nS/ÿ0,$$

where L is the length of the spiral turn; n is the number of spiral turns; ÿ0 — length waves in free space.

The input resistance of the spiral is determined by the formula, Ohm:

$$Rvx ÿ 140(L/ÿ0).$$

The spiral antenna retains its directional properties in the wavelength range 0.7ÿopt ... 1.2ÿopt, where ÿopt is the wavelength, for which antenna dimensions are optimal.

The use of *conical* spirals instead of cylindrical ones can provide broadband in approximately double the wavelength range. With the same number of turns as the cylindrical spiral, the conical a spiral antenna forms a wider radiation pattern than a cylindrical one. This is explained by the fact that when excited currents along the spiral wire effectively radiate only part of the turns conical spiral, the length of which is close to the wavelength. As the wavelength decreases, the active region of the spiral moves towards turns with a smaller diameter.

In *flat* spiral antennas, a traveling current wave is also excited. Unlike cylindrical and conical spirals, they in the absence of a screen, they emit circularly polarized waves in two directions, namely in directions perpendicular to the planes of the spiral. To obtain unidirectional radiation, a flat the spiral is placed on one side of the dielectric plate, the other side of which is metallized. Surrounding the spiral with a closed screen and connecting it with screen *2* spirals (Fig. 6.15), we get coaxial line with a spiral inner conductor. To maintain the traveling wave mode, the free end of the spiral is removed out through the RF connector and loaded onto a resistor with resistance, equal to the wave one. A test tube with an object is placed inside the spiral. In this case, the input resistance of the spiral coaxial line will increase due to a decrease the wavelength ÿÿ = ÿÿ close to 100 at D = 0.6–0.7 cm, S $\frac{\text{in}}{= 0.2–}$ and amounts to a large 0.3 cm and L ÿ 2 cm.

In such a situation, it is advisable to install a small one instead of a resistor tuning capacitor with air dielectric.

The choice of values of D and d is determined by formulas [78]. In Fig. 6.16 shows the design of a cylindrical microirradiator at a frequency of 915 MHz for irradiating liquid media in a duct.

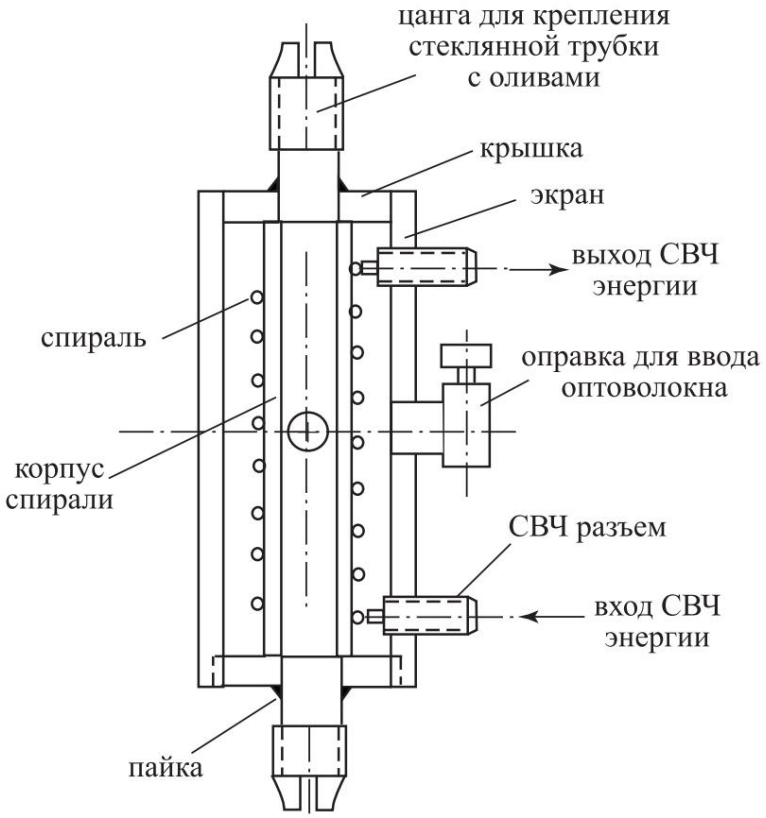

Rice. 6.16. Cylindrical microirradiator for irradiation of liquids in the duct

The spiral is made of silver-plated copper wire with a diameter of 0.8 mm and is tightly wound onto a plexiglass body. The spiral pitch is 2–2.5 mm. A glass tube is passed through the body of the coil
and is fixed in the collets with clamping nuts (not shown in the figure).
The collets are used from tuning potentiometers SP-1 (SP-2).
The screen and covers are made of brass. All joints are made by soldering.

In Fig. Figure 6.17 shows the design of a cylindrical microirradiator for irradiating liquid media in a test tube (frequency 915 MHz).
To register excited mechanical vibrations, the microirradiator is supplemented with a piezoreceiver, consisting of a housing with a cap
nut for connecting to the screen, piezoelectric sensor made of barium titanate with a diameter of 20 mm and a thickness of 0.5 mm and a connector for outputting an alternating electrical signal from a piezoelectric sensor.

In Fig. Figure 6.18 shows the design of a point microirradiator with conical helix antenna.

Dimensions of microirradiators: D = 2 cm; l = 5 cm; ÿS = 0.2 cm; d = = 0.9 cm; L = 2 cm.

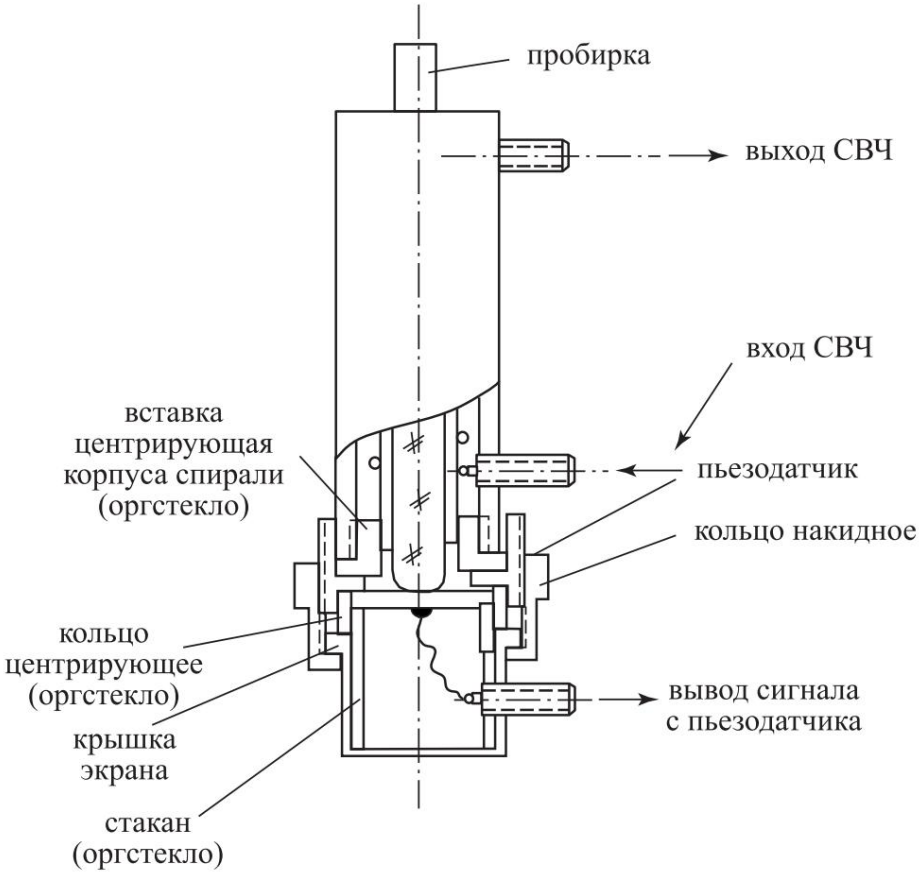

Rice. 6.17. Cylindrical microirradiator for irradiation of liquid media in a test tube

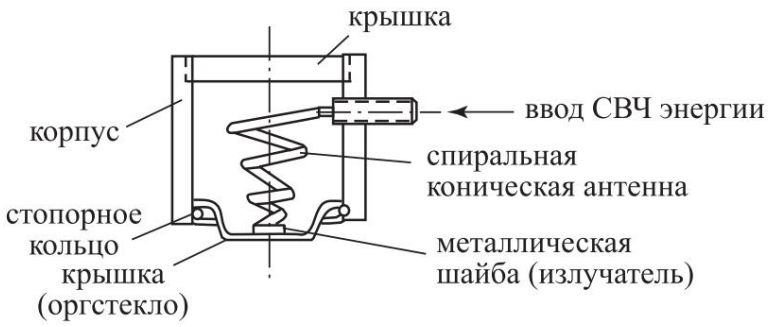

Rice. 6.18. Point microirradiator with conical antenna

Chapter 7

CONDITIONS FOR CONDUCTING EXPERIMENTS ON BIOEFFECTS OF MICROWAVE

7.1. Emission limits and standards frequencies

As shown above, experiments on the bio-effects of high-frequency electromagnetic fields often require powers of the order of tens and hundreds of watts. The high-frequency installations used by experimenters operate at different frequencies, which is explained by technical capabilities. At the same time, many technical services use frequency ranges located near the frequencies (or their harmonics) at which research work is carried out on the effect of high-frequency electromagnetic fields on biological objects. Naturally, the question arises about the permissible levels of radiation from high-frequency research installations in order to avoid interference with the work of technical services, as well as about the choice of frequencies at which these installations operate. Therefore, before starting work on a high-frequency installation, it is necessary to familiarize yourself with the relevant documents on the normalization of radiation into free space, as well as on the selection of frequencies allowed for operation. These provisions apply to both standard serial equipment and the modernization of existing or newly created ones. In the USSR (and in Russia), standards for permissible industrial radio interference [237] have been introduced for each frequency range for all high-frequency installations, approved by the State Commission for Radio Frequencies of the USSR (SCRF). This document regulates all types of possible radiation, including from high-frequency installations for scientific research. In addition, GOST 23450-79 dated January 29, 1979 on radio interference, including from scientific high-frequency installations, was put into effect [238]. The frequencies allocated for scientific work are indicated in [239]. The procedure for registering high-frequency installations, issuing permits for the acquisition, construction and operation of radio-electronic equipment and high-frequency installations are given in [239].

7.2. Issues of constructing shielded rooms

Shielding a certain amount of free space when
conducting research on the bioeffects of high-frequency electromagnetic fields aims to exclude the spread of these
fields in the entire space, or rather, a decrease in the level of high-frequency electromagnetic radiation to the value provided for
current standards. Hence, when designing and constructing
screened premises must be guided by certain requirements, the implementation of which will ensure in the future
compliance with these standards.

Let's consider the requirements that shielded rooms (ES) must meet. At the same time, the author did not seek to provide a design for a specific shielded room that would allow certain biophysical or electrophysiological tests to be carried out in it.

experiments, but was only limited to considering the necessary general
considerations. Most studies do not require the direct presence of an experimenter near the object. However
During the experiment, constant monitoring of parameters is required
fields, both power and time, adjustment of these parameters, change in irradiation mode, change in environmental parameters,
in which the object is located, control and registration of parameters of the functional state of the object itself, that is, control is necessary
experiment. Therefore, for most experiments it is possible
propose the following EP scheme: a high-frequency installation, including a high-frequency oscillation generator, a communication cable and an irradiator, a system of artifact-free electrodes for removing bioelectrical activity (in some cases, for stimulating an object),

the object itself and the object's life support system are located on the screen.
The experiment is controlled externally using the system
remote control. The shielded volume and the remote control system are connected through barrier devices,
excluding the leakage of electromagnetic energy from the shielded volume into free space. Shielded room
must be equipped with a hatch through which equipment and objects are placed in a shielded room. During the experiment
the hatch must be tightly closed. All necessary communications
(energy supply, air supply and exhaust, gas, water) must be
entered into the shielded room also through barriers
devices. The dimensions of such a shielded room are determined, first of all, by the dimensions of the equipment and the length used
radiation waves. In the wavelength range 10 ÷ 50 cm using
approximate dimensions of the generators and irradiators described above
the following: height - 150 cm, depth - 100 cm, length - 200 cm.

In experiments where the object of research is a person, the requirements for a shielded room can be supplemented by the presence two-way wired communication and a television installation for video monitoring of a person's condition. It is also necessary to have a second an emergency hatch for emergency evacuation from a shielded room if necessary. The approximate dimensions of the screened bathroom can be as follows: length - 3 m, width - 2 m, height - 2.5 m. An essential point is the location of the shielded room inside the laboratory in such a way so that the minimum clearance between the walls of the laboratory room and the shielded room was more than 1 m. The clearance between the floor laboratory room and the bottom of the shielded room should be also at least 1 m. This value is established by safety standards and, in addition, allows, if necessary, carry out repairs to the shielded room. Ventilation of the shielded room must ensure a threefold change in volume indoor air in 1 hour. The most complex (in terms of volume work) is the design of a shielded room in which, According to the conditions of the experiment, the presence of an experimenter is necessary. Such a shielded room must satisfy all the requirements of the above-described shielded rooms and in addition have an internal screen separating the experimenter from the control and recording equipment from a high-frequency installation. Both The compartments are connected by a door that ensures an acceptable radiation level of no more than 10 ÿW/cm2 at the experimenter's workplace. When conducting experiments using an open irradiator inside a shielded room, it is also necessary to provide for remote control of the experiment. Approximately The dimensions of such a shielded room can be as follows: length - 5 m, width - 3 m, height - 3 m. Given here the dimensions of the shielded rooms are taken from the experience of the author's work and, Naturally, they are not decisive. They only allow you to get a general idea of the dimensions of these structures and can be adjusted by researchers whose work will require the use of certain shielded rooms.

Thus, shielded rooms can be divided into into three classes:

— non-stationary shielded rooms with remote control experiment management;

— small screened, stationary rooms with remote control control of the experiment;

- large screened, stationary rooms with double shielding with local and remote control of experimental volume.

7.3. Materials and elements used shielding room designs

Sheet metal can be used to shield the room
copper, brass, steel. Strict requirements for the amount of permissible
level of radiation of high-frequency energy into free space
eliminate the joining of sheets with each other using collapsible or
permanent connections such as screws, bolts, rivets, etc. The only way to
ensure the necessary attenuation is soldering or welding. The frame of the
shielded rooms of the first
two classes can be served by a welded frame made of steel angle
followed by sheathing with steel 1–2 mm thick and welding of joints
in an environment of argon or carbon dioxide. Gas welding with acetylene
leads to warping of the sheet and does not provide absolute reliability
weld, stresses arise in the metal after cooling,
leading to seam rupture. From the inside of the shielded
placing bolted steel corners forming the frame onto the shelves
wooden blocks are attached to which boards are sewn with nails
(preferably unplaned), forming solid walls. To the boards
A radio-absorbing material, which is necessarily non-flammable, is attached
to KN-2 or “88” glue. This measure is necessary since the shielded
the room is a large resonator, which will contribute, especially in the
decimeter range, to the formation of standing
waves, and this, in turn, will lead to strong field inhomogeneity
inside the volume and loss of information about the magnitude incident on the object
power. The frame of the screened room can be assembled
also entirely made of planks. The outside of the boards is sheathed with
sheet brass or copper on nails. The sheets are laid overlapping,
the seams are soldered with POS grade solder, the most suitable flux
30-40% phosphoric acid is suitable. The seam turns out reliable,
there is practically no slag, which ensures the absence of fistulas and adhesion
strong. Careful soldering of the fastening caps is also necessary.
nails with the surface of the sheet. In case of using steel or
galvanized steel nails should be used as flux
zinc chloride. The inside of the boards is also covered with RPM. Outside
It is advisable to paint in 2-3 layers with conductive HF paint.

The frames of shielded rooms of the third class should be made only
of metal (steel angle 60 × 60 or 60 × 90)
and sheathed with steel sheet 2-2.5 mm thick by welding.
If these rooms are large and loaded with a large amount of equipment,
wooden beams can give a slight deflection, which will lead to rupture of the
skin and leakage of high-frequency
electromagnetic energy into the surrounding space. Stationary
shielded rooms are installed on a welded belt made of steel channel No.
12-16 on the same racks. From below to the ends of the racks

support steel platforms measuring 200 × 200 mm are welded
8-10 mm thick. The most crucial point in the construction of shielded rooms is the sealing of doors and hatches
reusable. The hatch or door must fit tightly
along the entire perimeter to the main screen. This is achieved by using loops with eccentrically located axes. Seals are used of the standard type - knife, petal, using conductive rubber (see, for example, Harvey). Because the front door

shielded room can only have external control
(additional compaction due to clamping with screws or other power elements), then an emergency exit is necessary
in case of emergency evacuation. This problem can be solved quite simply by using a disposable hatch. On the screen
an opening is left in a place convenient for exiting the shielded room; it is attached around the perimeter of this opening using soldering
a sheet of thin metal foil. Foil if necessary
It breaks easily and the person leaves the room without hindrance. After to eliminate an emergency situation, the opening is closed with a new sheet foil. In all cases, the shielded room must be ventilated. In a non-stationary shielded room this task
most simply solved due to natural supply and exhaust
ventilation system. To prevent leakage of high-frequency electromagnetic energy from a shielded room through
ventilation system, the latter is made in the form of the necessary number of metal tubes of sufficiently small internal diameter and the required length, welded or soldered to the outer
sheathing In order for these tubes not to transmit high-frequency electromagnetic energy, in other words, they would provide
large attenuation, it is necessary that the inner radius of the tube R was 10–15 times less than the operating wavelength [40]. In this case the tube will be a transcendental waveguide and its linear
attenuation (in decibels per centimeter) on the lowest wave type H11 can be approximately estimated using the formula

$$L = \frac{16}{R} \text{ dB/cm},$$

and the total attenuation with tube length l becomes equal to 16l/R dB. Let's consider a numerical example. According to the standards given in the documents specified in clause 7.1 of this chapter, a shielded room must provide attenuation no worse than 120 dB. At wavelength radiation 10 cm and inner tube radius 0.8 cm tube length
will be equal

$$l = \frac{LR}{16} = \frac{120 \cdot 0{,}8}{16} = 6 \text{ cm}.$$

To ensure the calculated open cross-section of the supply and exhaust ventilation openings, the required number of tubes

hits the block. The tubes on both sides are welded to the collectors.
A fan is connected to one of the collectors, the second collector
welded to the screen. As a high-frequency filter
The electromagnetic energy of the element can also be served by a metal mesh. The supply of water and gas to the screened room is carried out using metal pipes welded into the screen. Because the
The line length is usually several meters; these communications strongly absorb high-frequency electromagnetic energy
and cannot be a source of interference. The most labor-intensive and responsible moment can be considered the introduction of electricity, wired communications, alarms, etc. into the shielded room, as well as
ensuring the required amount of filtering of high-frequency electromagnetic energy by an intermediate screen separating inside
screened room with two compartments. As a filter
element it is most convenient to use a volumetric absorber, inside
which the electrical wire of one or another electrical
chains. The filter design is a coaxial system
two pipes: the outer one is made of steel, the inner one is made of porcelain or glass. The space between the pipes is filled with volumetric
an absorber consisting of a mixture of cement, sand and graphite with a ratio of parts of 3 : 9 : 1, respectively. Porcelain tube attached
the inside is steel with dielectric spacers. The steel pipe is welded to the screen of the room. The necessary attenuation is ensured
choosing a system of a certain length. The conductor is passed through porcelain tube. The number of such filters is set according to the number conductors that need to be introduced into the shielded room.
A detailed description of all issues related to the construction, installation and operation of shielded premises can be found in [240].

Literature

1. Tigranyan R.E., Parsadanyan A.Sh. The effect of low-intensity pulsed microwave EMF on the rhythm of contractions of the frog's heart. Biological effect of electromagnetic fields. Abstracts of reports of the All-Union Symposium. Pushchino, ONTI NTsBI AN USSR, 1982. 2. Tigranyan
R. E., Tyazhelov V. V. Effect of pulsed microwave EMF on the parameters of excitation along the nerve. Biological effect of electromagnetic fields. Abstracts of reports of the All-Union Symposium. Pu-schino. ONTI NCBI AS USSR. 1982.

3. Tyazhelov V.V., Alekseev S.I., Grigoriev P.A. Change in the conductivity of phospholipid membranes modified with alamethicin under the influence of a high-frequency electromagnetic field // Biophysics, **23,** 732–733, 1978. 4. Chersky P . // TIEER, 1975,
vol. 63, no. 11, p. 4–10.
5. Tyashelov V. V., Tigranian R. E., Khizhniak E. P., Akoev I. G. Some pecu-liarities of auditory sensation evoked by pulsed microwave fields // Radio Sci., 1979, v. 14, 6S, p. 259–63.
6. Corelli JC, Gutmann RJ, Kohazi S., Levy J. // J. Microwave Power, v. 12, No. 2, p. 141–144, 1977. 7. Guy A. // In
the world of science. 1986, No. 11. 8.
Biological effects of EMF. Issues of their use and normalization. Sat. scientific works. Pushchino ONTI NTsBI AN USSR, 1986.
9. Schwan H.P., Forster K.R. // TIIER, 1980, vol. 68, No. 1. 10.
Tigranyan R.E., Parsadanyan A.Sh. Biological effect of electromagnetic fields. — In: Abstracts of reports of the All-Union Symposium. Pushchino, ONTI NTsBI AN USSR, 1982.
11. Tigranyan R. E., Khafizov R. Z., Tyazhelov V. V. Biological effect of electromagnetic fields. — In the collection: Abstracts of reports of the All-Union Symposium. Pushchino, ONTI NTsBI AN USSR, 1982.
12. James C., Lin. Ph. D. Microwave auditory effects and application (USA). 13. Eidi
U. R. // TIIER, 1980, v. 68, no. 1. 14. Tigranyan
R. E., Shorokhov V. V. Frequency range of the auditory effect of microwave // Biophysics, 1988. V. 33. Issue. 2. pp. 349–350.
15. Tyazhelov VV, Tigranian RE, Khizhniak EP, Akoev IG — Science, 1979, v. 14, No. 6S, p. 259–263.
16. Mason W. Physical acoustics. T.V. - M.: Mir, 1973.
17. Andrews JM, Strankberg MWP // Proc. IEEE, 1966, No. 54, p. 523. 18. Tulsky
S.V. et al. - V. collection: Molecular biophysics. - M.: Nauka, 1965, p. 41–43.

19. Foster K. R., Finch E. D. // Science, 1974, v. 185, p. 256–258.
20. Joseph C., Sharp, H. Mark Grove, and OM P. Gaudhi. // IEEE trans., 1974, v. 22, p. 583–584.
21. White R. M. // J. Appl. Phys., 1963, v. 34, p. 3559–3567.

22. Tigranyan R. E., Tyazhelov V. V. Biological effect of electromagnetic fields. — In: Abstracts of reports of the All-Union Symposium. Pushchino, ONTI NTsBI AN USSR, 1982. 23. Veprintsev B. N. Dis. for the job application uch.
step. Ph.D. biol. Sci. - M.: MSU, 1960.
24. Kamensky Yu. I. // Biophysics, 1964, vol. IX, issue. 6.
25. Donald S., Mc Ree and Howard Wachtel. // Radiation Research 82, 1980, p. 536–546.
26. Tigranyan R. E. Issues of balneology, physiotherapy and physical therapy // Medicine, No. 6, 1986, p. 11–14.
27. Heintzen P. // Pflugers Archive, ges. Physiol., 1954, v. 259, No. 5, p. 381–399.
28. Trautwein WU, Gottstein and Pederschmidt K. // Pflug. Arch. ges. Phys-iol., 1954, v. 258, No. 3, p. 242. 29. Tigranyan R.E., Parsadanyan
A.Sh. Biological effect of electromagnetic fields. — In: Abstracts of reports of the All-Union Symposium. Pushchino, ONTI NCBI AN USSR, 1982. pp. 13–14.
30. Tyazhelov V.V., Tigranyan R.E. Phase biosynchronizer. Auto. date No. 497011. Publ. 12/30/1975. Bulletin No. 48.
31. Fry W. J., Tucker D. // Acoust. Soc. Amer., 1951, v. 23, p. 627.
32. Fry W. J., Tucker D., Fry E. J. // Acoust. Soc. Amer., 1951, v. 23, p. 364.
33. Fry W. J., Wulff V. J. // Acoust. Soc. Amer., 1950, v. 22, p. 682.
34. Fry W. J., Wulff V. J., Tucker D. // Acoust. Soc. Amer., 1950, v. 22, p. 867.
35. Wall P. D., Tucker D., Fry F. I., Mosberg W. H. // Acoust. Soc. Amer., 1953, v. 25, p. 281.
36. Coronini C., Lassmann G. Congress report of the Erlau ultrasound conference. 1149, S. 72.
37. Coronini C., Lassmann G., Skudrzyk E. // Act. neuroveg., 1950, No. 1, p. 342.
38. Lehmann J., Becker G., Jaenicke W. // Strahlentherapie, 1950, v. 83, p. 311.
39. Sarvazyan AP, Pashovkin TN // Proc. of UB IOMED - IV, v. 1, Viseg rad, Hungary, 1979, p. 103–105. 40. Pchelnikov Yu. N., Sviridov
V. T. High frequency electronics. — M.: Radio and communication, 1981.
41. Jung ÿ. // Klin. Wschr., 1942, v. 21, p. 917.
42. Barth G., Erlhof H., Streibl P. // Strahlentherapie, 1950, No 81, ÿ. 129.
43. Theismann H., Wallhauser KH // Natural Sciences, 1950, v. 37, p. 185.
44. Haussmann HG, Kehler H. // Optik, 1950, v. 7, p. 321.
45. Haussmann H.G., Kehler H., Koch A. // Zs. Hygiene, 1952, v. 134, p. 565. 46. Gavrilov L.P. //
Acoustic zhurn., 1974, vol. 20, p. 27–32.
47. Carstensen EL, Miller MW, Linke CA // J. Biol. Phys., 1974, v. 2, p. 173–192.
48. Kazarinov K.D., Sharov V.S., Putvinsky A.V. Biological effect of electromagnetic fields. — In the collection: Abstracts of reports of the All-Union Symposium. Pushchino, ONTI NTsBI AN USSR, 1982.
49. Schmitz W., Hoffmann D. // Acta Neurovegetatica, 1952, v. 4, p. 99. 50. Kholodov Yu.
A. // Success. physiol. Sciences, 1982, No 2. 51. Valitov R. A.,
Khizhnyak N. A., Zhidkov BC et al. Ponderomotor action of an electromagnetic field. — M.: Sovetskoe radio, 1975.

52. Alexander R. Biomechanics. - M.: Mir, 1970. 53. Krasilnikov V. A. Sound and ultrasonic waves. - M.: Fizmatgiz, 1960.

54. Elpiner I. E. Ultrasound. — M.: Gos. published. phys.-mat. lit., 1963. 55. Mason W. Physical acoustics. T. I, ch. B. — M.: Mir, 1973. 56. Sarvazyan A. P. Dis. on demand. uch. step. Dr. Phys.-Math. sciences. — Pushchino: IBF, 1983.

57. Hughes DE, Nyborg WL // Science, 1962, v. 138, p. 108.

58. Tyashelov VV, Alekseev SA, Faizova L.Kh., Chertishchev VV — URSI Symposium "Electromagnetic Waves and Biology", Jong-en-Josas, July, 1980.

59. Gournay LS Conversion of Electromagnetic to Acoustic Energy by Surface Heating // J. Acoust. Soc. Amer. 1966. V. 40. No. 6. P. 1322–1330. 60. Danilovskaya V. I. // Applied mathematics and mechanics. 1950. T. XIV. P. 316–344.

61. Danilovskaya V. I. // Applied mathematics and mechanics. 1952. T. XIV. P. 341–344.

62. Guo T. C., Guo W.W., Larsen L. E. Microwave-Induced Thermoacoustic Effect in Dielektrics and its Coupling to External Medium. // IEEE Trans. Microw. Theory Tech. 1984. V. 32. No 8. P. 835–843.

63. Lin J. C. Theoretical Analysis of Microwave-Generated Auditory Effects in Animals and Man. — Biological Effects of Electromagnetic Waves. Selected Papers of the USNC/URSI Annual Mecting // Boulder, CO. 1975. V. 1. P. 36–47.

64. Akhadov Ya.Yu. Dielectric properties of binary solutions. - M.: Science, 1977.

65. Tyurin A. M., Stashkevich A. P., Taranov E. S. Fundamentals of hydroacoustics. — L.: Shipbuilding, 1966.

66. Tigranyan R.E. Hypothesis about the acoustic nature of the mechanism of biological action of pulsed microwave fields. Preprint, Pushchino, ONTI NCBI AN USSR, 1984.

67. Brazhnikov N. I. Ultrasonic methods. - M.-L.: Energy, 1965. 68. Bergman L. Ultrasound and its application in science and technology. — M.: Mir, 1957.

69. Sarvazyan A. P. Some general issues of the biological action of ultrasound. Preprint. Pushchino, ONTI NTsBI AN USSR, 1981. 70. Ackerman Yu. Biophysics. - M.: Mir, 1964. 71. Romanov S. N. Biological effect of mechanical vibrations. — L.: Science, 1983.

72. Aidy W. R. // TIIER, 1980, 68 No 1 140–147. 73. Kim Yu. A., Kasimbekov I. K., Fomenko B. S., Tigranian R. E. // Biological Sciences, No 11, 37–40, 1986.

74. D¨oring H. I., Frey A. Changes in the Mechanical Activity of Heart, Skeletal and Smooth Muscle Induced by Hydrodynamic Pressure Pulses. // J. of Low Frequency Noise and Vibration, 1982, vol. 1, No 3, p. 135–148. 75. ÿÿÿÿÿÿ ÿ. ÿ. ÿÿÿÿÿÿ ÿ ÿÿÿÿÿÿÿÿ // ÿÿÿÿÿÿÿ ÿÿ ÿÿÿÿ, ÿ 8, 97–107, 1984.

76. Lebedev I.V. Microwave equipment and devices. // Higher school, 1973. 77. Andrushko L. M., Fedorov N. D. Electronic and quantum devices. — M.: Radio and communication, 1981.

78. Vambersky M.V., Kazantsev A.I., Shelukhin S.A. Transmitting devices Microwave quality. - M.: Higher School, 1984.
79. Tigranyan R. E., Shorokhov V. V. Physical basis of the auditory effect Microwave Pushchino, ONTI PNC, 1991
80. Chou C.-K., Galambos R., Guy A.W., Lovely R. H. Cochlear Microphonics Generated by Microwave Pulses // J. Microwave Power. 1975. V. 10, No 4. P. 361–367.
81. Guy A. W., Taylor E.M., Ahleman B. T., Lin I. C. Microwave Interaction with the Auditory Systems of Humans and Cats. Proc. Int. Microwave Symposium, Boulder, CO. 1973. P. 321–323.
82. Guy A.W., Chou C.-K., Lin J.C., Christeusen D. Microwave-Induced Acoustic Effects in Mammalian Auditory Systems and Physical Materials // Annals of the New York Academy of Sciences, 1975. V. 247. P. 194 –218. 83. Landau L. D., Livshits E. V.
Theoretical physics, vol., Hydrodynamics. - M.: Nauka, 1986.

84. Crawford F. Berkeley course in physics, vol. 3. Waves. — M.: Science, 1984.
85. Ivens I., Skalak R. Mechanics and thermodynamics of biological mem- selected — M.: Mir, 1982.
86. Zinin P. V., LevineW. M., Maev R. D. // Biophysics, 32, No. 1, 185–191, 1987.
87. Dwight G. B. Table of integrals. - M.: Nauka, 1977.
88. Ashmore JF A fast motile response in guinea-pig outer hair cell: the cellular basis of the cochlear amplifier / Ibid. - 1987. - 388. - P. 323–347. 89. Pasechnik V.I. Mechanisms of the cochlea of the
hearing organ. Results of science and technology. Physiology of humans and animals. T. 39. - M.: 1988. 90. Levenshtein V. Excitation and inactivation in the receptor
membrane. Modern problems of electrobiology. - M.: Mir, 1964. - P. 181–210.

91. Bolshakov M. A., Khizhnyak E. P., Tyazhelov V. V. Change in the conductivity of modified phospholipid membranes caused by electromagnetic fields of the decimeter range. — In the collection: Abstracts of reports of the All-Union Symposium “Biological effect of electromagnetic fields.” Pushchino, ONTI NTsBI AN USSR, 1982, p. 7–8. 92. Tigranyan R. E. Amplification of non-ionizing
radiation by periodic biological structures. Abstracts of reports. Pushchino, 1987, p. 28–29. Symposium “Mechanisms of action of electromagnetic radiation.”

93. Frey A. H. Auditory System Response to Radiofrequency Energy // Aerospace Medicine. 1961. V. 32. No 12. P. 1140–1142.
94. Airborne Instruments Laboratory. An Observation on the Detection by the Ear of Microwave Signals // Proc. IRE. 1956. V. 44, No 10. P. 2A.
95. Frey A. H. Human Auditory System Response to Modulated Electromag-netic Energy // J. Appl. Physiol. 1962. V. 17. No 4. P. 689.
96. Frey A. H. Some Effects on Human Subjects of Ultra-High-Frequency Radiation // Amer. J. of Medical Elecronics. 1963. V. 2. P. 28–31.
97. Frey AH Human Perception of Illumination with Pulsed Ultra-Frequency Electromagnetic Energy // Science. 1973. V. 181. P. 356–358. 98.
Tyazhelov V.V., Tigranyan R.E., Khizhnyak E.P. Study of sound effects of high-frequency electromagnetic pulse-modulated field // VINITI, Dep. No. 2049 -77. 1977.

99. Tyazhelov V.V., Alekseev S.N. Problems of forming ideas about the primary mechanisms of the biological action of high-frequency electromagnetic fields // Problems of experimental and practical electromagnetobiology. Pushchino: ONTI NCBI AN USSR, 1983. 100. Khizhnyak E. P., Tyazhelov V. V. Auditory effects under the action of pulsed EMR // Biological effects of electromagnetic fields. Issues of their use and regulation. Pushchino: ONTI NCBI AN USSR, 1986. pp. 49–68.

101. Khizhniak E. P., Tyazhelov V. V., Shorokhov V. V. Some Peculiarities and Possible Mechanisms of Auditory Sensation Evoked by Pulsed Electromag-netic Irradiation // Activ. Nerv. Sup. (Praha), 1979. V. 21. No 4. P. 247–251.
102. Khizhniak EP, Shorokhov VV, Tyazhelov VV Two types of Microwave Auditory Sensation and their Possible Mechanisms // URSI Symposium “Electromagnetic Waves and Biology”. Joui-en-Josas. Paris, July, 1980.
103. Bilsen F. A., Ritsma R. J. Some Parameters influencing the Perceptibility of Pitch // J. Acoust. Soc. Amer. 1970. V. 47. P. 469–475.
104. Frey A. H., Eichert E. S. Psichophysical Analysis of Microwave Sound Perception // J. Bioelectricity. 1985. V. 4. No 1. P. 1–14.
105. Schouten JF, Ritsma RJ, Cardozo BL Pitch of the Residue // J. Acoust. Soc. Amer. 1962. V. 34. P. 1418–1424.
106. Kitsovskaya I. A. Study of the relationships between the main nervous processes in rats exposed to microwaves of different intensities. On the biological effect of ultrahigh frequencies. - M.: Nauka, 1960. P. 75.

107. Frey A. H. A Restraint Device for Cats in a UHF Electromagnetic Energy Field // Psico-Physiology. 1966. V. 2. P. 381–383.
108. Frey A. H. Biological Function as Influenced by Low-Power Modulated RF Energy // IEEE Trans. MTT. 1971. V. MTT-19. No 2. P. 153.
109. Frey A. H., Feld S. R. Avoidance by Rate of Illumination with Low Power Nonionizing Electromagnetic Energy // J. Comparative and Physiological Psichology: 1975. V. 89. No 2. P. 183–188.
110. Hjersen D. L., Phillips R. D., Lovely R. H. Perseption and Response to Pulsed Microwave Radiation by Rats // Abstracts Annual Meeting URSI. Amherst, Mas., 1976.
111. Jonson R. B., Myers D. I., Guy A. W., Lovely R. H., Galambos R. Dis-criminative Control of Appetitive Behavior by Pulse Microwave Radiation in Rats // Biological Effect of Electromagnetic Waves. Selected Papers of the USNC/URSI Annual Meetings, Boulder, CO, Oct., 20–30; NEW Publication (FDA) 77 —8010. 1976. V. 1. P. 238–247.
112. King N. W., Juste D. R., Clarke R. L. Behavioral Sensitivity to Microwave Radiation // Science. 1971. V. 172. P. 398–401.
113. Stverak I., Marha K., Pafkova G. Some Effects of Various Pulsed Fields on Animals with Audiogenic Epilepsy // Biologic Effects and Health Hazards of microwave Radiation. Ed. P. Czersky et al., Polish Medical Publishers. Warsaw 1974. P. 141–144.
114. Lamb G. Dynamic theory of sound. - M.: Fizmatgiz, 1960. 115.
Romanenko E. V. Physical foundations of bioacoustics. - M.: Nauka, 1974. 116.
Tigranyan R. E. Physico-technical practice of biological experiment with microwave radiation. Pushchino: ONTI NCBI AN USSR, 1985, 130 p.

117. Tigranyan R. E. Microwave generators with broadband pulse modulation for biological research based on medical microwave therapy devices // Devices and laboratory equipment for scientific research in new directions of biology and biotechnology. Pushchino, ONTI NCBI AN USSR, 1986. pp. 66–70. 118. Tigranyan R. E., Mashkin P. V. Ibid. Tube microwave generators for

biological research. pp. 70–76.

119. Tigranyan R. E., Shorokhov V. V. On the issue of physical modeling of acoustic effects under the action of microwave fields on biological systems // Biophysics. 1985. T. 30. Issue. 5. pp. 894–899. 120. Shorokhov V.V., Tigranyan R.E., Mashkin I.V. Study of

the features of the radio sound effect using a spherical model // Biophysics. 1986. T. 31. Issue. 4. pp. 695–700.

121. Lin J. C. Microwave Auditory Effects and Applications. Springfield, Illinois: Charles C. Thomas, 1978.

122. Constant P. C. Hearing EM Waves. Digest of the 7th International Confer-ence on Medical and Biological Engineering. Stockholm, Sweden, August, 14–19. 1967. P. 349.

123. Atsuko M., Masao S. Microwave Auditory Effects // J. Acoust. Soc. Jap. 1983. V. 39. No 4. P. 262–265.

124. Physiology of sensory systems. Guide to Physiology Part 2. - L.: Nauka, 1972.

125. Chou ÿ.-ÿ., Guy A. W. Microwave-Induced Auditory Response: Cochlear Microphonics // Biological Effects of Electromagnetic Waves, edited by C. C. Johnson and M. J. Shore, Bureau of Radiological Health FDA (77 —8010). Rochville, Maryland, 1977.

126. Seaman R. L., Lebovitz R. M. Auditory Unit Responses to Single-Pulse Microwave Stimuli // Hearing Research. 1987. V. 26. P. 105–116.

127. Wilson B. S., Zook J.ÿ., Joines W. T., Casseday J. H. Alterations in Activity at Auditory Nuclei of the Rat Induced by Exposure to Microwave Radi-ation: Autoradiographic Evidence Using [l4C]-2-deoxy-D-Glucose // Brain Research. 1980. V. 187. P. 291–306.

128. Wilson B. S., Kobler J. B., Casseday J. H., Joines W. T. Spectral Content of Microwave-Induced Auditory Stimuli as Demonstrated by [14C]-2-deoxy-D-Glukose Uptake at the In ferior Colliculus // Bioelectromagnetics Abstracts, 1983, v. 5, p. 46.

129. Wilson B. S., Joiness H. T. Mechanism and Physiologic Significance of Microwave action on the Auditory System // J. Bioelectricity. 1985. V. 4. No 2. P. 495–525.

130. Young I. M., Lowry L. D., Menduke H. A Bekesy Descenting-Only Proce-dure: Effects of Attenuation Rate and Step Size, and Starting Level // J. Auditory Res. 1985. V. 25. P. 201–208.

131. Engin A. E., King L. J. Axisymmetric Response of a Fluid-Filled Spherical Shell in Free Vibrations // J. Biomechanics. 1970. V. 3, No 1. P. 11–22.

132. Chou C.-K., Guy A.W., Galambos R. Characteristics of Microwave-Induced Cochlear Microphonics // Radio Science. 1977. V. 12, No 6(S). P. 221–227.

133. Lin J. C. On Microwave-Induced Hearing Sensation // IEEE Trans. Microw. Theory Tech. 1977. V. MTT-25. No 7. P. 605–613.

134. Sagalovich B. M., Melkumova G. G. Study of the effect of electromagnetic waves of ultra-high frequency on evoked potentials of auditory centers

in connection with the prospects for using inadequate auditory stimulation // Vestn. otorhinol. 1974. T. 4. pp. 3–8.

135. Anne A., Saito M., Salti O. M., Shvan H. P. Relative Microwave Absorption Cross Sections of Biological Significance. In: Biological Effect of Microwave Radiation. V. 1. N. Y., Plenum Press, 1961. P. 153–176.

136. Ho H. S., Hagan G. J., Foster M. R. Microwave Irradiation Design Using Dielectric Lenses // IEEE Trans. Microw. Theory Tech., 1975. V. MTT-12. P 1058–1061.

137. Kritikos H. N., Schwan H. P. Hot Spots Generated in Conducting Spheres by Electromagnetic Waves and Biological Implications // IEEE Trans. Biomed. Eng. 1972. V. BME-19(1). P. 53–58.

138. Lin J.C. Auditory effect on microwave // TIEER. 1980. T. 68, No. 1. 139.

Shutilov V. A. Fundamentals of ultrasound physics. - L.: Publishing house Leningradsko-University, 1980.

140. Chou C.-K., Guy AW, Galambos R. Microwave-Induced Cochlear Micro-phonics in Cats // J. Microwave Power. 1976. V. 11. No 2. P. 171–173. 141. Malikova

S. I., Malyshev V. L., Balakireva V. N., Gorban L. G. Influence-influence of decimeter waves on the temperature of the brain and adjacent fabrics. // Issues of balneology, physiotherapy and pulmonary physical culture. 1982. T. 2. pp. 18–22.

142. Olsen R. G., Lin J. C. Microwave Pulse Induced Acoustic Resonances in Spherical Head Models // IEEE Trans. Microw. Theory Tech. 1981. V. MTT-29. No 10. P. 1114–1117.

143. Wilson J. J., Johustone J. R. Basilar membrane and middle ear vibration in guinea-pig measured by capasitive probe // J. Acoust Soc. Amer. 1975. V. 57. P. 705–715.

144. Anzelus A. The Effect of an Impact on a Spherical Liquid Mass // Acta Pathology Microbiology Scandinavica. 1943. V. 488. P. 153–159.

145. Hu ÿ.-L. Spherical Model of an Acoustical Wave Generated by Rapid Laser Heating in a Liquid // J. Acoust. Soc. Amer. 1969. V. 4. No 3 (part 2). P. 728–736.

146. Mc Ivor I.ÿ., Sonstegard D. A. Axisymmetric Response of a Closed Spher-ical Shell to a Nearly Radial Impulse // J. Acoust. Soc. Amer. 1966. V. 40 No 6. P. 1540–1547.

147. Wilkinson J. P. Natural Frequencies of Closed Spherical Shells // J. Acoust. Soc. Amer. 1965. V. 38. P. 367–368.

148. Khalil T. B., Viano D. C., Smith D. L. Experimental Analysis of the Vibra-tional Haracteristics of the Human Skull // J. Sound and Vibrations. 1979. V. 63. No 3. P. 251–376.

149. Khalit T. B., Viano D. C. Comparison of Human Skull and Spherical Shell Vibrations Implication for Head Injury Modeling // J. Sound and Vibrations. 1982. V. 82. No 1. P. 95–110.

150. Tondorf J., Jahn A. F. Velosity of Propagation of Bone-Conducted Sound in a Human Head // J. Acoust. Soc. America. 1981. V. 70. No 5. P. 1294–1297.

151. Zwisloski J. J. Acoustic Attenuation between Ears // J. Acoust. Soc. Amer. 1963. V. 25. P. 752–759.

152. Olsen R. G., Lin J. C. Microwave-Induced Pressure Waves in Mammalian Brains // IEEE Trans. Biomed. Eng. 1983. V. BME-30. No 5. P. 289–293.

153. Kolomiychenko A. I., Sheiman N. S. Atlas of tonal audiometric studies. (Manual for practitioners and students). Kyiv: GMI of the Ukrainian SSR, 1962.

154. Carhart ÿ. Clinical Application of Bone Conduction Audiometry // Archives of Otolaringology. 1950. V. 51. P. 797–808.

155. Dirks D. D., Libarger S. F., Olsen W. O., Billings B. L. Bone Conduction Calibration: Currents Status // J. Speech and Hear. Disord. 1979. V. 44. No 2. P. 143–155.

156. Queller J. E., Khanna S. M. Changes in Bone Conduction Thresholds with Vibrator Contact Area // J. Acoust. Soc. Amer. 1982. V. 71. No 6. P. 1519– 1526.

157. Whittle LS A Determination of the Normal Threshold of Hearing by Bone Conduction // J. Sound and Vibration. 1965. V. 2. No. 3. P. 227–248. 158. Sagalovich B. M., Melkumova G. G.

The ratio of hearing thresholds during air and bone conduction of sounds in humans is normal // Bulletin of Otorhinolaryngology. 1967. T. 2. pp. 78–83.

159. Shunichi K., Suzuki ÿ., Sone T. Some Consideration on the Auditory Perseption of Ultrasonic and its Effects on Hearing // J. Acoust. Soc Jap. 1985. E6. No 1. P. 3–8.

160. Bednin F.V., Sagalovich B.M. Equivalent thresholds of human audibility during bone conduction of sounds, measured using an “artificial mastoid” device in an extended frequency range // Acoustic Journal. 1975. T. 21, issue. 5. pp. 673–678. 161. Bednin F.V., Sagalovich B.M. The ratio of human hearing thresholds

skill in air and bone conduction of sounds in an extended frequency range // Acoustic Journal. 1984. T. 30, issue. 5. pp. 589–593. 162. Sagalovich B. M.. Simbirtseva O. I. Age characteristics of equivalence

tape thresholds of human hearing during bone conduction of sounds in an extended frequency range // Akust. magazine 1978. T. 24, no. 2. pp. 307–309.

163. Brinkman ÿ., Richter U. The determination of the normal hearing threshold for bone conduction with different bone conduction headphones // Audiol. Acoust. 1983. V. 22. No 4. P. 114–118.

164. Corso J. F. Bone-Conduction Thresholds for Sonic and Ultrasonic Frequen-cies // J. Acoust. Soc. Amer. 1963. V. 35. No 11. P. 1738.

165. Fenstein S. N., Hollien H., Hollien R. Diver Auditory Sensitivity: Another Look at Bone Conduction // J. Acoust. Soc. Amer. 1972. V. 52. No 1 (part 1). P. 170.

166. Nixon C.M., von Gierke H. E. Experiments on the Bone-Conduction Threshold in a Free Sound Field // J. Acoust. Soc. Amer. 1959. V. 31. No 8. P. 1121–1125.

167. Young I. M., Lowry L. D. Ascending and Descending Thresholds of Pure Tones // J. Acoust. Soc. Amer. 1986. V. 80, Suppl. 1, p. 123.

168. Zwislocki J. In Search of the Bone-Conduction Threshold in a Free Sound Field // J. Acoust. Soc. Amer. 1957. V. 29. No. 7. P. 795. 169. Sagalovich B. M., Bednin F. V.,

Gorshkov V. G., Stamov-Vitkovsky A. V. Bone telephone for the study of hearing acuity and hearing aids // BI. 1974. No. 42, Author. St. No. 449713. 170. Handbook of radio engineering / Ed. B. A. Smirenina. — M.-L.: GEI,

1950.

171. Sagalovich B. M., Bednin F. V. “Artificial mastoid” device for calibrating bone telephones in an extended frequency range // Med. technique. 1981. No. 1. P. 28–31. 172. Molchanov A.P., Babkina L.V. Electrical models of snail

mechanisms

organ of hearing. — L.: Nauka, 1978.

173. Human anatomy / Ed. S. S. Mikhailova. - M.: Medicine, 1984.

174. Goss S. A., Johnston R. L., Dunn F. Complication of Empirical Ultrasonic Properties of Mammalian Tissues. II // J. Acoust. Soc. Amer. 1980. V. 68. No 1. P. 93–108.

175. Ludvig G. D. The Velocity of Sound through Tissues and Acoustic Impedance of Tissues // J. Acoust. Soc. Amer. 1950. V. 22. No 6. P. 862–866.

176. Lagutin V.V., Molchanov A.P. Models of hearing mechanisms. - M.: Energia, 1973.

177. Belotserkovsky G. B. Fundamentals of radio engineering and antennas. Part I. - M.: Soviet radio, 1969.

178. Mechanisms of hearing // Problems of physiological acoustics. T.VI. — L.: Science, 1967.

179. Glinsky B.A., Gryaznov B.S., Dynin VS, Nikitin E.P. Modeling as a method of scientific research. - M.: Moscow State University Publishing House, 1965. 180. Prager V.

Introduction to continuum mechanics. - M.: IL, 1963.

181. Holmes M. H., Cole J. D. Cochlear mechanics: Analysis for a pure tone // J. Acoust. Soc. Amer. 1984. V. 70. No 3. P. 767–768.

182. Robles L., Ruggero M. A., Rich N. C. Basilar Membrane Mechanics at the Base of the Chinchilla Cochlea. I. Input-Output Function, Tunning Curves, and Response Phases // J. Acoust. Soc. Amer. 1986. V. 80. No 5. P. 1364– 1374.

183. Johnstone B. M., Yates G. K. Basilar membrane tuning curves in the guinea-pig // J. Acoust. Soc. America. 1974. V. 55. P. 389–390.

184. Rhode W. S., Diesler C. D. Measurement of the amplitude and phase of vibration of the basilar membrane using the Mosbauer effect // J. Acoust. Soc. America. 1970. V. 47. P. 60.

185. Labutin V.K., Molchanov A.P. Hearing and signal analysis. — M.: Energy, 1967.

186. Tigranyan R. E., Shorokhov V. V., Gorokhov A. L. Double-circuit resonant model of the auditory effect of pulsed microwave fields. Abstract. // Biophysics. 1988. T. 33. Issue. 3. P. 536. VINITI. Dep. No. 2506—B88.

187. Schouten JF // Proc. or Royal Netherlands Academy of Arts and Sciences shelves. 1940. V. 43. No 3. P. 356.

188. Schouten JF // Proc. or Royal Netherlands Academy of Arts and Sciences. 1940. V. 43. No 3. P. 991.

189. Shouten JF // Philips. Techn. Rev. 1940. V. 5. P. 286. 190. Experimental

psychology // Ed. S. S. Stevens. — M.: IL, 1963.

191. Zwicker E.. Feldkeller R. The ear as a receiver of information. — M.: Communication, 1971.

192. Shakhparonov M. I. Methods for studying the thermal motion of molecules and structure of liquid. - M.: Moscow State University Publishing House, 1963.

193. Vartanyan I. A., Tsirulnikov. Touch the invisible, hear the inaudible. - L.: Science, 1985.

194. Shkurin G.P. Handbook on measuring and radio measuring instruments. Radio measuring instruments. Album of schemes. - M.: Military Publishing House of the Ministry of Defense of the USSR, 1960.
195. Shkurin G.P. Handbook on electrical and radio measuring instruments. Radio measuring instruments. - M.: Military Publishing House of the Ministry of Defense of the USSR, 1960.

196. Tigranyan R. E. Physico-technical practice of biological experiment with microwave radiation. Pushchino: ONTI NTsBI, 1985. 197. Harvey A. F. Microwave technology. T. 2. - M.: Sov. radio, 1965, p. 422–440. 198. Krylova V. A., Yuchenkova T. V. Protection from electromagnetic radiation. - M.: Soviet Radio, 1972. 199. Nefedov E. I., Fialkovsky A. T. Strip transmission lines. - M.: Nauka, 1980. 200. Koltun S.V., Tigranyan R.E. In the collection: Instruments and laboratory equipment for scientific research in new directions of biology and biotechnology. Pushchino: ONTI NCBI AN USSR, 1987, p. 56–64. 201. Valitov R. A., Popov I. A. Radio transmitting devices on semiconductor diodes. Design and calculation. - M.: Soviet Radio, 1973. 202. Gvozdev V.I., Nefedov E.I. Volumetric microwave integrated circuits. - M.: Nauka, 1985.

203. Mariani EA, Heizman CP, Agrios J.R., Cohn SB // IEEE Trans. Microwave Theory and Techn., 1969, v. 17, No 12, p. 1091–1096.
204. Atabekov G.I. Linear electrical circuits. Part I. - M.: Energia, 1978; Part II, III, 1979, 592, 432 p. 205. Aizenberg G. Z. Ultrashort wave antennas. - M.: State. publishing house Department on Communications and Radio, 1957.
206. Harvey A.F. Ultrahigh frequency technology. T. I, II. — M.: Sovetskoe radio, 1963
207. Feldshtein A. L., Yavich L. R., Smirnov V. P. Handbook on elements of waveguide technology. - M.: Soviet Radio, 1967. 208. Neiman M. S. Course of radio transmitting devices. - M.: Soviet radio, 1958.
209. Mobile device for DCV therapy “Volna-2”. Passport. 210. Ivanov A. B., Sosnovkin L. N. Microwave pulse transmitters. - M.: Soviet radio, 1956.
211. Andreevsky M. N. Designs of decimeter and meter wave generators. - M.: Oborongiz, 1956.

212. Frey AM Biological Function as Influenced by Low-Power Modulated RF Energy. Microwave theory and techniques, vol. MTT -19, 2, 1971. 213. The influence of microwave radiation on the human body and animals. Ed. acad. USSR Academy of Medical Sciences prof. I. R. Petrova. - Medicine, Leningrad branch, 1970.

214. Electrovacuum devices. Directory. — M.–L.: Gosenergoizdat, 1956.
215. Vereshchagin E. M. Modulation in microwave generators. — M.: Soviet radio, 1972.
216. Device for microwave therapy “Luch-3”. Passport. 217. Device for microwave therapy “Luch-58-1”. Passport. 218. Portable microwave therapy device “Romashka”. Passport.

219. Liventsev N. M. Electromedical equipment. — M.: Medicine, 1964.

220. Starikov V.D. Methods of measurement in the microwave using a measuring device ny lines. - M.: Soviet radio, 1972.

221. Tyashelov V. V., Tigranian R. E., Khizhniak E. P. New artifact free elec-trodes for recording of biological potentions in strong electromagnetic fields. // Radio Sci., 1977, v. 12/6S. 222.

Tigranyan R. E., Tyazhelov V. V. Effect of pulsed microwave EMF on the parameters of excitation along the nerve. Biological effect of electromagnetic fields. Abstracts of reports of the All-Union Symposium. Pushchino, ONTI NTsBI AN USSR, 1982.

223. Buresh J., Petran M., Zakhar I. Electrophysiological research methods. - M.: IL, 1962. 224. Tasaki I. Conduction of a nerve impulse. -

M.: IL, 1957. 225. Parsadanyan A.Sh., Khafizov R.Z., Tigranyan R.E. Methodology for

recording the electrogram of the heart of a whole frog under microwave irradiation conditions. // Biological Journal of Armenia, Academy of Sciences of the Armenian SSR, vol. XXX, No. 7, Yerevan, 1977.

226. Presman A. S.. Electromagnetic fields and living nature. — M.: Science, 1968.

227. David R. Introduction to biophysics. - M.: Mir, 1982. 228. Koltun

S.V., Tigranyan R.E. Fundamentals of the theory of calculation and design of microwave microgenerators for biophysical research. Preprint, Puschino, 1989.

229. Cohn SB IEEE Trans. Microwave Theory and Techniques, v. MTT-17, No. 10, p. 768, 1969. 230. Handbook on the

calculation and design of microwave strip devices. Ed. Volmana V.I. - M.: Radio and communications, 1982. 231. Komar G.I., Shestopalov V.P. // Radio engineering and

electronics, vol. XXXII, no. 7, p. 1345, 1987.

232. Cohn S. B. // IEEE Trans. Microwave Theory and Techniques, v. MTT-20, No 2, p. 172, 1972.

233. Mariani E. A., Heinzman C. P., Agrios J. P., Cohn S. B. // IEEE Trans. Microwave Theory and Techniques, v. MTT-17, No 12, p. 1091, 1969.

234. Handbook Chemist, vol. 3. - L.: Chemistry, 1965, p. 664. 235. Johnson

K, Guy A . // TIIER, 1972, t. 60, p. 49. 236. Lavrov A. S., Reznikov G.

B. Antenna-feeder devices. — M.: Soviet radio, 1974. 237. All-Union norms of permissible industrial radio interference. — M.:

Communication, 1973.

238. Industrial radio interference from industrial, scientific and medical high-frequency installations. GOST 23450-79. State USSR Committee on Standards. - M.: Standards Publishing House, 1979.

239. Instructions on the procedure for issuing permits for the acquisition, construction (installation) and operation of radio-electronic equipment and HF installations. - M.: Communication, 1977. 240. Recommendations

for the use, design and installation of shielded rooms and cabins. - M.: Communication, 1966.